Ministry of Education
Department of Higher Education
East Yangon University

East Yangon University Research Journal

Vol. 9, No. 2 March, 2023

Ministry of Education
Department of Higher Education
East Yangon University

East Yangon University Research Journal

Vol. 9, No. 2 March, 2023

Ministry of Education
Department of Higher Education
East Yangon University

Research Journal 2023, Vol. 9, No. 2

Editorial Board

Editor in Chief

Dr. Nay Win Oo	Rector, East Yangon University
Dr. Aye Aye Ko	Pro-Rector, East Yangon University
Dr. Wah Wah Lwin	Pro-Rector, East Yangon University
Dr. Thidar Aung	Pro-Rector, East Yangon University

Editors

Dr. Thin Thin Soe	Professor and Head, Department of Myanmar
Dr. Aung Kyi	Professor and Head, Department of English
Dr. Nyein Nyein Win	Professor and Head, Department of Geography
Dr. Wah Wah Thein	Professor and Head, Department of History
Dr. Tin Tin Sein	Professor and Head, Department of Philosophy
Dr. Htar Htar Khin	Professor and Head, Department of Psychology
Dr. Thi Thi Lwin	Professor and Head, Department of Law
Dr. Thi Thi San	Professor and Head, Department of Oriental Studies
Dr. Min Thaung	Professor and Head, Department of International Relationship
Dr. Nan Nyo Nyo Win	Professor and Head, Department of Anthropology
Dr. Saw Mya Kyi Thar	Professor and Head, Department of Library and information
Dr. Myo Myo Myat	Professor and Head, Department of Chemistry
Dr. Naing Naing Oo	Professor and Head, Department of Physics
Dr. Sandar Maw	Professor and Head, Department of Mathematic
Dr. Ohn Mar Ohn	Professor and Head, Department of Zoology
Dr. Htay Htay Lwin	Professor and Head, Department of Botany
Dr. Than Than Thwe	Professor and Head, Department of Geology
Dr. Khin Thida Win	Professor and Head, Department of Industrial Chemistry

CONTENTS

No	Title	Page
28.	**DATA LOGGING SYSTEM USING INFLUX DB CLOUD AND ESP 32** *Dr. Su Su Aung, Professor, Department of Physics*	260
29.	**INVESTIGATION ON STRUCTURAL, SURFACE MORPHOLOGICAL AND OPTICAL PROPERTIES OF TRANSPARENT CONDUCTIVE OXIDE FILMS BY PRECIPITATION METHOD** *Dr. Nyo Nyo Myint, Associate Professor, Department of Physics*	271
30.	**RELIABLE AND USER FRIENDLY ELECTRONIC BALLOT SYSTEM** *Daw ThaZin Hlaing, Demonstrator, Department of Physics*	278
31.	**INVESTIGATION OF HEAVY METAL CONCENTRATION IN FLOWERS, LEAVES AND BARKS OF MANGROVE TRUMPET TREE (THAKUT)** *Daw Myint Zu Thin, Demonstrator, Department of Physics*	288
32.	**COMPARISON AND INVESTIGATION OF THE DIELECTRIC PROPERTIES OF UN-DOPED AND AI-DOPED TITANIA THIN FILMS** *U Shine Ko Ko, Demonstrator, Department of Physics*	296
33.	**INTELLIGENT ROOM LIGHT CONTROL AND ELECTRICAL POWER SAVING SYSTEM UTILIZING PERIPHERAL INTERFACE CONTROLLER** *Daw Phyu Thel Ei, Demonstrator, Department of Physics*	307
34.	**STUDY ON WINDOW CURTAIN DRIVING SYSTEM USING ARDUINO UNO** *Daw Kay Zin Win, Demonstrator, Department of Physics*	315
35.	**COMPARATIVE STUDY OF THE SOLAR POWER UTILIZATION AND DEVELOPMENT , IN KHAYAN AND THANLYIN TOWNSHIPS** *Daw Ngu Wah Hlaing, Demonstrator, Department of Physics*	324
36.	**GEODETIC NUMBER OF A CONNECTED GRAPH HAVING THE UNIQUE DIAMETRAL PATH** *Dr. Kyaw Lin Aung*, Lecturer, Department of Mathematics	336
37.	**A STUDY ON THE VALUATIONS OF DEEPLY RAMIFIED ON A FIELD** *U Zaw Myo Thant, Tutor, Department of Mathematics*	343
38.	**LINEAR FUNCTIONALS ON A FINITE DIMENSIONAL INNER PRODUCT SPACE** *Daw Aye Thandar Aung, Tutor, Department of Mathematics*	351

No	Title	Page
39.	**COMPARATIVE STUDY ON MORPHOLOGICAL APPEARANCE OF BLOOD CELLS IN SOME MAMMALS FROM YWAR THAR GYI SLAUGHTER-HOUSE, YANGON REGION** *Dr. Thida, Associate Professor, Department of Zoology*	361
40.	**THE NESTING ECOLOGY OF SOME TERRESTRIAL BIRDS IN THE CAMPUS OF EAST YANGON UNIVERSITY, THANLYIN TOWNSHIP, YANGON REGION** *Dr. Khin Maw Maw Myint, Associate Professor, Department of Zoology*	373
41.	**SPECIES COMPOSITION AND CATCH WEIGHT OF FISHES FROM DIFFERENT WHOLESALES IN KALAGWEL VILLAGE, THANLYIN TOWNSHIP** *Daw Aye Aye Mu, Demonstrator, Department of Zoology*	382
42.	**SEASONAL PREVALANCE RATE AND LARVAL OCCURRENCE OF *AEDES AEGYPTI* (LINNAEUS,1762) IN THREE QUARTERS OF THARKAYTA TOWNSHIP, YAGON REGION** *Daw Wint Yee Phyo, Demonstrator, Department of Zoology*	390
43.	**A STUDY OF THE DIFFERENT TOXICITY OF VIPER'S VENOM IN KAUNGYANGON TOWNSHIP,YANGON** *Daw Zin Moe Swe, Demonstrator, Department of Zoology*	401
44.	**A COMPARATIVE STUDY OF OPERCULAR APPRATUS OF SOME SILURID FISHES FROM MYOMA MARKET, THANLYIN TOWNSHIP** *Daw Thiri Nwe, Demonstrator, Department of Zoology*	410
45.	**ASSESSMENT OF MARINE FISH SPECIES DIVERSITY (ORDER-PERCIFORMES) FROM YANBYE TOWNSHIP, RAKHINE STATE** *Daw Yee Yee Khin, Demonstrator, Department of Zoology*	421
46.	**INVESTIGATION OF SOME EDIBLE GASTROPOD SPECIES IN NATIONAL RACES VILLAGE AT THARKAYTA TOWNSHIP** *Daw Su Hlaing Myint, Demonstrator, Department of Zoology*	433
47.	**EFFECTS OF DIFFERENT DIETS ON THE GROWTH AND SURVIVAL RATE OF COMET GOLDFISH, *CARASSIUS AURATUS AURATUS* LINNAEUS, 1758.** *Daw Myat Su Aung, Demonstrator, Department of Zoology*	443
48.	**SOME ECONOMIC FISH PRODUCTS FROM MYOMA MARKET IN KYAUKTAN TOWNSHIP, YANGON REGION** *Daw Yu Mon Khaing, Demonstrator, Department of Zoology*	456

No	Title	Page
49.	**OCCURRENCE OF SOME CEPHALOPODS SPECIES IN NYAUNG TAN JETTY, PAZUNDAUNG TOWNSHIP, YANGON REGION** *Daw Seinn lae Phyu, Demonstrator , Department of Zoology*	463
50.	**FECUNDITY AND NUTRITIONAL VALUE OF MEALWORM BEETLE *TENEBRIO MOLITOR* LINNAEUS, 1758** *Daw Mya Myo Marn, Demonstrator, Department of Zoology*	472
51.	**SEASONAL VARIATION OF SOME EDIBLE FROG SPECIES AROUND SI KONE VILLAGE, THANLYIN TOWNSHIP** *Daw Su Myat Win, Demonstrator, Department of Zoology*	480
52.	**MORPHOMETRIC AND REPRODUCTIVE PARAMETERS OF *JOHNIUS COITOR* (HAMILTON,1822) AND *POLYNEMUS PARADISEUS* LINNAEUS, 1758 IN MYOMA MARKET OF THANLYIN TOWNSHIP** *Daw Aung Thu Zar Tun, Demonstrator, Department of Zoology*	491
53.	**DIFFERENT TYPES OF TAIL AND CAUDAL SKELETONS OF SOME BONY FISH FROM MYOMA MARKET, THANLYIN TOWNSHIP** *Daw Pa Pa Win, Demonstrator, Department of Zoology*	500
54.	**COMPARISON OF MORPHOLOGICAL, PHYTOCHEMICAL CHARACTERIZATION AND ANTIMICROBIAL ACTIVITIES ON TWO SPECIES OF GENUS *JUSSIAEA*** *Dr. Htay Htay lwin, Professor and Head, Department of Botany*	512
55.	**EFFECT OF POSTHARVEST TREATMENTS ON SHELF-LIFE OF *LYCOPERSICON ESCULENTUM* MILL** *Dr. Su Latt Win, Associate Professor, Department of Botany*	420
56.	**STUDY OF PLANT SPECIES DIVERSITY IN DIFFERENT SITES OF THANLYIN AREA** *Dr. Myat Su Hlaing, Associate Professor, Department of Botany*	530
57.	**ANTIPYRETIC EFFECT OF *KAEMPFERIA GALANGA* L. RHIZOMES** *Dr. Phyo Moh Moh Zin, Lecturer, Department of Botany*	541
58.	**LITHOFACIES ASSOCIATIONS OF KALAW FORMATION IN WESTERN PART OF THE SHAN PLATEAU** *Dr. Than Than Thwe, Professor and Head, Department of Geology*	555
59.	**ENGINEERING GEOLOGICAL INVESTIGATION OF MYO GYI MULTIPURPOSE DAM PROJECT, YWA-NGAN TOWNSHIP, SHAN STATE (SOUTH)** *Daw Myint Myint Soe, Lecturer, Department of Geology*	562

No	Title	Page
60.	**HYDROCARBON EXPLORATION TARGETS IN SECOND LINE OF STRUCTURE MAGWE AND MANADALAY REGIONS** *Daw Kay Khine Yu, Lecturer, Department of Geology*	572
61.	**CARBONATE PETROLOGY AND LEAD MINERALIZATION OF THE BAW BYU-TAUNG AND NYAUNGLWE AREA, KALAW TOWNSHIP, SHAN STATE (SOUTH), MYANMAR** *U Zaw Moe Lwin, Demonstrator, Department of Geology*	580
62.	**DISTRIBUTION AND ECOLOGY OF RECENT FORAMINIFERA IN THE MYEIK COASTAL AREA, TANINTHARYI REGION, MYANMAR** *U Thet Paing Soe, Demonstrator, Department of Geology*	592

DATA LOGGING SYSTEM USING INFLUXDB CLOUD AND ESP 32

Su Su Aung[1], Khet Khet Tun[2]

Abstract

This research is based on sensor data logging system using ESP32 and InfluxDB. Physical quantities can be detected and stored by processing with the aid of ESP32 microcontroller which is internet – enable device which composed of dual-core processor, Wi-Fi module and Bluetooth. In this research, DHT 11 is used as a sample sensor. Weather data such as temperature, humidity, heat index and dew point are detected from DHT11 sensor. InfluxDB is an open source platform. It has high -performance time series database (TSDB). Each data which are submitted to the database is attached with a certain timestamp. Another advantage is that it can store large amount of data with timestamp per second. Nowadays, it becomes popular for data logging internet of things (IoT) research. The 40-bit sensor data of DHT11 are detected and processed to transform the readable data values by using ESP32. InfluxDB account is created by using Gmail. The credentials such as Wi-Fi name, Wi-Fi password, URL of Influx DB, Influx DB token and bucket are included in program. ESP32 can interface to InfluxDB with the aid of ESP8266 InfluxDB library. Sensor data is sent to InfluxDB through ESP32 from DHT11 sensor. InfluxDB composes of dashboard tools to display the sensor data in the different format such as graph, charts, gauge, table and histogram. InfluxDB account with free charge can retain the data for up to 30days while commercial InfluxDB account can retain sensor data for unlimited duration. This research is used for any database purpose like weather station and for monitoring system in industrials.

Key words: InfluxDB, ESP32, bucket, tag, dashboard.

Introduction

Time series data is different from the normal data in the research work. The main characteristic is the illustration at which point in time data samples are collected. This research is dealt about (i) the sending sensor data to cloud (ii) visualizing data with the help of dashboard tool on personal computer and tablet using IoT cloud and (iii) stored the data for a specified time duration. Among the various IoT platforms, Influx DB is one of IoT clouds used in this research. Physical parameters such as temperature, humidity, heat index and dew point are detected by using DHT11 sensor. DHT 11 sensor produces the 40-bit digital sensor output. ESP32 processes to convert these outputs to the readable sensor values. As ESP32 is a microcontroller attached with Wi-Fi and Bluetooth, it can be enabled to connect to internet with its Wi-Fi. Influx DB is an open-source time series database (TSDB) that can be enable to use in monitoring the data on the dashboard in form of graph, chart, widgets, table and histogram, real time data analysis and storing the data accompanying with timestamp. The special characteristics of Influx DB is that a huge amount of data can be logged every second with timestamps.

There are two essential parts to implement this research. These are hardware and software sections. On the hardware parts, the device which is enable to connect IoT such as ESP32, ESP8266. In this research, ESP32 is used as memory size and speed are higher than another compatible microcontroller. And then, DHT 11 sensor is used to obtain the temperature, humidity and other parameters related with them. On the software tools, ESP8266 InfluxDB library, DHT library and InfluxDB account are required. The program can be uploaded by Arduino IDE or VS code studio. ESP boards are needed to install in Arduino IDE because these boards are not included as default. The complete mechanism of this research is illustrated as block diagram in Figure 1.

[1] Dr, Professor, Department of Physics, East Yangon University.
[2] Dr, Associate Professor, Department of Physics, East Yangon University

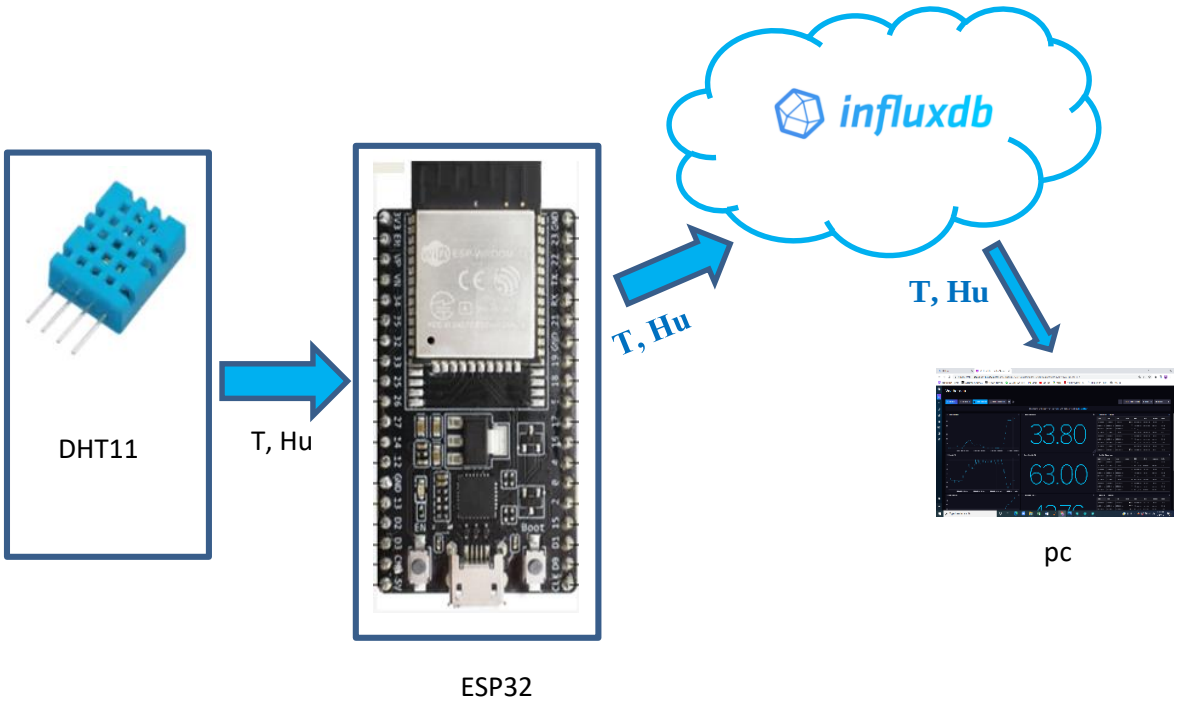

Figure 1. Block diagram of sensor data transporting via InfluxDB

Materials and Methods

DHT 11 mainly produces temperature and humidity in the format of 40- bit digital output. ESP32 detected and sends these values to InfluxDB through internet access. InfluxDB composes of dashboard tool which visualizes sensor data in the form of graph, gauge and table. Data is logged with timestamp for specified period.

ESP32

ESP32 is a microcontroller with dual-core 32 –bit microprocessor. Its operation speed is **80 to 240 MHz** adjustable clock frequency. ESP32 is attached with Wi-Fi transceiver, classic Bluetooth and Bluetooth low energy (BLE) capabilities. ESP32 can not only connect to a Wi-Fi network and interact with internet as station (STA) mode but also it can setup an own network as soft access point (AP) mode. It comprises of 448 kB of ROM, 520 kB of SRAM and 4 MB of flash memory which are sufficient to implement web pages, JSON / XML, (JavaScript Objects notation /Extensible Markup Language) data and everything used in IoT devices.

There are many ESP32 development boards in the local market. ESP32 Development Board with pin assignment used in this research is shown in Figure 2. There are many multiplexed I/O pins in ESP32. They are (1) 1 I2C interface, (2) 3 SPI interface, (3) UART interface, (4) I2S interface, (5) 15 ADC channels (6) 2 DAC channel, (7) 25 PWM outputs, (8) 9 touch pads. A single general-purpose input / output (GPIO) pin can multiplex as PWM / SPI / I2C. Two built-in sensors- Hall effect sensor and temperature sensor are also integrated in it. [1]

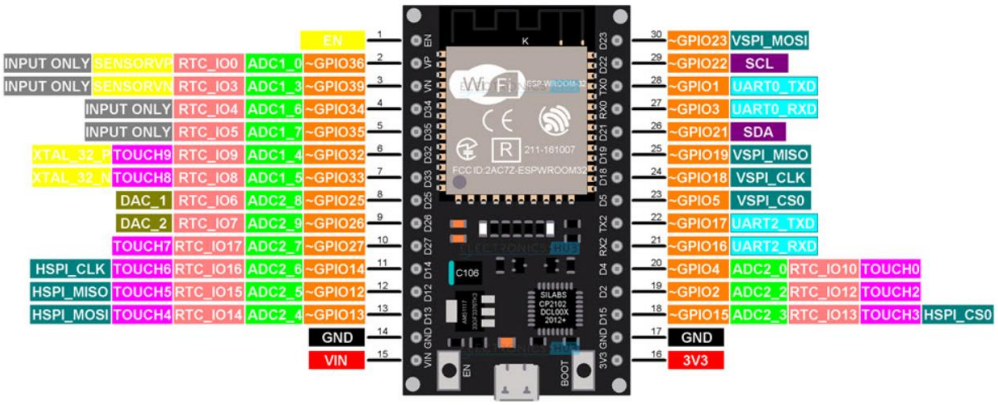

Figure 2. ESP 32 development board with pin assignment

DHT 11 Sensor

DHT sensor directly produces the temperature and the humidity. The parameters such as heat index and dewpoint are obtained from calculation based on two values of temperature and humidity indirectly. DHT11 has a humidity sensing component and a negative temperature coefficient (NTC) temperature sensor (or thermistor). Its construction is illustrated in Figure 3.

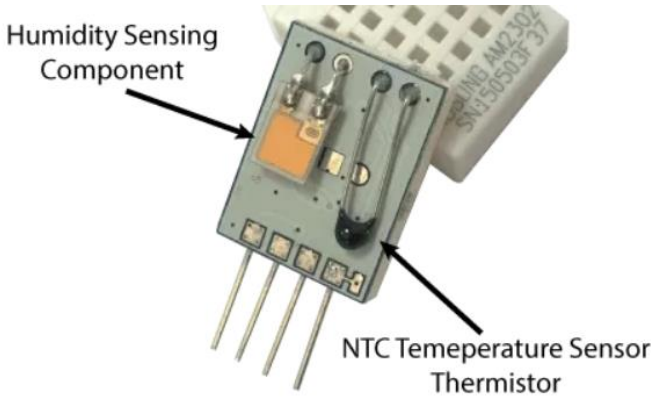

Figure 3. Internal parts of DHT sensor

Thermistor sensor is made up of semiconductor ceramics whose resistance is changed in large even if the temperature is changed in very little. The humidity sensor of DHT 11 is a capacitor whose moisture holding substance is sandwiched between two electrodes as dielectric medium as shown in Figure 3. If the change of the humidity level, the dielectric value is changed and the capacitance value is also changed. The output signal of DHT11 is calibrated due to the change in resistance of thermistor and capacitance of humidity sensor. Figure 4 depicts the internal structurer of humidity sensor.

The value of both temperature and humidity are produced as 40-bit serial data which is in the order of 8-bit humidity integer data, 8-bit the Humidity decimal data, 8-bit temperature integer data, 8-bit fractional temperature data, 8-bit parity bit. The connection of DHT11 to ESP32 is shown in Figure 5.

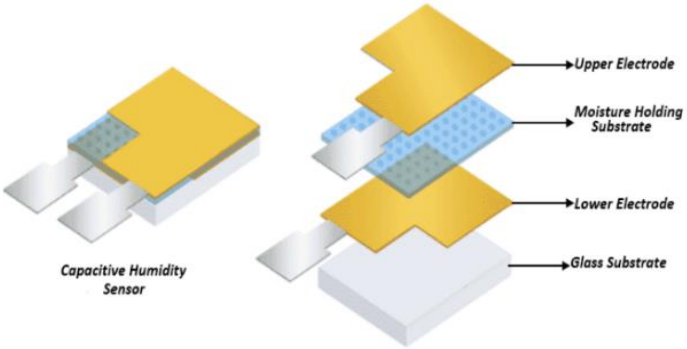

Figure 4. Internal structurer of humidity sensor

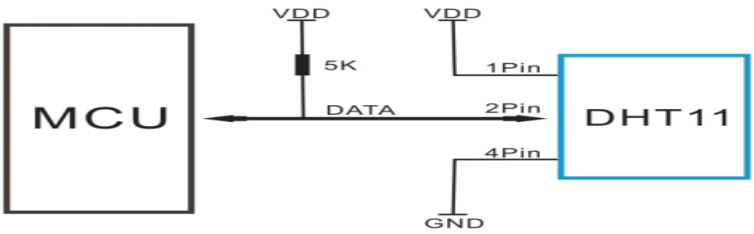

Figure 5. DHT connection to ESP32

Setting Up InfluxDB Database

InfluxDB is open-source database with timestamp. One of the advantages of implementing with InfluxDB is the vast amount of data per second can be logged in timestamp over a pre-determined period of time. Firstly, the InfluxDB account is created in the website https://www.influxdata.com/ as shown in Figure 6. Select Google cloud option where data is saved. (shown in Figure 7). And then, keep the free account and data are retained for 30 days plan as shown in Figure 8. Choose the bucket name as in Figure 9.

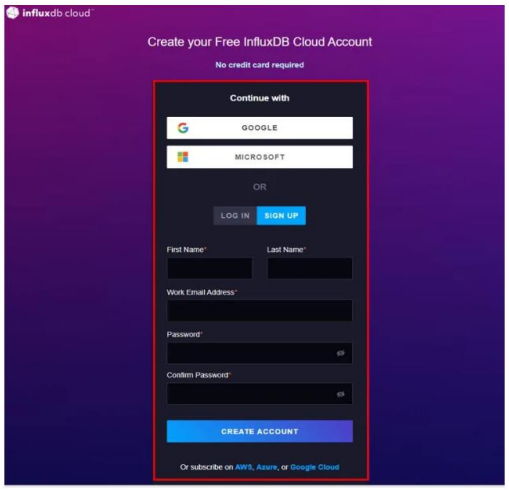

Figure 6. InfluxDB cloud account

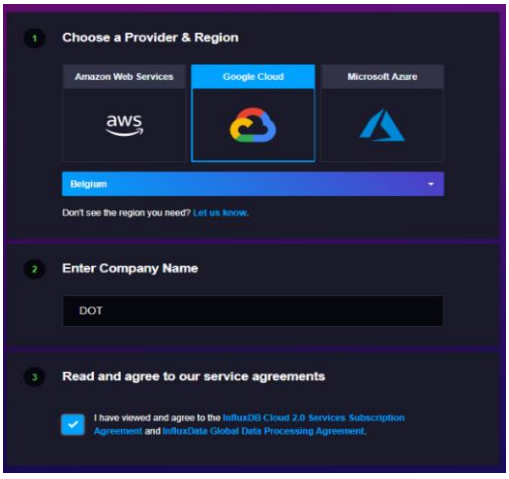

Figure 7. Choosing provider as Google cloud

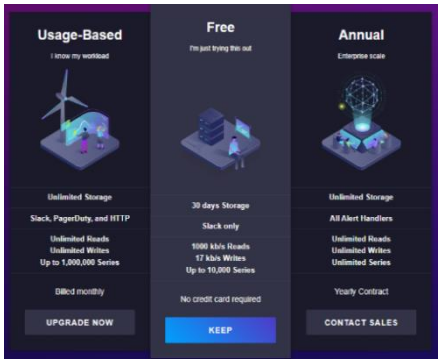

Figure 8. Select free InfluxDB plan

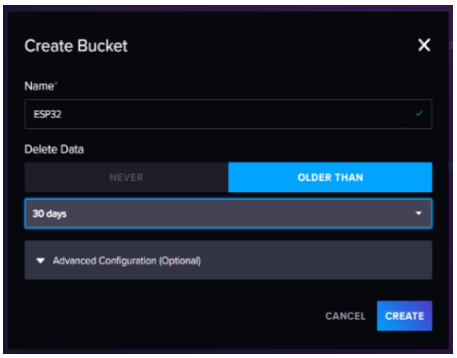

Figure 9. Choose the bucket name

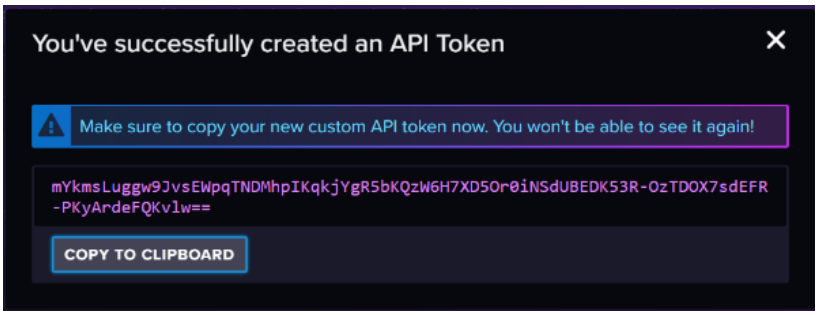

Figure 10. Creation of API token

InfluxDB Server URL, InfluxDB Organization, InfluxDB Bucket Name and application programming interface (API) Token are created and noted for listing in code. API token created in InfluxDB is shown in Figure 10. As InfluxDB key terms, bucket is name of location where data is saved. A set of data is logged in table format. Data in row of table are points which have measurement, tag, field key, field value and timestamp.[3]

Hardware Set up and Code Explanation

Power (V_{cc}), ground and data of DHT11 are connected to 5V, ground and GPIO 4 of ESP32 respectively. The circuit connection is illustrated in Figure 11. Program is listed with C^{++}. As ESP32 is compatible with Arduino IDE, the compilation and uploading are carried out with Arduino IDE. Initially, all libraries, serial communication and port are initialized. The program is listed for using both ESP32 and ESP8266. Moreover, multi Wi-Fi system is used in this code.

It can find out the network which is the strongest Wi-Fi intensity level in the surrounding. InfluxDB credentials such as Wi-Fi service set identifier (SSID) and pass word, InfluxDB_URL, InfluxDB ORG, InfluxDB token and bucket are defined in the code. InfluxDB detects whether these InfluxDB parameters are true or false and examine whether the network is strongest among other networks or not. If the detection is successfully completed, the process is continued for detecting sensor data and connecting to Wi-Fi. ESP 32 is connected to InfluxDB cloud with internet access. Using the “addtag ()” device and Wi-Fi SSID are included. Tag is the column of data table. To synchronize the time with network time protocol, “timeSync ()” function. For Yangon, “timeSync (TZ_INFO "<+0630>-6:30")” is included. And then, using “addField ()” on the point, temperature, humidity, heat index and dew point are uploaded as “sensor.addField ("humidity", h);” where first argument is key and second argument is value. The same instruction is listed for another parameters. InfluxDB

receives the sensor data and it processes to store and visualize the data inInfluxDB dashboard. The flowchart of Data logging system using InfluxDB is illustrated in Figure 12. [4,5,6]

Results

After uploading the code to ESP32, InfluxDB website is logged in with the specified Gmail. The bucket "ESP32DHT" is chosen in data explorer in graph option. Temperature, humidity, heat index and dew point are expressed in graph as shown in figure 13. Temperature, humidity, heat index and dew point are illustrated in graph, in single stat and in table respectively are shown in Figure 14 and Figure 15. Figure 16 shows the histogram of temperature. It interprets a graphical presentations of temperature points in specified range.

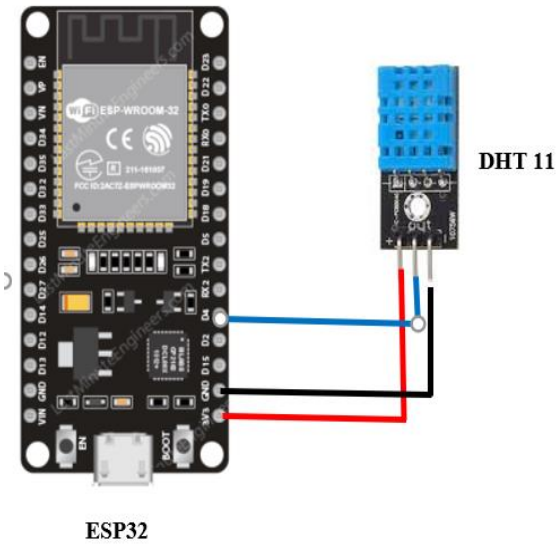

Figure 11. Circuit connection

The individual graph of temperature, humidity and dew point are illustrated in Figure 17, Figure 18 and Figure19 respectively.

As soon as ESP32 is connected to InfluxDB, sensor data is displayed on serial monitor with the words of "successful connection" and "writing data to InfluxDB". (in Figure 20) Sensor data is refreshed every 10 seconds.

The individual sensor data can be saved in Microsoft Excel as shown in Figure 21.

Discussion

In the most dashboards or display of IoT clouds, the single parameter can be displayed. But, in the InfluxDB dashboard, the single parameter as well as all parameters to be monitored can display on the dashboard. Sensor data can be visualized in the form of live graph, table, gauges, single stat and histogram. Data collecting time range can be determined as shown in Figure 22. It is one of the advantages of InfluxDB. There is no limit of amount of data for a parameter. The write per second depends on the numbers of cores in PC and size of memory RAM.

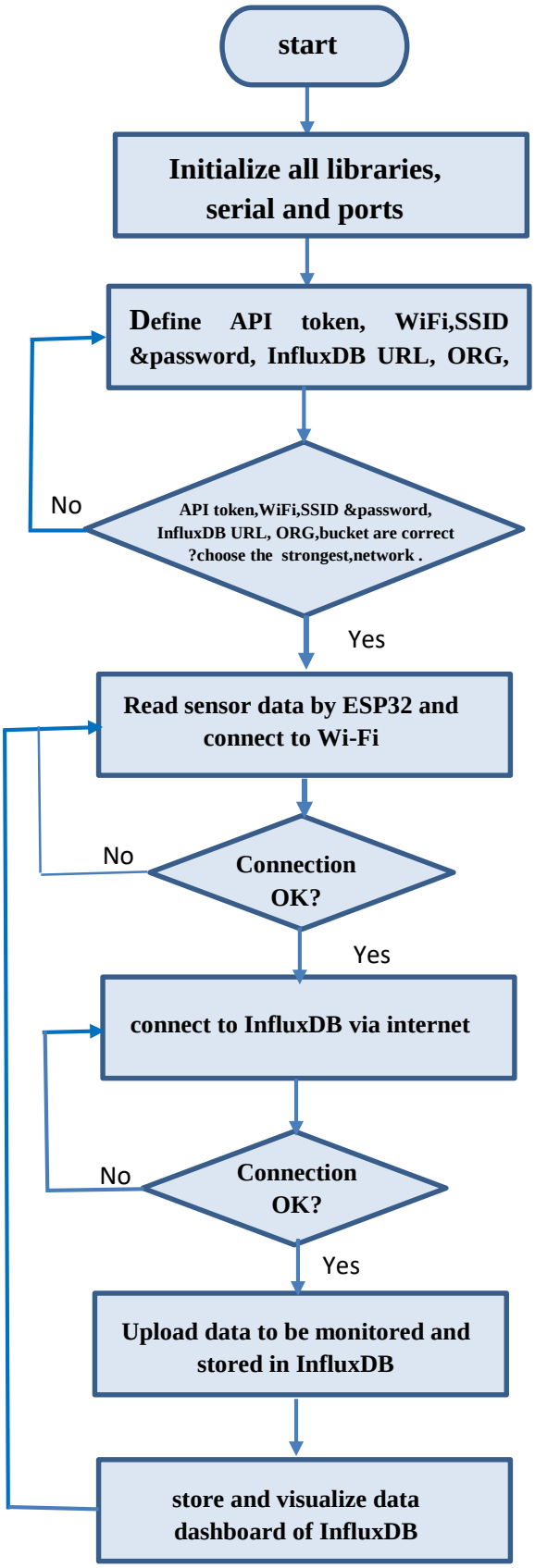

Figure 12. Flowchart

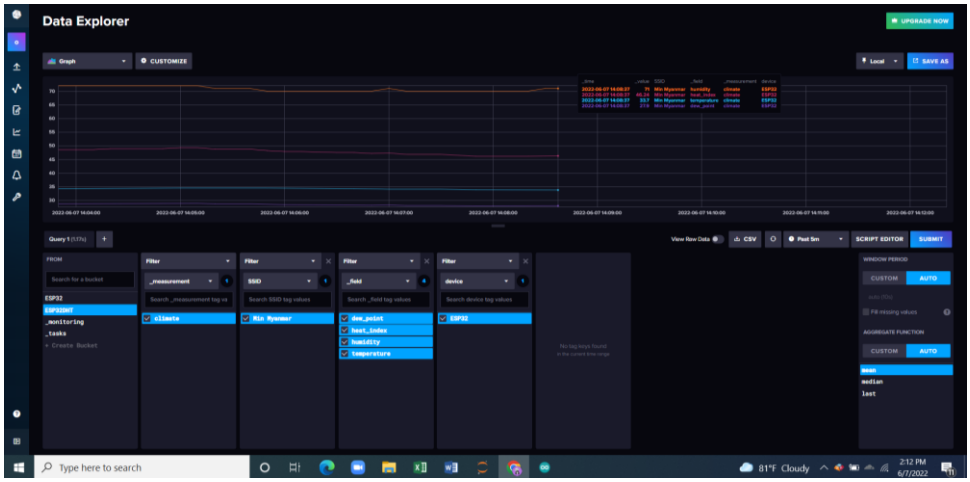

Figure 13. Graph of 4 parameters with timestamp

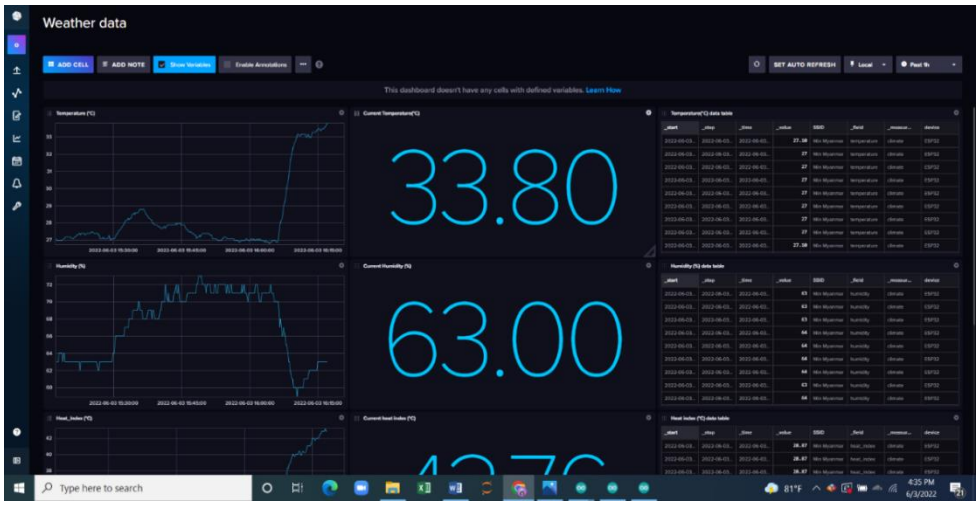

Figure 14.Temperature and humidity in graph, in single stat and in table.

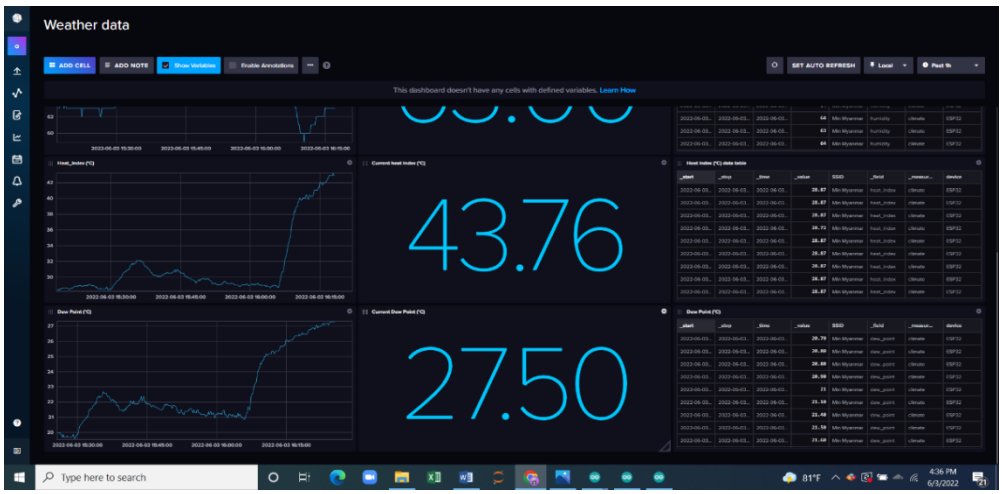

Figure 15. Heat index and dew point in graph, in single stat and in table.

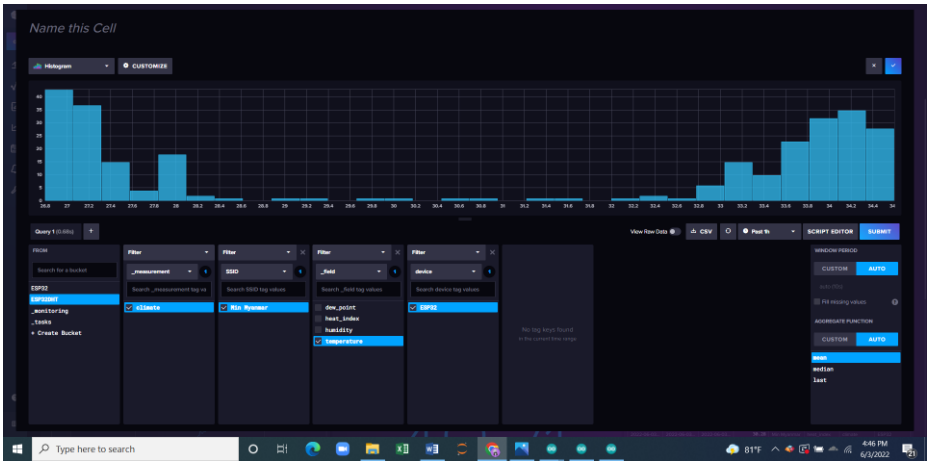

Figure 16. Histogram for temperature

Figure 17. Temperature graph with timestamp

Figure 18. Humidity graph with timestamp

Figure 19. Dew point graph with timestamp

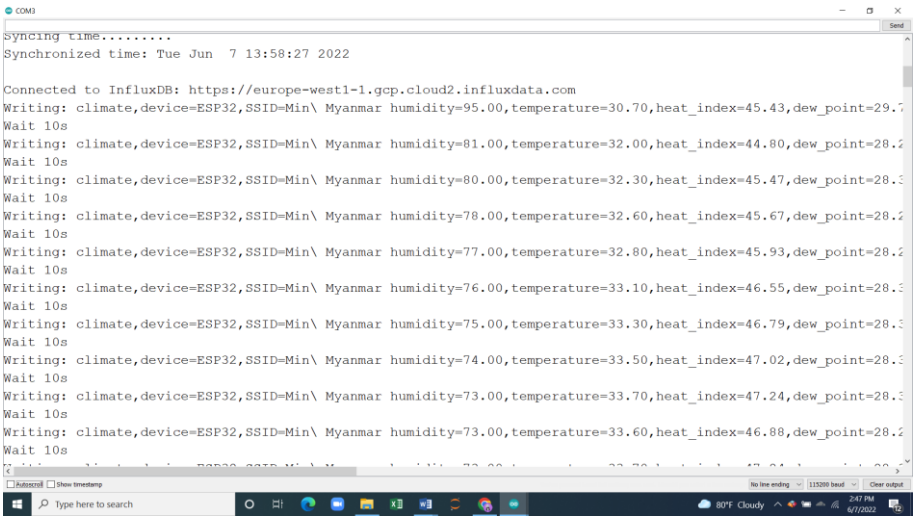

Figure 20. Sensor data on serial monitor

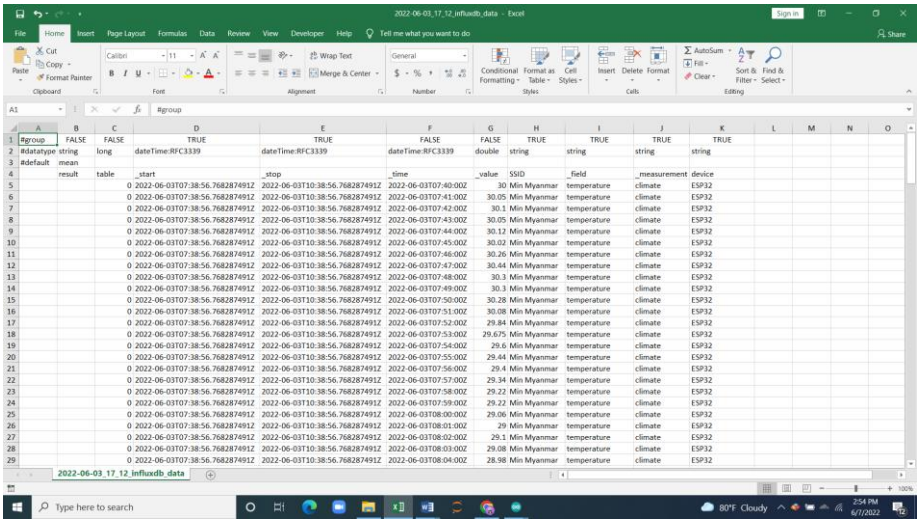

Figure 21. Sensor data on Excel spread sheet

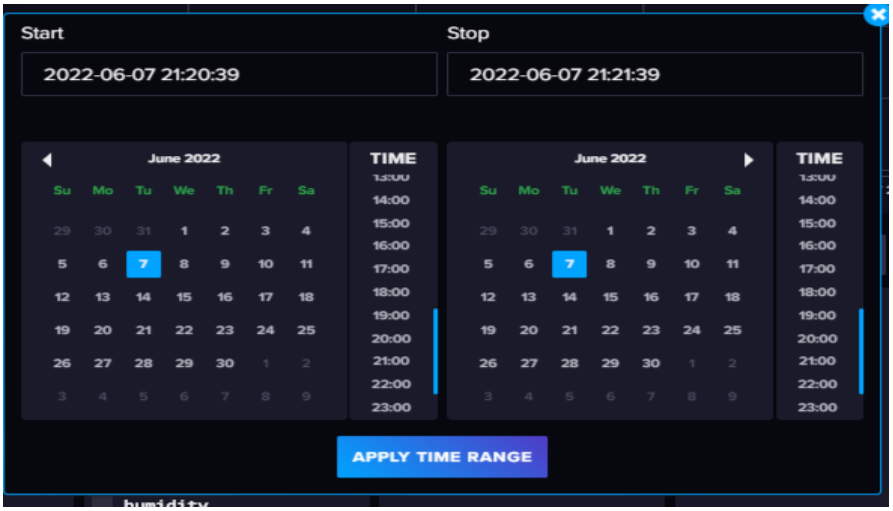

Figure 22. Adjustable time range to be measured

Conclusion

There are many technologies in this research. They are Internet of Things (IoT), Influx DB and ESP32. ESP32 is not only microcontroller but it is internet- enable device. Basic meaning of Internet of Things (IoT) is the interface of hardware and software via internet access. Influx DB used in this research is one of ideal data logging technologies. Dashboard design is not fixed. It can be created by researcher's option. Other advantages of using Influx DB are man-power conserving, adjustable time range for monitoring, familiar with upcoming technologies, and also cost-effective. The essential requirement of internet access is disadvantage of this system. In brief, Influx DB is one of the ideal database technologies for research field.

Acknowledgements

I am very grateful to Rector Dr Nay Win Oo, East Yangon University, for his permission to work this research. I would like to thank Pro-Rector Dr Aye Aye Ko, Po-Rector Dr War War Lwin, Pro-Rector Dr Thida Aung, East Yangon University, for their permissions to work on the present topic. I am greatly indebted to Professor Dr Naing Naing Oo, Head of Department of Physics, East Yangon University, who provides with generous help and kind permission in this research paper.

References

[1] https://www.electronicshub.org/esp32-pinout/
[2] https://components101.com/sensors/dht11-temperature-sensor
[3] https://w2.influxdata.com/blog/getting-started-arduino-influxdb/
[4] Rui Santos, (2020)" ESP 32 troubles shooting guide" Random Nerd Tutorial Lab,
[5] Rui Santos, (2020)" Learn ESP32 with Arduino IDE" Random Nerd Tutorial Lab, Porto, Portugal.
[6] Rui Santos, (2020)" Build Web Server with ESP32 and ESP8266" 2nd Edition, Random Nerd Tutorial Lab,Porto, Portugal.

INVESTIGATION ON STRUCTURAL, SURFACE MORPHOLOGICAL AND OPTICAL PROPERTIES OF TRANSPARENT CONDUCTIVE OXIDE FILMS BY PRECIPITATION METHOD

NYO NYO MYINT*

Abstract

The ZnO particles were synthesized by dissolving zinc acetate dehydrate in NaOH by precipitation method. The ZnO solution were prepared by dissolving ZnO particles in 2-methoxyethanol solvent. Transparent semiconductor thin films of zinc oxide (ZnO) were deposited onto glass substrates by the spin-coating technique. The as-coated films were heated at 400 ^{o}C and 500 ^{o}C for 1 h. The structural, optical and surface morphological properties of ZnO films were investigated by X-ray diffraction (XRD), ultra violet visible (UV-VIS) spectroscopy and scanning electron microscopy (SEM).

Key words: ZnO, XRD, UV-VIS, SEM

Introduction

ZnO is high electrical conductivity and low toxicity of attract researchers' attention since it is a transparent conductive oxide. Metals were used as compound materials or dopants. These materials have a multifunctional character with good electrical conductivity and optical transparency, so they can be used in conductive electrodes and solar cell surfaces, among others [5]. Transparent thin films and materials are some of the most commonly used materials that we depend on for a wide range of applications. Most of these applications need as conductive and transparent a TCO as possible [2]. Transparent conductive oxide (TCO) has high optical transmission at visible wavelengths and electrical conductivity close to that of metals [1,3]. Many new transparent conduction oxide (TCO) materials have been developed in recent years, most practical TCO applications employ doped oxides of indium (In), tin (Sn), zinc (Zn) [1]. Transparent conduction oxides (TCOs) are electrical conductive materials with a comparably low absorption of light. They are usually prepared with thin film technologies and used in opto-electrical devices such as solar cell, flat panel displays, optoelectronic devices, liquid crystal devices, torch screens, automobile window deicing and defogging and circuitries [6]. Transparent conduction oxide (TCO) based on indium doped zinc oxide films in the nano scale were successfully prepared using combination between dip coating and thermal decomposition process structural investigations confirm the polycrystalline ZnO hexagonal wurtzite phase grown along with nano crystallite size about 10 nm [4]. The wide band gap is responsible for high optical transmittance and free electrons increase electrical conductivity. TCOs are generally n-type wide band gap semiconductors (although p-type materials are now being developed) with a relatively high concentration of free electrons in the conduction band [6]. In this study of the deposition parameters that affect strongly on the transport and optical characteristics of ZnO films deposited by dip coating as low cost, wide area productivity and good film quality in order to compete with the other sophisticated preparation techniques.

Materials and Method

Preparation of the Sample

ZnO particles were formed by mixing (1.1 M) of zinc acetate dehydrate {Zn $(CH_3COO)_2 .2H_2O$} and (0.32 M) of sodium hydroxide (NaOH) with dehydrate iodine water (DIW) (50 ml). This solution was stirred at 960 rpm and heated at 120 ^{o}C by hotplate with magnetic stirrer for 2 h. After stirring, its solution was formed by clear and homogeneous.

* Dr., Associate Professor, Department of Physics, East Yangon University, Yangon, Myanmar

Then, it was heated at 80 ºC for 9 h and bulk ZnO was formed. After crushing into powder phase was examined by X-ray diffraction (XRD). As a result, ZnO powder was absolutely formed. Thus, the ZnO crystalline powder was successfully appeared. To change from ZnO powder phase into sol phase, 2-methoxethanol solvent was added into ZnO powder. The mixture solution was also annealed at 120 ºC for 3 h under stirring. After cooling at room temperature, ZnO sol-gel was formed. Then, the glass substrates were cleaned by using acetone and DIW as repeated time. The substrates were dried at ambient temperature by a few minutes. This solution was coated onto glass substrate rotated at 5000 rpm for 30 s by spin-coating method. ZnO were obtained and annealed at 400 ºC and 500 ºC in the furnace for 1 h. Hence, ZnO the film was appeared. The structure of ZnO film was characterized by X-ray diffraction (XRD). The optical properties of ZnO film were studied by UV-VIS spectroscopy. The morphology of ZnO film was examined by scanning electron microscopy (SEM). Figure 1 showed the flow diagram of the sample preparation procedure steps for ZnO films.

Results and Discussion

Powder Analysis by XRD

Zinc Oxide powder was thus obtained and examined its structural properties (crystal structure and phase identification) of ZnO powder. Figure 2 showed the XRD spectrum of ZnO powder. The sample was scanned between 10 deg to 70 deg. Two profiles were found on XRD spectrum. Seven diffracted peaks were significantly formed on observed profile. The upper site indicates the observed profile while the lower site represented the JCPDS (Joint Committee on Powder Diffraction Standard) library file (89-1397 > ZnO-Zinc Oxide). They were (100), (002), (101), (102), (110), (103) and (112) reflections. The highest peak or dominant peak was observed to be (101) peak. The ZnO powder was said to be polycrystalline. There were nine peaks on ZnO standard pestle. Accordingly, seven of nine peaks were matched well with those of ZnO standard. Thus, it is confirmed that the sample is Zinc oxide (ZnO). Table 1 showed the observed and standard Bragg angle (2θ) of Zinc oxide powder. The observed and standard interplaner spacing (d-space) of ZnO powder were listed in Table 2. The lattice parameters and lattice distortion of ZnO powder were recorded in Table 3 and also the crystallite size of ZnO powder were described in Table 4.

Table 1. Observed and standard 2θ of ZnO powder

Sr No.	Peaks	Diffraction angles, 2θ (deg)	
		Observed	Standard
1	(100)	31.680	31.736
2	(002)	34.341	34.378
3	(101)	36.241	36.214
4	(102)	47.478	47.483
5	(110)	56.582	56.534
6	(103)	62.810	62.775
7	(112)	67.837	67.866

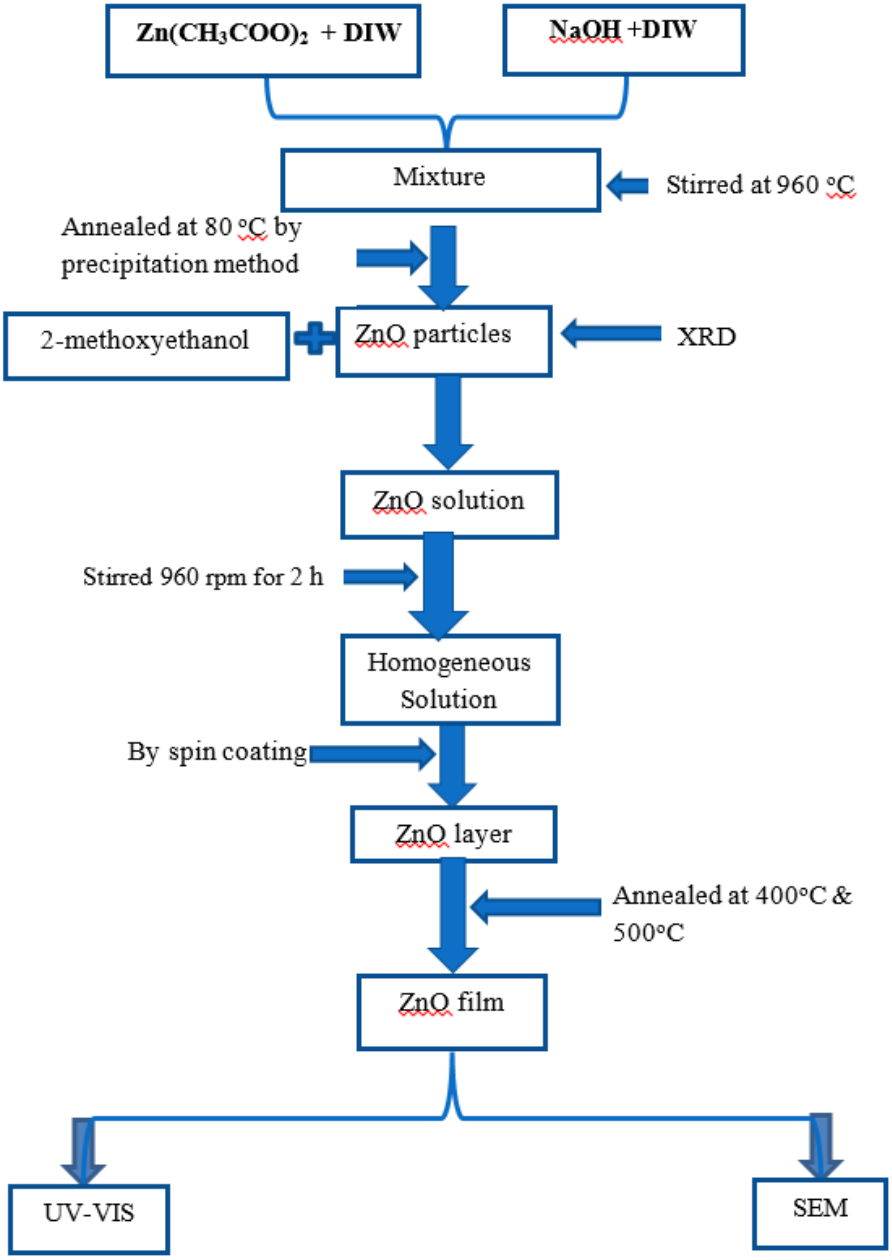

Figure 1. Flow diagram of the sample preparation procedure for ZnO films

Table 2. Observed and standard d-space of ZnO powder

Sr No.	Peaks	Interplaner spacing (d-space)	
		Observed	Standard
1	(100)	2.7734	2.8172
2	(002)	2.6054	2.6065
3	(101)	2.4793	2.4784
4	(102)	1.9086	1.9132
5	(110)	1.6271	1.6265
6	(103)	1.4767	1.4790
7	(112)	1.3778	1.3799

Table 3. Lattice parameters and lattice distortion of ZnO

ZnO	Lattice parameters (Å)		Lattice distortion (c/a)
	a-axis	c-axis	
Standard	3.18700	5.1056	1.6020
Observed	3.23870	5.1931	1.6043

The crystallite size of ZnO powder was determined by Debye Scherrer formula

$$G = \frac{\beta\lambda}{FWHM \times \cos\theta_B} \quad \text{----------(1)}$$

where G = Crystallite size (nm)
θ_B = Bragg angle (deg)
β = Scherrer constant (0.899)
λ = Wavelength of Cuk_a (λ = 1.54056 Å)
B = FWHM (Full Width at Half Maximum (deg))

Table 4 . Described the crystallite size of ZnO powder

Sr No.	Peaks	FWHM (deg)	Crystallite size (nm)
1	(100)	0.206	69.885
2	(002)	0.247	58.687
3	(101)	0.219	66.541
4	(102)	0.167	90.598
5	(110)	0.299	52.603
6	(103)	0.182	89.164
7	(112)	0.273	61.134
Average crystallite size= 69.8017nm			

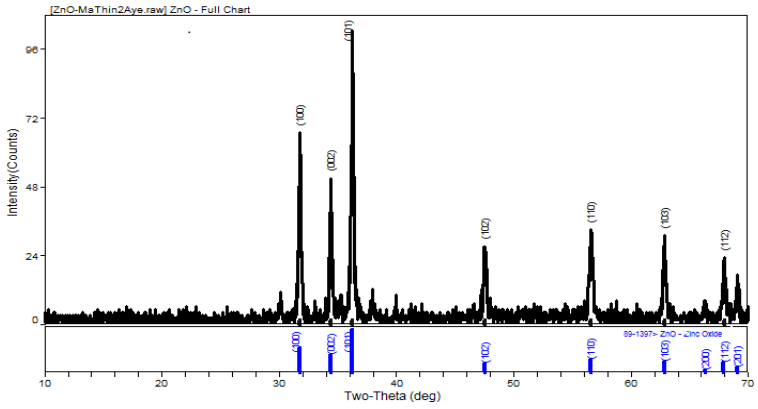

Figure 2. XRD spectrum of ZnO powder

UV-VIS Analysis

Band gap measurement by direct method

The absorption spectrum of ZnO film was obtained by using UV-VIS spectrum. The wavelength range of spectrum laid between 190 nm to 1100 nm. The UV-VIS absorbance spectra of ZnO film showed at 400 ºC and 500 ºC in figure 3 a and b. The measured and calculated values of UV-VIS spectra were described in Table 5. The optical band gap energy was calculated by following equation,

$$E_g = \frac{hc}{\lambda} \quad \text{----------} \quad (2)$$

where E_g = optical band gap energy (eV)
h = Plank's constant (6.625×10^{-34} Js)
c = velocity of light (3×10^{8} ms^{-1})
λ = cut off wavelength (nm)

Table 5. Optical band gap energy of ZnO film at 400 °C and 500 °C

Temperature (°C)	Cut-off wavelength(nm)	Optical band gap energy(eV)
400	315.28	3.94
500	334.82	3.71

Band gap measurement by Lambert-Beer law

The optical band gap measurement was performed for ZnO film by using Lambert-Beer law. Figure 4 a and b indicated the $(\alpha h\nu)^2$ and $h\nu$ characteristics curve of ZnO film at 400 °C and 500 °C. By extrapolating the curve onto X-axis $(\alpha h\nu)^2 = 0$, at point optical band gap was obtained. They were found to be 3.81 eV and 3.60 eV for ZnO film at 400 °C and 500 °C respectively. The comparative study on optical band gap of ZnO film obtained from two methods was collected and listed in Table 6.

Table 6 . Comparison on optical band gap of ZnO film by two different methods

ZnO film (substrate temperature) (˚C)	Optical band gap (eV)	
	Direct method	Lambert-Beer method
400	3.94	3.81
500	3.71	3.60

SEM Analysis

SEM analysis was performed to examine the microstructure surface morphology and film quality of ZnO film. In figure 5 a and b were shown SEM monographs of ZnO film at 400 ºC and 500 ºC. According to the SEM images the densities of both images were observed to be high and the shape of grain was found to be circular shaped for both samples. Grains were uniformly distributed on the examined areas of SEM image. The size of grain could be measured by bar code and its length was 1 μm for both samples. The average grains sizes were estimated to be 0.3272 μm and 0.4491 μm for ZnO film at 400 ºC and 500 ºC respectively. Some porosity was formed on both SEM images and they were porous structures.

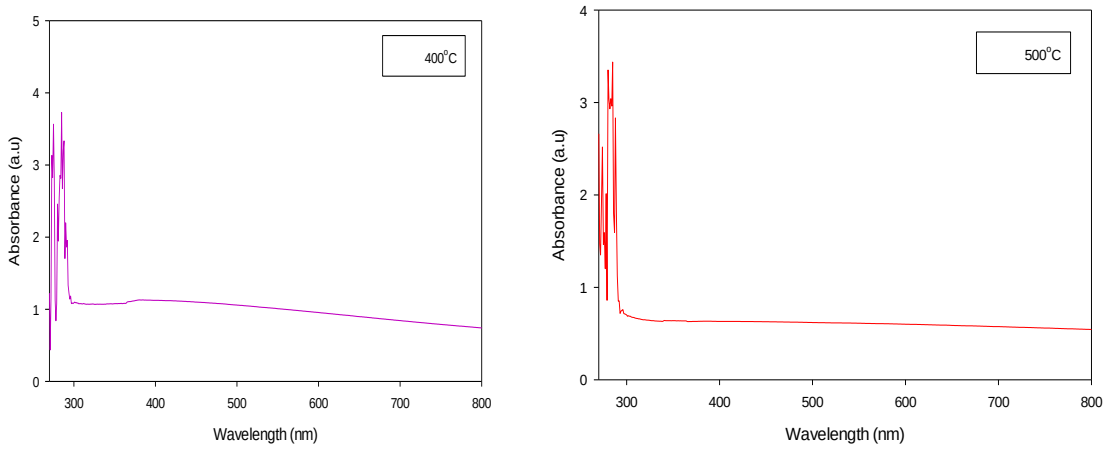

Figure 3. UV-VIS absorbance spectrum of ZnO film at (a) 400 °C and (b) 500 °C

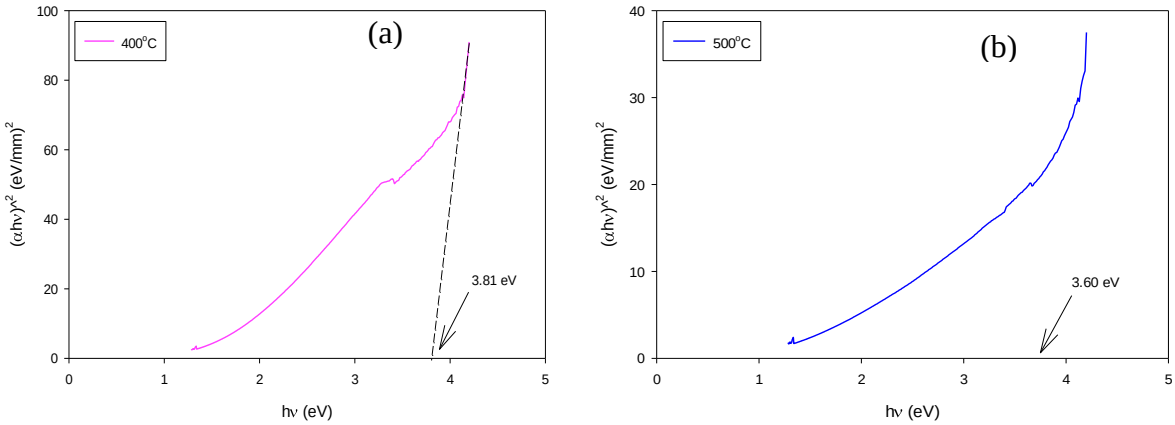

Figure 4. Optical band gap for ZnO at (a) 400 °C and (b) 500 °C

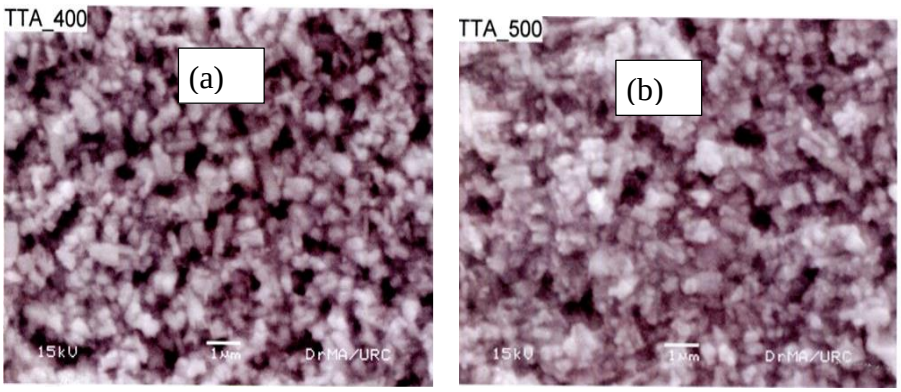

Figure 5. The SEM photographs of the ZnO film at (a) 400 °C and (b) 500 °C

Conclusion

Fabrication of ZnO film and their microstructural and optical properties have been investigated. Before the film preparation, ZnO powder was examined by XRD. As a result, ZnO powder was successful formed by precipitation method. The lattice distortion (hexagonally) (c⁄a) of ZnO powder (1.6) was matchal with 97 % with ZnO standard (c/a =1.633). So, ZnO polycrystalline powder was obtained with hexagonal symmetry. From UV-VIS analysis, the absorption peak was formed at 389 nm and 381 nm for ZnO film at 400 ^{o}C and 500 ^{o}C. These values were ranged in visible light (380 nm - 780 nm). The optical band gaps of ZnO films were calculated to be 3.94 eV and 3.71 eV at 400 ^{o}C and 500 ^{o}C. These vibes were futile acceptable compared to standard value of ZnO (3.37 eV). From SEM investigation, ZnO films at 400 ^{o}C and 500 ^{o}C were successfully deposited onto glass substrate. The microstructures were quite acceptable for film fabrication technology. Around the examined area of SEM image, if was found that good micrograins were formed at both temperatures. The detail analysis of SEM image showed a good and acceptable microstructure without formation in terms of microcracus. According to the above reasons, ZnO materials system is promising under focus is a good candidate for optoelectronic applications such as the manufacture of solar cells with transparent electrodes.

Acknowledgement

I wish to express my sincere thanks to Rector Dr Nay Win Oo and Pro-Rectors Dr Aye Aye Ko, Dr Wah Wah Lwin and Dr Thida Aung of East Yangon University for their permission to write this research paper. I would also like to thank Professor and head Dr Naing Naing Oo and Professor Dr Su Su Aung, for their suggestion throughout this paper.

References

1. Arico, A.S., Bruce, P., Scrosati, B., Tarascon, J.M. & Shalkwijk, W. (2005). Nanostructured materials for advanced energy conversion and storage devices. *Nature*, 4, pp 366-377.
2. Dler Adil Jameel et al., (2015) “Thin Film Deposition Processes” International Journal of Modern Physics and Applications Vol. 1 (4), pp 193-199.
3. Haetering G. H. (1999): " Ferroelectric materials: History and Technology " Journal of American CeramicSociety, Vol 82 (4), pp 797 - 818
4. Perkgoz N. K. et al., (2011). Photocatalytic hybrid nanocomposites of metal oxide nanoparticles enhanced towards the visible spectral range. Applied Catalysis B: Environmental 105, 77 -105.
5. Rayerfrancis A. et al(2017) “Sputtered AZO thin films for TCO and back reflector applications in improving the efficiency of thin film a-Si:H solar cells”, vol. 9 (1), pp 31–38.
6. Ranabhat K et al., (2016) " An Introduction to Solar Cell Technology ", Jour Appl Engg Sci, vol 14(4), pp 481 -491.

RELIABLE AND USER FRIENDLY ELECTRONIC BALLOT SYSTEM

Thazin Hlaing[1], Thet Mar Oo[2], Aye Aye Thwe[3], Thein Than Htay[4], Hsu Po Po Myint Sein[5]

Abstract

Voting is made to select winner of an election for a country or school council or making decision for a company. But there are many difficulties and arguments it is fair and trusted in an election. Therefore, an innovative design of voting system is introduced. It is "Reliable and User Friendly Electronic Ballot System". The system was designed to be very easy to vote for voters. Moreover, the system is reliable and voters cannot make illegal votes after one successful vote is made for a candidate. The results of vote counts can be saved in a micro SD card for data record. The maximum counting of each candidate is limited up to 65535 counts since integer type variables are used in the system. The system design consists of an Arduino Uno development board, an alphanumeric liquid crystal display, a micro SD card read/write module, a rotary encoder switch, a piezo buzzer, a few input switches and light dependent resistors (LDRs) for visitor sensor. The system is intended to solve most of the arguments in counting votes and protect illegal voting in an election.

Keywords: Arduino Uno, 16x4 LCD, Piezo Buzzer, Rotary Encoder, LDRs

Introduction

Ballot design is very important in an election. Poor design leads to confusion and potentially chaos if large numbers of voters spoil or mismark a ballot. Therefore, well designed and user friendly ballot system is very important in an election. Moreover, the votes counting is also important to be easy and fast. But there are many difficulties and arguments in paper ballot voting and counting systems. Therefore, an innovative design of Reliable and User Friendly Electronic Ballot System (RUFEBS) is introduced.

The system design was based on an eight-bit microcontroller development board as shown in Figure 1. It is Arduino Uno. The board was chosen for large amount of program memory, reasonable amount of I/O pins for the circuit design and easy to develop. The system comprises a 16 characters 4 lines alphanumeric liquid crystal display to illustrate the names of candidates or groups or teams to vote. The display was chosen for its properties of clear and large scale character display than other types of LCD displays. The design is made to be simple and easy for voters by using a rotary encoder switch. Both selecting and voting can be easily made by using rotary encoder switch. The voting results are permanently stored on a micro SD card by using a micro SD card read/write module. A piezo buzzer is added in the system to acknowledge the action of switches. Two light dependent resistors are used to detect the presence of a voter in the voting cell. The most important thing is restriction of votes for voters, one voter can make only one success vote at a time and no more illegal voting can be made on the system.

The system will be a great help and very useful in government elections or voting for a decision in a company or in many voting processes. The vote counting is very simple and counted results are automatically stored on a micro SD card. Therefore, it is not necessary for vote counting. Just read the memory card and results can be display to audience or public. It is very simple, reliable and user friendly system. The system can be operated by a power bank or 5 V USB power supply from android phone chargers.

[1,] Demonstrator, Department of Physics, East Yangon University
[2] Demonstrator, Department of Physics, East Yangon University
[3] Demonstrator, Department of Physics, East Yangon University
[4] Demonstrator, Department of Physics, East Yangon University
[5] Demonstrator, Department of Physics, East Yangon University

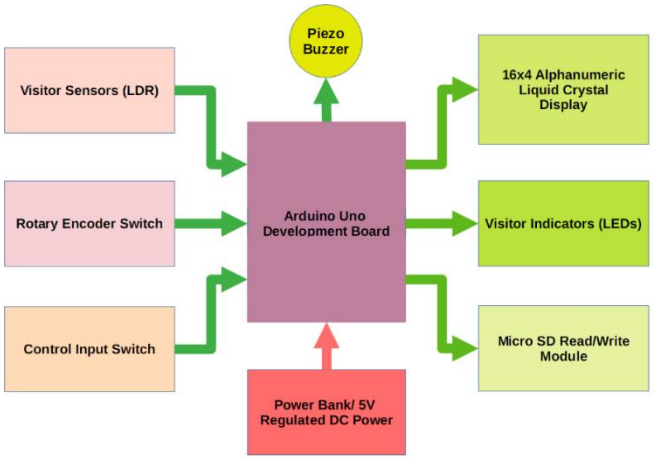

Figure 1. Block diagram of Reliable and User Friendly Electronic Ballot System

Introduction to Arduino Uno BoardArduino Uno is a microcontroller board based on 8-bit ATmega328P microcontroller. Along with ATmega328P, it consists other components such as crystal oscillator, serial communication, voltage regulator, etc. to support the microcontroller. Arduino Uno has 14 digital input/output pins (out of which 6 can be used as PWM outputs), 6 analog input pins, a USB connection, A Power barrel jack, an ICSP header and a reset button. Photo of Arduino Uno development board as shown in Figure 2 [1].

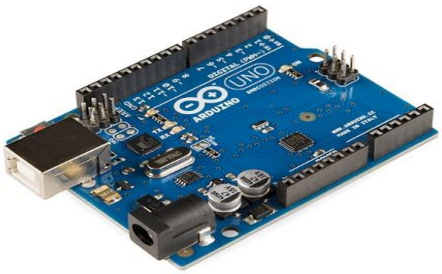

Figure 2. Photo of Arduino Uno development board

Arduino Uno Technical Specifications

Microcontroller	ATmega328P -8bit AVR family microcontroller
Operating Voltage	5 V
Recommended Input Voltage	7 - 12 V
Input Voltage Limits	6 - 20 V
Analog Input Pins	6 (A0 –A5)
Digital I/O Pins	14 (Out of which 6 provide PWM output)
DC Current on I/O Pins	40 mA
DC Current on 3.3V Pin	50 mA
Flash Memory	32 KB (0.5 KB is used for Bootloader)
SRAM	2KB
EEPROM	1KB
Frequency (Clock Speed)	16MHz [2].

Alphanumeric Liquid Crystal Display

The alphanumeric liquid displays are widely used in various applications. The most popular LCD interface is the Hitachi 44780 based LCD controller chip which provides a fairly easy to work with interface and low power consumption. Hitachi 44780 Compatible 2X16 characters display is used in this mode . There are six main pins in this LCD controller. Pin-1 and Pin-2 are ground and supply (V_{cc}) pins of controller. Next pin is for adjusting contract of LCD is required to connect a variable resistor as voltage divider reference. Typical Connections of LCD Display as shown in Figure 3 .

Figure 3. Typical Connections of LCD Display

Liquid Crystal Display Technical Specification

1	Vss	Ground
2	Vdd	+ve supply
3	Vee	Contrast
4	RS	Register Select
5	R/W	Read/Write
6	E	Enable
7	D0	Data bit 0 (8 bit)
8	D1	Data bit 1 (8 bit)
9	D2	Data bit 2 (8 bit)
10	D3	Data bit 3 (8 bit)
11	D4	Data bit 4
12	D5	Data bit 5
13	D6	Data bit 6
14	D7	Data bit 7
15	A	Back Light LED Anode
16	K	Back Light LED Cathode

Micro SD Card Module

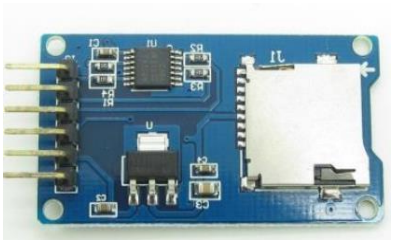

(a)

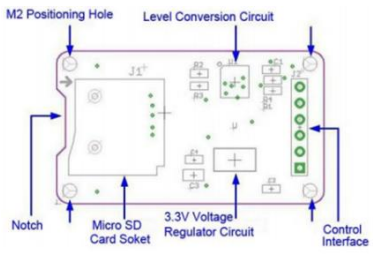

(b)

Figure 4. (a) Components side of micro SD module, (b) Components layout of micro SD module

The module (Micro SD Card Adapter) is a Micro SD card reader module for reading and writing through the file system and the SPI interface driver, SCM system can be completed within a file Micro SD card.

Support Micro SD Card, Micro SDHC card (high speed card). Level conversion circuit board that can interface level is 5 V or 3.3 V. Power supply is 4.5 V ~ 5.5 V, 3.3 V voltage regulator circuit board. Communications interface is a standard SPI interface. 4 M2 screws positioning holes for easy installation.

Control Interface utilized a total of six pins (GND, VCC, MISO, MOSI, SCK, CS), GND to ground, VCC is the power supply, MISO, MOSI, SCK for SPI bus, CS is the chip select signal pin; 3.3 V regulator circuit: LDO regulator output 3.3 V for level conversion chip, Micro SD card supply. Components side of micro SD module and Components layout of micro SD module as shown in Figure 4 (a) and (b) .

Rotary Encoder Switch

A rotary encoder is a type of position sensor that converts the angular position (rotation) of a knob into an output signal that is used to determine what direction the knob is being rotated. Due to their robustness and fine digital control; they are used in many applications including robotics, CNC machines and printers.

There are two types of rotary encoder – absolute and incremental. The absolute encoder gives us the exact position of the knob in degrees while the incremental encoder reports how many increments the shaft has moved. The rotary encoder used in this thesis is of an incremental type.

Rotary Encoders are the modern digital equivalent of the potentiometer and are more versatile than a potentiometer. They can fully rotate without end stops while a potentiometer can rotate only about 3/4 of the circle. Potentiometers are best in situations where you need to know the exact position of the knob. However, rotary encoders are best in situations where you need to know the change in position instead of the exact position. Inside the encoder is a slotted disk connected to the common ground pin C, and two contact pins A and B, as shown in the Figure 5.

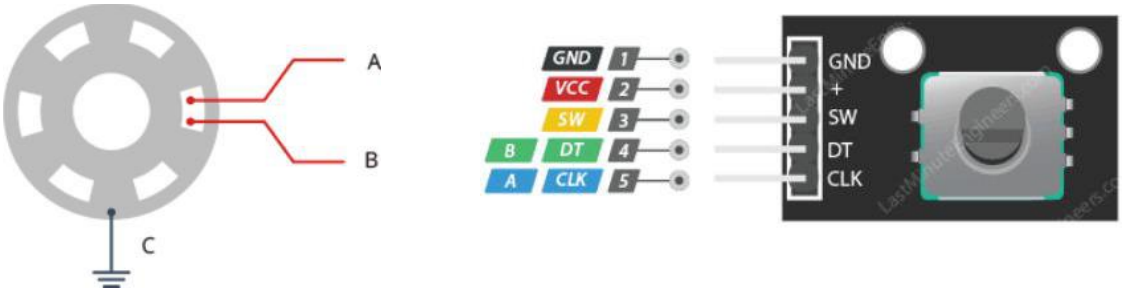

Figure 5. Slotted disk and contact pins for A, B and ground C in a rotary encoder

When you turn the knob, A and B come in contact with the common ground pin C, in a particular order according to the direction in which you are turning the knob. When they come in contact with common ground they produce signals. These signals are shifted 90° out of phase with each other as one pin comes in contact before the other pin. This is called quadrature encoding. Clockwise Rotation and its output timing diagram , Signal Comparison on clockwise timing diagram as shown in Figure 6 (a) and(b) .

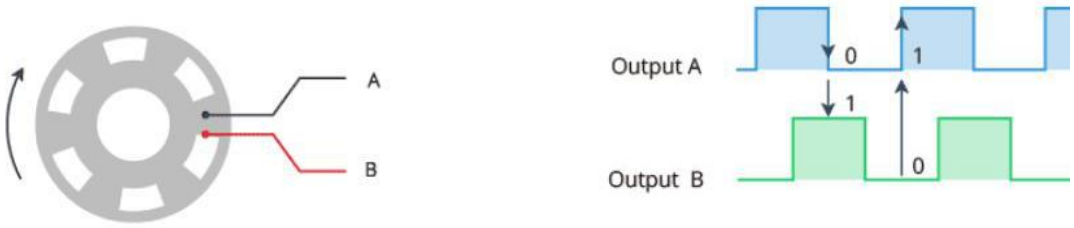

(a) (b)

Figure 6. (a)Clockwise Rotation and its output timing diagram
(b)Signal Comparison on clockwise timing diagram

(a) (b)

Figure 7. (a)Counter Clockwise Rotation and its output timing diagram,
(b)Signal Comparison on counterclockwise timing diagram

When you turn the knob clockwise, the A pin connects first, followed by the B pin. When you turn the knob counterclockwise, the B pin connects first, followed by the A pin. By tracking when each pin connects to and disconnects from the ground, we can use these signal changes to determine in which direction the knob is being rotated. You can do this by simply observing the state of B when A changes state as shown in Figure 7 (a) and (b) [3].

if B! = A, then the knob was turned clockwise.
if B = A, then the knob was turned counterclockwise.

Piezo Buzzer

Piezo buzzer is an electronic device commonly used to produce sound. Light weight, simple construction and low price make it usable in various applications like car/truck reversing indicator, computers, call bells etc. Piezo buzzer is based on the inverse principle of piezo electricity discovered in 1880 by Jacques and Pierre Curie. It is the phenomenon of generating electricity when mechanical pressure is applied to certain materials and the vice versa is also true. Such materials are called piezo electric materials. Piezo electric materials are either naturally available or manmade. Piezoceramic is class of manmade material, which poses piezo electric effect and is widely used to make disc, the heart of piezo buzzer. When subjected to an alternating electric field they stretch or compress, in accordance with the frequency of the signal thereby producing sound. A piezo electric element is a crystal or ceramic that deforms slightly when a voltage is applied to it. In this case, the voltage signals applied to the piezo ceramic disc causes mechanical expansion and contraction in radial direction. This causes the metal plate to bend in opposite direction. When metal plate bends and shrinks in opposite direction continuously it produces sound waves in the air. Front view and side view photos of a piezo buzzer as shown in Figure 8.

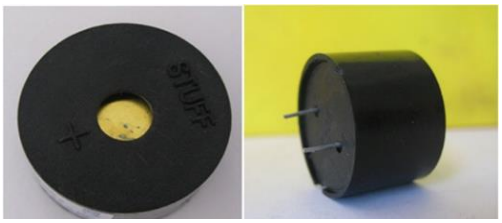

Figure 8. Front view and side view photos of a piezo buzzer

Light Dependent Resistor

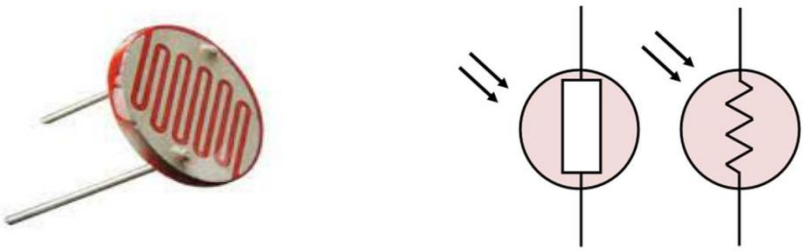

Figure 9. Photo and Symbol of an LDR

A light dependent resistor works on the principle of photo conductivity. Photo conductivity is an optical phenomenon in which the materials conductivity is increased when light is absorbed by the material. When light falls i.e. when the photons fall on the device, the electrons in the valence band of the semiconductor material are excited to the conduction band. These photons in the incident light should have energy greater than the band gap of the semiconductor material to make the electrons jump from the valence band to the conduction band. Hence, when light having enough energy strikes on the device, more and more electrons are excited to the conduction band which results in large number of charge carriers. The result of this process is more and more current starts flowing through the device when the circuit is closed and hence it is said that the resistance of the device has been decreased. This is the most common working principle of LDR as shown in Figure 9.

Circuit Construction

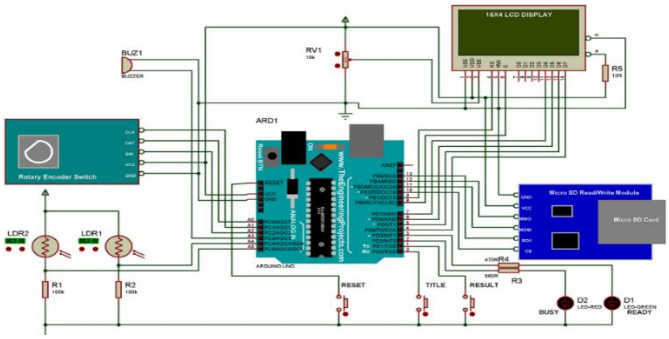

Figure 10. Schematic diagram of RUFEB System

This system design operation was completed eight different portion on the circuit as shown in Figure 10 . They are Arduino Uno, light dependent resistor, LED indicators, control input switches, rotary encoder, micro SD card read/write module, a 16 characters 4 lines

alphanumeric liquid crystal display and a piezo buzzer. Components illustration of the circuit board as shown in Figure 11.

The Arduino Uno is the heart of the circuit and it is connected with all other components on the circuit. It is loaded with a program code to control the circuit. The board consist a 5 V onboard voltage regulator circuit, 32 kB of flash program memory and 20 I/O pins. All the 20 I/O pins are used in the circuit design.

Two LDRs are connected with 100 kΩ resistors in series between the 5 V power line and ground line to become two pairs of sensors. Their junction is connected with analog input pins A4 and A5. If only one sensor is shaded, the system will not operate for voting. It will only be operated for voting if both sensors are shaded. There are two LEDs (Red and Green) on the circuit. They are connected with digital pins 2 and 3. They are used to indicate the voting cell conditions for the voters. If there is no one in the voting cell the Green LED will be illuminating and meaning that the voting cell is empty and ready for a new voter. When the voting cell is occupied by a visitor, the Red LED will be illuminated. In this case, new voter has to wait until the current voter finished voting and leave the voting cell. Adjusting the contrast of LCD display as shown in Figure 12 (a), (b) and (c).

There are two control input switches and a reset switch on the circuit. The title switch is used to display the title of the circuit and result switch is used to display the voting results. All the three switches must be hidden and can be used only by election committee. The reset switch is connected between reset pin of Arduino and ground line. The result switch is connected between digital pin 1 and ground line. For selection of candidates and voting, a rotary encoder switch is used. The switch can be rotating clockwise and counterclockwise to select various candidates. The switch can also be pressed to vote for selected candidate. There are five pins on the rotary encoder switch, the CLK, DAT and SW pins are connected with A1, A0 and A2 respectively. Display of searching various candidates as shown in Figure 13.

To record the proof of voting results, a micro SD card and micro SD card Read/Write module is used in the design. The module utilizes Serial Peripheral Interface (SPI) connection. Therefore, there are four SPI pins and two power pins on the module. The MISO pin is connected with the digital pin 12 of Arduino Uno. The MOSI pin is connected with the digital pin 11 of microcontroller. The SCK pin is connected with the digital pin 13 of microcontroller and the CS pin is connected with the digital pin 10 of the microcontroller respectively. The VCC pin is connected with the 5 V power line of the circuit and GND pin is connected with the ground line of the circuit. A micro SD card can be inserted on the card slot on the module.

Voting condition and result will be displayed on the LCD screen. The display is capable of illustrating alphanumeric characters for 16 characters and 4 lines. There are a total of 16 pins on the LCD and the first three pins are power pins. The VSS and VDD are connected with the ground line and 5 V line of the circuit. The V0 or VEE is contrast adjust pin and it is connected with the adjust pin of a 10 kW variable resistor. The other two pins of variable resistor is connected with the 5 V line and ground line of the circuit. The next three pins are control pins. They are RS, RW, and En pins. The RS and En pins are connected with digital pin 9 and 8 of the Arduino. But RW pin is directly connected with the ground line. The next pins D0 to D7 are parallel 8 bit data pins. But to save the pins on microcontroller, only four pin connection methods is used. D4 to D7 are connected with digital pin 7, 6, 5 and 4 of the Arduino respectively. The last two pins on the LCD is Anode and Cathode pins. Actually, it is the LED pin used to illuminate the backlight of the LCD. The Cathode pin is directly connected with the ground line of the circuit. The Red LED keeps on when voter is not leaving from the voting cell and the green LED switch on when the voter leaves the voting cell as shown in Figure 14 (a) and (b).

A piezo buzzer is added in the circuit design. It is connected between pin A3 and ground line of the circuit. The buzzer is used to acknowledge the used of switches on rotary encoder and button press condition. If any of the switch is active, two successive beep sound will generate.

The whole system can be safely operated by using a power bank or any 5 V, 2 A USB charger of android phone. Voting conditions and result will be displayed on the LCD screen.

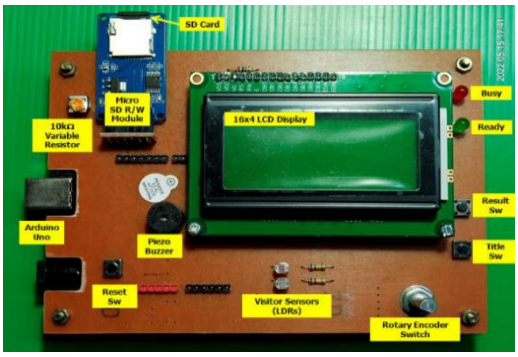

Figure 11. Components illustration of the circuit board

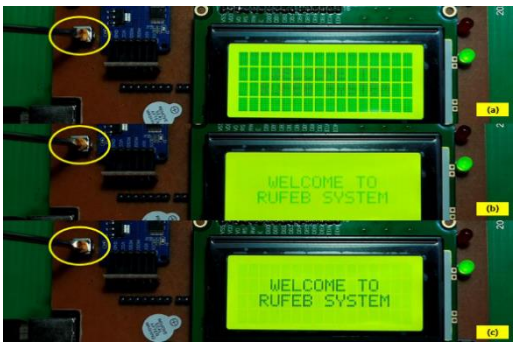

Figure 12. Adjusting the contrast of LCD display

(a) Turning variable resistor to the far right became very dark

(b) Turning to the far left fainted and cannot see the characters

(c) Adjust in the middle of somewhere results the best character illumination

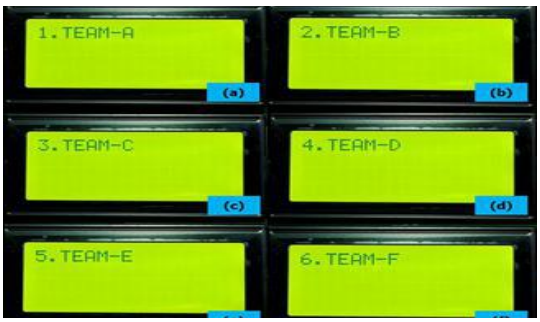

Figure 13. Display of searching various candidates

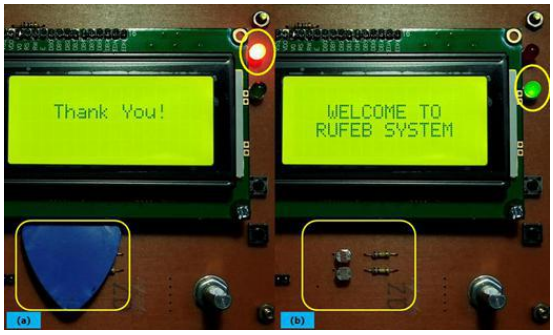

Figure 14. (a) The Red LED keeps on when voter is not leaving from the voting cell
(b) The Green LED switch on when the voter leaves the voting cell

Results and Discussion

In this circuit design, all the components are installed on a single printed circuit board to be compact and unity in presentations. But in the real application, it is required to build a voting cell. Only the LCD display and rotary encoder switch must be exposed for voter and build on the table. Moreover, the visitor sensors must be hidden somewhere, which can easily detect the presence of voter in the cell. The two LEDs can be installed on the door frame of voting cell entrance to easily seen by public. The most important thing is reset switch, voting result display switch and micro SD card. They are required to be hidden or locked and only access by authorities of election council. The use of two sensors in hardware and voting done flag (vdf) in program coding ensures the only one successful vote count for a voter and no one can make illegal voting on this system. Moreover, the system can check presence of micro SD card while voting. If the micro SD card is removed from the card Read/Write module and voting was made as shown in Figure 15 (a), (b) and (c), the display will prompt for "Cannot Vote" and ask "Insert SD Card". Some voting results after voting were illustrated with a photo on Figure 16 and text file displayed on Figure 17.

Figure 15. (a) SD card is removed from the module after voting
(b) Voting was made for Team-C
(c) Cannot vote on removing of SD card
(d) System ask to "Insert SD Card"

Figure 16. Photo of voting results

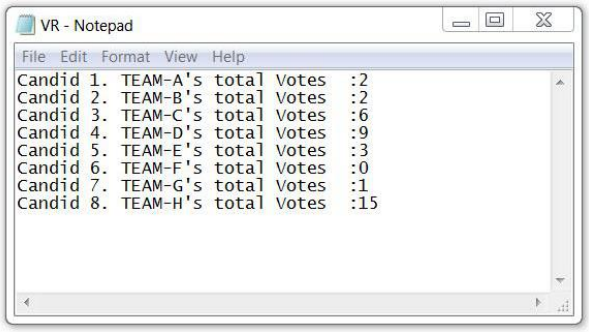

Figure 17. Screen capture image of voting results from micro SD card

Conclusion

The innovative design of Reliable and Friendly Electronic Ballot System is constructed and tested repeatedly to achieve final prototype model. The vote count is reliable and fast. The system no longer needs to count paper ballots manually. The process required a lot of human resources, time consuming and faulty. Moreover, all the candidates' votes are automatically started with zero when the power supply is initialized or system is reset by using reset switch. Therefore, the vote counts are fair and trusted. One more thing is no one can make illegal voting, such as pressing vote switch more than one time. The system will not count any illegal votes while the voter is in the voting cell. The system makes sure for voter can make only one successful vote for a candidate. The system can be built with locally available components and number of candidates can easily extend by editing the program codes. Vote counter variables use integer type variables; therefore, each candidate can be count up to 16-bit value starting from 0 to 65535. If larger count is required, it can be replaced with long type variables which can store up to 32 bit counts. Moreover, the system can be operated with power banks or 5 V dc supply when electricity is not available in the countrysides.

Acknowledgements

We would like to express our sincere gratitude to Rector Dr Nay Win Oo , East Yangon University, Pro-Rectors of Dr Aye Aye Ko , Dr Wah Wah Lwin and Dr Thida Aung, East Yangon University for allowing to submit this research paper in East Yangon University Journal. We would like to express our deepest gratitude to Professor Dr Naing Naing Oo, Head of Department of Physics, Professor Dr Su Su Aung, Department of Physics , East Yangon University, for her suggestions and critical reading of the manuscript .

References

[1] Arduino homepage on Arduino Uno [online]. Available: http://arduino.cc/en/Main/arduinoBoardUno

[2] "Atmega328 datasheet", [online]. Available: http://www.atmel.in/Images/doc7810.pdf

[3] Rotary Encoder.pdf (handsontec.com)

INVESTIGATION OF HEAVY METAL CONCENTRATION IN FLOWERS, LEAVES AND BARKS OF MANGROVE TRUMPET TREE (THAKUT)

Myint Zu Thin[1], Thu Thu[2], Thazin Oo[3], Ye Lin Tun[4], May Mi Tun[5]

Abstract

In this research work, the elemental concentration of flowers, leaves and barks of mangrove trumpet tree have been analyzed by using EDXRF (energy dispersive X-Rays fluorescence) method. It is found that the flower-powder sample of mangrove trumpet tree contained twenty-two kinds of elements. In the leave-powder sample, there are twenty- one kinds of elements and in the bark–powder sample contained twenty-seven kinds of elements. Among them, the concentrations of heavy metal were analyzed. They are Fe, Zn, Pb, Cu, Ni, Mn, Co, Cr and As elements. The flowers and leaves of mangrove trumpet tree can help to reduce the depression, Type II diabetes, asthma, hypertension and heart disease, osteoporosis and cardiovascular disease, cancers of the colon, rectum, and prostate and formation of kidney stones. The bark can be used as liniment to treat dysentery and rheumatism. The flowers and leaves of mangrove trumpet tree are suitable to eat as traditional food as well as medicine. And then, the observed data compare with International Permissible Limits of WHO data.

Keywords: Mangrove Trumpet tree, Powder sample, EDXRF, Heavy metal concentrations

Introduction

The scientific name *Dolichandrone spathacea*, including in *Bignoniaceae* family, common named mangrove trumpet tree is known as Thakut or Thatkutma in Myanmar as shown in figure 1. They are salt-tolerant tree and shrubs that fringe intertidal areas of tropical and sub-tropical coastline. This species is found in most of Southeast Asia, India and Sri Lanka. They contain a complex salt filtration system and a complex root system to cope with saltwater immersion and wave action. It is about 5 m tall tree. Leaves made up of 2-4 pairs of leaflets eye-shaped thin arranged opposite one another. Generally, 3 pairs of leaflets are found at the tip. Usually, leaves are slightly pinkish and somewhat sticky. At times the tree may be nearly leafless. The plant produces bisexual flower that develop on flowering shoots. Flowers are borne on short, terminal, few-flowered racemes. Calyx is 4 to 5 centimeters long. Corolla is white, with a rather slender, cylindrical tube 9 to 11 centimeters long, becoming funnel-shaped or bell-shaped above, 5 to 7 centimeters in diameter. Flowers are in clusters of 2-10 flowers [3]. The flowers in the cluster bloom one at a time and are very fragrant. Fruit is a capsule, somewhat cylindrical or slightly compressed, 30 to 40 centimeters long, 2 to 2.5 centimeters thick, with numerous, rectangular, winged seeds. Seeds are dark grey, squarish, with thick corky wings. In Myanmar, the dried flowers and new leaves are edible in tradition. The study of elemental concentration in flowers, leaves and barks of mangrove trumpet tree was made by using EDXRF method.

Energy Dispersive X-ray Fluorescence (EDXRF) Technique

EDXRF spectrometry is an analytical technique widely used for elemental analysis in both industrial and research laboratories. The Rigaku NEX-CG combines secondary target excitation with a high performance SDD detector, to deliver optimal EDXRF sensitivity for the measurement of metals in aerosols on air filters. The NEX-CG analyzer is capable of

[1] Demonstrator, Department of Physics East Yangon University
[2] Demonstrator, Department of Physics East Yangon University
[3] Demonstrator, Department of Physics East Yangon University
[4] Demonstrator, Department of Physics East Yangon University
[5] Demonstrator, Department of Physics East Yangon University

elemental analysis from sodium (Na) to uranium (U), making the XRF technique ideal for other elements on air filters, as well and in concentration ranging from a few part per million (ppm) to 100% [5]. Instrument control and data analysis are performed by a personal computer (PC) that is connected to the system. Instrument control and data analysis are performed by a personal computer (PC) that is connected to the system. The schematic major instrumental components of an EDXRF analyzer as shown in figure 2. In present work, the samples were placed in the sample chamber of Rigaku spectrometer, which can measure fifteen samples at a time. A large sample chamber with an automatic opening and closing door was used. The atmosphere used is helium mode routine operation helium (gas) pressure was about 0.66 liter per minute. Each sample was run for about 600 seconds and the spectra were analyzed in PC using NEX-CG software. Secondary targets all measurements were carried out under the helium atmospheric condition.

Figure 1. *Dolichandrone spathacea* (Mangrove Trumpet Tree)

Methodology

Energy Dispersive X-ray Fluorescence (EDXRF) Technique

EDXRF spectrometry is an analytical technique widely used for elemental analysis in both industrial and research laboratories. The Rigaku NEX-CG combines secondary target excitation with a high performance SDD detector, to deliver optimal EDXRF sensitivity for the measurement of metals in aerosols on air filters. The NEX-CG analyzer is capable of elemental analysis from sodium (Na) to uranium (U), making the XRF technique ideal for other elements on air filters, as well and in concentration ranging from a few part per million (ppm) to 100% [5]. Instrument control and data analysis are performed by a personal computer (PC) that is connected to the system. Instrument control and data analysis are performed by a personal computer (PC) that is connected to the system. The schematic major instrumental components of an EDXRF analyzer as shown in figure 2. In present work, the samples were placed in the sample chamber of Rigaku spectrometer, which can measure fifteen samples at a time. A large sample chamber with an automatic opening and closing door was used. The atmosphere used is helium mode routine operation helium

(gas) pressure was about 0.66 liter per minute. Each sample was run for about 600 seconds and the spectra were analyzed in PC using NEX-CG software. Secondary targets all measurements were carried out under the helium atmospheric condition.

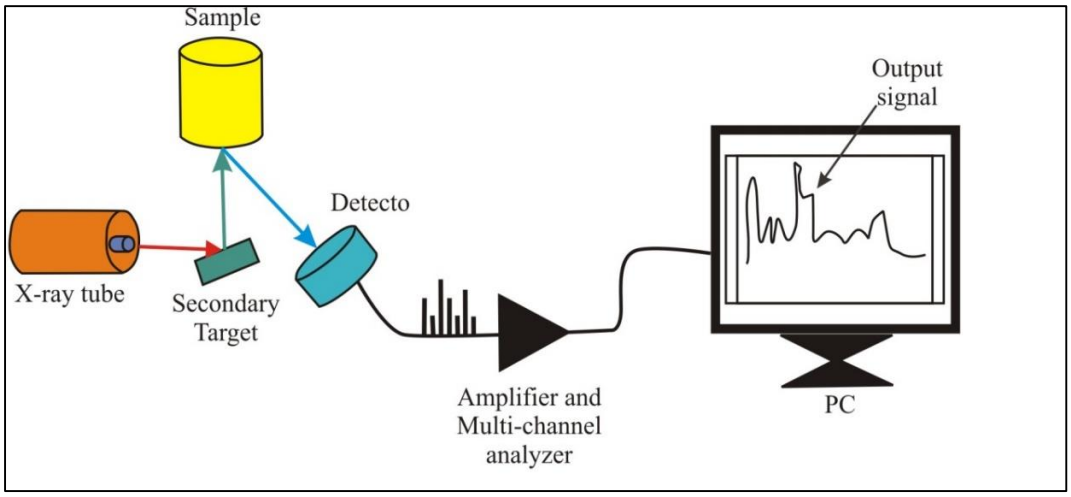

Figure 2. The Schematic Major Instrumental Components of an EDXRF Analyzer

Experimental Procedure

Sample Location, Collection and Sample Preparation

The samples were collected from Yahtaung village, Pwintbyu Township, Magway Region, Myanmar. Magway is situated at North latitude 20.15˚, East longitude 94.02˚ and 1968 feet elevation above the sea level. The flowers, leaves and barks of Mangrove Trumpet were dried at room temperature for 15 days. Then they were ground into the fine powder by using grinding machine. After sieving them with a mesh of size 150, they were grounded by agate mortar for one hour to become homogeneous powder. After getting very fine powder, the sample was weighed nearly 5g and were prepared as pellets. The size of the pellet is 32 mm. The resulted three powder samples of flower, leave and bark were shown in figure 3 a, b and c respectively.

Figure 3.(a) Dried flowers of Mangrove Trumpet and flower powder

Figure 3.(b) Dried leaves of Mangrove Trumpet and leave powder

Figure 3.(c) Dried barks of Mangrove Trumpet and bark powder

Results and Discussion

In this research, the elemental concentrations in three kinds (flowers, leaves and barks) of mangrove trumpet tree samples were analyzed with EDXRF-720 method at Y Center in Taunggyi University. It is found that the powder samples contain Fe, Mg, K, Ca, Zr, Si, Cl, S, Al, Eu, Tm, Zn, Gd, Pb, Sb, Pa, Cu, Hf, Ni, Os, Rb and Br elements. From observed data, the heavy metals are Fe, Zn, Pb, Cu, Ni, Mn, Co, Cr and As. According to the experimental results, it is seen that Fe is maximum concentration and As element is minimum concentration. The comparison of heavy metal concentration in sample with WHO as shown in Table (1).

Table (1) Comparison of heavy metal concentration in powder samples with WHO

Sr.No	Symbol	Element	Flower-powder(ppm)	Leave-powder(ppm)	Bark-powder(ppm)	WHO/FAO (ppm)
1	Fe	Iron	0.00924	0.4168	1.005	0.5
2	Zn	Zinc	0.00254	0.00417	0.00488	3
3	Pb	Lead	0.00026	0.00026	0.00039	0.01
4	Cu	Copper	0.00145	0.00265	0.00233	1
5	Ni	Nickel	0.0006	0.00021	0.00013	0.02
6	Mn	Manganese	0.00191	0.00674	0.00414	0.5
7	Co	Cobalt	0.0003	0.0003	0.0003	0.01
8	Cr	Chromium	0.00072	0.00107	0.00155	0.05
9	As	Arsenic	0.00008	0.00013	0.00018	0.5

Iron is required for the production of red blood cells.A lack of red blood cells is called iron deficiency anemia. They are very essential to maintain good health for human beings. By having the flowers and leaves of mangrove trumpet tree regularly, it can reduce the probability of depression, Type II diabetes, asthma, hypertension and heart disease[4].

Second major element is zinc. Znic is a mineral that human body uses for fighting off infections and producing cells. It's important for healing injuries and creating DNA, the genetic blueprint in all of cells. If zinc is not enough in diet, may have side effects such as hair loss, lack of anertness, and a reduced sense of taste and smell. High blood pressure is a leading cause of cardiovascular disease. It accounts for two-thirds of all strokes and half of heart disease[4].

And third major element is lead. Lead in the body is distributed to the brain, liver, kidney and bones. It is stored in the teeth and bones, where it accumulates over time.Human exposure is usually assessed through the measurement of lead in blood. Lead in bone is released into blood during preganacy and becomes a source of exposure to the developing fetus. So the bark should be used as liniment to treat dysentery and rheumatism.

The major elements contained in flowers and leaves of mangrove trumpet tree are the essential elements required for body. The graphs of elemental concentration in flowers, leaves and barks of Mangrove Trumpet tree are shown in Figures. From the table, comparison of heavy metal concentration of flowers, leaves, and barks of Mangrove Trumpet tree with WHO data as shown in Figure 7.

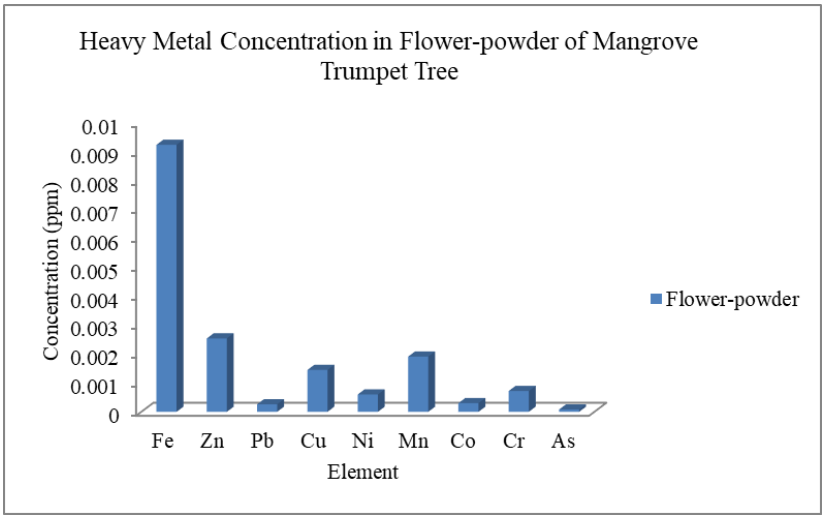

Figure 4. Heavy metal concentration in flower-powder of Mangrove Trumpet tree

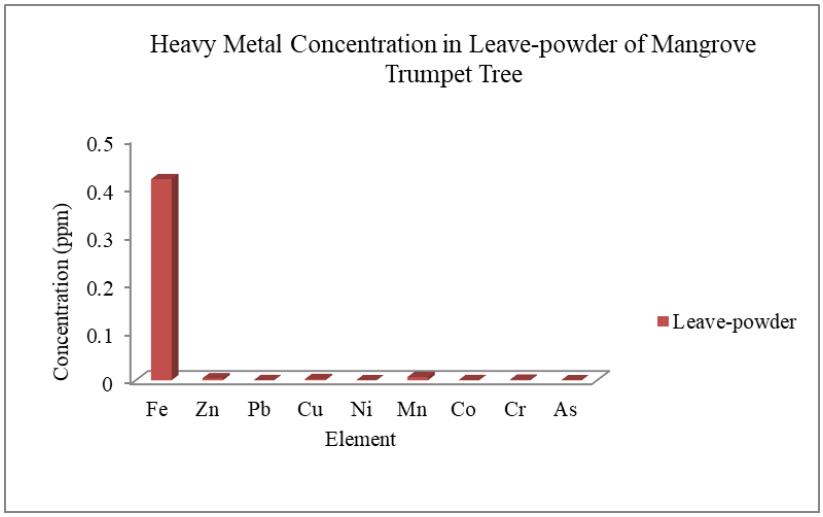

Figure 5. Heavy metal concentration in leave-powder of Mangrove Trumpet tree

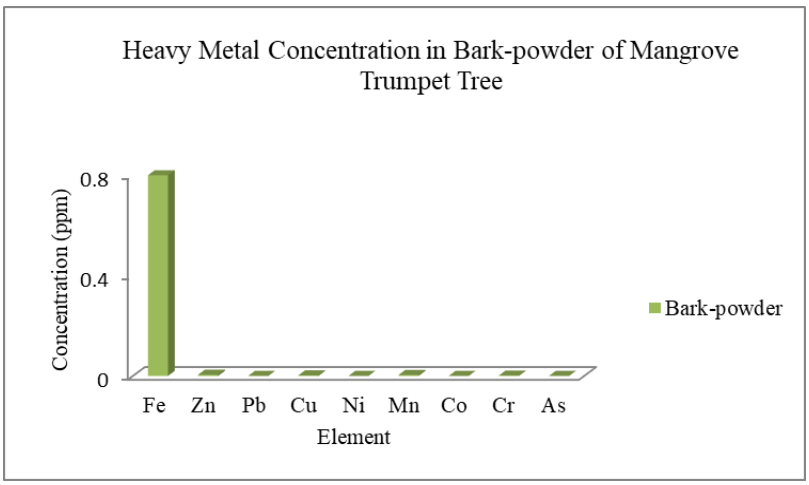

Figure 6. Heavy metal concentration in bark-powder of Mangrove Trumpet tree

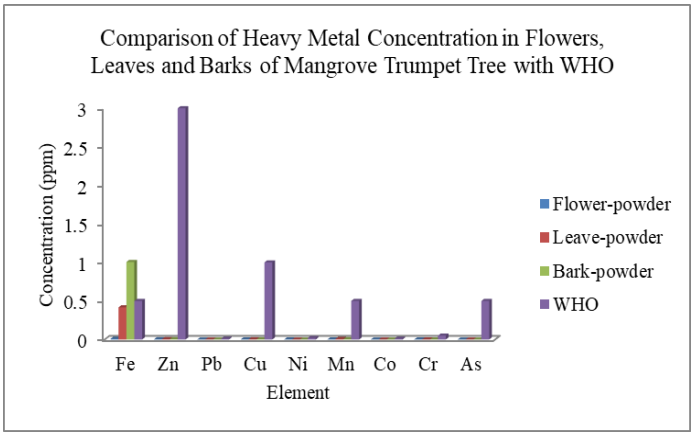

Figure 7. Comparison of heavy metal concentration in flowers, leaves and barks of Mangrove Trumpet tree with WHO

Conclusion

According to the experimental results it is found that Fe and Zn contain as major elements in powder samples. In this research, Fe is the main contaminant element from 0.00924 ppm to 1.005 ppm in powder samples. Fe was found to be present at the highest concentration of 1.005 ppm in bark powder sample.The presence of Fe in leave and bark is slightly exceeded than the permission level 0.5 ppm. The amount of iron needed is 8 mg a day for men and 18 mg a day for women. Up to 60% of patients with colon cancer have iron deficiency at diagnosis, probably due to chronic blood loss. The World Health Organization (WHO) estimates that approximately half of the 1.62 billion cases of anemia worldwide are due to iron deficiency. Thus, flowers and leaves of mangrove trumpet tree may reduce the probability of colon cancer and anemia**.** The leaves of mangrove trumpet tree may be one of the important medicinal leaves for liver and for treating to fight against bacterial infection. The flowers and leaves of mangrove trumpet tree are suitable to eat as traditional food as well as medicine and the bark can be used as liniment. Thus, Mangrove Trumpet tree (Thakut) should be taken to get minerals which are benefical for human health.

Acknowledgements

We would like to express our sincere thanks to Rector Dr Nay Win Oo, Pro-Rectors Dr Aye Aye Ko, Dr Wah Wah Lwin and Dr Thida Aung, Professor Dr Naing Naing Oo , Head of Department of Physics and Professor Dr Su Su Aung , from East Yangon University for their kind permission to carry out this research paper.

References

[1] Institute of Medicine. Food and Nutritrition Board, “Dietary Reference Intakes for VitaminA, VitaminK,
Arsenic, Boron, Chromium, Copper, Iodine, Iron, Manganese, Molybdenum, Nicle, Silicon, Vanadium, and Zinc:a Report of the Panel on Micronutrients” , Washington, DC: National Academy Press; 2001

[2] He Fj, MacGregor GA. “A Comprehensive review on salt and health and current experience of worldwide salt reduction programmes”, 2009

[3] Committee to Review Dietary Reference Intakes for Vitamin D and Calcium, Food and Nutrition Board,Institute of Medicine. Dietary Reference Intakes for Calcium and Vitamin D. Washington, DC: National
Academy Press, 2010.

[4] https://www.flowersofindia.net/catal/slides/Mangrove% 20Trumpet%20 Tree.html Dolichandrone spathacea- Mangrove Trumpet Tree

[5] http;//specek.co.in/products/x-ray fiuorescence spectrometers/bench top-edxrf-2/Bench top EDXRF Spectek

[6] www.ancient-minerals.com > health
[7] www.Articles.mercola.com/sites/articles/arch
[8] https;//www.researchgate.net/figure/Guideline- for- safe-limits of heavy metals tbl2-262604015 Table2.Guideline for heavy metal
[9] http://www.researchgate.net/figure/Permissible limits of heavy metals in soil and plants tbl1 304347101

COMPARISON AND INVESTIGATION OF THE DIELECTRIC PROPERTIES OF UN-DOPED AND Al-DOPED TITANIA THIN FILMS

Shine Ko Ko[1], Wint Wah Soe[2], Su Myat Yadanar[3], Khin Hlaing Htay[4], Su Pon Chit[5]

Abstract

The Al-doped and un-doped TiO_2 thin film were investigated on a glass substrate by using spin coating technique through a sol-gel route. The wt % 1:3 of Al-doped were used to dissolve in H_2SO_4 solution. In order to get the Al-doped TiO_2 sol-gel, $Al_2(SO_4)_3$ solution was added drop by drop into the $Ti(SO_4)_2$ solution during stirring at 60 °C on mixed for 4 days. The un-doped TiO_2 sol-gel was formed by using 1:2 weight % of TTIP and 2-methoxyethanol. And then, these obtained sol-gels were used to produce the thin films by spin coating technique with 2000 rpms. The average crystallize sizes and natures of Al-doped and un-doped TiO_2 thin films were not too much difference which were about 29.56 nm and 36.2 nm at 700 °C, according to the XRD results. Energy Dispersive X-ray Fluorescence (EDXRF) showed that the concentrations of 29.29 % of Al and 69.89 % of TiO_2 were contribute to form Al- doped TiO_2 particles on these thin films. The dielectric properties of these films were examined with the Digital Impedance Analyzer (insteak:8110G LCR Meter). The dielectric properties of the un-doped and Al-doped TiO_2 thin films were well stored electrical charges between the frequencies range 3 kHz and 10 kHz. The surface morphologies of Al-doped and un-doped TiO_2 thin film were also observed with Scanning Electron Microscopy (SEM).

Keywords–SEM, EDXRF, LCR meter, sol-gel, Spin coating

Introduction

The TiO_2 as a photocatalytic material was analyzed by Fujishima and Honda in 1972, who observed the photocatalytic splitting of water on TiO_2 electrodes (A Fujishima et al,1972) [1]. TiO_2 thin film for photocatalytic application has the most common ones being Rutile, Anatase and Brookite states. According to the XRD result, the three different types of TiO_2 were at (400-600) °C is Anatase, at (600-700) °C is Rutile and at above 700 °C is Brookite phases. TiO_2 is activated by illumination with (UV) light having an energy higher than the band gap. The band gap of Anatase is Eg = 3.2 eV and Rutile is Eg = 3.0 eV for this corresponds to wavelengths below 387 nm and 413 nm, respectively. Most research with respect to photocatalysis is performed using Anatase, while in all other aspects Rutile has been much more thoroughly characterized (e.g. electronic behavior, bulk structural investigations) [2]. In recent years, applications to environmental cleanup have been one of the most active areas in heterogeneous photocatalysis. Here one looks at the photo-degradation of hydrocarbons either in water or in air using suspended small particles or thin films of TiO_2 [3]. The advantages of TiO_2 is low price, chemical solidity, non-toxicity, highly photoactive, self–regeneration and can easily be recycled. While TiO_2 powders or films obtained at low temperatures are finely grained (nanocrystalline) because little grain growth can occur, grain growth at temperatures above 800 °C can be substantial [4]. Therefore, depending on the preparation method, the nature of the TiO_2 particle or film surface, as well as the active surface area are usually very different for Anatase and Rutile powders. Since for a catalyst its active surface area is important, differences in surface area must be taken into account when comparing the activity of different materials [5].The two methods of thin film deposition are wet chemical and vapor deposition. The wet chemical technique used most

[1] Demonstrator, Department of Physics, East Yangon University
[2] Demonstrator, Department of Physics, East Yangon University
[3] Demonstrator, Department of Physics, East Yangon University
[4] Demonstrator, Department of Physics, East Yangon University
[5] Demonstrator, Department of Physics, East Yangon University

often is sol-gel technique. Furthermore, the development of sol-gel technique has led to procedures which can yield crystalline.

In this research journal, the characterization of un-doped and Al-doped TiO_2thin films with the temperature of 400 °C and 700 °C will be investigated by XRD, SEM, EDXRF. Finally, the comparative study of the dielectric properties of these films will also be illustrated by using Digital Impedance Analyzer (insteak: 8110G LCR Meter) [6].

Materials and Methods

Preparation of un-doped TiO_2 Thin Film

Titanium–isopropoxide (TTIP) and 2-methoxyethanol with the weight percent of 1:2 was used as the starting chemical materials for TiO_2 sol-gel to perform the un-doped TiO_2 thin film. These two materials were mixed together in a closed- beaker by using the magnetic stirrer with the temperature at 45 °C to get the homogeneous solution. During the stirring process, some drops of acetic acid were used again to get the transparent solution. In order to control the viscosity of this solution, De-ionized water was used. TTIP and 2-methoxyethanol sol-gel were performed on as desired chemical materials to develop the un-doped TiO_2 thin film by using spin coating method. Non electrolytic glass substrate must be etched with acetone and DI water for releasing the contaminations. Furthermore, the diffusion of TiO_2 particles on the substrate was carried by a hot- plate with the temperature 50 °C at 10 min. And then the obtained TiO_2 sol-gel was placed on a substrate by using spin-coating making with a speed- rate of 2000 rpms to form the un-doped TiO_2 thin films. Finally, these thin films were placed in the oven at 400 °C and 700 °C at 30 min to pass the crystallization of TiO_2 thin film. Figure 1 showed the flow chart of the un-doped TiO_2 thin film preparation [7].

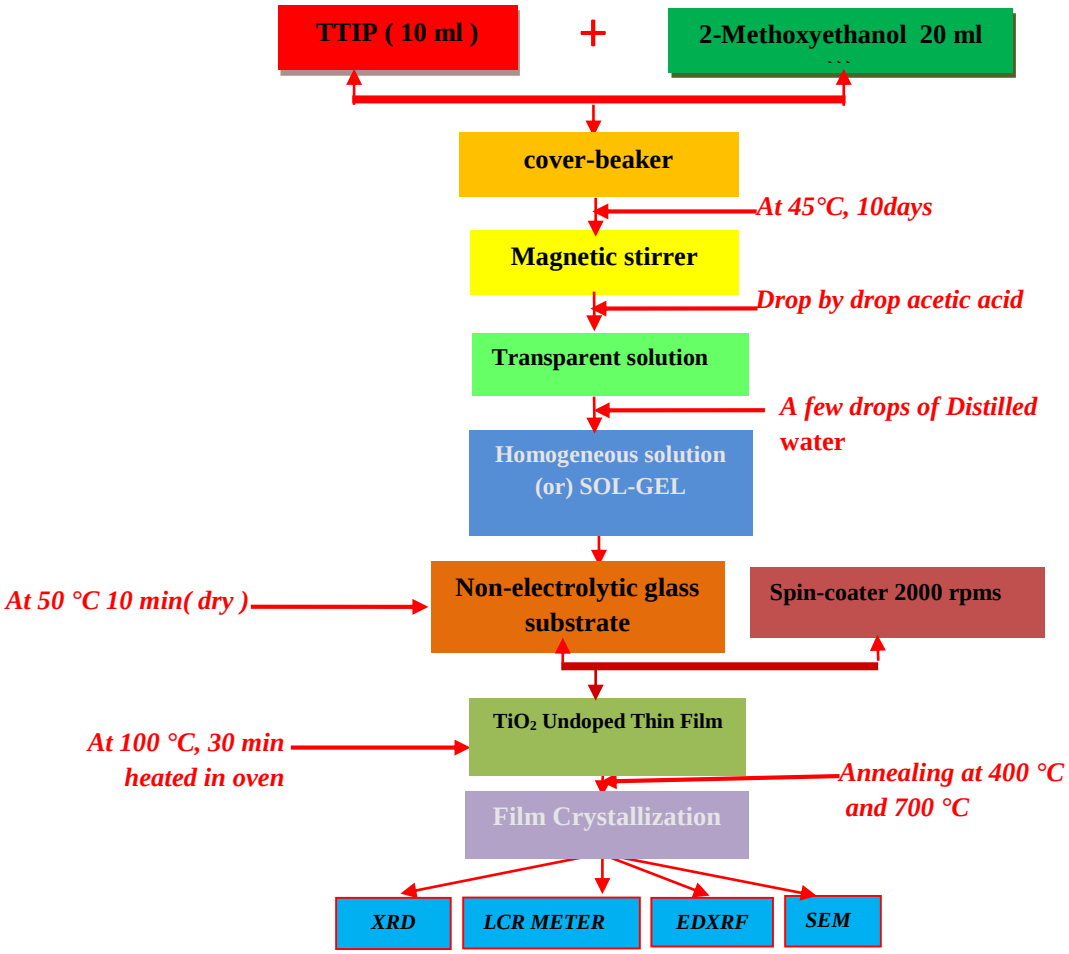

Figure 1. The flow chart of the un-doped TiO_2 thin film preparation

Preparation of Al-doped TiO_2 Thin Film

The 99 percent purities of TiO_2 powder and Al powder with the weight percent of 1:3 was used as the starting chemical materials to get the Al-doped TiO_2 sol-gel. Before making the Al-doped TiO_2 sol-gel, TiO_2 powder and H_2SO_4 diluted sulfuric acid were combined in a closed beaker first. The magnetic stirrer with the temperature of 55 °C was use to get the titanium–sulphate $Ti(SO_4)_2$ homogeneous solution about 4 days. Similarly, Al powder and diluted sulfuric acid H_2SO_4 were combined in a closed beaker again. The magnetic stirrer with the temperature of 75 °C was used to produce the homogeneous aluminium–sulphate $Al_2(SO_4)_3$ solution about 4 days. After investigation of these two solutions, the few drops of $Al_2(SO_4)_3$ solution was added to the $Ti(SO_4)_2$ solution in a closed beaker to perform Al-doped TiO_2 sol-gel for about 4 days with the help of the magnetic stirrer at temperature of 55 °C. The obtained Al–doped TiO_2 sol-gel was used again to investigate the thin film on the non-electrolytic glass substrate with the spin coating machine. The spin coating speed of 2000 rpms was made to obtain Al-doped TiO_2 thin films. These films were held on the oven at the temperature of 100 °C at 30 min to get the dry condition of Al and TiO_2 crystal. And then, these two films of 400 °C and 700 °C were annealed in the furnace to obtain the Al-doped TiO_2 thin film crystallization. Figure 2 showed the flow chart of the Al – doped TiO_2 thin film preparation [8].

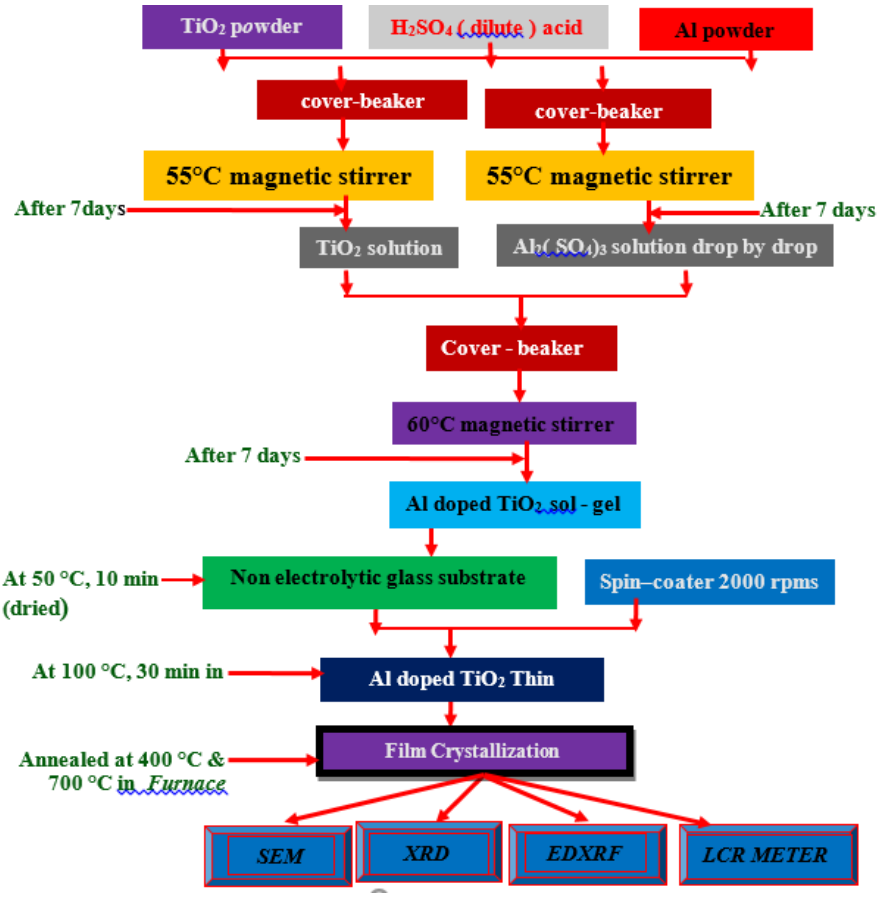

Figure 2. The flow chart of the Al – doped TiO_2 thin film preparation

Results and Discission

Characterization of un-doped and Al-doped TiO_2 particles and thin films by XRD

The ultra-fine un-doped and Al-doped TiO_2 powders were investigated to know the crystalline state of thin films by annealing the un-doped sol-gel and Al-doped TiO_2 sol-gel at

400 °C and 700 °C. The crystallite diameters 'D' were obtained from XRD peaks according to the Debye-Scherrer equation: $\boldsymbol{D = \frac{0.89\lambda}{\Delta W cos\theta}}$, where λ is the wavelength of X-ray beam (λ = 1.5405 Å of Cu-K_α radiation), $'\theta'$ is the Bragg's angle, ΔW *is* the width of X-ray peak in radians (rads). The data obtained from XRD spectrum was shown in Tables 1 to 4. It was observed that the crystalline nature of pure anatase phase at 400 °C and rutile phase at 700 °C for un-doped TiO_2 powders. From XRD diffraction technique, at 400 °C the tetragonal peaks of crystalline planes are (101), (004), (200), (211) and (213). At 700 °C, the powder changed to their actual rutile phase but the intensity was still increased as shown in Figures 5 and 6. The crystallite diameter came from dominant plane (101) for 400 °C and (110) for 700 °C which was calculated from above equation were 7.88 nm and 33.17 nm. The average crystallize sizes were 8.42 nm at 400 °C and 36.20 nm at 700 °C for un-doped TiO_2 particles on the thin film. The thickness of the un-doped TiO_2 thin films for both temperatures was about 595 nm as shown in Figure 12. Even though the Al diffused or doped into TiO_2 particles on the thin film, tetragonal structure of TiO_2 phase were remained unchanged as shown in Figures 3 to 4. The crystallite diameter of dominant plane (101) at 400 °C and 700 °C were calculated data are 28.38 nm and 22.27 nm for Al-doped TiO_2 particles on the Al-doped TiO_2 thin film. Simultaneously, the average crystallize sizes were also about 31.54 nm at 400 °C and 29.56 nm at 700 °C for these both thin films. These crystallite sizes were not too much difference for both 400 °C and 700 °C for Al-doped TiO_2 thin films, Al-doped TiO_2 particles would compared than the un-doped TiO_2 particles on the TiO_2 thin films. The thickness of the Al-doped TiO_2 thin film was about 714 nm for both temperatures as shown in Figure 13.

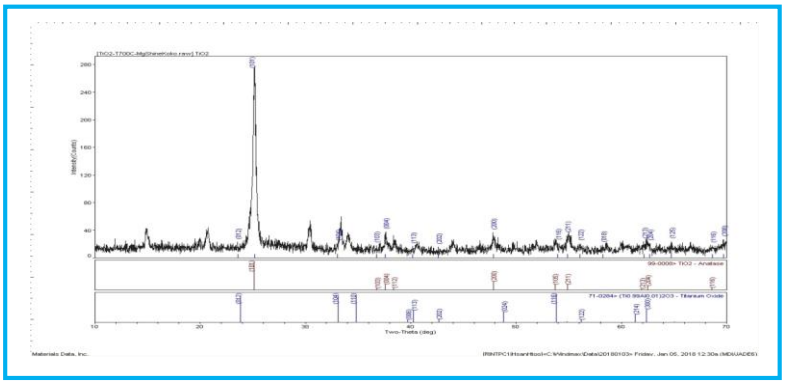

Figure 3.The data analyse of the Al-doped TiO_2 thin film at 700°C

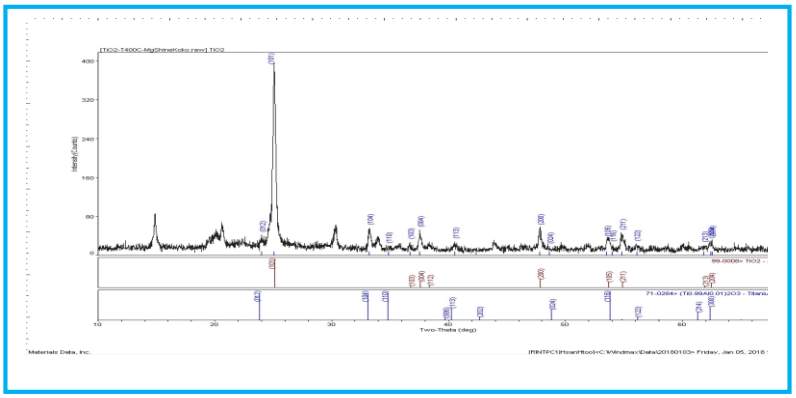

Figure 4.The data analyse of the Al-doped TiO_2 thin film at 400°C

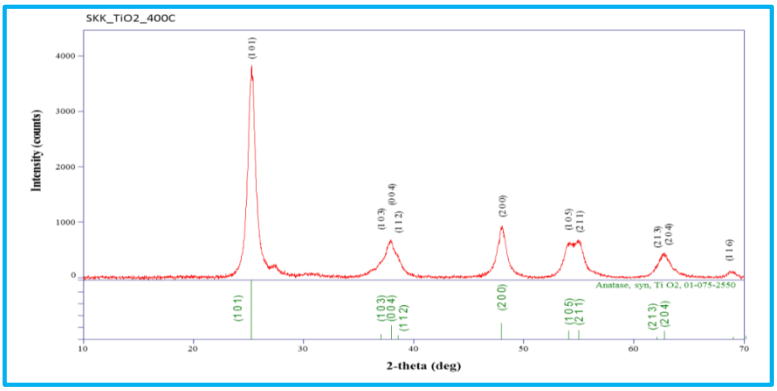

Figure 5. The data analyse of the un-doped TiO_2 thin film at 400°C

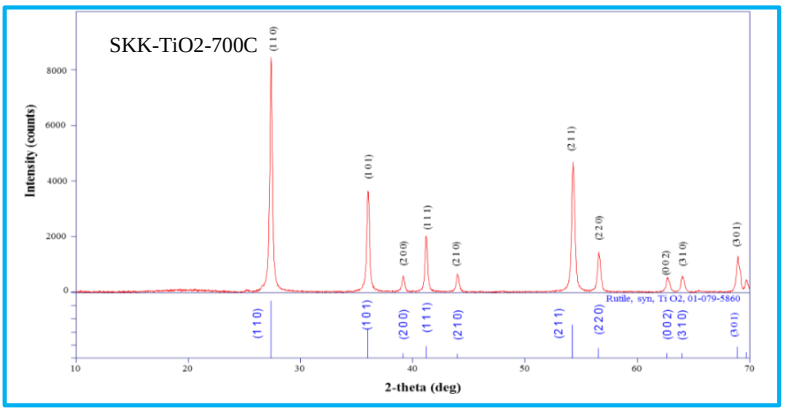

Figure 6. The data analyse of the un-doped TiO_2 thin film at 700°C

Table1. The average crystallize size of un-doped TiO_2 particles at 400 °C

No	20 Degree	FWHM	Plane Direction	Crystallize Sizes (nm)
1	25.2869	1.0224	101	7.88
2	37.9924	1.0224	004	8.14
3	47.9564	1.0224	200	8.42
4	62.1005	1.0224	211	8.67
5	62.7555	1.0224	213	8.98
	Average crystallize sizes of un-doped TiO_2 particles			8.42

Table 2. The average crystallize size of un-doped TiO_2 particles at 700 °C

No	20 Degree	FWHM	Plane Direction	Crystallize Sizes (nm)
1	25.4045	0.2440	110	33.17
2	36.0363	0.2289	101	36.12
3	41.1896	0.2249	111	37.35
4	54.2533	0.2361	211	37.42
5	56.5563	0.2416	220	36.95
	Average crystallize sizes of un-doped TiO_2 particles			36.20

Table 3. The average crystallize size of Al-doped TiO_2 particles at 400 °C

No	20 Degree	FWHM	Plane Direction	Crystallize Sizes (nm)
1	25.077	0.284	101	28.38
2	37.545	0.171	004	47.15
3	47.818	0.325	200	26.36
4	62.540	0.501	211	17.09
5	62.531	0.236	204	38.72
	Average crystallize sizes of un-doped TiO_2 particles			31.54

Table 4. The average crystallize size of Al-doped TiO_2 particles at 700 °C

No	20 Degree	FWHM	Plane Direction	Crystallize Sizes (nm)
1	25.170	0.362	101	22.27
2	36.739	0.177	103	45.56
3	37.596	0.237	004	34.02
4	47.833	0.349	200	24.55
5	54.859	0.427	211	21.39
	Average crystallize sizes of Al-doped TiO_2 particles			29.56

Characterization of un-doped and Al-doped TiO_2 particles and thin films by EDXRF

Energy Dispersive X-ray Fluorescence (EDXRF) was performed to confirm the Al-doping concentration on the Al-doped TiO_2 thin film as shown in Figure 7. From the results, the concentration of the TiO_2 peak is 68.89 %, Al peak concentration is 29.29 % and other peak concentrations are 1.41, 0.36 and 0.03 percents which can be neglected amount in Al-doped TiO_2 or $Al_2(TiO_2)_3$. In spite of the suitable amount of Al concentration diffused into the TiO_2 to make the Al-doped TiO_2, a few amount of the other contaminations was also diffused. This is because of the uncontrolled ambient conditions for Al-doped TiO_2 or $Al_2(TiO_2)_3$ thin films during the investigation process of these films. Figures 2 and Table 5 showed the following EDXRF data.

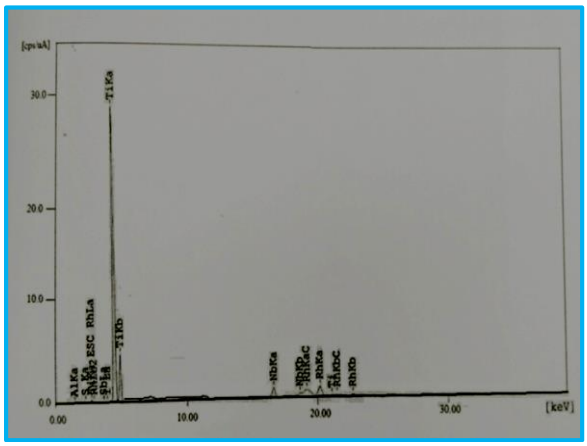

Figure 7. The investigated of EDXRF data of the Al-doped TiO_2 thin film

Table 5. The results of Aluminum concentrated in Al-doped TiO_2 with EDXRF

Analyte	**Concen-tration (%)**	**Test Line**	**Intensity (cps/µA)**
Ti	68.89	Ti (K_α)	198.05
Al	29.29	Al (K_α)	10.13
S	1.41	S (K_α)	0.44
Nb	0.36	Nb (K_α)	0.88
Zn	0.03	Zn (K_α)	0.28
Cu	0.03	Cu (K_α)	0.22

Characterization of un-doped and Al-doped TiO_2 particles and thin films by SEM

The surface morphologies of the TiO_2 particles on the un-doped and Al-doped particles on the Al-doped TiO_2 thin films are shown in Figures 8 to 13. SEM technique was used again. According to the SEM results, the crystallite diameters of un-doped and Al-doped TiO_2 thin films at 400 °C were almost identical with the previous XRD results as shown in Figures 8 and 9. At 700 °C, the agglomeration of Al-doped TiO_2 thin films were increased as shown in Figures 10 to 11. The crystal linearity also was not inhomogeneous. But the crystallite diameters were not changed as Al-doped TiO_2thin films at 400 °C. Cause of highly diffusion of Al-atoms in TiO_2 particles at high temperature, Al-doped TiO_2 particles were strongly combined with each other. The grain boundaries of these particles, therefore, were increased up to 1 μm as shown in figures 8 and 10. Figures 12 and 13 also showed the value of thickness of un-doped and Al-doped TiO_2 thin films. The value of the thickness of Al-doped thin films were increased about 714 nm as the Al-atoms diffused strictly to the TiO_2 particles on the thin film as shown in Figure 13.

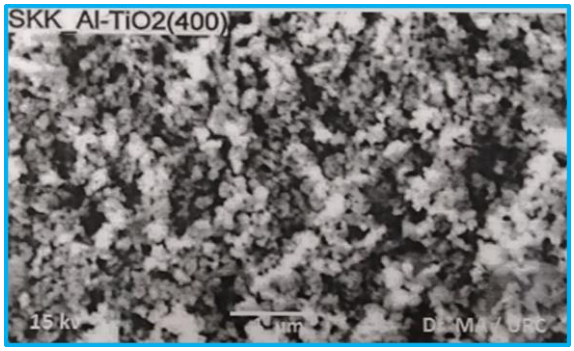

Figure 8.SEM image investigated for Al-doped TiO_2 thin film at 400 °C

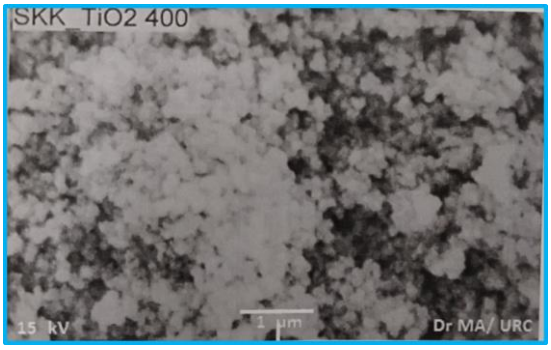

Figure 9.SEM image investigated for un-doped TiO_2 thin film at 400 °C

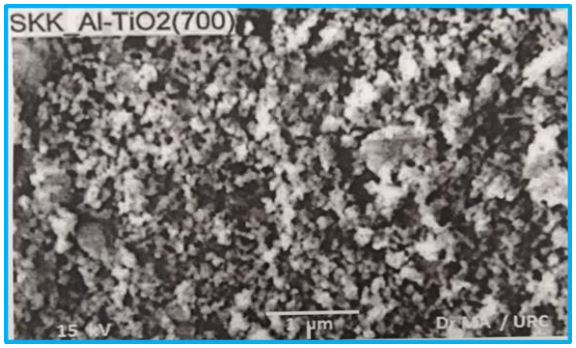

Figure 10. SEM image investigated for Al-doped TiO_2 thin film at 700 °C

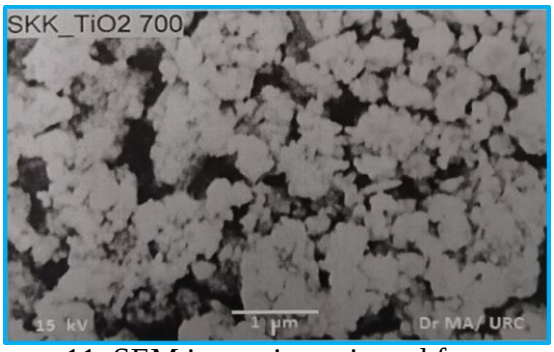

Figure 11. SEM image investigated for un-doped TiO_2 thin film at 700 °C

Figure 12. SEM image investigated for the 'thickness'of the Un-doped TiO_2 thin film at 400 °C and 700 °C

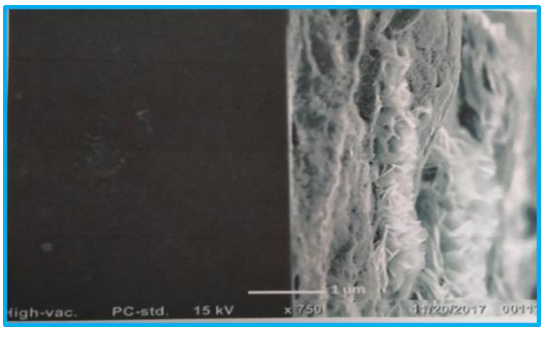

Figure13. SEM image investigated for the 'thickness'of the Al-doped TiO_2 thin film at 400 °C and 700 °C

In order to realize the characterization for dielectric properties of un-doped and Al-doped TiO_2 thin film investigation was carried out by using Digital Impedance Analyzer (insteak: 8110G LCR Meter), the dielectric properties of un-doped and Al-doped TiO_2 thin films were measured over the frequency range between 100 Hz to 100 kHz. The dielectric constant and dissipation factor were calculated by the following equation $\varepsilon_r = Cd/(\varepsilon_\circ A)$, $\tan\delta = D/\varepsilon r$, where ε_r is dielectric constant, C is capacitance measured, d is the thickness of the thin film, A is area of the top electrode, D is dielectric loss, tan δ is dissipation factor. The thicknesses of un-doped and Al-doped TiO_2 thin films were about 595 nm and 714 nm, as shown in Figures 12 and 13. The change in capacitance and dissipation factor with various frequencies at temperatures of 400 °C and 700 °C for TiO_2 un-doped and Al-doped TiO_2 thin films were presented in Tables 6 to 9.According to the results, when the low frequency (<100Hz) was applied to the TiO_2 thin films, the change in capacitance and dielectric loss were not detected in both un-doped and Al-doped thin films but when the high frequency (>3 kHz) was applied to the TiO_2 thin flims, the change in dielectric constant, capacitance and dissipation factor were found to be decreased as shown in Figures 14 to 17. In addition, when the frequencies range between 3 kHz and 10 kHz were applied to both un-doped and Al-doped thin films, they would well response and maintain the electrical charges as shown in Tables 6, 7 and 8. However, the frequencies ranges between 10 kHz and 100 kHz, these films cannot good store the electrical charges. Therefore, the optimum frequencies ranges for these films were between 3 kHz and 10 kHz.

Table 6. Frequency, dielectric constant and dissipation factor for un-doped TiO_2 at 400 °C

No.	Frequency (F) Hz	Capacitance (C)pF	Dielectric Loss(D)	Thickness, d (m)	Area(A) m^2	Dielectric Constant, ε_r	Dissipation Factor (tanδ)
1	3031.27	3.21	66.27	5.95E-07	1.00E-06	13.84	4.78
2	4041.36	2.66	0.62	5.95E-07	1.00E-06	0.18	3.52
3	5051.45	1.81	0.39	5.95E-07	1.00E-06	0.12	3.26
4	9091.81	1.79	2.47	5.95E-07	1.00E-06	0.97	2.60
5	16162.45	1.44	0.12	5.95E-07	1.00E-06	0.08	1.41
6	17172.54	1.38	0.06	5.95E-07	1.00E-06	0.07	0.81

Table 7. Frequency, dielectric constant and dissipation factor for Al-doped TiO_2 at 400 °C

No.	Frequency (F) Hz	Capacitance (C)pF	Dielectric Loss(D)	Thickness, d (m)	Area(A) m^2	Dielectric Constant, ε_r	Dissipation Factor (tanδ)
1	9091.82	8.82	2.10	7.14E-07	1.00E-06	0.65	3.23
2	14142.27	1.37	0.23	7.14E-07	1.00E-06	0.09	2.55
3	19192.73	1.09	0.18	7.14E-07	1.00E-06	0.08	2.25
4	49495.45	1.04	0.13	7.14E-07	1.00E-06	0.07	1.86
5	79798.20	1.01	0.03	7.14E-07	1.00E-06	0.06	1.33
6	84848.67	1.00	0.03	7.14E-07	1.00E-06	0.05	0.68

Table 8. Frequency, dielectric constant and dissipation factor for un-doped TiO_2 at 700 °C

No.	Frequency (F) Hz	Capacitance (C)pF	Dielectric Loss(D)	Thickness, d (m)	Area(A) m^2	Dielectric Constant, ε_r	Dissipation Factor (tanδ)
1	9091.82	2.83	2.13	5.95E-07	1.00E-06	0.65	3.24
2	14142.27	2.09	0.20	5.95E-07	1.00E-06	0.08	2.53
3	49495.45	1.09	0.15	5.95E-07	1.00E-06	0.07	2.21
4	79798.20	1.04	0.11	5.95E-07	1.00E-06	0.06	1.83
5	84848.67	8.38	0.12	5.95E-07	1.00E-06	0.07	1.68
6	80899.14	1.49	0.05	5.95E-07	1.00E-06	0.07	0.76

Table 9. Frequency, dielectric constant and dissipation factor for Al-doped TiO_2 at 700 °C

No.	Frequency (F) Hz	Capacitance (C)pF	Dielectric Loss(D)	Thickness, d (m)	Area(A) m^2	Dielectric Constant, ε_r	Dissipation Factor (tanδ)
1	15152.36	1.84	0.62	7.14E-07	1.00E-06	0.35	5.00
2	16162.45	1.61	0.39	7.14E-07	1.00E-06	0.10	3.55
3	19192.72	1.47	0.26	7.14E-07	1.00E-06	0.09	3.07
4	96969.79	1.44	0.27	7.14E-07	1.00E-06	0.08	3.22
5	97979.89	1.30	0.20	7.14E-07	1.00E-06	0.07	2.72
6	98989.98	1.21	0.16	7.14E-07	1.00E-06	0.06	2.12

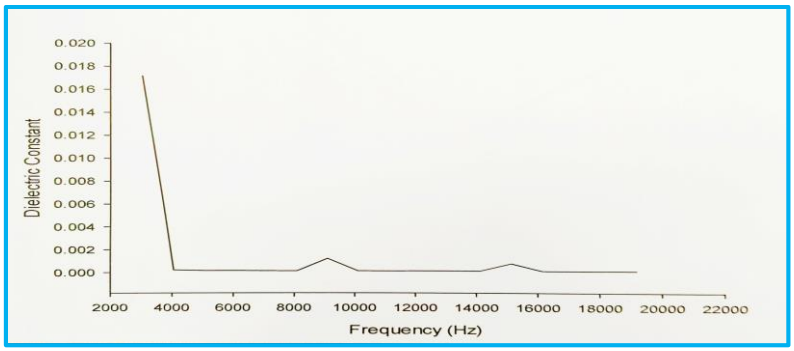

Figure 14. The variation of the dielectric constant
frequency for un-doped TiO2 thin film at 400°C

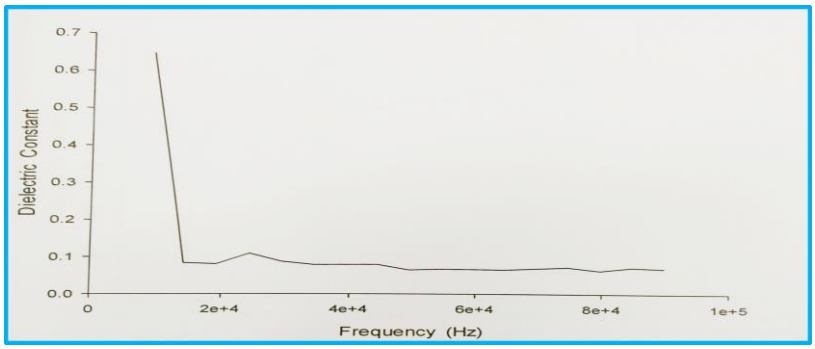

Figure 15. The variation of the dielectric constant and frequency
for Al-doped TiO2 thin film at 400 °C

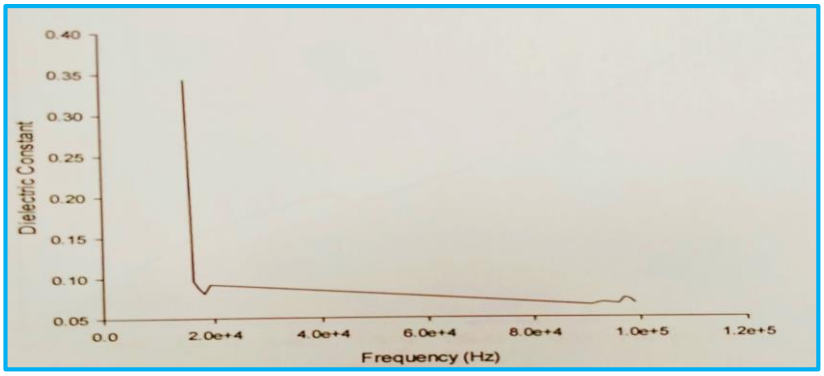

Figure 16. The variation of the dielectric constant and frequency

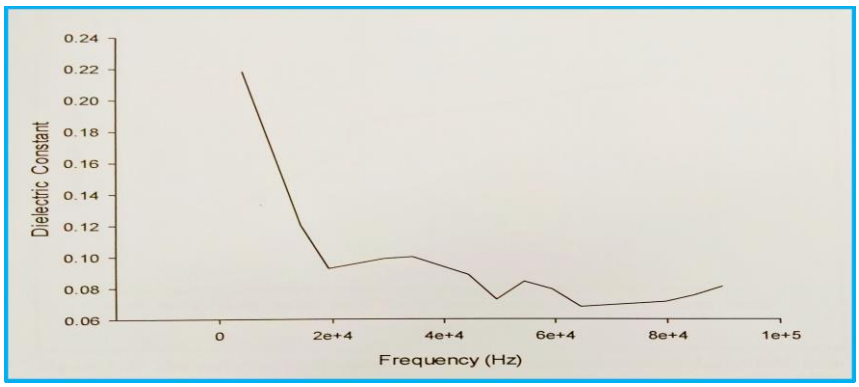

Figure 17. The variation of the dielectric constant and frequency for Al-TiO_2 thin film at 700 °C

Conclusion

The weight percent 1:2 of Titanium–isopropoxide (TTIP) and 2-methoxyethanol were used for TiO_2 sol-gel to perform the un-doped TiO_2 thin film with the help of spin coating technique. The obtained un-doped TiO_2 particles on the TiO_2 film were analyzed with XRD to show its crystallize sizes and natures at 400 °C and 700 °C. Meanwhile, the few drops of $Al_2(SO_4)_3$ solution and $Ti(SO_4)_2$ solution were also used to form Al-doped TiO_2 sol-gel for making the Al-doped TiO_2 sol-gel for making the Al-doped TiO_2 thin film with spin coating technique again. The obtained Al-doped TiO_2 particles on the TiO_2 film were also analyzed with XRD to show its crystallized size and nature at 400 °C and 700°C, again. Scanning Electron Microscopy SEM analysis was also performed to realize the crystallized size and nature of un-doped TiO_2 and Al-doped TiO_2 particles on the TiO_2 films.

According to the XRD results, the average crystallize sizes were 8.42 nm at 400 °C and 36.2 nm at 700 °C for un-doped TiO_2 particles before spin coating. After coating the un-doped TiO_2 thin films, these crystallize sizes at 400 °C and 700 °C for Al-doped TiO_2 particles were almost the same as before spin coating. This is because of the Al-atoms diffusion onto the Al-doped TiO_2 thin films. These Al-doped TiO_2 particles would strictly held to each other and the crystallite sizes were not too much changed compared than the TiO_2 particles on the un-doped TiO_2 thin films. The thickness of un-doped and Al-doped TiO_2 thin films were also about 595 nm and 714 nm for both temperatures.

Besides, EDXRF analysis was used to ensure the Al-doping concentration on the Al-doped TiO_2 thin films. The concentration of TiO_2 peak was 68.89 % whereas the Al-peak concentration was 29.29 % with other ignored amount concentration of S, Nb, Zn and Cu. Due to the necessity of annealing of these films, the small amount of other contamination were negligible. In order to realize the surface morphologies, SEM investigation was carried out again.

Moreover, the dielectric characterizations were showed that the electrical charge strong capability of these films. They were measured by the Digital Impedence Analyzer (Insteak: 8110G LCR Meter). When the low frequency (<100 Hz) was applied to the TiO_2 thin films, the changes in capacitance and dielectric loss were not detected in both un-doped and Al-doped thin films. When the high frequency (> 3 kHz) was applied to the TiO_2 thin films, the change in dielectric constant and capacitance were found to be decreased. Moreover, the dissipation factor was also decreased with various frequencies at different temperatures. In addition, when frequencies ranges between 3 kHz and 10 kHz were applied to both un-doped and Al-doped thin films, they would well response and store the electrical charges. The optimum frequencies ranges must be between 3 kHz and 10 kHz for both films. Therefore, they can also used in high power gain, low noise performance, optoelectronics

devices, micro and nano-science and engineering. And then, I must again rework carry out this research for my future tasks, researches and I must do to get the available electrodes and solar cells.

Acknowledgements

We would like to express our heartfelt thanks to Rector Dr Nay Win Oo and Pro-Rectors Dr Aye Aye Ko, Dr Wah Wah Lwin and Dr Thida Aung, East Yangon University, for their kindly permission to perform this research paper work. Furthermore, We really special thanks to Professor Dr Naing Naing Oo, Head of Department of Physics, East Yangon University for her warmly advising and supporting throughout to do my research. Finally, We actually wish to thanks Professor Dr Su Su Aung, Department of Physics, East Yangon University for her valuable guidelines and helpfulness to carry out this research.

References

[1] A Fujishima and K J Honda, 1972, J Chem Soe Japan 74, 355
[2] C Kittle, 1960, "Photoconductivity of Solids", Jhon Wiley and Sons Inc (New York)
[3] D Schwarzenbach 1996 "Crystallography" New York: Wiley)
[4] H Faouzi, B Yacine, K Fouad, and B Abderrahmane, 2013, Int J Nanoparticles, 6, 132
[5] M Abdel Aziz. I Yahia, L Wahab, M Fadel and M A fifi, 2006, J Appl Surf Sci, 252, 23, 8168
[6] M Sylvanin, H C Doo, H Romain, A Dinesh and L Michael, 2013, J Int Creamics, 39, 299
[7] Nay Myo Tun, Than Than Win and Yin Maung Maung 2011 "Formation of TiO_2 ElectrospumUltrafine Fibres", 11th MAS conference, Yangon University (Bet Paper Award)
[8] Nay Myo Tun, Than Than Win and Yin Maung Maung 2011 "Preparation and Characterization of TiO_2 Electrospum Nano fibres", 2nd ICSE conference, Sedona Hotel, Yangon (Best Paper Award)

INTELLIGENT ROOM LIGHT CONTROL AND ELECTRICAL POWER SAVING SYSTEM UTILIZING PERIPHERAL INTERFACE CONTROLLER

Phyu Thel Ei[1] , Khin Myat Mon[2], Hnin Ei Hlaing[3], Wutt Yi Zaw[4], Zuly Moe[5]

Abstract

In this research paper, an intelligent room light control system is designed to be smartly operated by a microcontroller circuit. The objective of this research is to prevent home electrical hazards and reduce electricity consumption. The system design consists of optical sensor, room light intensity monitoring sensor, LCD display, relay circuit and PIC 16F877A microcontroller. Program for the whole system is based on PIC microcontroller with PIC Basic Pro programming language. This project is proposed to monitor and control lights on/off action that depend on human existence and light intensity inside the room. By this way, it will reduce human efforts and also it will save electricity. The proposed system is very useful for such situation that is forgotten to turn off lights while leaving a room. Such system can be implemented in the living rooms, office rooms, conference halls and classrooms, etc. This research project is a perfect choice for caring about electrical security and also electrical power saving as well.

Keywords: 16F877A microcontroller, LCD display, Relay circuit, LDRs

Introduction

Wasting energy has become one of the most challenging problems that are having a struggle at the present time. The most common waste of energy comes from the unnecessary use of the electrical energy in daily life [6]. In home, school, office, university, college and industry, the lights are stayed on even when there are in the absence of people inside the room. This often happens because of negligence or forgetfulness to turn off lights while leaving a room [6]. To keep away such situation, the author has proposed the system called "Intelligent Room Light Control and Electrical Power Saving System Utilizing Peripheral Interface Controller". In this research paper, the design of intelligent room light control system is demonstrated by using microcontroller PIC 16F877A. This system can be described with the help of following block diagram in Figure 1.

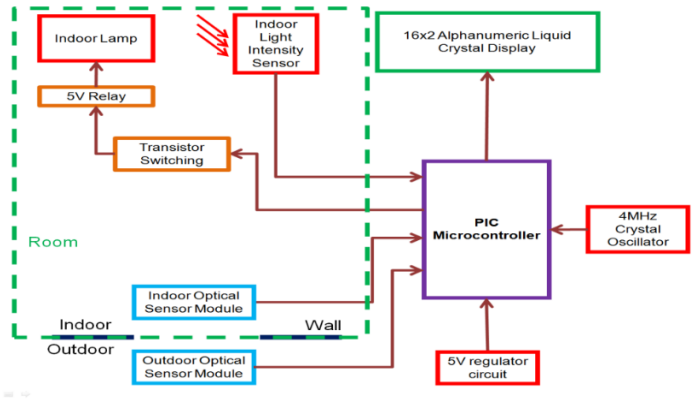

Figure 1. The block diagram of the system

---

[1] Demonstrator, Department of Physics, East Yangon University

[2] Demonstrator, Department of Physics, East Yangon University

[3] Demonstrator, Department of Physics, East Yangon University

[4] Demonstrator, Department of Physics, East Yangon University

[5] Demonstrator, Department of Physics, East Yangon University

Methodology of the System

In this intelligent room light control and electrical power saving system, the whole design consists of six sections, the controller circuit, the indoor light intensity sensor circuit, the power supply circuit, the lamp relay switching circuit, the indoor visitor detector circuit and the outdoor visitor detector circuit. The microcontroller PIC 16F877A is programmed in such a way that the lightning in the room is controlled by the passage of individuals in or out of the room using optical sensor (Light Dependent Resistor). Then decide for the automatic light bulb switching on and off as instructed in the program. The indoor light intensity is displayed on the LCD by reading the indoor light intensity monitoring sensor. The total number of person inside the room is also displayed on the LCD. The light bulb is ready to switch on if there is at least one visitor, but it will not operate if there is plenty of light of in the room. If the luminous in the room is not enough, the light bulb will automatically switch on. By this way, the system operates the room light automatically and smartly according to the sensors.

Hardware and Software Requirements of Circuit Construction

Microcontroller PIC 16F877A

The PIC16F877A is one of the most renowned microcontrollers in the industry [4]. The PIC16F877A microcontroller is designed using RISC architecture, manufactured by Microchip and is used in embedded projects. It belongs to the mid-range family of the PIC microcontroller devices. It can be used in remote sensors, security and safety devices, home automation and many industrial instruments [4]. It can be operated with 20MHz clock input and it contains 8K x 14 words of FLASH Program Memory, 368 x 8 bytes of Data Memory and 256 x 8 bytes of EEPROM Data Memory. It has five ports on it, starting from PORT A to PORT E [5]. The device consists of 14 interrupts and both serial and parallel communication features [3]. The PIC16F877A comes in 40 pin packages as shown in Figure 2.

Figure 2. PIC 16F877A Microcontroller

Light Dependent Resistor (LDR)

A Light Dependent Resistor (LDR) or a photo resistor is a device whose resistivity is a function of the incident electromagnetic radiation. Hence, they are light sensitive devices. They are also called as photo conductors, photo conductive cells or simply photocells. They are made up of semiconductor materials having high resistance. A light dependent resistor (LDR) whose resistance is decreased when light falls on it and that is increased in the dark [2]. The photograph of light dependent resistor is shown in Figure 3.

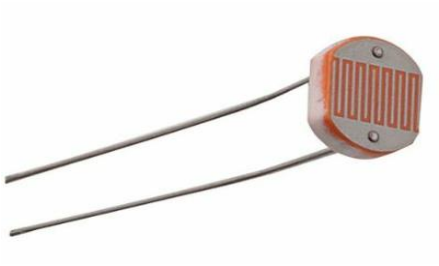

Figure 3. Light Dependent Resistor (LDR)

Hitachi 44780 Compatible LCD Display

The alphanumeric liquid displays are widely used in various applications. The most popular LCD interface is the Hitachi 44780 based LCD controller chip which provides a fairly easy to work with interface and low power consumption. Hitachi 44780 Compatible 2x16 characters display is used in this project. The photograph of 2x16 LCD Display which can show two rows of 16 characters as shown in Figure 4.

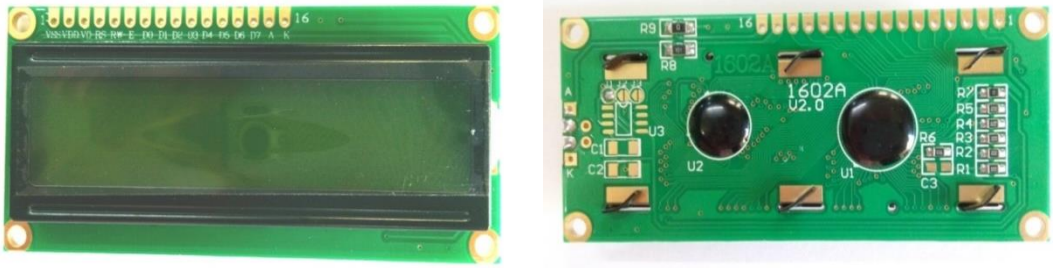

Figure 4. Photographs of front side and back side of 16 characters x 2 lines LCD display

Relay

A relay is a switch used to turn other circuits on or off. It is useful if we want (i) a small current in one circuit to control another circuit containing a device such as a lamp or electric motor which needs a large current, or (ii) several different switch contacts to be operated simultaneously [1]. The photograph of 5V DC Relay is shown in Figure 5.

Figure 5. Photograph of 5V DC Relay

Designing and Etching Printed Circuit Board

The printed circuit board was designed with computer aided software, Niche PCB software. The software can be easily downloaded from the internet. It is very easy to design a printed circuit board. The software consists of two layers only to design the circuit, the soldering side and the component side. The soldering side and the components side are expressed with the red and blue color track-lines respectively. The drawings of the circuit are illustrated as shown in Figure 6. The printed circuit boards after etched are as shown in Figure 7.

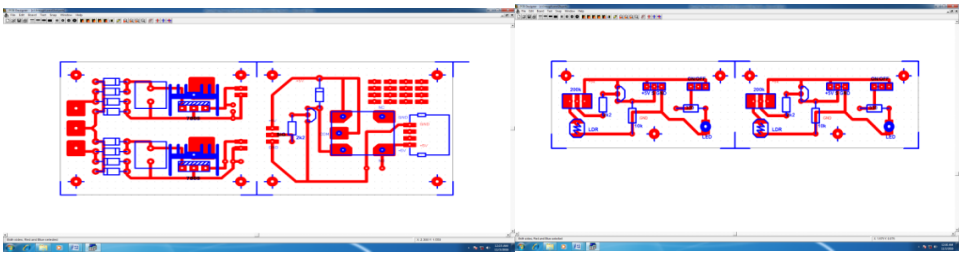

Figure 6. The both side view of PCB drawing for the relay & power supply circuit and indoor & outdoor sensors circuits

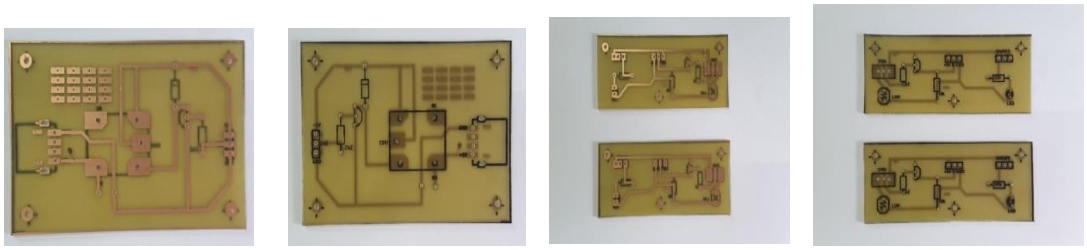

Figure 7. Soldering side and component side photos of relay circuit board and sensor circuit boards after etching

Programming for PIC 16F877A Microcontroller

The program source code is created with the PIC Basic Pro programming language. The structure of the program is illustrated with a flowchart diagram. The program flow chart of the proposed intelligent room light control and electrical power saving system is shown in Figure 8.

Circuit Operation of System

The whole circuit operation was stimulated and designed using electronic circuit stimulation software called Proteus software. The simulation designing of the whole system on Proteus software is shown in Figure 9. The PIC 16F877A is the heart of the circuit and it is preprogrammed with the program coding created with PIC Basic Pro language. The Port B pins are connected with the LCD display. The supply pins of LCD are directly connected with the GND and +5V line of the circuit. In this circuit, the LCD will display the textual information such as luminous and amount of visitors in the room. The RD2 pin is used as an output pin and it is used to operate the indoor lamp with a 5V relay. Instead of directly controlling the relay, an NPN transistor (BC547) is used to operate the relay. The emitter of the transistor is directly connected with the ground line and the collector is connected with the supply line through the relay coil. But there is a rectifier diode added parallel with the relay coil to protect the back EMF, which can greatly damage parts of the circuit.

The two visitor sensor circuits are designed as active high sensors. They will generate logic LOW in normal condition and change to logic HIGH whenever a visitor is detected. The sensor circuits are constructed by using two LDRs and transistors. The photograph of the whole system is illustrated in Figure 10. The whole circuit before power connection is demonstrated in Figure 11.

As soon as the power supply is connected, the LCD display illuminates the luminous level of room light intensity. The limited value for room light intensity level is 1000 lux. The light intensity level in the room is about 868 lux while operating the circuit which is not a suitable light condition for a visitor. If there is a visitor in front of the door, the LCD display changes and is described as “OUTDOOR DETECT”. If the visitor is leaving first outdoor

sensor and keep going in, the display illuminated as “CHECKING INDOOR”. If the visitor is leaving opposite to indoor sensor, the visitor counter has not achieved a successful count. If the visitor keeps coming inside, the indoor sensor detected and then the display illuminated as “VISITOR = 01”. Meanwhile, the indoor luminous was under 1000 lux and so the lamp operated as shown in the Figure 12.

If the visitor inside the room is near the indoor sensor to go out, the display illuminated as “INDOOR DETECT”. If the visitor is leaving from the indoor sensor then the display changes to “CHECKING OUTDOOR”. If the visitor is not really going out, the successful decrement cannot make. If the visitor is passed through the door, the successful decrement is made. If there is no visitor, the lamp will automatically switch off.

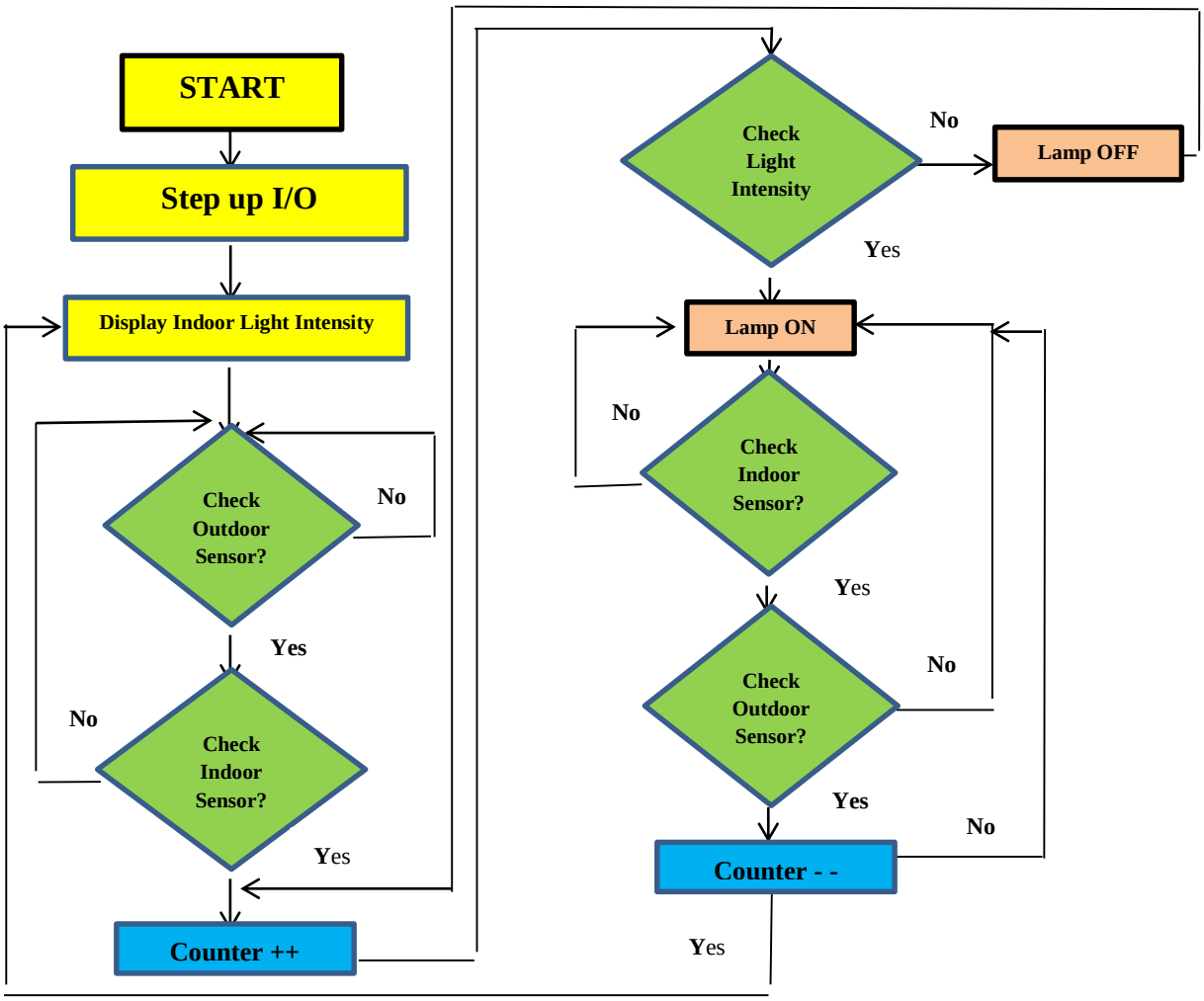

Figure 8. Program flow chart of the proposed intelligent room light control and electrical power saving system

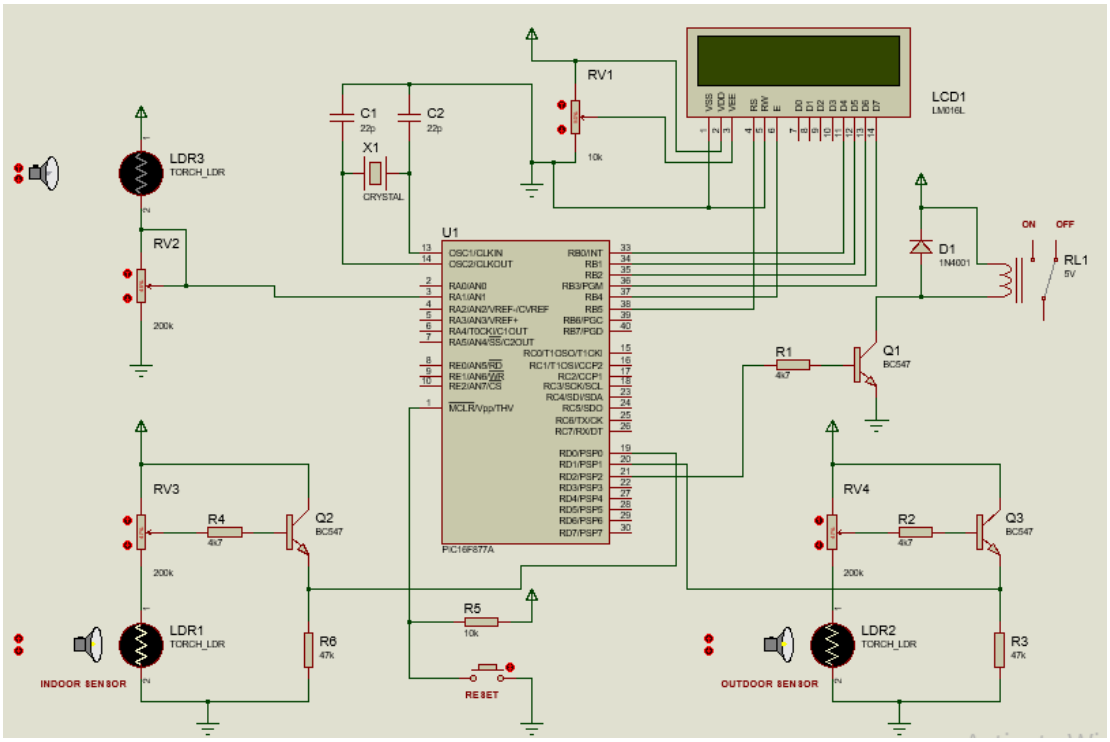

Figure 9. Schematic diagram of the intelligent room light control and electrical power saving system

Figure 10. Photograph of intelligent room light control and electrical power saving system

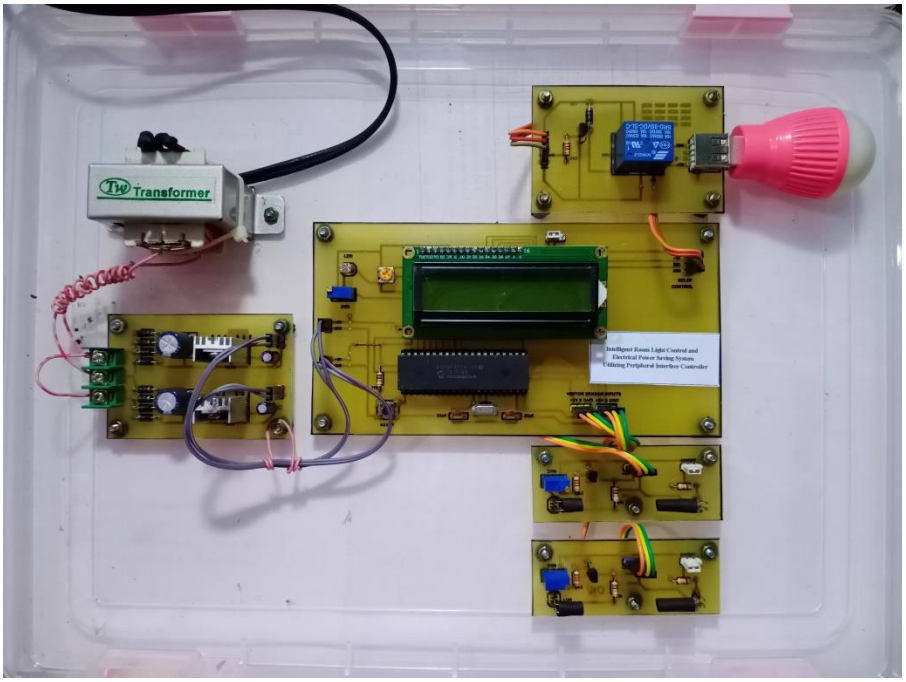

Figure 11. Photograph of the circuit board in a plastic box

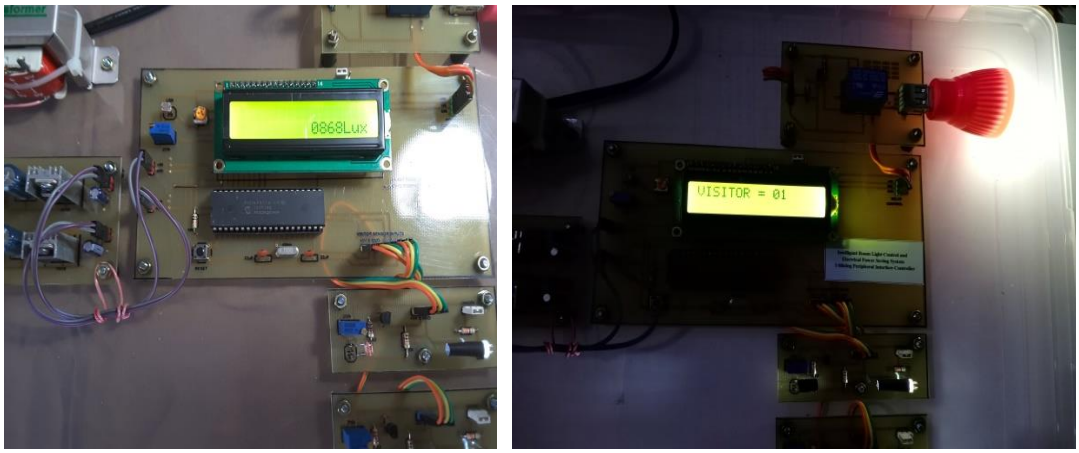

Figure 12. Photographs of the circuit operation

Results and Discussion

The step by step operation procedures are illustrated and explained with photos. Since the whole circuit is installed in a plastic box and decorated like a house, it is very smart and impressive. For better and safer to carry and keep the circuit, the whole circuit is housed in a plastic file box which is large enough to keep the five separate circuits and a transformer.

The power supply card and transformer are on the left side of the box. The controller circuit is the largest and it is in the middle of the box. The microcontroller circuit is required to put in the middle because it is interconnected with all other circuits. The relay circuit is on the upper right of the box and it consists of a USB terminal to operate a 5V/5W USB lamp. The two visitor sensors for indoor and outdoor are kept near its control terminal. Therefore, they are at the lower side of the box. The wire connections to each circuit are made by using

female to female cables. After inserting the LCD on its position, the circuit is ready to test with PIC microcontroller.

This system can be used for a 10 x10 square feet room. This project proposes a basic one that can be smart, comfort, energy saving and reduce human efforts for the users. Since it is a research project, this circuit can be upgraded by many modifications for future research and development. This system can be installed in bathrooms, laundry and rooms in the house and can also be used in public areas like public bathrooms, conference rooms, classrooms, offices and seminar halls, staircases, storage rooms and warehouses, etc.

Conclusion

This research paper presents the implementation of an intelligent room light control and electrical power saving system. This system is constructed with the PIC microcontroller 16F877A and other electronics components. As soon as the power switch is on, the system will automatically detect the number of visitors and luminous in the room. The indoor light intensity is displayed on the LCD by reading the voltage divider output of LDR circuit in analog value. The indoor and outdoor sensors are used for detection of incoming or outgoing visitors according to sensor priority. If the visitor coming in, the number of visitor is increased. Otherwise, the visitor is decreased. The total number of persons inside the room is also displayed on the LCD display. The lamp is ready to switch on if there is at least one visitor, but it will not operate if there is plenty of light in the room. If the luminous in the room is not enough for a visitor, the lamp will automatically switch on. In this way, the system operates the room light automatically and smartly according to the sensors. Turning the lights off when leaving the room is necessary to help saving electricity bills and also extend the life of the light bulbs. This system will be a solution for the problems of wasting electricity and electrical hazards. The author expects that this research project has a vast scope in future applications.

Acknowledgements

We are very grateful to Rector Dr Nay Win Oo, East Yangon University, for his permission to work this research. We would like to thank Pro-Rectors Dr Aye Aye Ko, Dr Wah Wah Lwin and Dr Thida Aung, East Yangon University, for their permissions to work on the present topic. We are greatly indebted to Professor Dr Naing Naing Oo, Head of Department of Physics, East Yangon University, who provides with generous help and kind permission in this research paper. We are also deeply grateful to Professor Dr Su Su Aung, Department of Physics, East Yangon University, for her help and guidance in this research work.

References

[1] Kratika Dixit, Juhi Pal Shyaliga V. Karatangi and Amrita Rai, "Automatic Room light System for Power Saving" (ISSN No: 2279) Volume 07, April 2019

[2] Balaji M "International Research Journal of Engineering and Technology" (IRJET) Volume 06, Mar 2019

[3] Microchip Technology Incorporated 1999 "PIC 16F877A Instruction Set" (New York : MicrochipTechnology)

[4] https://microcontrollerslab.com/pic16f877a-introduction-features/

[5] https://www.theengineeringprojects.com/2017/06/pic16f877a.html

[6] https://www.electronicshub.org/automatic-room-lighting-system-using-microcontroller/

STUDY ON WINDOW CURTAIN DRIVING SYSTEM USING ARDUINO UNO

Kay Zin Win[1], Phyo Hsu Mon Kyaw[2], Aye Thandar Oo[3], Thiri Naing[4]

Abstract

A kind of window curtain driving system is designed and constructed. The system can be operated wirelessly with a 4-keys remote control unit. The system design is constructed with electronic circuit and mechanical window curtain. The electronic circuit composed with an Arduino Uno development board, a stepper motor driver circuit, limit switches, LED display, and a 4-keys remote control transmitter and receiver circuit. The mechanical window curtain is included the stepper motor with pulley belt, limit switches on each sides of the window frames and curtain cloth. The remote control can be used within about 8 feet. The circuit is quite useful and it is innovative for modern living room with automation functions.

Keywords: Arduino Uno, Stepper Motor, Switches, LED, Remote

Introduction

Nowadays, modern technology becomes an important part in our daily life. Technology is making daily life in a better way. Without technology, life is difficult. New devices and applications are improving every day according to user demands. Even in modern architecture designs, automations and controls are added in newly designed apartments and houses. But there are a variety of control systems and they are expensive such as radio control systems or wi-fi control systems or network-based control systems. Only the luxury can afford their accommodations.

In this research paper, the window curtain driving system is designed and constructed. The system consists of two different control modes, fully open/close mode and custom open/close mode. The system design consists of a unipolar stepper motor, two limit switches, a 4-channel remote control transmitter and receiver, ULN2003 IC, Li-Ion battery, LED indicators and an Arduino Uno development board. The Arduino Uno is a microcontroller board based on the ATmega328. It was chosen for consisting of 14 digital input/output pins and 32 k Bytes of program memory [4]. The microcontroller on the board is programmed using the Arduino programming language (based on wiring) and the Arduino development environment (based on processing). Unipolar stepper motor is used in this circuit to move the window curtain. The ULN2003 is a seven NPN Darlington transistor pair IC with high voltage and current capability. It is used to drive the stepper motor.

The circuit design is simple and easy to build, since it is developed with a microcontroller. Moreover, it is cheaper than any foreign imported curtain controllers. The circuit design can also be applied in other applications such as sliding gate door or door control system.

Methodology

The project is made up of seven components in the circuit; Arduino Uno, 4-keys remote transmitter and 4-keys remote receiver, a Darlington transistor pair IC (ULN2003), a unipolar stepper motor, two display LEDs and two limit switches. The Arduino Uno is the heart of the whole circuit and it consists of power supply outputs and digital input/output pins. The digital I/O pins received user commands and transmitted control signals to operate

[1] Demonstrator, Department of Physics, East Yangon University

[2] Demonstrator, Department of Physics, East Yangon University

[3] Demonstrator, Department of Physics, East Yangon University

[4] Demonstrator, Department of Physics, East Yangon University

the other components on the circuit. The four keys remote transmitter is a remote-control unit and consist of four control keys, A, B, C and D. It is a separate component and not wired with the circuit. The 4-keys remote receiver circuit is a receiver module circuit and there is a total of 7 pins. The right most two pins are +V and GND pins [1]. They are connected with the +5 V power supply line and ground line respectively.

The signal pins are named as C, B, A and D according to the function order of remote transmitter key press. They are connected with pin 7 to 4 of Arduino digital I/O pins directly. The last pin on the far left of receiver module is not connected. The ULN2003 is the Darlington transistor pair IC and it consists of 7 Darlington transistors integrated as an integrated circuit [2]. But only four pairs are utilized in the circuit. The pin 1 to pin 4 of ULN2003 connected with the pin 13 to pin 10 of Arduino Uno respectively. The output of Darlington IC is connected with the four pairs of a unipolar stepper motor. The pin IC is connected with the blue color pin of stepper motor, the pin 15, pin 14 and pin 13 are also connected with the pink, yellow and orange color wires of the stepper motor. The red pin of stepper motor is a common pin of the stepper motor and it is directly connected with the 5 V supply line on the circuit. The motor rotation speed and directions are generated by Arduino Uno output pins. The two display LEDs utilize both blue color LEDs. They are used to indicate rotation direction of the stepper motor. They indicate the window curtain is opening or closing. The cathodes of both LEDs are connected with ground line through 330 Ω resistors. But the anodes of LEDs are connected with pin 2 and 3 of Arduino Uno.

Moreover, there are two limit switches on each door side of the window to detect the curtain movements, the left limit switch and the right limit switch. The switches and a resistor are connected in series between power supply line and ground line. The junction of each pair is connected with the pin 9 and 10 of Arduino board as left limit switch and right limit switch respectively. There is a reset switch on the left end of the schematic. The whole circuit is powered by two 3.7 V Lithium ion batteries. The circuit diagram of window curtain driving system is shown in Figure 1.

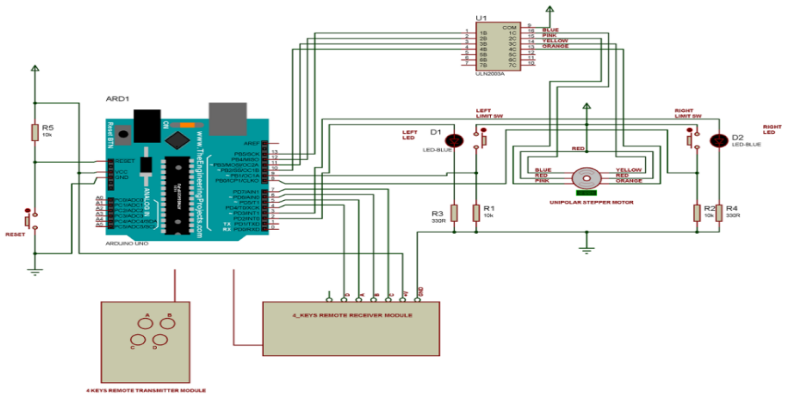

Figure 1. Schematic diagram of window curtain driving system

Hardware and Software RequirementsArduino Uno

The Arduino Uno is a microcontroller board based on the ATmega328 (datasheet). It has 14 digital input/output pins (of which 6 can be used as PWM outputs), 6 analog inputs, a 16 MHz crystal oscillator, a USB connection, a power jack, an ICSP header, and a reset button. It contains everything needed to support the microcontroller; simply connect it to a computer with a USB cable or power it with a AC to DC adapter or battery to get started. The Uno differs from all preceding boards in that it does not use the FTDI USB-to-serial driver chip. Instead, it features the Atmega8U2 programmed as a USB to serial converter [4].

"Uno" means one in Italian and is named to mark the upcoming release of Arduino 1.0. The Uno and version 1.0 will be the reference versions of Arduino, moving forward. The Uno is the latest in a series of USB Arduino boards, and the reference model for the Arduino platform; for a comparison with previous versions, see the index of Arduino boards [4]. Arduino Uno board is illustrated as shown in Figure 2.

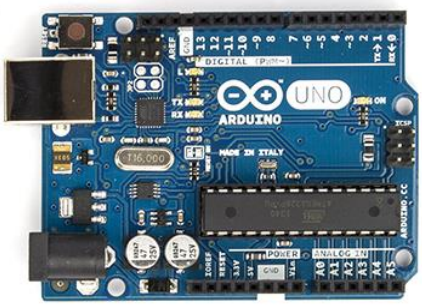

Figure 2. Arduino Uno board

The Arduino Uno can be powered via the USB connection or with an external power supply. The power source is selected automatically. External (non-USB) power can come either from an AC to DC adapter or battery. The adapter can be connected by plugging a 2.1 mm center-positive plug into the board's power jack. Leads from a battery can be inserted in the GND and VIN pin headers of the POWER connector. The board can operate on an external supply of 6 to 20 V. If supplied with less than 7 V, however, the 5 V pin may supply less than 5 V and the board may be unstable. If using more than 12 V, the voltage regulator may overheat and damage the board. The recommended range is 7 to 12 V [4].

The Arduino Uno has polyfuse that protects your computer's USB ports from shorts and overcurrent. Although most computers provide their own internal protection, the fuse provides an extra layer of protection. If more than 500 mA is applied to the USB port, the fuse will automatically break the connection until the short or overload is removed.

The ATmega328 has 32 KB of flash memory for storing code (of which 0.5 KB is used for the bootloader); It has also 2 KB of SRAM and 1 KB of EEPROM (which can be read and written with the EEPROM library). Each of the 14 digital pins on the Uno can be used as an input or output, using pin Mode (), digital Write (), and digital Read () functions. They operate at 5 V. Each pin can provide or receive a maximum of 40 mA and has an internal pull-up resistor (disconnected by default) of 20 - 50 kOhms [4].

The Uno has 6 analog inputs, each of which provide 10 bits of resolution (i.e. 1024 different values). By default they measure from ground to 5 V, though is it possible to change the upper end of their range using the AREF pin and the analog Reference () function.

Wireless Remote Control For Arduino (4 Keys Remote)

There is an interesting pair of complementary Integrated Circuits, PT2262/PT2272 that make basic wireless remote control rather easy to implement. They are commonly used in inexpensive wireless devices to control garage doors, fans, toys and even some alarm systems. These ICs utilize fixed address codes and no inherent encryption so they are not high security devices but are maybe about as secure as the average home’s inexpensive door lock. There are several iterations of these chips sold under slightly varying names with PT2262/PT2272 and SC2262/SC2272 being the most common. The PT2262/PT2272 version is manufactured by Princeton Technology Corporation of Taipei, Taiwan, while the SC2262/SC2272 is manufactured by Silvan Chip Electronics Tech.Co.Ltd. of Shenzhen,

China. Both are identical although the Princeton chips are more common and better documented [3].

There is a resistor in both the 2262 and 2272 that controls an internal oscillator that controls the pulse width of the amplitude modulation and these resistors must be set to complementary values. For example, if the 2262 uses a 4.7 MΩ resistor, then the mating 2272 must use an 820 kΩ resistor. The three most commonly used values are 1.5, 3.3 and 4.7 MΩ.

The PT2262 encoder sends out a serial string with a sync pulse and then data represented by pulse-width modulation, repeated four times. The PT2272 must match the addresses in two pulse trains to its own address, to accept. One bit is represented by 32 clock cycles. Figure 3 showed the 4 keys remote.

Figure 3. 4 keys remote

Transistor ULN2003 IC

The transistor ULN2003 is a monolithic IC consisting of seven NPN Darlington transistor pairs with high voltage and current capability. It is commonly used for applications such as relay drivers, motor, display drivers, led lamp drivers, logic buffers, line drivers, hammer drivers and other high voltage current applications. It consists of common cathode clamp diodes for each NPN Darlington pair which makes this driver IC useful for switching inductive loads [2].

The output of the driver is open collector and the collector current rating of each Darlington pair is 500 mA. Darlington pairs may be paralleled if higher current is required. The driver IC also consists of a 2.7 kΩ base resistor for each Darlington pair. Thus, each Darlington pair can be operated directly with TTL or 5 V CMOS devices. This driver IC can be used for high voltage applications up to 50 V. Transistor ULN2003 is widely used in relay driving and stepper motor driving applications. Transistor ULN2003A IC is illustrated as shown in Figure 4.

Figure 4. Transistor ULN2003A IC

Stepper Motors

Stepper Motors are classified into two, based on its winding arrangement.

1. Unipolar Motors
2. Bipolar Motors

A unipolar motor contains center tapped windings. Usually center connection of coils is tied together and used as the power connection. By using this arrangement, a magnetic pole

can be reversed without reversing the direction of current. Thus, the commutation circuit can be made very simple [5]. Figure 5 showed unipolar stepper motor.

Bipolar motors have no center tap connections. Current through a winding should be reversed to reverse the magnetic poles. Therefore, the driving circuit should be more complicated. This can be solved by using a H-bridge connection or by using ready-made chips such as L293D. Bipolar motors can be distinguished from unipolar motors by measuring the coil resistance. In bipolar motors we can find two wires with equal resistance [5]. Figure 6 showed bipolar stepper motor.

In this circuit, 28-BYJ48 stepper motor is used. The stepper motor 28-BYJ48 is shown in Figure 7.

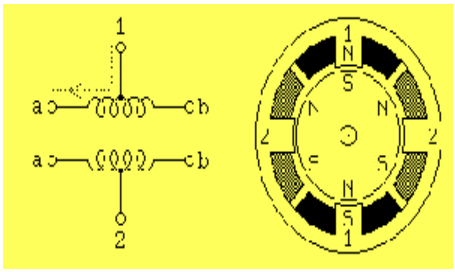

Figure 5. Unipolar stepper motor

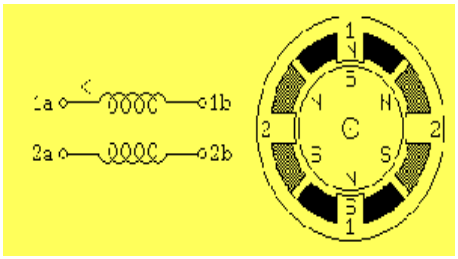

Figure 6. Bipolar stepper motor

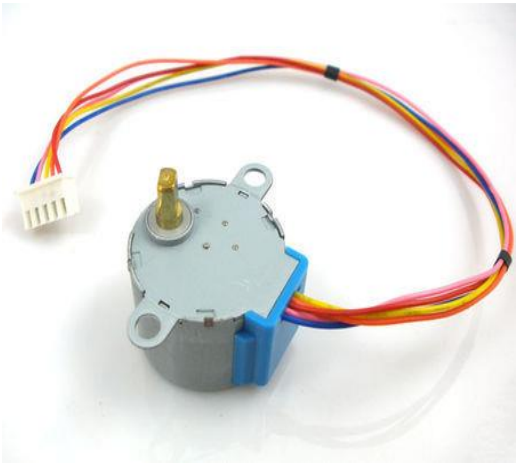

Figure 7. 28-BYJ48 stepper motor

Circuit Operation of System

The operation of window curtain driving system is very simple and easy to use. Completely assembled control circuit is illustrated as shown in Figure 8. The stepper motor, the remote transmitter, remote receiver, Arduino Uno is on the back of the printed circuit board, and battery package are ready to test the program control results.

Before, testing the circuit, the microcontroller in the Arduino Uno is required to upload the written program code. Therefore, a personal computer and the Arduino Uno are connected with a USB cable. Then upload the edited program code from pc by using Arduino IDE software. When uploading is done, it is ready to test. Therefore, the USB connection between the pc and Uno are disconnected. Then the batteries are installed with correct polarity in their housing, then connect the 2.1 mm dc jack with Arduino Uno power input.

The two LEDs on the board flash four times, as the program directed. It is used to indicate the power supply is properly installed and the program code in the microcontroller is initiated. At the moment, the stepper motor is in stop position.

Then the user command is ready to transmit from the remote transmitter unit. There are 4 keys on the remote and it is known as 4 keys remote control. The keys are labeled with A, B, C and D. In the program coding, the key A is used as manual left or manual open switch. The key B is used as manual right or manual close switch. The key C is used as open all switch. The key D is used as close all switch.

The test running started by pressing key A (manual open switch). As soon as the switch is pressed, the stepper motor starts rotating to the left. To observe clearly for rotation, a blue cable tight is attached on the rotor of stepper motor as pointer. The blue pointer rotation continues when the key A is kept pressing. Releasing the remote button stop the stepper motor rotation immediately.

Then test with another key input button B. In this case, the stepper motor rotates opposite direction, to the right, to close the window curtain. The rotation can be observed on the blue pointer on the rotor of stepper motor. The rotation continues, until the button is released. When the switch is released, the stepper motor stops at the point.

Therefore, the two upper buttons of the remote transmitter are used as manual open and manual close switch to operate the window curtain. The other two are also tested for their operations. When the switch button C is pressed, the motor rotates to the left. The rotation continues, although the button C is released from the remote control. In this case, the open limit switch and close limit switches are designed to attach on the left side and right side of window. To simulate these input limit switches, a wire is installed on the common pin of four green terminal pins beside the stepper motor connecting green terminals. The first two are the open limit switch input and the second two are close limit input.

Therefore, the other end of common wire is touched with the second green terminal to activate the open limit switch. Then the stepper motor stops rotation immediately. Similarly, the last key button D on the remote is pressed and made observations. In this case, the motor rotate to the right until the close limit switch is touched with common wire. Therefore, the window curtain movement control operation is successful for its driving functions in either manual open/close or open all/ close all operations.

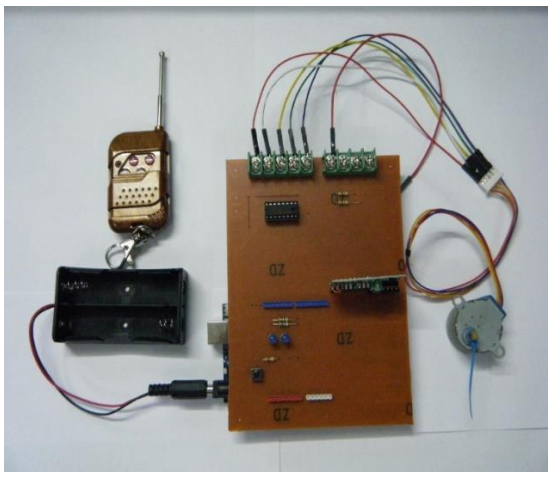

Figure 8. Completely assembled window curtain driving control circuit

Results and Discussion

Physical output result is provided for the operation of window curtain driving system. Before connecting the external power supply, the Arduino Uno board is connected with the pc via USB printer cable. It is used to upload the created program sketch into the memory ROM of ATmega328. After successfully uploaded the code, the USB cable is disconnected and battery unit is connected with the power terminal on the Arduino Uno board as shown in the Figure 9. Series connection of two lithium ion batteries are 7.4 V and it is the most suitable stable power supply for the Arduino development board. There are no other voltage regulator circuits in the construction design, since the Arduino Uno consists of built in two voltage regulator ICs, a 5 V regulator IC and a 3.3 V voltage regulator IC. The 3.3 V power supply output is used to support the voice module. But the other components utilized 5 V supply. When the power supply is connected, all the LEDs run once, showing the system power is initiated.

In this research work, the system looping was started by switch off for the stepper motor sequence and checks the input signal of four remote key functions alternately, until one of them are initiated. The window curtain motor driving in opening function is shown in Figure 10 and opening position and closing position of the window curtain are shown in Figures 11 and 12.

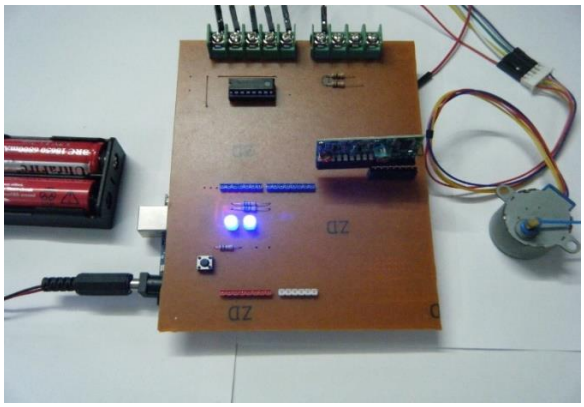

Figure 9. The two LEDs illuminate on power connection

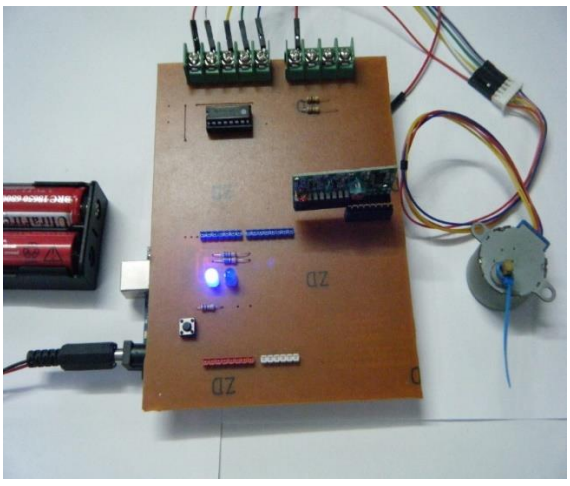

Figure 10. The window curtain motor driving in opening function

Figure 11. Opening position of the window curtain

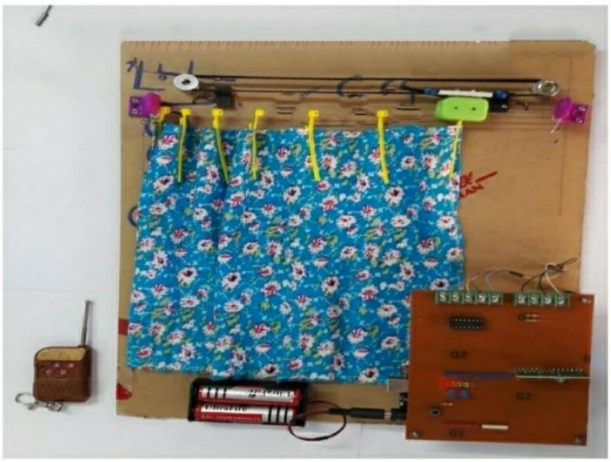

Figure 12. Closing position of the window curtain

Conclusion

The design of window curtain driving circuit is constructed. The program coding is created with Arduino IDE software and loaded into the memory of ATmega328. Various compilations are made to achieve successfully operating codes. The system can be operated with a distance between transmitter and receiver by using four keys remote control. The remote control can be used within about 8 feet.

Acknowledgement

We would like to express great indebtedness to Rector Dr Nay Win Oo, Pro Rectors Dr Aye Aye Ko, Dr Wah Wah Lwin and Dr Thida Aung, East Yangon University, for their encouragement to make present research paper. We wish to express my genuine thanks Professor Dr Naing Naing Oo, Head of Department of Physics, East Yangon University, for her kind permission to carry out this research. We would like to express thankful to Dr Su Su Aung, Professor of Physics Department, East Yangon University, for guidance with this research.

References

[1] Jeetender Singh Chauhan (2018), " International Journal of Engineering Research and Applications" (IJERA)
ISSN: 2248-9622

[2] Nick Dossis (3/2002), "Everyday Practical Electronics"(London: Wimborne Publishing)

[3] www.atmel.com/literature

[4] www.instructables.com/id/Beginner-Arduino

[5] www.wikipedia.org/wiki/Stepper-motor

COMPARATIVE STUDY OF THE SOLAR POWER UTILIZATION AND DEVELOPMENT, IN KHAYAN AND THANLYIN TOWNSHIPS

Ngu Wah Hlaing[1], Su Myat Mon[2], Lai Lai Htay[3], Thazin Phyo[4]

Abstract

The development level of a nation determines the energy consumption. Today, the technology of converting solar energy into direct electricity using photovoltaic system is developing. In this research, the two 50 W solar panels were used for average solar energy accepted at home system in Aye Ywa village of Khayan township and Phayar Kone village of Thanlyin township, Yangon division. Day to day solar radiation was collected from January to December in 2020 by deploying solar photovoltaic technology. In May, the highest solar irradiation was found 9.75 kWh/m^2/day in Khayan township and the lowest was 4.78 kWh/m^2/day in August. In Thanlyin township, the annual daily average solar radiation was found between 4.33 kWh/m^2/day and 8.94 kWh/m^2/day. According to the measurement results, it was found that average daily solar radiation intensity more than 5 kWh/m^2/day for two studied areas were perceived during the dry season. This study indicates that Aye Ywa village in Khayan township and Phayar Kone village in Thanlyin township were the best regions for developing solar photovoltaic system. In Khayan township, Aye Ywa village was more excellent than Phayar Kone village in Thanlyin township. It is also wanted to get the welfare the development and utilization of solar energy for people in these studied areas. If so the annual solar radiation on the earth's surface is tremendous, and then it is now one of the world's largest and cleanest energies that can be developed.

Keywords-photovoltaic system, photovoltaic technology, solar panel, utilization, cleanest energies

Introduction

Solar power come from the sun is energy. It converted into thermal or electrical energy. Solar energy is the cleanest and most abundant renewable energy source available, and the U.S. has some of the richest solar resources in the world. Solar energy is the energy obtained by capturing heat and light from the sun. Solar radiation has a potential to be converted into power, but due to dependence on weather conditions and seasonal change [1].This energy can be used in villages, detached houses, water pumping, and refuges. Human life is inseparable from the sun, and the vast majority of energy human need is directly or indirectly from the sun. The development and application of solar energy is mainly reflected in the following areas: solar water heaters, refrigeration and heating systems assisted by solar absorption, solar heating system, solar construction, passive solar houses, solar light, photovoltaic system [2]. Solar power is the resources of much energy, for example, the wind power, chemical energy, potential energy of water and other are all converted by the solar power. The solar power is the world's fastest growing energy source. Solar panel is reliable, affordable, easy to install and causes no pollution. The specific objective of in this research is to know the utilization development of solar energy in two selected areas. There are many ways to use solar power, and this research is about how to use solar power to produce electricity [3]

[1] Demonstrator, Department of Physics, East Yangon University
[2] Demonstrator, Department of Physics, East Yangon University
[3] Demonstrator, Department of Physics, East Yangon University
[4] Demonstrator, Department of Physics, East Yangon University

Materials and Methods

In this research, small-scale solar home system was used. The suitable areas such as Aye Ywa village of Khayan township and Phayar Kone village of Thanlyin township at Yangon region were selected to collect solar radiation from January to December in 2020. The solar radiation data collected area in Aye Ywa village of Khayan township and Phayar Kone village of Thanlyin township are given in Figures 1 and 2. The 50 W (3.178 ft^2 or 0.295 m^2) solar panels used for solar photovoltaic system I and II were fixed in Aye Ywa village of Khayan township and Phayar Kone village of Thanlyin township. Solar panel checker was used to check for output solar power received in a day for a month [4]. Nowadays, most PV systems are grid-connected and off-grid systems. PV panels are cells that convert sunlight into electricity; each cell contains layers of semi-conducting material [5]. The functional block diagram of the solar photovoltaic (PV) system is shown in Figure 3**.**

Figure 1. The solar radiation data collected Area in Aye Ywa village of Khayan township

Figure 2. The solar radiation data collected area in Phayar Kone village of Thanlyin township

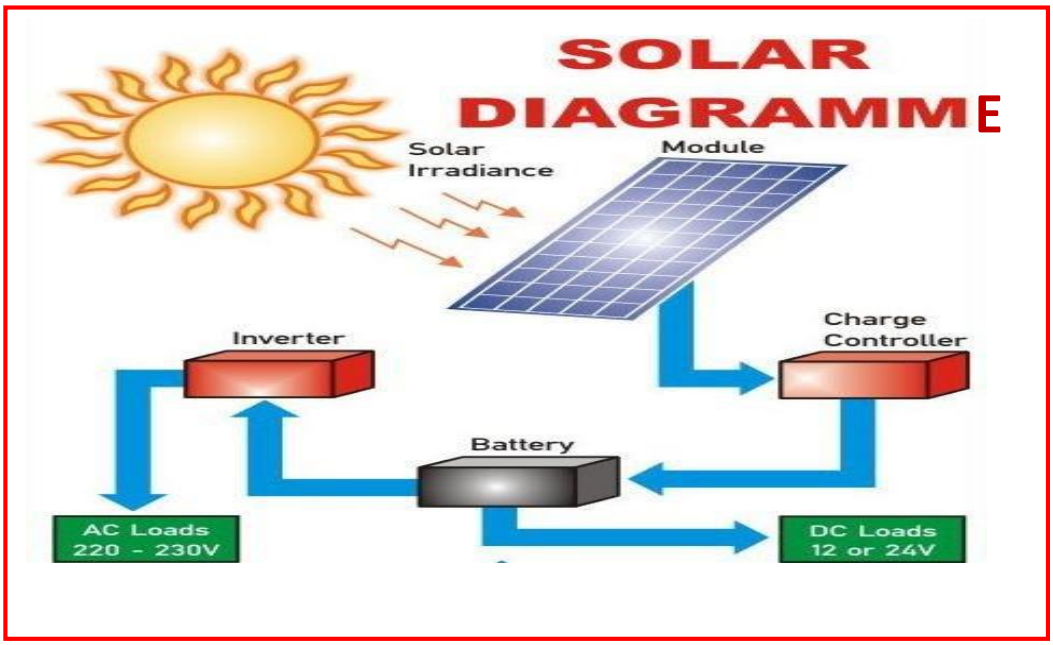

Figure 3. The functional block diagram of the solar photovoltaic (PV) system

When certain materials are exposed to light, they absorb photons and release free electrons. This phenomenon is called the photoelectric effect. When a solar cell is illuminated by sun-light, photons energy of the incident light is converted to direct current electricity through the process of photovoltaic effect of the solar cell.

Results and Discussion

The monthly average solar radiation data such as the total output power (P), the average solar energy (E_{av}) and the average solar energy per area per day (E/A) were calculated by mathematical method. The daily solar radiation value was obtained for every one hour and its summation for one day. The monthly average daily solar radiation records for the number of days in one month were calculated. The hourly solar output power from 50 W solar panel for Khayan township is given in Table 1. Figure 4 shows the solar power output data of hour-pairs at Khayan township. At 12 noon, when most of the sunlight hits the solar cell in Khayan township, the power output from the solar cell is up to 48 W. The hourly solar output power from 50 W solar panel for Thanlyin township is shown in Table 2. The solar output power recorded data with hour-pairs at Thanlyin township is illustrated in Figure 5. In Thanlyin township, when solar energy hits a solar cell at 12 noon, it can generate more than 45 W. In these results, the two regions studied had an average of eight hours of total sunlight per day was observed. Solar irradiation is the sun's radiant energies incident on a surface of unit area, expressed in units of kWh/m².

Table 1. The hourly Solar Output Power from 50 W Solar Panel for Khayan township

Hours	Jan	Feb	Mar	Apr	May	Jun	Jul	Aug	Sep	Oct	Nov	Dec
	Solar Output Power from 50W Solar Panel (W)											
6:00-7:00 AM	0	0	12	12	10	10	10	0	0	0	0	16
7:00-8:00 AM	20	24	20	22	20	26	14	14	13	22	16	20
8:00-9:00 AM	28	34	28	28	28	30	18	22	28	30	26	26
9:00-10:00 AM	35	40	34	34	40	32	24	32	35	36	32	30
10:00-11:00 AM	41	42	40	40	47	30	30	30	28	42	38	40
11:00-12:00 PM	45	44	46	46	48	18	36	36	29	48	44	44
12:00-1:00 PM	38	40	42	42	48	18	30	28	30	42	40	36
1:00-2:00 PM	34	32	34	34	40	20	24	24	23	34	34	31
2:00-3:00 PM	28	24	28	28	32	10	19	16	13	30	28	22
3:00-4:00 PM	20	15	14	18	20	0	0	0	0	18	20	14

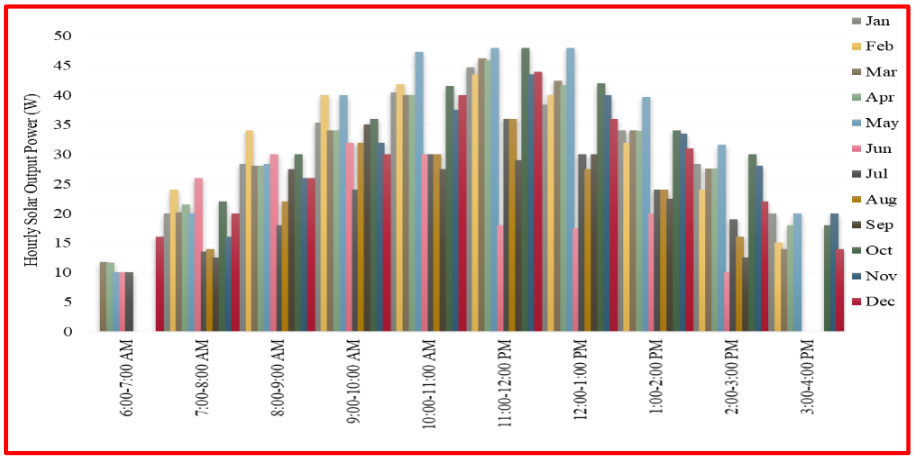

Figure 4. The solar output power recorded data with hour-pairs at Khayan township

Table 2. The hourly Solar Output Power from 50 W Solar Panel for Thanlyin township

Hours	Jan	Feb	Mar	Apr	May	Jun	Jul	Aug	Sep	Oct	Nov	Dec
	Solar Output Power from 50W Solar Panel (W)											
6:00-7:00 AM	0	0	0	0	0	0	0	0	0	10	12	10
7:00-8:00 AM	10	16	18	20	20	10	10	12	16	14	24	18
8:00-9:00 AM	14	22	28	28	30	35	18	20	20	20	30	24
9:00-10:00 AM	22	30	34	34	40	40	20	30	26	28	36	28
10:00-11:00 AM	30	38	41	39	45	45	28	32	42	41	40	32
11:00-12:00 PM	38	46	44	46	48	45	30	38	44	38	32	28
12:00-1:00 PM	34	42	38	42	49	25	36	27	34	36	24	22
1:00-2:00 PM	29	38	32	32	39	20	24	24	28	32	18	18
2:00-3:00 PM	22	28	24	26	30	20	18	14	10	26	14	13
3:00-4:00 PM	13	16	16	18	19	10	0	0	0	10	0	0

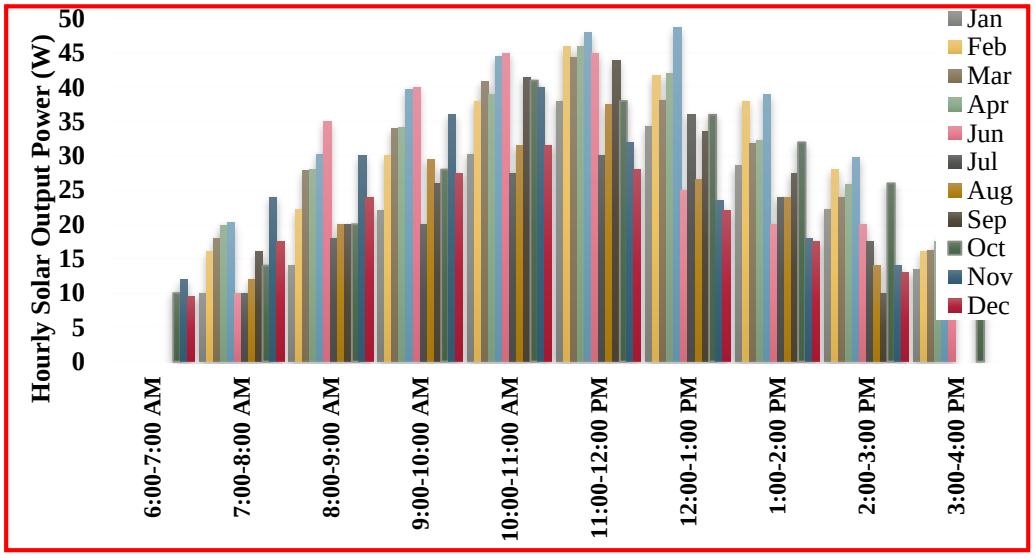

Figure 5. The solar output power recorded data with hour-pairs at Thanlyin township

Solar energy is equal to the average solar power multiplied by time (E_{av} = P t). The monthly average daily solar radiation records for the number of days in one month were calculated. Monthly average daily solar radiation results for Khayan township are given in Table 3. The daily variation of solar energy received in one day from Khayan township is shown in Figure 6. In Khayan township, the highest amount of average solar irradiation was 2.88 kWh in May and lowest of 1.41 kWh in August. Table 4 shown monthly average daily solar radiation results for Thanlyin township. The daily variation of solar energy received in one day from Thanlyin township is illustrated in Figure 7. The measurement result of average solar irradiation varies from 2.64 kWh in May to 1.28 kWh in July for Thanlyin township. The average solar energy per area per day (E/A) received on the system I and II (50 W solar panels) were calculated from the experimental recorded data of solar energy. Solar irradiation is the sun's radiant energy incident on a surface of unit area in one day, expressed in units of kWh/m²/day. Table 5 shown the monthly average solar energy received per area per day for Khayan township. The relation between the average solar energy received per area per day and months for Khayan township is given by Figure 8. In Khayan township, the highest amount of average solar irradiation was 9.75 kWh/m^2/day in May and lowest of 4.78 kWh/m^2/day in August. The monthly average solar energy received per area per day for Thanlyin township is shown in Table 6. The variation of the average solar energy received per area per day with months for Thanlyin township is illustrated by Figure 9. The measurement result of average solar irradiation varies from 4.33 kWh/m^2/day in July to 8.94 kWh/m^2/day in May for Thanlyin township.

The comparative results of solar energy received in one day for two studied areas are shown in Table 7 and Figure 10. According to all the results, the highest amount of solar energy received from Aye Ywa village of Khayan township in May was higher than Phayar Kone village of Thanlyin township. According to these findings, the amount of solar energy received from Khayan township was lowest in August and from Thanlyin township in July. The comparison results of solar energy received per area per day in two studied areas are given in Table 8 and Figure 11. Therefore, according to all solar radiation data, solar energy received per area per day was higher than 5 kWh/m^2 /day of the solar energy data. Myanmar Electric Power Enterprise (MEPE) experimental measurements indicate that irradiation

intensity of more than 5 kWh/m^2 was observed during the dry season. The example of the uses of home appliances for 50 W solar panel in Figure 12.

Table 3. Monthly average daily solar radiation results for Khayan township.

Months	Total solar power output in one day P (W)	Total sunshine hours in one day t (hrs)	Solar energy received in one day E_{av} (kWh)
January	290	8	2.32
February	294	8	2.43
March	298	9	2.57
April	302	9	2.61
May	332	9	2.88
June	194	8	1.55
July	205	8	1.53
August	202	7	1.41
September	197	8	1.57
October	302	8	2.42
November	277	8	2.21
December	279	9	2.37
Average	264	8	2.16

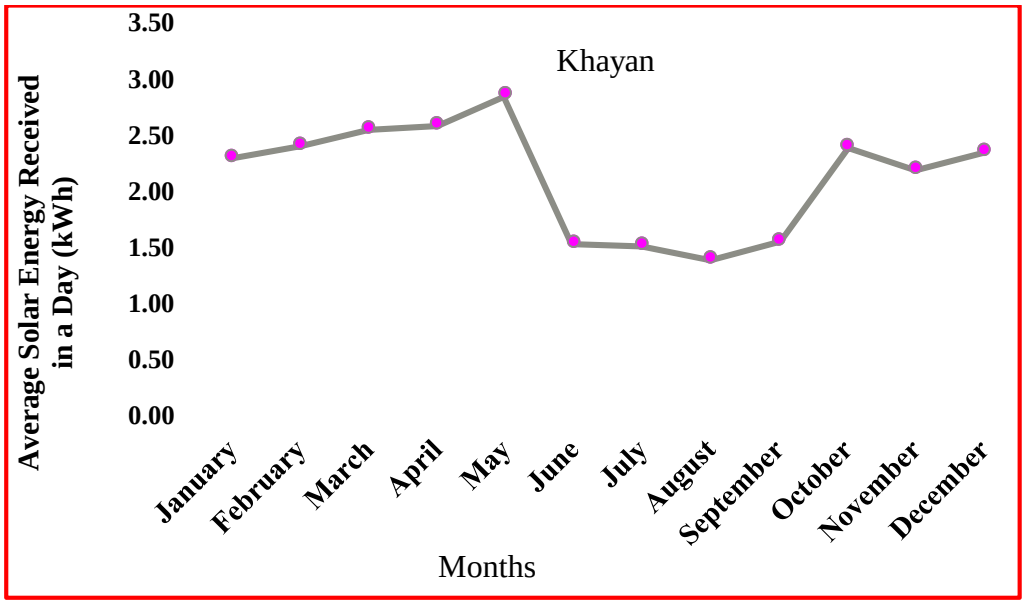

Figure 6. The daily variation of solar energy received in one day from Khayan township.

Table 4. Monthly average daily solar radiation results for Thanlyin township.

Months	Total solar power output in one day P (W)	Total sunshine hours in one day t (hrs)	Solar energy received in one day E_{av} (kWh)
January	213	8	1.60
February	276	8	2.21
March	275	8	2.20
April	285	8	2.35
May	320	8	2.64
June	250	8	2.00
July	183	7	1.28
August	195	7	1.36
September	219	8	1.64
October	255	9	2.16
November	230	8	1.84
December	191	8	1.53
Average	238	8	1.89

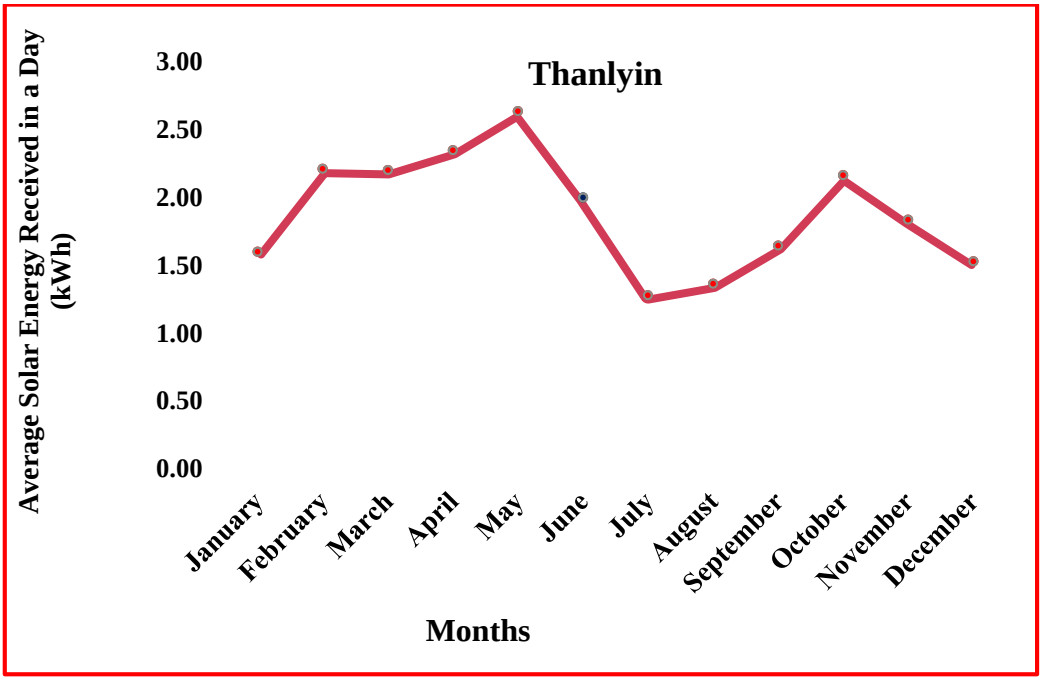

Figure 7. The daily variation of solar energy received in one day.

Table 5. The monthly average solar energy received per area per day for Khayan township.

Months	Solar Energy obtained in one day E_{av}(kWh)	The area of roof–mounted solar cell A (m^2)	Average Solar Energy Received per area per day E/A ($kWh/m^2/day$)
January	2.32	0.295	7.86
February	2.43	0.295	8.23
March	2.57	0.295	8.72
April	2.61	0.295	8.84
May	2.88	0.295	9.75
June	1.55	0.295	5.26
July	1.53	0.295	5.20
August	1.41	0.295	4.78
September	1.57	0.295	5.33
October	2.42	0.295	8.19
November	2.21	0.295	7.50
December	2.37	0.295	8.04
Average	2.16	0.295	7.31

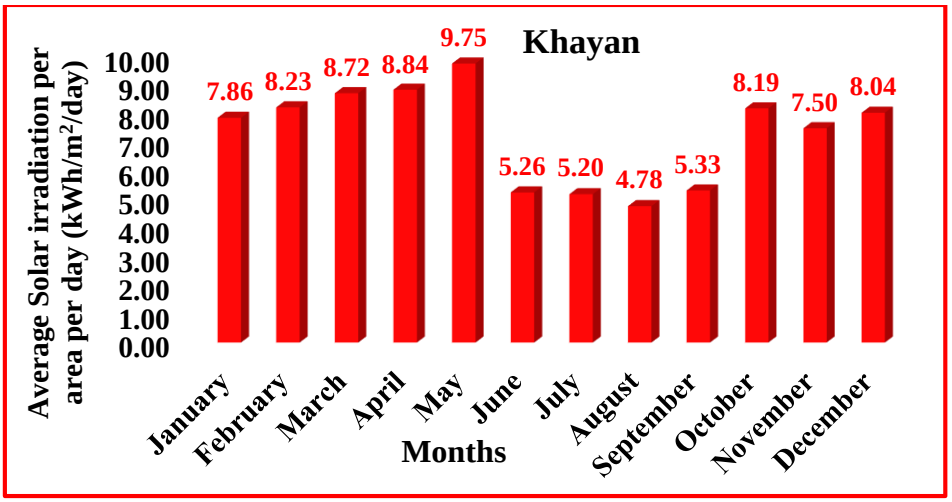

Figure 8. The relation between the average solar energy received per area per day and months for Khayan township.

Table 6. The monthly average solar energy received per area per day for Thanlyin township.

Months	Solar Energy obtained in one day E_{av}(kWh)	The area of roof–mounted solar cell A (m^2)	Average Solar Energy Received per area per day E/A (kWh/m^2/day)
January	1.60	0.295	5.42
February	2.21	0.295	7.49
March	2.20	0.295	7.46
April	2.35	0.295	7.96
May	2.64	0.295	8.94
June	2.00	0.295	6.78
July	1.28	0.295	4.33
August	1.36	0.295	4.62
September	1.64	0.295	5.57
October	2.16	0.295	7.33
November	1.84	0.295	6.22
December	1.53	0.295	5.18
Average	1.89	0.295	6.40

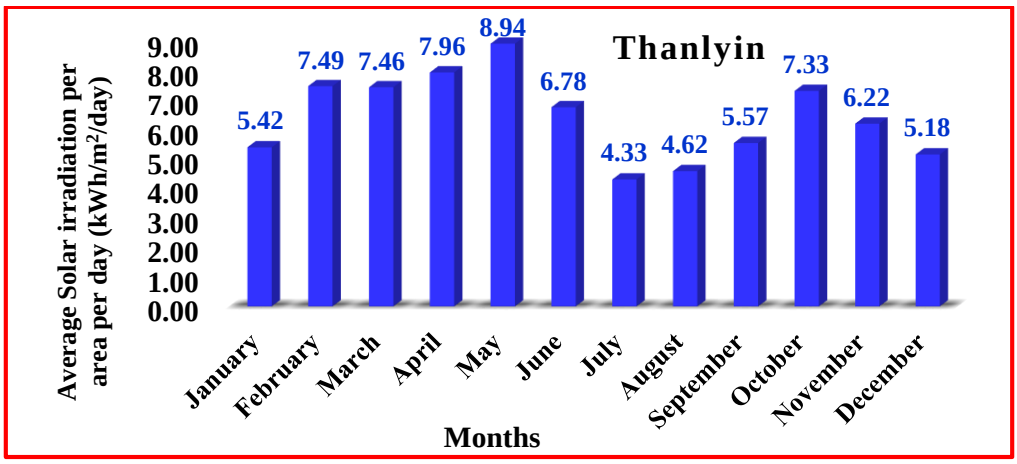

Figure 9. The relation between the average solar energy received per area per day and months for Thanlyin township

Table 7. The comparison results of solar energy received in one day for two studied areas.

Months	Solar Energy received in one day E_{av}(kWh)	
	Thanlyin	Khayan
January	1.60	2.32
February	2.21	2.43
March	2.20	2.57
April	2.35	2.61
May	2.64	2.88
June	2.00	1.55
July	1.28	1.53
August	1.36	1.41
September	1.64	1.57
October	2.16	2.42
November	1.84	2.21
December	1.53	2.37
Average	1.90	2.15

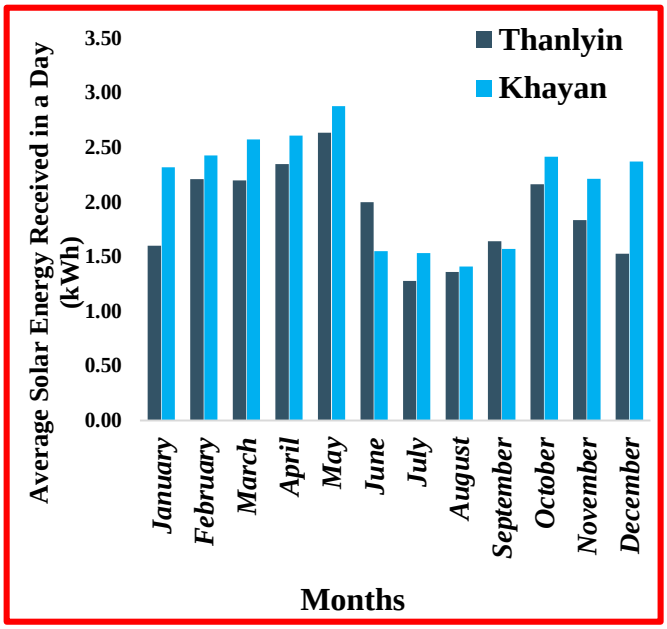

Figure 10. The comparison results of solar energy received area per day in two studied areas.

Table 8. The comparison results of solar energy received per area per day in two studied areas.

Months	Average Solar Energy Received per area per day E/A (kWh/m^2/day)	
	Thanlyin	Khayan
January	4.14	7.86
February	7.49	8.23
March	7.46	8.72
April	7.96	8.84
May	8.94	9.75
June	6.78	5.26
July	4.33	5.20
August	4.62	4.78
September	6.31	5.33
October	7.33	8.19
November	6.22	7.50
December	5.18	8.04
Average	6.44	7.28

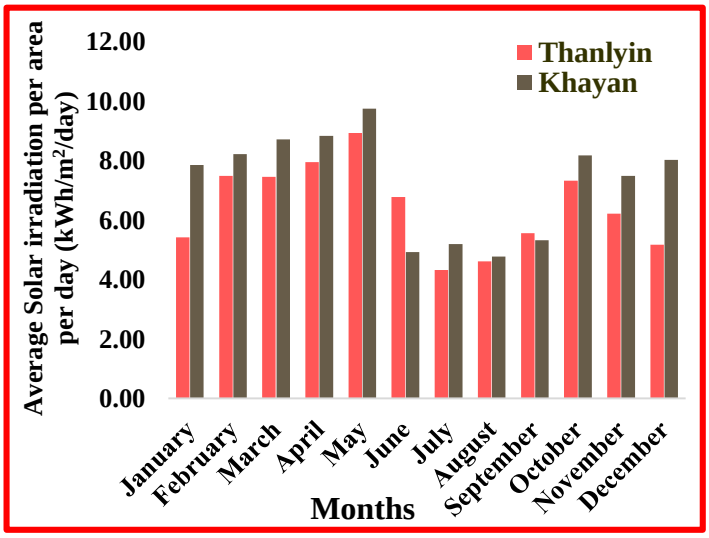

Figure 11. The comparison results of solar energy received area per day in two studied areas

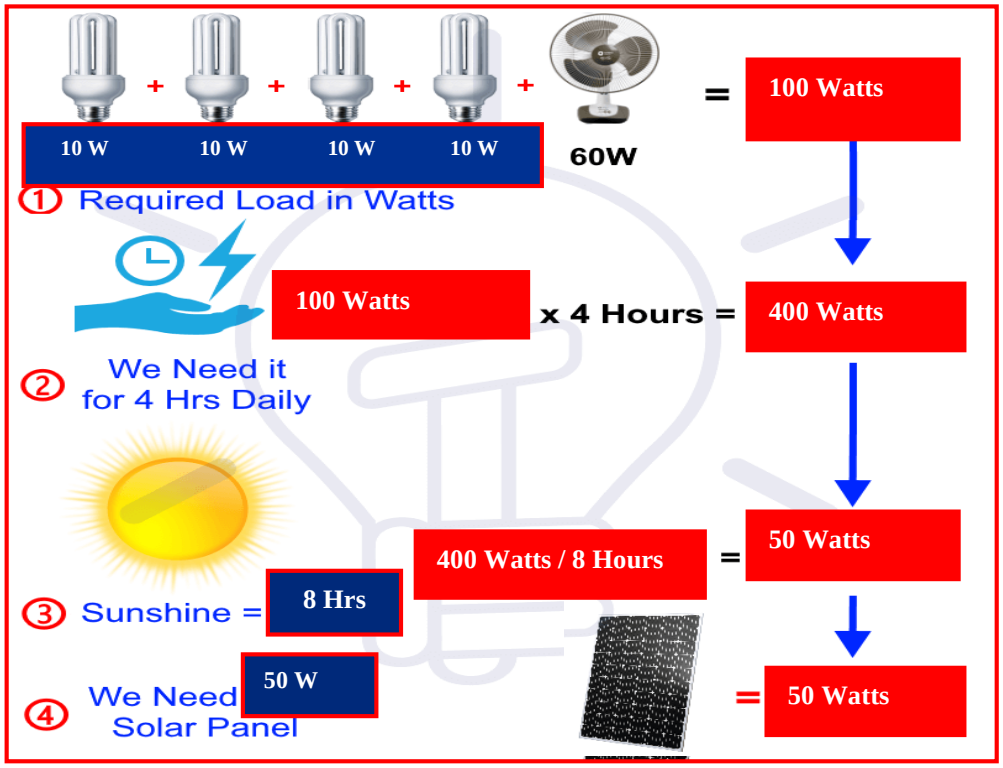

Figure 12. Example of uses of home appliances for 50 W solar panel

Conclusion

In this research journal, the solar photovoltaic system could be estimated the average solar irradiation rate received per day. These studied areas have the average received about 8 hours of sunshine per day. In all measurement records, it was found that the monthly average daily solar radiation results of Aye Ywa village in Khayan township were more than that of Phayar Kone village in Thanlyin township. Therefore, according to most of results, Aye Ywa village in Khayan township was the best regions for solar photovoltaic system because the average daily solar radiation intensity was more than 5 kWh/m^2/day for these studied areas. In this work, solar 50 W off-grid solar system was used for lighting, mobile charging and battery charging for studied areas.

The amount of electricity generated from solar energy depends upon the available sunlight. With the development of society and the solar photovoltaic technology, solar photovoltaic power generation involves many aspects. Energy consumption is one of the indices in determining the levels of development of a nation. Myanmar is a land of plentiful sunshine. If so the annual solar radiation on the earth's surface is enormous, and then it is now one of the world's largest and cleanest energies that can be developed. Solar Panels are one of the best options for renewable energy. This data obtained in this study may be useful to produce electricity from solar photovoltaic system of the study area.

Acknowledgements

We would like to express thanks to our Rector Dr Nay Win Oo and Pro-Rectors Dr Aye Aye Ko, Dr Wah Wah Lwin and Dr Thida Aung, East Yangon University for their valuables permission to do this research. And then, we also special thanks to Professor Dr Naing Naing Oo, Head of Department of Physics, East Yangon University for her kindly supporting and encouraging to carry out this research. Finally, we actually wish to thanks Professor Dr Su Su Aung, Department of Physics, East Yangon University for her very interested guidelines and warmly helpfulness to make this research.

References

[1] Abedelhak Ben Jemaa et.al., (2013) "Estimation of Global Solar Radiation Using Three Simple Methods", University of Reims Champagne-Ardenne, Energy Procedia 42, PP 406 – 415.

[2] Basic Research Needs for Solar Energy Utilization, (2005) "Report of the Basic Energy Sciences Workshop on Solar Energy Utilization".

[3] Henry A., (2013) "Improving the Efficiency of Solar Photovoltaic Power System", University of Rhode Island. Li Xie, Suyao Liu, (2013) "Investigation of Solar Energy Utilization in China", University of Gävle.

[4] Ms. Ei Ei Thar, (2018) "Studying on Average Hourly and Monthly Solar Radiation at Myintkyina in Myanmar", International Journal of Science, Engineering and Technology Research (IJSETR), Volume 7, Issue 12, ISSN 2278-7798.

[5] R. R. King, (2009) "24th European Photovoltaic Solar Energy Conference", Hamburg, Germany, 21-25. Thet Thet Han Yee, Su Su Win, and Nyein Nyein Soe, (2008) "Solar Energy Potential and Applications in Myanmar", World Academy of Science, Engineering and Technology.

GEODETIC NUMBER OF A CONNECTED GRAPH HAVING THE UNIQUE DIAMETRAL PATH

Kyaw Lin Aung[1], Nilar Myo Thwin[2], Su Myat Noe[3]

Abstract

The aim of this paper is to find the geodetic number $g(G)$ of a connected graph G having the unique diametral path of length d. As an introduction, the basic definitions and notations of the graph theory are stated. The concepts of $g(G)$ of G and some properties of $g(G)$ are studied. The connected graph G with the unique diametral path plays a major role in this paper. Based on induced subgraphs of G are isomorphic to paths P_3, it is extended to subgraphs of G which are isomorphic to paths P_m ($3 \leq m < d$), and the bounds of $g(G)$ of G are investigated. Finally, the algorithm for finding the bounds of $g(G)$ of G having the unique diametral path is proposed.

Keywords: geodetic cover, geodetic basis, geodetic number, extreme vertex, diametral path

1. Introduction

Geodetic covering problems are widely researched topic in graph theory. One such problem is geodetic problem introduced by Frank Harary who was widely recognized as one of the 'fathers' of modern graph theory. There are many applications research to geodetic sets for urban street network and communication network designs. In this paper, we try to extend the upper bound of geodetic number in the result of [4] and [1].

Throughout this paper, the concepts of the terminologies and notations of the graph theory are based on [2, 3] .A *graph* G is an ordered triple ($V(G)$, $E(G)$, ψ_G) consisting of a nonempty set $V(G)$ of *vertices*, a set $E(G)$, disjoint from $V(G)$, of *edges*, and an *incidence function* ψ_G that associates with each edge of G an unordered pair of (not necessarily distinct) vertices of G. If e is an edge and u and v are vertices such that $\psi_G(e) = uv$, then e is said to *join* u and v; the vertices u and v are called the *ends* of e. If $\psi_G(e) = uv$ and $u = v$, then e is called a *loop*, otherwise e is a *link*. We write $e = uv$ and say u and v are *adjacent* vertices. A *walk* in a graph G is a finite non-null sequence $W = v_0e_1v_1e_2v_2 \ldots e_kv_k$, whose terms are alternatively vertices and edges, such that, for $1 \leq i \leq k$, the ends of e_i are v_{i-1} and v_i. We say that W is a *walk* from v_0 to v_k, or a v_0v_k-*walk*. The vertices v_0 and v_k are called the *origin* and *terminus* of W, respectively, and $v_1, v_2, \ldots, v_{k-1}$ its *internal vertices*. The integer k is the *length* of W. If the edges $e_1, e_2, \ldots, e_k$ of a walk W are distinct, W is called a *trail*. A v_0v_k-walk is said to be *closed* if $v_0 = v_k$. A closed v_0v_k-trail whose origin and internal vertices are distinct is said to be a *cycle* C_k if $k \geq 3$ and $v_0e_1v_1e_2v_2 \ldots e_{k-1}v_{k-1}$, where $v_0, v_1, \ldots, v_k$ are distinct, is a v_0v_k *-path*. If there is a uv-path in G for any two distinct vertices u and v of G, then G is said to be *connected*; otherwise G is *disconnected*. The *distance* between two vertices u and v in G, denoted by $d_G(u,v)$, is the length of a shortest uv-path in G, if there is no path connecting u and v, we define $d_G(u,v)$ to be infinite. A shortest uv-path is called a *uv-geodesic*. The *eccentricity* of v, denoted by $e(v)$, is the distance to a vertex farthest from v. Thus $e(v) = max\{d_G(u,v): u \in V(G)\}$. If $e(v) = d_G(u,v)$, then u is called an *eccentric vertex* of v and the shortest uv-path is called the *eccentric path* of v. The *radius* $r(G)$ of G is the minimum eccentricity of vertices in G, whereas the *diameter* $d(G)$ of G is the maximum eccentricity. A vertex v in G is a *peripheral vertex* if $e(v) = d(G)$, and the *periphery* of G is the set of all

[1] Dr., Lecturer, Department of Mathematics, East Yangon University,

[2] Associate Professor, Department of Mathematics, East Yangon University,

[3] Tutor, Department of Mathematics, East Yangon University.

peripheral vertices. A *diametral path* in G is a geodesic of length $d(G)$ joining two peripheral vertices u and v. Hence, a diametral path is a path of length $d(G)$ that is an eccentric path for its end vertices. A graph is called a *simple* graph if it has no loop and no two of its links join the same pair of vertices. A graph H is a *subgraph* of a graph G if the vertex set of H is a subset of the vertex set of G and the edge set of H is a subset of the edge set of G. The order of the vertex set V is the number of vertices in V and denoted by $|V|$. Suppose that V' is a nonempty subset of V. The subgraph of G whose vertex set is V' and whose edge set is the set of those edges of G that have both ends in V' is called the subgraph of G *induced* by V' and is denoted by $G[V']$; we say that $G[V']$ is an *induced subgraph* of G. The *degree* $d(v)$ of a vertex v in G is the number of edges which are incident with v, where every loop is counted twice. A vertex of degree one is called a *pendant vertex* or *end vertex* or *leaf*. A *cut vertex* of a graph G is a vertex whose removal increases the number of components of G. A vertex of a graph G is called an *extreme vertex* if the subgraph of G induced by the set of its adjacent vertices is complete.

We refer to the letter G to denote a simple graph in our paper. Moreover, one graph is under discussion we usually denote that graph by G.

2. Geodetic Number of a Connected Graph

In this section, we study on the geodetic number of a connected graph G [4] and state some properties of the geodetic numbers of G.

2.1 Definition. Let G be a finite connected simple graph. A *geodetic cover* of G is a set $S \subseteq V$ such that every vertex of G is contained in a geodesic joining some pair of vertices in S. The *geodetic number* $g(G)$ of G is the minimum order of its geodetic covers, and any geodetic cover of order $g(G)$ is a *geodetic basis*.

2.2 Remark. For any connected graph G with n vertices, it is obvious that $2 \leq g(G) \leq n$.

2.3 Example. For the graph G in Figure 1, the geodetic number $g(G)$ is stated below.

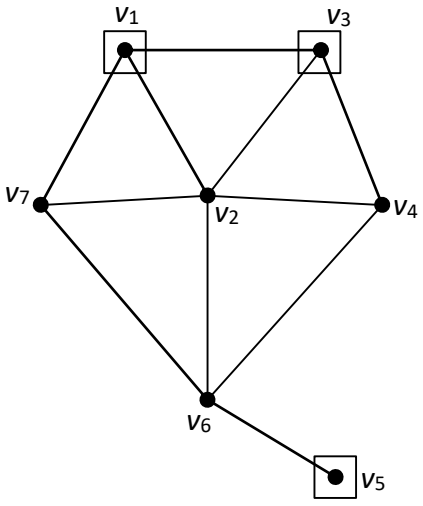

Figure 1. A graph G with $g(G) = 3$.

Any vertex set S containing two vertices from $\{v_1, v_2, v_3, v_4, v_5, v_6, v_7\}$ is not a geodetic cover. Thus, $g(G) \geq 3$.

Consider $S = \{v_1, v_3, v_5\}$. It can be checked that S is a geodetic cover of G. Thus $g(G) \leq 3$ and hence $g(G) = 3$.

2.4 Theorem. [4] For any connected graph G, every extreme vertex of it belongs to the geodetic basis of it. In particular, every pendant vertex of G belongs to the geodetic basis of it.

2.5 Corollary. If a connected graph G with n vertices contains r extreme vertices, then $g(G) \geq max\{2, r\}$.

2.6 Theorem. [4] For any connected graph G, no cut vertex of it belongs to the geodetic basis of it. If the graph G has n vertices and q cut vertices, then the geodetic number of it is $max\{2, r\} \leq g(G) \leq n - q$.

Proof. Let G be a connected graph, x be a cut vertex of G and $W \subseteq V$ be a geodetic basis of G. Suppose that $x \in W$. Since x is a cut vertex, $G - x$ is disconnected and suppose that $G - x$

consists of k components $C_1, C_2, C_3, \ldots, C_k$ where $k \geq 2$. Obviously W contains at least one vertex y_i of each component C_i, $i = 1, 2, \ldots, k$. Otherwise, W will not be a geodetic cover of G.

Consider the set $W \setminus \{x\}$ and any vertex $u \in V$. Then u is on a shortest vw-path in G where $v, w \in W$. If $v \neq x$ and $w \neq x$, then u lies on a shortest vw-path where $v, w \in W \setminus \{x\}$.

Suppose $v = x$ and $w = y_i$ where $y_i \in C_i$. Then u is on a shortest xy_i-path, say P. Consider the vertex y_j of C_j where $j \neq i$. Let Q be a shortest y_jx-path.

Then the union of P and Q is a shortest y_iy_j-path say R, both x and u lie on R. It follows from these discussions that $W \setminus \{x\}$ is a geodetic cover of G. This contradicts to the hypothesis that W is a geodetic basis of G.

So $x \notin W$.

It follow that $g(G) \leq n - q$.

2.7 Theorem. The geodetic number of a path is 2.

Proof. Every path P_n with n vertices has two extreme vertices and $(n - 2)$ cut vertices.

By Corollary 2.5 and Theorem 2.6,

$max\ \{2, 2\} \leq g\ (P_n) \leq n - (n - 2)$

$2 \leq g\ (P_n) \leq 2$

Hence, $g\ (P_n) = 2$.

3. Bounds of the Geodetic Number of a Connected Graph Having the Unique Diamentral Path

In this section, the extension to the upper bound of the geodetic number of a connected graph with the unique diamentral path are discussed in Theorem 3.2 and Theorem 3.3.

The following theorem is the result of G. Chartrand, F. Harary and P. Zhang [4] which states the upper bound of the geodetic number of a connected graph in terms of its diameter.

3.1 Theorem. [4] If G is a graph of order n and diameter d, then $g(G) \leq n - (d - 1)$.

By adding some conditions to Theorem 3.1, S. Bermudo, J. A. R. Velazquez, J. M. Sigarreta and I. G. Yero [1] obtained the more better bound of the geodetic number of a connected graph, shown in the following theorem.

3.2 Theorem. [1] Let G be a graph of order n and diameter d, and let A be the set of all vertices on the unique diametral path. If $V \setminus A$ contains subsets S_i, $i \in \{1, 2, \ldots, k\}$, such that $S_i \cap S_j = \emptyset$, $i \neq j$, and the induced subgraphs $[S_i]$ are isomorphic to P_3, then $g(G) \leq n - (d - 1) - k$.

We consider the path $P_m (m \geq 3)$ instead of P_3 in Theorem 3.2. Thus we get the upper bound of the geodetic number of a connected graph. By combining this result with Corollary 2.5, we get the bound of the geodetic number of a connected graph, it is shown in the following theorem.

3.3 Theorem. Let G be a graph of order n, r extreme vertices and has the unique diametral path P of length d (see Figure 2). Let A be the set of all vertices on P. If $V \setminus A$ contains subsets S_i, $i \in \{1, 2, \ldots, k\}$, such that $S_i \cap S_j = \emptyset$, $i \neq j$, and the induced subgraphs $[S_i]$ are isomorphic to some path $P_m (3 \leq m < d)$ and p_m is the number of path P_m, then

$$max\ \{2, r\} \leq g(G) \leq n - (d - 1) - \sum_{3 \leq m < d} (m - 2)\, p_m.$$

Proof. Suppose that

(a) G be a connected graph of order n, r extreme vertices and diameteral path P of length d,

(b) $A = \{u_0, u_1, \ldots, u_d\}$ where $u_0, u_1, \ldots, u_d$ lie on the path P of G,

(c) For $i \in \{1, 2, \ldots, k\}$ the induced subgraphs $[S_i]$ are isomorphic to some paths

P_m $(3 \leq m < d)$ and p_m is the number of the paths P_m, $\sum p_m = k$ and $S_i \cap S_j = \emptyset$, $i \neq j$.
Then by Theorem 2.7, $\{v_1^i, v_m^i\}$ is a geodetic basis of each $v_1^i v_m^i$-path.
Let $S = V \setminus \{ v_2^1, ..., v_{m-1}^1, v_2^2, ..., v_{m-1}^2 ..., v_2^k, ..., v_{m-1}^k, u_1, u_2, \ldots, u_{d-1}\}$.
Then it is clear that S is a geodetic cover (see Figure 2), and

$$g(G) \leq n - (d-1). \qquad (1)$$

Again by Corollary 2.5,

$$g(G) \geq \max\{2, r\}. \qquad (2)$$

From (1) and (2), we get $max\{2, r\} \leq g(G) \leq n - (d-1) - \sum_{3 \leq m < d} (m-2) p_m$. ■

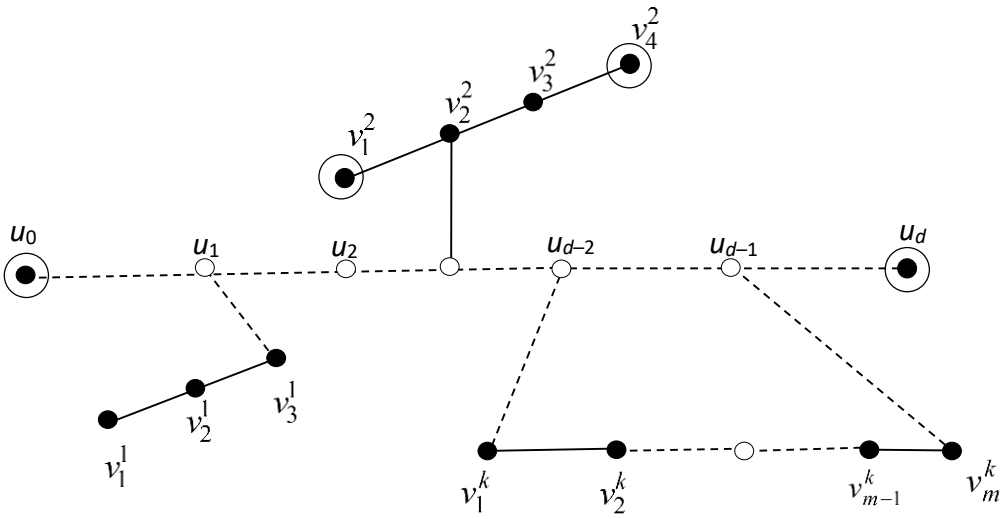

Figure 2. A Graph G with $S = V \setminus \{ v_2^1, ..., v_{m-1}^1, v_2^2, ..., v_{m-1}^2 ..., v_2^k, ..., v_{m-1}^k, u_1, u_2, \ldots, u_{d-1}\}$

3.4 Example. Consider the graph G of order 36 shown in Figure 3.

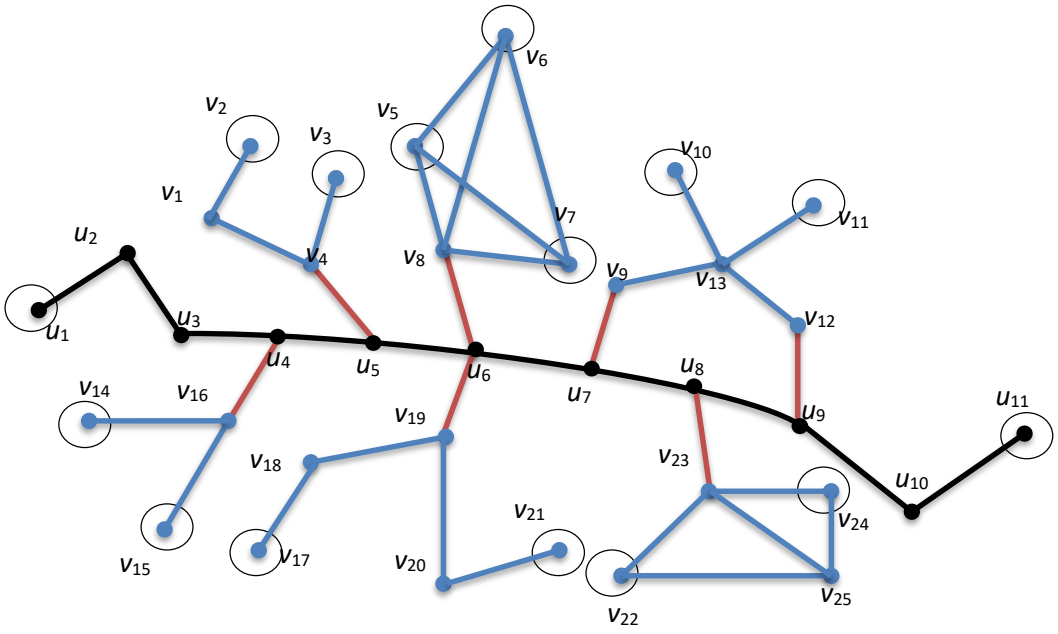

Figure 3. A Graph G with $n = 36$, $r = 15$, $d = 10$

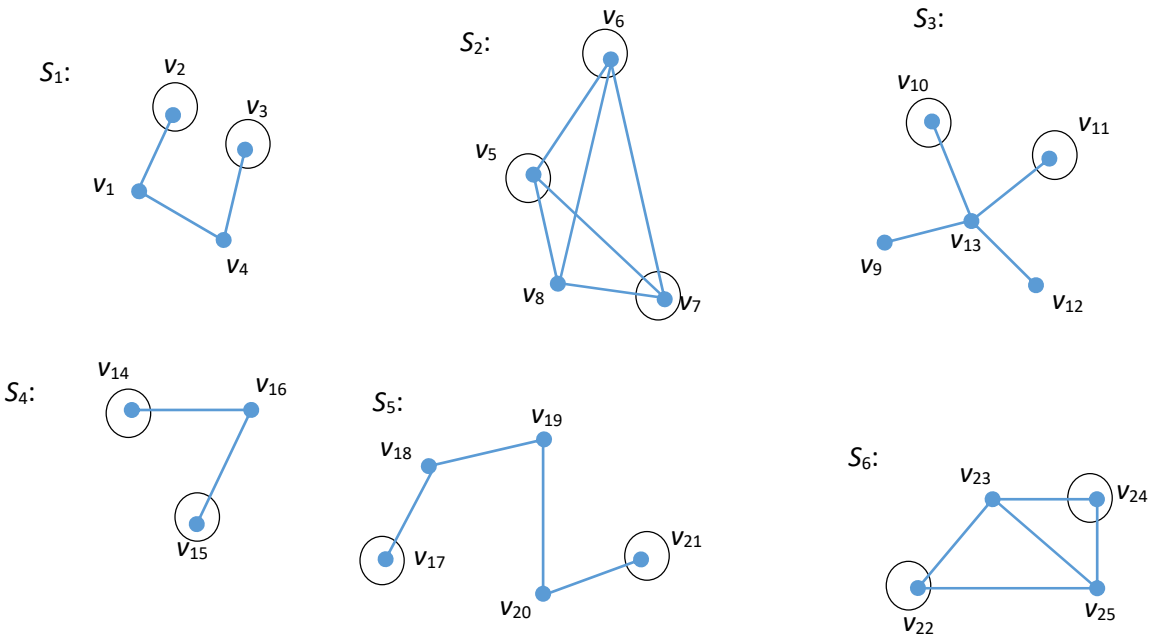

Figure 4. $V \setminus A$ **where** $A = \{u_1, u_2, ..., u_{11}\}$

The graph G contains 15 extreme vertices and has a unique diametral path of length 10. The vertices $u_1, u_2, u_3, ..., u_{10}, u_{11}$ lie on the diametral path (i.e., u_1u_{11}- path) of G.

If $A = \{u_1, u_2, ..., u_{11}\}$, we get six components S_i $(i = 1, 2, \ldots, 6)$ in $V \setminus A$ where $S_1 \cong P_4$, $S_4 \cong P_3$, $S_5 \cong P_5$, S_2, S_3 and S_6 are isomorphic to no path (see Figure 4).

From Figure 3 and Figure 4, we get $n = 36$, $r = 15$, $d = 10$ and $p_3 = p_4 = p_5 = 1$.

By Theorem 3.3,

$$max\ \{2, r\} \leq g(G) \leq n - (d-1) - \sum_{3 \leq m < d} (m-2)p_m$$

$$max\ \{2, 15\} \leq g(G) \leq 36 - (10-1) - [(3-2)\,p_3 + (4-2)\,p_4 + (5-2)\,p_5]$$

$$max\ \{2, 15\} \leq g(G) \leq 21$$

Now we find $g(G)$ practically.

Let $S = \{u_1, u_{11}, v_2, v_3, v_5, v_6, v_7, v_{10}, v_{11}, v_{14}, v_{15}, v_{17}, v_{21}, v_{22}, v_{24}\}$(See Figure 3).

It can be checked that S is a geodetic basis of G. Thus, $g(G) = 15$.

4. Proposed Algorithm

In this section, the proposed algorithm for finding the bound of the geodetic number of a connected graph having the unique diametral path is discussed.

4.1 Definition. The matrix associated with a graph G is the *adjacency matrix*; this is the $v \times v$ matrix $\boldsymbol{A}(G) = [\ a_{ij}\ ]$, in which a_{ij} is the number of edges joining v_i and v_j.

4.2 Remark.

(1) The graph are commonly stored in computers like in the form of *adjacency matrix*.

(2) The graph can be drawn from the adjacency matrix by using some computer software.

4.3 Example. For the graph G in Figure 1, the adjacency matrix of G is shown in Table 1. The graph G can be stored in computer in the form $\boldsymbol{A}(G)$.

Table 1. $A(G)$

	v_1	v_2	v_3	v_4	v_5	v_6	v_7
v_1	0	1	1	0	0	0	1
v_2	1	0	1	1	0	1	1
v_3	1	1	0	1	0	0	0
v_4	0	1	1	0	0	1	0
v_5	0	0	0	0	0	1	0
v_6	0	1	0	1	1	0	1
v_7	1	1	0	0	0	1	0

4.4 Example. Consider the graph G in Figure 1, we will find the eccentricity of each vertex in G, the diametral path of G and the extreme vertex of G.

The distance between every two vertices of G (see Table 2) can be obtained from Figure 1 of G or from Table 1 of the adjacency matrix $\boldsymbol{A}(G)$. The eccentricities of all vertices of G are $e(v_i) = 2$, $i = 2, 4, 6, 7$ and $e(v_i) = 3$, $i = 1, 3, 5$.

Table 2. The distance between two vertices v_i and v_j of G

	v_1	v_2	v_3	v_4	v_5	v_6	v_7
v_1	0	1	1	2	3	2	1
v_2	1	0	1	1	2	1	1
v_3	1	1	0	1	3	2	2
v_4	2	1	1	0	2	1	2
v_5	3	2	3	2	0	1	2
v_6	2	1	2	1	1	0	1
v_7	1	1	2	2	2	1	0

From the eccentricities of the vertices, it can be seen that G has four diametral paths of length 3. These paths are P_1: $v_1\ v_2\ v_6\ v_5$, P_2: $v_1\ v_7\ v_6\ v_5$, P_3: $v_3\ v_2\ v_6\ v_5$ and P_4: $v_3\ v_4\ v_6\ v_5$. There is only one extreme vertex v_5 in G.

4.5 Proposed Algorithm for Theorem 3.3. For the graph G with the given vertices,

(1) Let n = the number of given vertices.
(2) Draw the adjacency matrix of G, $\boldsymbol{A}(G)$.
(3) By using $\boldsymbol{A}(G)$, draw the table which states the distance between any two vertices of G.
(4) From the table, find the eccentricity of each vertex of G. Find the diametral paths of G.
(5) If G has the unique diametral path then the path: $u_0\ u_1\ u_2\ ....\ u_d$ and d = the length of the path. Else stop.
(6) Remove all vertices on the unique diametral path: $u_0\ u_1\ u_2\ ...\ u_d$ and count the number of path P_m for $3 \le m < d$. Let p_m = the number of path P_m.
(7) Find the extreme vertex of G and count the number of extreme vertices. Let r = the number of extreme vertices.
(8) Use the formula $max\ \{2, r\} \le g(G) \le n - (d - 1) - \sum_{3 \le m < d} (m-2)p_m$.

4.6 Remark. (1) We can apply the proposed algorithm 4.5 only for the graph which has the unique diametral path.

(2) In practical, it is difficult to draw the adjacency matrix and the table which states the distances between vertices of the graph when G has many vertices (see the graph G in Figure 3). It takes so many long time and too spaces in paper. If the matrix and the table can be drawn in computer by using computer software, it will be more efficient.

4.7 Example. By using the proposed algorithm 4.5, we find the geodetic number $g(G)$ of G in Figure 1 as follows:

(1) $n = 6$

(2) $A(G)$ of G can be seen in Figure 5.

(3) By using $A(G)$, the table in Figure 6 can be drawn.

(4) From the table, we get the eccentricities of vertices; $e(v_i) = 2$, i = 2, 4, 6, 7 and $e(v_i) = 3$, $i = 1, 3, 5$.We also get the four diametral paths of length 3.

(5) Since G has four diametral paths, stop.

Thus, we could not find the geodetic number $g(G)$ of G in Figure 1 by using the proposed algorithm 4.5.

Conclusion

In this paper, the concepts of the geodetic number $g(G)$ of a connected graph G and some properties of $g(G)$ of G are studied. For the graph G with the unique diametral path of length d and induced subgraphs of G isomorphic to the path P_m ($3 \leq m <$ d), the bounds of $g(G)$ are also discussed. Moreover, the algorithm for finding the bound of $g(G)$ of G having the unique diametral path is proposed. With the aid of program, it may be more easy and efficient for finding the bound of $g(G)$ of G having the unique diametral path although G contains so many vertices.

Acknowledgements

We would like to express our deepest gratitude to Dr. Nay Win Oo, Rector of East Yangon University and Dr. Aye Aye Ko, Dr. Wah Wah Lwin and Dr. Thida Aung, Pro-Rectors of East Yangon University for their kind consent to the preparation and submission of this paper. We would also like to express our gratitude to Professor and Head Dr. Sandar Maw, and Professor Dr. Phyu Phyu Aung of Department of Mathematics, East Yangon University, for their encouragement and interest to this paper.

References

[1] Bermudo, S., J. A. R. Velazquez, J. M. Sigarreta and I. G. Yero, "On geodetic and *k*-geodetic sets in graphs", *ARS Combinatoria* 96(2010), pp. 469-478.

[2] Bondy, J. A. & U.S.R. Murty, (1982) *Graph Theory with Applications*, Fifth Printing, American Elsevier, New York.

[3] Buckley, F. & F. Harary, (1990) *Distance in Graphs*, Addison Wesley, New York.

[4] Chartrand, G., F.Harary and P. Zhang, "On the geodetic number of a graph", *Networks* **39** (2002), pp.1-6.

A STUDY ON THE VALUATIONS OF DEEPLY RAMIFIED ON A FIELD

Zaw Myo Thant[1]

Abstract

In this paper, surveys the absolute values and valuations of deeply ramified on a field. The basic definitions and some results about absolute values, valuations of field are studied. These notions give two basic examples: the trivial absolute values and the set of rational number Qp with the p- adic absolute values. Then, the equivalence conditions for a field to be an absolute values and valuations are discussed. Next, the definitions of artin constant, non - archimedean and archimedean and their related results are studied with examples and lemmas. I also focus on the differences between absolute values and valuations base on a field. The notion of a valuation of a field arises when one attempts to assign magnitudes to the elements of a field. The classical case is that of the absolute value in the field of real numbers and in the field of rational numbers.

Keywords: field, absolute values, valuations, equivalence.

Introduction

The basic definitions of absolute values and valuations with examples base on a field are introduced. Then, the equivalence of absolute values and some results about of absolute values are discussed. Next, the equivalence of valuations and some results about of valuations are studied. Throughout this paper, I have mainly referred to [1] and [2].

1. Basic Definition of Field

A **field** is a set F with two operations, called addition and multiplication, which satisfy the following axioms:

(1) If $x \in F$ and $y \in F$, then $x + y \in F$. (closed under addition)

(2) $x + y = y + x$ for all $x, y \in F$. (commutative under addition)

(3) $(x + y) + z = x + (y + z)$ for all $x, y, z \in F$. (associative under addition)

(4) F contains an element 0 such that $0 + x = x$ for every $x \in F$. (existence of additive identity)

(5) To every $x \in F$ corresponds an elements $-x \in F$ such that $x + (-x) = 0$. (existence of additive inverse)

(6) If $x \in F$ and $y \in F$, then $xy \in F$. (closed under multiplication)

(7) $xy = yx$ for all $x, y \in F$. (commutative under multiplication)

(8) $(xy)z = x(yz)$ for all $x, y, z \in F$. (associative under multiplication)

(9) F contains an element $1 \neq 0$ such that $1 \cdot x = x$ for every $x \in F$. (existence of multiplicative identity)

(10) If $x \in F$ and $x \neq 0$ then there exist an element $\frac{1}{x} \in F$ such that $x \cdot \frac{1}{x} = 1$. (existence of multiplicative inverse)

(11) $x(y + z) = xy + xz$ and $(y + z)x = yx + zx$, for all $x, y, z \in F$. (distributive law)

---

[1] Tutor, Department of Mathematics, East Yangon University

1.1 Definition[1]. Let F be a field. An ***absolute value*** $|\ |$ on F is a real - valued function $x \mapsto |x|$ on F satisfying the following three properties:

(i) We have $|x| \geq 0$ for all $x \in F$, and $|x| = 0$ if and only if $x = 0$.

(ii) For all $x, y \in F$, we have $|xy| = |x|\,|y|$.

(iii) For all $x, y \in F$, we have $|x + y| \leq |x| + |y|$.

1.2 Some Examples of Absolute Values

(1) On any field F, define

$|\ |\ : F \to \mathbb{R}^{\geq 0}$ by $0 \mapsto 0$, $x \in F \setminus \{0\} \mapsto 1$.

This is an absolute value on F, called the ***trivial absolute value***.

(2) Let Q_p be the set of rational numbers with the p-adic absolute value, defined by the formula

$$\left| p^r \frac{m}{n} \right|_p = \frac{1}{p^r}$$

where p is a prime and r is an integer and m, n are integers $\neq 0$, not divisible by p. This is an absolute value on Q_p .

Indeed, Let $x = p^r \frac{a}{b}$, $|x| = \frac{1}{p^r}$ where p is a prime and r is an integer and a, b are integers $\neq 0$, not divisible by p.

Let $y = p^s \frac{c}{d}$, $|y| = \frac{1}{p^s}$ where p is a prime and s is an integer and c, d are integers $\neq 0$, not divisible by p.

$x \neq 0$, $|x| = 0 \Leftrightarrow \frac{1}{p^r} = 0$, which is impossible.

So $|x| = 0 \Leftrightarrow x = 0$.

Next,

$$xy = p^r p^s \frac{a}{b}\frac{c}{d}$$

$$= p^{r+s} \frac{ac}{bd}$$

$$|xy| = \left| p^{r+s} \frac{ac}{bd} \right|$$

$$= \frac{1}{p^{r+s}}$$

$$= \frac{1}{p^r p^s}$$

$$= \frac{1}{p^r}\frac{1}{p^s}$$

$$= |x|\,|y|$$

and $$|x+y| = \left| p^r \frac{a}{b} + p^s \frac{c}{d} \right|$$

$$\leq \left| p^r \frac{a}{b} \right| + \left| p^s \frac{c}{d} \right|$$

$$|x+y| \leq |x| + |y|.$$

1.3 Lemma. Let F be a field. Let $|\ |$ be an absolute value on F. We have

(i) $|1| = 1$

(ii) $|\eta| = 1$, for all $\eta \in F$ with $\eta^d = 1$ for some $0 \neq d \in \mathbb{N}$ (η is a root of unity).

(iii) $|x^{-1}| = |x|^{-1}$, for $x \in F$

(iv) $||x| - |y|| \leq |x - y|$.

(v) $|-1| = 1$

(vi) $|-x| = |x|$

Proof: (i) $|1|^2 = |1^2|$

$= |1| \Rightarrow |1| = 1.$

(ii) $|\eta|^d = |\eta^d|$

$= |1|$

$= 1 \Rightarrow |\eta| = 1.$

(iii) $1 = |xx^{-1}|$

$= |x||x^{-1}| \Rightarrow |x^{-1}| = |x|^{-1}$ for $x \in F$.

(iv) Let $x, y \in F$.

Since $x = x - y + y$, the triangle inequality gives

$$|x| \leq |x - y| + |y|,$$

so that $|x| - |y| \leq |x - y|$.

Similarly $|y| - |x| \leq |x - y|$.

Since $|x| - |y|$ is a real number we have either

$||x| - |y|| = |x| - |y|$ or

$||x| - |y|| = |y| - |x|$.

In either case, we have show that

$$||x| - |y|| \leq |x - y|.$$

(v) $|-1| = |-1|^2$

$= |(-1)^2| = |1| = 1$

(vi) $|-x| = |-1 \cdot x|$

$= |-1||x| = 1|x| = |x|$.

2. Equivalence of Absolute Values

2.1 Definition [2]. Let F be a field. $|\ |_1$, $|\ |_2$ are two absolute values on a field F. They are ***equivalent*** if there exists $\alpha \in \mathbb{R}^{>0}$ such that $|\ |_2 = |\ |_1^{\alpha}$. We denoted by $|\ |_1 \sim |\ |_2$.

2.2 Lemma. This $\sim$ in definition 2.1 is an equivalence relation.

Proof: For $|\ |_1 = |\ |_1^1$ (choose $\alpha = 1$).

Hence $|\ |_1 \sim |\ |_1$.

Therefore, $\sim$ is reflexive.

Also, assume $|\ |_1 \sim |\ |_2$.

Then $|\ |_2 = |\ |_1^{\alpha}$, where $\alpha \in \mathbb{R}^{>0}$.

$|\ |_2^{1/\alpha} = |\ |_1$

$|\ \ |_1 = |\ \ |_2^{1/\alpha}$

Hence $|\ \ |_2 \sim |\ \ |_1$.

Therefore , $\sim$ is symmetric.

Finally, Let $|\ \ |_1 \sim |\ \ |_2$, $|\ \ |_2 \sim |\ \ |_3$.

Then $|\ \ |_2 = |\ \ |_1^{\alpha}$ and $|\ \ |_3 = |\ \ |_2^{\beta}$ where $\alpha, \beta \in \mathbb{R}^{>0}$.

Thus $|\ \ |_2 = |\ \ |_1^{\alpha}$

$|\ \ |_2^{\beta} = |\ \ |_1^{\alpha\beta}$

$|\ \ |_3 = |\ \ |_1^{\alpha\beta}$ where $\alpha\,\beta \in \mathbb{R}^{>0}$.

Hence $|\ \ |_1 \sim |\ \ |_3$.

Therefore, $\sim$ is transitive.

2.3 Definition [2]. For an absolute value $|\ \ |$ on a field F, we define the ***Artin constant*** C_k to the infimum of all $C \in \mathbb{R}^{>0}$ such that $|\ \ |$ satisfies:

$$|x| \le 1 \Rightarrow |x + 1| \le C \text{ , for all } x \in F .$$

2.4 Lemma [2]. Let F be a field and $|\ \ |$ an absolute value, and $C \in [1, \infty)$. Then the followings are equivalent:

(i) for all $x \in F$, $|x| \le 1 \Rightarrow |x + 1| \le C$.

(ii) for all $x, y \in F$, $|x + y| \le C \max(|x|, |y|)$.

Proof: Assume (i) and let $x, y \in F$.

We may assume that $0 < |x| \le |y|$.

Then $\left|\frac{x}{y}\right| \le 1$,

so $\left|\frac{x}{y} + 1\right| \le C$.

$\left|\frac{x+y}{y}\right| \le C$.

Multiplying through by $|y|$ gives

$|y|\left|\frac{x+y}{y}\right| \le C|y|$

$|x + y| \le C|y| = C \max(|x|, |y|)$.

Assume (ii) and let $x \in F$ be such that $|x| \le 1$.

Then , $|x + 1| \le C \max(|x|, |1|)$

$= C \max(|x|, 1)$

$= C$.

2.5 Definition [2]. An absolute value is ***non-Archimedean*** if the Artin constant is equal to 1 (the smallest possible value). If the Artin constant is greater than 1, we say that ***Archimedean***.

2.6 Example. The sets Q of all rational numbers, $\mathbb{R}$ of all real numbers and $\mathbb{C}$ of all complex numbers with the usual Euclidean norms are Archimedean valuated fields.

3. Valuations of a Field

3.1 Definition [3]. Let F be a field. An absolute value is called **non-Archimedean** if we have

$$|x + y| \le \max\{|x|, |y|\}, \ \forall x, y \in F$$

Alternatively, the absolute value is called **Archimedean**. [See 2.3 and 2.4]

3.2 Example. On $F = Q$, p-adic norm $|\ \ |_p$ is non-Archimedean.

Proof :

Let Q_p denote the p-adic absolute value on the rational numbers.

We must show that for all $x, y \in Q$.

Then $|x + y| \leq \max\{|x|, |y|\}$.

If $x = 0$ or $y = 0$ or $x + y = 0$, the result is trivial, as follows:

Let $x = 0$. Then $x = 0 \Rightarrow |x| = 0$ and $\max\{|x|, |y|\} = |y|$.

So $|x + y| \leq \max\{|x|, |y|\}$.

Let $y = 0$.Then $y = 0 \Rightarrow |y| = 0$ and $\max\{|x|, |y|\} = |x|$.

So $|x + y| \leq \max\{|x|, |y|\}$

Let $x + y = 0$, then

$|x + y| = 0 \quad (\because |x| \geq 0, |y| \geq 0)$

$\leq \max\{|x|, |y|\}$.

Let $x, y \in Q$, $x + y \in Q$.

Then

$|x + y| = \frac{1}{p^{(x+y)}} = p^{-(x+y)}$

$\leq \max\{p^{-(x)}, p^{-(y)}\} = \max\{|x|, |y|\}$.

3.3 Definition [1]. Let Γ be a multiplicative commutative group. We shall say that an ***ordering*** is defined in Γ if we are given a subset S of Γ closed under multiplication such that Γ is the disjoint union of S, the unit element 1, and the set S^{-1} consisting of all inverses of elements of S.

If $a, b \in \Gamma$ we define $a < b$ to mean $ab^{-1} \in S$. We have $a < 1$ if and only if $a \in S$. One easily verifies the following properties of the relation $<$:

1. For $a, b \in \Gamma$ we have $a < b$ or $a = b$, or $b < a$ and these possibilities are mutually exclusive.
2. $a < b$ implies $ac < bc$ for any $c \in \Gamma$.
3. $a < b$ and $b < c$ implies $a < c$.

3.4 Definition [1]. Let F be a field. By a ***valuation*** v of F we shall mean a map $x \mapsto v(x)$ of F into an ordered group Γ, together with the extra element 0, such that:

(i) $v(x) = 0$ if and only if $x = 0$ for all $x \in F$.

(ii) $v(xy) = v(x)\, v(y)$ for all $x, y \in F$.

(iii) $v(x + y) \leq \max(v(x), v(y))$ for all $x, y \in F$.

3.5 Remark

(1) We see that a valuation gives rise to a homomorphism of the multiplicative group K^* into Γ where K^* is F different the set of zero .

(2) The valuation is called **trivial** if it maps K^* on 1.

3.6 Example. Let F be a field and v a valuation on F. Then a valuation is trivial if and only its value group is $\{1\}$.

Proof: Assume that valuation is trivial.

Then, the image of K^* under this valuation is $\{1\}$.

Conversely, its value group is $\{1\}$.

This mean that the valuation is restricted to an order subgroup of Γ.

Thus the valuation map onto $\{1\}$.

4. Equivalence of Valuations

4.1 Definition [1]. Two valuations v_1 and v_2 of F with valuation group Γ_1 and Γ_2, respectively are said to be **equivalent** if there is an order-preserving group isomorphism $\phi : \Gamma_1 \to \Gamma_2$ such that $v_2(a) = \phi(v_1(a))$ for all a in K^*.

4.2. Lemma. This ~ in definition 4.1 is an equivalence relation.

Proof: ~ is reflexive.

There is an identity mapping

$$I : \Gamma_1 \to \Gamma_1, \text{ such that}$$
$$v_1(a) = I(v_1(a)) \text{ for all } a \in K^*$$

Thus I is an order-preserving group isomorphism.

Hence $v_1 \sim v_1$.

Also, ~ is symmetric.

Assume, $v_1 \sim v_2$.

Then, there is an order-preserving group isomorphism $\varphi : \Gamma_1 \to \Gamma_2$ such that

$$v_2(a) = \varphi(v_1(a)) \text{ for all } a \in K^*$$

Thus $\varphi^{-1} : \Gamma_2 \to \Gamma_1$ such that

$$v_1(a) = \varphi^{-1}(v_2(a)) \text{ for all } a \in K^*.$$

Let $a, b \in \Gamma_2$.

Let $a < b$ then $ab^{-1} \in S_2$.

Then $\varphi^{-1} : \Gamma_2 \to \Gamma_1$ by

$$ab^{-1} \mapsto \varphi^{-1}\left(ab^{-1}\right) = \varphi^{-1}(a)\varphi^{-1}\left(b^{-1}\right)$$
$$= \varphi^{-1}(a)\left(\varphi^{-1}(b)\right)^{-1} \in S_1.$$

So $\varphi^{-1}(a) < \left(\varphi^{-1}(b)\right)^{-1}$.

Thus φ^{-1} is also an order-preserving group isomorphism.

Hence, $v_2 \sim v_1$.

Finally, assume $v_1 \sim v_2$ and $v_2 \sim v_3$.

Then, there are order-preserving group isomorphisms $\varphi : \Gamma_1 \to \Gamma_2$ such that $v_2(a) = \varphi(v_1(a))$ for all $a \in K^*$ and $\psi : \Gamma_2 \to \Gamma_3$ such that $v_3(a) = \psi(v_2(a))$ for all $a \in K^*$.

Thus $(\psi \cdot \varphi) : \Gamma_1 \to \Gamma_3$ such that

$$(\psi \cdot \varphi)(v_1(a)) = \psi(\varphi(v_1(a)))$$
$$= \psi(v_2(a))$$
$$= v_3(a)$$

Let $a < b$ then $ab^{-1} \in S_1$.

Then $(\psi \cdot \varphi) : \Gamma_1 \to \Gamma_3$ by

$$ab^{-1} \mapsto (\psi \cdot \varphi)\left(ab^{-1}\right) = (\psi \cdot \varphi)(a)\left((\psi \cdot \varphi)\left(b^{-1}\right)\right.$$
$$= (\psi \cdot \varphi)(a)\left((\psi \cdot \varphi)(b)\right)^{-1} \in S_3.$$

So $\left((\psi \cdot \varphi)(a)\right) < \left((\psi \cdot \varphi)(b)\right)^{-1}$.

Thus $\psi \cdot \varphi$ is also an order preserving group isomorphism.

Therefore, $v_1 \sim v_3$.

Hence ~ is an equivalence relation.

4.3 Remark: Two valuations v_1 and v_2 on F are **equivalent** if there exists a real $s > 0$ such that $v_1 = sv_2$.

5. Alternative Notion of Valuations

5.1 Definition [3]. A **valuation** on F is a function

$$v : F \to \mathbb{R} \cup \{\infty\}$$

satisfying these properties, for all $a, b \in F$.

1. $v(a) = \infty \Leftrightarrow a = 0$,
2. $v(ab) = v(a) + v(b)$,
3. $v(a + b) \geq \min\{v(a), v(b)\}$.

Note that if we set $v(a) = 0$ for all $0 \neq a \in F$ and $v(0) = \infty$, we have a valuation on F, called the **trivial valuation**.

5.2 Lemma: Let F be a field. Let v be a valuation on F. We have

(i) $v(1) = 0$

(ii) $v(\eta) = 0$, for all $\eta \in F$ root of unity,

(iii) $v(a^{-1}) = -v(a)$, $\forall a \in K^*$

(iv) if $a, b \in F$ and $v(a) \neq v(b)$, $v(a + b) = \min\{v(a), v(b)\}$.

Proof:

(i)
$$\begin{aligned} v(1) &= v(1^2) \\ &= v(1) + v(1) \\ v(1) - v(1) &= v(1) \\ v(1) &= 0. \end{aligned}$$

(ii) Let $\eta \in F$ with $\eta^d = 1$ for some $0 \neq d \in \mathbb{N}$.

Then
$$\begin{aligned} dv(\eta) &= v(\eta^d) \\ &= v(1) \\ &= 0 \end{aligned}$$

Therefore $v(\eta) = 0$.

(iii)
$$\begin{aligned} 0 &= v(1) \\ &= v(aa^{-1}) \quad \forall a \in K^*. \\ &= v(a) + v(a^{-1}). \\ v(a^{-1}) &= -v(a). \end{aligned}$$

(iv) We can assume that $v(a) > v(b)$ and so $b \neq 0$.

If $a = 0$, obvious.

Assume that $a \neq 0$.

Then $v(a + b) \geq \min\{v(a), v(b)\} = v(b)$.

We have
$$\begin{aligned} v(b) &= v(b + a - a) \\ &\geq \min\{v(a + b), v(a)\}. \end{aligned}$$

Assume that $\min\{v(a + b), v(a)\} = v(a)$, then $v(a) > v(b) \geq v(a)$ and we get a contradiction.

So, $\min\{v(a + b), v(a)\} = v(a + b)$
$$v(a + b) \leq v(b)$$

Therefore, $v(a + b) = \min\{v(a), v(b)\}$.

Conclusion

A valuation is a function on a field that provides a measure of size and multiplicity of elements of the field. The valuation is used to calculate the total amount of energy used. The theory of absolute value on field was originally developed as a means of generalizing the work of German Mathematicians on p-adic numbers. The absolute value is used in the real world in calculations of changes in temperature and travel distances. It also used in physics and calculus to define certain situations.

Acknowledgements

I would like to express my greatest thanks to Dr. Nay Win Oo, Rector, East Yangon University for his permission to work on the present research. I would like to express my profound gratitude to Dr. Aye Aye Ko, Dr. Wah Wah Lwin and Dr. Thida Aung, Pro-Rectors, East Yangon University, for their kind permission to present my research work. I also would like to thank Professor and Head Dr. Sandar Maw and Professor Dr. Phyu Phyu Aung, Department of Mathematics, East Yangon University, for their invaluable suggestions, encouragements and comments.

References;

[1] Lang, S.,(2002) *Algebra:Graduated Texts in Maths*, Revised Third Edition, Springer-Verlag, New York.

[2] Milne, J.S., (2020) *Algebraic Number Theory*, New Zealand.

[3] Neukirch, J.,(1999) *Algebraic Number Theory*, Springer-Verlag, New York.

[4] Stichtenoth, H.,(1993) *Algebraic Function Fields and Codes*, Springer-Verlag, New York.

Linear Functionals on a Finite Dimensional Inner Product Space

Aye Thandar Aung[1]

Abstract

This research paper, the linear functions on a finite dimensional inner product space are presented. The notation of inner product spaces and the basic properties of inner product spaces are expressed. The inner product space $\mathbf{R}^n$ is often called ***n-dimensional Euclidean space.*** The inner product space $\boldsymbol{C}^n$ is often called ***n-dimensional unitary space***. The inner product of two vectors in the space is a scalar, denoted with angle brackets such as in $\langle a, b \rangle$. Two vectors are orthogonal to each if their inner product is zero. The proofs of a number of mathematical theorems rely on the Cauchy- Schwarz Inequality. An elementary example of the Cauchy- Schwarz Inequality in action can be found in the proof of the Triangle inequality. The theorems relating to Pythagorean Theorem and Generalized Pythagorean Theorem are expressed. Moreover, the orthogonal set, orthonormal set and orthonormal basis of inner product spaces are discussed. Every linear transformation has a unique adjoint. The concepts of the adjoint of a linear operator on inner product spaces with some examples are discussed.

Keywords: norm, inner product space, finite dimensional, linear functional.

Introduction

Definitions of norm and inner product space are introduced. The concept of a general norm, which measures the length of vectors. Two vectors are orthogonal if their dot product is 0. Two vectors are orthonormal if their dot product is 0 and their lengths are both 1. The notion of orthogonality and the Pythagorean Theorem holds in any inner product space are proved. Throughout this paper is mainly referred to [1] and [2].

1. Basic Definition of Norm

Let **F** denote either **R** or **C**. Let V be a vector space over **F**. A ***normed linear space*** is a vector space V equipped with a ***norm***. A norm is a function V → **R,** denoted by ||.|| , which satisfies the following properties.

(i) For all $v \in$ V, for all $\alpha \in \mathbf{F}$, $\| \alpha v \| = | \alpha | \, \| v \|$.

(ii) For all $v \in$ V with $v \neq 0$, $\| v \|$ is a positive real number; $\| v \| > 0$.
And $v = 0$ if and only if $\|v\| = 0$.

(iii) For all $v, w \in$V, $\|v + w \| \leq | v | + | w |$

1.1 Example. Let $x = (x_1, \ldots, x_n) \in \mathbf{R}^n$.

Define the 2-norm on $\mathbf{R}^n$ by

$$||x||_2 = \sqrt{x_1^2 + \cdots + x_n^2} .$$

So, for $n = 1$, we have $||x||_2 = | x |$.

Define the 1-norm on $\mathbf{R}^n$ by

$$||x||_1 = \sum_{i=1}^{n} | x_i | .$$

Define the ∞ -norm on $\mathbf{R}^n$ by

$$||x||_\infty = max_{i=1,\ldots,n} |x_i| .$$

---

[1] Tutor, Department of Mathematics, East Yangon University

We will show that the triangle inequality for the 1-norm.

Indeed ,

let $x , y \in \mathbf{R}$. Then $| x + y | = \| x + y \|_1 \leq \| x \|_1 + \| y \|_1 = | x | + | y |$.

1.2 Definition [1]. Let **F** denote either **R** or **C**. Let V be a vector space over **F.** An **inner product space** is a vector space V equipped with an **inner product**. An inner product is a function $V \times V \rightarrow \mathbf{F}$, denoted by $\langle .,. \rangle$, which satisfies the following properties .

(i) For all $v, v', w \in V$. $\langle v + v', w \rangle = \langle v , w \rangle + \langle v', w \rangle$.

(ii) For all $v , w \in V$, for all $\alpha \in \mathbf{F}$. $\langle \alpha v, w \rangle = \alpha \langle v , w \rangle$.

(iii) For all $v \in V$, if $v \neq 0$, then $\langle v, v \rangle$ is a positive real number; $\langle v , v \rangle > 0$.

(iv) For all $v , w \in V$, $\langle v , w \rangle = \overline{\langle w, v \rangle}$; $(v) > 0$.

1.3 Remark. If $\mathbf{F} = \mathbf{R}$, then property (iv) says that $\langle v, w \rangle = \langle w, v \rangle$.

1.4 Examples . (i) Let $x = (x_1, ..., x_n) \in \mathbf{R}^n$ and $y = (y_1, ..., y_n) \in \mathbf{R}^n$.

Define the standard inner product (or dot product) on R^n by

$$\langle x , y \rangle = \sum_{i=1}^{n} x_i y_i .$$

The inner product space R^n is often called ***n-dimensional Euclidean space***.

(ii) Let $x = (x_1, ..., x_n) \in \mathbf{C}^n$, and let $y = (y_1, ..., y_n) \in \mathbf{C}^n$.

Define the standard inner product (or dot product) on $\mathbf{C}^n$ by

$$\langle x, y \rangle = \sum_{i=1}^{n} x_i \overline{y_i}.$$

The inner product space $\boldsymbol{C}^n$ is often called ***n-dimensional unitary space***.

(iii) The vector space C [a , b] of all continuous complex-valued functions on the closed interval [a , b] is a complex inner product space under the inner product

$$\langle f, g \rangle = \int_a^b f(x) \overline{g(x)}\, dx .$$

1.5 Theorem. Let V be an inner product space , then

(i) For all $v , v', w \in V$, $\langle w , v + v' \rangle = \langle w , v \rangle + \langle w, v' \rangle$.

(ii) For all $v, w \in V$, for all $\alpha \in \mathbf{F}$, $\langle v, \alpha w \rangle = \overline{\alpha} \langle v, w \rangle$.

(iii) For all $v \in V$, $\langle v , 0 \rangle = \langle 0, v \rangle = 0$.

(iv) $\langle v, v \rangle = 0$ if and only if $v = 0$.

Proof . (i) Suppose $v , v', w \in V$, then

$$\langle w , v+ v' \rangle = \overline{\langle v + v', w \rangle} = \overline{\langle v + w \rangle + \langle v', w \rangle} = \overline{\langle v, w \rangle} + \overline{\langle v', w \rangle} = \langle w , v \rangle + \langle w , v' \rangle.$$

(ii) Suppose $v , w \in V$, and $\alpha \in \mathbf{F}$. Then

$$\langle v , \alpha w \rangle = \overline{\langle \alpha w, v \rangle} = \overline{\alpha \langle w, v \rangle} = \overline{\alpha}\, \overline{\langle w, v \rangle} = \overline{\alpha} \langle v, w \rangle.$$

(iii) Suppose $v \in V$, then $\langle v , 0 \rangle = \langle v, v + (- v) \rangle = \langle v , v \rangle - (v , v) = 0$.

Similarly $\langle 0 , v \rangle = 0$. Thus $\langle v , 0 \rangle = \langle 0 , v \rangle = 0$.

(iv) Suppose $v \in V$, then $\langle v , v \rangle = 0 \Leftrightarrow v . v = 0 \Leftrightarrow v = 0$.

1.6 Definition . Let V be an inner product space, and let $v, w \in V$. We say that v, w are ***orthogonal*** if $\langle v , w \rangle = 0$.

1.7 Lemma (Cauchy – Schwarz Inequality)

Let V be an inner product space. Then, for any $v , w \in V$,

$$|\langle v, w \rangle| \leq \sqrt{\langle v, v \rangle} \sqrt{\langle w , w \rangle} .$$

Proof . If $w = 0$, then both sides of our inequality are zero , so the inequality holds , and assume that $w \neq 0$. So , $\langle w , w \rangle > 0$. Define $\alpha = \frac{\langle v,w \rangle}{\langle w,w \rangle}$ .By conjugate – symmetry of the inner product ,

$$\langle v , w \rangle \langle w , v \rangle = \langle v , w \rangle \overline{\langle v , w \rangle} = |\langle v , w \rangle|^2.$$

Also , by positivity of the inner product ,

$$\langle v - \alpha w , v - \alpha w \rangle \geq 0 ,$$

$$\Rightarrow \langle v , v \rangle + \langle v , -\alpha w \rangle + \langle -\alpha w , v \rangle + \langle -\alpha w , -\alpha w \rangle \geq 0$$

$$\Rightarrow \langle v , v \rangle - \langle v , w \rangle - \alpha \langle w , v \rangle + |\alpha^2| \langle w , w \rangle \geq 0$$

$$\Rightarrow \langle v , v \rangle - \frac{|\langle v,w \rangle|^2}{\langle w,w \rangle} - \frac{|\langle v,w \rangle|^2}{\langle w,w \rangle} + \frac{|\langle v,w \rangle|^2}{\langle w,w \rangle} \geq 0.$$

We get $\langle v , v \rangle - \frac{|\langle v,w \rangle|^2}{\langle w,w \rangle} \geq 0$.

Thus $|\langle v, w \rangle| \leq \sqrt{\langle v, v \rangle} \sqrt{\langle w , w \rangle}$.

1.8 Lemma . Let $\langle . , . \rangle$be an inner product on a vector space V. Then the function ||.|| V→R defined by $||v||= \sqrt{\langle v, v\rangle}$ is a norm on V.

Proof . Let $v \in$ V , for all $\alpha \in$ **F**.

Then $|| \alpha v ||^2 = \langle \alpha v, \alpha v\rangle = |\alpha|^2 \langle v, v\rangle$.

Thus $||\alpha v|| = |\alpha| ||v||$.

Let $v \in$V, $v \neq 0$, then $||v|| = \sqrt{\langle v, v\rangle} > 0$.

And if $v = 0$, $\Leftrightarrow ||v|| = \sqrt{\langle 0, v\rangle} = 0$

Again $|| v + w ||^2 = | \langle v + w , v + w \rangle|$

$= |\langle v ,v\rangle+\langle w ,w\rangle+\langle v ,w\rangle+\langle w ,v\rangle|$

$\leq |\langle v ,v\rangle|+|\langle w ,w\rangle|+|\langle v ,w\rangle|+|\langle w ,v\rangle|$

$\leq ||v||^2+||w||^2+2||v||||w||$

$= (||v||+||w||)^2$.

Thus ||.|| is a norm on V.

2. Orthogonality

2.1 Definition . Let V be an inner product space and let $\{v_1, \dots, v_n\}$be a collection of vectors in V. The set of vectors $\{v_1, \dots, v_n\}$ is said to be ***orthogonal*** if $\langle v_i, v_j\rangle = 0$ for all $i, j \in \{1,\dots,n\}$ with $i \neq j$. If additionally $\langle v_i, v_i\rangle = 1$ for all $i \in \{1, \dots,n\}$, the set of vectors $\{v_1, \dots, v_n\}$ is called ***orthonormal***.

2.2 Definition . Let V be an inner product space. An ***orthonormal basis*** of V is a collection $\{v_1, \dots, v_n\}$ of orthonormal vectors that is also a basis for V.

2.3 Lemma. Let V be an inner product space. Suppose $v \in$ V is orthogonal to each of the vectors $v_1, \dots, v_n \in$ V. Then v is orthogonal to any linear combination of $v_1, \dots, v_n$.

Proof. Since $\langle v, v_i \rangle = 0$ for all $i \in \{1, \dots, n\}$, if $\alpha_1, \dots, \alpha_n \in$ **F**, then

$\langle v, \sum_{i=i}^{n} \alpha_i v_i \rangle = \langle v, \alpha_1 v_1 + \cdots + \alpha_n v_n \rangle$

$= \langle v, \alpha_1 v_1 \rangle + \ldots + \langle v, \alpha_n v_n \rangle$

$= \overline{\alpha_1} \langle v, v_1 \rangle + \ldots + \overline{\alpha_n} \langle v, v_n \rangle$

$= \sum_{i=i}^{n} \overline{\alpha_i} \langle v, v_i \rangle$

$= 0.$

Thus v is orthogonal to any linear combination of $v_1, \ldots, v_n$.

2.4 Theorem (Pythagorean Theorem)

Let V be an inner product space, and let $v, w \in V$ be orthogonal.Then $\|v + w\|^2 = \|v\|^2 + \|w\|^2$.

Proof. $\|v + w\|^2 = \langle v + w, v + w \rangle$

$= \langle v, v \rangle + \langle w, w \rangle + \langle v, w \rangle + \langle w + v \rangle$

Since v and w are orthogonal, we have $\| v + w \|^2 = \| v \|^2 + \| w \|^2$.

2.5 Theorem (Generalized Pythagorean Theorem)

Let V be an inner product space, and let $v_1, \ldots, v_n \in V$ be orthogonal to each other. That is, $\langle v_i, v_j \rangle = 0$ for all $i, j \in \{1, \ldots, n\}$ with $i \neq j$. Then

$$\|\sum_{i=1}^{n} v_i\|^2 = \sum_{i=1}^{n} \|v_i\|^2.$$

Proof. We induct on n.

Suppose the assertion is true for a fixed n.

Then, let $v_1, \ldots, v_{n+1}$ be orthogonal to each other.

From **Lemma 2.3**, v_{n+1} is orthogonal to $\sum_{i=1}^{n} v_i$.

So, applying **Theorem 2.4** to $v_{n+1}$and $\sum_{i=1}^{n} v_i$, and then using the inductive hypothesis,

$$\|v_{n+1} + \sum_{i=1}^{n} v_i\|^2 = \left\|v_{n+1}\right\|^2 + \|\sum_{i=1}^{n} v_i\|^2$$

$$= \left\|v_{n+1}\right\|^2 + \sum_{i=1}^{n} \|v_i\|^2.$$

Thus $\|\sum_{i=1}^{n} v_i\|^2 = \sum_{i=1}^{n} \|v_i\|^2$.

2.6 Corollary. Let V be an inner product space, and let $v_1, \dots, v_n \in$ V be orthogonal to each other. That is, $\langle v_i, v_j \rangle$=0 for all i , $j \in \{1 \dots n\}$ with $i \neq j$. Let $\alpha_1, \dots, \alpha_n \in \mathbf{F}$. Then

$$\|\sum_{i=1}^{n} \alpha_i v_i\|^2 = \sum_{i=1}^{n} |\alpha_i|^2 \big||v_i|\big|^2.$$

Proof. If $\langle v_i, v_j \rangle$ =0, then $\langle \alpha_i v_i, \alpha_j v_j \rangle = 0$ 0. So, apply **Theorem 2.5** to the set of vectors $\alpha_1 v_1, \dots, \alpha_n v_n$.

2.7 Corollary. Let V be an inner product space, and let $v_1, \dots, v_n \in$ V be an orthogonal set of vectors. Then

$$\|\sum_{i=1}^{n} \alpha_i v_i\|^2 = \sum_{i=1}^{n} |\alpha_i|^2.$$

2.8 Corollary. Any set of orthonormal vectors is linearly independent.

2.9 Corollary. Let V be an n-dimensional inner product space. Let $\{v_1, \dots, v_n\}$ be an orthonormal set in V. Then $\{v_1, \dots, v_n\}$ is an orthonormal basis of V.

Proof. By **Corollary 2.8**, $\{v_1, \dots, v_n\}$ is linearly independent. If we have n linearly independent vectors in an n -dimensional space, then these vectors form a basis of V.

2.10 Theorem. Let V be an inner product space. Let $\{v_1, \dots, v_n\}$ be an orthonormal basis of V. Then, for any v∈ V, we have v = $\sum_{i=1}^{n} \langle v, v_i \rangle v_i$.

Proof. Let $v \in$ V. Since $\{v_1, \dots, v_n\}$ is a basis of V, there exist $\alpha_1, \dots, \alpha_n \in \mathbf{F}$ such F such that

$$v = \sum_{i=1}^{n} \alpha_i v_i \ (*)$$

So, we need to show that $\alpha_i = \langle v, v_i \rangle$ for all $i \in \{1,2, \dots, n\}$. $Let\ j \in \{1,2, \dots, n\}$

Taking the inner product of both sides of (*) with v_j, and then applying orthonormality,

$$\langle v, v_j \rangle = \langle \sum_{i=1}^{n} \alpha_i v_i, v_j \rangle = \sum_{i=1}^{n} \alpha_i \langle v_i, v_j \rangle = \alpha_j \langle v_j, v_j \rangle = \alpha_j.$$

3. Linear Functionals

3.1 Definition[2]. Let V be a vector space over a field **F**. A ***linear functional*** is a linear transformation T: V → **F**.

3.2 Examples.

(i) Define T: $\mathbf{R}^3 \to \mathbf{R}$ by T $(a, b, c) = a + 2b + 3c$. Then T is a linear functional.

(ii) Define T: C ([0, 1], **R**) → **R** by T $(f) = \int_0^1 f(t)\,dt$. Then T is a linear functional.

(iii) Define T: C ([0, 1], **R**) → **R** by T $(f) = f\left(\frac{1}{3}\right)$. Then T is a linear functional.

(iv) Let V be a finite-dimensional inner product space over **R**. Let $w \in$ V, and define T: V → **R** by T $(v) = \langle v, w \rangle$. Then T is a linear functional.

3.3 Theorem. Let V be a finite-dimensional inner product space over **F**. Let T: V → **F** be a linear functional. Then there exists a unique vector $w \in V$ such that, for all $v \in V$, T$(v) = \langle v, w \rangle$.

3.4 Lemma. Let **F** denote **R** or **C**. Let V be a finite-dimensional inner product space over **F** with inner product $\langle , \rangle_v$, and let W be a finite-dimensional inner product space over **F** with inner product $\langle , \rangle_w$.Let T: V → W be a linear transformation. Given any w ∈ W, define a linear functional.

Let T_w: V→**F** by $T_w(v) = \langle T(v), w \rangle_w$.

Then T_w is a linear functional.

Proof. Let $v, v' \in$V let $\alpha \in$ **F.** Then

$$T_w(v + v') = \langle T(v + v'), w \rangle_w$$

$$= \langle T(v), w \rangle_w + \langle T(v'), w \rangle_w$$

$$= T_w(v) + T_w(v').$$

Next, $T_w(\alpha v) = \langle T(\alpha v), w \rangle_w = \alpha \langle T(v), w \rangle_w = \alpha T_w(v)$.

Thus, $T_w$is a linear functional.

3.5 Definition. Let $T_w : V \to \mathbf{F}$ is a linear functional, then we can apply Theorem 3.3 to get a unique vector in V, which we denote by T* (w), such that for all $v \in V$,

$$T_w(v) = \langle v, T^*(w) \rangle_w.$$

As we will see shortly, T* is linear transformation from W to V, which we call the **adjoint** of T. Also, recalling the definition of T_w , we have

$$\langle T(v), w \rangle_w = \langle v, T^*(v) \rangle_v.$$

3.6 Remark. We note that T: V→W, whereas T* : W → V.

3.7 Lemma. Let T: V→W be a linear transformation between finite- dimensional inner product spaces. Then T: W→V is a linear transformation.

Proof. Let $w, w' \in W$ and let $\alpha \in \mathbf{F}$. We will first show that

$$T^* \langle w + w' \rangle = T^*(w) + T^*(w').$$

By the definition of T* , for all $v \in V$,

$$\langle T(v), w + w' \rangle = \langle v, T^*(w + w') \rangle.$$

So, rearranging things and applying the definition of T* again,

$$\langle v, T^*(w + w') \rangle = \langle T(v), w \rangle + \langle T(v), w' \rangle$$

$$= \langle v, T^*(w) \rangle + \langle v, T^*(w') \rangle$$

$$= \langle v, T^*(w) + T^*(w') \rangle.$$

By the uniqueness part of the Theorem 3.3, we therefore have

$$T^*(w + w') = T(w) + T^*(w').$$

We now show that $T^*(\alpha w) = \alpha T^*(w)$.

$$\langle v, T^*(\alpha w) \rangle = \langle T(v), \alpha w \rangle = \overline{\alpha} \langle T(v), w \rangle = \overline{\alpha} \langle v, T^*(w) \rangle = \langle v, \alpha T^*(w) \rangle.$$

By the uniqueness part of the Theorem 3.3, we therefore have

$$T^*(\alpha w) = \alpha T^*(w).$$

3.8 Theorem. Let **F** denote **R** or **C** Let T: V→W, S: V→W and let R: U→V be a linear transformation between inner product spaces U, V, W over **F**. Then

(i) (T+ S)*

(ii) For all α∈ **F**, (αT)*= $\overline{\alpha}$ T*

(iii) (T*)* = T

(iv) (TR)* = R*T*

Proof. (i) If $v \in V$ and $w \in W$, then

$\langle v., (T + S)^* (w) \rangle = \langle (T + S) (v), w \rangle$

$= \langle T (v), w \rangle + \langle S (v), w \rangle$

$= \langle v, T^* (w) \rangle + \langle v, S^*(w) \rangle$

$= \langle v, T^* (w) + S^* (w) \rangle$.

Thus, $(T + S)^* (w) = T^* (w) + S^* (w)$, as desired.

(ii) Suppose $\alpha \in \mathbf{F}$. If $v \in V$ and $w \in W$, then

$\langle v, (\alpha T)^* (w) \rangle = \langle (\alpha T) v, w \rangle = \alpha \langle T (v), w \rangle = \alpha \langle v, T^* (w) \rangle = \langle v, \overline{\alpha} T^* (w) \rangle$.

Thus, $(\alpha T)^* (w) = \overline{\alpha} T^* (w)$, as desired.

(iii) If $v \in V$ and $w \in W$, then

$\langle v, (T^*)^* (w) \rangle = \langle T^*(v), w \rangle = \langle \overline{w, T * (v)} \rangle = \langle \overline{T(w), v} \rangle = \langle v, T (w) \rangle$.

Thus, $(T^*)^* (w) = T (w)$, as desired.

(iv) If $v \in V$ *and* $w \in W$, *then*

$\langle v, (TR)^*(w) \rangle = \langle (TR)(v), w \rangle = \langle R(v), T^*(w) \rangle = \langle v, R^*(T^*(w)) \rangle$.

Thus, $(TR)^*(w) = R^* ((T^*(w))$, as desired.

Conclusion

The more special concept of an inner product, which measures the angle between two vectors. The length of a vector with two elements is the square root of the sum of each element squared. Normed of a vector is always positive or zero $||x|| \geq 0$. The Cauchy-Schwarz Inequality also important because it connects the notion of an inner product space with the notion of length. The Generalized Pythagorean Theorem in any inner product space is proved. All linear functionals on a finite- dimensional inner product space. A linear functional gives you a scalar value from some field **F.** On the other hand a linear transformation gives you another vector. Linear transformations are often used in machine learning applications. They are useful in the modeling of 2D and 3D animations, where an

object's size and shape needs to be transformed from one viewing angle to the next. Therefore, a linear functional is a special case of a linear transformation which gives you a vector with only one entry.

Acknowledgements

I would like to express my deepest gratitude to Dr. Nay Win Oo, Rector of East Yangon, University and Dr. Aye Aye Ko , Dr. Wah Wah Lwin and Dr. Thida Aung, Pro-Rectors of East Yangon University, for their kind permission to present my research work. I also would like to give my greatest thanks to Professor and Head Dr. Sandar Maw and Professor Dr. Phyu Phyu Aung, Department of Mathematics, East Yangon University, for their invaluable suggestions, encouragements and comments.

References

[1] Axler, S., (2015) *Linear Algebra Done Right, Undergraduate texts in Mathematics*, Springer, New York.

[2] Heilman, S., (2015) *Linear Algebra*, Department of Mathematics, University of California, Los Angeles, Spring.

[3] Roman, S., (2008) *Advanced Linear Algebra, Graduate texts in Mathematics*, Springer, New York.

COMPARATIVE STUDY ON MORPHOLOGICAL APPEARANCE OF BLOOD CELLS IN SOME MAMMALS FROM YWAR THAR GYI SLAUGHTER-HOUSE, YANGON REGION

Thida[1], Khin Maw Maw Myint[2], Thet Thet Lwin[3]

Abstract

The blood samples were collected from the 20 numbers for 10 samples of cows namely *Bos taurus* and 10 samples of pigs namely *Sus scrofa domesticus* from Ywar Thar Gyi Slaughter-House, Yangon Region. The study period was from October 2017 to August 2021. Stained blood smears using wedge smear technique and Leishman stain was prepared. Blood cells were examined by X 1000. Cells types were identified based on well shape and mean size in diameter and staining properties. In the present study, the largest mean diameters of red blood cell (5.99μm), basophil (12.83μm), eosinophil (12.7μm) neutrophil (12.16μm), lymphocyte (11.81μm), monocyte (12.67μm) and platelet (2.15μm) were found in pig and the smallest red blood cell (5.2μm), basophil (11.07μm), eosinophil (11.33μm), neutrophil (10.86μm), lymphocyte (10.08μm), monocyte (12.04μm) and platelet (1.47μm) were found in cow. The mean diameters of pig blood cells were larger than of cow blood cells. The hematological analysis was conducted at laboratory of Zoology Department, East Yangon University. The morphological and cytochemical features of erythrocytes, leukocytes and platelets of studied species were compared and discussed.

Key words: Erythrocytes, Leukocytes, Platelets, Mammals and mean size in diameter

Introduction

Blood circulates throughout the body and is well adapted for its various functions in transporting nutrient, oxygen, waste products, carbon dioxide, hormones, cells and other substances. Plasma (55%) is the fluid portion, called serum when depleted of fibrin and fibrinogen. The formed elements of blood (45%) include Erythrocytes (Red Blood Cells), Leukocytes (White Blood Cells) and Platelets (Thrombocytes) (Sina, 2014).In all vertebrates, the blood comprises (1) nearly colorless plasma (2) white blood cells or leukocytes (3) red blood cells or erythrocytes (4) platelets or thrombocytes (Tibbo, 2004).

The red blood cells of domestic mammals are non-nucleated and biconcave discs. The average diameter of erythrocytes varies with the species. The erythrocytes are the largest in the dog (7μm), while those of the goat are the smallest (4.1μm) (Sina, 2014).

There are two main types of white blood corpuscles, according to the structure of nuclei and presence or absence of granules in their cytoplasm. They are granulocytes and non-granular leukocytes. Granulocytes have numerous granules in cytoplasm and the nucleus is segmented into two or more lobes, they are of three types, basophils, eosinophils and neutrophils. Non-granular leukocytes may or may not have small granular of neutral nature but the nucleus is never segmented into lobes, lymphocytes and monocytes (Jordon, 2004). Basophil only a small percentage of the leukocytes of domestic mammals is basophils. Hence, they are not often found in blood smears. Basophil nucleus may be irregular, bilobed or highly segmented. They are often fairly large, oval to round, and stain dark purple to reddish purple (Sina, 2014). They are 14-16μm in diameter (www. Histology.leeds.ac.uk > blood, 2021). Eosinophil has many large granules; nucleus has two lobes connected by a thread. The cytoplasm, pale blue (Sina, 2014). These cells are 12-17μm in diameter (www.Histology.leeds.ac.uk > blood, 2021). Neutrophil or heterophil in birds, reptiles and some mammals is the predominant granulocyte. Neutrophils have white cytoplasm with small pink granules (Sina, 2014). There is a single nucleus, which is multilobed, and can have

[1] Dr., Associate Professor, Department of Zoology, East Yangon University
[2] Dr., Associate Professor, Department of Zoology, East Yangon University
[3] Dr., Associate Professor, Department of Zoology, Pathein University

between 2 and 5 lobes. The neutrophils are 12-14μm diameter (www.Histology.leeds.ac.uk > blood, 2021).

Lymphocyte has single large round nucleus with a thin rim of clear cytoplasm. The cells range in size from six to 15 mm. Most of lymphocytes in carnivores, horses and pigs are small (Sina, 2014).The monocytes are the largest of the leukocytes (15 to 20μm in diameter) (www.Histology.leeds.ac.uk > blood, 2021). The shape of the nucleus is highly variable and may be irregular, oval, irregular, kidney-shaped or horseshoe-shapes (Sina,2014).

Platelets serve a vital function in the formation of blood clots. They are not cells. Platelets are small and pale blue. Platelets are called thrombocytes in avian (Sina, 2014).

The blood is the major tool in the hands of veterinary practitioners. The blood examination is performed routinely to assess health and diagnosis of various pathological conditions on domestic animals (Suresh and Ishwar, 2014).Thus, the good and healthy poultry farms may be breed in Myanmar. So, hoping to get the normal blood cell types and diameter from the studied species. The study was undertaken to determine and compare the morphology of blood cells in cow and pig. The present study was conducted for the following objectives:

- to examine the composition of blood cell types and their morphology
- to investigate and measure the mean diameter of the blood cells
- to compare the obtained data between the studied species

Materials And Methods

Study area and study period

The blood samples of twenty individuals, ten samples of cows, namely *Bos taurus* and ten samples of pigs, namely *Sus scrofa domesticus* were taken from Ywar Thar Gyi Slaughter-House, (16°54'10" N 96°14'50" E), Yangon Region (Fig.1). The study period lasted from October, 2017 to August, 2021.

Blood sample collection and preparation

This study was carried out on twenty individuals (ten cows and ten pigs) in order to study the influence of breed on blood cells morphology. Blood samples were taken from the jugular vein (cow) and ear vein (pig).The blood was drawn smoothly into a three ml syringe with an 18-gauge needle. One ml of collected blood sample were transferred into vacutainer tube containing ethylenediamine tetra acetic acid (EDTA).The blood was mixed with the anticoagulant by gentle rotation or inversion. EDTA treated samples are preferred for general haematological work. Basic experiments on haematology were done using routine thin blood film preparation and staining. The method was followed after Dacie and Lewis (1975) (Plate 1 and 2).The hematological analysis was done at laboratory of Zoology Department, East Yangon University.

Staining of thin blood film

Leishman stain was carefully dropped onto the thin blood film to cover the whole thin blood film. The stain on the thin blood film was left for about 2 minutes. Then distilled water was added to the stain on the thin blood film to dilute. When a treat pipette, the diluted stain is then sucked up and down to mix it thoroughly. A correct dilution of the fluid had a thin greenish scum. The diluted stain was allowed to act for 10 minutes after which it was washed off with distilled water, stand the slides for two stain an end to dry. When dry, a liberal drop of immersion oil in the surface of the smear and proceeded with the examination by oil immersion. The diameters of the blood cells were measured under a digital binocular microscope at a magnification of immersion (x1000). (Model: NLCD – 307B, RATING: AC 100-240V 50 HZ/ 60 HZ, LAMP:S-LED WI, T 250V 500 mA, No. 1400040).The method in this study was after Lewis (2000) (Plate 2).

Formula of Leishman's stain

Leishman's powder ---------- 0.2 gm
Methanol ---------- 100ml

0.2 gm of powdered dye was weighted out and transferred to a conical flask of 200-250 ml capacity. 100ml of methanol were added and the mixture was warmed to 50˚C for 15 minutes with occasional shaking. The solution was filtered. It was them ready for use, but had improved on staining (Lewis, 2000).

Measurement of the blood cells

Mature erythrocytes, leukocytes and platelets were measured for diameter in each sample of individual (cow and pig) and their mean diameter values in microns were calculated in each sample followed after Murry (1992).

Formula for calculation of standard deviation

$$\bar{x} = \frac{\sum x}{n}$$

$$\hat{s} = \sqrt{\frac{\sum(x-\bar{x})^2}{N-1}}$$

$\hat{s}$ = Standard deviation

x = Diameter of one blood cell

$\bar{x}$ = Average diameter of blood cell

N = Total number of blood cell

Identification of blood cells in cow and pig

Morphological identification of erythrocytes, leukocytes and platelets were followed after Schermer (1958) and Thein Htut (1979).

Fig. 1 Map of the study area (Source: Google Earth, 2021

A. Blood collection from jugular vein of cow B. Blood collection from ear vein of pig C. Materials for analyzing sample D.Blood sample mixing with EDTA

Plate 1 Collection of blood samples of the studied species

A. Drawing of the thin blood film B. Stained blood films of studied species C. Staining of thin blood films of studied species D.Digital binocular electric microscope

Plate 2 Preparing of equipment for study blood smear

RESULTS

The morphological characters of the erythrocytes, leukocytes and platelets (thrombocytes) in cows and pigs were described.

The blood cells of *Bos taurus* (cow)

Erythrocytes (RBC)

The red blood cells were round and flat disc with little or no central depression. They do not contain a nucleus. The mean diameter of erythrocyte was 5.2μm (Table 1 and 3, Fig. 2 and Plate 3).

White blood cells or Leukocytes (WBC)

Two main types of leukocytes; granulocytes and non-granulocytes were investigated.

Granulocytes:

(1) The basophil had round granules and the nucleus was segmented with dark purple color. The cell had numerous small dark purple cytoplasmic granules obscuring part of the nucleus. The mean diameter of basophil was 11.07μm.

(2) The eosinophil had round and very large. The nucleus had bi-lobed with dark purple. The eosinophil had round to oval reddish granule in the cytoplasm obscuring part of the nucleus. The mean diameter of eosinophil was 11.33μm.

(3) The neutrophil had round (irregular shape) and cytoplasm with light pink granules. The nucleus had segmented with purple color. The mean diameter of neutrophil was 10.86μm (Table 1 and 3, Fig.2 and Plate 3).

Non-granular Leucocytes:

(1) The lymphocytes had round with rim of light blue cytoplasm. The nucleus had large round with purple color. The mean diameter of lymphocyte was 10.08μm.

(2) The monocytes had large and round and its nucleus was bean-shaped with purple color. The cytoplasm had blue gray color. The mean diameter of monocyte was 12.04μm (Table 1 and 3, Fig.2 and Plate 3).

Platelets

The platelets were small round and pale blue color. Platelets have purple central granules in stained blood smears. The mean diameter of platelet was 1.47µm. (Table 1 and 3, Fig. 2 and Plate 3).

The blood cells of *Sus scrofa domesticus* (pig)

Erythrocytes (RBC)

The red blood cells were non-nucleated, biconcave shaped. They are purple. The mean diameter of erythrocyte was 5.99µm (Table 2 and 3, Fig.2 and Plate 3).

White blood cells or Leukocytes (WBC)

Two main types of leukocytes; granulocytes and non-granulocytes were investigated.

Granulocytes:

(1) The basophil had round in shape and the nucleus was segmented with dark purple color. The cytoplasm had numerous granules occupying whole of the cytoplasm. The mean diameter of basophil was 12.83µm.

(2) The eosinophil had round and very large. The nucleus had bi-lobed and connected with thick chromatin strands. The eosinophil had large pinkish granules in the cytoplasm. The mean diameter of eosinophil was 12.7µm.

(3) The neutrophil had round and the pale gray cytoplasm with light pinkish granules was distributed. The nucleus had segmented with purple color. The mean diameter of neutrophil was 12.16µm (Table 2 and 3, Fig.2 and Plate 3).

Non-granular Leukocytes:

(1) The lymphocytes had round with rim of light blue cytoplasm. The nucleus had large round with purple color. The mean diameter of lymphocyte was11.81µm.

(2) The monocytes had large and round and its nucleus was kidney shaped with purple color. The cytoplasm had pale greyish-blue color. The mean diameter of monocyte was 12.67µm (Table 2 and 3, Fig.2 and Plate 3).

Platelets

The platelets were irregular in shape. Platelets granules were stained in pink-red. The mean diameter of platelet was 2.15µm (Table 2 and 3, Fig.2 and Plate 3).

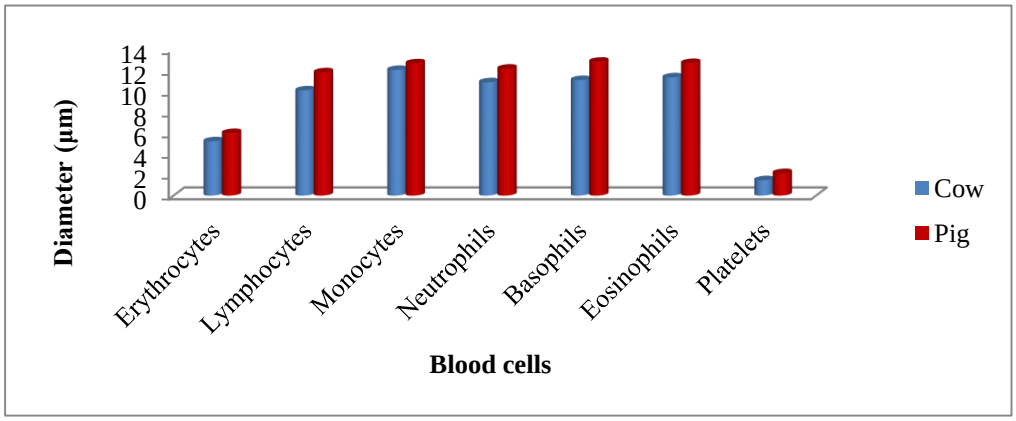

Fig. 2 Comparison of mean diameter (µm) of blood cells of cow and pig

Table 1 Mean morphometric measurement of the blood cells diameter (μm) of the collected cow species

Sr	RBC	Platelets	Lymphocyte	Monocytes	Neutrophils	Basophils	Eosinophils
1	5.9	1.2	8.6	11.1	8.9	13.1	10.5
2	5.8	1.5	9.8	10.8	11.5	10.3	11.9
3	5.8	1.9	10.4	15.2	12.2	10.6	11.2
4	5.7	1.9	11.2	14.2	11.1	12.1	16.2
5	5.4	1.6	11.7	12.5	12.3	11	12.5
6	5.1	1.2	10.6	10.6	10.4	10.2	8.9
7	5.1	1.3	9.1	13.6	9.4	9.6	10.1
8	4.5	1.4	10.1	11.1	10.1	11.5	11.1
9	4.4	1.5	8.8	10	12.3	11	10.8
10	4.3	1.2	10.5	11.3	10.4	11.3	10.1
S.D.	0.620035841	0.266874919	1.016311413	1.744324129	1.219471652	1.008904797	1.982731001
Mean	5.2	1.47	10.08	12.04	10.86	11.07	11.33
Mean ± S.D.	5.2 ± 0.62	1.47 ± 0.27	10.08 ± 1.02	12.04 ± 1.75	10.86 ± 1.22	11.07 ± 1.09	11.33 ± 1.98

Table 2 Mean morphometric measurement of the blood cells diameter (μm) of the collected pig species

Sr	RBC	Platelets	Lymphocyte	Monocytes	Neutrophils	Basophils	Eosinophils
1	6.3	1.7	9.7	10.6	12.1	13.2	12.1
2	5.4	2.4	12.9	13.2	13.7	11.9	12.5
3	6.3	2.1	14.1	10.4	12.8	13.9	12.9
4	5.9	2.3	9.9	13.8	11.8	12.3	13.1
5	6.1	1.9	10.2	13.2	12.3	13.5	11.9
6	6.2	2.3	12.7	13.2	11.9	12.1	13.3
7	5.9	2.1	11.2	12.9	12.2	13.2	12.8
8	5.8	2.8	11.9	13.1	10.5	12.9	12.7
9	5.8	1.8	12.7	13.4	11.9	11.8	13.4
10	6.2	2.1	12.8	12.9	12.4	13.5	12.3
S.D.	0.284604989	0.320589734	1.493281249	1.172888173	0.808565259	0.749888881	0.501109879
Mean	5.99	2.15	11.81	12.67	12.16	12.83	12.7
Mean ± S.D.	5.99 ± 0.28	2.15 ± 0.32	11.81 ± 1.50	12.67 ± 1.17	12.16 ± 0.89	12.83 ± 0.75	12.7 ± 0.50

Table 3 Comparison of mean diameter (μm) of blood cells of cow and pig

Sr no.	Blood cell type	Parameters	n	Cow	Pig
1	Erythrocyte	Cell	10	5.2 ± 0.62	5.99 ± 0.28
2	Leucocyte	Basophil	10	11.07 ± 1.09	12.83 ± 0.75
		Eosinophil	10	11.33 ± 1.98	12.7 ± 0.50
		Neutrophil	10	10.86 ± 1.22	12.16 ± 0.89
		Lymphocyte	10	10.08 ± 1.02	11.81 ± 1.50
		Monocyte	10	12.04 ± 1.75	12.67 ± 1.17
3	Platelet	Cell	10	1.47 ± 0.27	2.15 ± 0.32

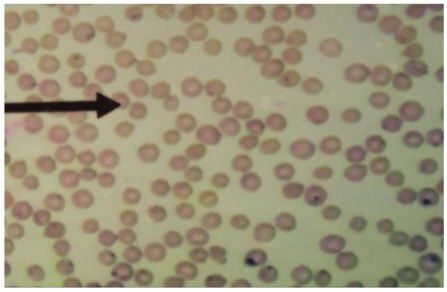

A. Red blood cell (cow)

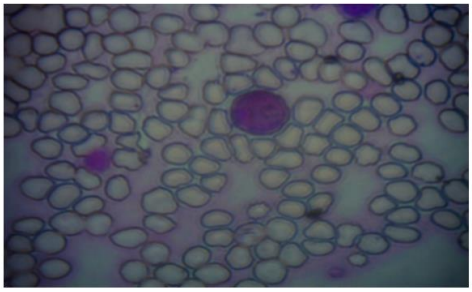

B. Red blood cell (pig)

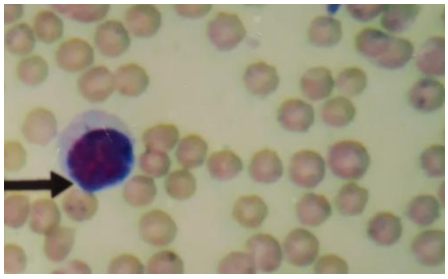

C. Lymphocyte (cow)

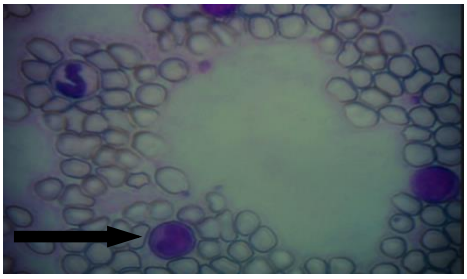

D. Lymphocyte (pig)

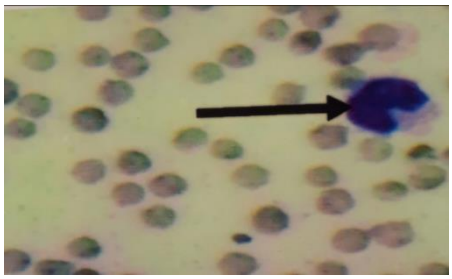

E. Monocyte (cow)

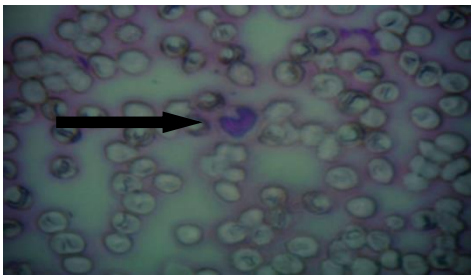

F. Monocyte (pig)

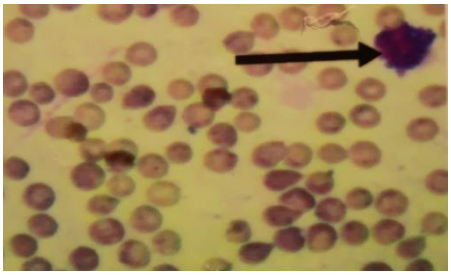

G. Basophil (cow)

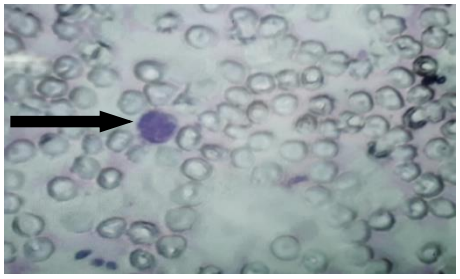

H. Basophil (pig)

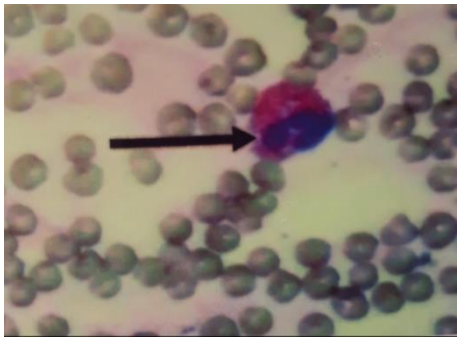

I. Eosinophil (cow)

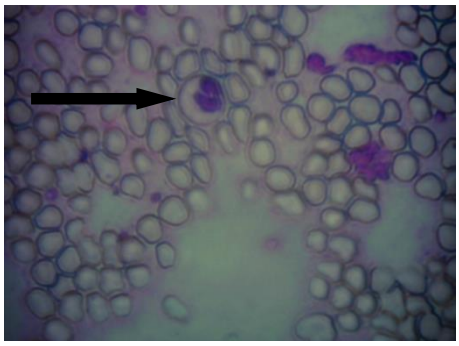

J. Eosinophil (pig)

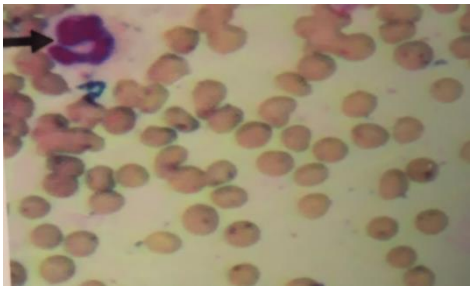

K. Neutrophil (cow)

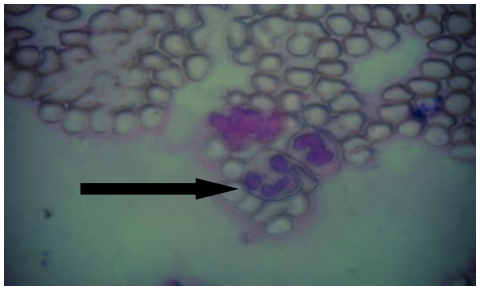

L. Neutrophil (pig)

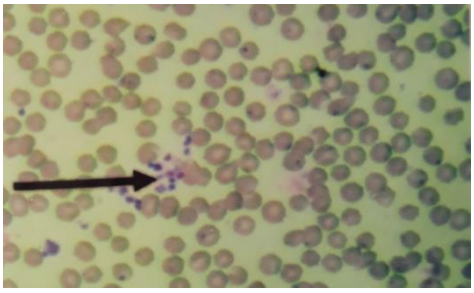

M. Platelets (cow)

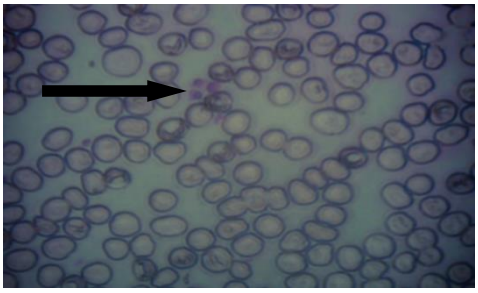

N. Platelets (pig)

K. Neutrophil (cow)

Discussion

The present study was conducted on twenty samples for cytomorphological studied on blood cells. Among them, 10 samples were domestic cows and another 10 samples were domestic pigs. From these samples, the morphological characters of the erythrocytes, leukocytes and platelets were described.

In mammals, the erythrocytes are circular, biconcave and non-nucleated (Jordon, 2004). In the previous report, the mature red blood cell of the adult cattle is biconcave in shape. Erythrocytes have an average diameter of 5-6 μm in cattle (Roland *et al*., 2014). In

Myanmar, the erythrocytes of the domestic cows were found to be round, flat disc with no central depression. Average diameter was six μm (Khin Sabae Htut *et al*., 2014). Hsu Htoo (2018) observed that the erythrocytes in cows were 5.38 μm.

In the present study, the red blood cells of *Bos taurus* (cow) were found to be round and flat disc with little or no central depression. The mean diameter of red blood cell had 5.2 μm .

The mature red blood cells of domestic mammals are non-nucleated biconcave discs. In pig and goat, red blood cells have no biconcavity and therefore appear as flattened discs (www.histology.leeds.ac.uk > *blood* Blood). Red blood cells have an average diameter of 4-8μm in pig (Hidetaka and Thomas, 2009).

In the present study, *Sus scrofa domesticus* (pig) red blood cells have non-nucleated and biconcave. The mean diameter of red blood cell had 5.99 μm .

The mean diameter of red blood cell of *Sus scrofa domesticus* (5.99μm) was larger than of *Bos taurus* (5.2μm).

In cows, the cell with the segmented nucleus and numerous, small purple granules in the cytoplasm is a basophil (Foitikvth. yolasite.com. 2013). In Myanmar, Khin Sabae Htut *et al*., (2014) described that the mean diameter of basophils were observed 12.76 μm in domestic cow. Hsu Htoo (2018) recorded that mean diameter of cow basophil was 11.44 μm .

In the present study, basophil of *Bos Taurus* (cow) had segmented with dark purple color and their cells have numerous small dark purple granules in the cytoplasm. The mean diameter had 11.07μm.

Suresh and Ishwar (2014) reported that pig basophils were roughly round in shaped and 13.25μm in size. The nuclei had 2-3 lobes, which were connected with chromatin strand.

The present work also found that basophil of *Sus scrofa domesticus* (pig) had round in shaped and the nucleus was segmented with dark purple color. The cytoplasm had numerous granules occupying whole of the cytoplasm. The mean diameter had 12.83μm.

The mean diameter of basophil of *Sus scrofa domesticus* (12.83μm) was also larger than *Bos taurus* (11.07μm).

In cow, the mean diameter of eosinophil had 12-15μm. The nucleus elongated and small, round reddish granules in the cytoplasm (vetsci-co.uk. 2018). In Myanmar, Khin Sabae Htut *et al*., (2014) described that the mean diameter of eosinophil were observed 12.91μm in domestic cow. Hsu Htoo (2018) observed that eosinophil of cow had diameter 12.01μm.

In the present study, the eosinophil of *Bos taurus* (cow) had round, nucleus bi-lobes with dark purple. The mean diameter of eosinophil was 11.33μm.

Suresh and Ishwar (2014) studied that the mean diameter was observed 12.25μm eosinophil of pig. The nuclei had 2-4 lobes. The cytoplasm was darkly stained.

In the present study, the eosinophil of *Sus scrofa domesticus* (pig) had round and very large. The nucleus had bi-lobed and connected with thick chromatin strands. The eosinophil had larger pinkish granules in the cytoplasm. The mean diameter of eosinophil was 12.7μm.

The mean diameter of eosinophil of *Sus scrofa domesticus* (12.7μm) was also larger than *Bos taurus* (11.33 μm).

In cow, segmented neutrophils are typically 10 to 12 μm in diameter. The cell with a segmented nucleus and light pink cytoplasm (foitikvth. yolasite,com, 2018). In Myanmar, Khin Sabae Htut *et al*., (2014) described that the mean neutrophils were observed 13.28 μm in domestic cow. Hsu Htoo (2018) observed that neutrophils of cow had diameter 10.13 μm.

The present work also found that the neutrophil of *Bos taurus* (cow) had round (irregular shape) and cytoplasm with light pink granules. The nucleus had segmented with purple color. The mean diameter of neutrophil was 10.86μm.

In pig, the neutrophils were round in shaped and 12.00 μm in size. The number of lobes varied from 2 to 5. The pale gray cytoplasm of neutrophil was light pinkish granules (Suresh and Ishwar, 2014).

In the present study, the neutrophil of *Sus scrofa domesticus* (pig) had round and pale gray cytoplasm with light pinkish granules. The nucleus had segmented with purple color. The mean diameter of neutrophil was 12.16μm.

The mean diameter of neutrophil of *Sus scrofa domesticus* (12.16 μm) was larger than of *Bos taurus* (10.86 μm).

In cows, lymphocyte cells size range from six to 15 μm. The cell had round and nucleus with small amounts of light blue cytoplasm (foitikvth. yolasite,com, 2018). In Myanmar, Khin Sabae Htut *et al*.,(2014) described that the mean diameter of lymphocytes were observed 12.8 μm in domestic cow. Hsu Htoo (2018) observed that lymphocyte of cow had diameter 10.17 μm.

In this study, the lymphocyte of *Bos taurus* (cow) was round with rim of light blue cytoplasm. The nucleus had large round with purple color. The mean diameter of lymphocyte had 10.08 μm.

The lymphocytes were the predominant leukocytes in pig, which were round in shape. The small medium and large sized lymphocytes were observed. Most of the lymphocytes were small sized with mean diameter 7.44 μm, medium sized 9.65 μm and large sized were 12.05 μm. In pig, most of the lymphocytes are small at about 6-9 μm in diameter. The rest are larger, about 10-14 μm in diameter (www.histology. Leeds.ac.uk > blood)).

In the present study, the lymphocyte of *Sus scrofa domesticus* (pig) had round with rim of light blue cytoplasm. The nucleus had large round with purple color. The mean diameter of lymphocyte was 11.81μm.

The mean diameter of lymphocytes of *Sus scrofa domesticus* (11.81 μm) was larger than of *Bos taurus* (10.08 μm).

In cow, monocytes are the largest size among leukocyte (15 μm to 20 μm). The shape of the nucleus may be oval, irregular, kidney-shaped and horseshoe-shaped. The cytoplasm is blue-gray (vetsci.co.uk, 2018). In Myanmar, Khin Sabae Htut *et al*., (2014) described that the mean diameter of monocytes were observed14.91μm in domestic cow. Hsu Htoo (2018) observed that monocyte of cow had diameter 12.45 μm.

In the present study, the monocyte of *Bos taurus* (cow) nucleus was bean-shaped with purple color. The cytoplasm has blue gray color. The mean diameter of monocyte of had 12.04 μm.

In pig, monocytes are the largest of the leukocyte (15 μm to 20 μm in diameter). The shape of the nucleus is highly variable and may be oval, irregular, kidney-shaped or horseshoe-shaped. The cytoplasm is pale gray-blue color (Sina, 2014).

In the present study, the monocytes of *Sus scrofa domesticus* (pig) had large and round and its nucleus was kidney-shaped with purple color. The cytoplasm had pale greyish-blue color. The mean diameter of monocyte was 12.67μm.

The mean diameter of monocytes of *Sus scrofa domesticus* (12.67 μm) was larger than of *Bos taurus* (12.04 μm).

In cows, platelets play an important role in hemostasis. Platelets are small and pale blue color. Platelets are non-nucleated cell 2-4 μm in diameter (leukocytes-VetSic, 2018). In Myanmar, Khin Sabae Htut *et al*., (2014) described that the mean diameter of platelets were observed 2.13 μm in domestic cow. Hsu Htoo (2018) observed that the mean diameter of platelets were 1.59μm in cow.

In the present study, the platelets of *Bos taurus* (cow) were small round and pale blue color. Platelets have purple central granules in stained blood smears. The mean diameter of platelet was 1.47μm in cow.

In pig, platelets have a diameter of 2-4 μm and are round or spindle-shaped (August *et al*., 2013). Platelets of pigs are small and pale blue. They have purple central granules in stained smears (Sina, 2014).

In the present, the platelets of *Sus scrofa domesticus* (pig) were irregular in shape. Platelets granules were stained in pink-red. The mean diameter of platelet was 2.15μm.

The mean diameter of platelets of *Sus scrofa domesticus* (2.15 μm) was larger than of *Bos taurus* (1.47μm).

Conclusion

The study was conducted to determine normal blood cell types in the two species (cows and pigs). Blood samples from 10 number of each species were used for the determination of hematological indices values. The morphological essays obtained in the present study were red blood cells, three granular white blood cells consisting basophils, neutrophils and eosinophil and non-granular white blood cells consisting lymphocyte and monocytes. Blood cells types are often helpful in the diagnosis of a disease.The morphometric study of blood cell show that the diameter has a significant influence on the determination the species of domestic animals. In the present study, two species (cows and pigs) were found to have normal blood cell types and normal diameter. In addition, the observing data from this work would also partially from the basis for further research on their blood.

Acknowledgements

We are greatly indebted to Dr Nay Win Oo, Rector of East Yangon University for his permission to carry out this research. We would like to express our deepest gratitude to Dr Aye Aye Ko (Pro-Rector), Dr Wah Wah Lwin (Pro-Rector) and Dr Thida Aung (Pro-Rector), East Yangon University for their kind permissions to perform this research. We wish to express our greatly indebted to Dr Ohn Mar Ohn, Professor, Head of Zoology Department, East Yangon University, for her invaluable guidance and editing of the manuscript to complete this research work.

References

August, S., H. Wilkens., B. Vollmerhaus., and K.H. Habermehl. (2013) *The circulator system, the skin and the cutaneous organs of the domestic mammals.*

Cytomorphological characterization of agranulocytes of pig www. *researchgate. net >publication* Accessed 1.7.2021

Dacie, J.V., and S.M. Lewis. (1975) *Practical Haematology*. 5th Edition. Churchill Livingston; Edinburgh London and New York, pp 13-581

Foitikvth. yolasite.com > resources > Blood Accessed 22.3.2018

Hidetaka, H., and E. Thomas, (2009) "*Genetically engineered pig red blood cells for clinical transfusion: initial in vitro studies*." Transplantation Institute, University of Pittsburgh Medical Center. Transfusion / Volume 49, Issue 11 / p.2418-2429

Hsu Htoo (2018) *Comparative morphological profile of blood cells in hybrid cattle species in Pyinmapin dairy farm, Mingaladon Township, Yangon Region*. MSc. Thesis, Department of Zoology, East Yangon University.

Jordan, E.L. (2004) *Chordate Zoology*.3.Chand & Co Delhi, New Delhi Jullunder-Lucknow, Bombay. Pp.806 813.

Khin Sabae Htut, Khin Cho Myint, Ĺe Ĺe Naing, and Kyi Kyi Than, (2014) "Haematological profiles of domestic animals from markets and slaughter house of Yangon Region." *Research Paper*. Department of Zoology, Dagon University.

Lewis, S.M. (2000) *Guidelines on Standard Operating Procedures for Haematology*. World Health Organization, South East Asia, New Delhi, pp.23-32.

Leukocytes-VetSci. *Vetsci.co.UK > learn-leukocytes* Accessed 22.3.2018

Murry, R.S. (1992) *Theory and problems of statistics*. 2nd Edition. Mc Graw - Hill Book Company: New York. Pp.198.

Roland, L., M. Drillich., and M. Iwersen, (2014) "Hematology as a diagnostic tool in bovine medicine." *Journal of Veterinary* Diagnostic investigation. Vol 26.

Schermer, S. (1958) *The Blood Morphology of Laboratory Animals*. 3rd Edition. F.A Davis Company, Philadephia, pp. 1-118.

Sina, T, (2014) "Veterinary Histology of Blood." Slide Share A Zad University of Tabriz, Veterinary Medicine Faculty. *www. slidesharee . net > Sina Taefehshokr*

Suresh, M. and S. Ishwar, (201 4) "Cytomorphological studies on granulogytes of pig." *Veterinary Science Research Journal, Volume 5*| Issue| &2|Apr.& Oct.,2014|18-2|

Thein Htut (1979) *The blood cells of some vertebrates*. M.Sc. Thesis, Department of Zoology, University of Yangon.

Tibbo, M, (2004) "Factor affecting haematological profil in three Ethiopan indigenous goat breeds." *Intern. J.Appl. Res. Vet. Med*.2 (4): 297-309

Vetsci. co.uk > learn leukodytes Accessed 22.3.2018

*www.histology.leeds.ac.uk>blood*Blood:The histology Guide. Accessed 13.4.20221

THE NESTING ECOLOGY OF SOME TERRESTRIAL BIRDS IN THE CAMPUS OF EAST YANGON UNIVERSITY, THANLYIN TOWNSHIP, YANGON REGION

Khin Maw Maw Myint[1], Thida[2], Aye Aye Than[3]

Abstract

Nesting ecology of some terrestrial bird species were studied in the Campus of East Yangon University, Thanlyin Township and Yangon Region during January to December 2020. A total of six types of nests were observed. Out of these the cup shaped nests were built by six species and it was the highest number. Slender nest was built by one species in lowest number. The nesting materials of recorded birds were grasses, leaves, cotton, plastics and coconut shells. The nesting behaviors of recorded birds were solitary and colonial behaviors. The nesting sites of *Apus affinis*, *Passer domesticus* and *Pycnonotus cafer* were artificial sites. The nests of ten species were found in wet season**.** The nests of *Passer domesticus* were found in all seasons. The nests of *Pycnonotus jocosus*, *Pycnonotus cafer* and *Pycnonotus blanfordi* were found in hot season.

Key words: Nesting birds, Nests types, Materials, Behavior, Nesting sites and seasons

Introduction

A nest is a structure built by certain animals. Nests are constructed by members of vertebrates. Each species has a distinct type of nests. Nest buildings are adaptive advantage among birds. They build in a greatest variety of forms with variety of materials, and on a variety of sites. Birds can create many different types of nests and to protect their eggs and fledglings not only predators but also from adverse weather during the breeding season. Many birds build isolated hidden nests (Gill, 2001).

Birds are the most skilled nest builders. They make nests of many different materials. Bird nests are amazing structures that come in wide range of size and shapes. The types of nest vary from simple to elaborate; platform, open cup nest, hole nest, pensile nest, dome shape nest, floating platform nest, sandy scrape nest, and mud nest. A good nesting site generally provides protection against predators, offers adequate stability. The various kinds of materials including twigs, grass, leaves were used for the nesting. These materials may help to camouflage the nests or may provide some level of insulation; they may also help to keep the eggs in place (Collias and Collias, 1984).

Durability of nests was depending on the types of materials used and nesting sites. Birds mainly used materials which are long lasting such as sticks. Cotton, feathers are soft materials used for protection against impact and provide comfort to the eggs in the nests. Nest site selection can be influenced by several factors, including nest predation risk, physiological tolerance to abiotic factors and competition (Lack, 1968).

The number of nesting birds in the study area is indicator of ecological change. The terrestrial nesting birds are a main part of terrestrial ecosystem. The types of nest differed according to the different species of the birds. The various types of nest also influence the risk of predation. Dome type nest was more safety than the other nest. The amazing nest types of *Orthotomus sutorius* Common Tailor Birds built their nest with grass, cotton and leaves by sewing their beaks. Thus, their name implies common tailor birds. The successful breeding time of birds required nesting materials. Plants matter is the

[1] Dr., Associate Professor, Department of Zoology, East Yangon University
[2] Dr., Associate Professor, Department of Zoology, East Yangon University
[3] Dr., Professor, Department of Zoology, Dawei University

most common construction materials for nests thus habitat is important. The organic nesting materials used for their nests are sticks, leaves, cotton, feathers and inorganic materials as plastics (Kyaw Nyunt Lwin and Khin Ma Ma Thwin, 2003).

Although extensive work on avian composition, diversity, population density, morphomatric of birds have been done previously. The information on nesting behavior of birds has not been carried out in East Yangon University campus. Thus nest types and nesting behavior of some bird species in East Yangon University Campus was conducted with the following objectives:

- to study the types of nest and nesting materials
- to analyze the nesting behavior of study birds
- to examine nesting sites and nesting seasons

Materials And Methods

Study area

East Yangon University campus is located at 16˚ 44' 14"North and 96˚ 17' 09" East at the southern district of Yangon region (Fig. 1).

Study period

The present research was conducted during January to December 2020.

Data collection

Data collection was carried out twice a week. The nests were carefully studied between 7:00 am to 12:00 pm by using binoculars throughout the study period but sometimes the whole day was spent for searching the nests. The photographs of the birds and their nests were taken by using digital cannon camera *sx*65*HS* (Fig. 2 A).

Identification of nesting terrestrial birds

The bird species were identified by Smythies 1953.The nest types, nesting materials and behavior were studied according to the Kyaw Nyunt Lwin and Khin Ma Ma Thwin, 2003 and nesting sites and nesting seasons were studied by Robson, 2013 (Fig. 2 B).

Fig. 1 Map of Study area

Fig. 2 A Binocular and camera

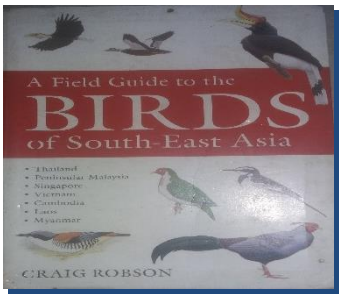

Fig. 2 B Field guide book

Results

Recorded nesting birds in East Yangon University Campus

A total 13 species belonging to 11families, four orders of nesting birds were recorded at East Yangon University Campus. Among them order Passeriformes was the highest number of the nine bird species followed by the two species of order Piciformes and by one species of Order Apodiformes and Columbiformes (Fig. 3, Table 1).

Types of nests

The cup, platform, hole, dome, irregular and slender nests were found in the study. The cup nests were built by the four species and it was the highest, followed by the irregular nests by three species, the hole and dome nests by two species each, platform and slender nests by one species each (Fig. 4, Table 2).

The nests of *Rhipidura albicollis* White-throated Fantail, *Pycnonotus jocosus* Red-whiskered Bulbul, *Pycnonotus cafer* Red-vented Bulbul and *Pycnonotus blanfordi* Streak-eared Bulbul were cup type (Plate 1).

The nest of *Streptopelia chinensis* Spotted Dove was platform type (Plate 2).

The nest of *Megalaima haemacephala* Coppersmith Barbet and *Dendrocopos analis* Spot-breasted Woodpecker were hole type (Plate 3).

The nests of *Lonchura striata* White-rumped Munia and *Ploceus hypoxanthus* Asian Golden Weaver were dome type (Plate 4).

The nests of *Apus affians* House Swift, *Passer domesticus* House Sparrow and *Acridotheres tristis* Common Myna were the irregular type (Plate 5).

The nest of *Orthotomus sutorius* Common Tailorbird was slender type (Plate 6).

The nesting materials of recorded birds

In the present study, except hole nests, resulting nesting bird species used organic materials such as coconut shell, cotton, leaves, feathers, sticks, grass and sometimes inorganic materials such as plastics for their nests (Table, 2).

The nesting behavior of recorded birds

The nesting behavior of *Apus affians* House Swif, *Passer domesticus* House Sparrow and *Ploceus hypoxanthus* Asian Golden Weaver were colonial nesting behavior and *Streptopelia chinensis* Spotted Dove, *Megalaima haemacephala* Coppersmith Barbet, *Dendrocopos analis* Spot-breasted Woodpecker, *Rhipidura albicollis* White-throated Fantail, *Lonchura striata* White-rumped Munia, *Acridotheres tristis* Common Myna, *Pycnonotus jocosus* Red-whiskered Bulbul, *Pycnonotus cafer* Red-vented Bulbul, *Pycnonotus blanfordi* Streak-eared Bulbul and *Orthotomus sutorius* Common Tailorbird were solitary nesting behavior (Table, 2).

Nesting sites

Different species of birds used different nesting sites to build their nests. Some birds used natural nesting sites such as trees (*Lagerstroemia spp*. Pyinma tree, *Samanea saman* rain tree, *Pterocarpus macrocarpus Kurz.* Padauk tree, *Mangifera indica* mango tree, *Pithecellobium dulce* manila tamarind tree, *Trientalis borealis* star-flower tree, *Euphobia milii* Kiss-me-quick flower plant, *Citrus lemon* lemon plant (Hundley and Chit Ko Ko, 1987). Some other birds used artificial nest sites such as ceiling, lamppost and wall. The nest site of *Apus affians* House Swift was ceiling at convocation hall, the nest site of *Passer domesticus* House Sparrow was in the telephone wire box at lamppost and the nest of *Pycnonotus cafer* Red-vented Bulbul were found at the wall of building number 1 in the study (Table 3).

Nesting season of recorded birds

Nesting season differs according to the different species of birds. Among the recorded bird nests of *Streptopelia chinensis* Spotted Dove and *Apus affinas* House Swift, *Megalaima haemacephala* Cppersmith Barbet, *Dendrocopos analis* Spot-breased Woodpecker, *Rhipidura albicollis* White-throated Fantail, *Lonchura striata* White-rumped Munia, *Ploceus*

hypoxanthus Asian Golden Weaver, *Acridotheres tristis* Common Myna *Orthotomus sutorius* Common Tailorbird were found in wet season.

The nests of *Rhipidura albicollis* White-throated Fantail, *Pycnonotus jocosus* Red-whiskered Bulbul, *Pycnonotus cafer* Red-vented Bulbul, *Pycnonotus blanfordi* Steak-eared Bulbul were found and hot season. The nests of *Passer domesticus* House Sparrow were recorded in the all seasons (Fig. 5, Table 3).

Table 1 Recorded nesting birds in East Yangon University Campus

No.	Order	Family	Species	Common name
1	Columbiformes	Columbidae	*Streptopelia chinensis*	Spotted Dove
2	Apodiformes	Apodidae	*Apus affinis*	House Swift
3	Piciformes	Megalaimidae	*Megalaima haemacephala*	Coppersmith Barbet
4	Piciformes	Picidae	*Dendrocopos analis*	Spot-breasted Woodpecker
5	Passeriformes	Rhipididuridae	*Rhipidura albicollis*	White-throated Fantail
6	Passeriformes	Estrilididae	*Lonchura striata*	White-rumped Munia
7	Passeriformes	Passeridae	*Passer domesticus*	House Sparrow
8	Passeriformes	Ploceidae	*Ploceus hypoxanthus*	Asian Golden weaver
9	Passeriformes	Sturnidae	*Acridotheres tristis*	Common Myna
10	Passeriformes	Pycnonotidae	*Pycnonotus jocosus*	Red-whiskered Bulbul
11	Passeriformes	Pycnonotidae	*Pycnonotus cafer*	Red-vented Bulbul
12	Passeriformes	Pycnonotidae	*Pycnonotus blanfordi*	Streak-eared Bulbul
13	Passeriformes	*Sylvidae*	*Orthotomus sutorius*	Common Tailorbird

Table 2 Nest types, materials and nesting behavior of recorded birds

No.	Species	Nest types	Nesting materials	Nesting behavior
1	*Streptopelia chinensis*	platform	sticks, leaves	solitary
2	*Apus affinis*	irregular	leaves, feathers	colonial
3	*Megalaima haemacephala*	hole	nil	solitary
4	*Dendrocopos analis*	hole	nil	solitary
5	*Rhipidura albicollis*	cup	coconut shells	solitary
6	*Lonchura striata*	dome	grass	solitary
7	*Passer domesticus*	irregular	grass, leaves	colonial
8	*Ploceus hypoxanthus*	dome	grass	colonial
9	*Acridotheres tristis*	irregular	grass	solitary
10	*Pycnonotus jocosus*	cup	grass, leaves	solitary
11	*Pycnonotus cafer*	cup	grass, plastics	solitary
12	*Pycnonotus blanfordi*	cup	grass	solitary
13	*Orthotomus sutorius*	slender	leaves, cotton	solitary

Table 3 Nesting sites and season of recorded birds

No.	Species	Nesting site		Nesting season		
		Natural	Artificial	Hot	Wet	Cool
1	*Streptopelia chinensis*	Pyinma tree	-	-	√	-
2	*Apus affinis*	-	ceiling	-	√	-
3	*Megalaima haemaecphala*	Padauk tree	-	-	√	-
4	*Dendrocopos analis*	Rain tree	-	-	√	-
5	*Rhipidura albiocollis*	Star-flower tree	-	-	√	-
6	*Lonchura striata*	Lemon tree	-	-	√	-
7	*Passer domesticus*	-	lamp post	√	√	√
8	*Ploceus hypoxanthus*	Manila tamarind tree	-	-	√	-
9	*Acridotheres tristis*	Mango tree	-	-	√	-
10	*Pycnonocus jocosus*	Kiss me quick plant	-	√	-	-
11	*Pycnonotus cafer*	-	wall	√	-	-
12	*Pycnonotus blanfordi*	Star-flower tree	-	√	-	-
13	*Orthotomus sutorius*	Mango tree	-	-	√	-
	Total			4	10	1

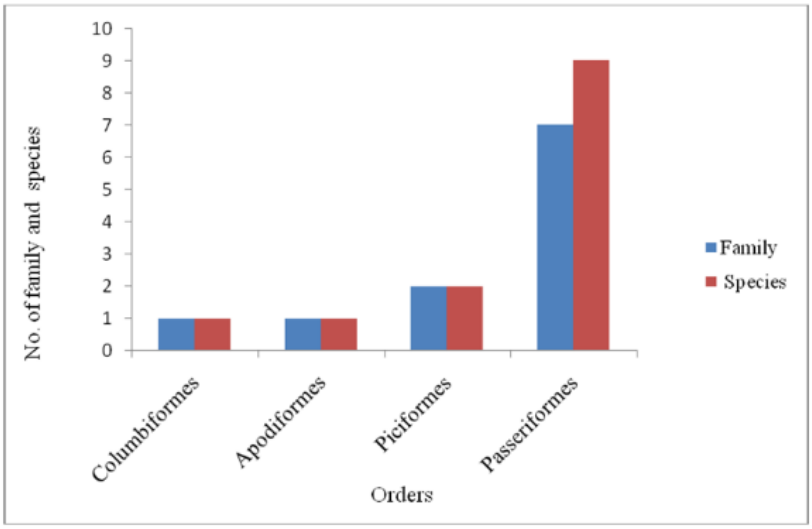

Fig. 3 Numbers of recorded nesting terrestrial birds during the study

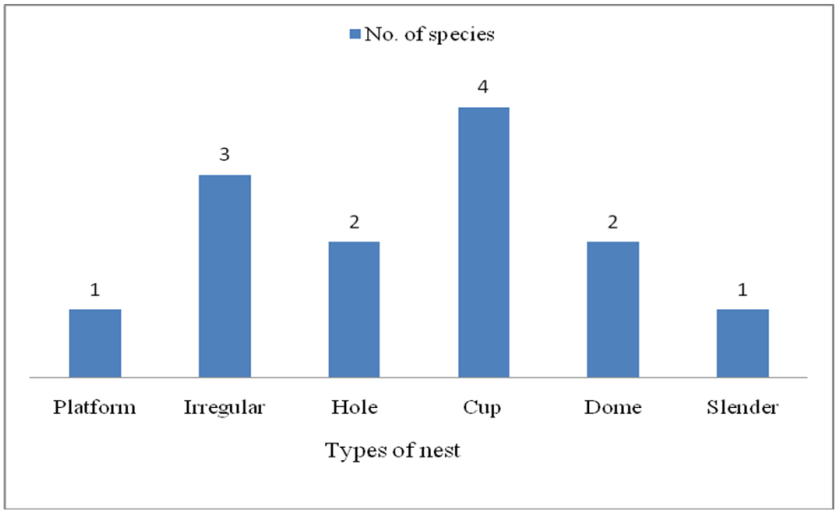

Fig. 4 Nest types of recorded terrestrial birds during the study

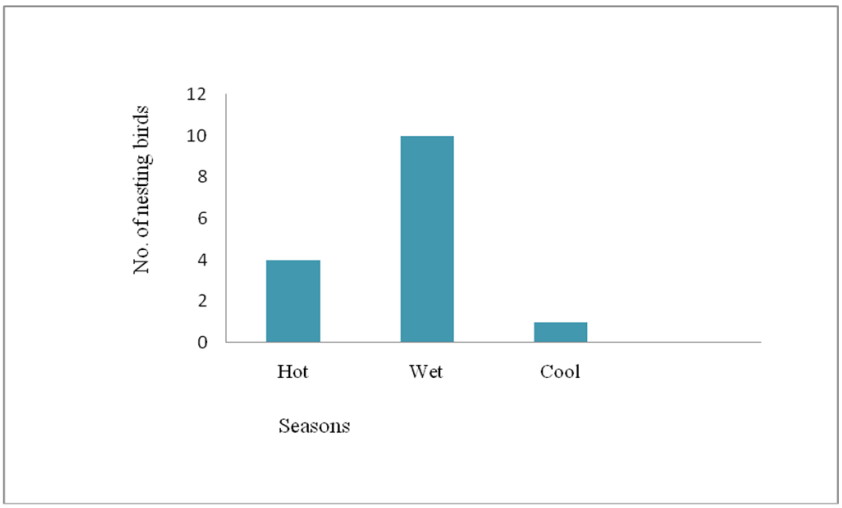

Fig. 5 Relationship between the nesting terrestrial birds with the season

A *Rhipidura albicollis* B *Pycnonotus jocosus* C *Pycnonotus cafer* D *Pycnonotus blanfordi*

Plate 1 Cup type of recorded nesting birds

Plate 2 Platform type of *Streptopelia chinensis*

A *Megalaima haemaecphala* B *Dendrocopos analis*

Plate 3 Hole type of recorded nesting birds

A *Lonchura striata* B *Ploceus hypoxanthus*

Plate 4 Dome type of recorded nesting birds

A *Apus affinis* B *Acridotheres tristis* C *Passer domesticus*.

Plate 5 Irregular type of recorded nesting birds

Plate 6 Slender type of *Orthotomus sutouris*

Discussion

The presence of colonial nesting birds indicate that East Yangon University Campus support the required energy for the nesting birds. The colonial nesting birds such as *Apus affinis* House Swift, *Ploceus hypoxanthus* Asian Golden Weaver and *Passer domesticus* House Sparrow are very important as vital signs of the health of our university campus. These birds must acquire large quantities and high quality of food during their nesting season as they select mates, build nests and lay eggs and rear fledglings. The advantages of colonial nesting behavior are susceptible to disturbance and predation pressure. Solitary nesting behavior has some disadvantages because predators especially domesticated animals

(cat and dogs) can destroy their nests and fledglings. The selection of nesting sites was determined by the availability of food and safety of nesting birds. Trees and shrubs habitats were essential for nesting birds.

U Tin Htut (2010) recorded that seven types of nest are found in Thongwa Township. Among them cup nest was the most common in his study. He also stated that the different species of birds built the different types of nests with the sticks, leaves, cotton, plastics and grass. The most nests were recorded in wet season.

In the present study, six types of nest were recorded and cup nestwas the common. The nesting materials were sticks, leaves, grass, cotton and plastics. The most nesting birds were found in the wet season. This finding agrees with above author. This may be assumed that both study area (habitats, topography and climate) located in same district.

The nesting species, *Pycnonotus jocosos* Red-whiskered Bulbul, *Pycnonotus cafer* Red-vented Bulbul and *Pycnonotus blanfordi* Strek-eared Bulbul were frugivorous birds. The nests of these species were found in hot season. These may be due to fruits (such as mango, banyan, banana and guava) were abundant in this season in the study area.

Li *et al*. 2009 revealed that the arthropods (insects) were more distributed in the wet season. In ecosystem, birds are tremendous importance because of indicators of environmental conditions.

The recorded nesting birds *Apus affinis* House Swift, *Megalaima haemacephala* Coppersmith Barbet, *Dendrocopus analis* Spot-breasted Woodpecker, *Rhipidura albicollis* White-throated Fantail, *Lonchura striata* White-rumped Munia, *Ploceus hypoxanthus* Asian Golden Weaver and *Orthotomus sutorius* Common Tailorbird were found in wet season. These birds were said to be insectivorous birds.

The Campus of East Yangon University provides the natural habitat for the shelter of the nesting birds. Because of the study area get the tropical monsoon climate with three seasons. The wet season was prolonging from mid-may to October (Department of Meteorology and Hydrology, Yangon Region, 2020). Trees were full of canopy in wet season. This may be assumed that habitat during wet season provide more safety than other seasons for nesting birds.

The study area posses the trees, shrubs and small wetlands. Thus these areas provide shelter, feeding and nesting places not only for bird species but also insects, amphibians and reptiles. Although some human activities disturbed their nests, birds selected their nest sites near human activities for the safety of their nests which reduced the chance of predation by predatory birds like crow.

According to Law of Forest Department 2009, the recorded nesting birds were seasonally protected birds species. These species must be protected from human disturbances during their breeding time.

Conclusion

For the conservation of nesting birds, conservation of nesting sites is necessary. Birds are sensitive indicators of pollution in all ecosystems. They are the best monitors of environmental changes. By studying the nesting of birds one can predict natural disasters such as earthquakes storm and flooded by heavy rain. The study of nesting birds would share the conservation knowledge between birds and their habitats for the students. Thus the loss of habitats and disturbance of birds should be conserve priority.

Acknowledgements

We are very grateful to Dr Nay Win Oo, Rector of East Yangon University for his permission to present this research paper. We are also indebted to Pro-Rector Dr Aye Aye Ko, Pro-Rector Dr Wah Wah Lwin and Pro-Rector Dr Thida Aung, East Yangon University for their permission to present this research paper.

We would like to express my profound gratitude to Dr Ohn Mar Ohn, Professor and Head of Zoology Department, East Yangon University, for her suggestions during the course of research.

References

Collias, N.E. & E.C. Collias. (1984). *Nest building and bird behaviour*. Princeton University Press, Princeton, New Jersey.

DMH, 2020. Department of Meteorology and Hydrology, Kabaraye Branch, Yangon Region. https://www.moezala.gov.mm. Downloaded 15th January 2020. Forest Department, 2009. *Fourth National Report to The United Nation as Covention of Biological Diversity, Ministry of Forestry*. Government of the Union of Myanmar.

Forest Department, 2009. *Fourth National Report to The United Nation as Covention of Biological Diversity, Ministry of Forestry*. Government of the Union of Myanmar.

Gill, F.B. (2001) *Ornithology* 2nd ed. W.H. Freeman and Company, New York, 766Pp.

Hundley, H.G. & Chit Ko Ko. (1987) *List of trees, shrubs, herbs and principle climbers, at recorded from Burma with Vernacular Names of fourth Revised Edition*. Government Printing Press. Yangon

Kyaw Nyunt Lwin and Khin Ma Ma Thwin. (2003) *Birds of Myanmar*, Swiftwinds Services Co., Ltd, Yangon, Myanmar.

Lack, D. (1968) *Ecological adaptation for breeding in birds*. Methuen, London, 409 Pp.

Li, J., L., You-quing, H., Tong-yi, S., Juan, C.,Yu-jie, and K. Heliovaara, (2009) "Diversity and dominant species of arthropods in different forests of Aeshan, Inner Mongolia". *Forestry Studies in China*, Vol.11, No.1:1-8(Abstract only).

Robson, C. (2013) *A field Guide to the Birds of South-East Asia*. UK: new Holland Publisher.

Symthies, B. E. (1953). *The Birds of Burma*.Third Edition Nimrod press Ltd and Silvio Matta chehione and Co. Ltd.

Tin Htut (2010) *Breeding Ecology of Bird Species in Thongwa Township,Yangon Division*. Ph.D Dissertation, Yangon University.

SPECIES COMPOSITION AND CATCH WEIGHT OF FISHES FROM DIFFERENT WHOLESALES IN KALAGWEL VILLAGE, THANLYIN TOWNSHIP

Aye Aye Mu [1]Nyo Mie Kyaing[2]

Abstract

The study area was chosen at Kalagwel Village, Thanlyin Township for observation on the spatial fluctuation of some fishes in different wholesales. This study was carried out during the period from December, 2018 to September, 2019. Three fish wholesales were selected as the study sites. They are Ma Aye fish wholesale (Site I), Ngwe Nagna fish wholesale (Site II) and Khin Htar Kyi wholesale (Site III). A total of 10 species under 10 genera and 10 families belonging to five orders of fishes were recorded. Clupeiformes (one species), Siluriformes (four species), Perciformes (three species) Gobiiformes (one species) and Mugiliformes (one species) were recorded. *Tenualosa ilisha* (263 kg) had highest catch weight followed by *Pangasius pangaisus* (219 kg) while *Rhinomugil corsula* (16 kg) was the lowest.Total catch weight of Site II (501 kg) was the highest followed by Site I (348 kg), while that of Site III (212 kg) was the smallest.

Key words: wholesale, catch weight, spatial fluctuation.

Introduction

Myanmar is well-known for its richness of natural resources including extensive inland water bodies which can provide freshwater, brackish water and marine fish population. (Pereira, 2000). Fish is crucial in Myanmar people while it is certainly recognized that fish is second only to rice in the diet of Myanmar (DoF, 2007). An Inland fishery, Myanmar is one of the top ten countries in terms of production in the world (Coates, 2002).

Freshwater and brackish water fish fauna is abundant in Thanlyin Township. Kalagwel Village is located in Thanlyin Township. It is situated along the river. Rural populations are closely linked with Bago River as an integral part of their livelihood approaches. This feature undoubtedly reflects a bearing on inland fisheries. Kalagwel village is well developed in the transportation sector and arrived driving by car about one and half hours from Yangon. Most of the aquatic products are exported to Yangon through fish wholesales. Therefore, this area was chosen to study the spatial fluctuation of some fishes in different wholesales.

The present study was conducted with following objectives;

- to study and identify the collected fish species from the study sites
- to assess the catch weight of the collected species

Materials And Methods

Study area and study sites

Kalagwel Village was chosen as the study area. It is located between 16° 56' N and 95° 96' E. Three fish wholesales were selected as the study site. They were Ma Aye fish wholesale (Site I, 16° 49' 12´´N and 96° 17' 19´´E), Ngwe Nagna fish wholesale (Site II, 16° 49' 14´´N and 96° 17' 23´´E) and Khin Htar Kyi fish wholesale (Site III, 16° 49' 13´´N and 96° 17' 27´´E) (Fig. 1 and Plate 1).

Study period

[1] Demonstrator, Department of Zoology, East Yangon University
[2] Dr, Associate Professor, Department of Zoology, East Yangon University

The study period lasted from December, 2018 to September, 2019.

Specimen collection

Monthly data collection was carried out in each study site. Specimens were recorded in fresh and were subjected to study immediately before discoloured. Scaled photographs were instantly taken to get natural size and colour. Interview surveys were performed to obtain the necessary data such as local name and catch weight for each species.

Identification of fish species

Identification was followed after Talwar and Jhingran (1991).

Fig.1 Map of study area

Source: Department of Geography (East Yangon University)

A. Site I

B. Site II

C. Site III

Plate 1 Study sites

Results

Collected some fish species from the study area

A total of 10 species under 10 genera and 10 families belonging to five orders of fishes were collected from the study area during the study period.

There were one species of fish representing in each family Clupeidae *Tenualosa ilisha*, Siluridae *Wallago attu*, Bagridae *Mystus guilo*, Pangasiidae *Pangasius pangasius*, Ariidae *Arius thalassinus*, Sciaenidae *Chrysochir aureus*, Polynemidae *Polynemus paradiseus*, Centropomidae *Lates calcarifer*, Oxudercidae *Apocryptes bato* and Mugilidae *Rhinomugil corsula* respectively (Table 1, Plate 2).

Among the recorded species of percentage level, the composition of order Siluriformes (40%) was the highest followed by order Perciformes (30%), while orders Clupeiformes, Gobiiformes, Mugiliformes (10% for each) were the smallest (Fig.2).

Table 1 Collected some fish species in study area

Order	Family	Sr. No	Study Species (Scientific Name)	Common Name	Local Name
Clupeiformes	Clupeidae	1	*Tenualosa ilisha* (F. Hamilton, 1822)	Hilisa shad	Nga Tha Lauk
Siluriformes	Siluridae	2	*Wallago attu* (Bloch, 1801)	Helicopter catfish	Nga Bud
	Bagridae	3	*Mystus guilo* (Hamilton, 1822)	Long whiskered catfish	Nga ZinYaing
	Pangasiidae	4	*Pangasius pangasius* (Hamilton, 1822)	Pangas catfish	Nga Dan
	Ariidae	5	*Arius thalassinus* (Ruppell, 1837)	Giant cat fish	NgaYway
Perciformes	Sciaenidae	6	*Chrysochir aureus* (Richardson, 1846)	Croker	Nga Poke Thin
	Polynemidae	7	*Polynemus paradiseus* (Linnaeus, 1758)	Mango fish	Nga Pon Nar
	Centropomidae	8	*Lates calcarifer* (Bloch, 1970)	Giant sea perch	Ka Ka Tit
Gobiiformes	Oxudercidae	9	*Apocryptes bato* Valenciennes, 1837	Mud skipper	Nga Byat
Mugiliformes	Mugilidae	10	*Rhinomugil corsula* Hamilton, 1822	Mullet	Nga Zing

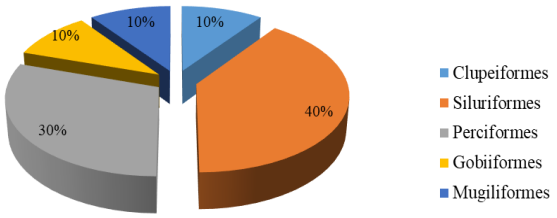

Fig.2 Percent composition of collected species in respective orders

Monthly catch weight (kg) of collected species from the study sites

During the study period, catch weight of collected species were observed from three fish wholesales. All collected species were found in all three study sites in December and January. *Tenualosa ilisha*, *Wallago attu* and *Pangasius pangasius* were found at all study sites in all months involved during study period. *Rhinomugil corsula* was not found at all study sites in all months except December and January (Table 2, 3, 4).

In site I, monthly catch weight was highest (64 kg) in July (Table 2). In site II, June had high recorded catch weight (92 kg) than other months (Table 3). In site III, monthly catch weight was highest (38 kg) in January (Table 4).

In total catch weight of collected species from different study sites, the highest total catch weight was recorded in *Tenualosa ilisha* (263 kg). The lowest catch weight of *Rhinomugil corsula* (16 kg) was recorded (Table 5).

A. *Tenualosha ilisha Pangasius* B. *Wallogo attu* C. *Mystus gulio* D. *Pangasius pangasius*

E. *Arius thalassinus* F. *Chrysochir aureus* G. *Polynemus paradiseus* H. *Lates calcarifer*

I. *Apocryptes bato* J. *Rhinomugil corsula*

Plate 2 Recorded species

Comparison of total catch weight (kg) from different study sites

Comparatively, total catch weight obtained from Site II (501kg) was the highest followed by Site I (348 kg), while that of Site III was the lowest (212kg) during the study period (Table 6).

Table 6 Comparison of total catch weight (kg) from different study sites

Sr.No	Study site	Total catch weight (kg)
1	Site I	348
2	Site II	501
3	Site III	212

Table 2 Monthly catch weight (kg) of collected species at Site I

Sr. No	Species	December	January	February	March	April	May	June	July	Total (kg)
1	*Tenualosa ilisha*	13	13	13	12	12	12	8	7	90
2	*Wallago attu*	3	2	3	2	3	7	10	10	40
3	*Mystus gulio*	2	2	3	-	-	-	10	10	27
4	*Pangasius pangasius*	8	8	8	10	10	8	13	13	78
5	*Arius thalassinus*	2	3	2	-	-	-	-	-	7
6	*Chrysochir aureus*	3	3	-	-	-	10	5	12	33
7	*Polynemus paradiseus*	5	5	-	-	7	10	8	8	43
8	*Lates calcarifer*	3	3	-	-	-	-	-	2	8
9	*Apocryptes bato*	2	2	3	-	-	5	3	2	17
10	*Rhinomugil corsula*	3	2	-	-	-	-	-	-	5
	Total	44	43	32	24	32	52	57	64	348

1viss = 1.63kg

Table 3 Monthly catch weight (kg) of collected species at Site II

Sr. No	Species	December	January	February	March	April	May	June	July	Total (kg)
1	*Tenualosa ilisha*	16	16	16	16	13	10	8	8	103
2	*Wallago attu*	5	5	5	3	3	12	12	12	57
3	*Mystus gulio*	2	2	3	3	3	13	12	10	48
4	*Pangasius pangasius*	10	10	10	8	12	12	15	15	92
5	*Arius thalassinus*	2	3	3	-	-	-	-	-	8
6	*Chrysochir aureus*	5	5	5	3	10	13	13	10	64
7	*Polynemus paradiseus*	5	5	5	7	7	16	16	5	66
8	*Lates calcarifer*	3	2	-	-	-	-	8	8	21
9	*Apocryptes bato*	2	2	2	3	3	8	8	8	36
10	*Rhinomugil corsula*	3	3	-	-	-	-	-	-	6
	Total	53	53	49	43	51	84	92	76	501

1viss = 1.63kg

Table 4 Monthly catch weight (kg) of collected species at Site III

Sr. No	Species	December	January	February	March	April	May	June	July	Total (kg)
1	*Tenualosa ilisha*	12	12	10	10	8	8	5	5	70
2	*Apocryptes bato*	2	2	2	-	-	-	3	3	12
3	*Wallago attu*	2	2	2	3	3	5	7	7	31
4	*Mystus gulio*	2	2	-	-	-	-	10	10	24
5	*Pangasius pangasius*	5	5	7	7	3	2	10	10	49
6	*Arius thalassinus*	2	2	-	-	-	-	-	-	4
7	*Chrysochir aureus*	2	3	-	-	-	-	-	-	5
8	*Polynemus paradiseus*	3	5	-	-	-	-	-	-	8
9	*Lates calcarifer*	2	2	-	-	-	-	-	-	4
10	*Rhinomugil corsula*	2	3	-	-	-	-	-	-	5
	Total	34	38	21	20	14	15	35	35	212

1viss = 1.63kg

Table 5 Total catch weight of collected species from different study site

Sr. No	Species	Site I	Site II	Site III	Total (kg)
1	*Tenualosa ilisha*	90	103	70	263
2	*Wallago attu*	40	57	31	128
3	*Mystus gulio*	27	48	24	99
4	*Pangasius pangasius*	78	92	49	219
5	*Arius thalassinus*	7	8	4	19
6	*Chrysochir aureus*	33	64	5	102
7	*Polynemus paradiseus*	43	66	8	117
8	*Lates calcarifer*	8	21	4	33
9	*Apocryptes bato*	17	36	12	65
10	*Rhinomugil corsula*	5	6	5	16
	Total	348	501	212	1061

1viss = 1.63kg

Discussion

A total of 10 species under 10 genera and 10 families belonging to five orders of fishes were recorded from the study area. The collected species number may be said to be few in number because of limited duration of study period and study area. Although number of species caught was few; all were found to be commercially important.

Wint Naing Aung (2017) studied economic importance of some fishes in different depots of Maubin Township, Ayeyarwady Region. In her study, 15 species under 15 genera and 13 families belonging to four orders of fishes were recorded from the study area. Three species of present study such as *Wallago attu, Mystus guilo* and *Pangasius pangasius* were similar to the fishes which recorded by Wint Naing Aung (2017).

Species occurrence and economic importance of some marine fish in Phyapon Township, Ayeyarwady Region was studied by Thiri Shwe Sin (2018). She reported that a total of 18 species of 16 genera belonging to 14 families of five orders were described from her study sites. Only one sepcies, *Tenualosa ilisha* recorded by Thiri Shwe Sin (2018) was also recorded in the present study.

According to species composition, order Siluriformes (46.67%) was the highest followed by order Perciformes (33.33%) were recorded in the catch (Wint Naing Aung, 2017). Based on finding data, species composition of Siluriformes (40%) followed by order Perciformes (30%) were recorded to be of highest percentage in different study sites during the study period. This data is in agreement with the reported by Wint Naing Aung (2017).

Thiri Shwe Sin (2018) reported that Perciformes (11 species, 61%), Clupeiformes (two species, 11%), Siluriformes (two species, 11%), Carcharhiniformes (two species, 11%) and Pleuronectiformes (one species, 6%) were observed. In the present study, four species of fish in order Siluriformes (40%) was the highest number species in Thanlyin Township, Yangon Region. Order Perciformes (three species, 30%) was also observed. It is not agree with the finding of Thiri Shwe Sin (2018). It could be assumed that fishes of order Perciformes were abundant in Phyapon Township, Ayeyarwady Region.

According to catch weight of collected species, the highest total catch weight was recorded in *Tenualosa ilisha* (263 kg) in the present study. Wint Naing Aung (2017) reported that the high total catch weight was recorded in *Channa striatus* (19715 kg). It was not similar to the present study.

According to the data described in a comparison of total catch weights from different study sites, the highest catch weight 501 kg was present in site II, while 348 kg in site I and lowest catch weight 212 kg in site III. So, it may be assumed that the given price for fishes at the Site II is higher than other Site. So, most of the fishermen sold their caught fish to Site II.

According to the result, it was found that Kalagwel Village is also famous as one of the good fisheries grounds and as the important centre of fishery sector in Myanmar. The result and finding of present work will give some important information about species and monthly catch weight of collected fish species to both academic field and fisheries workers. Moreover, findings of the present surveys would be shared the information about the livelihood of local communities in chosen study sites and aided in conducting further extensive research processes.

Conclusion

In the present study, *Chrysochir aureus*, *Tenualosa ilisha*, *Apocryptes bato* and *Pangasius pangasius* were found to be collected from all three study sites in all months involved during study period. Thus, this species may be regarded as predominant species. *Tenualosa ilisha* and *Pangasius pangasius* were found in the high classes of large-scale

fishery process. It was found that these species were now more popular and attractive export marketing species.

Acknowledgements

We would like to express our profound gratitude to Dr Nay Win Oo, Rector of East Yangon University for his keen interest and also for his permission. We are indebted to Dr Aye Aye Ko, Pro-Rector, Dr Wah Wah Lwin, Pro-Rector and Dr Thida Aung, Pro-Rector, East Yangon University for their supports, permitting to conduct this work and confidence in the implementation of this research. We would like to express our profound gratitude to Dr Ohn Mar Ohn, Professor and Head of Zoology Department, East Yangon University, for her valuable suggestions and encouragement. We are greatly indebted to Dr Aye Thida Than, Professor, Department of Zoology, East Yangon University, for her valuable suggestions given throughout the research work.

References

Coates, D, 2002. *Inland capture fishery statistics of Southeast Asia*: current status and information needs. Asia - Pacific Fishery Commission, FAO, Regional Office for Asia and the Pacific, Bangkok, Thailand.

DoF**,** 2007. Fishing gears and methods of introduction in rural of Myanmar (internet). (cited 2007 November 8). Available from http://map.seafdec. Org /monograpy… Myanmar/ Marine.php.Cached.

Pereira, G., 2000. Women in fisheries in Latin America. Accessible at http://www.Iied.org/ docs/ Sarl/ sust, 25 January 2005.

Talwar, P.K. and Jhingran, A.G., 1991. *Inland fishes of India and adjacent countries*, Vol.I and II. Oxford and IBH Publishing Co.Pvt Ltd, New Delhi.

Thiri Shwe Sin**,** 2018. Species occurrence and economic importance of some marine fishes in Phyapon Township, Ayeyawardy Region. *MSc Thesis*, Department of Zoology, Maubin University.

Wint Naing Aung, 2017. Economic importance of some fishes in different depots of Maubin Township, Ayeyawardy Region. *MSc Thesis*, Department of Zoology, Maubin University.

SEASONAL PREVALANCE RATE AND LARVAL OCCURRENCE OF *AEDES AEGYPTI* (LINNAEUS, 1762) IN THREE QUARTERS OF THARKAYTA TOWNSHIP, YANGON REGION

Wint Yee Phyo[1], Khin Maung Oo[2]

Abstract

The life cycle and seasonal occurrence of *Aedes aegypti* were studied in Ten North, Two North and Six West quarters in Tharkayta Township. During December 2018 to October 2019. The numbers and lengths of different stages during life cycle of *Aedes aegypti* were found in relevant tables and photographs. The prevalence rates of larva of *Aedes aegypti* in different container categories in three quarters of Tharkayta Township found to be the survival rate of different stages in life cycle of *Aedes aegypti* may be depending on cool, hot and rainy seasons. The present results show that HI, BI and CI values of both study sites were highest in monsoon period (rainy season) and gradually decrease cool season period and the lowest values in hot season. Ten North quarter was found higher positive major containers than Two North quarter and Six West quarter in all surveys. Six West quarter was found higher positive minor containers than Two North quarter and Ten North quarter all surveys. Six West quarter was found lowest positive miscellaneous containers than Two North quarter and Ten North quarter all surveys.

Keyword: Seasonal occurrence, prevalence rates, different container, index value, *Aedes aegypti*

Introduction

Aedes aegypti is one of the world's most widely distributed mosquitoes and considerable medical importance as a vector of dengue and yellow fever (Service, 1992). *Aedes aegypti* is the only proven vector of dengue in the western hermisphere, and studies of the epidemiology of the disease in panama by Rossen would indicate that it is probably the only vector in America.

Aedes aegypti is a major vector of dengue, dengue hemorrhagic fever and dengue shock syndrome (DF/DHF/DSS) in many subtropical and tropical countries. In human, dengue infection ranged from simple fever to much more severe and sometimes fetal dengue hemorrhagic fever (DHF) and dengue shock syndrome (DSS) (Halsteas, 1980). In Southeast Asia, dengue hemorrhagic fever (DHF)is a major cause of mortality among children (Halsted,1980) while dengue fever (DF) occurs epidemically and affecting older children and adults (WHO,1980). The age group between 5-9 yeas is mainly affected by DHF followed by the age groups of 1-4 and 10-14 years.

In Myanmar, a severe outbreak of DHF occurred for the first time in Yangon during 1970. The disease has spread to Rakhine State during 1957 and now occurs in all states and regions except Kayah State (VBDC, 1990). The highest number of DHF cases was recorded in July (the rainy season) corresponds to high densities of *Aedes aegypti* mosquitoes, the vectors of DHF (Tin Mar Yi Tun, 2007).

It is important to recognize the vulnerable time in the life cycle of a vector and correct forecast of population increase number known environmental condition. This information provides a sound basis for the planning of an effective control programmed. Before any attempt is made to employ either chemical or biological control, the ecology of vector mosquito and the mechanism of disease transmission must be understood.

Preventive vaccines are not yet available commercially. Thus prevention of mosquito bite by personal protection and control of the vectors are the only methods available to prevent Dengue/DHF: In drawing up strategies for *Ae. aegypti* control, it is essential that

[1] Demonstrator, Department of Zoology, East Yangon University
[2] Dr, Professor/head (Retired) Department of Zoology, Myitkyina University

detail biology and ecology of the mosquito should be studied. As the DHF cases are correlated to the density of *Aedes aegypti* of the locality, factors influencing the seasonal abundance of the vector needed to be studied in detail.

Water storage practices in Tharkayta Township provide breeding sites become established only in the rainy season. The present study was to determine the prevalence and bionomics of immature *Aedes aegypti* in different container categories to provide larval densities in study areas.

The present study was to determine the prevalence and bionomics of immature *Aedes aegypti* in different container categories and types at selected areas in order to provide basic information on the larval densities in areas.

This study is aimed to determine the role of the vector *Aedes aegypti* based on larval density and indicates the impact of Dengue fever in Tharkayta Township.

The outcome of this study would be applied for mosquito control. For that reason, the present study included in survival rate in different stages of progeny of each female mosquitoes in laboratory and the larval abundance with substrate preference of field survey in three quarters of Tharkayta Township.

Therefore, this study was aimed to carry out with the following objectives:

- to investigate the substrate preference of *Aedes aegypti* from breeding sources
- to examine the larval abundance of studied area from Tharkayta Township
- to study the different stages of life cycle of *Aedes aegypti* in the laboratory

Materials And Methods

Study Area

Ten North, Two North and Six West quarters were chosen as study sites. It is located between Latitude 16° 48′ N to16° 48′ N and Longitude 96° 12 ′ E to 96° 14 ′ E (Fig. 1).

Study period

The study was conducted during December 2018 February 2019 (cool season), March 2019 to May 2019 (hot season) and June 2019 to October 2019 (rainy season) using nonintervention descriptive field investigation method.

Larva positive containers

Larva positive containers of different containers categories and types were recorded and compared in association with the seasons (Plate 1).

The breeding sources were divided into major and minor sources. Metal drums (half or full drums), glazed or unglazed earthen jars (up to a size 30 litters), old can and discarded car tyres were considered as major sources. Other sources such as flower vases, small glazed earthen jars and ant-guards were considered as minor sources. Miscellaneous container categories contain discarded utensils and hollow bamboo pole (Plate 2).

Larval Indices Larval survey was carried out in the selected sites. Larval examination method of Sheppard, Mac Donald, *et al.* (1969) was used to confirm the presence of larvae in the containers.

Two North Quarter

Ten North Quarter

Six West Quarter

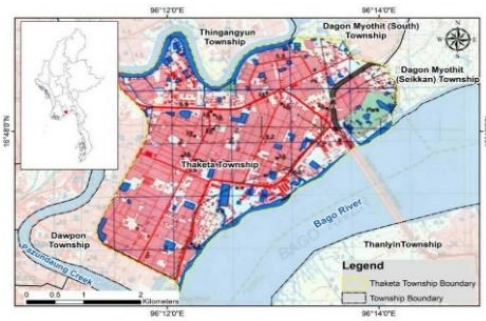

Fig. 1 Map of three quarters in Tharkayta(source-civil map)

A. Various plastic cups rearing different stages of lifecycle of *Aedes aegypti* mosquito

B. Light microscope

Plate 1 Laboratory experiment apparatus and examining larval stages

A. Major container B. Minor container C. Miscellaneous

Plate 2 Larval survey in study sites

Larval indices were calculated as follow;

Container Index (CI) = $\frac{\text{No. of positive containers x 100}}{\text{No. of houses positive for } \textit{Aedes}}$

House Index (HI) = $\frac{\text{Total number of containers}}{\text{Total number of house examined}}$

Breteau Index (BI) = No. of positive container per 100 house

(Bang.1984)

Laboratory experiments

DHF vector, *Aedes aegypti*, larvae in high risk areas within study sites were collected and checked for the taxonomic status. Some were reared in the laboratory conditions.

For the laboratory experiment, newly hatched larvae from Ten North quarter were randomly put into white cups to compare the developmental processes of larvae in relation to different types. The number of pupae and emerged adult males and females were recorded. Egg, first, second, third and fourth stages of larvae were randomly measured for their total length under light microscope.

Results

Systematic position

The classification of *Aedes aegypti* was followed after Knight and Stone, 1997.

Phylum	-	Arthropoda
Class	-	Insecta
Order	-	Diptera
Suborder	-	Nematocera

Super family	-	Culicoidea
Family	-	Clicidae
Genus	-	*Aedes*
Species	-	*Aedes aegypti* (Linnaeus, 1762)

Distinctive characters of adult *Aedes aegypti*

It has very characteristic thoracic marking that almost alone serve to distinguish it. In addition, the marking of the mid-femur, a white line on the anterior surface extending from the base almost to the tip is peculiar to this species of Stegomyia. There is a patch of white scales on each side of the clypeus in the female, the clypeus of male is usually, however, bare or has only a few scales (Fig. 2).

Adult *Aedes* mosquitoes are distinguished from other types of mosquitoes by their narrow and typically black body, unique patterns of light and dark scales on the abdomen and thorax, and alternating light and dark bands and the legs. Females are further distinguished by the shape of the abdomen, which usually comes to a point at its tip and by their maxillary palps, which are shorter than the proboscis. *Aedes* mosquitoes characteristically hold their bodies low and parallel to the ground with the proboscis angled downward when landed. (Source: https//www.britannica.com>animal)

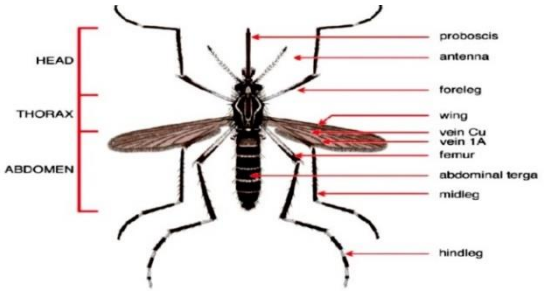

Fig. 2 External features of *Aedes aegypti* (Source: https://en.m.wikipedia.org > wiki)

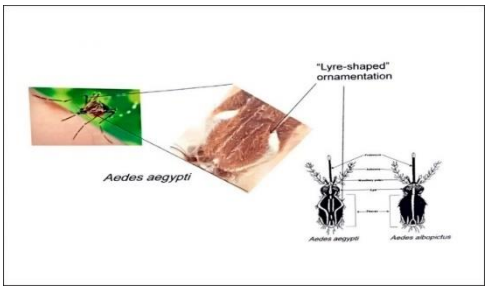

Fig. 3 Prominent feature of *Aedes aegypti* (Source:VBDC)
VBDC – Vector Borne Disease Control

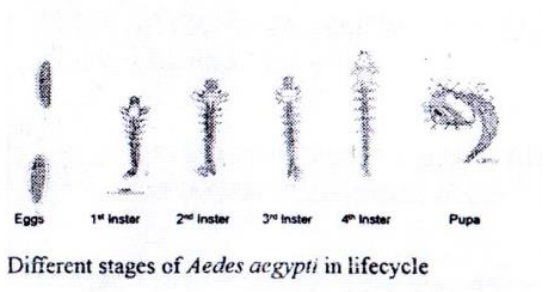

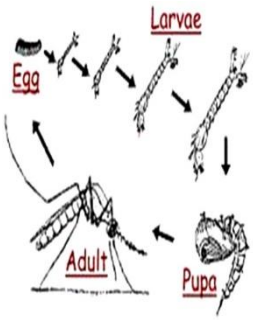

Fig. 4 Different stages in life cycle of *Aedes aegypti* (Source: intownhawk.com)

Different stages of *Aedes aegypti* in lifecycle (Fig. 4,5 and 6)

Four stages in the lifecycle of *Aedes aegypti* namely, egg, larva, pupa and adult. Eggs are white and soft when newly laid but later turn black and become the first instar is recognized by the presence of an egg-breaker on the dorsum of the head. The second instar larva is same in length as the first instar but is bulkier. The third instar larva has prominent structure of tail comb-spine. The fourth instar larva shows the rudiments of the pupal respiratory trumpets. Pupae are comma shaped and also called tumblers.

Egg laying habit

Aedes aegypti were not laid on dry surface. They preferred wet surface and on water surface. The laid on wet filter paper or wet sponge in laboratory conditions. Egg may be laid freely on water where they float ventral surface up wards. When eggs were laid on water there were usually a certain number which sank to the bottom as well as some float on the surface. The eggs laid on wet surface anchored the substrate with their sticky chorionic pad.

Description of the egg

The eggs are small, intensely black, elongate oval seed-like bodies. Under the microscope they appeared somewhat torpedo-shaped with one end, the anterior rather thicker. At the anterior pole is the micropyle, indicated pole has not special modification of structure. The egg had flattened upper surface and a more convex lower surface. These two surfaces further differ not only in shape but also in other respects. Both are covered with polygonal marking which under certain circumstance stood out conspicuously as a network of milky white lines.

The first instar larva

The first instar when newly hatched measured about a millimeter in length, but grew to reach nearly twice of that measurement. The duration of first instar was one day. The first instar can be identified by the presence of the egg breaker on the dorsum of the head.

The second instar larva

The second instar after ecdysiast was much the same length as the fully grown first instar, but was bulkier and the swollen head was enormous. The tracheal trunks were enlarged and lined with aecidia and the terminal portions in the siphon were ballooned. As in the previous instars the head darkened and the body became long and cylindrical, whist with increase in size. During the sound instars larval stage, it grew in length 3 to 4 mm the duration of second instar was one to two days.

The third instar larva

The third instar had certain characters of its own. Head measurements of this stage were more variable than any another stages having different sizes of head. The head capsule contained ecdysial lines. The pre ecdysis stage is rather long and thin and size was 5 to 7 mm. The duration of third instar was one to two days.

The fourth instar larva

The size of fourth instar was 7 to 7 mm and became much stouter due to development of the thoracic marginal buds and accumulation of fat body. The larval had relatively large head, very long lateral hairs, longer siphon. The duration of fourth instar was one to two days.

The pupa

Aedes aegypti pupa consisted of a large globular anterior portion, cephalothorax, and a narrow articulated abdomen which was normally kept flexed under the cephalothorax and was used to propel the insect when swimming. This outward appearance was largely a simulacrum, the result of gluing together of head, body, wing and legs.

At the front of the cephalothorax was the flattened head with the trunk like a keel. Conspicuous on the sides of the head were the large compound eyes and behind these the five ocelli. In front of the compound eyes were antennae. Thorax had respiratory trumpet, wing roots and their pairs of legs. The duration of pupa was one to two days.

Seasonal larval surveys

Seasonal larval surveys were inspected Ten north, Two north and Six west quarters. In three study sites, high risk area of DHF due to highest index values of Site 3; HI (113.09), BI (81.49) and CI (50.09) were found in cool season (first survey). In three study sites, high

risk area of DHF due to highest index values of Site 3; HI (54.6) and CI (24.25), Site 1; BI (46.62) was found in hot season (second survey) and high risk area of DHF due to highest index values of Site 1; HI (169.02) and CI (60.37), Site 3; BI (91.86) was found in rainy season (third survey) (Table 1).

Seasonal larval surveys were inspected from Ten North, Two North and Six West quarters. In three study sites, Ten North quarter was high risk area of DHF due to high Index values of HI (169.02) and CI (60.37), Six West was high risk area of DHF due to high Index values of BI (91.86) in rainy season (Table 2).

In cool season (first survey), House Index (HI) value, Breteau Index (BI) value and Container Index (CI) value of Two North quarter were higher than Six West quarter and Ten North quarter. In hot season (second survey), HI and CI values of Two North quarter was higher than those of the Ten North quarter while BI value was higher than in Ten North quarter Even in rainy season (third survey), HI, BI and CI values of Two North quarter were higher than Ten North and Six West quarter (Table 2)

Table 1 The larval indices of three study sites in Tharkayta Township

(A) HI, BI and CI values of first survey (cool season)

	HI	BI	CI
Site 1	49.97	32.88	17.54
Site 2	80.47	62.58	33.96
Site 3	113.09	81.49	50.09
Average	81.18	58.98	33.86

(B) HI, BI and CI values of second survey (hot season)

	HI	BI	CI
Site 1	47.81	46.62	18.82
Site 2	28.43	21.72	11.51
Site 3	54.6	41.74	24.25
Average	43.61	36.7	18.2

(C) HI, B1 and CI values of third survey (rainy season)

	HI	BI	CI
Site 1	169.02	86.7	60.37
Site 2	108.71	64.11	43.86
Site 3	128.53	91.86	42.86
Average	135.42	80.89	49.03

Site 1 - Ten north quarter

Site 2 - Two north quarter

Site 3 - Six west quarter

Table 2 Seasonal surveys of HI, BI and CI in three study sites

(A) House Index (HI) of three study sites in first, second and third surveys

House Index(HI)	Cool Season	Hot Season	Rainy Season
Ten North	49.97	47.81	169.02
Two North	80.47	28.43	108.71
Six West	113.09	54.6	128.53

(B) Breteau Index (BI) three study sites in first, second and third surveys

Breteau Index(BI)	Cool Season	Hot Season	Rainy Season
Ten North	32.88	46.62	86.7
Two North	62.58	21.72	64.11
Six West	81.49	41.74	91.86

(C) Container Index (CI) of three study sites in first, second and third surveys

Containers Index(CI)	Cool Season	Hot Season	Rainy Season
Ten North	17.54	18.82	60.37
Two North	33.96	11.51	43.86
Six West	50.09	24.25	42.86

The percentage of various positive containers

The percentages of positive major containers in Ten North quarters the first surveys were 55.71%, second and third were 25.35%, and 26.31% respectively. The Two North quarter in first, second and third surveys were 50.84%, 12.9% and 51.89% respectively. The Six West quarter in first, second and third surveys were 42.85, 18.68 and 43.33% respectively.

The percentages of positive minor containers from Ten North quarter, the first survey were 65.21%, second and third were 11.11% and 0% respectively. The Two North quarter in first, second and third surveys were 40%, 10.52% and 35.71 respectively. The Six West quarter in first, second and third survey were 41.66%, 30.76% and 62.5% respectively.

The percentage of positive Miscellaneous containers from Ten North quarter in first, second and third survey were 26.31%, 7.14% and 60% respectively. The percentage of positive Miscellaneous containers from Two North quarter in first, second and third survey were 14.28%, 11.11% and 40.74% respectively. The percentage of positive Miscellaneous containers from Six West quarter in first, second and third survey were 44.44%, 23.33% and 43.58% respectively (Table 3).

Table 3 Percentage of Major, Minor, Miscellaneous containers in study period

(A) Percentage of Major, Minor, Miscellaneous containers in first survey

	Major Containers		Minor Containers		Miscellaneous Containers	
	Inspected Containers	Positive Containers	Inspected Containers	Positive Containers	Inspected Containers	Positive Containers
Ten North quarter	76	20(26.31%)	11	0	38	10(26.31%)
Two North quarter	79	41(51.89%)	14	5(35.71%)	14	2(14.28%)
Six West quarter	60	26(43.33%)	8	5(62.5%)	18	8(44.44%)

(B) Percentage of Major, Minor, Miscellaneous containers in second survey

	Major Containers		Minor Containers		Miscellaneous Containers	
	Inspected Containers	Positive Containers	Inspected Containers	Positive Containers	Inspected Containers	Positive Containers
Ten North quarter	71	18(25.35%)	45	5(11.11%)	38	6(7.14%)
Two North quarter	93	12(12.9%)	38	4(10.52%)	27	3(11.11%)
Six West quarter	91	17(18.68%)	13	4(30.76%)	30	7(23.335)

(C) Percentage of Major, Minor, Miscellaneous containers in third survey

	Major Containers		Minor Containers		Miscellaneous Containers	
	Inspected Containers	Positive Containers	Inspected Containers	Positive Containers	Inspected Containers	Positive Containers
Ten North quarter	70	39(55.71%)	23	15(65.21%)	25	15(60%)
Two North quarter	59	30(50.84%)	15	6(40%)	27	11(40.74%)
Six West quarter	84	36(42.85%)	36	15(41.66%)	39	17(43.58%)

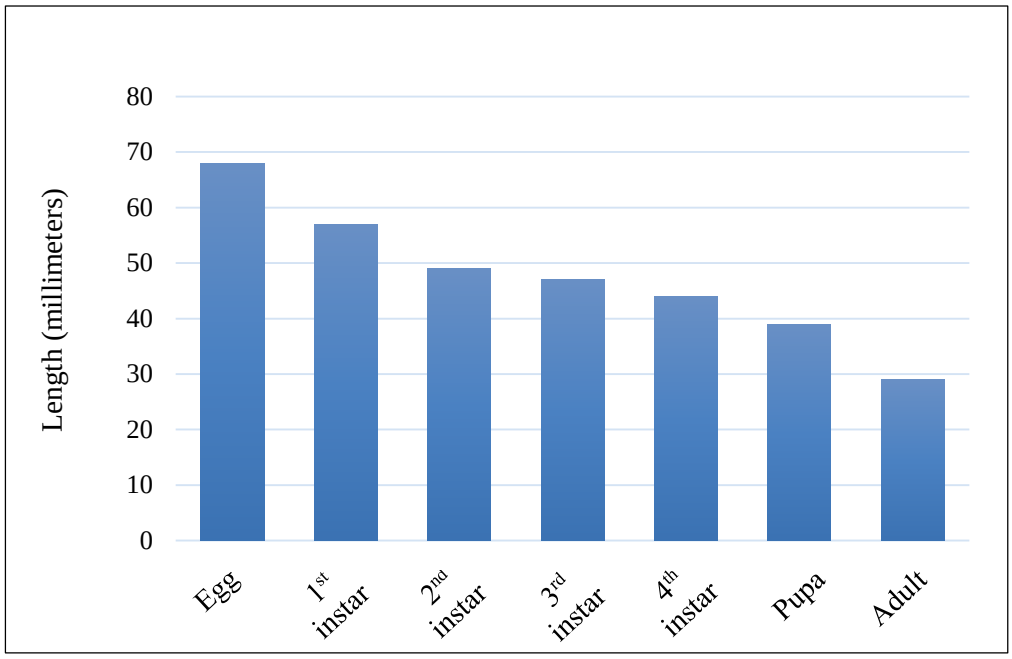

Fig. 5 Population numbers of different stages of *Aedes aegypti* during life cycle

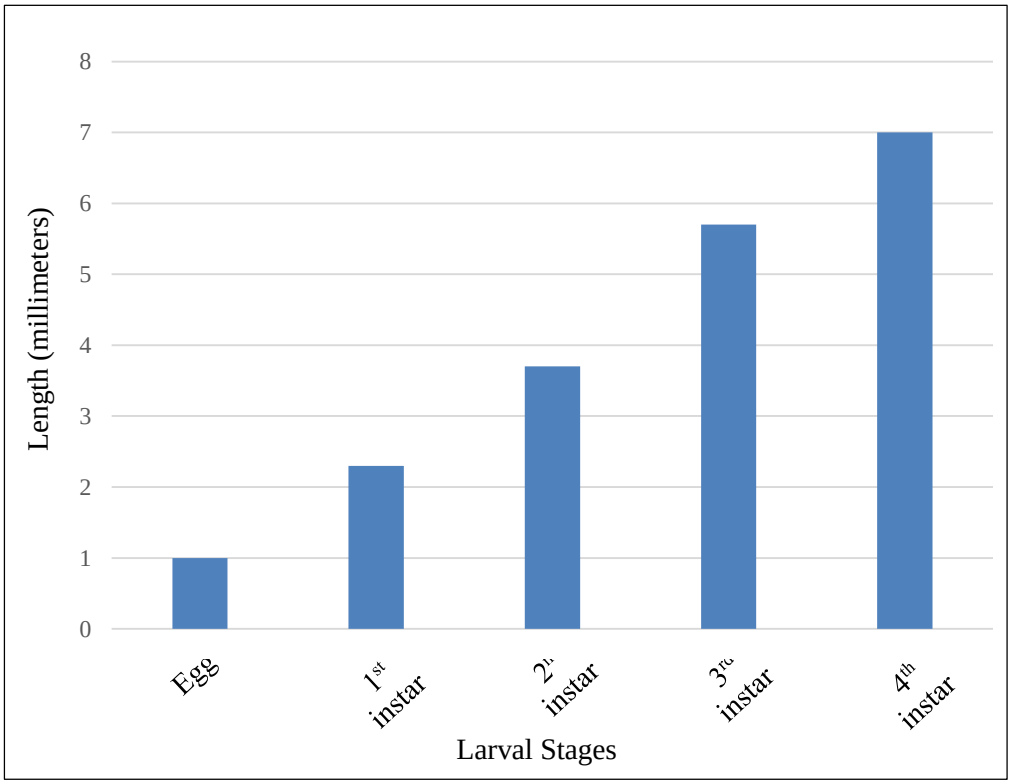

Fig. 6 Comparison between growth lengths in millimetres different stages in life cycle

Discussion

The present results showed that the populations of different stages of life cycle were gradually decreased and the higher stages of life cycle were coincided the higher growth length.

The present study emphasizes on the life cycle of *Aedes aegypti* based on this knowledge effective control strategies should emphasize on travel source reduction which will be an important achievement for long term vector control. The population numbers, growth length and other attributes of *Aedes aegypti* from different stages in their life cycle since these were focal points, which were target in control activities. The present results show that the populations of different stages in life cycle were gradually decreased.

The survival rate of different stages in life cycle of *Aedes aegypti* may be depend on cool, hot and rainy seasons.

Aedes aegypti larvae were mainly found in plastic drums and concrete tanks, which are the major water containers. Breeding sites of *Aedes aegypti* larvae were different from one area to another. The larval population size of *Aedes aegypti* was high in major domestic containers which were more productive than indoor containers due to the fact that the large containers were kept without any covers while the indoor containers were kept covered.

For the development of community based vector control programs for dengue prevention, one of the key components is to formulate an adequate classification scheme for the different containers in which immature *Aedes* mosquitoes develop. Such a standardized scheme would permit more efficient targeting of efforts and resources in the most productive way possible.

The present study emphasizes on the lifecycle of *Aedes aegypti.* Based on this knowledge effective control strategies should emphasize on larval source reduction which will be and important achievement for long-term vector control.

Ten North quarter was found higher positive major containers than Two North quarter and Six West quarter in all surveys.

Ten North quarter was highest density breeding area of DHF vector of *Aedes aegypti* because of high in major and miscellaneous containers for breeding source of *Aedes aegypti.*

The population numbers, growth length and other attributes of *Aedes aegypti* from different stages in their lifecycle were studied since these focal points, which were target in DHF control activities. In the present study there was a significant increase in total positive premises and positive containers as well as all three types of container categories in the monsoon season. The larvae were found developing in the containers even in cool season and increased in number during monsoon season when containers were filled with rainwater. Six West quarter was found higher positive minor containers than Two North quarter and Ten North quarter all surveys. Ten North quarter was found higher positive miscellaneous containers than Two North quarter and Six West quarter in all surveys. Various water storages containers were found increase in urbanization which provided breeding places for *Aedes aegypti* mosquitoes, the vector of DHF.

Phyu Nyein Aye (2012) described that HI, BI and CI values were highest in pre monsoon period (rainy season) and gradually decrease in post monsoon period and the lowest values in cool season in Sittway, Rakhine Region.

The present results agree with Phyu Nyein Aye and show that HI, BI and CI values of both study sites were highest in rainy season and gradually decrease in cool season and hot

season. The high in HI, BI and CI values indicated to high density of DHF vector. Thus, rainy season was found in the highest density of *Aedes aegypti* mosquitoes and this period was needed to control the DHF, especially in 10 North quarter following to Two North and Six West quarter in Tharkayta Township.

Phyu Nyein Aye (2012) found that Pyi-daw-thar was higher positive major containers (major breeding source) than Ywa-gyi-myauk in all surveys and so Py-daw-thar was highest density breeding area of DHF vector of *Aedes aegypti* in Sittway, Rakhine Region.

The present results also found that Ten North quarter was found higher positive major containers than Two North quarter and Six West quarter in all surveys. Ten North quarter was highest density breeding area of DHF vector of *Aedes aegypti* because of high in major and miscellaneous containers for breeding source of *Aedes aegypti* in Tharkayta Township, Yangon Region.

Conclusion

The survival rate of different stages in life cycle of *Aedes aegypti* may depend on cool, hot and rainy seasons. Seasonal occurrence of *Aedes aegypti* larvae in some major, minor and miscellaneous containers has been studied. Ten North quarter was found higher positive major containers than Two North quarter and Six West quarter in all surveys. Comparative study of *Aedes aegypti* prevalence in HI, BI and CI values in some high risk areas of three quarters in Tharkayta Township seasonally.

Acknowledgements

We are very grateful to Dr. Nay Win Oo, Rector of East Yangon University for his permission to work this research. We would like to thank Dr. Aye Aye Ko, Dr. Wah Wah Lwin and Dr. Thida Aung, Pro-Rectors, East Yangon University, for their permission to work on the present topic. We are grateful appreciated to Professor Dr. Ohn Mar Ohn, Head of Zoology Department, East Yangon University, for her valuable suggestion during the observation of this work and criticism the manuscript. I would like to express my deep gratitude to Dr. Aye Thida Than, Professor of Zoology Department, East Yangon University, for her kind helps and cooperation throughout the research work.

References

Britannica, 2022. https// www. britannica.com > animal accepted date 21 oct 2022.

Halstead, S.B. 1980. *Aedes aegypti.* Why can't we control it? *Bull Soc vector Ecol*, 13:304-311

Halstead, S.B. 1980. Dengue haemorrhagic fever a public health problem and a Field for research. *Bull. Wld. Hlth* Org., 58: 1-21

Phyu Nyein Aye, 2012. Life cycle and seasonal occurrence of *Aedes aegypti* (Linnaeus 1762) in some areas of Sittway Environs, Rakhine State.

Service, M.W. 1992. Importance of ecology in *Aedes aegypti* control. *South East Asia Journal* of Trap. Med. Pub. Hlth 23(4); 221-226.

Sheppard, P.M, W. W, Mae Donald, R.J. Tonn and B.Grab., (1969). The dynamics of an adult population of *Aedes aegypti* in relation to dengue haemorrhagic fever in Bangkok. *Journal of Animal Ecology*, 38:661-702

Tin Mar Yi Tun, 2007. Biology and some ecological aspects of *Aedes aegypti* (Linnaeus, 1762) in some high risk of areas of Yangon City.

Vector Borne Disease Control, 1990. *Dengue haemorrhagic fever in Myanmar*.

WHO, 1980. *Guide for diagnosis, treatment and control of dengue hemorrhagic fever* (second edition).

A STUDY OF THE DIFFERENT TOXICITY OF VIPER'S VENOM IN KAUNGYANGON TOWNSHIP, YANGON

Zin Moe Swe[1], Ni Lar Than[2]

Abstract

Vipers from different localities of highest snake bite cases in Myanmar collected by Myanmar Pharmaceutical Factory MPF were morphologically identified. All collected specimens were *Daboia siamensis.* This species is the most important cause of life-threatening snake bite and acute renal failure in Myanmar. This resarch was carried out at the laboratory of Myanmar Pharmaceutical Factory (MPF), Hmawbi Branch, Yangon during the period of December, 2018 to September, 2019. The venom of 20 specimens (including males and females) from study area was extracted and the toxicity and lethality of venom LD_{50} (50% Lethal Dose) were calculated. The results of this study showed that LD_{50} of *D. siamensis* lies between 3.4 to 4.3 μg/mouse in intravenous injection of dilution. The findings of this study showed that venoms of *D. siamensis* in the study areas can be neutralized and be effective to human.

Key words: vipers, venom, toxicity, Myanmar Pharmaceutical Factory

Introduction

The serpent, or snake, is one of the oldest and most wide spread mythological symbols. The word is derived from Latin serpents, a crawling animal or snake. Snakes have been associated with some of the oldest rituals known to mankind (Robbins et al., 2007) and represent dual expression of good and evil (Eward, 2007).

Snakes rely on venom to disable prey and aid in the digestive process. Snake venom is the poisonous, typically yellow fluid and it is stored in the modified salivary glands of venomous snakes. There are hundreds of venomous snake species that rely on the venom they produce to debilitate and immobilize their prey. Venom is composed of a combination of proteins, enzymes, and other molecular substances. Protein constitutes more than 90% of snake venom. Each type of venom contains more than a hundred different proteins. These toxic proteins cause the most harmful effects. It also contains enzymes, which help to speed up chemical reactions that break chemical bonds between large molecules. These enzymes aid in the breakdown of carbohydrates, proteins, phospholipids, and nucleotides in prey. Toxic enzymes also function to lower blood pressure, destroy red blood cells, and inhibit muscle control. An additional component of snake venom is polypeptide toxin. Polypeptides are chains of amino acids, consisting of 50 or fewer amino acids. Polypeptide toxins disrupt cell functions leading to cell death. Some toxic components of snake venom are found in all poisonous snake species, while other components are found only in specific species (Bailey, 2018).

Snake venom has been classified into three main types: cytotoxin, neurotoxin, and haemotoxin. Other types of snake toxins affect to some types of cell and it include cardiotoxins, myotoxins and nephrotoxins. Viperine venom is typically haemotoxic (blood toxins), necrotising (death of tissue), and anticoagulant (preventing the blood from clotting), although a neurotoxic component is present in the venom of some species (Bailey, 2018).

These toxics substances work to destroy cells, disrupt nerve impulses, or both. Snakes use their venom cautiously, injecting amounts sufficient to disable prey or to defend against predators. Snake venom can destroy the cells and tissues and it can lead to paralysis, internal bleeding, and death to the victim. For venom to take effect, it must be injected into tissues or enter the blood stream. Although the snake venom is poisonous and deadly, researchers find to use snake venom components to develop drug to treat human disease (Bailey, 2018).

[1] Demonstrator, Department of Zoology, East Yangon University
[2] Dr, Professor Head, Department of Zoology, Pathein University

The assessment of snake venom median lethal doses (LD_{50}) is an important step for an accurate evaluation of the toxic activity of specific venom, and is also regularly used to select the relevant anti-venom batch, as well as to establish the neutralizing capacity of each vial. According to the WHO, venom lethality is expressed as median lethal dose (LD_{50}). LD_{50} is the dose of venom, injected into the tail vein, which kills 50% of mice over 24 hours (WHO, 2010a). The LD_{50} value is defined as the amount of a substance (or venom) causing death of 50% injected mice. The LD_{50} for snake venom was first determined in mice by Meier and Theakston in 1986. For calculating LD_{50} by any one method: Find out the least tolerated (smallest) dose (100% mortality) and most tolerated (highest) dose (0% mortality) by hit and trial method. Once these two doses are determined, select at least 5 doses in between them, and observe mortality due to these doses. Apply correction factor to 0% and 100% mortality group (for 0% dead = 100 [0.25/n] and for 100% dead = 100x (n-0.25/n), where n= number of death). The percentage mortality values are converted to probit values by reading the corresponding probit units from the probit table. Plot the probit value against log doses and read LD_{50} value as the dose that corresponds to probit.

Therefore, the statistic data for *Dabioa* spp. in relation with the gradients of their venoms and their localities are needed to study in Myanmar. The faunal diversity of major groups of snakes in Myanmar has not been carefully studied. The aim of this study was to provide the knowledge in order to manufacture highly potent and cost-effective anti-snake venom serum by the determination of LD_{50} tend to manufacture the most appropriate antivenoms for the different localities in Kaungyangon Township, Yangon Myanmar. For the above reasons, the present study was conducted with the following objectives:

- to calculate the toxicity and lethality of venom LD_{50} of *Dabioa siamensis* in the study area
- to find the gradients of the venom of *Dabioa siamensis* in Kaungyangon Township

Material And Methods

Study area and the study site

Vipers from Kaungyangon Township, Yangon Region that were collected by Antivenom production plant in Myanmar Pharmaceutical Factory (MPF) was studied for investigation of their toxicity. Myanmar Pharmaceutical Factory was formerly known as BPI (Burma Pharmaceutical industry). (Plate 1)

Study period

The present research work lasted from December, 2018 to September, 2019.

Identification and Classification

The classification and identification of recorded snakes were followed after Smith (1943), Cox *et al*. (1998), Leviton *et al*. (2003) and Das *et al*. (2010).

Method of venom neutralizing potency tests

Laboratory mice were used for preclinical testing of new or existing antivenoms for essential medium Lethal venom Dose (LD_{50}) determination. Taxonomic identity and geographical origin of each individual animal used for venom production was recorded.

Extraction of snake venom

Venom was extracted from batch (20 snakes) for testing. Twenty collected snakes (males and females) from Kaungyangon Townships were used for obtaining venom for the experiment. Strong and healthy specimens was used for milking venom. Those were undergoing quarantine, or were gravid, undergoing treatment for sickness or injury, or in the process of sloughing their skins were avoid for venom production.

Storage of snake venom

About 8.0ml of venom (about 0.4ml/snake) per one batch were extracted from the snakes and frozen at (-80°C) as soon as after extraction. It took for 24 hours and dried in the freeze dryer (- 40°C) for three days. After three days, about 30mg of dry venom pounder were weighted by using the digital balance and preparing for dilution.

Preparation of snake venom solution to be used in LD_{50} experiments

The dry venom was diluted with five different levels of normal saline to inject into the intravenous vein of tail of the mice. The five tubes of diluted normal saline with venom were shaken five times by hand. Then, these tubes were kept in the incubator for 30 minutes. After that, the tubes were placed at room temperature for 30 minutes. The preparation for dilution was completed and one tube of normal saline with venom was used for injection into the one group of mice (five individuals).

The dry venom was diluted with five different levels of normal saline to inject into the intravenous vein of tail of the mice. The five tubes of diluted normal saline with venom were shaken five times by hand. Then, these tubes were kept in the incubator for 30 minutes at 37°C. After that, the tubes were placed at room temperature for 30 minutes. The preparation for dilution was completed and one tube of normal saline with venom was used for injection into the one group of mice for LD_{50} test. The mice of ICR strain weighted by 19 gm were used for experiments of LD_{50} test.

Injection for LD_{50} test

Deaths are recorded at 24 hours. A range of venom doses causing 0% to 100% lethality was established. Totally 120 mice (30 mice for one locality) were used in this experiment. For one locality, 30 mice were divided into five groups, each group consisting of six mice of defined weight (19 gm) for one level dose. Various venom doses were prepared using saline solution as dilutes and aliquots of a precise volume (0.2 ml) of each dose was injected using one mouse per dose, by the intravenous route in the tail vein. Doses were fluctuated from level one to five with the amount of each dose increasing until 100 percent mortality with the highest potency doses. Different level of dose were used by 50% and 100% venom solution. The minimal amount of venom LD_{50} causing death in 50% of the mice injected. All study species death injected by 100% venom solution were recorded. The study species died within 24 hours was recorded and LD_{50} was calculated by Spearman-Karber method. LD_{50} was expressed by µg/ mouse. The amount of LD_{50} (µg/mouse) was expressed the potency of the venom of specific species.

The LD_{50} was calculated by Spearman and Karber method, (Spearman and Karber, 1981; WHO recommended method of LD_{50}).

M (Log LD_{50})	=	$X_{100} \pm d/n (\Sigma r\text{-}n/2)$
M	=	Log LD_{50}
X_{100}	=	Log dose giving 100% death and having 100% death for all higher dose
n	=	number of mice used at each dose level
r	=	number of mice dying at each dose level
Σ	=	Summation of overall dose
d	=	Log dose interval (constant)

Mixture of snake venom solution for injection (LD_{50})

For the preparing of solution for LD_{50} test, the dry powder venom 30mg was mixed with 15ml normal saline solution. Therefore, the amount of venom in the solution was 2mg/ml. This preparation was named as stock (I).

For the stock II solution, 1ml of solution were extracted from stock (I) and added with 39ml of normal saline solution. So, the mixture of venom and saline solution were 40ml and the concentration of venom in the mixture might be 0.05mg/ml. The solution with 0.05mg/ml

amount of venom was used for calculating to determine the different level doses to mice until 1

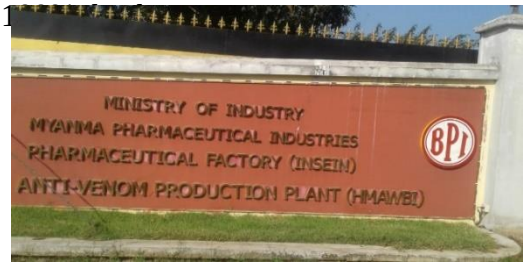

Plate 1. Myanmar Pharmaceutical Factory (MPF)

A. Snake room

B. A snake box

Plate 2. Snake room and snake box

A. Preparing for milking

B. Cup of venom milk

C. Extracting venom from a viper

D. The bottles with venom in the refrigerator

E. Dry freezing

F. Weighting the dry venom

Plate 3.Venom extracting, dry freezing and weighting the dry venom

A. Diluting with normal saline solution

B. Shaking the bottle

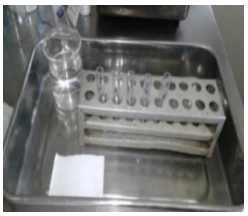

C. Preparing venom solution for injection

D. Incubating the tubes at 37° C

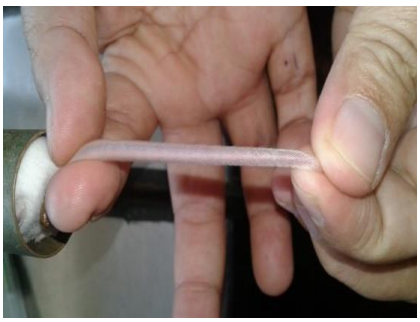

E. Caudal vein of a mouse

F. Injection the diluted venom into the caudal vein of a mouse

Plate 4. Diluting and injecting of venom into the tail vein of mouse

Results

A total of 20 individuals of different sexes of *Daboia siamensis* from Kungyangon Township, Yangon Region were collected and tested for LD_{50} during the study period.

Systemic position of *Daboia siamensis*

Kingdom	-	Animalia
Phylum	-	Chordata
Class	-	Reptilia
Order	-	Squamata
Suborder	-	Serpentes
Family	-	Viperidae
Sub family	-	Viperinae
Genus	-	*Daboia*
Species	-	*D. siamensis* (Smith, 1917)

The dose of venom when injected into the animals produced death in at least half of the number of animals objected within 24 hours is defined as LD_{50}. The amount of venom which may die a mouse within 24 hours was the gradient of venom of viper in this locality. It can be shown by µg / ml or µg/ mouse. According to the experiments, the LD_{50} for Kaungyangon townships was 3.4µg/mouse.

Preparation of venom stock solution for LD_{50} test

Stock number	Venom	Normal saline	Concentration of Venom in solution
Stock (I)	30mg	15ml	2mg/ml
Stock (II)	1ml (stock I)	39ml	0.05mg/ml

LD_{50} Test for *Daboia siamensis* from Kaungyangon Township

Name	- Viper venom (lyophilized)
Locality	- Kaungyangon
Log 1.1	- 0.0414
Interval	- 1.1
Test Animal	- mice (5 individuals for one group)
Weight of mice	-19gm

Preparation of venom solution for injection

For Level I

venom solution 1ml = 0.05mg venom x 1000

= 50µg venom

venom solution 1ml = 50µg venom

Preparation for 0. 50ml = $\frac{50 \times 0.50}{1}$

= 25 µg / ml venom

2ml = 25 µg / ml

0.2 ml dose = $\frac{25 \times 0.2}{2}$

= 2.5 µg / ml

Log of 2.5 = 0.397940009

For Level II

venom solution 1ml = 0.05mg venom x 1000

= 50µg venom

venom solution 1ml = 50µg venom

Preparation for 0.60ml = $\frac{50 \times 0.60}{1}$

= 30 µg / ml venom

2ml = 30 µg / ml

0.2 ml dose = $\frac{30 \times 0.2}{2}$

= 3 µg / ml

Log of 3 = 0.477121255

For Level III

venom solution 1ml = 0.05mg venom x 1000

= 50µg venom

venom solution 1ml = 50µg venom

Preparation for 0.72ml = $\frac{50 \times 0.72}{1}$

= 36 µg / ml venom

2ml = 36 µg / ml

0.2 ml dose = $\frac{36 \times 0.2}{2}$

= 3.6 µg / ml

Log of 3.6 = 0.556302501

For Level IV

venom solution 1ml = 0.05mg venom x 1000

= 50µg venom

venom solution 1ml = 50µg venom

Preparation for 0. 86ml = $\frac{50 \times 0.86}{1}$

= 43µg / ml venom

2ml = 43 µg / ml

0.2 ml dose = $\frac{43 \times 0.2}{2}$

= 4.3 µg / ml

Log of 4.3 = 0.633468456

For Level V

venom solution 1ml = 0.05mg venom x 1000

= 50µg venom

venom solution 1ml = 50µg venom

Preparation for 1.03 ml = $\frac{50 \times 1.03}{1}$

= 51.5 µg / ml venom

2ml = 51.5µg / ml

0.2 ml dose = $\frac{51.5 \times 0.2}{2}$

= 5.15µg / ml

Log of 5.15 = 0.711807229

Calculation:

M (Log LD_{50}) = $X_{100} \pm d / n (\Sigma r\text{-}n/2)$

= $0.6021 \pm \frac{0.0414 (0+1+2+3+5-5/2)}{5}$

= 0.6021± 0.0083(11-5/2)

= 0.6021 ± 0.0083(8.5)

= 0.6021 ± 0.0706

= 0.5315 antilog ⟶ 3.400

LD_{50} = 3.4µg/mouse

= 3.4 µg/mouse

Therefore, the gradient of the venom of *Daboia siamensis* from Kaungyangon Township was 3.4µg/mouse.That is why, the gradient of venom of *Daboia siamensis* from Kaungyangon Township = 3.4

Table 1. Different level doses of venom solution for injection to mice until 100% death (Kaungyangon Township)

Sr No	Venom Solution(ml)	Normal Saline (ml)	Total	Route of injection	Injected Volume (ml)	Number of mice used	Survival (number of mice)	Death (number of mice)	Expected LD_{50} µg/mouse	Log LD_{50} µg/ mouse
1	0.50	1.50	2	I.V	0.2	6	6	0	2.50	0.3979
2	0.60	1.40	2	I.V	0.2	6	5	1	3.00	0.4771
3	0.72	1.28	2	I.V	0.2	6	4	2	3.60	0.5563
4	0.86	1.14	2	I.V	0.2	6	1	5	4.30	0.6335
5	1.03	0.97	2	I.V	0.2	6	0	6	5.15	0.7118

Discussion

In the present study, a total of 20 vipers were collected from Kaungyangon Township to test for LD_{50}.

The toxicity and lethality of the snake venom varies from species to species and even within the species depending upon geographical location, route of venom injection, age, size, locality, health, body temperature and even mood of the snake. There may be wide variation in venom composition through the geographical range of a single species (WHO guideline, 2018).

LD_{50} is the lethal dose that kills 50% of the animals in laboratory testing. The current study is based upon the calculation of LD_{50} of venom of viper in the study area and its evaluation in terms of LD_{50}.

Parveen *et al.* (2017) determined that the LD_{50} of Russell's viper (*Vipera russelli*) in Pakistan is 5 to 6 µg/dose when injected intravenously. Maduwage *et al.* (2016) reported that venom concentrations measured in all vitro experiments in case of human envenoming was 1.7 mg/ml (µg /mouse) for *D. russelli*.

The LD_{50} of Russell's vipers at Taungdwingyi Township was 3.97 ± 2.42 µg /mouse and those at Nyaugdon Township was 6.44 ± 0.54 recorded by Tun Pe *et al.*, (1993).

In the present study, the LD_{50} of *D. siamensis* from Kaungyangon Townships was 3.4µg/ mouse. Therefore, the potents of venom would be 3.4 for this region.

Geographical variations of venom may be responsible for the discrepancy in clinical features of viper bites in different localities. Monospecific antivenom against *D. siamensis* prepared by MPF was used for treating Russell's viper bite patients throughout Myanmar.

Prior to importing antivenoms, national health authorities are able to carefully consider their regional threat from venomous snakes to guide their antivenom requirements.

Conclusion

A total of 20 vipers from Kaungyangon Township were selected to find out the potent of their venom (LD_{50}). The LD_{50} of *D. siamensis* in study area was 3.4µg/mouse. The potency of snake venom was 3.4 and it may assumed that the *D. siamensis* from the study area possesses a fairly higher grade of venom. The findings of this study will help in the production of highly potent and cost effective anti-snake venom serum in Myanmar.

Acknowledgements

We are very grateful to Dr Nay Win Oo, Rector of East Yangon University for his permission to work this research. We would like to thank Dr Aye Aye Ko, Pro-Rector, Dr Wah Wah Lwin, Pro-Rector and Dr Thida Aung, Pro-Rector, East Yangon University, for her permission to work on the present topic. We would like to express our heartfelt thanks to Dr Aung Zaw, General Manager, Myanmar Pharmaceutical Factory, Insein, Yangon for his kind permission to do experiments and supporting all necessities throughout the study period. Our special thanks goes to U Yè Win Naing, Assistant Manager, Hmawbi Branch, (MPF) for his help in during experiments. We are grateful appreciated to Professor Dr Ohn Mar Ohn, Head of Zoology Department, East Yangon University, for her valuable suggestion during the observation of this work and criticism the manuscript. We would like to express my deep gratitude to Dr Aye Thida Than, Professor of Zoology Department, East Yangon University, for her kind helps, cooperation and understanding throughout the research work.

Reference

Bailey, R. 2018. How does snake venom work? Science, technology and Math > Animal and Nature

Cox, M. J., Dijk, P. P, Nabhitabhata, J., Thirakhupt, K. 1998. A photographicGuide to Snake and other reptiles of *Thailand and South East Asia.* Asia Books, Bangkok.

Das, I. 2010. A field guide to the Reptiles of Thailand and South-East Asia. Asia Book Company Limited, Bangkok.

Eward, F. M., 2007. The Spiritual Technology of Ancient Egypt: Sacred Science and the Mystery of Consciousness. Inner Traditions/ Bear. Pp. 448.

Leviton, A. E., Wogan, G. O. U., Koo, M. S., Zug, G. R., Lucas, R. S and Vindum, J. V., 2003. The dangerously venomous snakes of Myanmar illustrated checklist with keys, Proceeding of the California Academy of Sciences, DC 20560; Vol 54, No.24 pp. 407-462, 80 figs.

Parveen, G., Khan, F., Ali, H., Ibrahim, T. and Shah, R., 2017. Determination of Lethal Dose (LD50) of Venom of four Different Poisonous Snakes foundin Pakistan. Biochemistry & Molecular Biology Journal.3、(3):18

Robbins, L. H., Campbell, A., Brook G. A, Michael L., Murphy, M. L., 2007. “World's Oldest Ritual Site? The" Python Cave" at Tsodilo Hills World Heritage Site, Botswana". NYAME AKUMA." the Bulletinof the Society of Africanist Archaeologists (67). Retrieved 1 (2010).

Smith, M.A., 1943. The Fauna of British India, Ceylon and Burma, Vol. III Serpentes. Tailor and Francis Ltd, Londan

Tun Pe, Sann Mya, Aye Aye Myint, Ki May Htwe, Khin Aung Cho and Teingie, 1993. Biological properties of Russell’s viper venom of upper and Lower Myanmar (BPI ± DMR).

WHO,2010. Guidelines for the production, control and regulation of snake Antivenom immunoglobulins. Aviable from: www.who.int/ bloodproducts/snakeantivenoms

WHO,2018. Guidelines for the production, control and regulation of snake Antivenom immunoglobulins. Aviable from: www.who.int/ bloodproducts/snakeantivenoms

A COMPARATIVE STUDY OF OPERCULAR APPRATUS OF SOME SILURID FISHES FROM MYOMA MARKET, THANLYIN TOWNSHIP

Thiri Nwe[1], Thet Thet Myaing[2]

Abstract

The studied species were collected from Myoma Market, Thanlyin Township. The study period lasted from December, 2018 to September, 2019. Total nine species were collected for this research. The fishes were collected in the rate of ten samples for each species. The sizes of species were collected randomly bought from fish mongers. Morphological characteristics, measurements, fin counts and photographing were made and recorded. Collected specimens were identified and classified according to Talwar and Jhingran (1991), Jayaram (1981). Entire and parts of opercular apparatus were recorded with photographs. Opercular bone is the largest bone. Among them, subopercular bone were absent in studied species except in *Clarias batrachus.* The numbers of opercular apparatus differ in different families of fishes.

Keyword: Entire of opercular apparatus, Parts of opercular bone, Order Siluriformes

Introduction

The skeleton system of the fishes exemplifies many evolutionary trends and adaptations. One group of these trends and adaptions deals with the formation of jaws and their supports and thus largely determines the facial appearance. The fish ancestors possessed no true jaws, but first evolved some skeletal structures for supporting the gills (Lagler, *et al*., 1962).

As the richness of fish species is high along with large population size, aquatic products of the inland rivers are important resources for the people of Myanmar. Fisheries sector plays an important role in the national economy in terms of income, food production, foreign exchange and employment to the rural population (ADB/NACA, 1998).

In fishes one of the obvious morphologic characters that distinguish the bony fishes from the sharks, skates and rays (Elasmobranchs) is the presence of a gill cover or operculum. It is a pair of broad plates that articulate vertically to the sides of the skull by ball and socket joints. It covers the gill chamber and can swing quite a large angle about the vertical axis through the joints (Nu Nu Yi, 1990).

One on each side of the skull, the series of opercular bones, that make the gill- cover and frame the cheek posteriorly. Their number and attachment differ in the different groups of fishes (Lagler, *et al*., 1977).

The opercular series contains four bone segments known as the preoperculum, suboperculum, interoperculum and operculum. The preoperculum is a crescent-shaped structure that has a series of ridges directed posterodorsally to the organisms canal pores. The preoperculum is located through an exposed condyle that is present immediately under its ventral margin; it is also borders the operculum, suboperculum, and interoperculum posteriorly. The suboperculum is rectangular in shape in most bony fishes and is located ventral side of the operculum. The interoperculum is a thinnest bone, out of the opercular series and is located directly above the gills. It is triangular shaped and borders the suboperculum posterodorsally and the anterodorsally of preoperculum. This bone is exposed to be short on the dorsal and ventral surrounding borders (Charles, *et al.*, 2008).

Operculum is the hard bone flap, protective plate on each side of a fish's head. It protects the gills; this is confused as being the gills. The rear edge of the operculum roughly marks the division between the head and the body in fish. In fish, the operculum is a bony flap

[1] Demonstrator, Department of Zoology, East Yangon University
[2] Dr,Professor/ Head (Retired), Department of Zoology, East Yangon University

covering the gills. It moves back and forth to move water over the gills, allowing the fish to breath, and also serves as protection against these sensitive parts of the fish (Charles, *et al*., 2008).

The opercular series is vital in obtaining oxygen. They open as the mouth closes, causing the pressure inside the fish to drop. Water then flows towards the lower pressure across the fish's gill lamellae, allowing some oxygen to be absorbed from the water (Charles, *et al*., 2008).

The gill flaps of fishes are composed of four bones which together make up the opercular series. The most posterior of these is the opercular. Variation in the form of the fulcrum and in the pattern of ossification over the opercular surface allows identification to species in many instances. The second major bone in this series is the preopercular. In most species the preopercular is roughly crescent shaped, and in some it bears spines or serrations along its lower edge. The preopercular is often thicker and more robust than the opercular and can, therefore, be useful in identification. The other two bones in this series are the subopercular and the interopercular. The subopercular lie beneath the opercular, covering the branchiostegal rays. In most species it is thin and flat, with few distinguishing features. However, in the siluriform fishes most of them are absent. The interopercular is a thin featureless plate of bone lying beneath the preopercular and separating it from the subopercular (Watt, *et al*., 1997).

The margins of the bones were named as dorsal, ventral, anterior and posterior respectively in accordance with their position in the articulated skull with opercular apparatus. Descriptive accounts of the bones are presented together with plates. The shapes of the opercular apparatus of the study species were compared.

Since, the different shapes and numbers of opercular apparatus are determined in the different groups of fishes. Therefore, the present study was investigated with the aim and the following objectives:

- to investigate the morphological structures of some silurid fishes
- to observe the relationship between the shape of opercular apparatus of different species of fishes

Materials And Methods

Study site

The specimens were collected from Myoma Market, Thanlyin Township. It is situated between 16°45′54″N to 96°14′44″E (Fig. 1, Plate 1 A).

Study period

The study period was lasted from December, 2018 to September, 2019.

Identification of specimens

Morphological characteristics, measurements, fin counts and photographing were made and recorded. The specimens were identified following that of Talwar and Jhingran (1991).

Preservation of the specimens and opercle extraction methods

Each specimen was washed in tap water. Then, the head of the fishes was cut behind the pectoral fin and were immersed in boiling water for five to ten minutes. The muscles and soft tissues were removed with forceps. The disarticulated opercular apparatus such as preopercular, opercular, subopercular and interopercular were taken off an entire bone. Each opercular bones were dried at room temperature. Entire and separated opercular apparatus were recorded with scaled photographs (Plate 1 B).

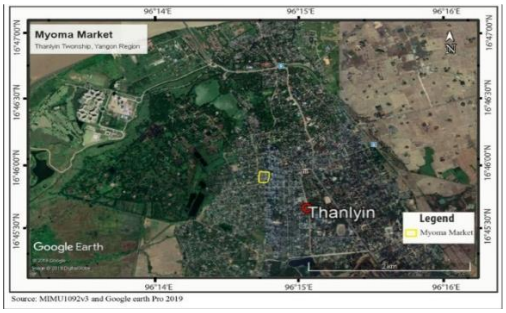

Fig. 1 Map of study area
(Source: Google Earth, 2019)

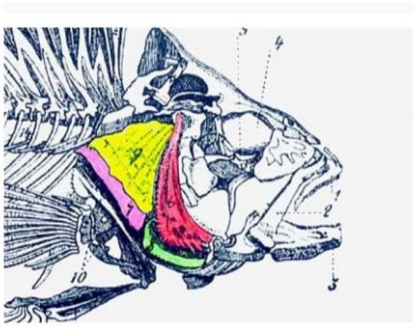

Fig. 2 Opercular series in bony fish:
operculum (yellow)
preoperculum (red)
interoperculum (green)
subopercular (pink)
(Source: https://en.m.Wikipedia.org)

A. Myoma Market, Thanlyin Township

B. Fish head prepared for boil

Plate 1 Specimen collection site and preparation for opercle extraction

Results

In the present study, a total of nine species, belonging to seven genera, five families and one order of fish were studied (Table 1).

Morphological structure of opercular apparatus

***Mystus cavasius* (Hamilton-Buchanan, 1822)**

Common name - Gangetic mystus
Local name - Nga- zin-yaing-phyu (Plate 1, A)
Fin formula - D I/ 7; A IV/ 7; P I/ 8; V I/ 5

Preopercular bone: It is an elongated and curved bone. It is narrow at the upper half but broad at the lower half. At about the middle the anterior margin bears a narrow and short anterior projecting plate. On the outer surface, there is a low longitudinal ridge running from the dorsal apex to the posterior margin near the lower end (Plate 1, C).

Opercular bone: It is a broad, thick bone somewhat triangular in shape. The anterior margin is shorter than the posterior margin and bears at the dorsal end a long and point opercular arm directing backwards. The postero-dorsal angle is narrow and rounded without a prominent auricular arm. The ventral angle is broad and truncate (Plate 1, D).

Interopercular bone: It is a short bone. It is narrow and pointed at the anterior end, broad and forked at the posterior end. On the outer surface, it bears a submarginal transverse dorsal ridge running from the anterior apex to the posterior margin (Plate 1, E).

Subopercular bone: It is absent in this fish (Table 2).

***Mystus gulio* (Hamilton-Buchanan, 1822)**

Common name - Long-whiskered catfish
Local name - Nga-zin-yaing-kyat-chay (Plate 2, A)
Fin formula - D I/ 7; A iii-iv/ 9-11; P I/ 8-10; V i/ 5
Preopercular bone: It is thick, elongated and somewhat crescentic in shape. The upper half is narrow, slender and bears a shallow opening at the apex. The lower half is flat, broad and pointed at the apex. In the middle, there is a broad anterior plate with irregular free margin (Plate 2, C).
Opercular bone: It is thick, flat and broad, somewhat triangular in shape. The anterior margin is straight and bears an inner articulating concavity near the dorsal end. The opercular arm is prominent, short and pointed (Plate 2, D).
Interopercular bone: It is a thick, flat and slightly elongated bone; it is broad at the posterior end, narrow at the anterior end. The remaining species it is pointed or bears small short process. The broad posterior end is broad and bilobed with a notch in the middle; the lobes are subequal and pointed (Plate 2, E).
Subopercular bone: It is absent in this fish (Table 2).

***Mystus leucophasis* (Blyth, 1861)**

Common name - Sittang mystus
Local name - Nga-pet-let (Plate 3, A)
Fin formula - D I/ 7; A ii-iii/ 7-8; P I/ 8-10; V i/ 5
Preopercular bone: It is slightly thick, elongated and somewhat crescentic in shape. The upper half is narrow, slender and bears a shallow opening at the apex. The lower half is flat, broad and pointed at the apex. In the middle, there is a broad anterior plate with irregular free margin (Plate 3, C).
Opercular bone: It is slightly transparent, flat and broad, somewhat triangular in shape. The anterior margin is straight and bears an inner articulating concavity near the dorsal end (Plate 3, D).
Interopercular bone: It is slightly transparent, flat and slightly elongated bone; it is broad at the posterior end, narrow at the anterior end. The pointed ventral lobe is larger than the rounded dorsal lobe (Plate3, E).
Subopercular bone: It is absent in this fish (Table 2).

***Mystus microphthalmus* (Day, 1877)**

Common name - Irrawaddy mystus
Local name - Nga- jaung (Plate 4, A)
Fin formula - D I/7; P I/9; V i/5; A iii/9
Preopercular bone: It is thin, solid, transparent and elongated. The tip of entire margin is blunt. The expanded anterodorsal margin is concave. The dorsal tip is blunt. Margin of posterior, posteroventral and ventral are mostly rounded and ventral margin is slanted (Plate 4, C).
Opercular bone: It is thin, transparent, and kite shape. Margin of anterior are slightly pointed. The posterior margin is blunt and thick. The dorsal margin is transparent (Plate 4, D).
Interopercular bone: It is irregular in shape. The tip of entire margin is blunt. The expanded anterodorsal margin is convex. The dorsal margin is transparent. The ventral margin is rought (Plate 4, E).
Subopercular bone: It is absent in this fish (Table 2).

***Ompok bimaculatus* (Bloch, 1797)**

Common Name - Indian-butterfly catfish
Local name - Nga-nu-than (Plate 5, A)
Fin formula - D 4; A ii-iii/57-58; P I/12-14; V i/7-8
Preopercular bone: It is elongated and irregular shaped, the posterior margin is blunt. Margin of anterior is rough. The dorsal margin is rough and slightly concave. The ventral margin is rough and transparent (Plate 5, C).
Opercular bone: It is small, transparent and thin. The posterior margin is rough. The antetior margin is blunt. The dorsal margin is rough. The ventral margin is slightly straight (Plate 5, D).
Interopercular bone: It is small and solid. The posterior margin is blunt. The anterior margin is rounded. The dorsal and ventral margins are rough (Plate 5, E).
Subopercular bone: It is absent in this fish (Table 2).

***Wallago attu* (Schneider, 1801)**

Common Name - Boal
Local Name - Nga-butt (Plate 6, A)
Fin formula - D 5; P I/13-15; Vi/7-9; A iii/74-93
Preopercular bone: It is small, solid and irregular-shaped. The posterodorsal region is expanded, and the tip of this region is rough. The posterior margin is blunt. The anterior margin is pointed. The dorsal margin is rough and concave. The ventral margin is slightly convex (Plate 6, C).
Opercular bone: It is large , with a solid and rough surface. The anterior margin is blunt. The posterior margin is concave. The ventral margin is rough and thicker than other part. The dorsal margin is transparent (Plate 6, D).
Interopercular bone: It is large, solid and irregular-shaped. The anterior margin is blunt and posterior margin is slightly pointed. The dorsal margin is concave. The ventral margin is slightly rough (Plate 6, E).
Subopercular bone: It is absent in this fish (Table 2).

***Pangasius pangasius* (Hamilton-Buchanan, 1822)**

Common name - Pungas
Local name - Nga-dan (Plate 7, A)
Fin formula - D I/ 6-7; A iv-v/ 26-29; P I/ 12-13; V I/ 5
Preopercular bone: It is large, thick, solid and elongated bone. The anterior margin is curved inward. The entire anterior margin is quadrate. The dorsal margin is tapered. The posterior margin is rough and wavy (Plate 7, C).
Opercular bone: It is thick, solid, rough, and convex outward and butterfly wing-like bone. This bone is largest and can be easily distinguished. The anterior margin is slanted outward. The anterodorsal region is slightly curved, blunt and flat. The dorsal region is concaving inward and slanted downward to the posterior. The posterior margin is rounded and wavy. The ventral margin is expanded and curved inward. The outer surface of the entire opercular bone is rough (Plate 7, D).
Interopercular bone: It is solid, thick, rough and convex outward, irregular in shaped. The anterior margin is pointed. The dorsal margin is slightly wavy and concave. The posterior margin is wavy. A posterior ventral is abruptly

downward and concave. The ventral margin is slanted upward anteriorly and slightly wavy. Interopercular bone is shorter than opercular bone (Plate 7, E).

Subopercular bone: It is absent in this fish (Table 2).

***Clarias batrachus* (Linnaeus, 1758)**

Common name - Magur
Local name - Nga-khu (Plate 8, A)
Fin formula - D 70-76; A 45-58; P I/8-11; V i/5

Preopercular bone: It is small, solid and sickle shaped. The posterior margin is blunt. The dorsal margin is straight and smooth. The anterior margin is blunt. The ventral margin is very rough and curved (Plate 8, C).

Opercular bone: It is pointed and solid. The posterior margin is blunt. The posterodorsal is expanded and dorsal margin is rough. The anterior margin is blunt. The ventral margin is slightly smooth and convex (Plate 8, D).

Interopercular bone: It is large, solid and irregular-shaped. The posterior margin is rounded and blunt. The anterior margin is rough, concave and pointed. The anterodorsal margin is curved. The ventral margin is very rough (Plate 8, E).

Subopercular bone: It is solid, hard, elongated and feather shape. The anterior part is taper. The dorsal margin is straight and smooth. The posterior margin is slanted downward and wavy. The ventral margin is curved inward (Plate 8, F).

***Heteropneustes fossilis* (Bloch, 1794)**

Common name - Stinging catfish
Local name - Nga-gyi (Plate 9, A)
Fin formula - D 6-7; A 60-70; P I/ 7; V i/ 5

Preopercular bone: It is a narrow and short bone with a low dorsal ridge along the central axis. It is broad at the dorsal end and narrow and pointed at the ventral end. The posterior margin is convex; the anterior margin is concave and bears a long and narrow anterior projecting plate which is constricted at the base (Plate 9, C).

Opercular bone: It is a thick and moderately large triangular shaped bone with a long and pointed postero-dorsal process. The anterior margin is short and straight and bears near the dorsal end an inner articulating concavity. The opercular arm is not prominent. The dorsal and posterior margins are long and straight and the auricular arm is long (Plate 9, D).

Interopercular bone: It is a flat bone which is broad and blunt at the posterior end, narrow, elongated and pointed at the anterior end. At the posterior end the dorsal and ventral angles are produced into short pointed processes (Plate 9, E).

Subopercular bone: It is absent in this fish (Table 2).

Table 4.1 Systematic position of collected some silurid fish species from Thanlyin Myom Market

Family	No.	Species	Common name	Local name
Bagridae	1	*Mystus cavasius*	Gangetic mystus	Nga-zin-yaing-phyu
	2	*Mystus gulio*	Long-whiskered catfish	Nga-zin-yaing-kyat-chay
	3	*Mystus leucophasis*	Sittang mystus	Nga-pet-let
	4	*Mystus microphthalmus*	Irrawaddy mystus	Nga-jaung
Siluridae	5	*Ompok bimaculatus*	Indian-butterfly catfish	Nga-nu- than
	6	*Wallago attu*	Boal	Nga-butt
Pangasiidae	7	*Pangasius pangasius*	Pungas	Nga-dan
Clariidae	8	*Clarias batrachus*	Magur	Nga-khu
Heteropneustidae	9	*Heteropneustes fossilis*	Stinging catfish	Nga-gyi

Table 4.2 Comparison between the shapes of the opercular apparatus of the studied species

No.	Species Name	Opercular apparatus			
		Preopercular bone	Opercular bone	Interopercular bone	Subopercular bone
1	*Mystus cavasius*	Elongated	Triangular	Short	Absent
2	*Mystus gulio*	Crescentic	Triangular	Slightly elongated	Absent
3	*Mystus leucophasis*	Crescentic	Triangular	Slightly elongated	Absent
4	*Mystus microphthalmus*	Elongated	Kite	Irregular	Absent
5	*Ompok bimaculatus*	Irregular	Small	Small	Absent
6	*Wallago attu*	Irregular	Large	Irregular	Absent
7	*Pangasius pangasius*	Large	Butterfly-wing-like	Irregular	Absent
8	*Clarias batrachus*	Sickle-shape	Pointed	Irregular	Feather-shape
9	*Heteropneustes fossilis*	Narrow	Moderately large triangular	Flat	Absent

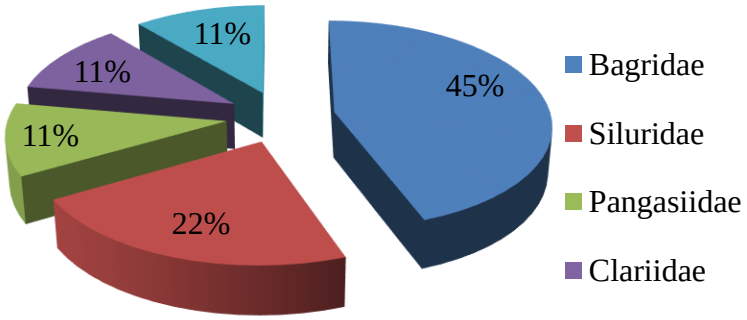

Fig. 3 Species composition of the studied fishes as shown in percentages

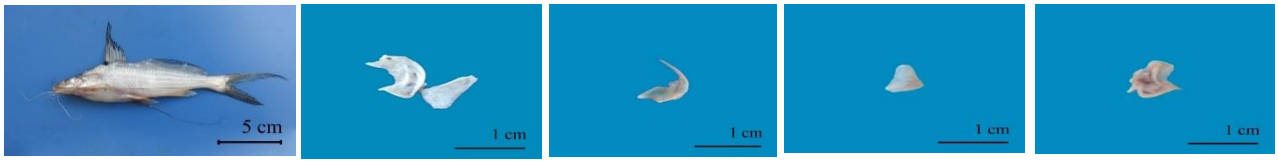

A. External feature B. Entire bone C. Preopercular bone D. Opercular bone E. Interopercular bone

Plate 1 External feature and opercular apparatus of *Mystus cavasius*

A. External feature B. Entire bone C. Preopercular bone D. Opercular bone E. Interopercular bone

Plate 2 External feature and opercular apparatus of *Mystus gulio*

A. External feature B. Entire bone C. Preopercular D. Opercular bone E. Interopercular bone

Plate 3 External feature and opercular apparatus of *Mystus leucophasis*

A. External feature B. Entire bone C. Preopercular bone D. Opercular bone E. Interopercular bone

Plate 4 External feature and opercular apparatus of *Mystus microphthalmus*

Plate 5 External feature and opercular apparatus of *Ompok bimaculatus*

A. External feature B. Entire bone C. Preopercular bone D. Opercular bone E. Interopercular bone

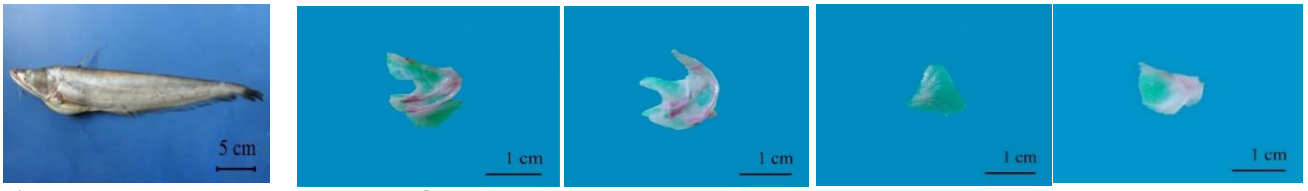

A. External feature B. Entire bone C. Preopercular bone D. Opercular bone E. Interopercular bone

Plate 6 External feature and opercular apparatus of *Wallago attu*

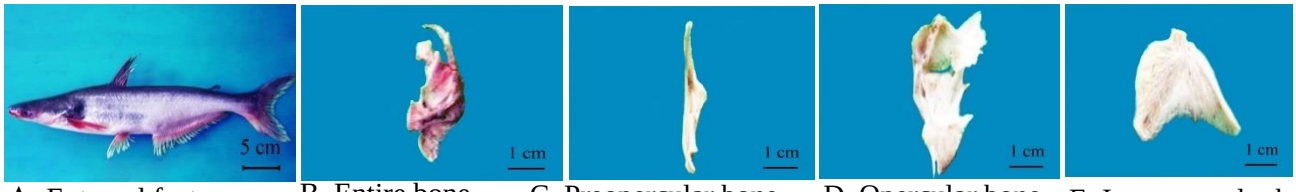

A. External feature B. Entire bone C. Preopercular bone D. Opercular bone E. Interopercular bone

Plate 7 External feature and opercular apparatus of *Pangasius pangasius*

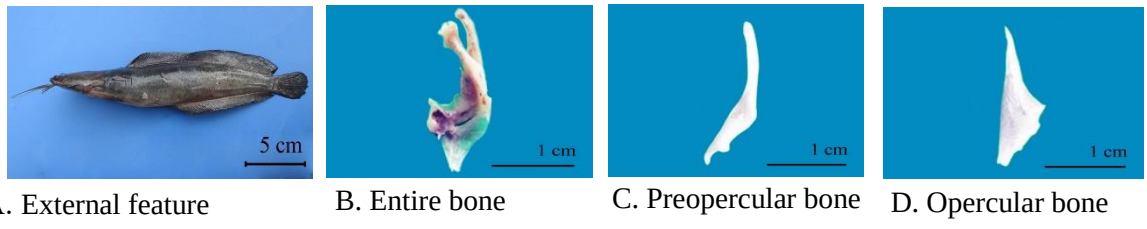

A. External feature B. Entire bone C. Preopercular bone D. Opercular bone

E. Interopercular bone F. Subopercular bone

Plate 8 External feature and opercular apparatus of *Clarias batrachus*

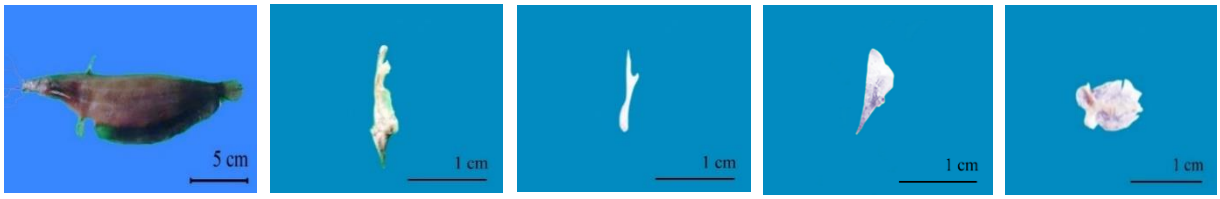

A. External feature B. Entire bone C. Preopercular bone D. Interopercular bone E. Interopercular bone

Plate9 External feature and opercular apparatus of *Heteropneustes fossilis*

Discussion

The opercle is typically the largest bone in the series and extends farthest posteriorly of the skull of the fish. (Lagler, *et al*.,1977).

The operculum is a series of bones found in bony fish that serves as a facial support structure and a protective covering for the gills; it is also used for respiration and feeding (Charles, *et al.*, 2008).

In the present study, opercle bone was found to be the largest bone in the series and posteriorly; a protective covering for the gills; used for respiration and feeding so that agree with Lagler, *et al*., 1977 and Charles, *et al.*, 2008.

There is no subopercular bone in eighteen studied species of Silurids, and the opercular plate is made up of only three bones. The Silurid group with three opercular apparatus and opercular bone is roughly triangular in shape (Nu Nu Yi, 1990).

There is no subopercular bone in nine studied species of Silurids, and the opercular plate is made up of only three bones and roughly triangular in shape. In my study species, agree above author.

Opercular apparatus are paired. Subopercular bones are absent in species of order Siluriformes except in *Clarias batrachus* (Ni Ni Tin, 1998).

In the present study, the opercle is also the largest and attached at the hindermost part of the opercular apparatus. The number of opercular apparatus of all study species are not the same; subopercular bone is absent in studied species, which composed of three bones contain all of four opercular apparatus except in *Clarias batrachus*. The findings of present study were similar with the findings of Lagler, *et al*., 1977, Moe Moe, 1985, Nu Nu Yi, 1990, Watt, *et al*., 1997 and Ni Ni Tin, 1998.

The preopercle of *Pangasius pangasius* can be regarded as the most straight among study species. Present study observed that the numbers of opercular apparatus differ in different families of fishes.

Nu Nu Yi (1990) stated that the shapes of preopercular bone was elongated, opercular bone was triangular, interopercular bone was flat and subopercular bone was absent in *Mystus cavasius.* In the present study, this result is confirmed with the observation of Nu Nu Yi. In *Mystus gulio*, the shapes of preopercular bone was crescentic, opercular bone was triangular, interopercular bone was slightly elongated and subopercular bone was absent.

Mystus leucophasis was showed that the shapes of preopercular bone was crescentic, opercular bone was triangular, interopercular bone was slightly elongated and subopercular bone was absent by Nu Nu Yi (1990). In the present study, this result is confirmed with the observation of Nu Nu Yi. But Ni Ni Tin (1998) was studied that the shapes of preopercular bone was elongated, opercular bone was wing like, interopercular bone was irregular and subopercular bone was absent. In this study, it is not confirmed with the observation of Ni Ni Tin.

Mystus microphthalmus was observed that the shapes of preopercular bone was elongated, opercular bone was triangular, interopercular bone was slightly elongated and subopercular bone was absent by Nu Nu Yi (1990). In the present study, the shapes of opercular bone was seen as kite and interopercular bone was irregular in *M. microphthalmus.* It is assumed that this result confirmed with the observation of Nu Nu Yi (1990).

Ompok bimaculatu was showed that the shapes of preopercular bone was irregular, opercular bone was small, interopercular bone was small and subopercular bone was absent by Nu Nu Yi (1990). In the present study, this result is confirmed with the observation of Nu Nu Yi. But Ni Ni Tin (1998) was studied that the shapes of preopercular bone was thin, opercular bone was flat, interopercular bone was rectangular and subopercular bone was absent. In this study, it is not confirmed with the observation of Ni Ni Tin.

Wallago attu was observed that the shapes of preopercular bone was elongated, opercular bone was large, interopercular bone was roughly rectangular and subopercular bone was absent by Nu Nu Yi (1990). In the present study, the shapes of preopercular bone was seen as irregular and interopercular bone was irregular in *W. attu.* It is assumed that this result confirmed with the observation of Nu Nu Yi (1990).

Pangasius pangasius was showed that the shapes of preopercular bone was large, opercular bone was butterfly-wing-like, interopercular bone was irregular and subopercular bone was absent by Ni Ni Tin (1998). In the present study, this result is confirmed with the observation of Ni Ni Tin.

Clarias batrachus was observed that the shapes of preopercular bone was elongated, opercular bone was roughtly triangular, interopercular bone was elongated and subopercular bone was absent by Nu Nu Yi (1990). But Ni Ni Tin (1998) was studied that the shapes of preopercular bone was irregular, opercular bone was polygonal, interopercular bone was small and subopercular bone was triangular. In the present study, the shapes of preopercular bone was sickle, opercular bone was pointed, interopercular bone was irregular and subopercular bone was feather. In this study, it is not confirmed with the observation of Ni Ni Tin and Nu Nu Yi.

Heteropneustes fossilis was showed that the shapes of preopercular bone was narrow, opercular bone was moderately large triangular, interopercular bone was flat and subopercular bone was absent by Nu Nu Yi (1990). In the present study, this result is confirmed with the observation of Nu Nu Yi.

Conclusion

Data collection was made from Myoma Market in Thanlyin Township, which lasted from December 2018 to September 2019. The opercular apparatus of order Siluriformes; among four opercular apparatus; preopercular bone, opercular bone, interopercular bone and subopercular bone. A total of nine species, *Clarias batrachus* was studied all of four opercular apparatus, the remaining eight species; three opercular apparatus were observed and subopercular bone were not found.

Acknowledgements

We are very grateful to Dr Nay Win Oo, Rector of East Yangon University for his permission to work this research. We would like to thank Dr Aye Aye Ko , Pro-Rector, Dr Wah Wah Lwin, Pro-Rector and Dr Thida Aung, Pro-Rector, East Yangon University, for her permission to work on the present topic. We are grateful appreciated to Professor Dr Ohn Mar Ohn, Head of Zoology Department, East Yangon University, for her supervision, for her valuable suggestion during the observation of this work and criticism the manuscript. We would like to express my deep gratitude to Dr Aye Thida Than, Professor of Zoology Department, East Yangon University, for her kind helps, cooperation and understanding throughout the research work.

References

ADB/NACA, 1998. *Aquaculture sustainability and the environment.* Bangkok. 491pp. Ecology and its Applications, 227-265.

Charles B. Kimmel; Windsor E. Aguirre; Bonnie Ullmann; Mark Currey; William A. Cresko, (2008). Allometric change accompanies opercular shape evolution in Alaskan threespine sticklebacks. *Fifth International Conference on Stickleback Behavior and Evolution. 145 (4/5): 669–691.*

Day, F**.,** 1978. *The Fishes of Indian*; being a natural history of fishes known to Inhabit the seas and waters of Indian, Barma and Ceylon. Vol. I and II, Today and Tomorrow's Book Agency, New Delhi.

Gregory, W.K**.,** 1938. *Fish skulls*; A study of the evolution of Natural Mechanisms. Eric Lundberg, L'aurel, Floridda.

Jayaram, K.C, 1981. *The freshwater fishes of India, Pakistan, Bangladesh, Burma and Sri Lanka*. Sri Aurobindo Press.

Lagler, K.F., J.E. Bardach and R.R. Miller, 1962. *Ichthyology*. The study of fishes. John Wiley & Sons, Inc., New York.

Lagler, K.F., Bardach, J.E., Miller, R.R and May Passino, D.R., 1977. *Ichthyology*. (Second Edition). John Wiley & Sons, Inc., New York. United State of America.

Ministry of Livestock Breeding and Fisheries, 1986-87. *Checklist of fishes of Burma*. Department of Fishes.

Moe Moe, 1985. Comparative study of the opercular bones of some bony fishes. *MSc. Thesis*. Rangon University.

Ni Ni Tin, 1998. Study of opercular apparatus in some bony fishes of the order Siluriformes, Channiformes and Perciformes. *MSc Thesis*. Department of Zoology, University of Yangon.

Nu Nu Yi. 1990. Comparative study on the opercular bones of freshwater fishes. *MSc Thesis*, Department of Zoology, University of Madalay.

Storer, T.I. and Usinger, R.L., 1975. *General Zoology*. Fifth edition. International student edition. Kogakusha Company Ltds, Tokyo.

Talwar, P.K. and A.G., Jhingran, 1991. *Inland fishes of India and adjacent countries.* Vol. 1-2, Oxford and IBH Publishing Co.PVD. Ltd, New Delhi. 1158pp.

Tin Mar Haling, 2013. Study on opercular apparatus in some bony fishes from Monywa Market. *MSc Thesis*, Department of Zoology, Monywa University.

Vashwanath, S. 1975. *A text book of Zoology*, Volume II (Chordates) S. Chand and Co., (Pvt.) Ltd., ram Nagar, New Delhi.

Watt, J., Pierce, G.J. and Boyle, P.R., 1997. Guide to the Identification of North Sea Fish Using Premaxillae and Vertebrae. Department of Zoology, University of Aberdeen, Scotland, United Kingdom. *ICES cooperative research report*, 220:1-6.

Yi Mon, 2017. Study on opercular apparatus in some bony fishes from Myoma Market. *MSc Thesis*, Department of Zoology, Pakokku University.

ASSESSMENT OF MARINE FISH SPECIES DIVERSITY (ORDER-PERCIFORMES) FROM YANBYE TOWNSHIP, RAKHINE STATE

Yee Yee Khin[1], Aye Aye Lwin[2]

Abstract

Marine fish species of Rakhine Coastal Area, Yanbye Township lasted from December, 2019 to August, 2020. Za Yat Pyin Village was chosen as the study site. Monthly samples of fish species including 57 species of 43 genera belonging to 27 families under (Order-Perciformes) were recorded. The sampling was carried out fortnightly for a period of nine months. Three types of fishing gears were categorized. Fish samples were taken from three fishing boats in each type of three fishing gears. Ecological indies such as Shannon-Wiener diversity index, equitability, species richness and Simpson's dominance index were calculated by using the three fishing gears. According to current observations, the fish species in the beach surrounding net are in a healthy condition and also most of them are equally distributed in it. The dominance indices values of three fishing gears are low categories. A uniformity index and small diversity indicates a high dominance of a species against other species. A total of 43 species were caught by boat seine net (Kyawt Pike), 22 species by bottom trawl net (Gyan Pike) and 31 species by beach surrounding net (Moyan Pike). Fish species diversity and richness coincided with maximum fish catch. According to the total catch, the highest quantity was caught by boat seine net which was followed by beach surrounding net. Moreover, commerson's anchovy (Nga Ni Tu) was noted to be caught by boat seine net (Kyawt Pike) in Yanbye Township.

Keyword: Monthly samples, Three types of fishing gears, Marine fish species diversity and richness, Order-Perciformes

Introduction

Myanmar is endowed with rich natural resources both in freshwater and marine fisheries. It has a long coastline and large marine territory. The coastline stretches from the Naf River, the dividing line between Bangladesh and Myanmar, to Kawthaung at the border with Thailand, 2,831 km to the south. Coastline formed several large estuarine, delta system and numerous offshore inland (DOF, 2018).

The coastal zones of Myanmar can be subdivided into three main areas, namely Rakhine Coast, Ayeyarwady Delta and Tanintharyi Coast. Many rivers flow into the coastal zones such as the "Mayu" and " Kaladan" rivers in the Rakhine Coastal area: the "Ayeyarwady", " Sittaung" and " Thanlwin " rivers in Delta coastal area and the "Ye", "Dawai", " Tanintharyi" and "Lenya" rivers in the Tanintharyi coastal area (Psomadakis et al., 2019).

The Rakhine Coastal Zone is bounded by the Bay of Bengal on the west and has a total land area of 367,780 sq.km. The Rakhine Coast stretches 740 km from the Naff River to Mawdin Point. The upper part of the coastline is shallow and deltaic. The southern part is more or less rocky. Two big islands namely "Yan-bye Kyune"(Ramee Island) and "Man-aung Kyune"(Cheduba Island), exist near the Sittwey valley off the Rakhine coast (Myint Pe, 2002).

Yanbye township is the main principal town of Ramree island of Rakhine coastal region. In Yanbye Township, 67.7 percent of the employed persons aged 15-64 are skilled agricultural, forestry and fishery workers. There are fishing villages or fishing communities along the coastline. The Za Yat Pyin village was chosen as the study site. It was a fishing village, located near the "Sin Tin Maw" fishing ground, with an economy based on catching

[1] Demonstrator, Department of Zoology, East Yangon University
[2] Dr, Lecturer, Department of Zoology, Dangon University

fish. Sand beaches along the coast, the fishing boats are loading the catch and young villagers carried the catch by buckets. And some are preparation for sun dried small fishes (most are anchovy) (Myanmar census, 2017).

FAO has always made efforts to standardize the number of marine stocks or species groups monitored and described for each major fishing area. The marine capture fishery comprises coastal or inshore fisheries, and offshore or deep-sea fisheries. The marine fisheries of Myanmar are demarcated into four main fishing areas i.e Rakhine, Ayeyarwady, Mon and Tanintharyi. Among them, Rakhine is the highest fish biomass (FAO, 2011).

In Rakhine area, the major fishing gears used are small purse seine operate by two boats, light boat and seine boat. About 18 crews on those two boats. Fishing activity is only one night at sea, leave from landing site at about 17:00 pm and come back in the early morning. Crew is searching for the fish school by the experience eye in the night time, then luring light to aggregate fish before net shooting. Fishermen generally operate only one or two time per night. Marine fishing activities are controlled by the licensing and registration system under the current Fisheries Law (Aung Htay Oo, 2009).

According to Froese and Pauly (2019), 40,000 species of fish, including approximately 20,000 marine species had been described in the world. In Myanmar, there are 536 freshwater fish species and 600 marine fish species. Almost 60.0% of the world fish catch is being fished from coastal ecosystems. Thus, the present paper was a study of fisheries with the purpose of maintaining the sustainable fish catch with different gill nets. The objectives of the study are as follows:

- to investigate the species composition of marine fish
- to assess the diversity of marine fish species

Materials And Methods

Study area and study site

Specimens were collected from the coastal area of Za Yat Pyin village in Yanbye Township, Rakhine State. It is located between Latitude 19º 04' 11" longitude 93º 39' 53" E. The distance from Yanbye Township to the study area at 26.97 kilometers in the south-west (fig.1).

Method of collection

The marine capture fishing comprises coastal or inshore fisheries and offshore or deep-sea fisheries. Approximately 30 fishing boats are conducting the fishing ground. Only six to eight fishing boats are going into the sea every day. The fish catch data was collected by using three sample boats in each type of three fishing gears.

Recorded fishing gears were classified after Khin Maung Aye *et al.* 2006. (1) boat seine net, (2) bottom trawl net and (3) beach surrounding net were used in the study period (Plate 2). The total catch from each sample boat was recorded and species wise quantity was recorded as soon as fishes are landed (Plate 1).

Indices of species diversity

Coast fish species diversity was calculated by using the Shannon-Wiener index in 1949.

$$H' = - \sum Pi \, LnPi$$

Where; Pi = the proportion of individuals in the species

The evenness or equitability of diversity was calculated from Pielou's index (Pielou, 1996) given as:

$$J' = H'/LnS$$

Where: J' = Pielou evenness index

H' = The observed values of Shannon Index

H max = LnS

S = Total number of species

Species richness was determined using Margalef index (1958) given as

SR = S-1/Ln(N)

Where; SR = Species richness

S = Total number of species in a sample

N = Natural log of total number of individuals of all species

The Dominance Index was calculated as Simpson's Index of Dominance defined by Simpson (1949).

$C = \sum [\![pi]\!]^2$

Where; C = Dominance Index

pi = The proportion of individuals fish species

Fig. 1 Map of Yanbye Township

Plate 1 Study site and Fishing boat

(A) Boat sein net

(B) Bottom trawl net

(C) Beach surrounding net

Plate 2 Three fishing gears

Table 1 Continued

Order	Family	No	Scientific Name	Common name
Perciformes	Siganidae	43	*Siganus canaliculatus*	White spotted spinefoot
		44	*S. fuscescens*	Mottled spinefoot
		45	*S. javus*	Streaked spinefoot
	Sphyraenidae	46	*Sphyraena obtusata*	Obtuse barracuda
		47	*S. putnamae*	Sawtooth barracuda
	Trichiuridae	48	*Trichiurus lepturus*	Largehead hairtail
	Scombridae	49	*Scomberomorus commerson*	Narrow barred Spanish mackerel
	Scombridae	50	*Scomberomorus guttatus*	Indo-Pacific king mackerel
		51	*S. lineolatus*	Streaked seerfish
		52	*S. tritor*	West African Spanish mackerel
		53	*Rastrelliger kanagurta*	Indian mackerel
	Stromateidae	54	*Pampus argentus*	Silver pomfret
	Gobiidae	55	*Glossogobius giuris*	Tank goby
		56	*Paratrypauchen microcephalus*	Comb goby

	Priacanthidae	57	*Priacanthus tayneus*	Purple-spotted bigeye

Results

Table 1 Recorded fish species from the study area Order-Perciformes

Order	Family	No	Scientific Name	Common name
Perciformes	Centropomidae	1	*Lates calcarifer*	Barramundi
	Serranidae	2	*Cephalopholis formosa*	Bluelined hind
	Serranidae	3	*Epinephelus areolatus*	Areolate grouper
		4	*E. coioides*	Orange-spotted grouper
		5	*E. marginatus*	Dusky grouper
	Terapontidae	6	*Terapon puta*	Small-scaled terapon
		7	*Pelates quadrilineatus*	Fourlined terapon
	Sillaginidae	8	*Sillaginopsis panijus*	Flathead sillago
	Apogonidae	9	*Jaydia truncata*	Flagfin cardinalfish
	Carangidae	10	*Megalaspis cordyla*	Torpedo scad
		11	*Parastromateus niger*	Black pomfret
		12	*Selaroides leptolepis*	Yellowstripe scad
		13	*Alepes djedaba*	Shrimp scad
		14	*Decapterus maruadsi*	Japanese scad
		15	*Scomberoides commersonnianus*	Talang queenfish
		16	*S. tol*	Needlescaled queenfish
		17	*Seriolina nigrofasciata*	Blackbanded trevally
	Menidae	18	*Mene maculata*	Moon fish
	Leiognathidae	19	*Gazza minuta*	Toothpony
		20	*Leiognathus longispinis*	Longspine ponyfish
		21	*Photopectoralis bindus*	Orangefin ponyfish
		22	*Secutor ruconius*	Deep pugnose ponyfish
	Lutjanidae	23	*Lutjanus fulvus*	Blacktail snapper
		24	*L. johnii*	John's snapper
		25	*L. russellii*	Russell's snapper
		26	*L. vitta*	Brownstripe red snapper
	Gerreidae	27	*Gerres filamentosus*	Whipfin silver-biddy
		28	*Pentaprion longimanus*	Longfin mojarra
	Lethrinidae	29	*Lethrinus lentjan*	Pink ear emperor
	Nemipteridae	30	*Nemipterus peronii*	Notchedfin threadfin bream
		31	*N. virgatus*	Golden thread fin bream
	Sciaenidae	32	*Johnius dussumieri*	Sin croaker
		33	*Boesemania microlepis*	Boeseman croaker
	Mullidae	34	*Upeneus moluccensis*	Goldband goatfish
	Mullidae	35	*Upeneus vittatus*	Yellowstriped goatfish
	Drepaneidae	36	*Drepane punctata*	Spotted sicklefish
	Rachycentridae	37	*Rachycentron canadum*	Cobia
	Echeneidae	38	*Echeneis naucrates*	Live sharksucker
	Scatophagidae	39	*Scatophagus argus*	Spotted scat
	Mugilidae	40	*Mugil cephalus*	Flathead grey mullet
	Polynemidae	41	*Eleutheronema tetradactylum*	Fourfinger threadfin
		42	*Leptomelanosoma indicum*	Indian threadfin

Table 2 Diversity indices of recorded marine fish species in boat seine net (December-April)

No	Species	Total	Pi	(Pi)^2	PiLnPi
1	*Terapon puta*	170	0.0193	0.0387	-0.0763
2	*Pelates quadrilineatus*	300	0.0341	0.0683	-0.1153
3	*Jaydia truncata*	100	0.0114	0.0228	-0.0509
4	*Megalaspis cordyla*	440	0.0501	0.1002	-0.1499
5	*Parastromateus niger*	162	0.0184	0.0369	-0.0736
6	*Selaroides leptolepis*	680	0.0774	0.1548	-0.1980
7	*Alepes djedaba*	740	0.0842	0.1684	-0.2084
8	*Decaptarus maruadsi*	660	0.0751	0.1502	-0.1945
9	*Scomberoides commersonnianus*	13	0.0015	0.0030	-0.0096
10	*S. tol*	16	0.0018	0.0036	-0.0115
11	*Seriolina nigrofasciata*	15	0.0017	0.0034	-0.0109
12	*Gazza minuta*	270	0.0307	0.0615	-0.1070
13	*Leiognathus longispinis*	320	0.0364	0.0728	-0.1206
14	*Photopectoralis bindus*	280	0.0319	0.0637	-0.1098
15	*Secutor ruconius*	630	0.0717	0.1434	-0.1890
16	*Gerres filamentosus*	160	0.0182	0.0364	-0.0729
17	*Pentaprion longimanus*	90	0.0102	0.0205	-0.0469
18	*Nemipterus peronii*	270	0.0307	0.0615	-0.1070
19	*N. virgatus*	80	0.0091	0.0182	-0.0428
20	*Johnius dussumieri*	210	0.0239	0.0478	-0.0892
21	*Boesemania microlepis*	240	0.0273	0.0546	-0.0983
22	*Upeneus moluccensis*	235	0.0267	0.0535	-0.0969
24	*Drepane punctata*	45	0.0051	0.0102	-0.0270
25	*Rachycentron canadum*	1	0.0001	0.0002	-0.0010
26	*Echeneis naucrates*	5	0.0006	0.0011	-0.0043
27	*Scatophagus argus*	60	0.0068	0.0137	-0.0341

Table 2 Continued

No	Species	Total	Pi	(Pi)^2	PiLnPi
28	*Mugil cephalus*	50	0.0057	0.0114	-0.0294
29	*Leptomelanosoma indicum*	50	0.0057	0.0114	-0.0294
30	*Siganus canaliculatus*	200	0.0228	0.0455	-0.0861
31	*S. fuscescens*	340	0.0387	0.0774	-0.1258
32	*S. javus*	100	0.0114	0.0228	-0.0509
33	*Sphyrena obtusata*	30	0.0034	0.0068	-0.0194
34	*S. putnamae*	8	0.0009	0.0018	-0.0064
35	*Trichiurus lepturus*	505	0.0575	0.1150	-0.1642
36	*Scomberomorus commerson*	4	0.0005	0.0009	-0.0035
37	*S. guttatus*	2	0.0002	0.0005	-0.0019
38	*S. lineolatus*	4	0.0005	0.0009	-0.0035
39	*S. tritor*	5	0.0006	0.0011	-0.0043
40	*Rastrelliger kanagurata*	560	0.0637	0.1275	-0.1755
41	*Pampus argentus*	6	0.0007	0.0014	-0.0050
42	*Paratrypauchen microcephalus*	150	0.0171	0.0341	-0.0695
43	*Pricanthus tayneus*	200	0.0228	0.0455	-0.0861
	Total individual	8786	1.0000	2.0000	-3.2427
				Shannon diversity index (H')	3.2427
				Pielou evenness index (J')	0.8621
				Species Richness (SR)	4.6251
				Dominance index (C)	2.0000

Table 3 Diversity indices of recorded marine fish species in bottom trawl net (May-August)

No	Species	Total	Pi	(Pi)^2	PiLnPi
1	*Epinephelus coioides*	5	0.0005	0.0009	-0.0036
2	*Pelates quadrilineatus*	75	0.0071	0.0142	-0.0352
3	*Sillaginopsis panijus*	157	0.0149	0.0298	-0.0626
4	*Megalaspis cordyla*	19	0.0018	0.0036	-0.0114
5	*Selaroides leptolepis*	145	0.0137	0.0275	-0.0589
6	*Alepes djedaba*	20	0.0019	0.0038	-0.0119
7	*Mene maculata*	125	0.0118	0.0237	-0.0525
8	*Gazza minuta*	150	0.0142	0.0284	-0.0605
9	*Photopectoralis bindus*	100	0.0095	0.0190	-0.0441
10	*Secutor ruconius*	350	0.0332	0.0663	-0.1130
11	*Gerres filamentosus*	30	0.0028	0.0057	-0.0167
12	*Nemipterus peronii*	30	0.0028	0.0057	-0.0167
13	*Johnius dussumieri*	3785	0.3587	0.7173	-0.3678
14	*Boesemania microlepis*	4985	0.4724	0.9448	-0.3543
15	*Drepane punctata*	60	0.0057	0.0114	-0.0294
16	*Scatophagus argus*	40	0.0038	0.0076	-0.0211
17	*Siganus canaliculatus*	50	0.0047	0.0095	-0.0254
18	*Siganus javus*	25	0.0024	0.0047	-0.0143
19	*Sphyrena obtusata*	24	0.0023	0.0045	-0.0138
20	*Trichiurus lepturus*	325	0.0308	0.0616	-0.1072
21	*Scomberomorus guttatus*	11	0.0010	0.0021	-0.0072
22	*Pampus argentus*	42	0.0040	0.0080	-0.0220
	Total individual	10553	1.0000	2.0000	-1.4494
				Shannon diversity index (H')	1.4494
				Pielou evenness index (J')	0.4689
				Species Richness (SR)	2.2667
				Dominance index (C)	2

Table 4 Diversity indices of recorded marine fish species in beach surrounding net (May-August)

No	Species	Total	Pi	(Pi)^2	PiLnPi
1	*Lates calcarifer*	312	0.0619	0.1238	-0.1723
2	*Cephalopholis formosa*	18	0.0036	0.0071	-0.0201
3	*Epinephelus areolatus*	21	0.0042	0.0083	-0.0228
4	*E. coioides*	13	0.0026	0.0052	-0.0154
5	*E. marginatus*	4	0.0008	0.0016	-0.0057
6	*Selaroides leptolepis*	185	0.0367	0.0734	-0.1213
7	*Decaptarus maruadsi*	80	0.0159	0.0318	-0.0658
8	*Gazza minuta*	180	0.0357	0.0714	-0.1190
9	*Leiognathus longispinis*	16	0.0032	0.0064	-0.0183
10	*Secutor ruconius*	275	0.0546	0.1091	-0.1587
11	*Lutjanus fulvus*	122	0.0242	0.0484	-0.0901
12	*L. johnii*	262	0.0520	0.1040	-0.1537
13	*L. russellii*	120	0.0238	0.0476	-0.0890
14	*L. vitta*	15	0.0030	0.0060	-0.0173
15	*Gerres filamentosus*	100	0.0198	0.0397	-0.0778
16	*Lethrinus lentjan*	8	0.0016	0.0032	-0.0102
17	*Johnius dussumieri*	110	0.0218	0.0437	-0.0835
18	*Boesemania microlepis*	60	0.0119	0.0238	-0.0528
19	*Drepane punctata*	55	0.0109	0.0218	-0.0493
20	*Scatophagus argus*	800	0.1588	0.3175	-0.2922
21	*Mugil cephalus*	165	0.0327	0.0655	-0.1120
22	*Eleutheronema tetradactylum*	382	0.0758	0.1516	-0.1956
23	*Siganus canaliculatus*	220	0.0437	0.0873	-0.1367
24	*S. fuscescens*	100	0.0198	0.0397	-0.0778
25	*S. javus*	355	0.0705	0.1409	-0.1869
26	*Sphyrena obtusata*	5	0.0010	0.0020	-0.0069
27	*S. putnamae*	13	0.0026	0.0052	-0.0154
28	*Trichiurus lepturus*	20	0.0040	0.0079	-0.0219
29	*Scomberomorus guttatus*	2	0.0004	0.0008	-0.0031
30	*Pampus argentus*	3	0.0006	0.0012	-0.0044
31	*Glossogobius giuris*	85	0.0169	0.0337	-0.0689
	Total individual	4106	0.8148	1.6297	-2.4647
				Shannon diversity index (H')	2.4647
				Pielou evenness index (J')	0.7178
				Species Richness (SR)	3.6056
				Dominance index (C)	1.6297

A. *Lates calcarifer*

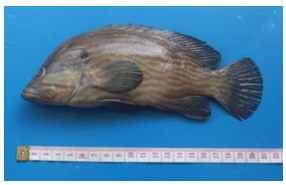

B. *Eephalopholis formosa*

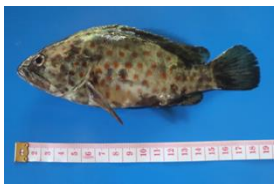

C. *Epinephelus areolatus*

D. *Epinephelus coioides*

E. *E. marginatus*

F. *Terapon puta*

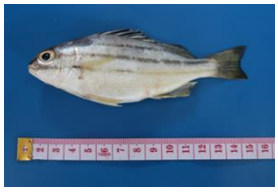

G. *Pelates quadrilineatus*

H. *Sillaginopsis panijus*

I. *Jaydia truncata*

J. *Megalaspis cordyla*

K. *Parastromateus niger*

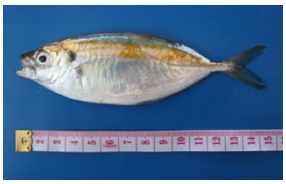

L. *Selaroies leptolepis*

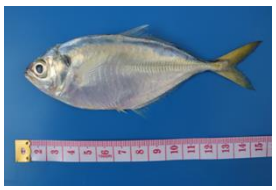

M. *Alepes djedaba*

N. *Decapterus maruadsi*

O. *Scomberoides commersonnianus*

P. *Scomberoides tol*

Q. *Seriolina nigrofasciata*

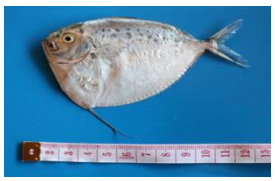

R. *Mene maculat*

S. *Gazza minuta*

T. *Leiognathus longispinis*

Plate 3 Fish species of Families Centropomidae, Serranidae, Terapontidae, Sillaginidae, Apogonidae,Carangidae, Menidae and Leiognathidae from Order Perciformes

A. *Photopectoralis bindus*

B. *Secutor ruconius*

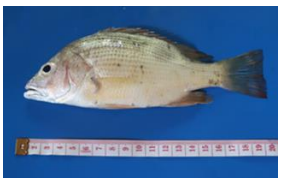

C. *Lutjanus fulvus*

D. *Lutjanus johnii*

E. *Lutjanus russellii*

F. *Lutjanus vitta*

G. *Gerres filamentosus*

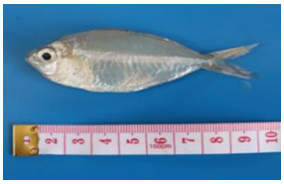

H. *Pentaprion longimanus*

I. *Lethrinus lentjan*

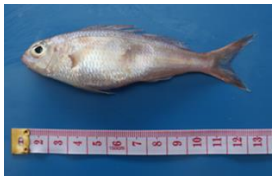
J. *Nemipterus peronii*

K. *N. virgatus*

L. *Johnius dussumieri*

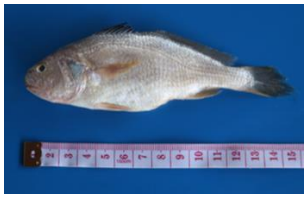
M. *Boesemania microlepis*

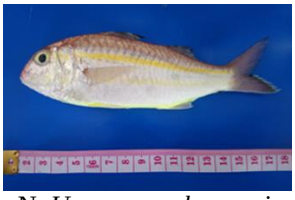
N. *Upeneus moluccensis*

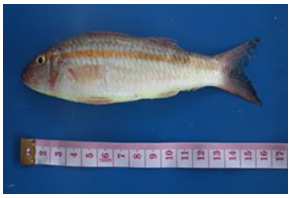
O. *Upeneus vittatus*

P. *Drepane punctata*

.

Q. *Rachycentron canadum*

R. *Echeneis naucrates*

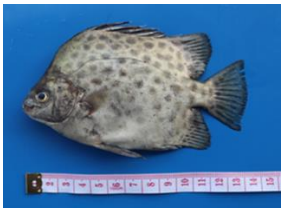
S. *Scatophagus argus*

T. *Mugil cephalus*

Plate 4 Fish species from Order Perciformes

A. *Eleutheronema tetradactylum*

B.*Leptomelanosoma indicum*

C. *Siganus canaliculatus*

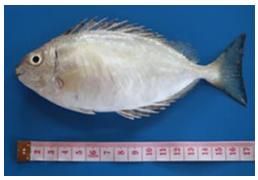
D. *Siganus fuscescens*

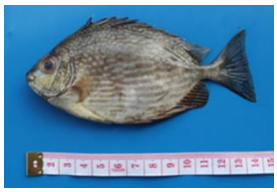
E. *Siganus javus*

F. *Sphyrena obtusata*

G. *Sphyrena putnamae*

H. *Trichiurus lepturus*

I. *Scomberomorus commerson*

J. *Scomberomorus guttatus*

K. *Scomberomorus lineolatus*

L. *Scomberomorus tritor*

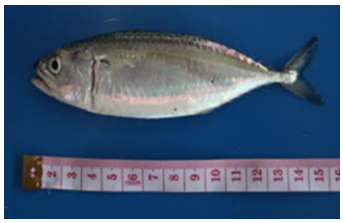
M. *Rastrelliger kanagurta*

N. *Pampus argentus*

O. *Glossogobius giuris*

P. *Paratrypauchen microcephalus*

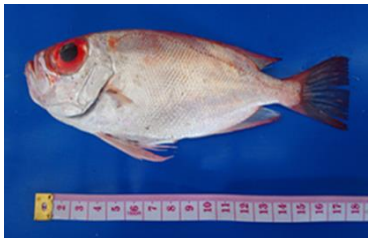
Q. *Pricanthus tayneus*

Plate 5 Fish species from Order Perciformes

Discussion

In this study, the recorded species differ from that of previous workers who have studied along the water ways of Rakhine State and its environs of study area. The fish species in Thandwe Township as surveyed by Aye Mi San (2008) included 45 species belonging to ten orders. Hnin Wai Phyo (2019) collected 93 species of 13 orders from Thandwe Township. Of these 16 were similar to those of Aye Mi San (2008). 39 species were similar to those of Hnin Wai Phyo (2019). Recorded numbers of species were different above the study works. That may be due to the different collection sites.

The fish population always shows fluctuation during the study period. This was due to the weather condition and types of gear. Yanbye township can be bit by depression and cyclones of the Bay of Bengal. Storms, tidal waves, strong winds and heavy rains can cause widespread damage to lives. The result of present study was similar with those of Hnin Wai Phyo (2019).

Three types of fishing gears: boat seine net (Kyawt Pike), bottom trawl net (Gyan Paik) and beach surrounding net (Moyan Pike) were mainly utilized in the study area. The main fishing gears was used in similar types apart from their sizes which depend on the sizes of the boats. Mesh size of the nets are changed mostly depending on targeted fish species as well as water body and also seasons.

In the present study, boat seine net (kyawt pike) was mostly employed. This net was banned from late April to October. This finding was similar with Hnin Wai Phyo (2019). Because the wind is a strong factor that cause just as much damage as water. So, another nets (bottom trawl net and beach surrounding net) could be change during the study period. Utilization of bottom trawl could cause depletion of deep-sea fish species since immature were recorded. Two types (boat seine and bottom trawl) were similar to Hnin Wai Phyo. That may be due to the different collection sites.

Diversity index states the circumstances of the organism's population to analyze the number of individuals in each growth in a habitat community. Shannon diversity index explains both variety and relative abundance of fish species. In the present study, the Shannon Diversity Index (H') value was 3.2427, 1.4494 and 2.4647 in boat seine net, bottom trawl net and beach surrounding net respectively. The indices were highly variation in different gears. Species diversity sampled with bottom trawl net and beach surrounding net

reached minimum values from May to August and boat seine net with maximum values from December to April. The calculated (H') value 3.2427 of boat seine net indicates its healthy status. In the present study, the diversity indices, evenness and species richness were good result from December to April with boat seine net. The present observed data of boat seine net is satisfactory.

Hnin Wai Phyo (2019) recorded three fishing gears: bottom trawl, beach seine and boat seine nets. She stated that fishing by boat seine net is carried out cool season (December to April) and the rainy season (June to August) is resting time. So bottom trawl net can be changed during the rainy season. The diversity indices, evenness and species richness were healthy status in rainy season only. The present finding was similar with Hnin Wai Phyo (2019).

Conclusion

Many marine fishes inhabit the Rakhine coastal region. In the present study, the type of fishing gear mostly employed was boat seine net. So, the mesh size is important for controlling casualties during fishing. Besides, utilization of trawl net could cause depletion of deep-sea fish species immature fish species were recorded in the catches by trawl net during this study. This factor should be taken into account from the aspect of conservation to maintain long-term sustainable food source. So majority fishing gears and methods recorded were found harmful for fish diversity and abundance. Thus, gear restrictions and over fishing were the most important factors for declining of fish diversity. Thus, local people need to be aware of declining fish population for long-term area of food sources.

Acknowledgements

We would like to express our profound gratitude to Dr Nay Win Oo, Rector of East Yangon University for his keen interest and also for his permission. We are indebted to Dr Aye Aye Ko, Dr Wah Wah Lwin and Dr Thida Aung, Pro-Rectors, East Yangon University for their supports, permitting to conduct this work and confidence in the implementation of this research. We would like to express our profound gratitude to Dr Ohn Mar Ohn, Professor and Head of Zoology Department, East Yangon University, for her valuable suggestions and encouragement. We are greatly indebted to Dr Aye Thida Than, Professor, of Zoology Department of Zoology East Yangon University.

References

Aung Htay Oo, 2009. *Status of deep-sea survey in Myanmar*. Fishery Resources Conservation Unit, R & D. Department of Fisheries.

Aye Mi San, 2008. Ecological aspect of fisheries in the environs of Thandwe Township, Rakhine State. *M.Sc Thesis*, Dangon University.

DOF, 2018. Fishery Statistics. The republic of The Union of Myanmar Ministry of Agriculture, livestock and Irrigation. Department of Fisheries Myanmar.

FAO, 2011. *Review of the state of world marine fishery resources*. FAO Fisheries and Aquaculture Technical Paper No. 569, 334 pp.

Froese, R. and Pauly, D. 2019. List of marine /brackish fishes for Myanmar available at http://www. Fishbase.org, version (12/2019).

Hnin Wai Phyo, 2019. Species composition, diversity and seasonal variation of marine fishes from Thandwe Township, Rakhine State. *M.Sc Thesis*, Department of Zoology, Dagon University.

Khin Maung Aye, Win Ko Ko and Siriraksophon, S. 2006. *Inland Fishing Gear and Methods in Southeast Asia*. (SEAFDEC) Training Department P.O. Box 97, Phrasamutchedi, Thailand.

Myanmar census, 2017. The 2014 Myanmar Population and Housing Census Rakhine State, Kyaukphyu District, Yanbye Township Report. The republic of the union of Myanmar. Department of Population Ministry of Labour, Immigration and Population.

Myint Pe, 2002. National Report of Myanmar On the Sustainable Management of The Bay of Bengal Large Marine Ecosystem (BOBLME) GCP/RAS/179/WBG. Department of Fisheries Grounds of Myanmar and Landing Sites.

Psomadakis, P.N., Htun Thein, Barry, C.R. and Mya Than Tun, 2019. *Field identification guide to the living marine resources of Myanmar*. FAO Species Identification Guide for Fishery Purposes. ISSN 1020-6868.

INVESTIGATION OF SOME EDIBLE GASTROPOD SPECIES IN NATIONAL RACES VILLAGE AT THARKAYTA TOWNSHIP

Su Hlaing Myint[1], Thet Thet Myaing[2]

Abstract

The present study was conducted to observe the investigation of edible snail species and their habitats of Tharkayta Township, during December 2018 to September 2019. A total of six gastropod species, four genera in three families and two orders were observed. Some gastropods species were collected by using plastic hand gloves and a pair of forces and dead specimens was keeping in dry plastic bottles. In this study area, six colleded gastropods among than one specie is land snail and other five species are aquatic species. For species composition and relative abundance calculated by using Brish *et al* 2004. Species composition of family Ampullariidae (67%) followed by family Achatinidae and Viviparidae (16.5% each). The most abundance specie was *Filopaludina bengalensis* (1612 inds.) very common and remaining five species were common. Collected gastropod species varied with different foraging habits and habitat types. In this study period, was found at six habitat types. *Filopaludina bengalensis* was found on four habitat types and remaining species were found three habitat types.

Keyword: Edible snails, Species abundance, Habitat types

Introduction

Mollusks are the second largest invertebrate group in abundance next only to insect (Abbott, 1989; Bouch *et al*., 1922). Estimates of the total number of valid described and undescribed mollusk species range from 50,000 to 200,000 (Van Bruggen, 1995). Among these 31,000-100,000 are marine, 14,000-35,000 terrestrial and about 5,000 freshwater species (Abbott, 1989; cited by Seddon, 2000).

Soft-bodied snails and slugs belong to the phylum Mollusca and the class Gastropoda. The Latin word mollusks mean soft and the class name, Gastropoda, originates from the Greek words gaster (belly) and podos (foot) (Martin, 2000).

Almost all species of snails can be identified by shell characters. In a few species of snails, the colour of the body is useful for identification (Godan, 1983).

The shell of gastropods is made of one part (univalve) and usually coiled into a spiral. The majority of shell were coiled to the right (dextral) and they normally coiled to the left (sinistral). If the mouth or aperture is on the right shell is dextral, in the reverse case it is sinistral (Pfleger, 1998).

Most recent estimates tend to favor the higher end of the range (e.g., Stork, 1999). Despite this uncertainty, and given the caveats mentioned above, we estimate that there are approximately 24,000 terrestrial and 7000 freshwater mollusk species for which valid descriptions exist. In addition, there are probably 11,000 to 40,000 undescribed terrestrial species and 3000 to 10,000 undescribed freshwater species (cited by Charles *et al.*, 2004).

The mollusks are richly represented in natural. The number of the species and individual numbers are also largely influenced by the diversity of the microhabitats. Snails are nocturnal but they active only when meteorological condition provide a relatively warm and moist environment (Solem, 1984).

The aim of the study is to contribute to an understanding of the value and shape and size of freshwater and land snails of different microhabitats, according to different areas and their foraging patterns.

[1] Demonstrator, Department of Zoology, East Yangon University
[2] Professor Head (Retired), Department of Zoology, East Yangon University

The objectives of the study were as follows:

- to record some species in study sites
- to study the habitat type of study area
- to investigate the relative abundance of some edible gastropod species in the study area

Materials And Methods

Study area and study period

The field surveys conducted and National Races Village in Tharkayta Twonship, Yangon Region, between 16º 48′ 10.81 ″ N and 96º 13′ 50.17″ E (Fig.1). Sampling was carried out from December 2018 to September 2019.

Specimen and data collection

National Races Village was occurring ditches, small ponds, leaf litter, trees, ground patches and mud. The study areas were searched for dead and living specimens. They were collected by using plastic hand gloves and a pair of forces from the respective habitats (Plate 1). Dead specimens were keeping in dry bottles (Plate 2).

Morphometric measurements

Specimens were collected from each study site and morphometric measurements were used caliper. The measurements were recorded for all collected specimens to confirm identification done by shell pattern, whorl (Wh), width (W), height (H), spire, apex, aperture umbilicus, suture and other characteristics (Plate 2).

Identification of specimens

Species were identified by taxonomic criteria according to Blandford and Godwin-Austen (1908); Vaught (1989), Marshall (1921), Gude (1914) and Subba Rao (1989). Different size of *Achatina fulica* such as small, medium and large size were classified according to Naggs and Raheem (2002).

Analysis of data

Species composition of gastropods in study area was conducted by using following formula designated by Bisht *et al*., 2004.

$$\text{Species composition} = \frac{\text{Number of individual of a species}}{\text{Total number of individual of all species}} \times 100$$

Recorded gastropods data were analyzed for relative abundance. The calculating method for relative abundance was followed after (Bisht *et al*., 2004).

$$\text{Relative abundance} = \frac{\text{Number of individual of a species}}{\text{Total number of individual of all species}}$$

uC = uncommon (having relative abundance less than 0.01)
C = common (having relative abundance of 0.01but less than 0.05)
vC = very common (having relative abundance of 0.05 and above)

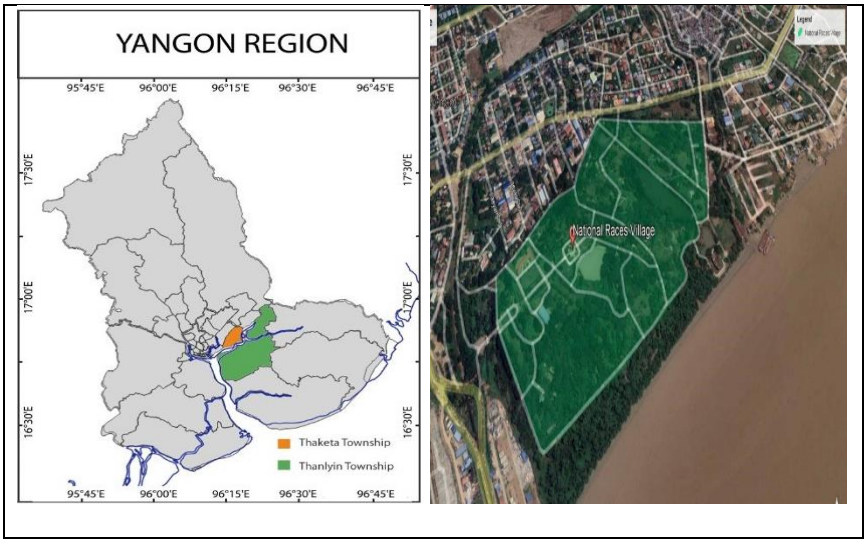

Fig.1 Map of the study site

Source: Google earth, 2019

A. Collected Gastropod species patches in ground

B. Collected Gastropod species in ditch

C. *Pomacea* spp. on the mud

D. *Filopaludina bengalensis* on the ground patches

Plate1 Site of Collected species

A. Cylindrical plastic box and bottle

B. Hand gloves and clipper

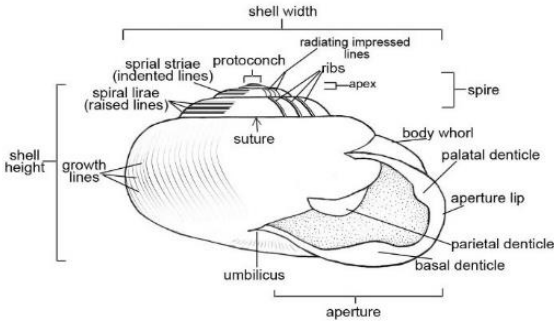

C. Identification and measurement of collected Species

D. Morphological structure of mollusks (followed after Penha and Burch, 2005)

Plate 2 Material used, maintain species and Morphological structure

Results

A total of six gastropod species belong to four genera and three families under two orders were collected from Tharkayta Township Yangon Region (Table 1, Fig. 1 and Plate 3). Study species were collected pulmonate and operculate species, one species of pulmonate and operculate was found in five species. One species is land snail and five species are aquatic snails.

Table 1 Systematic position of the collected gastropod species from study area

No	Order	Family	No	Scientific name	Common name	Type of snails
I	Stylommatophora	Achatinidae	1	*Achatina fulica*	Giant African snail	L.S
II	Architaenioglossa	Ampullariidae	2	*Pila ampullacea*	Apple snail	A.S
			3	*P. scutata*	Asian apple snail	A.S
			4	*Pomacea canaliculata*	Channeled or Golden apple snail	A.S
			5	*P. maculata*	Island apple snail	A.S
		Viviparidae	6	*Filopaludina bengalensis*	-	A.S

L.S=Land snail
A.S=Aquatic snail

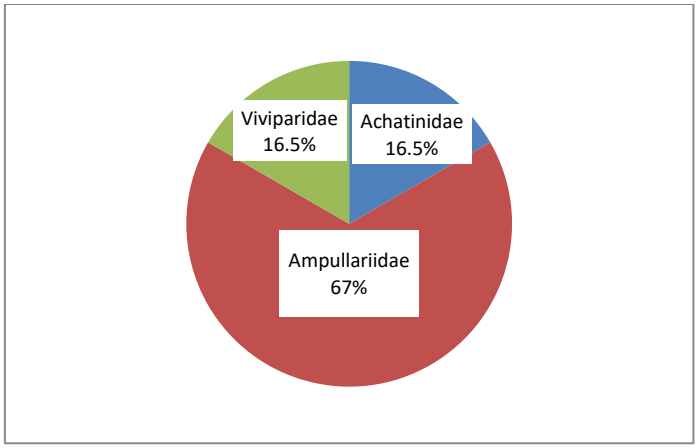

Fig. 2 Systematic position in different family of the collected gastropod species from study area

Table 2 Relative abundance of collected gastropod species in National Races Village

No	Scientific Name	Dec	Jan	Feb	Mar	Apr	May	Jun	Jul	Aug	Total	Relative Abundance	RAI
1	*Achatina fulica*	8	5	3	7	5	10	6	8	6	58	0.0295	C
2	*Pila ampullacea*	4	3	2	0	0	14	19	21	15	78	0.0396	C
3	*P. scutata*	4	4	1	0	1	14	20	23	17	84	0.0427	C
4	*Pomacea canaliculata*	0	1	0	0	0	11	13	19	15	59	0.0300	C
5	*P. maculata*	0	1	1	0	0	13	15	21	22	73	0.0371	C
6	*Filopaludina bengalensis*	147	472	382	39	99	149	124	109	91	1612	0.8203	vC
	Total Number of individual	163	486	389	46	105	211	197	201	166	1964		
	Total Number of species	4	6	5	2	3	6	6	6	6			

uC=0, C=5, vC=1 RAI = Relative Abundance Index

uC=uncommon , C =common , vC =very common

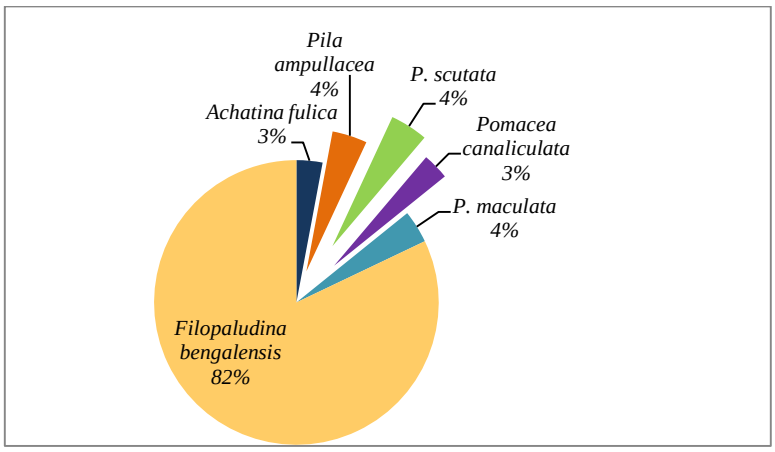

Fig. 3 Occurrence of collected gastropods individual numbers in relation with their each species as shown by percentages in study site

Table 3 Habitat types of collected species in study area

Scientific name	ditches	small ponds	leaf litter	trees	ground patches	mud	Total
Achatina fulica	-	-	√	√	√	-	3
Pila ampullacea	√	√	-	-	-	√	3
P. scutata	√	√	-	-	-	√	3
Pomacea canaliculata	√	√	-	-	-	√	3
P. maculata	√	√	-	-	-	√	3
Filopaludina bengalensis	√	√	-	-	√	√	4
Total species	5	5	1	1	2	5	19

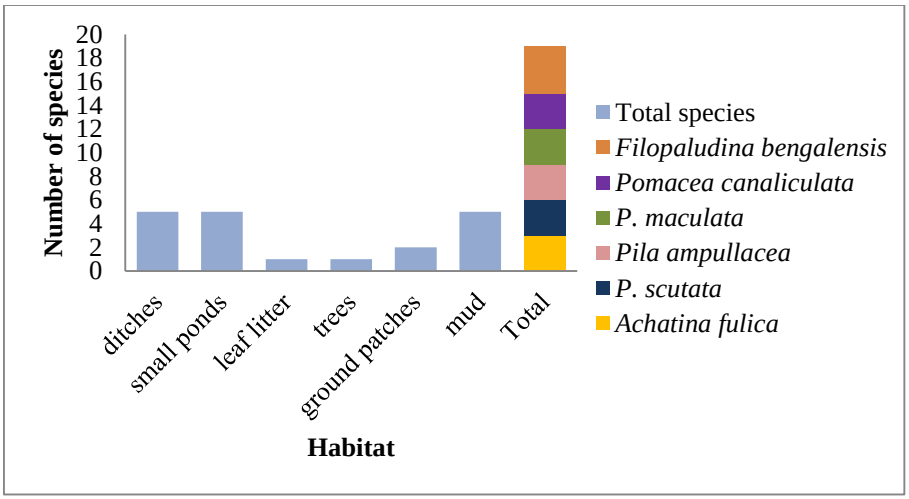

Fig. 4 Habitat types of collected species in study area

A. *Achatina fulica*

Aperture view

B. *Achatina fulica*

Abperture view

Family Achatinidae

C. *Pila ampullacea*
Aperture view

D. *Pila ampullacea*
Abperture view

E. *Pila scutata*
Aperture view

F. *Pila scutata*
Abperture view

G. *Pomacea canaliculata*
Aperture view

H. *Pomacea canaliculata*
Abperture view

I. *Pomacea maculata*
Aperture view

J. *Pomacea maculata*
Abperture view

Family Ampullariidae

E. *Filopaludina bengalensis*
Aperture view

F. *Filopaludina bengalensis*
Abperture view

Family Viviparidae

Plate 3 Gastropod species of Family Achatinidae, Ampullariidae and Viviparidae

Discussion

Survey of gastropod species was conducted in National Races Village at Tharkayta Township of Yangon Region, Myanmar. There are six habitat types in the study area. Land snail and aquatic snail species were observed under three families.

Class Gastropoda containing about 40,000 living and 15,000 fossil species (Hickman and Larson, 1993). A total of 13 mollusks species in nine families belonging to five orders were recorded. Species composition of family Ampullariidae was the largest (23.1%), followed by family Viviparoidae and Achatinidae were the lowest (7.7% each) respectively (Kay Zin Thwe, 2017).

In the present study, a total of six species, four genera under three families belonging to two orders were recorded. Species composition of family Ampullariidae (67%) followed by family Achatinidae and Viviparidae (16.5% each). Kay Zin Thwe and studied result is the same.

Brown (1913) stated that high relative humidity is also an important factor for snail and egg abundance. In the present study, the greatest monthly collected total individuals were found in January and the lowest total individual number was found in March from National Race Village. It could be due to climate factors that influences survive the snail population numbers.

Reheem, *et al*., 2008 stated that a substantial number of widespread and localized forest landsnail species can survive in garden. Moreover, *Achatina fulica* was the most widely distributed species. Outeiro, *et al*., (1993); Nekola (2010); De Winter and Gittenberger (1998) had stated that the effects of vegetation, climate, distribution and disturbance history was regulated with the species riches.

The results showed that *Achatina fulica* was found in home garden area, agricultural area. In the present study, *A. fulica* was found throughtout the study period. In the present study was found in plenty tree and fresh plants natural vegetation in study site, it would be generalist and agreed with Outeiro, *et al*., (1993); Nekola (2010); De Winter and Gittenberger (1998).

Freeland and Jazen (1974) stated that in choosing fresh plants and detritus plants gastropods have to trade-off between maximizing nutritional quality and minimizing secondary chemical contained in their food. *Pomacea canaliculata, P. maculata, Filopaludina* spp. and were not found in agriculture area. Regarding the foraging habits and habitats of gastropods and micro snail, in the present study, different species the foraging habits and habitat types were observed.

In this study, *Pila ampullacea*, *P. scutata*, *Pomacea canaliculata*, *P.maculata*, *Filopaludina bengalensis* was found in pond, ditch and plash. So this finding was agreed with the statement of the pervious author Freeland and Jazen (1974).

Albuquerque *et al*., 2006 stated that *Achatina fulica* was most active from the beginning of the evening until the mild morning. The result is similar to those obtained by Rauth and Baker (2002).

In the present study, most of the snails were nocturnal: active from the sunset until sunrise. However, snails were active depending on some cloudy and rainy days. Prior (1985) stated that they were active only in favored meteorological conditions, which provided a relatively warm and moist environment.

They generally do not live in brackish-water habitats. Ampullariids are regarded as amphibious because they possess both a well-developed gill and a lung and they often perform aquatic and aerial respiration simultaneously (Andrews, 1965; Berthold, 1991; McClary, 1964; Seuffert and Martín, 2009). Ampullariids are freshwater snails. Many ampullariids aestivate during dry periods (Lum-Kong and Kenny, 1989). When the habitat dries out, they bury themselves in the mud (Schnorbach, 1995, cited by Tietze, *et al*., 2012).

In the present study, ampullariids was found in pond, on land, ditches and mud, this statement that above authors. Seasonal abundance of collected highest individual numbers was found in winter, followed by rainy and lowest individual numbers was found in summer from National Races Village. In recorded species, *Pila ampullacea* was not found March and April, *P. scutata* was not found March, *Pomacea canaliculata* and *P. maculate* were not found December, February, March and April. *Achatina fulica* and *Filopaludina bengalensis* were found in monthly at National Races Village. In my study periods, *Filopaludina bengalensis* is very common and common are remaining five species. The result all collected species have not uncommon.

Conclusion

In study period, collected six edible gastropods species, one species is land snail and the rest species are aquatic snails. Monthly collected data in December (163 inds.), January (486 inds), February (389 inds), March (46 inds), April (105 inds), May (211 inds), Jun (197 inds), July (201 inds), August (166 inds) at National Races Village. As a result, total collected data can cause the abundance of species numbers change. The highest individual numbers in January and the lowest individual numbers in March were recorded. In study period, ditches, small ponds and mud (5 species), ground patches (2 species), leaf litter and trees (1 species) each respectively. *Filopaludina bengalensis* was found in four places and remaining five species was found in three places. *Pomacea* sp. is destroying in the paddy field. These edible snails are the

beneficial for human food source. So, more confirmation required to be identified in the National Races Village.

Acknowledgements

We are grateful to Dr Nay Win Oo, Rector of East Yangon University for his permission to carry out this research. We are greatly indebted to Dr Aye Aye Ko, Dr Wah Wah Lwin and Dr Thida Aung, Pro-Rectors East Yangon University for their encourage and permitting to conduct this work research. We are also grateful thanks to Professor Dr Ohn Mar Ohn, Head of Zoology Department, East Yangon University, for her kind permission to read the paper research and valuable advice. We are special thanks to Dr Aye Thida Than, Professor of Zoology Department, East Yangon University, for providing advices and support of this research paper. We highly acknowledge to office staffs from National Races Village.

References

Albuquerque, F.S., M.C. Pesop-Aguiar, and M.J.T. Assumcao-Albuquerque, (2006) "Distribution, feeding behavior and contril strategies of the exotic land snail *Achatina fulica* (Gastropoda: Pulmonta in the north of Brazil)." Braz. *J, Biol*, 68(4)-842.

Bisht, M. S., J. Kukreti, and Shantikhuson, (2004) "Relative abundance and distribution of bird fauna of Garhwal Himalaya." Eco. Env & Cons, 10 (4): 451-460

Brown, A.P., (1913) "Variation in two species of Lucidella from Jamaica." *Proceeding of the Academy of Natura Science Philadelphia* 63:3-21.

Blandford, W.T. F.R.S., and H.H. F.R.S. Godwin-Austen. (1908) *The Fauna of British India, incluing Ceylon and Burma*. Mollusca-I Testacellidae and Zonitidae. Printed by Taylor and Francis, Red Lion Court, Fleet Street. Calacutta: Thacker. Spinker & Co. Bombay Thacker & Co. Limited.

Charles, L., R. H. Cowie, F. P. Winston, E. B. Arthur, B. Philippe, A. C. Stephanie, S. C. Kevin, J. F. Terrence, G. Olivier, G. Ht. Dai, H. Robert, E. P. Kathryn, R. Barry, S. Mary, E. S Ellen., and G. T. Fred, (2004) "The Global Decline of Nonmarine Mollusks." *Article in BioScience*. April 2004 DOI: 10.1641/0006-3568 (2004) 054 [0321: TGDONM] 2.0.CO; 2· Source: OAI.

De Winter, A.J., and E. Gittenberger, (1998) "The land snail fauna of a square kilometer patch of rainforest in south western Cameroon: high species richness, low abundance and seasonal fluctuation." *Malacologia*. 40:231-250.

Freeland, W.J., and D.H. Jazen, (1974) "Strategies in herbivory by mammals-role of plant secondary compounds." *American Naturalist*, 108:265-289.

Godan, D. (1983) *Pest slugs and snails: Biology and Control.*1st Edition. Springer Verlag Berlin Heidelberg, 73-74:287- 293.

Gude, G.K. F.Z.S. (1914) *The Fauna of British India, incluing Ceylon and Burma*. Mollusca-II Trochomorphidae-Janellidae. Printed by Taylor and Francis, Bombay Thacker & Co…Limited.

Hickman, C.P., L.S. Roberts, and A. Larson. (1993) *Intergrated principle of Zoology*. Wm. C Brown Publishers. Oxford, Englan.pp. 412-447.

Kay Zin Thwe (2017) *Occurrence of some gastropod species in Kyauktaenvirons, Yangon.* MSc Thesis. Department of Zoology, Yangon University.

Marshall, G.A.K. (1921) *The Fauna of British India, incluing Ceylon and Burma*. Mollusca-III Cyclophoridae, Truncatellidae, Assimineidae, Helicinidae. Printed by Taylor and Francis, Red Lion Court, Fleet Street. Calacutta: Thacker. Spinker & Co. Bombay Thacker & Co…Limited.

Martin, S.M. (2000) *Terrestrial Snails Slugs (Mollusca: Gastropoda) of Maine*. Northeastern Naturalist 7:33-88. Mollusks (G.M. Barker, ed.), pp. 121-151. CABI Publishing. August 06, 2019 at

Naggs, F., and D. Raheem, (2002) "Land snail diversity in Srilanka." *The Natural History Museum*, London, UK.

Nekola, J.C., (2010) "Acidophilic terrestrial gastropod communities of North America." *J. of Moll. Stud*. New York, 76:144-156.

Outeiro, A., C. Aguera, and C. Parejo, (1993) "USA of ecological profiles in a study of the relationship of terrestrial gastropods and environmental factors." *J. of Conchology* 34:365-375.

Penha, S and Burch, J.B., 2005. An Introduction to the micro snails of Thailand, *malacological Review*, Vol.37/38:1-155.

Pfleger, D. (1998) *Afield Guide in Colour to Mollusks*. Blitz Edition, 216 pp.

Prior, D.J., (1985) "Water-regulatory behavior in terrestrial; gastropods." *Biological. Review* vol-60, p.403-429.

Raheem, C.D., F. Naggs, R.C. Preece, Y. Mapaumna, L. Kariyawasam, and P. Eggleton, (2008) "Structure and Conservation of Sri Lankan land-snail assemblages in fragmented lowland rainforest and village home graden." *Journal of Applied Ecology* 45: 1019-1028.

Rauth, S.K., and G.M. Baker, (2002) "Achatina fulica Bowdich and other Achatinidae as a pest in tropical agriculyure, Mollusks as Crop Pest." New Zealand: ED. By Land scare Research Hamilton. 472pp.

Seddon, M., (2000) "Molluscan Biodiversity and the Impact of Large Dams." *Report to IUCN Species Survial Commission*.

Solem, A., (1984) "A world model for land snail diversity abundance." *In*: *Worldwide snails: biogeographical; studies on non-marine Mollusca* A. Solem, and A.C. Van Burggen, eds, 6-12.E.J. Brill/W, Backhuys, Leiden.

Subba Rao N.V. (1989) *Freshwater molluscs of India*. Printed at: The Radiant Process Private Limited, Calcutta, India and published by the Director, Zoological Survey of India, Calcutta. 231pp.

Tietze, E., C.G. De Francesco, and V. Núñez, (2012) "Diversity, Habitat and Genetics." ISBN 978-1-61324-695-5 Editors: A. Bianchi et al. 2012, Published by Nova Science Publishers, Inc. New York. pp 1-35.

Vaught, K.C. (1989) *A classification of the living Mollusca*. (Eds. R.T. Abott and K.J. Boss). A, erocam malcogilsts, Melbourne, Florida 32902, USA.

EFFECTS OF DIFFERENT DIETS ON THE GROWTH AND SURVIVAL RATE OF COMET GOLDFISH, *CARASSIUS AURATUS AURATUS* LINNAEUS, 1758

Myat Su Aung[1], Aye Aye Than[2]

Abstract

This experiment was conducted to study the effects of different diets on growth and survival rate of *Carassius auratus auratus* (Comet goldfish). The study period lasted from December 2019 to August 2020. The effect of three types of formulated feeds containing different proportions of animal protein (fish meal) and plant protein (soybean meal) were evaluated and these compared with that of a commercially available pellet feed. The experiment was conducted in three glass aquaria to study the growth performance, survival rate, feed conversion ratio (FCR), specific growth rate. Diet D1 was prepared in combination with crude protein of fish meal (38.3%), Diet D2 was prepared in combination with crude protein of soy bean (28.58%). Diet D3 was ready made pellet (Tokyu) as a control experiment (32%) crude protein. In Comet goldfish fingerlings fed with diet D1 gained the highest body weight (5.88 ± 0.80 g), followed by diet D2 (5.87 ± 1.02 g) and D3 (5.58 ± 0.78g). The total length attained by fish was (6.31 ± 0.56 cm) on D1, (6.29 ± 1.07 cm) on D2 and (6.15 ± 0.59cm) on D3. The correlation coefficient 'r' was significant in all diets. The final stage of correlation coefficient between length and weight fed with different diets were highly significant at $p<0.01$ level. Higher survival rate was recorded in diet D1 (92.86%) compared to experimental diets D2 (85.71%) and D3 (92.86%). The FCR value of Comet goldfish fed with diet D1 (0.77) was better than diet D2 (0.81) and diet D3 (0.88). Specific growth rate of experimental diets D1 was (2.18%), D2 was (2.06%) while that of commercial diet D3 was (1.88 %). Diet D1 was better for the growth of the fish and D2 was less the effect on the fish growth. Thus, based on the result of growth performance and better FCR the fish meal diet D1 should be added to feed in the rearing of studied fish species. Fishkeeping hobbyists and aquarium fishery culture need to understand the feeding of fish to increase growth rate, promote health and facilitate reproduction. The finding of this study could be provided effective information for fishkeeping hobbyists and small aquarium fishery culture enterprise.

Key Words : formulated feeds, survival rate, feed conversion ratio, specific growth rate

Introduction

Ornamental fish is one of the important items among the various types of commercially important fishes marketed nationally and internationally. Only a few hundred of 4000-5000 ornamental fish species currently being kept as pet fish worldwide are very popular and commonly kept by a large number of fish hobbyists (Pannevis, 1993).

The Comet goldfish (*Carassius auratus auratus*) is one of the most popular breeds of goldfish in the United States. They are commonly found in pet stores as well as aquariums of all shapes and sizes. The Comet Goldfish is a beautiful, slender fish that has a similar body shape to that of the Common Goldfish. The Comet can be a variety of different colors and patterns. The most traditional coloration is the yellow-orange, orange-red color ranges. Comet Goldfish are omnivores so they will happily consume plant sources as well as meat sources (Anonymous, 2019).

Fish food consists of natural food and artificial feeds. When fish have balanced diet to eat, they grow fast and stay healthy. Fishes have various diets according to their feeding habits. DCorrect and suitable amount of diet produces healthy, colorful and disease-resistant fish. Healthy fish are more colorful than unhealthy one. Knowledge of feeding is very essential from the economical point of view (Lovell, 1987).

In ornamental fish, a correct formulation of the diet improves the nutrient digestibility and supplies the metabolic needs, reducing the maintenance cost and at the same time the

[1] Demonstrator, Department of Zoology, East Yangon University
[2] Dr Professor, Department of Zoology, Dawei University

water pollution. In aquarium, nutrition is critical because feed represents 40-50% of the production costs. Protein is the most expensive part of fish feed, it is important to accurately determine the protein requirements for each species and size of cultured fish (Houlihan *et al.*, 2001).

The crude protein requirements in many fish species generally range between 25 and 55%. There exists in a difference in optimum level of protein requirement between carnivorous and omnivorous fishes. Typically, carnivorous fish requires 40-55% dietary protein against only 35-45% protein requirement in omnivorous fishes (National Research Council, 1993).

Formulated feeds are complete feeds which supply all the nutrients necessary for optimal growth and health of the fish in culture practices. Fish nutrition has advanced dramatically in recent times with the development of new and balanced commercial feeds that promote optimal fish growth and health (Chong *et al.*, 2004).

Fish feed is hardly formulated without fish meal. Fish meal is produced either from the trash obtained from trawling or fish waste from the canning industry. The percentage protein depends on the source of fish product and method used in producing the fish meal. Soybean meal has a balanced amino acid profile and can replace a substantial part of fish meal. The use of this feedstuff is high fat content and presence of trypsin inhibitor (Zeitler, 1984).

The growth and feed conversion ratio (FCR) of a fish is remarkable tool to compute the acceptability of artificial feed. The proper information of FCR on locally available ingredients will provide the basis to develop acceptable feed, though the task of preparing acceptable and suitable artificial feed for fish is complex due to its feeding preferences (Jhingran,1991).

The main objective of the present study was to study the nutritional efficacy of three formulated feeds prepared with protein levels on growth rate and feeds conversion ratio. Among varieties of animal by-products such as fish meal and plant by-products such as soybean meal, rice bran, and wheat bran were chosen for these studies.

The present study was conducted with the following objectives;

- to access the content of crude protein, fat, ash and moisture
- to compare the effect of different diets on the growth rate of Comet goldfish, *Carassius auratus auratus*
- to analyze the survival rate, feed conversion ratio and specific growth rate of studied fish species

Materials And Methods

Study site and study period

The study site is Laboratory of Zoology Department, East Yangon University. Study period lasted from December 2019 to August 2020 (Plate 1).

Selection of ornamental fishes

Ornamental fish *Carassius auratus auratus* (Comet goldfish) was selected from families Cyprinidae. Two months old Comet goldfish are used for the experiment. The fishes were collected from the breeding pond of Lucky pet aquarium shop.

Preparation of Diets

Three diets (D1 to D3) were formulated by different feed ingredients. Diet D1 was prepared with animal based such as fish meal plus rice bran and wheat bran. Diet D2 was prepared with plant based such as soybean meal plus rice bran and wheat bran. Diet D3 was ready made pellet (Tokyu) as a control experiment. The ingredients of each diet were mixed and egg was added at the ratio of 3:4 (total weight of diet to egg). The mixture of diets made into

pellets and then sun dried for two days (Plate 2).
For the experiment

- Diet D1 (Fish meal 40% + rice bran 20% + corn 20% + wheat bran 10% + meat and bone meal 10%)
- Diet D2 (Soybean meal 40% + rice bran 20% + corn 20% + wheat bran 10%+meat and bone meal 10%)
- Diet D3 - Readymade pellet (Tokyu) as a control experiment.

Experimental set up

The experiment was done in three glass aquaria. The dimension of each aquarium was 90 x 45 x 45 cm^3. The experiment conducted *Carassius auratus auratus* (Comet goldfish) in Aquarium 1, 2 and 3. Each aquarium was stocked with 14 fingerlings. Aquarium 1 was given diet D1, those of Aquarium 2 with diet D2 and those in Aquarium 3 with diet D3. Prior to stocking, fishes were also weighed and measured individually. Glass aquaria which have been cleaned with salt for nearly two days were used to avoid the presence of toxic substances and placed under sunlight. During the experiment, every three days, three quarters of water of the aquarium was siphoned out and refilled with tap water. Aquaria were covered with plastic mosquito-net lids to prevent unnecessary disturbance and escape of fishes. Cleaning of three aquaria was done on a weekly basis.

Recording of water parameters

The water temperature of aquaria was noted twice a day with the use of common thermometer. The range of water temperature was applied between 28 - 31°C during study period by using heater.

Water pH was examined once a week using color matching method. In order to maintain stable water conditions, Dissolved Oxygen and pH in each aquarium was monitored by changing water daily and by using air pump (Table 1)

Table 1 Water parameters

Parameter	Unit	Tube well	Standard EPA value
pH		7.3	6.5 - 9
Total Alkalinity	mg/l	98	100-250
Total Hardness	mg/l	38	40 - 150
Dissolved Oxygen	mg/l	4.5	>5

Source for standard values; from U.S Environmental Protection Agency (EPA) Quality Criteria for water (1998)

Data recording

The morphometric characteristics i.e. body weight and total length was recorded to observe their growth performance. Standard length and body weight of ornamental fishes of each aquarium were measured to the nearest centimeter and gram. Measurements were taken monthly by using a scaled ruler and a weighting digital balance. The mean standard length and weight were calculated. Dead fish were removed and recorded. At the end of the experiment, weight gain, specific growth rate (SGR) and food conversion ratio (FCR) were calculated.

Analytical procedure

The composition of protein, fat, moisture and ash in each diet were examined at Analytical Laboratory Section, Department of Fisheries.

Water quality was assessed in the Laboratory of Freshwater Aquaculture Research Unit, Department of Fisheries (Table 1).

Comparison among three different diets in each experiment was done by Paired sample T-test. The relationships between the length and weight of fishes were calculated by the program of Microsoft Excel 2010 and Pearson Correlation Coefficient Test of SPSS version 11.5.

Growth rate, feed conversion ratio (FCR), specific growth rate (SGR) and survival rate were calculated as follows.

Feed conversion ratio $FCR = P/(W_k - W_p)$

Where P = Amount of food offered (g)

W_k = Final weight of fish in a aquarium (g)

W_p = Initial weight of fish in a aquarium (g) (Sadowski *et al.*, 1998)

$$\text{Specific growth rate SGR} = \frac{W_f - W_i}{T} \times 100$$

W_f = mean final weight

W_i = mean initial weight

T = total experiment days (Vasagam *et al.*, 2007)

The fish survival rate was calculated as the number of fishes harvested as percentage of the number of fish stocked.

$$\text{Survival rate} = \frac{\text{final fish number}}{\text{initial fish number}} \times 100$$ (Booth and Alquezar, 2002)

Identification of species

Species was identified according to Petrovicky`(1989).

Aquaria in Laboratory of Zoology Department

Aquarium (1)

Aquarium (2)

Aquarium (3)

Plate 1 Experiment aquaria in Zoology Department of East Yangon University

Plate 2 Formulated food

Results

Systematic position

The systematic positions of ornamental fish was identified according to Petrovicky`(1989)

Phylum - Chordata
Class - Actinopterygii
Order - Cypriniformes
Family - Cyprinidae
Genus - *Cyprinus*
Species - *C. auratus auratus* Linnaeus,1758
Common name - Comet goldfish
Local name - Shwe-nga

Morphological characteristics of studied ornamental fish species

Cyprinus auratus auratus Linnaeus,1758
Common name- Comet goldfish

Dorsal spines: 3 - 4; Dorsal soft rays: 14-20; Anal spines: 2-3; Anal soft rays: 4 - 7. Body stout, thick-set, caudal peduncle thick and short. Head without scales, broadly triangular, interorbital space broad, snout longer than eye diameter, maxillary reaching posterior nostril or not quite to eye, barbels lacking on upper jaw. Lateral line complete. Dorsal and anal fins with serrate bony spines, pelvic fins short, broad and thoracic. Nuptial tubercles of male fine, on opercle, sometimes on back and a few on pectoral fins. Caudal fin with 17-19 rays. The comet goldfish have the slightly smaller and slimmer body. The head is wide but short, mouth is small and its body tapers smoothly from its back and belly to the base of its caudal fin. Comet possess two sets of paired fins and three single fins. The caudal fin is long and deeply forked. They are primarily a reddish orange color, but they are also available in yellow, orange, white and red.

Nutrient values of fishmeal and soybean meal

Nutrient values of fishmeal formulated feed D1 contained crude protein 38.3%, fat 8.5%, ash 14.5%, moisture 4.5% and soybean meal formulated feed D2 contained crude protein 28.58%, fat 0.1%, ash 7.5%, moisture 5.1% and in D3 Tokyu pellet contained crude protein 32%, fat 4%, ash 10%, moisture 9% were analyzed (Table 2).

Mean body weight and length of Comet goldfish between four months study period

Mean body weight and length of Comet goldfish receiving three different types of diets were also differed.

Growth performance of Comet goldfish fed with Diet D1

Initial weight and length of Comet goldfish fed with D1 were 3.27 ± 0.77 g and 4.21 ± 0.73 cm, respectively which increased to 4.64 ± 1.23 g and 4.96 ± 0.53 cm at the end of first month. Then the weight and length of fish increased regularly to 5.02 ± 1.12 g and 5.28 ± 0.64 cm at the end of second month and 5.51 ± 0.86 g and 5.46 ± 0.63 cm at the end of third month and 5.88 ± 0.80 g and 6.31 ± 0.56 cm at the end of the fourth month (Table 3) (Fig. 1 and 2).

Growth performance of Comet goldfish fed with Diet D2

Initially the size of fish fed with D2 was 3.26 ± 0.91 g in weight and 4.21 ± 0.89 cm in length. After one month of feeding, the mean weight and length of fish was found to be 4.51 ± 0.83 g and 4.85 ±0.53 cm, respectively. It increased to 4.94 ± 0.89 g and 5.15 ± 0.42 cm at the end of the second month and 5.36 ± 0.89 g and 5.42 ± 0.91 cm at the end of third month and 5.87 ± 1.02 g and 6.29 ± 1.07 cm at the end of fourth month (Table 3) (Fig. 1 and 2).

Growth performance of Comet goldfish fed with Diet D3

Initially, weight and length of fish fed with D3 was 3.32 ± 0.44 g and 4.25 ± 0.32 cm, respectively. After one month of feeding, the fish grew to 4.47 ± 1.05 g in weight and 5.14 ± 0.49 cm in length. At the end of second month, it grew to 4.96 ± 0.6 g in weight and 5.24 ± 0.43 cm in length and 5.26 ± 0.64 g and 5.35 ± 0.63 cm at the end of third month. At the end of experiment, the fish increased to 5.58 ± 0.78 g and 6.15 ± 0.59 cm (Table 3) (Fig. 1 and 2).

Comparison of the effects of the three feed formulations on the growth of fish

The weight and length of fish at the beginning of the experiment was the same. Significant different was not fount between three Diets ($p<0.05$), (Table 4). At the end of experiment, the size of the fish received Diet D1 was significantly different from those provide with Diet D2 and D3. However, no significant different was found between the fish those fed with Diet D2 and D3 (Table 5).

Table 2 The composition of food ingredients

Ingredients	Crude protein (%)	Crude fat (%)	Moisture (%)	Ash (%)
Diet D1 Fish meal	38.3	8.5	4.5	14.5
Diet D2 Soybean meal	28.58	0.1	5.1	7.5
Diet D3 Tokyu pellet	32	4	9	10

(Analytical Laboratory Section, Department of Fisheries)

Table 3 Monthly growth performance of Comet goldfish using three different diets

	Initial state		First month		Second month		Third month		Fourth month	
	Weight (g)	Length (cm)	Weight (g)	Length (cm)	Weight (g)	Length (cm)	Weight (g)	Length (cm)	Weight (g)	Length (cm)
Diet (1)	3.27 ± 0.77	4.21 ± 0.73	4.64 ± 1.23	4.96 ± 0.53	5.02 ± 1.12	5.28 ± 0.64	5.51 ± 0.86	5.46 ± 0.63	5.88 ± 0.80	6.31± 0.56
Diet (2)	3.26 ± 0.91	4.21 ± 0.89	4.51 ± 0.83	4.85 ± 0.53	4.94 ± 0.89	5.15 ± 0.42	5.36 ± 0.89	5.42 ± 0.91	5.87 ± 1.02	6.29 ± 1.07
Diet (3)	3.32 ± 0.44	4.25 ± 0.32	4.47 ± 1.05	5.14 ± 0.49	4.96 ± 0.6	5.24 ± 0.43	5.26 ± 0.64	5.35 ± 0.63	5.58 ± 0.78	6.15 ± 0.59

Table 4 Comparison of initial standard length and body weight of Comet goldfish fed on three different diets

Condition	Growth	P. value	Remark
Diet (3) vs Diet (1)	Weight	0.05*	S
	Length	0.03	S
Diet (3) vs Diet (2)	Weight	0.20	NS
	Length	0.82	NS
Diet (1) vs Diet (2)	Weight	0.92	NS
	Length	0.45	NS

Table 5 Comparison of final standard length and body weight of Comet goldfish fed on three different diets

Condition	Growth	P. value	Remark
Diet (3) vs Diet (1)	Weight	0.000**	S
	Length	0.000**	S
Diet (3) vs Diet (2)	Weight	0.07	NS
	Length	0.10	NS
Diet (1) vs Diet (2)	Weight	0.01*	S
	Length	0.04*	S

Significant level **p<0.01 (Paired sample T-test)
*p<0.05
S= Significant, NS= Non significant

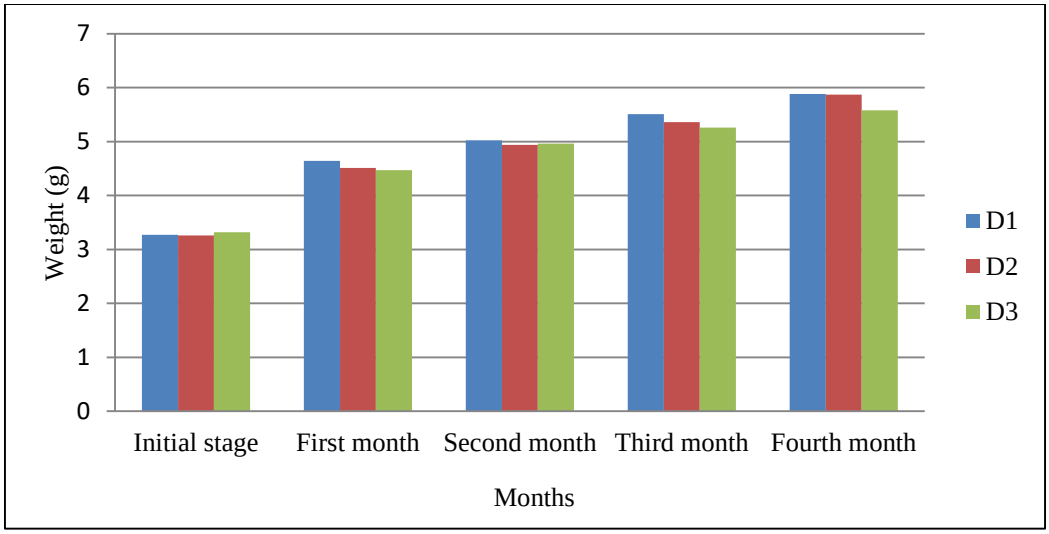

Fig. 1 Monthly growth (weight) performance of Comet goldfish using three different diets

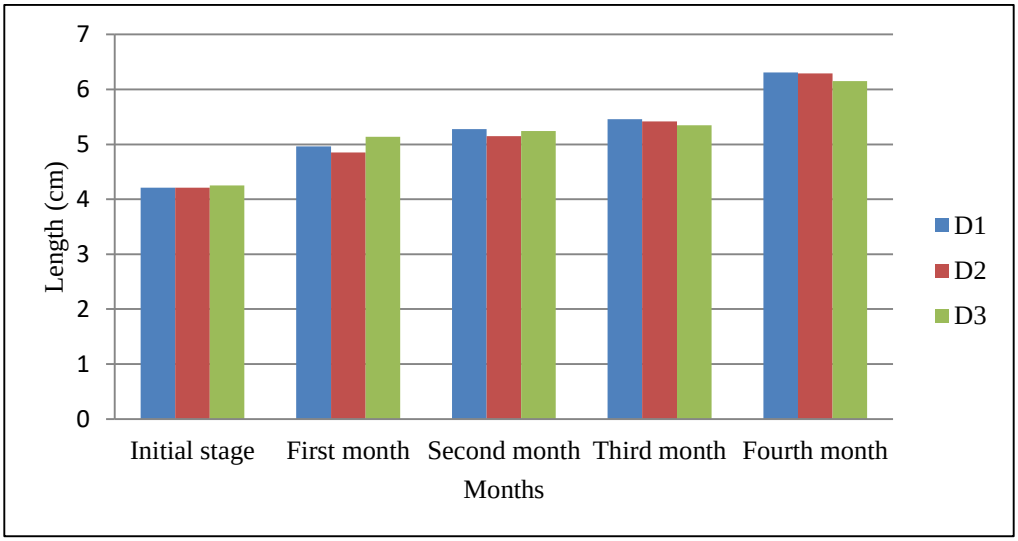

Fig. 2 Monthly growth (length) performance of Comet goldfish using three different diets

Correlation between length and weight of Comet goldfish fed with different diets

The initial stage of correlation coefficient between length and weight of Comet goldfish fed with diet D1 was r = 0.82, feeding with diet D2 was r = 0.67, and feeding with diet D3 was r = 0.71 (Table 6). Strong relationship was highly significant at $p<0.01$ level, a positive relationship between weight and length. The coefficient of determination reveals that (r^2) 51 % of the change in the weight is explained by change in length in diet D3, 68 % in diet D1 and 45% in diet D2 (Fig. 3).

At the end of the experiment, the correlation coefficient between length and weight of Comet goldfish fed with D1 was r = 0.96, feeding with diet D2 was r = 0.72, and feeding with diet D3 was r = 0.86 (Table 7). Significant positive relation between length and weight of Comet goldfish was observed in all three diets. The coefficient of determination reveals that (r^2) 74 % of the change in the weight is explained by change in length in diet D3, 93 % in diet D1 and 52 % in diet D2 (Fig. 4).

Survival rate, feed conversion ratio and specific growth rate of Comet goldfish

At the end of experiment (4 months), survival rate of Comet goldfish fed on diet D1 was 92.86 %, diet D2 was 85.71 % and diet D3 was 92.86 %. The formulated diet D1 was highest percentage and the same result was observed in control experiment of diet D3.

Feed conversion ratio (FCR) of Comet goldfish fed on diet D1 was 0.77, diet D2 was 0.81, and diet D3 was 0.88. The value of FCR was lower (better) in diet D1 than that of diet D2 and diet D3.

Specific growth rate of Comet goldfish fed on diet D1 was 2.18, diet D2 was 2.06 and diet D3 was 1.88 The specific growth rate show that fingerlings of Comet goldfish fed with diet D1 was the best, followed by diet D2 and D3 (Table 8).

Table 6 Correlations of initial body weight and length of Comet goldfish

	Weight Mean ± SD	Length Mean ± SD	Correlation coefficient (r)	P value
Diet (1)	3.27 ± 0.77	4.21 ± 0.73	$R^2 = 0.677$ $r = 0.822$	0.000**
Diet (2)	3.26 ± 0.91	4.21 ±0.89	$R^2 = 0.447$ $r = 0.669$	0.008**
Diet (3)	3.32 ± 0.44	4.25 ± 0.32	$R^2 = 0.506$ $r = 0.711$	0.004**

Table 7 Correlations of final body weight and length of Comet goldfish

	Weight mean ± SD	Length mean ± SD	Correlation coefficient (r)	P value
Diet (1)	5.88 ± 0.8	6.31 ± 0.56	$R^2 = 0.925$ $r = 0.961$	0.000**
Diet (2)	5.87 ± 1.02	6.29 ± 1.07	$R^2 = 0.524$ $r = 0.723$	0.003**
Diet (3)	5.58 ± 0.78	6.15 ± 0.59	$R^2 = 0.735$ $r = 0.857$	0.000**

Table 8 Survival rate, feed conversion ratio and specific growth rate of Comet goldfish

	Survival rate %	Feed conversion ratio (FCR)	SGR %
Diet (1)	92.86	0.77	2.18
Diet (2)	85.71	0.81	2.06
Diet (3)	92.86	0.88	1.88

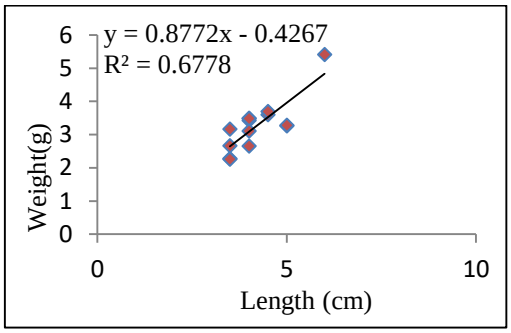

A. Diet D1

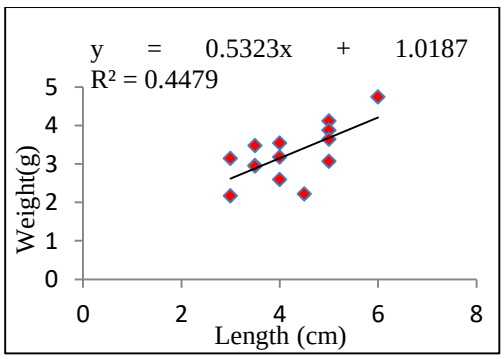

B. Diet D2

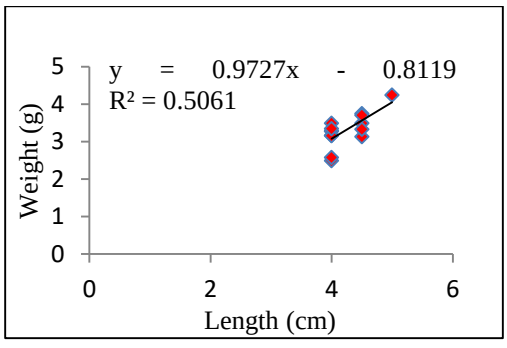

C. Diet D3

Fig. 3 Initial body length and weight relationshipin Comet goldfish feeding with different di

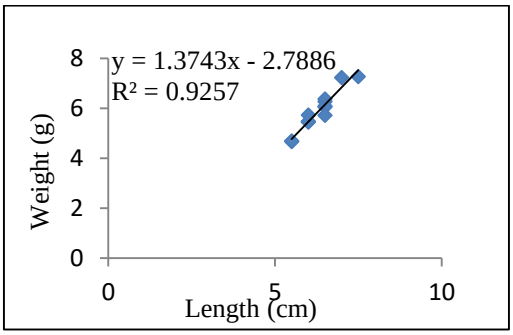

A. Diet D1

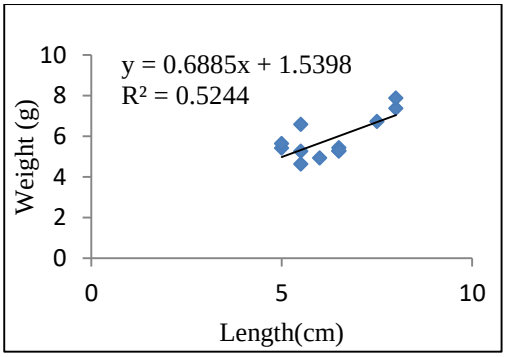

B. Diet D2

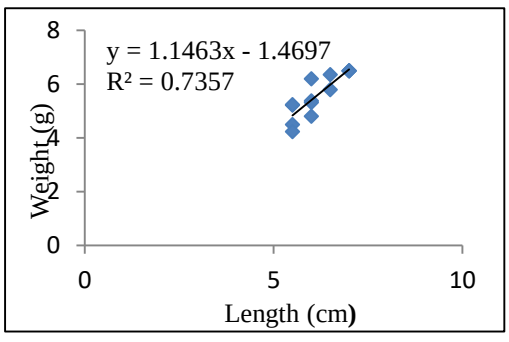

C. Diet D3

Fig. 4 Final body length and weight relationship in Comet goldfish feeding with different diets

Discussion

Ornamental fish keeping is one of the most popular hobbies in the world today. With the expansion of global ornamental fish trade, increased attention is being paid to the nutritional requirements of ornamental fish. Nutrition is one of the key factors of improving production efficiency of ornamental fish (Jagtap and Kulkarni, 2013).

The present study was undertaken to evaluate the effect of fish meal and soybean meal in studied fish species. Growth performance of fish species fed with three different types of diets found to differ from each other. At the end of experiment, body weight of Comet goldfish feeding with diet D1 was 5.88 g whereas feeding with Diet D2 was 5.87 g and diet D3 was 5.58 g. The growth performance of fish species fed with D1 was significant different from those fed with D2 and D3. It was clearly observed that species was well accepting the fish meal diet D1. In Comet goldfish, the highest weight gain (2.61 g) was recorded in D1 and the lowest weight gain (2.26g) was recorded in D3. It was assumed that D1 is the best food for the rearing of Comet goldfish fingerlings.

Atar and Secer (2003) stated that the length-weight relationships are important prerequisites to know the variations in weight from the known length indicating feeding, growth, breeding etc., and to estimate the population size of a stock for the purpose of its exploitation. In the present study, the linear plot based calculated values suggested that there is a direct relationship in length-weight relationships. The logarithmic relation between weight and length indicated a linear relationship signifying the increase in weight with increase in length. The correlation coefficient 'r' was significant in all diets. At the end of experiment correlation between length and weight of fish species fed with different diets were highly significant at $p<0.01$ level. Hansen (1997) described that the correlation coefficient 'r' can range from -1.0 to +1.0, with 0.0 indicating no linear relationship whatever. The present study has been found that correlations coefficient of final body weight and length of Comet goldfish species fed with Diet D1 was ($r = 0.96$), diet D2 was ($r = 0.72$), diet D3 was ($r = 0.86$). Thus, the result supported to Hansen (1997) and linear relationships were observed in studied fish species.

Food conversion ratio (FCR) is calculated as the weight of the feed fed to the fish divided by the weight of fish growth. As far as the value of FCR is concerned, the better (lower) feed conversion ratio of Comet goldfish was observed for fish meal (0.77), followed by soy bean meal (0.81) and diet D3 (0.88). Ali and Salim (2004) noted higher FCR value for rice polish (5.27), followed by fish meal (3.026) and sunflower meal (3.021). The FCR value of sunflower was comparatively higher than the value of present results. Thus, agreed with the previous author. This indicated that fish meal D1 is more acceptable fish feed for rearing in fingerlings of studied species. Significantly higher percent of survival rate was recorded in D1 than in D2. Specific growth rate of experimental diets D1 was (2.18%), D2 was (2.06%) while that of commercial diet D3 was (1.88 %). The value of FCR and SGR showed good condition in diet D1 than in diet D2 and D3. Steffens (1981) and Jauncy (1982) reported that best FCR recorded at certain protein level after which it increases. This is due to wider gap between protein and energy content of feed. FCR value decreased gradually with the increased protein level of the feed indicating better utilization of feed by juveniles at higher protein level. This is confirmed for the higher digestibility diet D1 at 38.3% crude protein in feed. Bureau (1997) stated that animal protein by products can be very useful complementary protein source in fish diets and it is important to use highly digestible products. Present findings agreed with the previous author.

In the present study, specific growth rate were the best in diet D1. According to the result, diet D1 could be considered as valuable food for studied fish species and it seems to be tasty than other diets because of the animal protein source. Moreover, ingredients of Diet D1 could be attracted the fish and these compounds seem to convert the food energy into

increase in growth performance.

Conclusion

The effect of food on the growth and survival rate of *Cyprinus auratus auratus* (Comet goldfish) was investigated in aquaria of Zoology Department, East Yangon University. Of the three formulated experimental diets, diet D1 had been given growth performance similar to the commercial pellet diet. The experiment revealed that diet D1 gave the best growth and survival rate. However, the fishes ate vigorously the diet D1 because the smells of fish meal that is able to attract than the other food. The value of FCR and SGR showed good condition in diet D1. Moreover, significantly higher percentage of survival rate was recorded in the experimental diets D1 than in the diet D2. Experimental diets formulated with locally available animal protein sources could be used in commercial production of studied fish species. Fishkeeping hobbyists need to understand the feeding of fish to increase growth rate, promote health and facilitate reproduction. The finding of this study could be provided effective information for hobbyists and small aquarium fishery culture enterprise. Thus, the present result could be contributed to the culture and management of these fish species.

Acknowledgements

We are very grateful to Dr Nay Win Oo, Rector of East Yangon University for his keen interest and also for his permission. We are indebted to Dr Aye Aye Ko (Pro-Rector), Dr Wah Wah Lwin (Pro-Rector) and Dr Thida Aung (Pro-Rector), East Yangon University for their supports, permitting to conduct this work and confidence in the implementation of this research. We are also grateful thanks to Dr Ohn Mar Ohn, Professor and Head, Department of Zoology, East Yangon University, for her valuable suggestions, constructive criticisms of the manuscripts and supervision.

References

Ali, T. and M. Salim (2004). Studies on the growth response and feed conversion ratio (FCR) of *Labeo rohita* fingerlings fed on rice polish, fish meal and sunflower meal. *Int. Journal. Agri. Biol.,* 6(5): 914-917.

Anonymous, (2019). About Fish Online. http://www.aboutfishonline.com Wikipedia, the free encyclopedia. Available from 2020 January 19

Atar, H.H. and S. Secer (2003). Width/length-weight relationships of the blue crab (*Callinectes sapidus* Rathbun, 1896) population living in Beymelek Lagoon Lake. Turkish *Journal of Veterinary Animal Science*., 27:443-447.

Booth, D and R. Alquezar (2002). Food Supplementation Increases Larval Growth, Condition and Survival of *Acanthochromis polyacanthus*. *Journal of Fish Biology*, 60: 1126-1133.

Bureau, D. (1997). *Fish Nutrition – An Overview*. Fish Nutrition Research Lab. Dept. Animal Poultry Science University of Guelph, Ontario. A few notes about the Fish Nutrition Research Lab.

Chong, A., S.D., Ishak, Z. Osman, and R. Hashim (2004). Effect of dietary protein level on the reproductive performance of female swordtails *Xiphophorus helleri* (Poeciliidae). *Aquaculture,* 234(1-4): 381-392.

Hansen, C.F.K. (1997). *Experimental Design and Analysis in Aquaculture*. 0.56670-274.

Houlihan, D., T. Bouiard and M., Jobling eds. (2001). *Food Intake in Fish*. Iowa State University Press. Blackwell Science Ltd.418 pp.

Jagtap, H.S. and S.S. Kulkarni (2013). Influence of live and dry diets on growth and survival of goldfish (*Carassius auratus*). *International Journal Science*. Res., 2 (7): 2277 – 8179.

Jauncy, K., (1982). The effect of varying dietary protein level on the growth, food conversion, protein utilization and body composition of juvenile tilapia (*Sarotherodon mossambicus*). Aquaculture, 27: 43-54.

Jhingran, V. G. (1991). *Fish and Fisheries of India*. 3rd Ed., Hindustan Publishing Co., Delhi, India.

Lovell, T., (1987). Nutrition and feeding of fish. Feeding formulation and processing. Yan Nostrant Reinhokld, New York. 229pp.

National Research Council. (1993). *Nutrient requirements of fish*. Washington, D.C., National Academy Press.

Pannevis, M.C.(1993). *Nutrition of Ornamental Fish*. The Waltham Book of Companion Animal Nutrition. Pergamon Press, Oxford, 85-96

Petrovicky`,I. (1989). *Aquarium Fish of the Worl*d. Crown Publishers, Inc., 225 Park Avenue South, New York.

Sadowski, J., J. Filipiak and R. Trzebiatowski (1998). Effects of Different Duration of Feeding on Results of Carp (*Cyprinus carpio*) Fry Cage Culture in CoolingWater. *Electronic Journal of Polish Agricultural Universities. Fisheries,* 1 (1)

Steffens, W. (1981). Protein utilization of rainbow trout *(Salmogairdneri)* and carp (*Cyprinus carpio):* a brief

review. *Aquaculture*, 23: 337-345.

USEPA. (1998). *Guidelines of United States*. Environmental protection Agency (Standard EPA values, 1998) for standard quality of river water. New York.

Vasagam,K.P.K., A. Shanmugam, and S. Rajagopal (2007). Dietary Effect on Fry Production and Growth Performance of Sailfin Molly, *Poecilla latipinna* in Salt Water. *Acta Ichthyologica Et Piscatoria*,37(1);

Zeitler, M.H., M., Kirchgessner, E.J. Schwarz (1984). Effects of different proteins and energy supplies on carcass composition of carp (*Cyprinus carpio* L.) *Aquaculture* 36:Pp.37-48. http://dx.doi.org/10.1016/0044-8486(84)90052-8.Vol.36, Issue 1-2,1 January 1984.

SOME ECONOMIC FISH PRODUCTS FROM MYOMA MARKET IN KYAUKTAN TOWNSHIP, YANGON REGION

Yu Mon Khaing[1], Nyo Mie Kyaing[2]

Abstract

Surveys on some economic products was carried out in Myoma Market of Kyauktan Township, Yangon Region, from December 2019 to August 2020. The economic fish products such as salted dried fish, unsalted dried fish, fish paste (Nga-pi), fish sauce (Ngan-pyar-yee), salted fish (Nga-pi-kaung) and fermented fish (Nga-chin) were prepared from various kinds of fish. A total of 15 species under 15 genera and 13 families belonging to 11 orders of fishes were recorded. The highest economic product was found with the use of salted dried fish (13 species) followed by unsalted dried fish (ten species), while fish sauce and salted fish (two species for each) were studied. Fish paste and fermented fish (one species for each) were also studied.

Key words: economic fish products, dried fish, salted fish, etc.

Introduction

People of Myanmar like fish and fishery products which are essential daily meals of them because fish sauce, fish and shrimp paste are the favorite dishes of Myanmar (DoF, 2006). The usefulness of perishable forms such as fresh fish is limited to points at which iced storage is available. Other forms can widely be utilized after being processed by traditional methods such as sun-drying, salting, or smoking and fermentation (Amano, 1991).

Freshwater and brackish water fish fauna is abundant in Hmaw Wun creek. Myoma Market is situated near this river. Fishery sector is the most important for local people because it provides the economic importance of local fisher families and fishery industry. In fish industry, most fresh and dry fish are traded in the whole country. Therefore, the study area is endowed with abundant fish resources and also abundant fish products. Thus, the economic importance of some fish products from Myoma Market in Kyauktan Township was conducted with the following.

Objectives;

- to examine the economic fish products from Myoma Market
- to identify the collected fresh fish species from the study area

Materials And Methods

Study area and study sites

Myoma Market was chosen as the study site. It is situated at Kyauktan Township in Yangon Region. It lies between 16˚ 37' 28" North and 96˚ 19' 58" East (Fig. 1 and Plate 1).

Study period

The study period lasted from December, 2019 to August, 2020.

Data collection

The specimens were collected from dry fish shops and fish mongers of market. Field surveys were conducted twice in each month. Fish products were collected from dry fish shops and recorded by photographs. Fresh specimens of each collected fish product were studied from fish mongers. The morphological and taxonomic characters were recorded from fresh specimen. Scaled photographs were instantly taken to get natural size and colour.

Identification of fish species

Identification was followed after Talwar and Jhingran (1991).

[1] Demonstrator, Department of Zoology, East Yangon University

[2] Dr, Associate Professor, Department of Zoology, East Yangon University

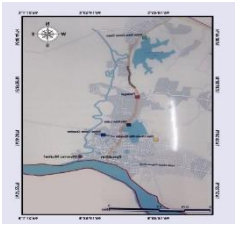

Fig. 1 Map of study area

Source: Department of Geography (East Yangon University)

(A) Myoma Market

(B) Dry fish shop

(C) Fish depot

Plate 1 Study sites

Results

Fish products from the study area

Fishes were used for different purposes in the study area. Economic fish products from Myoma Market were collected during the study period. They were salted dried fish, unsalted dried fish, fish paste (Nga-pi), fish sauce (Ngan-pyar-yee), salted fish (Nga-pi-kaung), and fermented fish (Nga-chin) (Table 1 and Plate 2-7)

Table 1 Economic fish products of collected fish species

Sr. No.	Species	Types of fish products					
		Salted dried fish	Unsalted dried fish	Fish paste	Fish sauce	Salted fish	Fermented fish
1	*Brevitrygon walga*	✓	✓	-	-	-	-
2	*Coilia dussumieri*	✓	✓	-	-	-	-
3	*Stolephorus indicus*	✓	✓	-	-	-	-
4	*Puntius sophore*	✓	✓	-	✓	-	✓
5	*Clarias batrachus*	-	-	-	-	✓	-
6	*Harpadon nehereus*	✓	✓	-	-	-	-
7	*Macrognathus zebrinus*	✓	-	-	-	-	-
8	*Lobotes surinamensis*	✓	✓	-	-	-	-
9	*Otolithes ruber*	✓	✓	-	-	-	-
10	*Trichiurus lepturus*	✓	-	-	-	-	-
11	*Rastrelliger kanagurta*	-	✓	-	-	-	-
12	*Scomberomorus guttatus*	✓	✓	-	-	-	-
13	*Channa striata*	✓	✓	✓	✓	✓	-
14	*Cynoglossus lingua*	✓	-	-	-	-	-
15	*Lagocephalus lunaris*	✓	-	-	-	-	-
	Total species	13	10	1	2	2	1

(√) Present

(-) Absent

A.*Brevitrygon walga*

B.*Coilia dussumieri*

C. *Stolephorus indicus*

D. *Puntius sophore*

E. *Harpadon nehereus*

F. Macrognathus *zebrinus*

G. *Lobotes surinamensis*

H.*Otolithes ruber*

I.*Trichiurus lepturus*

J.*Scomberomorus guttatus*

K.*Channa striata*

L.*Cynoglossus lingua*

M. *Lagocephalus lunaris*

Plate 2 Salted dried fishes

A. *Brevitrygon walga*

B.*Coilia dussumieri*

C.*Stolephorus indicus*

D. *Puntius sophore*

E. *Harpadon nehereus*

F.*Lobotes surinamensis*

G.*Otolithes ruber*

H.*Rastrelliger kanagurta*

I. *Scomberomorus guttatus*

J. *Channa striata*

Plate 3 Unsalted dried fishes

A.*Channa striata*

Plate 4 Fish paste

B.*Puntius sophore*& *Channa striata*

Plate 5 Fish sauce

A.*Clarias batrachus*

B.*Channa striata*

Plate 6 Salted fish

A. *Puntius sophore*

Plate 7 Fermented fish

Some collected fresh fish species from the study area

A total of 15 species under 15 genera and 13 families belonging to 11 orders of fishes were collected from the study area during the study period.(Table 2, Fig. 2 and Plate 8)

Table 2 Species composition of recorded fish species

Order	Family		Study Species	Local name
Myliobatiformes	Dasyatidae	1	*Brevitrygon walga* (Muller & Helen, 1841)	Nga-late-soon
Clupeiformes	Engraulidae	2	*Coilia dussumieri* (Valenciennes, 1848)	Nga-mee-tan-thwae
		3	*Stolephorus indicus* (van Hasselt, 1823)	Nga-ne-tu
Cypriniformes	Cyprinidae	4	*Puntius sophore* (F. Hamilton, 1822)	Nga-khoon-ma
Siluriformes	Clariidae	5	*Clarias batrachus* (Linnaeus, 1758)	Nga-ku
Aulopiformes	Synodontidae	6	*Harpadon nehereus* (F. Hamilton, 1822)	Nga-nut
Synbranchiformes	Mastacembelidae	7	*Macrognathus zebrinus* (Blyth, 1858)	Nga-mway-doh
	Lobotidae	8	*Lobotes surinamensis* (Bloch, 1790)	Nga-byin-ma
Perciformes	Sciaenidae	9	*Otolithes ruber* (Bloch & Schneider, 1801)	Nga-poke-thin
	Trichiuridae	10	*Trichiurus lepturus* Linnaeus, 1758	Nga-ta-khon
Scombriformes	Scombridae	11	*Rastrelliger kanagurta* (Cuvier, 1816)	Pa-lar-too
		12	*Scomberomorus guttatus* (Bloch & Schneider, 1801)	Nga-bee-zin
Anabantiformes	Channidae	13	*Channa striata* (Bloch, 1793)	Nga-yant
Pleuronectiformes	Cynoglossidae	14	*Cynoglossus lingua* Hamilton, 1822	Nga-khway-shar
Tetraodontiformes	Tetraodontidae	15	*Lagocephalus lunaris* (Bloch & Schneider, 1801)	Nga-pu-tin

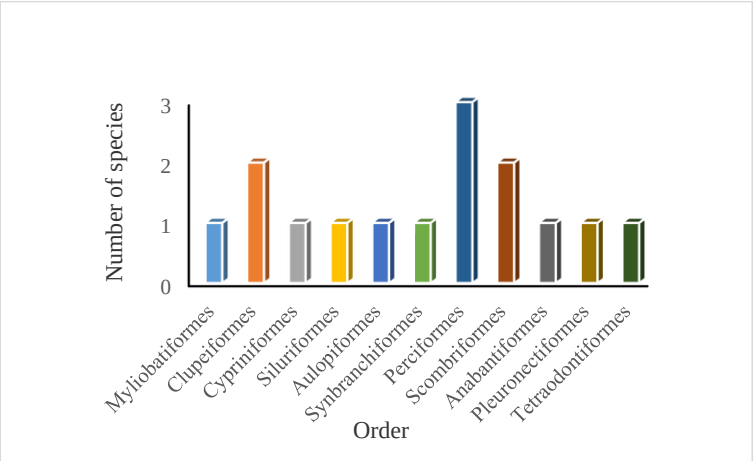

Fig. 2 Fish species composition of their respective orders

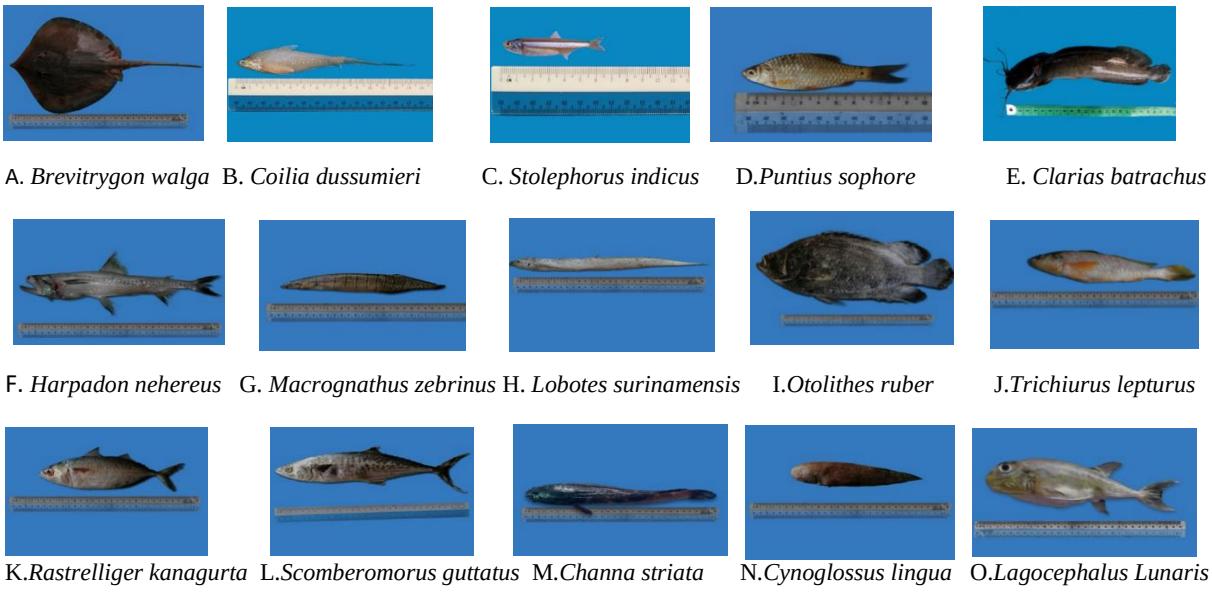

A. *Brevitrygon walga* B. *Coilia dussumieri* C. *Stolephorus indicus* D.*Puntius sophore* E. *Clarias batrachus*

F. *Harpadon nehereus* G. *Macrognathus zebrinus* H. *Lobotes surinamensis* I.*Otolithes ruber* J.*Trichiurus lepturus*

K.*Rastrelliger kanagurta* L.*Scomberomorus guttatus* M.*Channa striata* N.*Cynoglossus lingua* O.*Lagocephalus Lunaris*

Plate 8 Recorded species

Discussion

Some fish products were found to be important economically from Myoma Market observed in Kyauktan Township, Yangon Region.

Collected fish products were salted dried fish, unsalted dried fish, fish paste (Nga-pi), fish sauce (Ngan-pyar-yee), salted fish (Nga-pi-kaung), and fermented fish (Nga-chin). The highest fish products were found the salted dried fish (13 species) followed by unsalted dried fish (ten species), while fish sauce and salted fish (two species for each) were collected. Fish paste and fermented fish (one species for each) were the lowest fish products.

Phyu Sin Phwe (2013) studied socio-economic of fish products from some villages in Chaung-zon Township, Belugyun, Mon State. She reported that a total of collected 16 species used for various kinds of fishery products were described from her study sites. Among these

products, the highest economic product was salted dried fishes (13 species). Her observation was agreed with the present study.

Wint Naing Aung (2017) made a survey of economic importance of some fishes in different depots of Maubin Township. She described the highest economic products was found with the use of fresh eating followed by fish paste, dried fish, fermented fish while smoked fish, salted fish and fish sauce were the lowest. Her finding did not agree with the present study.

Regarding to species composition, only 15 species of fresh fishes were recorded from the study area. These fishes were identified and systematically placed under 11 orders, 13 families, 15 genera and 15 species during the study period. They are important as nutritional food requirements especially for every people of Myanmar.

Phyu Sin Phwe (2013) reported that a total of 16 fish species of 14 families under eight orders were recorded from Chaung-zon Township, Mon State. In the present study 15 species were recorded. Among them, four species *Coilia dussumieri, Clarias batrachus, Harpadon nehereus* and *Channa striata* were recorded species which were reported by Phyu Sin Phwe (2013).

Hnin Nyaint Nyaint Soe (2017) studied social and economic importance of some marine fishes from Chaungtha environs, Ayeyarwady Region. A total of 34 species belonging to 26 genera and 18 families under five orders were recorded during the study period. Two species were similar to the marine fishes which were recorded by Hnin Nyaint Nyaint Soe (2017). There are *Stolephorus indicus* and *Trichiurus lepturus.*

According to present results, order Perciformes included the most number of species (three species) among the collected fishes. The second most number of species (two species for each) were observed in Clupeiformes and Scombriformes, followed by orders Myliobatiformes, Cypriniformes, Siluriformes, Aulopiformes, Synbranchiformes, Anabantiformes, Pleuronectiformes and Tetraodontiformes (one species for each) were the least number of species.

Hnin Nyaint Nyaint Soe (2017) studied a total of 34 species which were recorded from Chaungtha environs. Order Perciformes was the most diverse group in which her study sites. Her observation was agreed with the present study.

Wint Naing Aung (2017) recorded a total of 15 fish species from the different depots of Maubin Township. Among 15 species recorded, the highest number of species was found in order Siluriformes. It did not agree with the present finding.

The result and finding of present work will give some important knowledge about recorded fish products and their fresh forms to people.

Conclusion

A total of six types of fish product were recorded and their fresh forms (15 species) noted in the present study. They were salted dried fish, unsalted dried fish, fish paste (Nga-pi), fish sauce (Ngan-pyar-yee), salted fish (Nga-pi-kaung), and fermented fish (Nga-chin). *Channa striata* was used for the popular economic important fish products such as salted dried fish, unsalted dried fish, fish paste, fish sauce and salted fish. As a result, it was found that all collected species were generally for the local market and home consumption in fresh form or fish products. Emphasis on the present finding of fishery surveys, all studied species could be regarded as commercially important species.

Acknowledgements

We would like to express our profound gratitude to Dr Nay Win Oo, Rector of East Yangon University for his keen interest and also for his permission. We are indebted to Dr Aye Aye Ko, Pro-Rector, Dr Wah Wah Lwin, Pro-Rector and Dr Thida Aung, Pro-Rector, East Yangon University for

their supports, permitting to conduct this work and confidence in the implementation of this research. We would like to express our profound gratitude to Dr Ohn Mar Ohn, Professor and Head of Zoology Department, East Yangon University, for her valuable suggestions and encouragement. We are greatly indebted to Dr Aye Thida Than, Professor, Department of Zoology, East Yangon University, for her valuable suggestions given throughout the research work.

References

Amano, K. (1991). The work of post-harvest technologists in our region. In: *Proceedings of the Seminar on Advances in Fishery Post-Harvest Technology in Southeast Asia*. Singapore, 6-11 May, 1991, 318 pp. Marine Fisheries Research Department, Southeast Asian Fisheries Development Centre.

DoF. (2006). *Fishery Statistics Year Book.* Department of Fisheries, Ministry of Livestock and Fishery. 103 pp.

Hnin Nyaint Nyaint Soe (2017). Social and economic importance of some marine fishes from Chaungtha Environs, Ayeyarwady Region. *MSc Thesis*, Department of Zoology, Pathein University.

Phyu Sin Phwe (2013). Socio-economic of fish products from some villages in Chaung-zon Township, Belugyun, Mon State. *MSc Thesis*, Department of Zoology, Mawlamyine University.

Talwar, P.K. and A.G. Jhingran (1991). *Inland fishes of India and adjacent countries*. Oxford and IBH Publishing Company PVT.Limited, New Delhi, Bombay. Volume I, II.158pp.

Wint Naing Aung (2017). Economic importance of some fishes in different depots of Maubin Township, Ayeyarwady Region. *MSc Thesis*, Department of Zoology, Maubin University.

OCCURRENCE OF SOME CEPHALOPODS SPECIES IN NYAUNG TAN JETTY, PAZUNDAUNG TOWNSHIP, YANGON REGION

Seinn Lae Phyu[1], Thet Thet Lwin[2]

Abstract

The present study was conducted in Nyaung Tan Jetty, Pazundaung Township, Yangon Region from December 2018 to September 2019. A total seven species belonging to one order, two families and three genera were identified and recorded during the study period. The highest species composition of cephalopods was found in December (seven species, 26%), followed by January (six species, 22%), February (five species, 18%), March (three species, 11%), April (one species, 4%) and May (five species, 19%) respectively. The Cephalopod species the highest species diversity occurred in Sepiidae. Of these, the most frequent occurrence of species was found in cool season and followed by dry season except raining season. The highest species was observed in December while the lowest species was found in April. June to September was closed fishing period. The findings were discussed supported by graphic presentation.

Keyword: Cephalopod species, Occurrence of species, Abundance

Introduction

The phylum Mollusca is one of the most diverse of animal's groups. It contains more than 35000 living species. The mollusks (soft bodied animals) which includes a variety of familiar animals and well known as decorative shells or as sea food. The phylum Mollusca is one of the few invertebrate groups that has attained much popularity with laymen and amateur collectors. Mollusca resources is found along the coast. In the numerous bays, brackish water, estuaries and in the sea around the subcontinent mollusks belonging to different taxonomic groups, such as mussels, clams, pearl-oysters, window-pane oysters, ark-shells, whelks, chanks, cowries, squids and cuttlefishes have been exploited since time immemorial for food, pearl and shells (Mohamed, 2012).

Cephalopods occur in all marine habitats: coral reefs, grass flats, sand, mud and rocks, epibenthic pelagic, epipelagic, mesopelagic, bathopelagic and benthopelagic species of the world Benthic forms were found in the open sea. Like benthic (e.g octopus), nectobenthic (cuttlefish, bottlesquid), neritic and ocenic (mainly squids) species constitute a primary marine predator such as fish, marine mammals or seabirds (Clarke 1996, Croxall and Prince 1996, Klages 1996, Smale 1996, Jereb and Roper, 2005).

Cephalopods are an important component of many marine ecosystems from tropics to poles (Jackson and O' dor, 2002). About 109 species under 31 families of cephalopods are occurring in the Western Atlantic Ocean and adjacent areas. Salinity is considered to be a limiting factors in squid's distribution. They are generally restricted to salinity concentration between 27% and 37%. As their habitat utilization, cephalopods are found in a wide range of aquatic habitats; some live in visually rich corals reefs while others live in the surface waters, or deep ocean where little or no light penetrates (Alves *et al.*, 2007).

Cephalopods are extremely important as food for human consumption and over 3 million metric tons are caught each year (Jereb *et al;* 2010). Four groups of cephalopods are squid, cuttlefish, octopus and chambered nautilus (Jereb and Roper 2005). Of them, the major orders are Octopoda, Sepioidea, Teuthoidea live on continental shelf (Boyle and Daly, 2000). They play an important role in the marine ecosystem as essential and valuable species in the world's sea and common food source in many countries, particularly in Asia. The species are abundant and ecologically important due to here, they are also extensively fished and consumed by humans (Amaratunga, 1983).

[1] Demonstrator, Department of Zoology, East Yangon University

[2] Dr, Lecturer, Department of Zoology, Mohnyin University

The cuttlefishes come under Sepioidea and are characterized by the presence of a shell (chitinous or calcareous), 10 circum oral appendages and the tentacles are retractile into pockets. Suckers have chitinous rings. Posterior fin lobes are free and not connected at midline. The cuttlebone is internal and located dorsally underneath the skin (Narasimham, 2005).

In Myanmar, fisheries sector plays an important role in the national economy in terms of income, food production, foreign exchange and employment to the rural population and the fourth source of foreign exchange earnings after timbers, mineral and rice (FAO, 1995 and ADB, 1998). There rich in natural resources including diverse Cephalopods. *Sepia, Loligo, Octopus* are edible mollusks along coastal area and economically important of Myanmar marine ecosystem (Thin Thin Maw, 2009).

The present study was conducted at Nyaung Tan Jetty where fishing vessels containing various cephalopods which are captured from Ayeyawaddy coastal areas, Rakhine coastal areas and Mon coastal areas. These areas are rich in fishery resource, it produced million tons of fishes and prawns. The rich of marine florals and faunas representing as marine resources area for our country. Fishery plays a significant role in the economic life of country. Therefore, the present study was carried out by the following objectives;

-to collect and identify some cephalopod species

-to assess monthly occurrence of some cephalopods in study area

-to record the abundance of some cephalopod species in study site

Materials And Methods

Study site

The specimens were collected from Nyaung Tan Jetty, Pazundaung Township in Yangon Region. It located between 96˚ 10′ 34″ East latitude and 16˚ 46′ 56″ North longitude where various species of cephalopods were captured from Myanmar coastal areas such as Ayeyawaddy coastal areas, Rakhine coastal areas and Mon coastal areas (Fig 1 and Plate 1, 2,3).

Study period

The study period lasted from December 2018 to September 2019. June to September was closed fishing period.

Data collection and morphometric measurement of collected specimens

The specimens were collected from fortnight visit to Fish Depot of Nyaung Tan Jetty. Collected samples were photographed and preserved in 10% formalin and preserved in 70% alcohol for further identification. A total of 10 individuals from seven species were weighed and measured (mantle length, total length). Body weight of each specimens was measured to the nearest gram.

Identification of the cephalopod species

The identification of collected specimens was done according to Jereb and Roper (2005) and Jereb *et al*., (2010).

Data analysis

Collected cephalopod species data were analyzed for species composition.

$$\text{Species composition} = \frac{\text{Number of species in each month}}{\text{Total number of species}} \times 100$$

Species composition was categorized according to Bisht *et al*., (2004).

Figure 1 Map of study site
Source: Google Earth

Plate 1 Nyaung Tan Jetty (Study Site)

A. Weight collection device B. Collection specimen C. Choosing specimen D. Taking sample container

Plate 2 Collecting data from Nyaung Tan Jetty

Results

A total of seven species belonging to one order, two families and three genera were collected from Nyaung Tan Jetty (Fig 1). They included six species from family Sepiidae (cuttlefishes), one species from family Sepiolidae (double-ear bobtail) (Table 1).

Sepia aculeata Van Hasselt, 1835

Common name - Needle cuttlefish
Mantle length - 11.4±2.25
Description - Head was large. The cuttlebone was elongate and oval. The fins were marginal border the mantle. Mantle about half as broad as long. The tentacular club was long and rather slender sub equal sucker in each across the club in males, 13 or 14 suckers across in female. Male and female arm length sub- equal. Left arm IV heterocotylied, about 12 normal suckers (three series) proximally (Plate 3).

Sepia prashadi Winckworth, 1963
Common name - Hooded cuttlefish
Mantle length - 12.7±2.31
Description - Head was medium. Cuttlebone was elongate and slightly flattened. Fins several millimeters shorter than mantle, narrow, separate, tentacular clubs short, broad; swimming keel broad, strong, slightly longer than the club (Plate 3).

Sepia vossi Khromov, 1996
Common name - Voss' cuttlefish
Mantle length - 9.5±2.45
Description - Head was medium. Cuttlebone was elongated. Fins were slightly short. Tentacular club with eight suckers differing markedly in size three to five suckers in middle of third longitudinal row extremely enlarged (Plate 3).

Sepia esculenta Hoyle, 1855
Common name - Golden cuttlefish
Mantle length - 8.3±1.78
Description -The head is large and has short sub equal arm. The cuttlebone elongates and oval and very flat. The tentacular club is long and moderately broad. Suckers are minute about equal in size (Plate 3).

Sepiella inermis (Van Hasselt,1835)
Common name - Spineless cuttlefish
Mantle length - 5.3±0.5
Description - Head is medium. Cuttlebone broadly oval, ventral surface strongly convex in lateral view, dorsal surface with low median rib. Fins were short. Mantle elongate, oval, a pigmented gland and pore at posterior tip of mantle on the ventral side. Tentacular club with 16 to 24 equal size minute suckers in transverse row. Arm stout, indistinctly keeled, and other arms with outer keel (Plate 3).

Sepiella japonica Sasaki, 1929
Common name - Japanese spineless cuttlefish
Mantle length - 6.23±0.95
Description - Head was large. Cuttlebone strongly convex, sulcus shallow, narrow, extends entire length of cuttlebone. Mantle oval, dorsal anterior margin triangular, obtuse Anterior dorsal edge of mantle with a tongue-like projection. Fins widen gradually posteriorly. Arms relatively short. Tentacular club elongated. Arms sucker tetraserial. Ventral two rows of suckers closed together, dorsal two rows separated. A large gland whose duct opens between the fins in front of red spots lieunder skin in postero-dorsal part of mantle. Hectotylus present on ventral arms (Plate 3).

Euprymna berryi Sasaki,1929
Common name - Double- ear bobtail
Mantle length - 4.2±0.58
Description - The head was united to the mantle over a broad area of the black of the neck. Individual soft his species share in common a broad round mantle which was bluntly rounded posterity and broad paddle – shaped lateral fins. Tentacles were long with slender stalks. The tentacular clubs were expanded and bear numerous minute suckers (Plate 3).

Monthly species composition of cephalopods at Nyaung Tan Jetty

The highest species composition of cephalopods was found in December(seven species, 26 %), followed by January (six species 22 %), February (five species, 18%), March (three species, 11%), April (one species, 4%) and May (five species, 19 %) respectively) (Table 2,3 and Fig 2).

Seasonal species occurrence of cephalopods in study area

The most occurrent cephalopod species were observed in cool season. Specimens were not observed in raining season. In dry season, cephalopods were studied the least occurrent cephalopod species (Table 4).

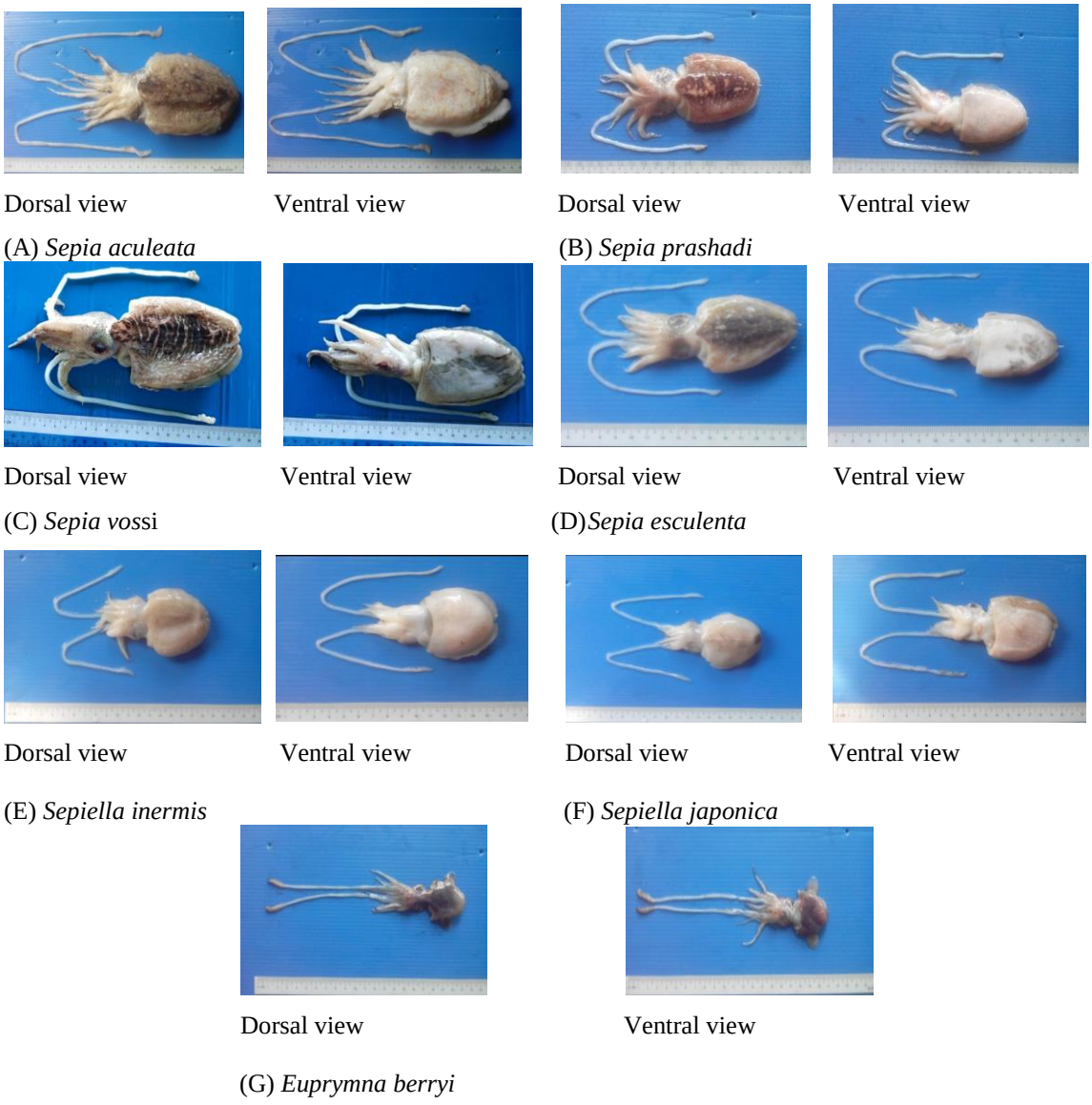

Dorsal view Ventral view Dorsal view Ventral view

(A) *Sepia aculeata* (B) *Sepia prashadi*

Dorsal view Ventral view Dorsal view Ventral view

(C) *Sepia vos*si (D)*Sepia esculenta*

Dorsal view Ventral view Dorsal view Ventral view

(E) *Sepiella inermis* (F) *Sepiella japonica*

Dorsal view Ventral view

(G) *Euprymna berryi*

Plate 3 Collected Cephalopods from study site

Table 1 Collected Some Cephalopods from Nyaung Tan Jetty

No.	Order	Family	Scientific name	Common name	Local name
1	Sepiida	Sepiidae	*Sepia aculeata*	Needle cuttlefish	Pyi gyi nga
2			*S. prashadi*	Hooded cuttlefish	Pyi gyi nga
3			*S. vossi*	Voss cuttlefish	Pyi gyi nga
4			*S. esculenta*	Golden cuttlefish	Pyi gyi nga
5			*Sepiella inermis*	Spineless cuttlefish	Pyi gyi nga
6			*S. japonica*	Japanese spineless cuttlefish	Pyi gyi nga
7		Sepiolidae	*Euprymna berryi*	Double-ear bobtail	Pyi gyi nga

Table 2 Monthly species occurrence of cephalopods from the study area

No.	Species	Dec	Jan	Feb	March	April	May	June	July	Aug
1	*Sepia aculeata*	+	+	+	+	+	+	-	-	-
2	*S. prashadi*	+	+	+	-	-	+	-	-	-
3	*S. vossi*	+	+	-	-	-	+	-	-	-
4	*S. esculenta*	+	+	+	-	-	+	-	-	-
5	*Sepiella inermis*	+	+	+	+	-	-	-	-	-
6	*S. japonica*	+	+	+	+	-	-	-	-	-
7	*Euprymna berryi*	+	-	-	-	-	+	-	-	-
	Total	7	6	5	3	1	5	0	0	0

Table 3 Monthly species composition of cephalopods at Nyaung Tan Jetty

No	Month	Number of species	Occurring Percentage of species
1	December	7	26%
2	January	6	22%
3	February	5	18%
4	March	3	11%
5	April	1	4%
6	May	5	19%
7	June	0	0%
8	July	0	0%
9	August	0	0%

Table 4 Seasonal species occurrence of cephalopods in study area

No.	Species	Rainy	Cold	Dry
1	*Sepia aculeata*	-	+	+
2	*S. prashadi*	-	+	+
3	*S. vossi*	-	+	+
4	*S. esculenta*	-	+	+
5	*Sepiella inermis*	-	+	+
6	*S. japonica*	-	+	+
7	*Euprymna berryi*	-	+	+

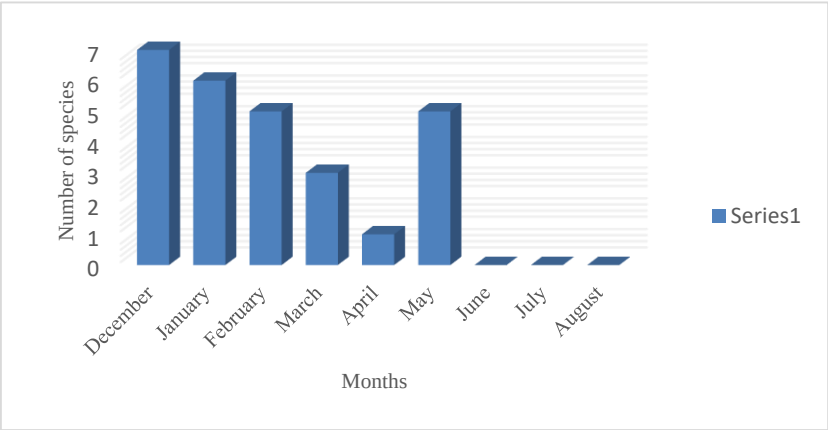

Fig. 2 Species Composition of Cephalopods from the study site

Discussion

In the present study a total of seven species belonging to two families and three genera were recorded at Nyaung Tan Jetty during study periods. Phyu Nyein Aye (2013) recorded that a total of six species belonging to two genera, two families were recorded at the study site. These present finding was similar family.

A total of 36 species cephalopods were recorded in Hong Kong area (Voss, 1971). Total 31 species of cephalopods were found in Thailand. There were only about 800 living species of cephalopods as reported by Carpenter (2002).

Mohamed (2012) stated that cephalopods from Indian Seas can be divided into three orders, among them Cuttlefishes (order Sepiida). The same order was collected in the present study.

In the present study were collected six species from cuttlefishes and one species of double-ear bobtail. Dominant cephalopods were *Sepia aculeata*, *Sepiella inermis*, and *Sepiella japonica*, these three species were recorded as commercially important cuttlefish.

Thin Thin Maw (2009) recorded four species of cephalopods: namely *Sepia aculeata*, *S. pharaonis*, *Sepiella inermis*, *Euprymna berryi* belonging to two families, Sepiidae (six species), Sepiolidae (one species) from some agents of Yangon Environ. Comparing to the present results three species *Sepia aculeata*, and *Sepiella inermis*, *Euprymna berryi* were same recorded in the present study area.

The remaining one species of cephalopods; *Euprymna berryi* was found in two months. Naw Mae May Phaw (2014) stated that genus *Euprymna* was found in two months in Chaung Tha Environs The present study is similar both findings because the salinity was similar in these habitats.

In present study, cuttlefish was recorded in all months and *Sepiella inermis* and *Sepiella japonica* were occurred in December to March. Jereb *et al.*, (2010), stated that maturing and matured animals were present in all months, showing prolonged and breeding in cuttlefishes. This finding is in agreement with the present study.

According to the seasonal occurrence of species, most species were recorded in cool season. In species diversity, the species of Cephalopods was probably abundance and largest numbers were collected in December to February for all species during the study period. Jereb and Roper (2005) suggest that it might be related to their breeding season among species.

In the present finding, three species of cephalopods; *Sepia aculeate, S. Prashadi* and *Sepiella inermis* were most abundant in the finding month. Three species of cephalopods;

Sepia vossi, *S. esculenta* and *Sepiella japonica* spawning concentration of species mostly occur between August and December along Pacific Coast as reported by Jereb *et al.*, (2010).

Voss (1971) stated that cephalopods were found all months of the year and particularly abundant in November to May, it may be probably due to many of the species in winter concentration. It is similar to the present finding, the captured of cuttlefishes were most abundance in cool season.

Conclusion

A total of seven cephalopod species belonging to three genera and two families were collected from Nyaung Tan Jetty. The lowest number of cephalopod one species (4%) were recorded in April and hightest number of cephalopods seven species (26%) were recorded in December. The highest species composition was found in December, followed by January, February, March, April and May. The most occurrent cephalopod species was observed in cool season while the least occurrent cephalopod species was found in dry season.

Acknowledgements

We are very grateful to Dr Nay Win Oo, Rector of East Yangon University for his permission to work this research. We would like to thank Dr Aye Aye Ko, Pro-Rector, Dr Wah Wah Lwin, Pro-Rector and Dr Thida Aung, Pro-Rector, East Yangon University, for their permission to work on the present topic. We are grateful appreciated to Professor Dr Ohn Mar Ohn, Head of Zoology Department, East Yangon University, for her valuable suggestion during the observation of this work and criticism the manuscript. We would like to express our deep gratitude to Dr Aye Thida Than, Professor of Zoology Department, East Yangon University, for her kind helps, cooperation and understanding throughout the research work.

References

ADB. 1998. *Aquaculture sustainability and the environment*. Bangkok.491Pp.

Alves, C., Chiche, R., and Boal, J.G.L. 2007. *Orientation in the cuttlefish Sepia officinalis*: response versus place learning.

Alves, C., Boal, J.G. and Dickel, L. 2007. *Short-distance navigation in cephalopods*: a review and synthesis, Marta Olivetti Belardinelli and Springer-Verlag, Cogn Process, DOI 10. 1007/s 10339-007-0192-9.

Amaratunga, T. 1983. *The role of cephalopods in the marine ecosystem.* In: J.F. Caddy (ed). Advances in assessment of world cephalopod resources. FAO fish Tech Pap 231:379-415.

Bisht, M.S., Kukreti, M., and Buhusans. 2004. Relative abundance and distribution of bird fauna of Garhwal Himalay. *Ecol. Environ Conserv*, 10 (4);451-460.

Boyle, P.R. and Daly, H.I. 2000. Fecundity and spawning in a deep-water cirromoph octopus. *Marine Biology*, 137:317-324.

Carpenter, K.E.2002. *FAO species identification guide for fishery purposes and American society of ichthyologists and herpetologists special publication No.5*, the living marine resources of the Western central Atlantic, Rome.

Clarke, M.R. 1996. The role of cephalopod in the world's ocean: general conclusions and the future. Philosophical Transactions of the Royal Society of London *B: Biological Science*, 351:1105-1112.

Croxall, J. P and Prince, P.A.1996. Cephalopods as pery. I. Seabirds. Philos Trans, *R., Soc Lond, B*. 351:1023-1043.

FAO. 1995. *Report on the region study of workshop on the environmental assessment and management of aqua cultural development*.

Jackson, G.D. and O' Dor, R. K.2002. Weeds of the sea and living life in the fast lane. *Vie Milieu*.

Jereb, P. and Roper, C.E.F. 2005. FAO Species Catalouge. Vol.I *Cephalopods of the world*, United Nations Development Progemme, Food and Agriculture Organization, united Nation.

Jereb, P., Vecchione, M. and Roper, C.F.E. 2010. Family *Loliginidae. In:* P. Jereb and C.F.E Roper, eds. *Cephalopods of the world.* An annotated and illustrated catalogue of species known to date. Volume 2. *Myopsid and Oegopsid Squids*. FAO Species Catalogue for Fishery Purposes. 4m (2): 38-117.

Klages, N.T.W. 1996. Cephalopods as prey. II. Seals. Philos trans, *R., Soc Lond*, B. 351:1045-1052.

Mohamed K.S. 2012. *Marine Molluscan Diversity in India-Exploitation and conservation Challenges in the 21st Century*.

Narasimham, K.A.2005. *Molluscan fisheries of India*. BR publications, New Delhi, 348p.

Naw Mae May Phaw.2014. Ecological aspects of Cephalopods Fauna from Chaung Tha Environs, *PhD Thesis*, Department of Zoology,University of Yangon.

Phyu Nyein Aye. 2013. Species Occurrence and Abundance of Cephalopods arriving at Nyaung Tan Fish Depot of Yangon Region, *MRes Thesis*, Department of Zoology, University of Yangon.

Smale, M.J.1996. *Cephalopods as prey*. IV. Fishews. Philos Trans, R., *Lond Ser*, B. 351:1067-1081.

Thin Thin Maw. 2009. Investigation of squid fishing and catch rate based on some Fishery Depots of Yangon Envion. *MSc Thesis*, Department of Zoology,Yangon University.

Voss.1971. *Cephalopod resources of the world*. Fish. Circ.149, FAO, Rome,75pp.

FECUNDITY AND NUTRITIONAL VALUE OF MEALWORM BEETLE *TENEBRIO MOLITOR* LINNAEUS, 1758

Mya Myo Marn [1], Myint Myint Naing[2]

Abstract

The present study was conducted in the laboratory of Zoology Department, East Yangon University. The study period lasted from December 2019 to August 2020. Two generation of *Tenebrio molitor* mealworm beetles were being reared in room temperature. Adults and larvae mealworm feed on three types of food as potato, cucumber and bread. Food of control group was potato, cucumber and bread. Fecundity of *T. molitor* was 151 eggs per female in F1, 149 eggs per female in F2 and 170 eggs per female in control group. Nutritional composition of *T. molitor* larvae, based on live weight was crude protein 20.36% and crude fat 10.02%, and based on dried weight 46.34% crude protein and 26.67% crude fat were recorded. In the present study, mealworm beetles were easily reared and had highly nutritional value.

Key words: *Tenebrio molitor*, mealworm beetle, nutritional value, fecundity

Introduction

Insects are the largest group, about 926,400 different species of animals on earth (Engel and Grimaldi, 2004). In order Coleoptera, superorder Endopterygota. Beetles create usable soil for vegetation by eating animal waste and rotten wood (Diego, 2020). Largest families are *Tenebrio molitor* comprising more than 15000 species which exhibit an extra ordinarily wide range of superficial dissimilarity in adult stage. Many are ground beetles, usually black and often bear a superficial resemblance to the Carabidae. *Tenebrio* are found in all stages in meal, flour and stored goods, their larvae being known as "mealworm" (Cotton and George, 1929).

Tenebrio is a genus of darkling beetles. They are nearly 12-18mm long and can live one to two years. The larvae are widely reared and sold as pet food, they are minor pest (David, 2020). Mealworm beetle larvae are easily reared and highly nutritious and used as feed for pests and many exotic animals to which they are usually served live, lyophilized or canned dried (Miranda *et al.*, 2002 and Veldkamp *et al*., 2012).

Insects become more considered as commonly acceptable food source for both human beings and domestic livestock in industrial countries, there will be a huge economical change involved (Defoliart,1992). The nutritive value of edible insect larvae, is as good as other animals or plants. In promoting insect larvae as human food, relative nutritive values should be taken into consideration to provide the maximum benefit to human consumers. Insect bodies are rich in various vitamin, element, protein, amino acids, fat and carbon hydrate. Therefore, insects offer an important nutritional resource for humans and are worthy of development (Chen *et al*.,2009).

Many researchers show that fresh yellow mealworm larvae contain about 15% fat and 20% protein. Not only do mealworm beetles utilize available food sources more efficiently than other livestock they can also breakdown low nutrient by products of common crops grown such as maize, wheat, millet and peanuts and quickly recycle then into high-quality food (Bodenheimer, 1951; Bukkens, 1996 and Johnson, 2010).

Mealworms are nutritious insects, they have high in protein and fat. Mealworm beetle are a good food for small animals, birds, reptiles and even people. Mealworms larvae can be

[1] Demonstrator, Zoology Department, East Yangon University
[2] Associate-Professor, Dr, Zoology Department, East Yangon University

eaten raw and alive, they can also be pan-fried and dry-roasting is often the tastiest (Rees, 2004).

Myanmar people have a long history of consuming insects but the nutritional value of edible insects is rarely known in Myanmar. The recorded data would be very useful for some information of sustainable food source and mealworm beetle rearing. The objectives of this work are as follows:

- to observe the fecundity of mealworm beetle
- to determine the nutrients composition of mealworm larvae

Materials And Methods

Study site

The present study was conducted in Laboratory of Zoology Department, East Yangon University. It was located at 16˚40′0″ N to 16˚50′0″N and 96˚15′0″E to 96˚25′0″E (Fig. 1).

Study period

The study period lasted from December 2019 to August 2020.

Mass rearing of *Tenebrio molitor*

F1 generation rearing data

Adult mealworms were purchased from the live pet food store. Three pairs of adult mealworms beetle were rearing for first stock (F1) in laboratory, Department of Zoology. It was difficult to distinguish the *Tenebrio molitor* mealworm male from female. So, directly after the first mating male and female pair was moved and placed in separate rearing box.

The first stock of adults *Tenebrio molitor* mealworm were kept in plastic containers measuring (173mm length×118mm width×36mm high) as three groups as (A), (B) and (C) with oatmeal and rice brans (25+25gm) were placed as soft ground substance for egg laying.

In the first stock of rearing box, mealworm adults and larvae were divided into three different dietary group as (A) slice of potatoes, (B) slice of cucumber and (C) slice of bread and cucumber (2.00 gm) each for every two days (Plate1, A to D).

From the first stock of adult mealworm beetles, numbers of egg and larvae were recorded (Plate2, A to C).

F2 generation rearing data

From the first stock of rearing data, 12 pairs of first generation of adult mealworm were collected and placed in three different dietary groups as (A) slice of potatoes, (B)slice of cucumber, (C) slice of potatoes, cucumber and control group was fed on potato, bread and cucumber. Four groups of rearing box were placed with oatmeal and rice barns (25+25g) as soft ground substance for egg laying. All the observations were made on three replicated in each group. During the study period, the ambient/prevailing temperature and relative humidity of laboratory were also First stock rearing (Plate 1, A to D).

From the F2generation of rearing beetle, numbers of egg and larvae were also recorded (Plate 2, A to C).

Fecundity of *Tenebrio molitor*

The Fecundity of *Tenebrio molitor* was determined as followed: when the female started to lay eggs, they were counted daily. The fecundity was computed using the following formula:

$$\text{Fecundity} = \frac{\text{Total number of eggs}}{\text{Total number of females}}$$

Chemical analysis

The determination and content of crude protein, crude fat, moisture and content of total ash from the mealworm larvae were done at Department of Fisheries Research and Development Division Yangon Region, Myanmar Analytical Laboratory Unit.

Identification of species

Identification of species, life cycle and terminology used in this work followed after Richard and Davies (1977) and Rees (2004).

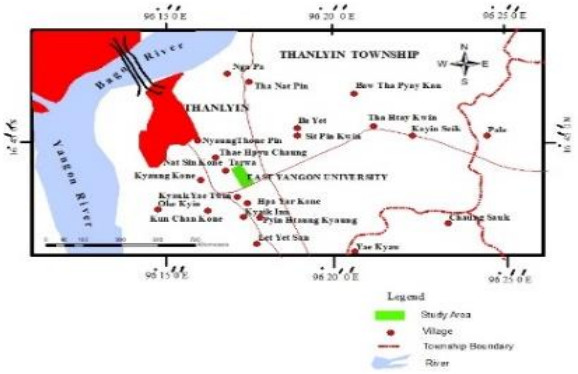

Source: Department of Geography, EYU, 2020)

Fig. 1 Map of study area

A.Rearing boxes B. Feeding on potato C. Feeding on cucumber D. Feeding on bread

Plate 1 Rearing boxes and three types of food

A. Eggs B. Larva

Plate 2 *Tenebrio molitor* eggs, larva and adult.

Results

Three pairs of *Tenebrio molitor* (mealworm beetle) were rearing for F1 generation and 10 pairs of mealworm were rearing for F2 generation.

Fecundity of *Tenebrio molitor* in F1 generation

In the present study three pairs of adult beetle *Tenebrio molitor* from the first stock were rearing as group A, group B and group C for the F1 generation (Plate 1A).

A total number of 453 eggs, 101(22.30٪) eggs in group A, 212 (46.80٪) eggs in group B, 140(30.90٪) eggs in group C were recorded.

Fecundity of mealworm beetle in F1 generation= $\frac{453}{3} = 151$eggs

The total fecundity of *Tenebrio molitor* varies from 101 eggs to 212 eggs with average of 151 eggs per female in F1 generation (Table 1, Fig.2).

Fecundity of *Tenebrio molitor* in F2 generation

Ten pairs of *Tenebrio molitor* from the F1 generation were rearing as group A, B, C and D (control) for F2 generation (Plate 1A).

Twelve pairs of *T. molitor* from the F1 generation were rearing as group A, B, C and D (control) for F2 generation.

A total number of 1341(average:447) eggs, 430 (ave: 143) (23.97٪) eggs in group A, 443 (ave:147) (24.69٪) eggs in group B, 468 (ave:156) (26.09٪) eggs in group C and 170 eggs in group D (control) were recorded (Table 1, Fig.2)

Fecundity of mealworm beetle in F2 generation = $\frac{1341}{9}$=149 eggs

The total fecundity of *Tenebrio molitor* varies from 143eggs to 156 eggs with average of 149eggs per female in F2 generation.

Nutritional value of *Tenebrio molitor* (mealworm beetle)

In the present study, chemical analysis of *Tenebrio molitor* (larvae) live and dried was examined by Kjeldahl technique (Pearson, 1970) and soxhlet method for crude protein, oven method for moisture content and temperature control oven muffle furnace for total ash content. As a result, nutritional composition of *T. molitor* larvae (live) was 66.46٪ moisture, crude protein 20.36٪, crude fat 10.02٪ and total ash 2.0٪. In the *Tenebrio molitor* larvae (dried) sample 8.5٪ moisture, 46.34٪ crude protein, 26.67٪ crude fat and 5.5٪ total ash was recorded (Table 2, Fig.3).

Usage of mealworm larva

The larvae of mealworm beetle are mostly used as food source not only for reptile, avian pest and fish bait but also for human as snack and street foods (Plate3 A to C).

Table 1 Number of eggs and larvae (live) of *Tenebrio molitor* in F1 and F2 generation

Group and Diet		F1 generation (Dec to March)		F2 generation (March to June)	
		Eggs	Larvae (live)	Eggs	Larvae (live)
Group (A)		101	98	430	392
P	(٪)	22.30٪	22.27٪	32.06٪	32.64٪
	Ave:			143	131
Group (B)		212	210	443	384
C	(٪)	46.80٪	47.73٪	33.04٪	31.97٪
	Ave:			148	128
Group (C)		140	132	468	425
B+C	(٪)	30.90٪	30.00٪	34.90٪	35.39٪
	Ave:			156	142
Total		453	440	1341	1201
	Ave;			447	401
Fecundity of egg		151		149	
Group (D) P+C+B(control)		-	-	170	154

P= Potato, C=Cucumber, B=Bread

Table 2 Proximate analysis of nutritional content in *Tenebrio molitor*

Types of sample	Nutritional contents			
	Moisture(٪)	Crude Protein(٪)	Crude fat(٪)	Total Ash(٪)
Tenebrio molitor Larvae (live)	66.46	20.36	10.02	2.0
Tenebrio molitor Larvae (Dried)	8.5	46.34	26.67	5.5

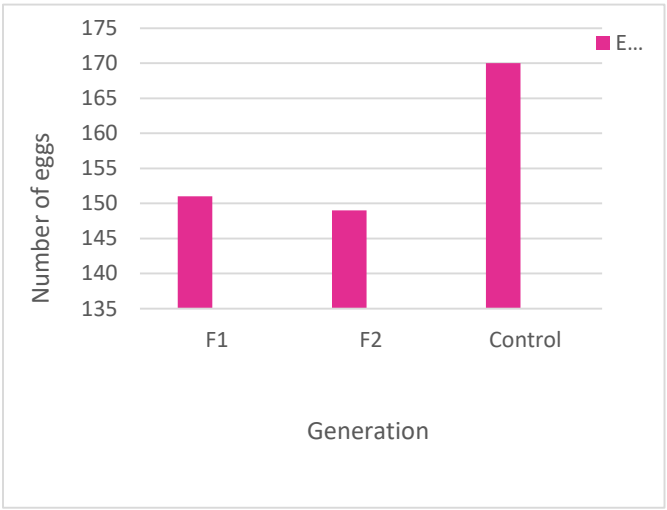

Fig.2 Fecundity of *T. molitor* egg in F1 and F2 generation

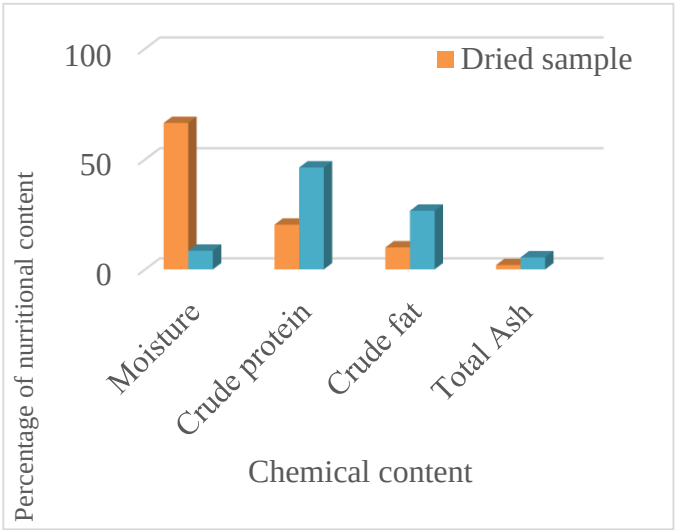

Fig.3 Percentage of chemical content in *T. molitor*

A Leopard Gecko eat mealworm

B. Bird eat mealworm larva

C. Fried mealworm larvae in plastic box

Source: Google and Purple rose online shop

Plate 3. Usage of mealworm beetle larvae

Discussion

Laboratory investigation of fecundity and nutritional value of mealworm beetle, T*enebrio molitor* was conducted in Zoology Department, East Yangon University. The study period lasted from December 2019 to August 2020.

In the present study, three pairs of *Tenebrio molitor* for F1 generation in December to March as cold season and ten pairs of mealworm beetle for F2 generation in March to June as hot season were rearing in this study period. A total of 453 eggs and 430 larvae (live) in F1 generation and 1341(Ave:447) eggs and 1201(Ave:401) larvae (live) in F2 generation were recorded. According to the result, fecundity of egg was 151 eggs per female in F1generation and 149 eggs per female in F2 generation.

Between the cold and hot season of rearing period, fecundity of egg number was nearly the same number in F1 and F2 generation. Present result showed that weather condition does not effect on eggs laying of mealworm.

ohnson (2020) stated that the female of darkling beetle lays hundreds of tiny eggs. Diego (2020) also reported that *T. molitor* female can lay between 70 and 100 eggs. The present finding showed that the number of eggs was more than previous authors.

According to the Anonymous (2020), mealworm beetle female typically produce 300 eggs at once. According to the Biologywise.com (2020) female of mealworm can lay around 500 eggs. The present study showed that the number of eggs was lesser than the previous authors. This finding of present study differ from previous statements. It may be assumed that number of eggs was varies in each statement because, temperature, food source and some other environmental factors were difference.

In the present study, three different types of food, potato, cucumber and cucumber + bread used for group (A), (B) and (C) respectively.Control group (D) of mealworm which feed on all these three types of food (potato, cucumber and bread).

Among three group of mealworm, number of eggs were vary 101 to 212 eggs in F1 and 143 to 148 eggs in F2 generation.Highest number of eggs found in group B (212 eggs, 46.80%) followed group C (140eggs, 30.40%) and group A (101eggs, 22.30%) of F1 generation in cold season. In F2 generation, highest number of eggs found in group C (156 eggs, 34.90%) followed the group B (148 eggs, 33.04%) and group A (143 eggs, 32.60%) in hot season.

In the present study period the best group and food for egg laying of mealworm was group B (cucumber) in F1 generation and group C (cucumber and bread) in F2 generation.The second best group was group C in F1 generation and group B in F2 generation.The third group was group A in F1 and F2 generation.

In the present rearing period, the best food for mealworm was cucumber in cold season and the best food of mealworm in hot season was cucumber + bread.Present results showed that mealworm more need and feed diet in hot season than cold season.It may be

assumed that cucumber is the best food for mealworm throughout the rearing period because available of water amount in cucumber is more than potato.So available of water is one of the important factor for mealworm rearing.

Number of eggs in control group was 170 eggs. So the number of eggs in control group was more than group of F1 and F2 generation because mealworm of control group feed on variety of food. Present finding showed that the available of food is one of the important factor for egg layng.

According to the chemical analysis data, the larvae of *T. molitor* contain 66.46% moisture, 20.36% crude protein, 10.02% crude fat and 2.0% ash (fresh weight basis) and 8.5% moisture, 46.34% crude protein, 26.67% crude fat and 5.5% ash (dry weight basis) were recorded in the present study period. Based on the dried weight, content of protein was more than fresh weight. Liu *et al.,* (2020) reported that larvae of *T. molitor* contain 64.1% moisture, 13.8% lipid, 17.6% protein and 1.5% ash base on fresh weight and 38.3% lipid, 49.1 protein and 4.1% ash base on dry weight. The finding of chemical analysis data in the present study is differ from the findings of them.

Ravzanaadii *et al.,* (2012) indicated that the larvae of *T. molitor* contain approxima -tely 46% protein and 33% fat (dry weight basis). The author also stated that lower protein content is 46%. In the present finding, protein content was similar to this report, but content of fat was lesser than previous statement. It may be assumed that protein content in the present finding is lower content.

Tran *et al.,* (2014) stated that *T. molitor* contain average crude protein 48.1%, ash 3.1% (base on dried sample) and crude protein 52.8% and ash 3.1% (base on fresh sample). The present finding disagreed with previous author because present data was lesser than that the statement. It may be assumed that food, temperature, humidity and environmental factor are one of the important factor for the nutritional value of mealworm beetle.

Present study showed that mealworm have been used as food and cheaper production due to their availability and easiness in raising that is much less burden some for environment than animal husbandary breeding. It also used as valuable protein sources for both human and animal.It may be concluded that present recorded data was very useful for mealworm beetle rearing and some information of sustainable food source for human.

Conclusion

In the present study fecundity and nutritional value of *Tenebrio molitor* were observed. Fecundity of *T. molitor* was vary, it laid 149 to 151 eggs per female. According to the different diet population number, it was vary maximum number was 210 individuals and minimum number was 98 individuals In nutritional value, dried sample of mealworm larva were higher than those of fresh sample. It was commonly used as pest food for reptile and avian, fish bait and snack food for human. Advantage of rearing mealworm larvae were valuable protein sources for food but it requires less space and generates less waste. It was concluded that mealworm beetle larvae use as sustainable food source for humans and domestic animals due to their favorable nutrient profile and low environmental impact.

Acknowledgements

We would like to express our sincere gratitude to Dr Nay Win Oo, Rector of East Yangon University for his valuable guidance and for his permission.We would like to give our warmest thank to Dr Aye Aye Ko, Pro-Rector, Dr Wah Wah Lwin, Pro-Rector and Dr Thida Aung, Pro-Rector East Yangon University for their advice in this research.We are deeply grateful to Professor Dr Ohn Mar Ohn, Head of Zoology Department, East Yangon University, for her kind permission, suggestion and providing facilities to work this research. We are also special thanks to Dr Aye Thida Than, Professor of Zoology Department, East Yangon University, for her valuable suggestions in this

research. We are also thanks to Daw Moe Thu Zar, Fishery Officer, In-charge of Nutrition lab, Chemical laboratory, Analytical Laboratory Unit, for her dutiful and helpful of test report in this research.

References

Anonymous. (2020) Life Cycle of a Mealworm. Available from: http://en.m.wikipedia.org/wiki/Mealworm Accessed 15.12.19.

Biologywise.com. (2020) Mealworm life cycle https// biologywise.com> mealworm Accessed 9 .12.2019.

Bodenheimer, F.S,(1951) *Insects as Human Food:* A Chapter of the Ecology of Man. W Junk Publishers, The Hague, Netherlands.

Bukkens, S.G.F.(1996) The nutritional value of edible insects. *Ecology of food and Nutrition*, 36:287-319pp.

Chen,V,Y. Feng and H. Zhang,(2009) *Review of nutritive value of edible insects*. Beijing, China Science and Technology Publishing House. In: Durst, P. B.*et al*., (ed). Forest insects as food: humans bite back, FAO. Bangkok, Thailand.

Cotton, R.T. and R.A.George,(1929)The meal worms, *Tech. Bull. U.S. Dept. Agric*., 95,37 pp.

David, S (2020) A Complete Guide On Mealworm Farming Enterprise. Mealworms breeding Website (internet) Available from: http://www.mealwormcarre.org.com Accessed 9.12. 2019.

Defoliart, G. R. (1992) *Insect as human food.* Gene Defoliart discusses some nutritional and economical aspects. Crop Prod., 11:394. DOF: 10.1016/0261-2194 (92) 90020-6

Dellinger, T.A. and E.R. Day. (2018) Darkkling Beetles and mealworms. Virginia cooperative Extensioin Virginia Tech. Virginia state university.www.ext.vt.edu Accessed 23.4. 2020.

Diego, S(2020) Animals and plants; Animals and plants Website (internet). Available from: http://www.animals,sandiegozoo.org.com Accessed 29.2.2020.

Engel, A., S.Michael, A. David and P.Grimaldi. (2004)˝ New light shed on the oldest insect˝.Nature427(6975:627630doi:10,1038/nature02201.PMID14961119.(http://www.nature.com/ nature/journal/v427/n6975/full/natureo2291.html Accessed 15.12. 2019.

Johnson, D.V(2010)The contribution of edible forest insects to human nutrition and forest management. In: Forest Insects as Food: Humans Bite Back. 5-22, FAO of the United Nation Region Office for Asia and the Pacific, Bangkok, Thailand.

Johnson, M(2020) Mealworm biology. Basic information on Mealworm, http://www.enchantedlearning.com/subjects/insects/beetles/mealworm/mealworm life cycle shtml Accessed 9.12.2019.

Liu, C.,J. Masri, V.Perez, C. Maya and G. Zhao(2020) Growth Performance and Nutrient Composition of Mealworm (*Tenebrio molitor*) Fed on Fresh Plant Materials- Supplemented Diets www.mdpi.com/journal/foods. 2000,9, 151;dio: 10-3390/ Foods 9020151.

Miranda, B.D. A**.,**M.G. Lopeq,C.E.Santana and B.A. Delarosa, (2002) characteristics of maize flour tortilla supplemented with ground *Tenebrio molitor* larvae. *Journal of Agricultural and food chemistry*, So: 192- 195.

Moran,D(2014) Mealworms. Biology Guide. Observation kit .www.FLUKERFARMS Accessed 23.4. 2020.

Pearson,D (1970) *The Chemical Analysis of foods Chemical,* Publishing Co. New York. 6th Edth PP7-11.

Ravzanadii, N.,S.H. Kim,W.H.,S.J. Choi and N.J. Kim, (2012) Nutritional Value of Mealworm, Tenebrio molitor as food source. *International Journal of Industrial Entomology* 25 (`1): 93-98.

Rees, D (2004) *Insects of stored products*. National Library of Australia, pp.112-133.

Richards, O.W. and R.G. Davies,(1977) *Imms' general textbook of entomology*. Tenth Edition Volume 2 Classification and Biology, pp.885-886.

Tran,G.,C. Gnaedinger and C. Melin (2014) Mealworm (*Tenebrio molitor*) http://www. feedipedia. org/ nude/16401 last updated on June 12, 2019, 13:29.Accessed 22 5.2020.

Veldkamp,T.,G. Van Duinkerken,V.Huis, A.Lakemond, E.Ohevanger, G.Bosch and I.M.A.J.S. Van Boeke, (2012) *Insects as sustainable feed ingredient in pig and poultry diets a feasibility study*. Report 638, Wageninger UR livestock Research.

SEASONAL VARIATION OF SOME EDIBLE FROG SPECIES AROUND SI KONE VILLAGE, THANLYIN TOWNSHIP

Su Myat Win[1] and Aye Thida Than[2]

Abstract

A total of six species, three genera belonging to two families under order Anura were studied in Si Kone village, Thanlyin Township, during December 2019 to August 2020. Collected some edible frog specimens were sorted and identified. Identification was done by using external morphological characteristics. The highest species numbers were found under family Dicroglossidae (four species, 81%) followed by Ranidae (two species, 19%). Monthly occurrence of anuran species were observed maximum numbers from August (six species) and minimum numbers of February were not found. According to seasonal variation results, the highest numbers of some edible frog species were found in rainy season (246 individuals, six species) and the lowest numbers of some edible frog species in winter season (27 individuals, two species).

Keyword: some edible frog, seasonal variation, monthly occurrence

Introduction

Amphibians are widely distributed, except Polar Regions, most oceanic islands and some desert regions. Amphibians use of both terrestrial and aquatic habitats, move between the two for reproduction and in search of suitable habitat, many amphibians effectively transport nutrients and energy between the two environments (Wilbur, 1980). In Myanmar, seven anurans families, Bufonidae, Dicroglossidae, Hylidae, Megophryidae, Microhylidae, Ranidae and Rhacophoridae are currently recognized. These families include 25 genera and 87 species. Only a single species of Hylidae, 7 species of Bufonidae, 11 species of Microhylidae and 24 species of Rhacophoridae are known (Zug, 2003).

Some frog species live on the ground, a few burrows in the soil. Some perch on shrubs or trees at varying height above the ground while others live in or by bodies of freshwater (Inger and Stuebing, 2005).

In recent time, amphibians form a very important link in evolutionary history of vertebrates. The word "amphibious" based upon Greek words and means "living a double life", they have evolved into three groups or orders. The first order of caecilians (Gymnophiona or Apoda), commonly called as limbless frogs. The second order of salamanders (Caudata or Urodela), commonly known as newts and salamanders. The third and largest order of modern amphibians (Salientia or Anura) to which frogs and toads belong (Duellman and Trueb, 1986). Amphibians are familiar to most people as frogs and toads, salamanders, and newts, and to a much smaller group of people as caecilians. All amphibians are members of the tetrapod vertebrate of class Amphibia (Stuart *et al*., 2008).

In tropical rainforests, frogs and caecilians are most diverse species, which provide an ideal combination of warm temperatures and abundant rainfall. Others live in deserts, where water is present only for very brief periods each year. Yet a few frogs live above the Arctic circle in both North America and Europe Salamanders are most common in the relatively cool, most forests of Eastern North America and the mountains of Central America, but others have [3]penetrated into local and tropical rainforests, deserts and even the tundra of Siberia (Wells, 2007).

Frogs and toads are integral parts of the food web in the ecosystem. As tadpoles, they graze on a variety of algae and detritus gleaned from the water column or found on the bottom substrates. On the other hand, they become food for predators, such as insects and fish. As adults, frogs and toads eat insects and other small invertebrates and vertebrates, and,

1 Demonstrator, Department of Zoology, East Yangon University
2 Dr, Professor, Department of Zoology, East Yangon University

in turn, are preyed upon by snakes, birds, humans and a host of other predators (Ibrahim, 2004).

Seasonal occurrence was the onset of wet seasons which are the breeding seasons of anurans. Another factor for more occurrence of frog and toad species may be due to an increase in availability of appropriate food sources. The highest number of individuals were observed in wet season when the rainfall was maximum and humidity was optimum for breeding. The lowest number of individuals were observed in hot season when the rainfall was minimum and humidity was low. Anurans thin skin, through which water was lost, most anurans which lived in humid regions were active only during wet season of the year. This may also be other seasons for their seasonal variation of activities (Hutchins, Duellman and Schlager, 2003).

Anurans of different species adapt to living in different habitat from intrinsic changes rather than extrinsic, by altering their physiology, behavior, and reproductive methods (Webb *et al*., 1981).

Frogs and toads are about 90% of all amphibians; they are an important link between human and ecosystem health and they are main components aquatic and terrestrial ecosystems (Delphin, 1954). In colder climates, the amphibian usually hibernates during the winter months, while in tropical countries where dry seasons intervene, they often bury themselves in the mud and remain in a state of temper till the return of the rain.

The present research was designated seasonal variation and occurrence some edible frog species in study areas of Si Kone village, Thanlyin Township. The present study areas include paddy field and vegetation area which greatly provides suitable habitats for different species of some edible frogs.

The objectives of present research are as follows:

- to examine the morphological characters and species occurrence in study area
- to observe the monthly and seasonal variation of studies species in Si Kone village, Thanlyin Township

Materials And Methods

Study area and study sites

Some edible frog species were collected from study sites in Si Kone village, Thanlyin Township. It is located between 16˚51′18.0″ N to 16˚ 51′ 46.8″ N and 96˚ 21′ 28.8″ E to 96˚ 21′ 57.6″ E (Fig. 1).

The study area was chosen study site I- paddy field and study site II vegetation area during study period (Plate 3 and 4).

Study period

The present study lasted from December 2019 to August 2020.

Specimen and data collection

Specimen collection was carried out twice per month by hand. Edible frog species were collected from study sites. Collected edible frog specimens were sorted and identified. Identification was done by using external morphological characteristics. Scaled photograph for each specimen will be taken before preservation (Plate 1).

Preservation of specimens

Collected specimens were fixed in 10% formalin for 24 h, placed in standing water for an additional 24 h and subsequently transferred to 70% ethanol for long-term storage (Heyer *et al*., 1994; Simmons, 2002) (Plate 2). The number of species and number of individuals investigated were noted. Some recorded some edible frog species data were analyzed for seasonal variation and composition occurrence.

Identification of collected frog species

The capture specimens were identified followed after Taylor (1962) and Delphin (1954), Zug, *et al.* (2003).

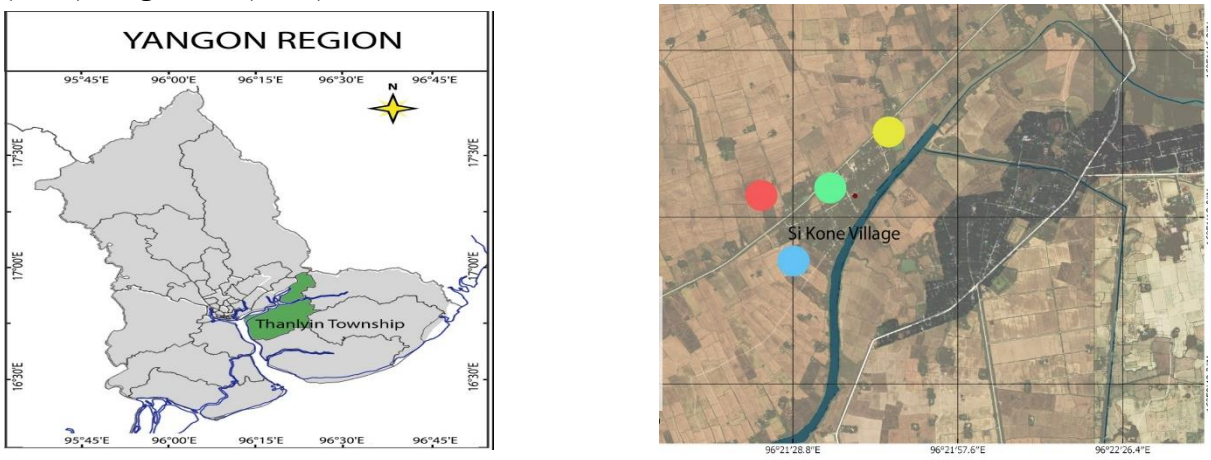

Fig. 1 Map of Thanlyin Township showing collection sites

Plate 1 Specimen capture and collection

Plate 2 Sample specimens and storage

Plate 3 Paddy field of study site I

Plate 4 Vegetatoin area of study site II

Results

Collected some edible frog species in study area

A total of six species of three genera under two families belonging to order Anura were recorded during the study period. In family Dicroglossidae; four species *Fejervarya cancrivora*, *F.limnocharis*, *Hoplobatrachus rugulosus* and *H. tigerinus*, family Ranidae; two species *Hylarana erythraea* and *H. macrodactyla* were observed in present study area (Table 1 and Plate 5).

The percentage of occurrence of families related to the studies species was observed during the study period with the highest species being Dicroglossidae 81% and Ranidae 19% from study sites (Fig. 1).

Morphometric characters of studied species

1. *Fejervarya cancrivora*

Common name -Rice field frog, grass frog
Local name -Hpar-kyar
Description
Head : head moderate as long as broad, snout oval.
Body and colour : body median-size; dorsal surface brown with large darks spot and ventral surface whitish.

2. *Fejervarya limnocharis*

Common name -Asian grass frog, rice field frog
Local name -Hpar-kyar, kyaw-san-kay
Description
Head : head as long as broad, snout pointed.
Body and colour : body with small tubercles, slender; dorsal surface brownish gray with darker blotches; a broad yellowish vertebral line present and ventral surface whitish.

3. *Hoplobatrachus rugulosus*

Common name -East Asian bullfrog
Local name -Sarr-hpar
Description
Head : head moderate, much depressed; snout pointed.
Body and colour : body median-sized, robust frog; dorsal surface with brownish and ventral surface brown dark spots.

4. *Hoplobatrachus tigerinus*

Common name -Asian bullfrog
Local name -Sarr-hpar
Description
Head : head moderate, much depressed; snout pointed, projecting more or less beyond the mouth.
Body and colour : body slender frog; dorsal surface with yellowish, green, olive, with dark spots and ventral surface white.

5. *Hylarana erythraea*

Common name -Green paddy frog, leaf frog
Local name -Hpar-thay-pann
Description
Head : longer than broad triangular shape, snout rather pointed.
Body and colour : body slender, slim and smooth; bright green above with two yellowish to whitish dorsolateral stripes; dorsal surface line pure white and ventral surface white.

6. *Hylarana macrodactyla*
Common name -Three-striped grass frog
Local name -Hpar-paung-shay
Description
Head : head long, narrow and elongate, snout pointed.
Body and colour : body slender frog with smooth skin; dorsal surface is dark brown with dull yellow and ventral surface white.

Monthly and seasonal variation of some collected edible frog species from study area

A total of six species representing 335 individuals under three genera belonging to two families were collected. Monthly distribution data, a total number of individuals and species were collected in December (11individuals and 2species), January (11individuals and 2species), February (5individuals and 1species), March (0individuals and 0species), April (1individuals and 1species), May (61individuals and 3species), June (92individuals and 4species), July (77individuals and 5species), August (77individuals and 6species). The highest number of individuals were observed in June (92individuals) and the lowest number of individuals in March (0individuals). The highest number of species were collected in August (6species) and the lowest number of species in March (0species).

Winter season consisting a total number of individuals and species (27 individuals and two species). According collected three season, the lowest number of individuals and species were observed in winter season.

Summer season consisting a total number of individuals and species (62 individuals and three species). According collected three season, the number of individuals and species were observed in summer season to be moderate.

Rainy season consisting a total number of individuals and species (246 individuals and six species). According collected three season, the highest number of individuals and species were observed in rainy season. The abundance sampled species was observed in the rainy season (Table 2 and Fig. 2, 3).

Species occurrence of collected some edible frog species in study area

Collected some edible frog species were recorded from two study area; paddy field site – I and vegetation area site – II in study sites during the study period. Although 335 individuals representing 6 species under eight genera were collected and identified from study Site I and Site II. During study area, 6 species were found in Site I and 5 species were found in Site II (Fig. 4).

Table 1 Collected some edible frog species in study area

No.	Family	No.	Scientific Name	Common Name	Local Name
I	Dicroglossidae	1	*Fejervarya cancrivora*	Rice field frog, grass frog	Hpar-kyar
		2	*F. limnocharis*	Asian grass frog, rice field frog	Hpar-kyar, kyaw-san-kay
		3	*Hoplobatrachus rugulosus*	East Asian bullfrog	Sarr-hpar
		4	*H. tigerinus*	Asian bullfrog	Sarr-hpar
II	Ranidae	5	*Hylarana erythraea*	Green paddy frog, leaf frog	Hpar-thay-pann
		6	*H. macrodactyla*	Three-striped grass frog	Hpar-paung-shay

Table 2 Monthly and seasonal variation of some edible frog species from study area

No	Family	Scientific Name	Winter Season				Summer Season				Rainy Season				All Total
			Dec	Jan	Feb	Total	Mar	Apr.	May	Total	Jun	Jul	Aug	Total	
1	Dicroglossidae	*Fejervarya cancrivora*	1	3	0	4	0	0	19	19	15	23	11	49	72
		F. limnocharis	10	8	5	23	0	1	41	42	48	38	42	128	193
		Hoplobatrachus rugulosus	0	0	0	0	0	0	0	0	0	0	1	1	1
		H. tigerinus	0	0	0	0	0	0	0	0	0	3	2	5	5
2	Ranidae	*Hylarana erythraea*	0	0	0	0	0	0	0	0	11	8	2	21	21
		H. macrodactyla	0	0	0	0	0	0	1	1	18	5	19	42	43
	Total number of individuals		11	11	5	27	0	1	61	62	92	77	77	246	335
	Total number of species		2	2	1	2	0	1	3	3	4	5	6	6	6
	All total number of individuals		27				62				246				335
	All total number of species		2				3				6				6

Table 3 Species occurrence of collected some edible frog species in study area

No.	Scientific Name	Sites		
		Paddy field site I	Vegetation area site II	Frequency
1	*Fejervarya cancrivora*	√	√	2
2	*F. limnocharis*	√	√	2
3	*Hoplobatrachus rugulosus*	√	-	1
4	*H. tigerinus*	√	√	2
5	*Hylarana erythraea*	√	√	2
6	*H. macrodactyla*	√	√	2
Total species		6	5	

√=observed, - =not observed

Fig. 1 Collected some edible frog species in relation with their families as shown by percentage in study area

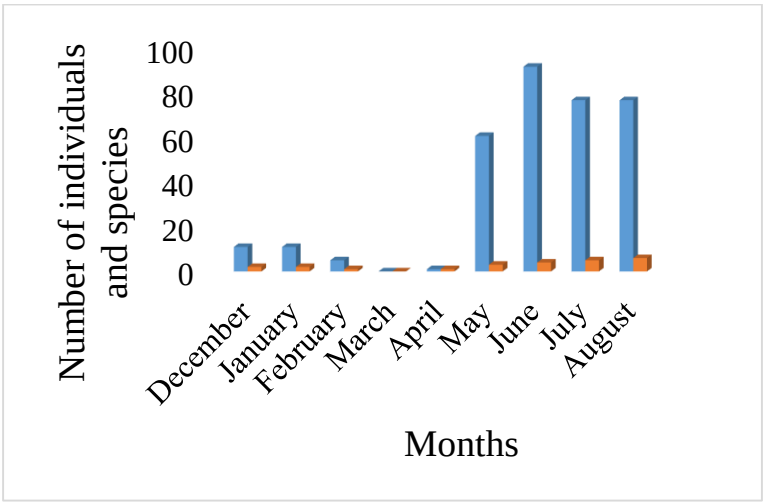

Fig. 2 Monthly occurrence of some edible frog species in study period

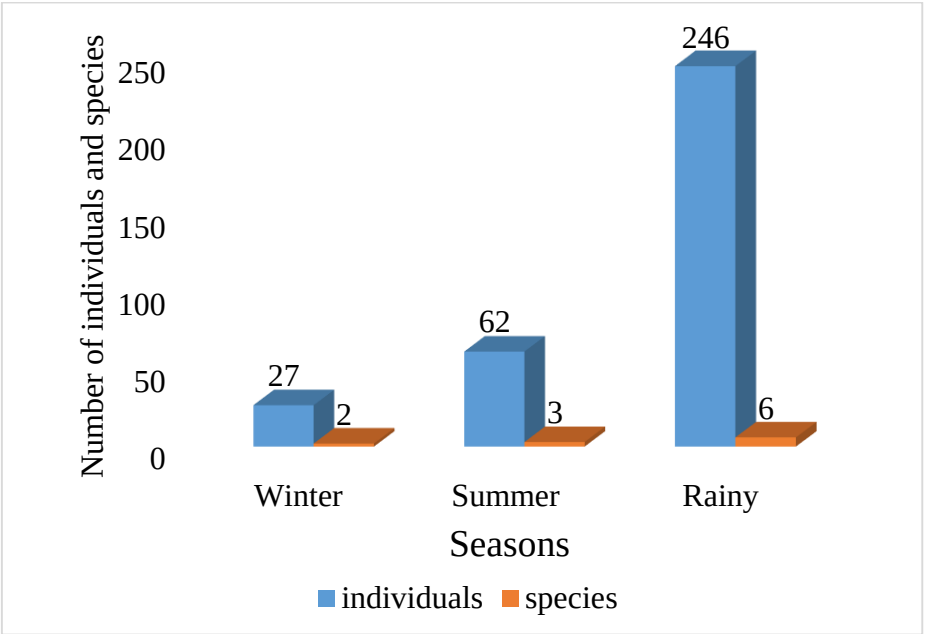

Fig. 3 Seasonal variation of some edible frog species from study area

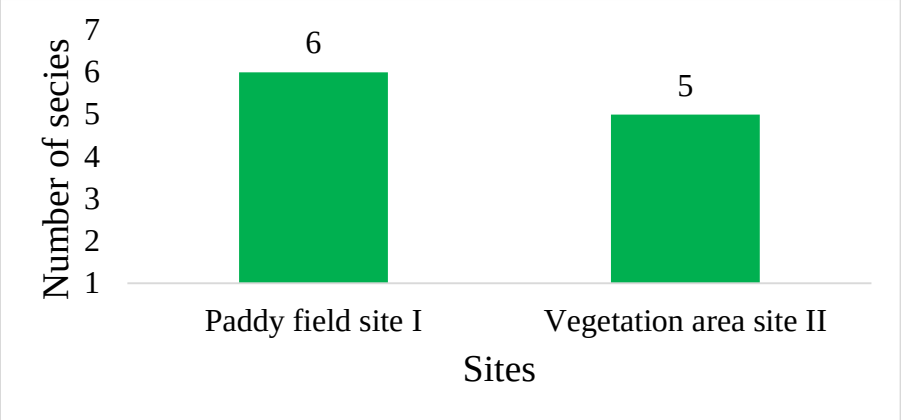

Fig. 4 Species occurrence of collected some edible frog species in study area

A. *Fejervarya cancrivora* (Dorsal)

B. *Fejervarya cancrivora* (Ventral)

A. *Fejervarya limnocharis* (Dorsal)

B. *Fejervarya limnocharis* (Ventral)

A. *Hoplobatrachus rugulosus*(Dorsal)

B.*Hoplobatrachus rugulosus* (Ventral)

A. *Hoplobatrachus tigerinus* (Dorsal)

B. *Hoplobatrachus tigerinus* (Ventral)

A. *Hylarana erythraea* (Dorsal)

B. *Hylarana erythraea* (Ventral)

A. *Hylarana macrodactyla* (Dorsal)

B. *Hylarana macrodactyla* (Ventral)

Plate 5 External features of collected some edible frog species

Discussion

The present study was focused on morphological characteristics and seasonal variation and occurrence of some edible frog species around Si Kone village, Thanlyin Township.

Frost, (2011) also stated that eight species of Bufonidae, 16 species of Dicroglossidae, 11 species of Microhylidae, 33 species of Ranidae and 24 species of Rhacophoridae were known in Myanmar.

In the present study a total of edible frog six species belonging to three genera under two families were recorded Dicroglossidae and Ranidae of order Anura. Four species of

Dicroglossidae and two species of Ranidae were observed in paddy field and vegetation area of the study site.

Frost, (2015) reported that a total of 93 species belonging to 40 genera under seven families of the order Anura were already described in Myanmar. Species composition of family Ranidae was the largest in Myanmar although that of family Dicroglossidae was the highest in the present study period. The present finding not similar with their statement.

According to the monthly distribution data, Aye Moe Moe (2018) stated that the maximum numbers of individuals were found in June (308 individuals) and the minimum numbers of individuals were found in April (4 individuals). The maximum numbers of collected edible frog species were found in May, June, July and August. The minimum numbers of collected edible frog species were found in December, January, February, March and April.

During the study period, the maximum numbers of individuals were found in June (92 individuals) and the minimum numbers of individuals were found in March (0 individuals) followed by April (1 individuals). In present results, the maximum number of collected edible frog species was found in May, June, July and August. The minimum numbers of collected edible frog species were found in December, January, February, March and April. This finding nearly similar with their statement.

Santos-Pereira, *et al.* (2011) reported that the population percentage of the family Dicroglossidae 58.2% and Ranidae 15.3%. The highest population was found in the family Dicroglossidae followed by Microhylidae.

In present study sites, the population percentage of the family Dicroglossidae 81% and Ranidae 19%. The highest population was found in the family Dicroglossidae followed by Ranidae. This finding not similar with their statement.

Santos-Pereira, *et al.* (2011) statement that we sampled a total of 96 frogs inhabiting the forest floor. The abundance, richness and density varied consistently among the four seasons sampled, with the highest values occurring in the spring and summer seasons.

Seasonal occurrence of 335 individuals related total number of individuals (27inds) in winter season and total number of individuals (62inds) in summer season and total number of individuals (246inds) in rainy season. The abundance sampled species was observed in the rainy season. During the study period in all seasons was recorded in the highest population size abundance in rainy season - the results contrary to above authors.

Kathy Htun, (2012), Naw Zarchi Linn, (2016) and Win Mar Khaing, (2007) also stated that the most abundant and dominant of the genus *Fejervarya* were observed from vegetation area (paddy field). During study period, *Fejervarya limnocharis* was the most abundant and dominant species in paddy field and vegetation area. The present finding also agreed with above authors.

In present study, only one number of *Hoplobatrachus rugulosus* was found once in nine months. This species was assumed near threaten (extinct) species in study sites. These species could be collected and there was needed to further study in paddy field of some edible frog of research.

Conclusion

The morphological characters of edible frog species in Si Kone village, Thanlyin Township were studied in present work. A total of six species, three genera under two families belong to order Anura were collected from the study area. There are *Fejervarya cancrivora*, *F. limnocharis*, *Hoplobatrachus rugulosus*, *H. tigerinus*, *Hylarana erythraea* and *H. macrodactyla*. The area of collection for the specimen of edible frog useful frog farming and beneficial from the commercial point of view. Commercial benefits of edible frog species for human should be evaluated.

Acknowledgements

We are very grateful to Dr. Nay Win Oo, Rector of East Yangon University for his permission to present this research paper. We would like to thank Dr. Aye Aye Ko, Pro-Rector, Dr. Thida Aung, Pro-Rector and Dr. Wah Wah Lwin, Pro-Rector, East Yangon University, for their permission to work on the present topic. We are grateful appreciated to Professor Dr. Ohn Mar Ohn, Head of Zoology Department, East Yangon University, for her supervision and valuable suggestion during the observation of this work and criticism the manuscript.

References

Aye Moe Moe, (2018) Occurrence and Habitat Preference of Anuran Around Thanlyin Township

Delphin, F. (1954) The frogs and toads of the Rangoon University Estate, *journal of Burma Research Society*.

Duellman, W.E. and L. Trueb, (1986) *Biology of Amphibians*. McGraw-Hill, Inc., New York. Pp 670

Frost, D. R. (2011) Amphibian Species of the World: an online References Version 5.5 (31, January, 2011). Electronic database accessible at. Amnh. org/ V7/ herpetology/ amphibian/ American Museum of Natural History, New York, USA.

Frost, D.R. (2015) Amphibian Species of the World: an online References Version 6.0 (31, January, 2015). Electronic database accessible at. Amnh. org/V7/ herpetology/ amphibian/ American Museum of Natural History, New York, USA.

Heyer, R., M. A., Donnelly, M. Foster, and R., Mcdiarmid, (1994) Measuring and monitoring biological diversity: standard methods for amphibians. *Smithsonian Institution*; Washington, D.C.: 1994.

Hutchins, M., W.E. Duellman and N. Schlager, (2003) True frogs (Ranidae), *Grzimek's animal life encyclopedia*, editions, Volume 6, *Amphibians*, Farmington Hill, Michigan, Gale Group: 245-264

Ibrahim, J. (2004) *Aspect of Biology and Ecology of Two Sympatric Frogs in Malaysia*. Yusran Publishing House. Sungai Petani, Malaysia. Pp 227

Inger, R.F. and R. Stuebing, (2005) *A Field Guide to the Frogs of Borneo.* Second Edition. A photographic guide. Natural History Publications (Borneo) Limited. Kota Kinabalu,

Kathy Htun, (2012) Species diversity, population abundance and habitat preference of amphibian fauna in Pathein environs. *PhD Thesis*, Zoology Department, University of Yangon.

Naw Zarchi Linn, (2016) Anuran diversity in Hpa-an and Kyain-Seikgyi, Townships of Kayin State. *PhD Thesis*, Zoology Department, University of Yangon.

Santos-Pereira, M., A., Candaten, D., Milani, F.B., Oliveira, J., Gardelin, F. D. Carlos, and C.F.D. Rocha, (2011) Seasonal variation in the leaf-litter frog community (Amphibia: Anura) from an Atlantic Forest Area in the Salto Morato Natural Reserve, southern Brazil. *Zoologia* (Curitiba) 28:6 Curitiba Dec. 2011.

Simmons, J. E. (2002) Herpetological collecting and collections management. *Herpetological Circular* No. 31. Society for the Study of Amphibians and Reptiles; Salt Lake City: 2002.

Stuart, S.N., M., Hoffmann, J.S., Chanson, N.A., Cox, R.J., Berridge, P. Ramani, and B.E. Young, (2008) *Threatened Amphibians of the World*. Lynx Editions, Barcelona, Spain; IUCN, Gland. Switzerland; and Conservation International, Arlington, Virginia, USA.

Taylor, E.H. (1962) *The amphibian fauna of Thailand*. University of Kansas Science Bulletin. 43: 265-599

Webb, J. E., J. H. Wallworkand Elgood, (1981) *Guide to Living Amphibians*. Pp 144

Wells, K.D. (2007) *The ecology and behavior of amphibians.* The University of Chicago Press. Pp.xii+1148

Wilbur, H.M. (1980) Complex life cycle. *Annual Review of Ecology and Syatematices.* 11:67-93

Win Mar Khaing, (2007) Community structure of ranid species in some areas of Myanmar, *PhD Thesis*, Zoology Department, University of Yangon.

Zug, G.R., A. E., Leviton, J.V., Vindum, G. O. U. Wogan and M.S. Koo, (2003) *Checklist of* the *amphibians and reptiles in Myanmar* available at http:// www/ calacademy. org/ research/ herpetology/ myanmar/checklist (30, March, 2020)

MORPHOMETRIC AND REPRODUCTIVE PARAMETERS OF *JOHNIUS COITOR* (HAMILTON, 1822) AND *POLYNEMUS PARADISEUS* LINNAEUS, 1758 IN MYOMA MARKET OF THANLYIN TOWNSHIP

Aung Thu Zar Tun*

Abstract

An investigation on the morphometric and reproductive parameters of *Johnius coitor* and *Polynemus paradiseus* was undertaken during the period of June 2017 to February 2018. Fish samples were weekly collected from Myoma Market of Thanlyin Township. A total 170 females; each of *Johnius coitor* and *Polynemus paradiseus* were collected for the monthly determination of fecundity, Gonadosomatic Index (GSI), Hepatosomatic Index (HSI), and Condition Factor (K value). The highest GSI value of *Johnius coitor* was found in July (11.15) and that of *Polynemus paradiseus* was found in August (10.66). HSI value of *Johnius coitor* was high in January (1.23) and that of *Polynemus paradiseus* was high in August (1.53). The highest value of condition factor (K) of *Johnius coitor* was found to be (0.92) in June and that of *Polynemus paradiseus* was (0.68) in November. GSI value and fecundity indicated that both species in present study reproduced between June to August.

Keyword: Gonadosomatic Index (GSI), Hepatosomatic Index (HSI), Condition Factor (K value), two female species, *Johnius coitor* and *Polynemus paradiseus*, morphometric parameters

Introduction

In the studies involving reproductive biology of fish, the degree of ovaries development is expressed as percent ovaries weight in relation to the body weight and usually termed as gonadosomatic index (GSI) (Lagler *et al*., 1962). Gonadosomatic index is a good indicator of gonad development and spawning season (Dadzie and Wangila, 1980). The gonadosomatic index is a suitable indicator of the ovaries development that can be used for determining the reproductive period, when increasing GSI values are associated with maturation and decrease with gamete extrusion or absorption (Le Cren, 1951).

Hepatosomatic index gives an idea of maturation and feeding intensity status, whether the food reserve in the liver is affected during the process of yolk formation or not (Oso *et al*., 2003).

Fecundity of any fish is related to egg size, length and weight of the female fish. The fecundity, among egg laying animals, is the number of eggs being laid for next spawning by the female (Royce, 1972). Fecundity appears to bear some broad relationship to care or nurture accorded to the eggs (Lagler, 1956). Knowledge on fecundity and breeding strategy is necessary to evaluate the reproductive potential of the spawning stock of individual fish species leading to management of the fisheries (Das, 1997).

In addition, condition factor (K) is calculated from the relationship between the weight of a fish and its length, with the intention of describing the "condition"of the individual fish (Froese, 2006). Different values in K indicate the state of sexual maturity, degree of food sources availability, age and sex and environmental conditions (Gomiero and Braga, 2005). In addition, condition factors of different population of the same species give some information about food supply, the timing and duration of breeding. The condition factor can also be used in assessing the well-being of fish. (Weatherly, 1972).

Johnius coitor is amphidromous fish to refer to fishes that regularly migrate between freshwater and the sea (in both directions), but not for the purpose of breeding, as in

* Demonstrator, Department of Zoology, East Yangon University

anadromous and catadromous species. Sub-division of diadromous migration should be cuclical and predictable and cover more than 100 km (Froese and Pauly, 2017).

Polynemus paradiseus Linn., the so -called mango-fish, which is marine inhabitat and migrate to the fresh and gradient zones of the estuaries during the pre-monsoon months for breeding. Though the species is of commercial importance and relished by different sections of people as a table fish, very little work relevant to its fishing dynamics has been worked out (Jones and Menon, 1953).

Hence, considering the economic importance, an investigation on the morphometric and reproductive parameters of *Johnius coitor* and *Polynemus paradiseus* was undertaken in the present study. The present study was investigated the following objectives;

- to examine the morphometric parameters of studied species
- to investigate reproductive aspect of female target fish species

Materials And Methods

Study area and study site

The study site was Myoma market, Thanlyin Township, Yangon Region. It is located at North latitude 16 º44' N to 16 º46' N and East longitude 96º 14' E to 96 º17' E (Fig. 1 and Plate 1).

Study period

The study period lasted from June 2017 to March 2018.

Specimen and data collection

Weekly fish samples were collected from the study site (Plate 1). A total of 170 female specimens each of two species (*Johnius coitor* and *Polynemus paradiseus*) were collected during June 2017 to February 2018 (Plate 3 A, B, C). Five fresh fish samples of each species were bought weekly from Myoma market, Thanlyin Township throughout the study period to investigate morphometric and reproductive parameters. Purchased specimens were brought from Myoma market to laboratory at Zoology Department of East Yangon University for further study. The collected fish were cleaned with tap water and removed excess water with blotting paper.

After cleaning the collected fish, total length (T.L) and body weight (B.W) were measured to the nearest centimeter and gram by using a ruler and a digital balance (Plate 2). Then, the specimens were dissected to remove out entire ovaries and liver (Plate 4). Ovary length (O.L), ovary weight (O.W) and liver weight (L.W) were recorded by using a ruler (nearest centimeter) and a digital balance (gram) for each species (Plate 4).

Preservation of specimens

Ovaries of two fish species were preserved in 5% buffer formalin. After a few days preserving, the ovaries were found to be harden so that counting of eggs can be done accurately and easily.

Data analysis

For the calculation of fecundity, the ovaries were sectioned out from anterior, middle and posterior region and weighing them. The eggs from each of the three sections were manually counted and the mean numbers of eggs were calculated (Plate 4). For each individual fish, the total numbers of eggs were calculated from the sample mean the total weight of ovaries (Das, 1997).

$$\text{Fecundity} = \frac{\text{Number of ova in the subsample of ovary}}{\text{Weight of the subsample}} \times \text{Weight of ovary in gm}$$

Gonadosomatic index (GSI) and hepatosomatic index (HSI) for each species were calculated according to the formulae of (Le Cren, 1951) and (Lagler, 1962).

$$\text{GSI} = \frac{\text{Ovaries weight}}{\text{Body weight}} \times 100$$

$$HSI = \frac{\text{Liver weight}}{\text{Body weight}} \times 100$$

Condition factor (K) was calculated according to the formula of Kader (1984).

$$\text{Condition factor (K)} = \frac{\text{Body weight – Gonad weight}}{(\text{Length})^3} \times 100$$

Relationship between fecundity and morphometric measurements (total length, body weight, gonad weight) and that of gonad weight and body weight of two fish species were investigated by using regression analysis. The recorded data were tabulated and graphs were drawn using Microsoft Excel Programme.

Identification of species

Fish species identification was made follow after Talwar and Jhingran (1991) and Jayaram (2010).

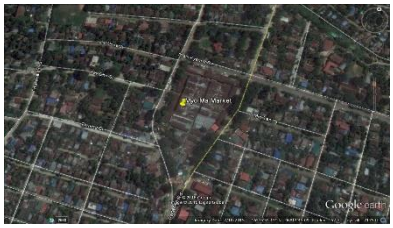

Fig.1 Map of the study site

Plate 1 Myoma Market, Thanlyin Township

(A)ruler and Petridis Dissecting apparatus

(B) Balance

(C) Digital balance

Plate 2 Materials used

(A) Studied fish species

(B) *Johnius coitor*

(C) *Polynemus paradiseus*

(D) Reproductive organs of *Johnius coitor*

(E) Reproductive organs of *Polynemus paradiseus*

Plate 3 Studied fish species and their reproductive organs

(A) Weighing of gonad

(B) Weighing of liver

(C) Counting of egg

Plate 4 Weighing of gonad and liver and counting of egg

Results

Mean morphometric and reproductive parameters of *Johnius coitor* and *Polynemus paradiseus* in Myoma Market of Thanlyin Township

Monthly mean morphometric parameters which concerning the reproductive aspects of *Johnius coitor* and *Polynemus paradiseus* were computed and based on these data, values of fecundity, GSI, HSI and K were calculated and are given in tables and graphs. (Table 1,2 and Fig. 2,3).

Morphometric and reproductive parameters of *Johnius coitor*

Mean total length of *Johnius coitor* which represent the study of reproductive aspect ranged from 25.6 cm (August) to 28.5 cm (December). Mean body weight of the studied specimens ranged from 134.0 g (October) to 187.0 g (June). Mean ovary weight ranged from 1.6 g (October) to 17.7g (July) was recorded. The range of mean ovary length was 5.8 cm (February) to 8.9 cm (August). Mean liver weight which represent the chosen fishes ranged from 0.7 g (October) to 1.8 g (January) (Table 1).

Mean GSI value of the species was found to be the highest in July (11.15) and the lowest in October (1.42). (Table 1. and Fig. 2, A).

Mean HSI value of the species was the highest in January (1.23) and the lowest in October (0.51) (Table 1. and Fig.2, A).

The condition factor (K) value of the species was the highest in June (0.92) followed by August (0.79) and January (0.74) while that was the lowest in July (0.69) (Table 1. and Fig. 2, A).

Mean fecundity of the species was highest in July (74324) and lowest in February (5730) (Table 1. and Fig. 2, B).

Morphometric and reproductive parameters of *Polynemus paradiseus*

Mean total length of *Polynemus paradiseus* which represent the study of reproductive aspect ranged from 18.6 cm (January) to 21.1 cm (February). Mean body weight of the studied specimens was found to be ranged from 40.5 g (January) to 63.5 g (February) was recorded. Mean ovary weight ranged from 2.8 g (January) to 5.5 g (August) was recorded. The range of mean ovary length was 4.4 cm (January) to 5.6 cm (August). Mean liver weight which represent the chosen fishes ranged from 0.4 g (September, October and January) to 0.7 g (August and February) (Table 2).

Mean GSI value of the species was the highest in August (10.66) and the lowest in January (6.87) (Table 2. and Fig. 3, A).

Mean HSI value of the species was the highest in August (1.53) and the lowest in September (0.77) (Table 2. and Fig. 3, A).

The condition factor (K) value of the species was the highest in November (0.68) followed by February (0.62) while that was the lowest in September and October (0.57) (Table 2 and Fig. 3, A).

Mean fecundity of the species was the highest in August (17419) and the lowest in January (8384). (Table 2. and Fig. 3, B).

Table 1 Monthly mean reproductive and morphometric parameters of *Johnius coitor* in Myoma Market of Thanlyin Township

Sr.No.	Parameter	Month								
		Jun	Jul	Aug	Sep	Oct	Nov	Dec	Jan	Feb
1	T.L (cm)	26.5	26.5	25.6	25.9	26.3	27.6	28.5	27.2	26.42
2	B.w (g)	187.0	153.0	138.5	135.0	134.0	156.0	175.0	158.0	134.5
3	O.w (g)	15.5	17.7	12.0	8.4	1.6	4.5	4.9	7.2	1.97
4	O.L (cm)	7.1	7.6	8.9	8.0	6.4	7.1	7.2	7.6	5.8
5	L.w (g)	1.4	1.1	1.0	1.1	0.7	1.5	1.2	1.8	0.98
6	Fecundity	59096	74324	65339	45042	19575	58288	51914	44941	5730
7	GSI (%)	8.59	11.15	8.47	6.12	1.42	2.68	2.77	5.17	1.47
8	HSI (%)	0.74	0.76	0.73	0.76	0.51	0.96	0.68	1.23	0.74
9	K	0.88	0.69	0.79	0.72	0.73	0.71	0.72	0.74	0.71

T.L =total length, B.W=body weight, O.W=ovary weight, O.L=ovary length, L.W=liver weight, GSI=gonadosomatic index, HSI=hepatosomatic index, K=codition factor

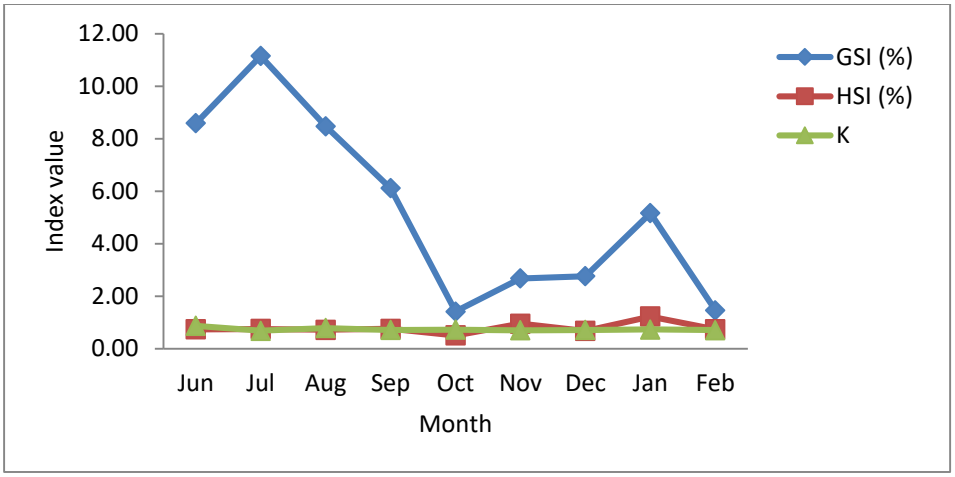

(A) Monthly values of GSI, HSI and K of *Johnius coitor*

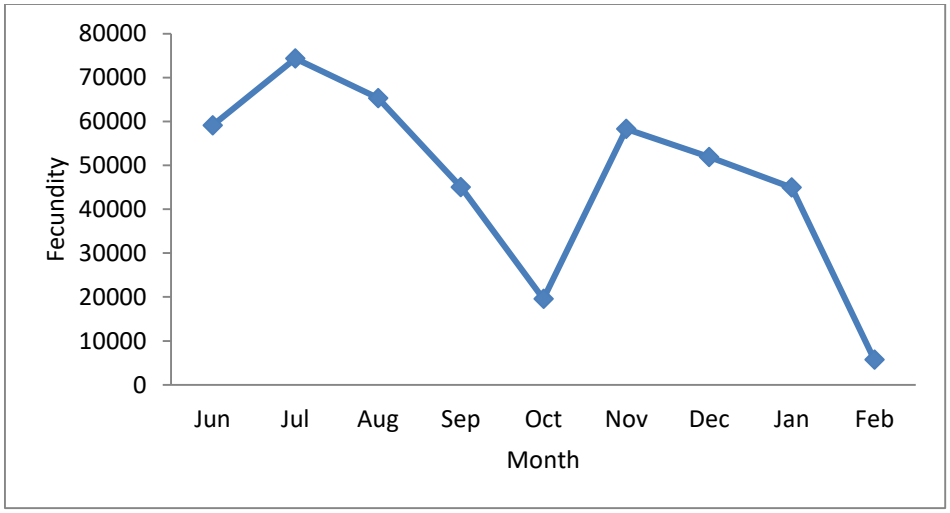

(B) Monthly fecundity of *Johnius coitor*

Fig. 2 Monthly values of GSI, HSI, K and fecundity of *Johnius coitor* in Myoma Market of Thanlyin Township

Discussion

To understand the gonadal capacity of any fish, gonadosomatic index is the most reliable and scientifically approved indicator because it gives a correct time span regarding season of spawning. (Bagenal, 1957). Gonad development indicates status of maturation of a particular fish and is essential for estimation of fecundity and spawning seasons (Nabi, 1994). Based on the results of GSI value and fecundity, it might be assumed to conclude that the study species *Johnius coitor* and *Polynemus paradiseus* reproduce from June to August.The fecundity of a fish is defined as the number of eggs that are likely to be laid during spawning season. The (GSI) values are higher in spawning period and declining in the post-spawning period (Bagenal, 1957). Fecundity is an important parameter to estimate the potentials of egg output by comparing its relation to female size (Chondar, 1977). To establish the length and weight at first maturity, fecundity and spawning time, which are essential for studies on population dynamics and the effects of fishing upon the exploitable fish in the population (Gupta, 1967). Knowledge on fecundity and breeding strategy is necessary to evaluate the reproductive potential of the spawning stock of individual fish species leading to management of the fisheries (Das, 1997). Thus, the findings of the study may provide information for future research in the field of Ichthyology.

Table 2 Monthly mean reproductive and morphometric parameters of *Polynemus paradiseus* in Myoma Market of Thanlyin Township

Sr.No.	Parameter	Month								
		Jun	Jul	Aug	Sep	Oct	Nov	Dec	Jan	Feb
1	T.L (cm)	19.8	19.3	19.7	19.5	19.1	19.4	19.4	18.6	21.1
2	B.w (g)	51.8	47.0	51.5	46.5	43.0	54.0	49.0	40.5	63.5
3	O.w (g)	5.3	3.6	5.5	3.8	3.9	4.4	3.8	2.8	4.5
4	O.L (cm)	5.2	5.2	5.6	5.3	5.2	5.2	5.3	4.4	5.4
5	L.w (g)	0.5	0.5	0.7	0.4	0.4	0.5	0.6	0.4	0.5
6	Fecundity	16835	9960	17419	11016	11999	13425	10549	8384	10880
7	GSI (%)	10.40	7.67	10.66	8.38	9.26	8.19	7.89	6.87	6.98
8	HSI (%)	0.95	0.99	1.53	0.77	0.87	0.93	1.15	0.94	0.92
9	K	0.60	0.61	0.60	0.57	0.57	0.68	0.61	0.59	0.62

T.L =total length, B.W=body weight, O.W=ovary weight, O.L=ovary length, L.W=liver weight, GSI=gonadosomatic index, HSI=hepatosomatic index, K=codition factor

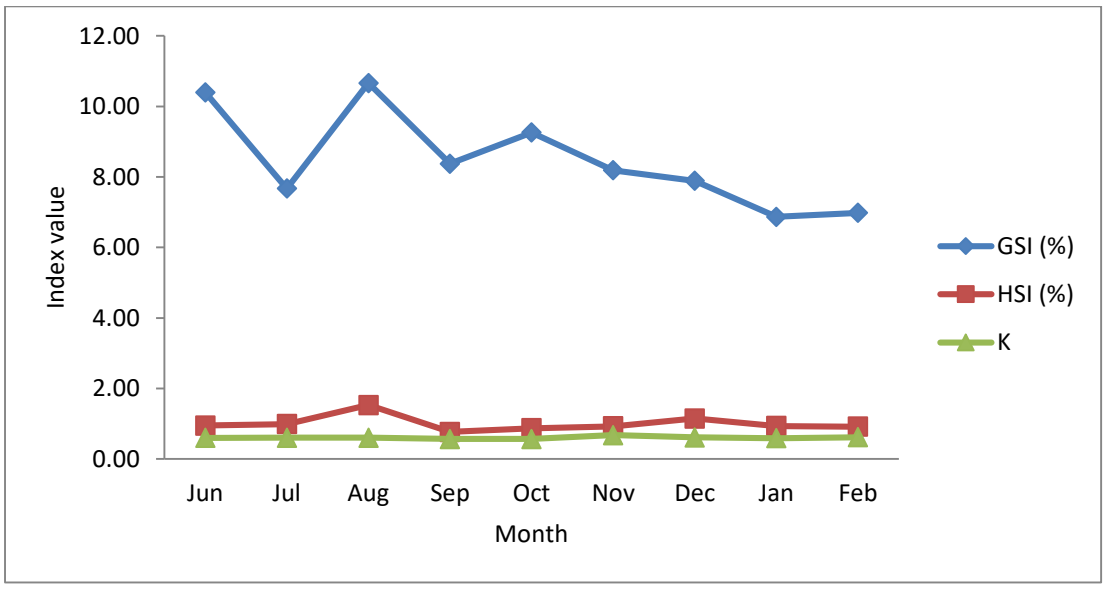

(A) Monthly values of GSI, HSI and K of *Polynemus paradiseus*

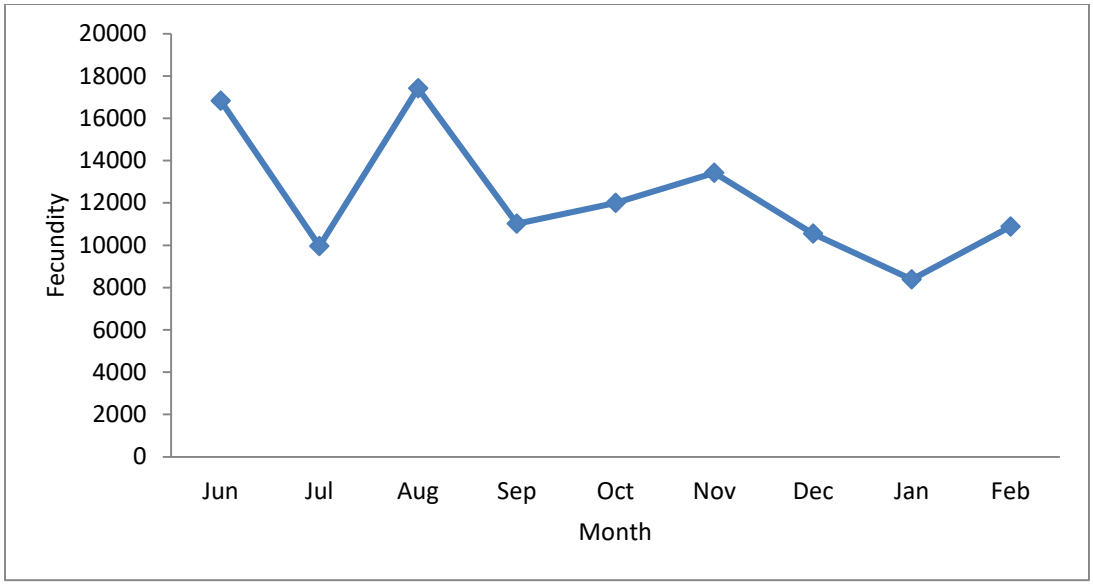

(B) Monthly fecundity of *Polynemus paradiseus*

Fig. 3 Monthly values of GSI, HSI, K and fecundity of *Polynemus paradiseus* in Myoma Market of Thanlyin Township

Conclusion

The highest fecundity of *Johnius coitor* was found in July and lowest in February that of *Polynemus paradiseus* was found in August and the lowest in January. The highest GSI value of *Johnius coitor* was found in July and lowest in October and that of *Polynemus paradiseus* was found in August and the lowest in January. The highest HSI value of *Johnius coitor* was found in January and lowest in October and that of *Polynemus paradiseus* was found in August and the lowest in September. The condition factor (k) value of *Johnius coitor* was found to be highest in June and the lowest in July and that of *Polynemus paradiseus* was highest in November and the lowest in September and October. GSI value and fecundity indicated that both species in present study reproduced between June to August.

Acknowledgements

I would like to express my profound gratitude to Dr Nay Win Oo, Rector of East Yangon University for his keen interest and also for his permission. I am indebted to Dr Aye Aye Ko, Dr Wah Wah Lwin and Dr Thida Aung, Pro-Rectors, East Yangon University for their supports, permitting to conduct this work and confidence in the implementation of this research. I am also grateful thanks to Professor Dr Ohn Mar Ohn, Head of Zoology Department, East Yangon University, for her valuable suggestions, constructive criticisms of the manuscripts and supervision. I am deeply thanks to Dr Aye Thida Than, Professor of Zoology Department, East Yangon University, for providing advices and support of this research paper.

References

Bagenal, T. B., 1957. Annual variations in fish fecundity. *Journal of Marine Biological Association*, United Kingdon, 36: 377-382.

Chondar, S. L., 1977. Fecundity and its role in racial studies of *Gudusia chapra* (Pices: Clupeidae). *The Proceedings of the Indian Academy Sciences*, 86:245-254.

Dadzie, S. and B. C. C. Wangila 1980. Reproductive biology, length-weight relationships and relative condition of pond raised *Tilapia zilli* (Gervais). *Journal of Fish Biology*, 17:243-253.

Das, H. P., 1997. The fecundity of gray mullet *Mugil cephalas* L. along the Goa Coast. *Mahaagar Bulletin of National Institute of Oceanography*, 10 (1and 2): 79-82.

Froese, R., 2006. Cube law, condition factor and weight-length relationships: History, meta-analysis and recommendations. *Journal of Applied Icthyology*, 22:241-253.

Froese**,** R. and D. Pauly 2017. FishBase: (cited 2017 February). Available from http://www.fishbase.org.

Gomiero, L. M. and F. M. S. Braga 2005. The condition factor of fishes from two river basins in Sao Paulo State, Southeast of Brazil. *Acta Scientiae Maringa*, 27: 73-78.

Gupta, M. V., 1967. *Observation on the fecundity of Polynemus paradiseus Linn. from the Hooghly estuarine system*. Central Inland Fisheries Research Institutes, Barrackpore.

Jayaram, K. C., 2010. *A Hand Book of Freshwater Fishes of India, Pakistan,Bangladesh, Burma and Sri Lanka*. Zoological survey of India Calcutta. Sir Aurobindo Press.

Jones, S. and P. M. G. Menon 1953. Notes on the breeding habits and developmental stages of some estuarine fishes. *J. Zool. Soc*. India. 5, 255-267.

Kader, M. A. 1984. Studies on *Gobioides rubicundus*Hamiton-Buchanan from the Karnafully estuary. *PhD Thesis*, University of Chittagong, 107p.

Lagler, K. F., 1956. Enumeration of fish eggs. *In:* In Freshwater Fishery Biology. 2nd ed. pp: 106-110. W.M.C. Brown Company, Dobuque.

Lagler, K. F., J. E. Bardach, and R. R. Miller 1962. *The Study of Fishes*. John Wiley and Sons, Inc., Toppan Printing Co. Ltd. New York. Pp.545.

Le Cren, E. D., 1951. The length–weight relationship and season cycle in gonad weight and condition in the perch (*Perca flavescens*). *Journal Animal Ecology*. 20: 201-219.

Nabi, M. R. U., 1994. On the Study of the threadfin *Polynemus paradiseus* from the landing centers and local market of Chittagong. *M.Sc Thesis*, Institute of Marine Science, University of Chittagong, Bangladesh, 67p.

Oso, J. A., E. O. Idown, T. S. Olaniran and B. E. Ayorinde 2003. Fecundity,condition factor and gonado-somatic index of *Hepsetus odoe* (African Pike) in a tropical reservoir, Southwest Nigeria. *World Journal of Fish and Marine Sciences*, 3(2): 112-116.

Royce**,** W. F., 1972. *Introduction to the Fishery Science*, Academic Press, New York, 251pp.

Talwar, P. K. and A. G. Jhingran 1991. *Inland fishes of India and Adjacent Countries*. Vol. I, II. Oxford and IBH Publishing, New Delhi, Bombay, Calcutta.

Weatherly, A. H., 1972. *Growth and Ecology of Fish Populations*. Academic Press, London.

DIFFERENT TYPES OF TAIL AND CAUDAL SKELETONS OF SOME BONY FISH FROM MYOMA MARKET, THANLYIN TOWNSHIP

Pa Pa Win[1], Myint Myint Soe[2]

Abstract

Caudal osteology of seven species collected from the Myoma Market, Thanlyin Township. The study period lasted from December 2017 to September 2018. The caudal skeleton is carried out 7 species of fishes Osteological peculiarities of caudal skeleton structures are discussed with the different types of tail shapes in Orders, Osteoglossiformes, Clupeiformes, Cypriniformes and Siluriformes. The studied fishes are *Notopterus notopterus, Tenualosa ilisha, Cirrhinus mrigala, Labeo rohita, Osteobrama cotio, Mystus bleekeri, Clarias batrachus.* Tail type were found in rounded shape of fishes are *Notopterus notopterus, Clarias batrachus.* Deeply forked shape of fishes are *Tenualosa ilisha, Cirrhinus mrigala, Labeo rohita, Mystus bleekeri.* Forked shape of fishes are *Osteobrama cotio*. Caudal bone structure of *Notopterus notopterus* can be discerned are the fused hypural complex which is in the form of a broad triangular structure. The dorsal caudal fin of *Tenualosa ilisha* is provided with the preural centrum1, neural crest, two ural centrum, three uroneurals, three epurals and three hypurals. The lower caudal fin is supported with three hypurals, last haemal spine, hypurapophysis and ridges of haemal spine. The dorsal lobe of caudal fin rays of *Cirrhinus mrigala* is supported by the epural and four hypurals. The lower lobe of caudal fin rays is supported by three hypurals. The caudal fins of *Labeo rohita* dorsal lobe are supported by the epural, the urostyle and three hypurals. The lower lobe of caudal fins is provided by two haemal spines, last haemal spines and three hypurals. The dorsal part of caudal bone of *Osteobrama cotio* is supported by the epural and hypural 2. The lower part consists of last haemal spine and two hypurals. The upper caudal lobe of *Mystus bleekeri* is supported with four hypurals, namely, hypural 6, 5, 4 and 3. The lower caudal lobe is provided with two hypurals. The upper part of caudal fin of *Clarias batrachus* is supported by one epural, one uroneural and three hypural. The lower part of caudal fin is supported by haemal spine of preural centrum 2, last haemal spine, two hypurals.

Key words: Collected species, Types of tail shape, Caudal skeleton

Introduction

The structure and development of the caudal fin of aquatic vertebrates have been studied by many authors. One of the most prominent characteristics of early vertebrates is the elongate caudal fin bearing fin rays. The caudal fin presents a fundamental design feature of the vertebrates that predates the origin of jaws and is found in both agnathans and gnathastomes. The caudal fin also represents the most posterior region of the vertebrate axis and is the location where fluid, accelerated by movement of the body anteriorly. Despite the extensive fossil record of the caudal fin, the use of caudal character for systematic studies and the importance of tail function for understanding locomotor dynamics in fishes, few experimental studies have been undertaken of caudal fin function. (Gorge, 2000). Study the caudal fins in the following specimens giving attention to the relation between the caudal vertebrae and the bony pieces supporting the tail. Generally, tails are divided into two; Heterocercal means that the vertebrae extend into the upper lobe of the tail, making it longer as in sharks. Most fishes have a homocercal tail, where the fin appears superfically symmetric but in fact the vertebrae extend for a very short distance into the upper lobe of the fin. This can be expressed in a variety of shapes (Kelvin, *et al.*, 1997). The design of the caudal fin of fishes has also attracted attention from workers interested in the mechanics and hydrodynamic of locomotion in fishes. (Dubios *et al.*, 1976). The caudal skeleton is assigned

[1] Demonstrator, Department of Zoology, East Yangon University
[2] Associate Professor, Department of Zoology, Pinlon University

to three caudal vertebrae, namely; the preural centrum3, preural cemtrum 2 and preural centrum1. They are counted from last centrum forward (Nag, 1967).

Preural centrum 1 is defined as the one bearing a laterally flanged last haemal spine. Neural crest arises from the upper portion of preural centrum1. Preural centrum is forms the posterior most end of the vertebral column, but in the lower teleost there may be one or two separately ossified centra behind it. These are called "ural centra". These ural centra become incorporated in preural centrum1 is advanced form Gosline (1968).

The unpaired epural lie above the neural crest of the preural centrum 1. Epural varifromone to three pieces. The paired uroneural are situated along the edge of the urostyle. The hypurals are plate-like bones which support the principle caudal rays. Hypurals varies from one to six pieces. The projection of the centrum was termed zygapophysis. Above two members were concerned with neural and were known as pre- and posterior neural zygapophysis. The other two of caudal bones below are pre- and posterior haemal zygapophysis respectively (Gosline, 1968). The main objectives of this study are as follows;

-to classify the studied fish species

-to distinguish the different caudal fin-shaped of studied fish species

-to determine the skeleton of the caudal fin of studied fish

Materials And Methods

Study site

The specimens for the present work were collected at the Myoma Market, Thanlyin Township, Yangon Region. It is located between North latitude 16°46'0"N and East longitude 96°16'40"E (Fig. 1).

Study period

The present study lasted from December 2017 to September 2018.

Specimen collection

Fish specimens for study caudal skeleton are collected from the study site.

Equipment

Collected specimens are supported by the aid of dissecting set, hot plate, wax tray, and solution of 20%KOH and H_2O_2.

Identification of studied fish species

The study fish are identified according to Talwar and Jhingran (1991).

Preparation of Specimens

Collected specimens are cut with knife to get the tail region. Firstly, caudal region of the fresh fish was boiled on the hot plate at 60˚C about five to ten minutes according to the specimen. Secondly, it was placed on the wax tray about ten minutes to cold. Then, skinned and removed the muscle with the aid of forceps and pointer, it was immersed into the 20% solution of KOH. Time interval depends on the size of the fish about 20 or more hours. Finally, caudal skeleton was picked up with the aid of forceps and placed it in a beaker. Then H_2O_2 was pourded until immersed the caudal bones to bleach the skeleton. (Gosline, 1968).

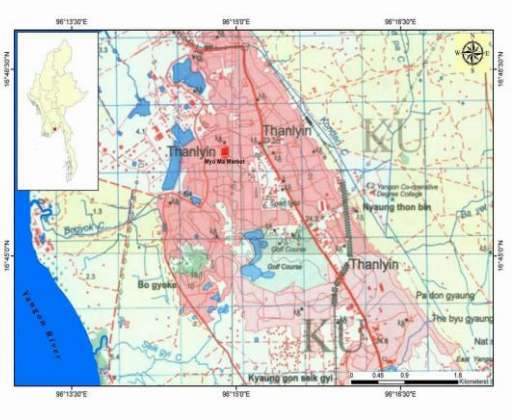

Fig .1 Map of the study area

Source: Department of Geography, Nationalities Youth Resources of Development Degree College

Results

A total of collected seven fish species belong to the four orders, five families and seven genera were observed in this study. They included seven species and they has different types of tail. In family Notopteridae and Clariidae are rounded fin shape, Clupeidae, two Cyprinidae and Bagridae are deeply forked and one Cyprinidae are forked. (Table 1).

Caudal skeleton of studied fish

Caudal skeleton of *Notopterus notopterus* (Pallas, 1769)

The caudal fin is rounded. The preural centrum 1 is a solid mass of bone with many of the characteristics of the vertebra and is reduced in many ways. Caudal bone structure can be discerned are the fused hypural complex which is in the form of a broad triangular structure. It bears an elongated hollow structure.Preural centrum 2 gives off a broad flat triangular shaped neural spine with a hollow at its distal end. The ventral portion baers a broad flat roughly triangular shaped haemal spine which is almost in line with the posterior edge of the hypural complex.Preural centrum 3 is an amphicoeleus cylindrical vertebra. It bears a short cylindrical neural spine on its dorsal side. On its ventral side gives off a haemal spine. The distal and bears a segment almost of an equal length. This segment ends short of its length from the distal edge of preural centrum 2.

Other typical structures like the epurals and uroneurals could not be detected (Plate1).

Caudal skeleton of *Tenualosa ilisha* (Hamilton, 1822)

The caudal fin shaped is deeply forked; upper and lower lobes are equal. The dorsal caudal fin is provided with the preural centrum1, neural crest, two ural centrum, three uroneurals,three epurals and three hypurals. The lower caudal fin is supported with three hypurals, last haemal spine, hypurapophysis and ridges of haemal spine.

Preural centrum 1 is stout bone and formed the last of vertebrae. Anterodorsal edge bears a pointed prezygapophysis, pointing towards the posterodorsal face preural centrum 2. The neural crest of preural centrum 1 is lancet-shaped. The base of the neural crest articulates with the base of uroneural 1. Postventral face of the preural centrum 1 partially fuses with the proximal end of the last haemal spine. The anterior face of preural centrum 1 articulates with the posterior face of pleural centrum 2. Ural centrum 1 is situated dorsally between the ventral edges of uroneural 1 and partially articulates anteriroly with the posterior face of preural centrum 1. The posterior face of ural centrum 1 partially fuses with hypural 2. Ural centrum 2 partially fuses with the dorsal face of ural centrum 1. The distal end of it is

bifurcated and partly articulates with the proximal end of hypural 4. The dorsal surface of ural centrum 2 is wedged between the ventral edges of uroneural 1 and uroneural 2.

Three epurals are arranged parallel to each other. All the epural are of the same size and length. The proximal end of eupral 1 and 2 are curved ventrally above the proximal end of epural 3. Epural 3 lies above the pained dorsal face of the proximal end of uroneural 1 and half of the length of uroneural 2. Uroneural 1 arises from the posterodorsal face of preural centrum 1 and articulates with dorsal face of ural centrum 1. The distal end of uroneural is pointed and is overlapped by the dorsal face of uroneural 2. One third distal end of uroneural 2 laterally covers uroneural 3 on each side.

Caudal skeleton consists five hypural 1, 2, 3, 4 and 5. Hypural 1 lies ventralmost along the dorsal edges of last haemal spine. The proximal end of last haemal spine partly fuses with the ventral face of preural centrum 1. Hypurapophysis is a long stout process. Hypural 2 is situated above the dorsal edge of hypural 1. The proximal end of its partly fuses with the posterior face of ural cemtrum 1. Hypural 3 lies along the dorsal margin of hypural 2. Hypural 4 is situates dorsal to the hypurals and its broad proximally and thin down distally. The proximal end of hypural 4 fits into the ventral face of the prolonged process of ural centrum 2. Hypural 5 lies dorsal to the hypural 4 and its fit into the dorsal noth of hypural 4. Hypural is slightly curved bone and lies dorsal to hypural 5. (Plate 2).

Caudal skeleton of *Cirrhinus mrigala* (Hamailton, 1822)

The caudal fin of *Cirrhina marigala* is deeply forked with equal upper and lower lobes. The dorsal lobe of caudal fin rays is supported by the epural and four hypurals. The lower lobe of caudal fin rays is supported by three hypurals. Each fin ray consists of two lateral halves joined together along their length except at the base where they form a cleft which fite over the hypurals are other supporting elements of the kind end of the vertebral column.

Neural spine of preural centrum 3 is long and slender. The haemal spine of preural centrum 3 is longer than the neural spine of preural centrum 3. The neural prezygapophysis of preural centrum 2 is fitted on the dorsal surface of preural centrum 3. On the preural centrum 2 have two neural spines. These two neural spines of preural centrum 2 are separated. The haemal spine of preural centrum 2 is based on the preural centrum 2. Neural crest is not broad and it tip is nearly pointed. It separated to the epural1. The epural 1 is elongated and based on the tip of the neural crest. Dorsal surface of uroneural is rather concave and it ventral surface is closely fused with in hypural 6. Tip of uroneural is pointed.

Caudal skeleton consists of six hypurals, hypural 1, 2, 3, 4, 5 and 6 respectively. The upper caudal lobe is supported with three hypurals, they are hypural 3, 4, 5 and 6. The lower caudal lobe is provided with two hypural 1, 2 which are also fused to the ultimate at their bases. The greatest bredth of hypural 1 is more than two times that of the hypural 1 and shorten than the hypural 3 separated from hypural 2. Hypural 3 is an elongated flat and base on the preural centrum1. Hypural 4 is greatest bredth of more than one time that of the hypural 5. Hypural 5 is lies in closely with hypural 4. Hypural 5 is lies in closely with hypural 4. The smallest hypural is hypural 6 and it based on epural 2 (Plate 3).

Caudal skeleton of *Labeo rohita* (Hamilton, 1822)

The caudal fin is deeply forked. The upper and lower lobe are equals. The caudal fins of dorsal lobe are supported by the epural, the urostyle and three hypurals. The lower lobe of caudal fins is provided by two haemal spines, last haemal spines and three hypurals. Each fin ray consists of two lateral halves joined together along their length expect at the base where they form a cleft which fits over the hypurals are other supporting elements of the hind end of

the vertebrae column. Two uroneural 1,2 are present. Dorsal surface of uroneural 2 is started from tip of the uroneural 1. Uroneural 2 is small and slender shaped.

Epural is longest and its base larger than the tip. Neural crest is triangle shaped and end of the tip is pointed. Epural 2 and 3 are absent. Caudal skeleton consists of six hypurals, hypural 1, 2, 3, 4, 5, 6. Hypural 1 is same side to hypural 2. It has smaller than the tip. Hypural 2 lies on the central side of the hypural 1 and it is articulated to uroneural. Hypural 3 is situated between hypural 2 and 4. It is long bone and triangle -shaped. Hypural 4 is the largest among the hypurals. The proximal end of hypural 4 is articulated to ural centrum 1. Hypural 5 is a long slender bone and it slightly curved and articulated to ural centrum2. Hypural 6 is small bone which is articulated to uroneural 2 on its ventral side.

A small pointed hypurapophysis present at the base of last haemal spine. Tip of the hypurapophysis reaches at dorsal margin of hypural 1. Ridge of the last haemal spine is present and close to the haemal spine of preural centrum 2 (Plate 4).

Caudal skeleton of *Osteobrama cotio (*Hamilton, 1822)

The caudal fin-shaped is forked. The dorsal part of caudal bone is supported by the epural and hypural 2. The lower part consists of last haemal spine and two hypurals. Neural spine of preural centrum 3 is long and slender shaped. Tip of the neural spine is pointed. Haemal spine of preural centrum 3 is longer than the neural spine of preural centrum 3. Its bone is slender shaped and tip is not pointed. One preural is present. The anterior dorsal surface of epural is pointerior and posterior dorsal surface is broad. Base of epural is placed a distance away from the dorsal surface of neural crest.Epural 2 and 3 are not present. The neural crest is triangle shaped and it base is broad. It is fused with preural centrum 1. Neural postzygapophysis and haemal postzygaphphysis of preural centrum 2 are closely fitted with dorsal and ventral surface of preural centrum 1. The preural centrum 1 consists with one neural crest, one epural, four hypurals.

Caudal skeleton consists of four hypurals, hypural 2,3,4 and 5. Hypural 3 lies on the ventral surface of hypural 4 and larger than hypural 4. Hypural 4 based on the dorsal surface of urostyle. It is broad triangular structure like structure and attached to the proximal end of the urostyle. Hypural 5 is attached with urostyle on its ventral side.

A broad hypurapophysis is present at the base of last haemal spine. The tip of hypurapophysis is pointed and reaches to the middle of neural centrum 1. Ridge of last haemal spine is smallet than the ridge of haemal spine of preural centrum 2. Ridge of haemal spine of preural centrum 2 is in the form of lobe (Plate 5).

Caudal skeleton of *Mystus bleekeri* (Day, 1878)

The caudal fin is deeply forked and the upper and lower lobes are equal. The neural crest of preural centrum 1 is lancet-shaped. The base of neural crest also articulated with the base of uroneural. Uroneurals stants from the posterodorsal face of preural centrum 1.

It is consisting of six hypurals. The upper caudal lobe is supported with four hypurals, namely, hypural 6, 5, 4 and 3. The lower caudal lobe is provided with two hypurals. They are hypural 2 and 1, which are also fused at the ultimate bases. The last haemal spine is a slender shaped bone. The distal end of hypurapophysis pointing to the anterolateral flange of last haemal spine. Hypural 1 lies above the dorsal edge of last haemal spine. Hypural 2 is a long bone which enlarges towards its proximal end. Hypural 3 is roughly triangular in shape and lies along the dorsal margin of hypural 2. Hypural 4 is separated and lies on dorsal to hypural 3. Hypural 4 is the smallest compact to the other hypurals. Hypural 5 is situated along the dorsal edge of hypural 4. Hypural 6 fits into the ventral side of uroneural. The caudal skeleton of *Mystus bleekeri* is basically similar to cyprinoids (Plate 6).

Caudal skeleton of *Clarias batrachus* (Linnaeus, 1758)

The caudal fin is rounded. The caudal fin is cannot be divided into dorsal and ventral lobe. The upper part of caudal fin is supported by one epural, one uroneural and three hypural. The lower part of caudal fin is supported by haemal spine of preural centrum 2, last haemal spine, two hypurals. Neural spine of preural centrum 3 is long and slender bone. Haemal spine of preural centrum 3 is long and slender shape. Anterior face of preural centrum 3 is firmly fused with the posterior face of preural centrum 2. Neural and spines of preural centrum 2 is long and slender bones. The prezygapophysis of preural centrum 1 is overlap on the postzygapophysis of preural centrum 2. Preural centrum is vertically rather broad towards the dorsal and ventral edges. Preural centrum 1 is articulated with preural centrum 2. Anterior edge of preural centrum possesses a small prezygapophysis like process. Neural crest is not present postventral face of preural centrum 1 is firmly fused with the last haemal spine, hypural 1 and 2. Epural is elongated and is situated between the ventral side of neural spine of preural centrum 2 and uroneural. Uroneural is long slender bone and entirely fuses with the posterodorsal face of pleural centrum. The ventral face of uroneural covers the dorsal margin of hyural 5.

Caudal skeleton consists of five hypurals, namely, hypural 1,2,3,4,5 and 6. Hypural 1 lies along the dorsal margin of last haemal spine. Hypural 2 lies along the dorsal margin of hypural 1. It proximally ends of which entirely fuses with the base of urostyle. Hypural 3 is smallest than among the hypural. It is situated between the dorsal surface of hypural 2 and ventral surface of hypural 4. Hypural 4 is long and lies on the dorsal surface of hypural 3. It is triangular shape and proximal end of which is articulated with the base of urostyle.Hypural 5 lies between along the dorsal margin of hypural 4 and ventral margin of uroneural.Hypural 5 is articulated with the ventral surface of urostyle . Hypurapophysis is absent (Plate 7).

A. *Notopterus notopterus*

B. Caudal fin shape of *Notopterus notopterus*

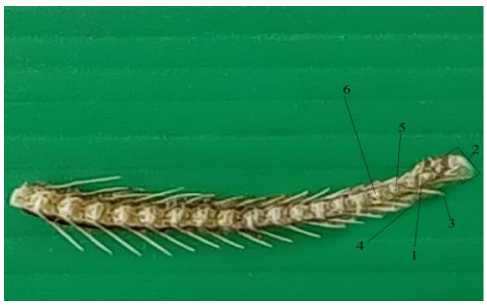

1. preural centrum1
2. fused hypural
3. last haemal spine
4. haemal spine preural centrum2
5. preural centrum 2
6. preural centrum 3

C. Caudal bones structure of *Notopterus notopterus*

Plate 1 Caudal skeleton of *Notopterus notopterus*

A. *Tenualosa ilisha*

B. Caudal fin shape of *Tenualosa ilisha*

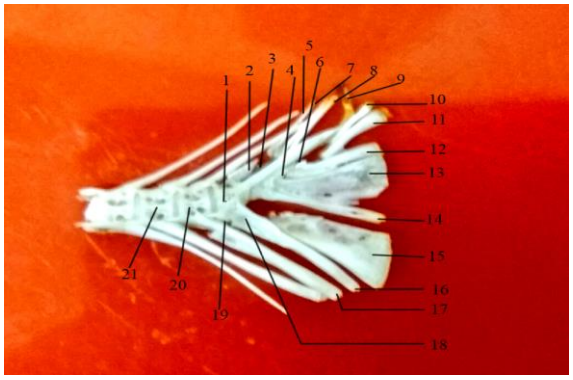

1. preural centrum1
2. neural crest
3. ural centrum 1
4. ural centrum2
5. uroneural 1
6. uroneural 2
7. epural 1
8. epural 2
9. epural 3
10. uroneural 3
11. hypural 5
12. hypural 4
13. hypural 3
14. hypural 2
15. hypural 1
16. haemal spine
17. haemal spine of preural centrum 2
18. ridge of haemal spine
19. hypurapophysis
20. preural centrum 2
21. preural centrum 3

C. Caudal bones structure of *Tenualosa ilisha*

Plate 2 Caudal skeleton of *Tenualosa ilisha*

A. *Cirrhinus mrigala*

B. Caudal fin shape of *Cirrhinus mrigala*

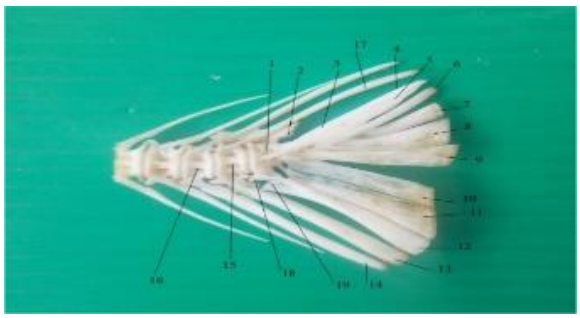

1. preural centrum 1
2. neural crest
3. uroneural 1
4. epsaaural 1
5. epural 2
6. hypural 6
7. hypural 5
8. hypural 4
9. hypural 3
10. hypural 2
11. hypural 1
12. last haemal spine
13. haemal spine of preural centrum 2
14. haemal spine of preural centrum 3
15. preural centrum 2
16. preural centrum 3
17. neural spine of preural centrun 2
18. haemal prezygapophysis
19. ridge of last haemal spine

C. Caudal bones structure of *Cirrhinus mrigala*

Plate 3 Caudal skeleton of *Cirrhinus mrigala*

A. *Labeo rohita*

B. Caudal fin shape of *Labeo rohita*

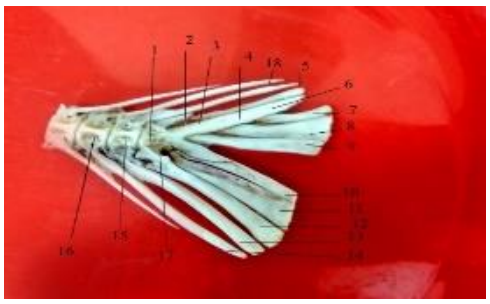

1. Preural centrum 1
2. neural crest
3. uroneural 1
4. uroneural 2
5. epural 1
6. epural 2
7. hypural 5
8. hypural 4
9. hypural 3
10. hypural 2
11. hypural 1
12. last haemal spine
13 haemal spine of preural centrum2
14 haemal spine of preural centrum3
15 preural centrum 2
16 preural centrum 3
17 hypurapophysis
18 neural spine of preural centrum 2

C. Caudal bones structure of *Labeo rohita*

Plate 4 Caudal skeleton of *Labeo rohita*

A. *Osteobrama cotio*

B. Caudal fin shape of *Osteobrama cotio*

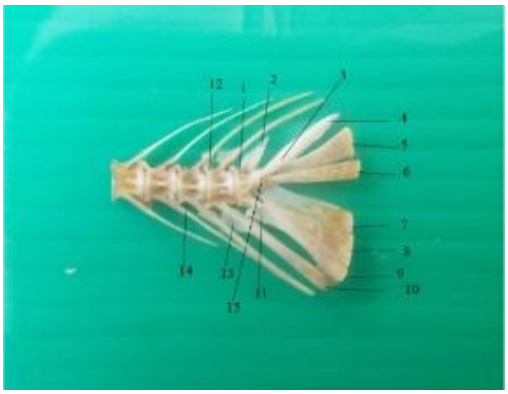

1.preural centrum 1
2.neural crest
3.uroneural 1
4.epural 1
5.hypural 4
6.hypural 3
7.hypural 2
8.hypural 1
9.last haemal spine
10.haemal spine of preural centrum 2
11.ridge of last haemal spine
12.neural postzygogapophysis
13.ridge of haemal spine of preural centrum 2
14.haemal prezygapophysis
15.hypurapophysis

C. Caudal bones structure of *Osteobtama cotio*

Plate 5 Caudal skeleton of *Osteobtama cotio*

A. *Mystus bleekeri*

B. Caudal fin shape of *Mystus bleekeri*

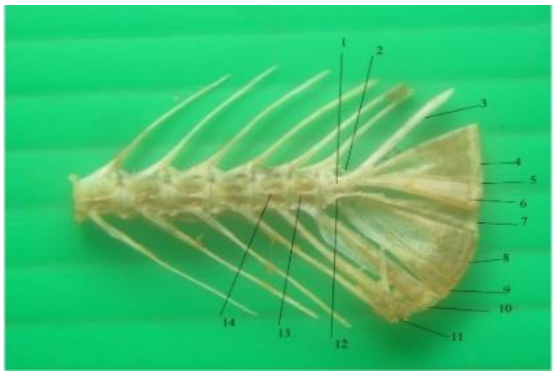

1. preural centrum 1
2. neral crest
3. uroneural
4. hypural 6
5. hypural 5
6. hypural 4
7. hypural 3
8. hypural 2
9. hypural 1
10. last haemal spine

C. Caudal bones structure of *Mystus bleekeri*

Plate 6 Caudal skeleton of *Mystus bleekeri*

A. *Clarias batrachus*

B. Caudal fin shape of *Clarias batrachus*

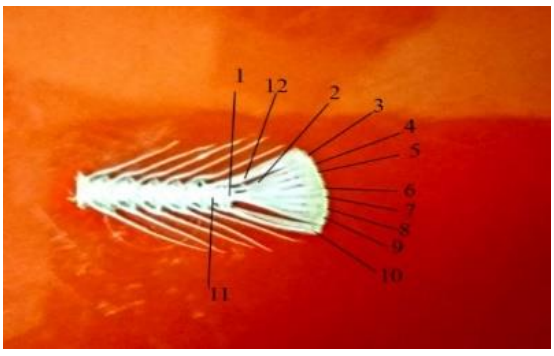

1. hypural 2
2. hypural 1
3. last haemal spine
4. haemal spine of preural centrum 2
5. preural centrum 2
6. neural spine of preural centrum 2
7. preural centrum 1
8. uroneural 1
9. epural 1
10. hypural 5
11. hypural 4
12. hypural 3

C. Caudal bones structure of *Clarias batrachus*

Plate 7Caudal skeleton of *Clarias batrachus*

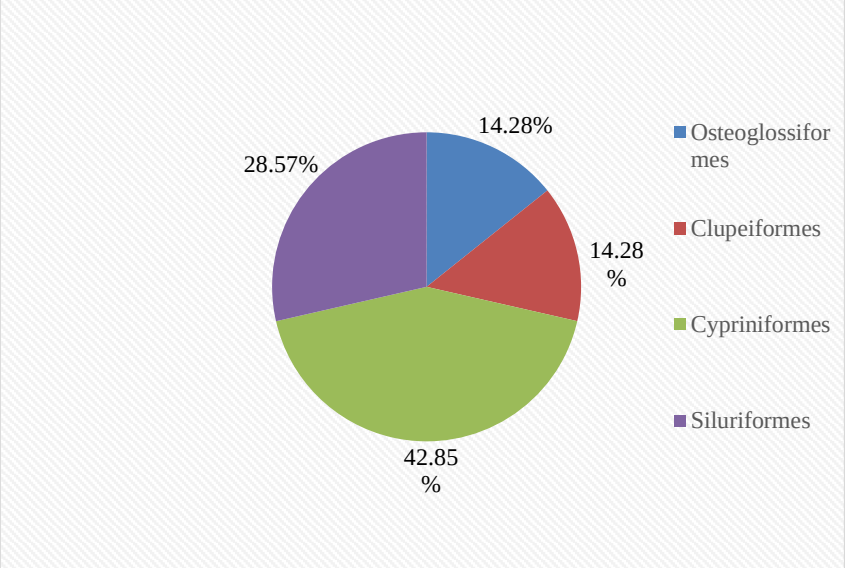

Fig. Species composition in different collected fish in orders

Table 1 The tail types of studied fish species from Myoma Market

Order	Family	Scientific name	Tail types
Osteoglossiformes	Notopteridae	*Notopterus notopterus*	Rounded
Clupeiformes	Clupeidae	*Tenualosa ilisha*	Deeply forked
Cypriniformes	Cyprinidae	*Cirrhinus mrigala*	Deeply forked
		Labeo rohita	Deeply forked
		Osteobrama cotio	Forked
Siluriformes	Bagridae	*Mystus bleekeri*	Deeply forked
	Clariidae	*Clarias batrachus*	Rounded

Table 2 Caudal bones of studied fish species

Collected fish species	Epurals	Uroneural	Hypurals	Hypurapophysis	Fin type
Notopterus notopterus	-	-	1	-	Rounded
Tenualosa ilisha	3	3	5	1	Deeply forked
Cirrhinus mrigala	2	1	6	1	Deeply forked
Labeo rohita	2	2	5	1	Deeply forked
Osteobrama cotio	1	1	4	1	Forked
Mystus bleekeri	-	1	6	1	Deeply forked
Clarias batrachus	1	1	5	-	Rounded

Discussion

The present study includes the different types of tail and caudal osetology of some bony fish were mentioned. The observation of collected fish species was classified according to Talwar and Jhingran (1991).

Tails were divided into two heterocercal means that the vertebrae extend into upper lobe of the tail, making it longer. Most fishes have a homocercal tail, where the fin appears superficially symmetric but in fact the vertebrae extend for a very short distance into the upper lobe of the fin. This can be expressed in a variety of shapes. Seven kinds of tail types

were found that (a)Truncate, (b) slightly emarginate, (c)Forked, (d)Deeply forked, (e)Rounded, (f)Lunate and (g) Lanceolate or spear-shaped (Kelvin, *et al*., 1997).

In this study, *Tenualosa ilisha*, *Cirrhinus marigala*, *Labeo rohita, Mystus bleekeri* were deeply forked. *Notopterus notopterus, Clarias batrachus* were rounded. *Osteobrama cotio* was forked.

The last three vertebrae of vertebral column designated as preural centrum 1, 2, 3. It includes neural crest, uroneurals, ural centra, last haemal spine, epurals and hypurals Nag, C (1967). The caudal skeleton in clupeoid fish, as mentioned earlier and was interesting because of its peculiar structure that differs with the other higher teleostean fishes (Gosline, 1965). Than Htoon U (1987) described that *Notopterus notopterus*, the caudal skeleton was massive one. The ultimate vertebra was fused to single broad hypural complex. This species lacks epural and uroneural bones. Soe Soe (1981) state that *Notopterus notopterus* the preural centrum 1 was solid mass of bone and reduced in many rays and its hypurals were complex.

In the recent study, the epural and uroneural bones were absent and hypural was fused to a fan-like processes in *Notopterus notopterus*. In family Clupeidae, Soe Soe (1981) described that the pair of uroneural, three epurals, six hypurals were present in *Hilsa ilisha*. In the present study *Tenualosa ilisha* comprises the epural 1, 2, 3 and uroneural three pairs and hypural 1, 2, 3, 4, 5 and 6. This result was the same as Soe Soe.

Than Htoon U (1978) described that about 36 species of cyprinoid fishes in Indawgyi Lake at Kachin State. Among 36 species only one cyprinoid Labeo *rohita* consist of one uroneural, one epural and seven hypural bones. In this study, six hypural bones were found. The caudal skeleton of *Cirrhinus mrigala* and *Labeo rohita*, *Rohtee coti* consists of two epural, two uroneural and six hypural bones were described by Mg Mg Tar (1983).

In the present study, caudal bones *of Cirrhiua mrigala, Labeo rohita* and *Osteobrama cotio* were observed. In *Cirrhinus mrigala*, caudal consists of one epural, one uroneural and six hypurals in *Labeo rohita*. In *Osteobrama cotio* were supported with two epurals, one uroneural and six hypurals. Thus, the present observed species were a little different from that than above the two authors.

In the order Siluriformes, Mg Mg Tar (1983) state that *Mystus bleekeri* and *Clarias batrachus* were supported with one epural, one uroneural bone and six hypural bone in *Mystus bleekeri* and five hypurals pieces in *Clarias batrachus*.

In the recent study above the two species of Siluriformes fish were the same structure of caudal bones were found.

Conclusion

A total of seven species, five families under four orders were collected from Myoma market in Thanlyin Township during December 2017 to September 2018.Species composition of 14.28% from family Osteoglossiformes, 14.28% of Clupeiformes, 42.85% of Cypriniformes and 28.57% of Siluriformes were observed. According to observed in four orders, three types of tail-shaped are collected. Study the caudal bones structure of collected fish species and recorded the bones attached to each other in differences are mentioned. Caudal bones are commonly found uroneurals, epurals, hypurals, last haemal spine and preural centrum in the study species.

Acknowledgements

We would like to express my profound gratitude to Dr Nay Win Oo, Rector of East Yangon University for his keen interest and also for his permission. We are indebted to Dr Aye Aye Ko, Dr Wah Wah Lwin and Dr Thida Aung, Pro-Rectors, East Yangon University for their supports, permitting to conduct this work and confidence in the implementation of this research. We are also grateful thanks to Professor Dr. Ohn Mar Ohn, Head of Zoology Department, East Yangon University, for her valuable suggestions, constructive criticisms of the manuscripts and supervision. We would also like to express our thanks to Dr Aye Thida Than, Professor of Zoology Department, East Yangon University, for providing advices and support of this research paper.

References

Dubois, A.B, G.A., Cavagna and RS.,Fox (1976). Locomotion of blue fish. *J. Exp Zool*, 195223-35.

Gosline, W. A, (1968). Some Osteological features of modern teleostean fishes. *Smithsonian, Musc. Coll*; 143; 1-42.

George, V, Lauder, (2000). *Function of the Caudal Fin during Locomotion in Fishes; Kinematics, Flow Visualization and Evolutionary Patterns.* Department of Ecology and Evolutionary Biology, University of California, Irvine, California 92697.

Kelvin, K.P, Lin and K.Y. Jeffery, Low, (1997). *A Guide to common marine fishes of Singapore*. Raffles Museum Biodiversity Research and Singapore Science Center.

Mg Mg Tar, (1983). A study on the fish caudal appendages of some freshwater fishes. *MSc Thesis*, Arts and Science University, Rangoon.

Nag. C, (1967). Functional morphology of the caudal region of certain Clupeiformes and Perciformes Fishes with references to the Taxonomy. *Journal of Morphology* 123, 529-558.

Soe Soe, (1981). On the study of the Osteology and Myology of the Caudal region of some Burmese Clupeiod fishes. *MSc Thesis*. Arts and Sciences University, Rangoon.

Tin May Yee, (1977). The comparative Myology of some percoid fishes. *MSc Thesis*. Arts and Science University, Rangoon.

Than Htoon U, (1978). On the study of the taxonomy and adaptive characters of fishes of Indawgyi Lake. *MSc Thesis*. Arts and Science University, Rangoon.

Talwar and Jhingran, (1991). *INLAND FISHES India and Adjacent* Countries. Volume 1 and 2 Oxford & IBH Publishing Co. PVT. LTD New Delhi Bombay Calcutta.

COMPARISON OF MORPHOLOGICAL, PHYTOCHEMICAL CHARACTERIZATION AND ANTIMICROBIAL ACTIVITIES ON TWO SPECIES OF GENUS *JUSSIAEA*

Htay Htay Lwin [1], Win Win Nu[2], Hnin Hnin Soe[3]

Abstract

The selected species of genus *Jussiaea* scientifically called *Jussiaea repens* L. (species 1) and *Jussiaea hyssopifolia* (G.Don) Exell (species 2) belong to the family Onagraceae locally known as Ye-ka-nyut and Taw-lay-hnyin which are wild species of medicinal plants. They are collected from Hpa-an Township, Kayin State. Verification of plants was done according to the literatures. In this research, phytochemical characterization and antimicrobial activities of collected plants were carried out. In morphological study, *Jussiaea repens* L. (species 1) is perennial herb, partly creeping in the mud and partly floating on the surface of tanks and pneumatophores are present. *Jussiaea hyssopifolia* (G.Don) Exell (species 2) is perennial herb or undershrub, growing usually in swamps. The phytochemical examination of *Jussiaea repens* L. (species 1) and *Jussiaea hyssopifolia* (G.Don) Exell (species 2) were showed the presence of alkaloids, α-amino acid, carbohydrates, flavonoids, glycosides, phenolic compounds, proteins, reducing sugar, saponins, starch, steroids, tannins and terpenoids. In the study of antimicrobial activity, the different solvent extracts (petroleum ether, chloroform, ethyl acetate, acetone, ethanol, methanol and watery) of powdered samples were also investigated six microorganisms such as *Aspergillus flavus*, *Bacillus subtilis*, *Candida albicans*, *Echerichia coli*, *Pseudomonas aeruginosa* and *Staphylococcus aureus*. According to the result, all extracts showed antimicrobial activity against *Aspergillus flavus*, *Candida albicans*, *Escherichia coli* and *Pseudomonas aeruginosa* in *Jussiaea repens* L. (species 1) and *Aspergillus flavus* and *Staphylococcus aureus* in *Jussiaea hyssopifolia* (G.Don) Exell (species 2).

Keywords: *Jussiaea repens* L. (species 1) and *Jussiaea hyssopifolia* (G.Don) Exell (species 2) morphological characters, phytochemical characterization, antimicrobial activity.

Introduction

Jussiaea repens L. (species 1) and *Jussiaea hyssopifolia* (G.Don) Exell (species 2) which belong to family Onagraceae. *Jussiaea repens* L. grows in fresh water, ponds, canals of road side and wetlands (Pradhan *et al*., 2014). In Myanmar, *Jussiaea repens* L. is commonly known as Ye-ka-nyut (Kress *et al*., 2003), water-primrose, creeping water-primrose, floating primrose-willow, red Ludwigia (Benson, 1957 and Al-Snafi, 2018). It was also used as diuretic, for the treatment of cough, Jaundice, gonorrhea, measles and erysipelas boils (Al-Snafi, 2018).

Jussiaea hyssopifolia (G.Don) Exell is semi-shrubby, erect perennial herb with tap root system (Kumar and Pranita, 2013). It is commonly known as Taw-lay-hnyin (Kress *et al*., 2003), Willow Primrose in English (Jacquin, 2013). The juice of the whole plant is useful to treat fever, jaundice, diarrhea, dysentery and diabetes (Kirtikar and Basu, 1935; Nadkarni, 1954, Chopra, 1956 and Saha *et al.*, 2000). The aim and objectives are to determine the phytochemical properties, to examine the antimicrobial activity from the plants *Jussiaea repens* L. and *Jussiaea hyssopifolia* (G.Don) Exell.

[1] Dr, Professor and Head, Department of Botany, East Yangon University
[2] Dr, Associate Professor, Department of Botany, East Yangon University
[3] Daw, Lecturer, Department of Botany, East Yangon University

Materials and methods

Identification of *Jussiaea repens* L. (Species 1) and *Jussiaea hyssopifolia* (G.Don) Exell (Species 2)

The collected plants were identified with the help of available literature Kirtikar and Basu (1935) and Backer (1965).

reliminary Phytochemical Investigation

Preliminary phytochemical investigation of the whole plants of *Jussiaea repens* L. (species 1) and *Jussiaea hyssopifolia* (G.Don) Exell (species 2) carried out at Botany Department, Hpa-an University by using the central council for Research in Unani Formulation (1987).

Antimicrobial activities of different solvent extracts from *Jussiaea repens* L. (species 1) and *Jussiaea hyssopifolia* (G.Don) Exell

Antimicrobial activities of different solvent extracts (petroleum-ether, chloroform, ethyl-acetate, acetone, ethanol, methanol and water) of *Jussiaea repens* L. and *Jussiaea hyssopifolia (G.Don) Exell* (species 2) were tested on six pathogenic microorganisms at Botany Department, Hpa-an University by using paper disc diffusion method.

Results

Table 1. Comparison of Morphological Characters of *Jussiaea repens* L. (species 1) and *Jussiaea hyssopifolia* (G.Don) Exell (species 2)

Characters	Species 1	Species 2	Figures	
Habit	Perennial herb, with white, erect, herb partly creeping in the mud and partly floating on the surface of tanks.	Perennial herbs and erect, well branches.	**Species 1**	**Species 2**
			Habit	Habit
Stems	The stem is floating.	Stem often 3 to 4 angled.	Stem	Stem
Roots	Pneumatophores in cluster at nodes of floating stems.	Tap root system.	Root	Root

Leaves	Leaves alternate, simple, both surface glabrous; stipulate.	Leaf simple, alternate, exstipulate, petiole short.	Leaves	Leaves
Inflorescences	axillary and solitary cymes.	axillary and solitary cymes.	Inflorescences	Inflorescences
Flowers	yellowish white, bisexual, actinomorphic, pentamerous, epigynous	Flowers yellow, bisexual, actinomorphic, tetramerous, epigynous .	L.S of Flower	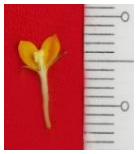 L.S of Flower
Calyx	Sepals 5, free, inner surface glabrous outer surface, glabrate, persistent.	Sepals 4, pubescent, persistent.	Calyx	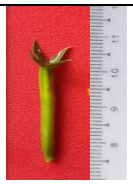 Calyx
Corolla	Petals 5, free, obovate, both surfaces glabrous, creamy-white with yellow base, caducous.	Petals 4, broadly oval, yellow glabrous, opposite the petals have hairs at the base, caducous.	Corolla	Corolla
Androecium	Stamen 5 + 5, free, anther dorsifixed, introrse longitudinal dehiscence.	Stamen eight anthers basifixed,extrorse, epipetalous, longitudinal dehiscence.	Androecium	Androecium
Gynoecium	Carpel 5, fused, pentacarpellary, axile placentation, one to many ovules in each locule, stigma capitate, ovary inferior.	Carpel 4, tetracarpellary, axile placentation, one to three ovules in each locule, stigma subglobose, ovary inferior.	Gynoecium	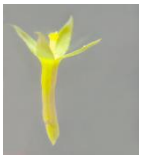 Gynoecium

Fruits	Capsule, oblong, pubescent.	Capsule not woody.	Fruit	Fruits
Seeds	Seeds many, quadrate, minute, glabrous.	Seeds in each locule several rows.	Seeds	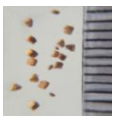 Seeds

Table 2. Comparison of Phytochemical Examination on *Jussiaea repens* L. (Species 1) and *Jussiaea hyssopifolia* (G.Don) Exell (Species 2)

Test	Extracts	Reagents	Observation	Results	
				Species 1	**Species 2**
Alkaloids	3% Acetic acid	Dragendorff's	Orange brown	+	+
		Hager's	Yellow ppt.	+	+
		Mayer's	White ppt	+	+
		Wagner's	Reddish brown	+	+
α-amino acid	H_2O	Ninhydrin	Purple spot	+	+
Carbohydrate	H_2O	Benedict's	Reddishbrown	+	+
Flavonoid	EtOH	HCl / Mg	Pink color	+	+
Glycosides	H_2O	10% lead acetate	Brown ppt.	+	+
Phenol	EtOH	1% $FeCl_3$	Deep blue ppt.	+	+
Protein	H_2O	Millon's reagent	red on heating	+	+
reducing sugar	H_2O	Feling A&B	Reddish brown	+	+
Saponins	EtOH	Distilled water	Frothing	+	+
Starch	H_2O	Iodine solution	Blue black	+	+
Steroid	EtOH	Chloroform + conc: H_2SO_4	Bluish green colour	+	+
Tannins	H_2O	$FeCl_3$	Brownish green	+	+
Terpenoid	EtOH	Chloroform + conc: H_2SO_4	Red colour	+	+

Table 3. Comparism of Antimicrobial Activity on *Jussiaea repens* L. (Species 1) and *Jussiaea hyssopifolia* (G.Don) Exell (Species 2)

Test Organisms / Solvents	*Aspergillus flavus*		*Bacillus subtilis*		*Candida albicans*		*Echerichia coli*		*Pseudomonas aeruginosa*		*Staphylococcus aureus*	
et-Ether	Species 1	Species 2	Species 1	Species 2	Species 1	Species 2	Species 1	Species 2	Species 1	Species 2	Species 1	Species 2
	14mm	30mm	-	-	12 mm	-	14mm	-	12mm	-	-	25mm
Chloroform	14mm	31mm	10 mm	25mm	14 mm	17mm	14mm	23mm	14mm	22mm	12 mm	31mm
Ethyl acetate	14mm	18mm	-	18mm	12 mm	17mm	14mm	32mm	14mm	-	-	17mm
Acetone	14 mm	25mm	12 mm	25mm	12 mm	17mm	12mm	-	12mm	-	-	25mm
Ethanol	14 mm	16mm	-	-	12 mm	-	14mm	-	16mm	25mm	-	17mm
Methanol	30 mm	25mm	18mm	18mm	28 mm	-	24mm	-	28mm	-	20 mm	24mm
Aqueous	18 mm	-	-	26mm	14 mm	28mm	14mm	-	14mm	32mm	12 mm	14mm

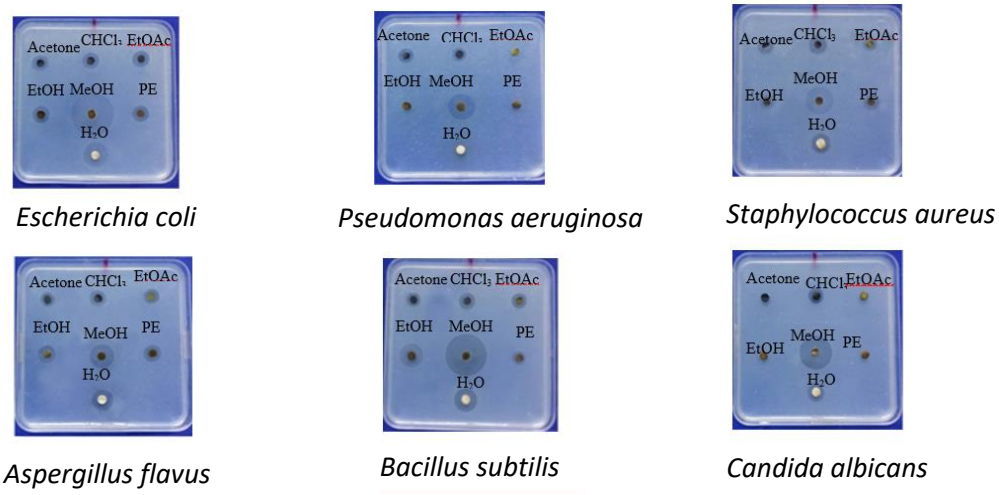

Fig. 1. Antimicrobial activity of different solvent extracts of *J. repens* L.

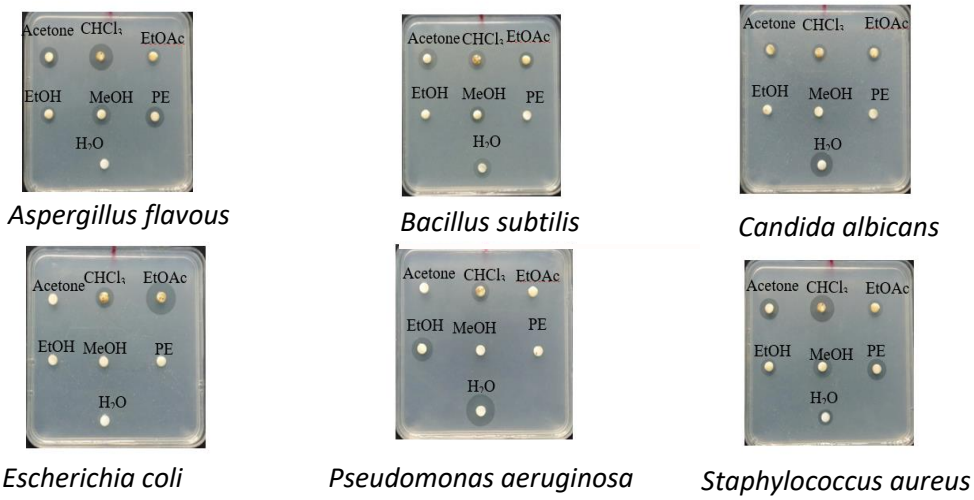

Fig. 2. Antimicrobial activity of different solvent extracts *J. hyssopifolia* (G.Don) Exell

Discussion

In this research, morphological characters, phytochemical investigation, and antimicrobial activity of two species of genus *Jussiaea* were carried out. Myanmar name Ye-ka-nyut is a floating aquatic herb and pneumatophores in clusters at nodes of floating stems are present. The plants are erect, perennial herbs and well branches. Taw-lay-hnyin is perennial herbs and erect, well branches. Leaves are alternate, simple, stipulate in *Jussiaea repens* L. Leaf simple, alternate, exstipulate in *Jussiaea hyssopifolia* (G.Don) Exell Inflorescences are axillary and solitary cymes in both species. Flowers are yellowish white, pentamerous and epigynous in *Jussiaea repens* L. Flowers yellow, tetramerous and epigynous in *Jussiaea hyssopifolia* (G.Don) Exell. Sepals are persistent in both species. Petals white and caducous in *Jussiaea repens* L. Petals yellow and caducous in *Jussiaea hyssopifolia* (G.Don) Exell. Stamens 5+5, introrse, anther dorsifixed in *Jussiaea repens* L. Stamen are eight, extrorse, basifixed in *Jussiaea hyssopifolia* (G.Don) Exell. Carpel 5, pentacarpellary and axile placentation, stigma capitate in *Jussiaea repens* L. Carpel 4, tetracarpellary and axile placentation in *Jussiaea hyssopifolia (*G.Don) Exell. These characters are agreed with those of Hooker (1885), Hutchinson (1926), Datta (1931), Henderson (1949), Cooke(1958), Gamble (1958), Backer (1965), Rendle (1967), Roxburgh (1971), Thompson (1990), Dassanayake (1995), Long (2007) and Pradhan *et al*., (2014). These mentioned characters can be used for identification of plants.

Saha *et al*., (2000) reported that *Jussiaea hyssopifolia* (G.Don) Exell showed presence of flavonoids, steroids, alkaloids and tannins.

Kumar and Pranita (2013) stated that the plant contain alkaloids, carbohydrate, saponins, proteins, α- amino acid, steroids, phenolic compounds and flavonoids.

In this research *Jussiaea repens* L. and *Jussiaea hyssopifolia* (G.Don) Exell showed presence of alkaloids, α-amino acid, carbohydrates, flavonoids, glycosides, phenolic compounds, proteins, reducing sugar, saponins, starch, steroids, tannins and terpenoids.

Al-Snafi (2018) stated that the methanolic extract of *Jussiaea repens* L. showed antibacterial activity against *Escherichia coli*.

In this experiment, the antimicrobial activities of *Jussiaea repens* L. and *Jussiaea hyssopifolia* (G.Don) Exell were tested with six different microorganisms (*Aspergillus flavus, Bacillus subtilis, Candida albicans, Escherichia coli, Pseudomonas aeruginosa and Staphylococcus aureus*) by using different solvent extracts such as pet-ether, chloroform, ethyl-acetate, acetone, ethanol, methanol and aqueous extracts.

In this study, chloroform and methanolic extract showed antimicrobial activity against tested organisms in *Jussiaea repens* L. and chloroform extract in *Jussiaea hyssopifolia* (G.Don) Exell. Among them, chloroform extract of *Jussiaea hyssopifolia* (G.Don) Exell showed the more significant antimicrobial activity against tested organisms than *Jussiaea repens* L.

In this study, all extracts showed antimicrobial activity against *Aspergillus flavus, Candida albicans, Escherichia coli* and *Pseudomonas aeruginosa* in *Jussiaea repens* L. and *Staphylococcus aureus* in *Jussiaea hyssopifolia* (G.Don) Exell. Ethyl acetate, ethanol, petroleum ether and aqueous extracts did not show antimicrobial activity against *Bacillus subtilis* in *Jussiaea repens* L. and ethanol and petroleum ether in *Jussiaea hyssopifolia* (G.Don) Exell. Ethanol, methanol and petroleum ether extracts did not show antimicrobial activity on *Candida albicans* in *Jussiaea hyssopifolia* (G.Don) Exell. Acetone, ethanol, methanol, petroleum ether and aqueous extracts did not show antimicrobial activity against *Escherichia coli* in *Jussiaea hyssopifolia* (G.Don) Exell. Acetone, ethyl acetate, methanol and petroleum ether did not show antimicrobial activity against *Pseudomonas aeruginosa* in *Jussiaea hyssopifolia (G.Don)* Exell. Ethyl acetate, acetone,

ethanol and petroleum ether extracts did not show antimicrobial activity against *Staphylococcus aureus* in *Jussiaea repens* L.

Conclusion

The plants *Jussiaea repens* L. and *Jussiaea hyssopifolia* (G.Don) Exell belongs to family Onagraceae. These plants contain alkaloids, α-amino acid, carbohydrates, flavonoids, glycosides, phenolic compounds, proteins, reducing sugar, saponins, starch, steroids, tannins and terpenoids. According to this experiment, different solvent extracts of *Jussiaea repens* L. indicated antimicrobial activity against *Aspergillus flavus*, *Candida albicans*, *Echerichia coli* and *Pseudomonas aerugino*sa. Therefore, it is effective in protecting against bronchitis caused by *Aspergillus flavus*, alimentary tract infection, cardiac infection, sores and inflammation by *Candida albicans*, diarrhoea, dysentery by *Echerichia coli*, urinary-tract infections, respiratory system infection caused by *Pseudomonas aeruginosa*. Different solvent extracts of *Jussiaea hyssopifolia* (G.Don) Exell indicated antimicrobial activity against *Staphylococcus aureus*. Therefore, it is effective in protecting against food poisoning, nausea, vomiting, illness, headache, transient change in blood pressure caused by *Staphylococcus aureus*. Therefore, *Jussiaea repens* L. and *Jussiaea hyssopifolia* (G.Don) Exell is effective on protection of diseases which caused by microorganisms.

Acknowledgements

I would like to express my special thanks to Dr Nay Win Oo, Rector, East Yangon University for his allowing me to do this research paper. I also wish to extend my gratitude to Dr Aye Aye Ko, Dr Wah Wah Lwin and Dr Thida Aung , Pro-Rectors, East Yangon University for their advice and encouragement in preparing this paper.

References

Al-Snafi A.E. (2018). *Constituents and Pharmacological Importance of Jussiaea repens L.* - A Review , Indo Am. J.P. Sci, 05(04).American Society Of Plant Taxonomists.

Backer, C.A., D.Sc. (1965). *Flora of Java*. Vol. I. Published under the Auspices of the Rijks herbarium, Leyden.Wolters.Noorhoff.N.V. and Groningen.The Netherlands.

Benson, L. (1957). *Classification.D.C.* Health and company, Boston, Printed in the United States of America.

Chopra, R. N. (1956). *Glossary of Indian Medicinal Plants*. Council of Scientific. Industrial Research, New Delhi.

Cooke, T., C.I.E. (1958). *Flora of the Presidency of Bombay*. Vol. I. Sri Gougange Press Private Ltd., 5, Chintameni; Das Lane, Calcutta -9.

Dassanayake, M.D. (1995). *A Revised Handbook to the Flora of Ceylon.* Vol. IX Published for the Smithsonian Intitution and the National Science foundation, Washington, D.C., by Amerind Publishing Co. Pvt. Ltd, New Delhi.

Datta, S.C. (1931). *A handbook of Systematic Botany*.Asia Publishing House, New York.

Gamble, J.S. (1958). *Flora of the Presidency of Madras*. Vol. I. Botanical survey of India. Calcutta. Government of India.

Henderson, M. R. (1949). *Malayan Wild Flowers*. Part II. Coxton Press. Kuahimpur, Malaysia.

Hooker, J. D. (1885). *Flora of British India*. Vol III. Reeve & Co; Ltd; London.

Jacquin, N.J. V. (2013). *Ludwigia octovalvis* Shrubby Water Primrose. Fourth Edition. Michael A. Arnold with all rights reserved; intended for future inclusion in Landscape Plants For Texas And Environs.

Kirtikar, K. F. and B. D. Basu. (1935). *Indian Medicinal Plants* Vol I. 2nd edition. Lallit Mohan Basu. All ahabad India

Kress, W.J. (2003). *A Checklist of the trees, shrubs, herbs and climbers of Myanmar*. Department of Systematic Biology. Botany, National Museum of Natural History, Washington, DC.

Kumar, A.,K. Pranita.(2013). *Pharmacognostical & Phytochemical Approach of Jussiaea suffruticosa Linn*. International Journal of Pharmacognosy and Phytochemical Research. ISSN: 0975-4873.

Long, M. C. (2007). *Flora of China*. 13: 400–404. 2007.

Nadkarni, A. K. (1954). *Indian Materia Medica*. 3rd edition. Published by G.R. Bhatkal for the Popular Book Depot (Regd) Lamington Road, Bombay 7 and Dhootapapeshwar Prakashan Ltd., Panvel.

Pradhan, N, I. Chakraborty and S. Ghosal. (2014). *Jussiaea repens* L. Acts as an Uterotonic Agent - An Invitro Study. Department of Physiology (Reproductive Biology Research Unit), Presidency University, 86/1 College Street, Kolkata, West Bengal, India.

Rendle. A.B. (1967). *The classification of flowering plants*. Vol. II. Cambridge at the University press.

Roxburgh, W, M.D. (1971). *Flora Indica or Descriptions of Indian Plants*. Today and Tomorrow's Printers and Publishers, 22B/5, Original Road, New Delhi.

Saha, B.P., T. Murugesan, L. Manikandan, K.B. Suresh and M. Pal. (2000). *Evaluation of diuretic potential of Jussiaea hyssopifolia (G.Don) Exell extract in rats*. Indian Journal of Pharmaceutical Science.

Thompson, J. (1990). *Flora Of Australla*. Volume 18. Podostemaceae to Combretaceae. © Commonwealth of Australia.

Central Council for Research in Unani Formulation. (1987). *Phytochemical standards of Unani Formulation part 2*, Ministry of Health and Family Welfare, Govt. of India, New Delhi.

EFFECT OF POSTHARVEST TREATMENTS ON SHELF-LIFE OF *LYCOPERSICON ESCULENTUM* MILL.

Su Latt Win[1], Myat Su Hlaing[2]

Abstract

Postharvest treatments of tomato *Lycopersicon esculentum* cv. padamyarni was conducted at postharvest fruit laboratory, Vegetable and Fruit Research Development Center (VFRDC). Tomato plants were cultivated for postharvest treatment in order to get uniformly mature fruits at the same date. Harvested fruits were immediately brought to the postharvest laboratory. There were 8 treatments; T_1 (control), T_2 (4% ethylene absorbent), T_3 (5% ethylene absorbent), T_4 (6% Ethylene absorbent), T_5 (6 pin-pricks + LDPEB), T_6 (10 pin-pricks + LDPEB), T_7 (6 pin-pricks + HDPEB) and T_8 (10 pin-pricks + HDPEB). The results of the experiment showed that T_7 gave the best result in fruit weight of 50.26 g, 14.6 cm in fruit roundness, 4.77 cm in fruit length, 1.95% weight loss, 2.37 $mmkg^{-1}$ peel firmness, 4.21 $mmkg^{-1}$ pulp firmness, 5.91°C Brix total soluble solid, 1.21% total acidity, 10R 5/10 in peel color and 32 days shelf-life. Among the postharvest treatments, modified atmosphere packaging was best due to its lesser weight loss, highest fruit weight, moderate in fruit length and width, peel and pulp firmness, total soluble solid, total acidity and shelf-life. Therefore, the discovery and utilization of modified atmosphere packaging treatment (6 and 10 pin-pricks + LDPEB and HDPEB) is an effective treatment that could have significant benefits for quality management of tomato fruits.

Keywords: *postharvest treatments, roundness, length, weight loss, firmness, total soluble solid, total acidity, peel color, shelf-life*

Introduction

Tomato originated in Western South America and it was introduced into European gardens in the early sixteenth century (Wien, 1997). Tomato is a member of the solanaceae family or night shade family. Other members of the family include potato, pepper, eggplant, tobacco. In a protected environment, tomato is a short-lived herbaceous perennial. Tomato is grown for its commercial importance (Decoteau, 2000). Tomato is a warm season crop. Tomato grows best in the dry season under day temperature of 21-25°C and night temperature of 15°C-20°C. The optimum range of day temperature is 20°-25°C and night temperature is 15°-25°C. Mean temperature below 16°C and above 27°C is not desirable. Lycopene which is responsible for red colour is highest at 21°-24°C. Tomato performs well in a soil having a pH of 6.0-7.0 but it is moderately tolerant to acid-soil of pH 5.5 (Mandal, 2006). Postharvest technology is essential to maximize the shelf-life of fruit for markets and utilization. Shelf-life is determined by the intensity of physiological activity or rate of metabolism. The metabolic rate of the commodity is essential for extending the shelf-life and maintaining consumer acceptance of harvested produce (FAO, 1989). Between 25-40% of produce can be lost due to postharvest spoilage, particularly if appropriate conditions for storage are not available. The two main causes of postharvest losses are physical damage and subsequent microbial infection, and natural or programmed senescence (Acedo and Weinberger, 2006). Ethylene is a ripening hormone, produced possibly by all higher plants.

It is of great importance in the postharvest physiology of perishable fruits and vegetables (Salunkhe and Desai, 1984). Modified atmosphere packaging (MAP) is referred to as a relationship between product respiration and gas exchange within any form of structural enclosure. Modified atmosphere packaging (MAP) technique can be used to maintain the postharvest quality of different fruits (Ding, 2002). The objectives of this

[1] Dr, Associate Professor, Department of Botany, East Yangon University
[2] Dr, Associate Professor, Department of Botany, East Yangon University

research are (1) to investigate the effects of ethylene absorbent on shelf life and tomato (2) to study the pinpricks containing LDPEB and HDPEB effects on shelf life of tomato.

Materials And Methods Experimental Site

The study was conducted in Fruit Laboratory of Vegetable and Fruit Research and Development Centre (VFRDC), Yemon village, Hlegu Township.

Collection, Sorting and Cleaning the Fruits

Mature green and fresh fruits were harvested from the experimental field of VFRDC. Firstly, harvested tomato fruits were sorted out based on the size and uniform peel color development. Secondly, the selected fruits were wiped thoroughly with wet cloth, then they were air-dried. After drying, were weighed the fruits for the treatments (Fig. 1, 2).

Fig. 1. Harvesting of the 55 days old mature fruits, preparing baskets, and fruits to carry to postharvest laboratory

Fig. 2. Harvested fruits, sorting fruit by using Munsell color chart and preparing sorted fruits for the experiment

Preparing materials for ethylene absorbent treatment

The standard concentration of ethylene absorbent was prepared by the mixing of one molecular weight of $KMnO_4$, half molecular weight of H_2SO_4 and 2 kg of burnt rice-husk. Then the mixture was put into the cotton bags for the treatments. The amount of ethylene absorbent in a bag was based on the weight of the fruit in each treatment. The ethylene absorbent used in this experiment was 4%, 5% and 6%, respectively (Fig. 3).

Fig. 3. Required materials and preparation of ethylene absorbent treatment

Preparation of modified atmosphere packaging (MAP)

The low and high density polyethylene bags (LDPEB and HDPEB) in the size of (10°C -15°C) were used in modified atmosphere packaging (MAP). These densities bags were prepared six and ten pin-pricks.

Experimental Layout

Eight treatments, each with 3 replications were set up in Complete Randomized Design (CRD) under the ambient temperature (28-30°C). Each treatment containing 15 fruits of approximately 750 g. Hence the total fruits were 120 and total fruit weight were 6000 g (Fig. 4).

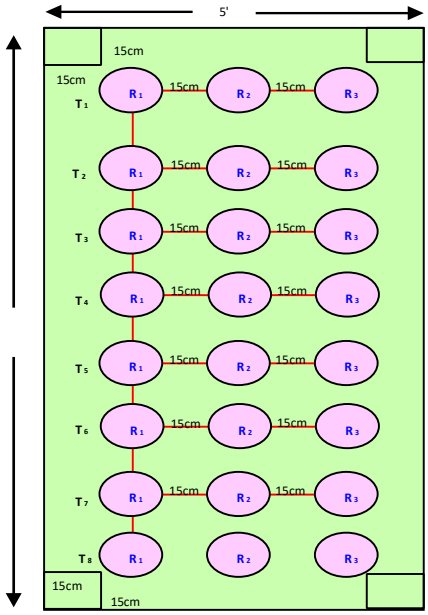
5'
15cm
15cm
15cm

2.50%, T_6 (10 pin-pricks + LDPEB) 2.58%, T_2 (4% ethylene absorbent) 3.00%, T_3 (5% ethylene absorbent) 3.14%, T_4 (6% ethylene absorbent) 3.29% and finally T_1 (control) 11.99% (Table 1, Fig. 5).

Table 1. Effect of postharvest treatments on weight and weight loss, fruit length and roundness of tomato under ambient temperature

Treatment	Weight (g)		Weight loss (%)	Fruit length (cm)		Fruit roundness (cm)	
	Initial	Final		Initial	Final	Initial	Final
T_1-(Control)	52.87	46.53	11.99	4.53	4.41	14.30	14.16
T_2-(4% Ethylene absorbent) + LDPEB	50.93	49.40	3.00	4.67	4.63	14.27	14.09
T_3-(5% Ethylene absorbent) + LDPEB	50.93	49.33	3.14	4.60	4.55	14.33	14.28
T_4-(6% Ethylene absorbent) + LDPEB	50.80	49.13	3.29	4.73	4.70	14.37	14.28
T_5-6 pin-pricks + LDPEB	50.80	49.53	2.50	4.70	4.63	14.13	13.98
T_6-10 pin-pricks + LDPEB	51.53	50.20	2.58	4.60	4.57	14.33	14.17
T_7-6 pin-pricks + HDPEB	51.26	50.26	1.95	4.77	4.72	14.60	14.52
T_8-10 pin-pricks + HDPEB	51.40	50.20	2.33	4.67	4.60	14.23	14.15
F–test			*	*	*	ns	ns	ns	ns
5% LSD	0.68	0.71	0.84	0.29	0.35	0.21	0.19	cv%		12.70	14.70
17.10	3.60	3.20	1.70	1.90							

* significant ns = non significant

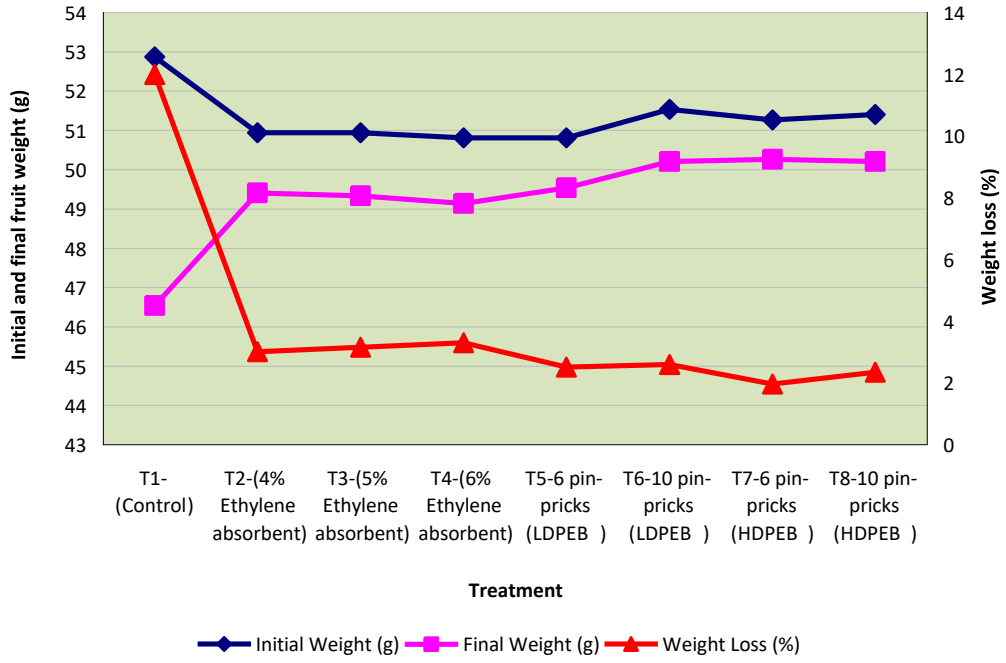

Fig. 5. Effect of postharvest treatments on fruit weight, weight loss of tomato under ambient temperature

Fruit length and roundness

The initial fruit length and roundness were measured at the first day (day 0) and these of the final were measured at the final day (day 36) of the experiment.

The results of the initial fruit length showed that the treatments were not statistically different from each other. But the individual results showed that T_7 (6 pin-pricks HDPEB) had higher fruit length 4.77 cm, followed by T_4 (6% ethylene absorbent) 4.73 cm, then T_5 (6 pin-pricks LDPEB) 4.70 cm. T_2 (4% ethylene absorbent) and T_8 (10 pin-pricks HDPEB) had 4.67 cm each and T_3 (5% ethylene absorbent) and T_6 (10 pin-pricks LDPEB) had 4.60 cm each. T_1 (control) had 4.53cm. The longest final fruit length of 4.72 cm was recorded from T_7 and the shortest final fruit length of 4.41 cm from the T_1.

The initial fruit roundness among the treatments showed that T_7 (6 pin-pricks HDPEB) had highest fruit roundness 14.60 cm, followed by T_4 (6% ethylene absorbent) which had 14.37 cm, T_3 (5% ethylene absorbent) and T_6 (10 pin-pricks LDPEB) had 14.33 cm each, T_1 (control) had 14.30 cm, T_2 (4% ethylene absorbent) had 14.27 cm, T_8 (10 pin-pricks HDPEB) had 14.23 cm and T_5 (6 pin-pricks LDPEB) and 14.13 cm, respectively. However, both the initial and final roundness were not statistically different from each other. The maximum final fruit roundness of 14.52 cm was recorded from treatment T_7 and the minimum final fruit roundness of 13.98 cm was recorded from treatment T_5 (Table 1, Fig. 6).

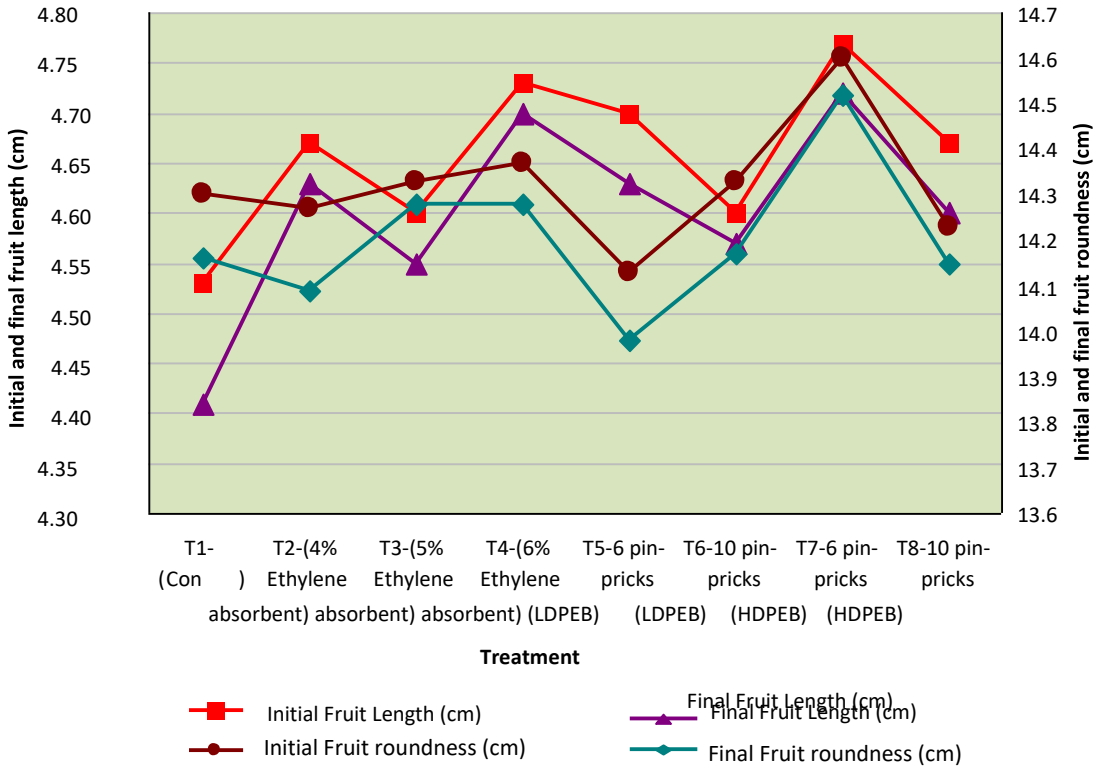

Fig. 6. Effects of postharvest treatments on initial and final fruit length and roundness of tomato under ambient temperature

Peel and pulp firmness

The firmness of peel and pulp at ripen stage expressed that the highest peel firmness 2.37 mm kg^{-1} was obtained from T_7 (6 pin-pricks HDPEB), followed by T_4 (6% ethylene absorbent) and T_8 (10 pin-pricks HDPEB) 2.31 mm kg^{-1} each, T_2 (4% ethylene absorbent) 2.17 mm kg^{-1}, T_3 (5% ethylene absorbent) 2.15 mm kg^{-1}, T_5 (6 pin-pricks LDPEB) 1.75 mm

kg^{-1}, T_6 (10 pin-pricks LDPEB) 1.33 mm kg^{-1} and T_1 (control) 1.30 mm kg^{-1}, respectively. Similarly, the highest pulp firmness 4.21 mm kg^{-1} was obtained from T_7 (6 pin-pricks HDPEB), followed by T_4 (6% ethylene absorbent) 4.08 $mmkg^{-1}$. T_5 (6 pin-pricks LDPEB) 4.03 $mmkg^{-1}$, T_3 (5% ethylene absorbent) 3.65 $mmkg^{-1}$, T_6 (10 pin-pricks LDPEB) 3.43 $mmkg^{-1}$, T_2 (4% ethylene absorbent) 3.42 mm kg^{-1}, T_8 (10 pin-pricks HDPEB) 3.27 mm kg^{-1} and finally T_1 (control) 3.03 mm kg^{-1}, respectively. The statistical analysis revealed that the peel firmness among treatments was significant but the pulp firmness was non-significant (Table 2, Fig. 7).

Total soluble solid and total acidity

Tomato is a highly perishable fruit and it is therefore essential to apply postharvest treatments to maintain the fruit quality especially to maintain the sweetness and acidity of the fruits. The results among the treatments showed that T_7 (6 pin-pricks HDPEB) fruits were sweetest (5.91°C Brix), followed by T_4 (6% ethylene absorbent) 5.88°C Brix, T_6 (10 pin-pricks LDPEB) and T_8 (10-pin-pricks HDPEB) 5.75°C Brix, T_2 (4% ethylene absorbent) 5.37°C Brix, T_5 (6 pin-pricks LDPEB) 5.24°C Brix, T_3 (5% ethylene absorbent) 5.21°C Brix and T_1 (control) which were less sweetness 4.81°C Brix.

The results of total acidity among the treatments showed that T_7 (6 pin-pricks HDPEB) has highest acid content 1.21%, followed by T_4 (6% ethylene absorbent) 1.01%, T_6 (10 pin pricks LDPEB) 0.91 %, T_5 (6 pin-pricks LDPEB) 0.77%, T_2 (4 % ethylene absorbent) 0.72%, T_8 (10 pin-pricks HDPEB) 0.69%, T_3 (5% ethylene absorbent) 0.48% and T_1 (control) 0.35%, respectively (Table 2, Fig. 7).

Table 2. Effects of postharvest treatment on firmness of peel and pulp, total soluble solid and total acidity content of tomato under ambient temperature

Treatment	Peel firmness (mm kg^{-1})	Pulp firmness (mm kg^{-1})	Total soluble solid (□Brix)	Total acidity (%)
T1 (Control)	1.30	3.03	4.81	0.35
T2 (4% Ethylene absorbent)	2.17	3.42	5.37	0.72
T3 (5% Ethylene absorbent)	2.15	3.65	5.21	0.48
T4 (6% Ethylene absorbent)	2.31	4.08	5.88	1.01
T5 6 pin–pricks (LDPEB)	1.75	4.03	5.24	0.77
T6 10 pin–pricks (LDPEB)	1.33	3.43	5.75	0.91
T7 6 pin–pricks (HDPEB)	2.37	4.21	5.91	1.21
T8 10 pin–pricks (HDPEB)	2.31	3.27	5.75	0.69
F–test	*	ns	*	*
5% LSD	0.19	0.24	1.21	0.86
cv%	14.70	18.90	12.90	6.20

* significant ns = non significant

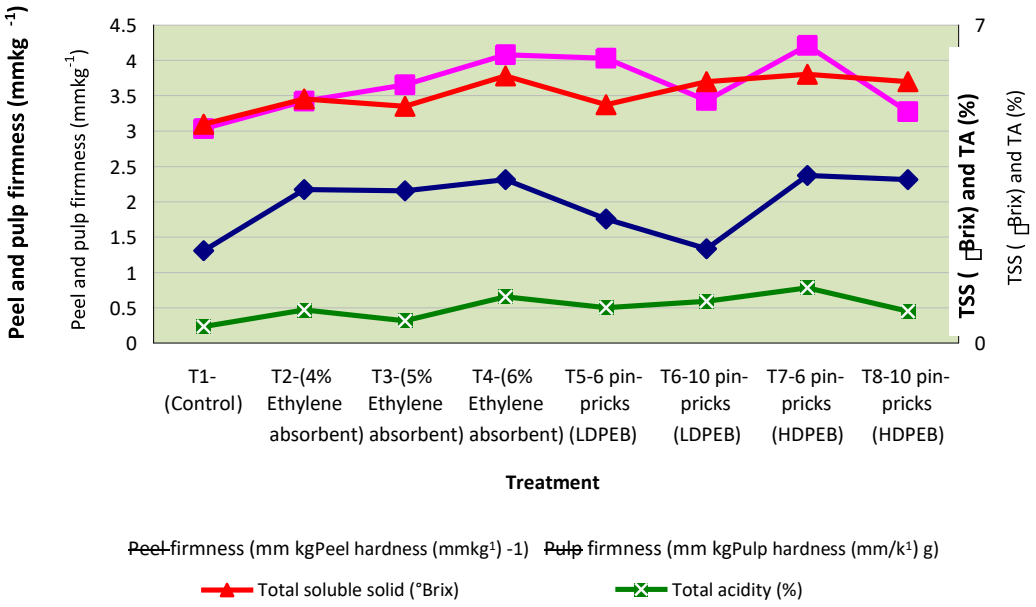

Fig. 7. Effects of postharvest treatment on firmness of peel and pulp, TSS and TA content of tomato under ambient temperature

Peel color development and shelf-life

The peel color development of fruits was due to the ripen condition and that condition effected on the shelf-life of tomato. The results of peel color development in initial stage of all treatments were 5GY 0/10. The stage of 5GY is the pure green color in Munsell color index chart. Chroma-notation (color scale) of 6/10 expressed that the fruits were not totally black based color meaning that the dark color mixed with white and they became pure green color. The color changes of the fruits were recorded in every three days interval. The shelflife of the fruits was decided when the peel color changes to pure red color. The results revealed that the red color development of peel (10R 6/10) of T1 (control) was at 16d, T5 (6 pin- pricks LDPEB) and T6 (10 pin-pricks LDPEB) at 20d, T2 (4% Ethylene absorbent), T3 (5% Ethylene absorbent) and T8 (10 pin-pricks HDPEB) at 24d. T4 (6% Ehtylene absorbent) at 28 d and T7 (6 pin-pricks HDPEB) at 32 d (Table 3, 4 and Fig. 8).

Table 4. Effects of postharvest treatments on shelf-life of tomato under ambient temperature

Treatment	Shelf-life (Day)
T1 (Control)	16
T2 (4% Ethylene absorbent)	24
T3 (5% Ethylene absorbent)	24
T4 (6% Ethylene absorbent)	28
T5 -6-pin–pricks (LDPEB)	20
T6 -10-pin–pricks (LDPEB)	20
T7 -6-pin–pricks (HDPEB)	32
T8 -10-pin–pricks (HDPEB)	24

Table 3. Effects of postharvest treatments on peel color development of tomato under ambient temperature

Treatment	Peel color development of Tomato (day)									
	0 d	4 d	8 d	12 d	16 d	20 d	24 d	28 d	32 d	36 d
T1 (Control)	5GY6/10	2.5GY7/8	2.5Y8/10	7.5YR8/10	10R6/10	10R6/10	10R8/10	10R8/10	10R8/12	10R8/12
T2 (4% Ethylene absorbent)	5GY6/10	5GY6/10	5GY8/10	7.5YR8/10	5YR6/10	5Y6/10	10R6/10	10R6/10	10R8/10	10R8/10
T3 (5% Ethylene absorbent)	5GY6/10	5GY6/10	5GY7/10	7.5YR6/10	5YR6/10	2.5Y6/10	10R6/10	10R6/10	10R6/10	10R6/10
T4 (6% Ethylene absorbent)	5GY6/10	5GY7/10	5GY8/10	2.5GY7/6	2.5GY8/10	2.5Y8/10	7.5YR8/10	10R6/10	10R6/10	10R6/10
T5 6 pin–pricks (LDPEB)	5GY6/10	5GY7/10	5GY8/12	2.5GY7/6	2.5YR8/10	10R6/10	10R6/10	10R6/10	10R8/10	10R8/10
T6 10 pin–pricks (LDPEB)	5GY6/10	5GY7/10	5GY8/10	2.5GY7/6	2.5YR8/10	10R6/10	10R6/10	10R6/10	10R8/10	10R8/10
T7 6 pin–pricks (HDPEB)	5GY6/10	5GY6/10	5GY7/6	2.5GY7/6	2.5GY8/10	2.5Y8/10	7.5YR8/10	7.5YR8/10	10R5/10	10R5/10
T8 10 pin–pricks (HDPEB)	5GY6/10	5GY7/10	5GY8/10	2.5Y8/10	7.5YR8/10	2.5YR8/10	10R6/10	10R6/10	10R8/10	10R8/10

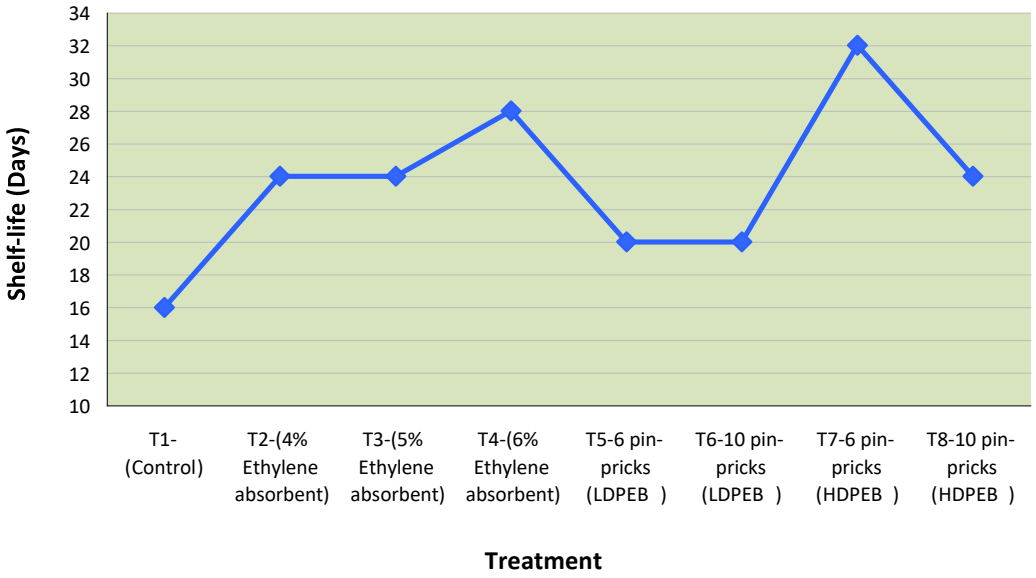

Fig. 8. Effects of postharvest treatments on shelf-life of tomato under ambient temperature

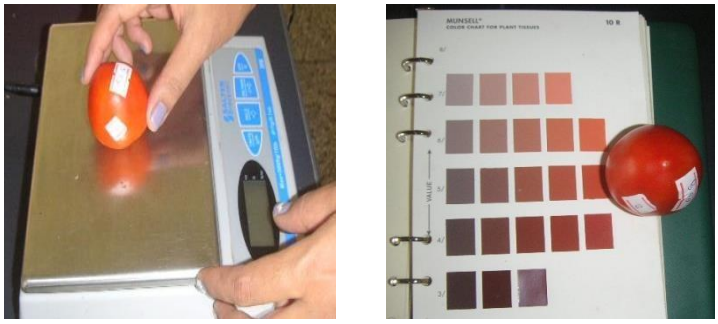

Fig. 9. Measuring the weight and color development of fruits at day 36

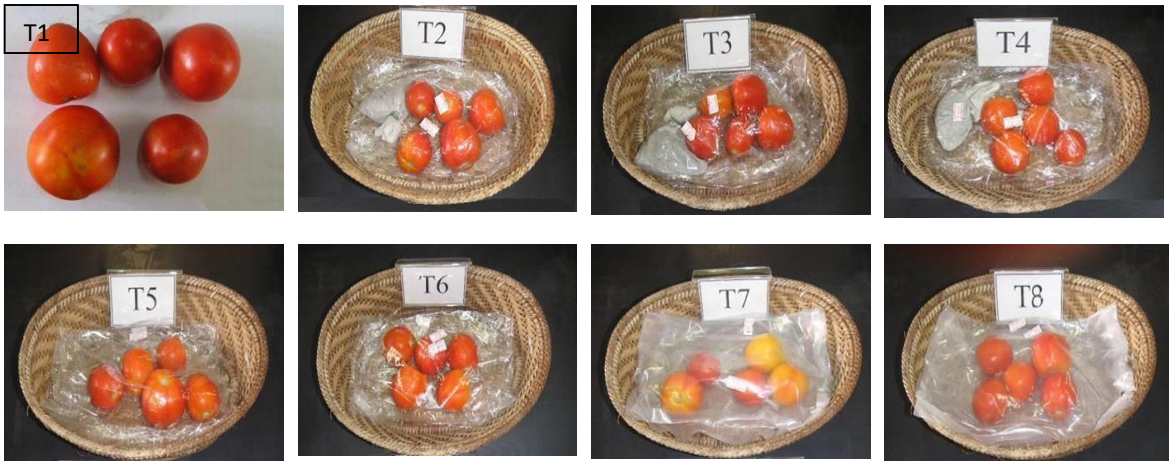

Fig. 10. Ethylene absorbent and modified atmosphere packaging treatments on shelf-life of tomato

Fig. 11. Effects of ethylene absorbent and modified atmosphere packaging treatments on peel color and pulp characteristics of tomato at day 36

Discussion and Conclusion

The purpose of storing fruits is to delay ripening and extend the shelf-life. One of the important factors for improving shelf-life is maturity index. Uniform harvest date is important for postharvest treatment and thus the fruits from cultivation field was harvested at the same day of maturity. The different techniques of prolonging postharvest shelf-life was tested under local facilities and these factors also influence the storage responses. The results of the modified atmosphere packaging treatments showed that T_7 (6 pin-pricks containing HDPEB) influenced the shelf-life of tomato at ambient temperature. The treatments were continuously carried out under ambient temperature. At the ripe stage, T_7

fruits developed the typical red peel color (color index of 10R 5/10) with lowest weight loss. The fruit roundness, fruit length, and fruit weight of T_7 were also superior than that of the other treatments. The disease symptoms were not developed in all treatments as well as in the control. Many vegetables including tomato produce high levels of ethylene that leads to the senescence and thus this experiment used the ethylene absorbent to minimize ethylene level during handling and storage. However, the effect of ethylene absorbent used in this experiment had less influence on controlling ripening of tomato than controlled atmosphere, that is, HDPEB. It might be lower concentration and small amount of ethylene absorbent were used in the experiment. However, it is still needed to investigate for obtaining more accurate results.

Vegetables are in a living state after harvest. Continued respiration gives off CO_2, moisture, and heat which influence the storage life and thus cold treatments and refrigeration were required. When respiration continues, it breaks down the storage carbohydrate of the fruits. The consequence of it was decrease carbohydrate in the fruits, which led to senescence. At ripening stage of fruits, the organic acid generally decreased due to utilization in the respiratory pathway (Ryall and Lipton, 1979). Respiration is the process by which plants take in oxygen and give out carbondioxide. Respiration rate was depended on a good air supply. Air contains about 20% of the oxygen that is essential to normal plant respiration, during which starch and sugars are converted to CO_2 and water vapour. When the air supply is restricted and the amount of available oxygen in the environment falls to about 2% or less, fermentation instead of respiration occurs (FAO, 1989). Reduction of acid content which influences firmness of fruit, since many of pigments are sensitive to acid and thus the fruit color is changed. For above reasons, controlled or modified atmosphere packaging technique (HDPE and LDPE) were require in the experiment. The results showed that 6 pin-pricks HDPE could maintain the fruits to longer shelf-life. It may be due to the reduced respiration, reduced transpiration, and thus higher carbohydrate and higher organic acid content.

In conclusion, the six pin-pricks HDPEB was the best for extending shelf-life of tomato. The second best was obtained from LDPEB. The ethylene absorbent gave inferior results than HDPEB and LDPEB, however, it still need to verify the results through another experimentation.

Acknowledgements

The author is indebted to Dr Nay Win Oo, Rector of East Yangon University and Dr Aye Aye Ko, Dr Wah Wah Lwin and Dr Thidar Aung, Pro-Rector of East Yangon University for their kind permission to carry out this research. Special thanks are also due to Professor and Head, Dr. Htay Htay Lwin, Botany Department of East Yangon University for her invaluable encouragement and suggestions.

References

Acedo Jr. A. L and K. Weinberger. (2006). *Improving rural livelighoods through development of vegetable base postharvest technologies.* RETA 6208 Postharvest technology Training and Development of Training Master Plan.

Decoteau, D. R. (2000). *Vegetable Crops.* Prentice Hall, Upper Saddle River, NJ 07458.

Ding, C. K. (2002). *Modified atmosphere packaging maintains postharvest quality of loquat fruit*. Postharvest Biology and Technology 24(3):341-348

FAO. (1989). *Preventions of postharvest food losses, fruits, vegetables and root crops, a training manual*. Food and Agriculture Organization of the United Nations. Printed in Rome, Italy.

Mandal. B. C. (2006). *Manual on Seed production of Major Vegetables of Myanmar*. Food and Agriculture Organization of United Nations, Office of Representative in Myanmar.

Ryall, A. L. and W. J. Lipton. (1979). *Handling, Transportation and Storage of Fruits and Vegetables*. Vol. 1, Vegetables and Fruit, AVI Publishing, Westport, Conn.

Salunkhe. D. K and B. B. Desai. (1984). *Postharvest Biotechnology of Vegetables*. Volume I. CRC Press, Inc. Boca Raton, Florida.

Wien, H. C. (1997). *The Physiology of Vegetable Crops, Science Comell University, Ithaca, NY, USA, 207 pp.*

STUDY OF PLANT SPECIES DIVERSITY IN DIFFERENT SITES OF THANLYIN AREA

Myat Su Hlaing[1], Su Latt Win[2]

Abstract

The present study was conducted in Thanlyin Township, Yangon Region. In order to obtain essential data for the vegetation analysis, four quadrats (15 × 15m) for trees, thirty six quadrats (5 × 5m) for herbs were set up in two different sites (Kyaik-Inn and Ah-Lel Ywar). All sample plants in the quadrat were recorded and counted. Then, density (D), relative density (R.D), frequency (F), relative frequency (R.F) were calculated. Some mathematical calculation concerning with species diversity; Shannon-Wiener diversity index (H), Simpson Index (D), Shannon-Wiener evenness (E) were also used. The Shannon-Wiener diversity index (H) of Kyaik-Inn were (1.5, 3.71) for trees and herbs respectively and (0.7, 3.2) in Ah-Lel Ywar. Simpson Index (D) of Kyaik-Inn showed (0.5, 0.88) for all layers and for (0.3, 0.9) in Ah-Lel Ywar. Shannon-Wiener evenness (E), the plant species of Kyaik-Inn and Ah-Lel Ywar showed (0.7) for trees and herbs respectively. Some of the dominant species from two sites were selected for calculation of relative density and relative frequency. Among them, In Kyaik-Inn, *Aristida depressa* Retz. (Thamin-mwe-myet) has the highest degree of density and frequency. The relative density of this species is (26.05%) and relative frequency is (7.91%). Similarly, *Mimosa pudica* L. (Tikayon) has the highest degree of density and frequency in Ah-Lel Ywar. The relative density of this species is (20.16%) and relative frequency is (9.28%). The recent study will give the plant species diversity that distributed in the study area.

Keywords : quadrats, Shannon-Wiener diversity index (H), Simpson Index (D), Shannon-Wiener evenness (E), Dominant species

Introduction

Ecology is the study of interaction between living organism and their environment and the pattern of distribution of plants and animals on the earth. It has been suggested that changes in plant species diversity affect several ecosystem processes, such as primary productivity, nutrient retention, and vegetation dynamics (Naeem *et al*., 1996, Tilman *et al*., 1996).

A vegetation is the sum total of plant covering an area which generally consist of a number of communities. A community is an association of different population of organisms that live and interact together in the same place at the same time. Forest vegetation is influenced by a number of abiotic and biotic environmental factors (Weaver and Clements, 1966).

Species diversity is one of the important specifications of bio-societies that are measured in different ways (Krebs, 1998). Traditionally, ecologists have been concerned with the concept of ecological diversity. Species diversity is the most commonly used representation of ecological diversity, but it is not the only measure. Niche width and habitat diversity are also key components of ecological diversity (Magurran, 1988).

The quadrat method, known also as the sample-plot method, is a basic method for many types of ecological investigations. If received the name 'quadrat method' from the square used as sample plots. The quadrat method is used for the purpose of detailed study. By the study of numerous quadrats a knowledge of the structure of vegetation may be obtained. In its simplest form, the quadrat is used in counting the individuals of each species to determine exact differences in the composition and structure of vegetation (Whittaker, 1980).

[1] Dr, Associate Professor, Department of Botany, East Yangon University
[2] Dr, Associate Professor, Department of Botany, East Yangon University

In order to accomplish the above mentioned important, a selected study sites have been chosen in Thanlyin Township: the species diversity using Shannon-Wiener and Simpson's indices; density, relative density, frequency and relative frequency were also calculated.

The main objectives in this study were to identify and classify the plant species that distributed in the study area and to calculate the species diversity, population density and frequency of study area.

Study Site and Methods

General Description of the Study Area

The different sites of Kyaik-Inn and Ah-Lel Ywar, Thanlyin Township was selected for this study. Thanlyin township is located at the southern bank of Bago river mouth in the Southern Province of Yangon Region, between Latitude (16° 40' - 16° 54" N) and Longitude (96° 15' - 96° 22" E). It is situated east by the Thon-khwa Township, south by Kyauk-tan Township and west and north by Bago River. The study area, Kyaik-Inn and Ah-Lel Ywar lies between 16° 42' - 05.371" to 16° 42' - 55.360" North latitude and 96° 17' - 40.373" to 96° 18' - 08.113" East longitude. The study area was situated in the left side of the Thanlyin-Kyauktan road and it was about 2-5 kilometers away from famous pagoda Kyaik-khaut. The location map of the study area is as shown in Fig. 1.

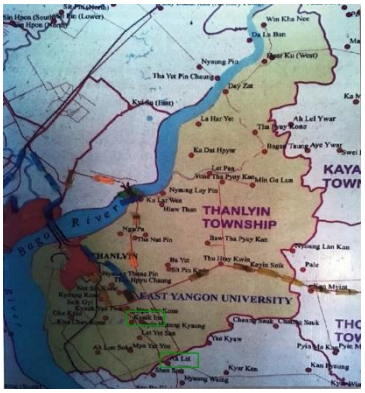

Fig. 1 Location Map of Study Area

Methodology

Preparation of sample plots in the study site

The field area (Kyaik-Inn and Ah-Lel Ywar) situated left side of the Thanlyin-Kyauk-tan road. To estimate the plant species present in the study site, 2 large quadrats for trees (15 × 15 meters) were set up. Then, each large was equally subdivided into 9 small quadrats (5 × 5 meters) for herbs in Kyik-Inn and Ah-Lel Ywar (Plate 1, 2, 3 and 4).

Specimen Collection and Species Identification

To estimate plant species in Kyaik-Inn and Ah-Lel Ywar, intensive collection of the specimens were undertaken. The number of species collected from each plot was listed and recorded. Plant specimens were also pressed for the preparation of herbarium sheets and the available literatures are used to get the correct specific name: Hooker, Vol. (I-VII), 1875-1885; Backer & Brink, Vol. (I-III), 1963-1968; Lawrence, 1969; and Hundley & Chit Ko Ko, 1961, "A checklist of Trees, Shrubs, Herbs and Climber of Myanmar" (Kress *et al*., 2003) whenever species were uncertain and verification is needed.

Soil Sampling and Chemical Analysis

To determine the composition and chemical characteristics of soil in the experimental field area was done by taking soil sample of two different location in the quadrats. Soil samples were taken by digging the hole up to 15 cm depth from two sites, kept in the air-tight

plastic containers and the samples were sent to Laboratory of Soil Analysis, Myanmar Agriculture Service (Land use), Insein. Soil analysis was done for textures, nutrient contents (N, P, K), pH of the soil, organic carbon and humus contents.

Measurement of plant species diversity and evenness

Plant Species Diversity

Species diversity is a measure of both species richness and evenness of a community. Species diversity varies greatly from one community to another. The diversity indices are better measures of the species diversity of a forest than the species density and more informative than species counts alone (Weidelt, 2000). Species diversity is often expressed by the Shannon-Wiener index (H), Evenness (E) and Simpson index (D) (Magurran, 1988).

Shannon- Wiener Index

$$H = -\sum_{i=1}^{s} (p_i)(\log_2 p_i)$$

H = index of species diversity
S = number of species
P_i = proportion of total sample belonging to the i^{th} species

Shannon-Wiener diversity index places more weight on the rare species while Simpson's diversity Index emphasis on the common species (Weidelt, 2000).

Simpson's Index

$$D = 1 - \sum_{i=1}^{s} (p_i)^2$$

D = Simpson's index of species diversity
S = number of species
P_i = proportion of species i^{th} in the community

Evenness (E)

Another measurement of species diversity is the species evenness, An ecosystem where all the species are represented by the same number of individuals has high species evenness. The value E is regard as a suitable dimension for recording the second diversity component evenness. E is between 0 and 1. The value 1 represents all species as equally abundant. The value of E gradually goes down to the zero (0) when the number of species decreases. Increasing evenness values mean a rise in diversity. Evenness was calculated by Shannon-Wiener function (1963), as follow:

$$E = \frac{H}{H_{\max}}$$

$$H_{\max} = Log_2 S$$

E = evenness (range 0 – 1)
H = index of species diversity
H_{max} = species diversity under conditions of maximal equitability
S = number of species

Calculation of Density, Relative Density, Frequency and Relative Frequency

The density of a species is the numerical representation of its individual in an unit area. The density of a species refers to the adequacy of its different requirement and the availability of space. Density is determined by-

$$\text{Density (D)} = \frac{\text{No. of individual of the species in all the sample plots}}{\text{Total no. of sample plots studied}}$$

$$\text{Relative density (R.D)} = \frac{\text{No. of individual of the species}}{\text{No. of individual of all the species}} \times 100$$

The frequency of a species is expressed as the percentage occurrence of its individuals in a number of observations. The frequency of different species is determined by-

$$\text{Frequency (F)} = \frac{\text{No. of sample plots in which the species occurs}}{\text{Total no. of plots sampled}}$$

$$\text{Relative frequency (R.F)} = \frac{\text{No. of occurrences of the species}}{\text{No. of occurrences of all the species}} \times 100$$

Results

Plant Species Diversity in Study Area

In the present study, total numbers of plant species in the study area is 55 species, including 53 genera and 33 families. Among them 12 are trees, 4 are small trees, 8 are shrubs, 21 are herbs, 3 are climbers, 6 are grasses and fern is only one (Table 1).

Plant Species Diversity in Kyaik-Inn

In Kyaik-Inn, composed of 39 species, 38 genera, and 24 families. Among them trees are 9, small trees are 3, shrubs are 3, herbs are 16, climbers are 2, grasses are 5 and fern is 1 (Table 2 and Fig. 2). The most abundance species is *Aristida depressa* Retz. (Thamin-mwe-myet). The less abundance species is *Celosia argentea* L. (Kyet-mauk-pan), *Flueggea virosa* (Roxb.ex.Willd.)Voigt (Ye-chinya), *Terminalia catappa* L. (Banda), etc.

Plant Species Diversity in Ah-Lel Ywar

In Ah-Lel Ywar, a total of 30 species, 29 genera, and 20 families. Among them trees are 6, shrubs are 8, herbs are 9, climbers are 2, grasses are 3, small tree and fern are 1 (Table 2 and Fig. 2). The most abundance species is *Mimosa pudica* L. (Tikayon). The less abundance species is *Commelina benghalensis* L. (Wet-kyok), *Ziziphus jujuba* Lam. (Zi), *Myrica nagi* Thumb. (Kat-pho), etc.

Species diversity indices

Shannon-Wiener and Simpson Indices

According to the result of Shannon-Wiener Index (H), it was observed that the diversity index of Kyaik-Inn were (1.5, 3.71) for trees and herbs respectively and (0.7, 3.2) in Ah-Lel Ywar. Simpson Index (D) of Kyaik-Inn showed (0.5, 0.88) for all layers and for (0.3, 0.9) in Ah-Lel Ywar. Kyaik-Inn was relatively higher than that of Ah-Lel Ywar in both layers (Table 2).

Evenness (E)

As the result of Shannon-Wiener evenness, the plant species of all layers in Kyaik-Inn and Ah-Lel Ywar showed (0.7) (Table 3). So, both layers of study area distributed evenly.

Density, Relative Density, Frequency, and Relative Frequency in Kyaik-Inn and Ah-Lel Ywar

To understand the density and frequency of plant species in study area, eight dominant species were chosen and calculated. *Aristida depressa* Retz. (Thamin-mwe-myet) has the highest degree of density and frequency in Kyaik-Inn. The relative density of this species is (26.05%) and relative frequency is (7.91%). (Table 4, 5 and Fig. 3, 4). *Mimosa pudica* L. (Tikayon) has the highest degree of density and frequency in Ah-Lel Ywar. The relative density of this species is (20.16%) and relative frequency is (9.28%) (Table 6, 7 and Fig. 5, 6).

Effect of soil on vegetation

The structure and nutrient content of the soil are important for plants because they affected the vegetation that grows on it, and in turn, can also affect the nature of vegetation. As the result of soil analysis, the soil pH in both sites possessed strongly acid (5.19%) to extremely acid (4.38%) nature were shown in (Table 8).

The soil texture of Kyaik-Inn showed Silt loam and Ah-Lel Ywar expressed Sandy loam. The nutrient contents of soil in Kyaik-Inn and Ah-Lel Ywar were quite different. Organic carbon content in Ah-Lel Ywar (0.94%) is higher than the Kyaik-Inn (0.77%) (Table 9).

Table 2. Total number of species, genera, families and their total % in two study sites

	Habit	Kyaik-Inn	Ah-Lel Ywar
1.	Trees	9	6
2.	Small trees	3	1
3.	Shrubs	3	8
4.	Herbs	16	9
5.	Climbers	2	2
6.	Grasses	5	3
7.	Fern	1	1
	Species	39	30
	Total %	70.9	54.55
	Genera	38	29
	Total %	71.7	54.72
	Families	24	20
	Total %	72.73	60.61

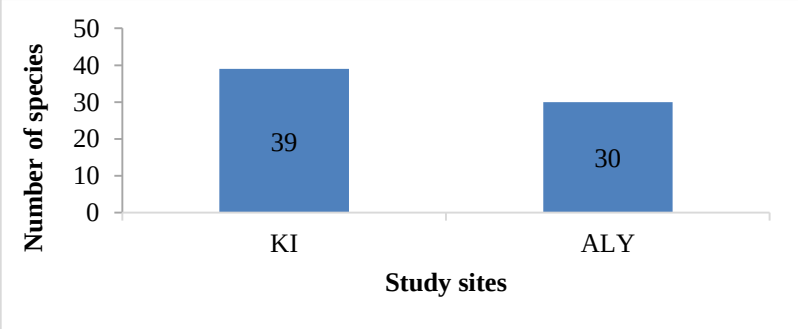

Fig. 2. Comparison of species diversity in two Study Sites

Table 1. List of Species in Study Area

No.	Scientific Name	Myanmar Name	Family	Habit
1.	*Abutilon indicum* (L.)Sweet	Bauk	Malvaceae	H
2.	*Acacia auriculiformis* A.Cunn.	Malaysia-padauk	Mimosaceae	ST
3.	*Acmella calva* (DC.) R.K.Jansen	Shadon-po	Asteraceae	H
4.	*Adenanthera pavonina* L.	Ywe-gyi	Mimosaceae	T
5.	*Alternanthera sessilis* (L.) R.Br.	Pazun-sar	Amaranthaceae	H
6.	*Amaranthus mangostanus* L.	Hin-nu-nwe	Amaranthaceae	H
7.	*Anacardium occidentale* L.	Thiho-thayet	Anacardiaceae	T
8.	*Aristida depressa* Retz.	Thamin-mwe-myet	Poaceae	G
9.	*Artocarpus heterophyllus* Lam.	Peinne	Moraceae	T
10.	*Blumea lacera* (Burm.f.) DC.	Lada-pabyin	Asteraceae	H
11.	*Carallia lancaefolia* Roxb.	Maniawga	Rhizophoraceae	T
12.	*Carica papaya* L.	Thinbaw	Caricaceae	ST
13.	*Celosia argentea* L.	Kyet-mauk-pan	Amaranthaceae	H
14.	*Citrus maxima* (Burn.) merr.	Kywe-gaw	Rutaceae	ST
15.	*Cleome viscosa* L.	Gant-galar	Capparaceae	H
16.	*Commelina benghalensis* L.	Wet-kyok	Commelinaceae	H
17.	*Crotalaria juncea* L.	Taw-paiksan	Fabaceae	S
18.	*Dichanthium caricosum* (L.) A.Camus	Padaw-ni	Poaceae	G
19.	*Digitaria adscendens* (Kunth) Henrard	Myet-hnankar	Poaceae	G
20.	*Echinochloa crus-galli* (L.) P.Beauv.	Myet-cho	Poaceae	G
21.	*Eleocharis acicularis* (L.) Roem. & Schult.	Myet 2	Cyperaceae	H
22.	*Eleusine indica* (L.) Gaertn.	Sin-ngo-myet	Poaceae	G
23.	*Eupatorium cannabinum* L.	Hkwe-thay-pan	Asteraceae	S
24.	*Eupatorium cordata* Burm.f.	Bizat-nwe	Asteraceae	C
25.	*Eupatorium odoratum* L.	Bizat	Asteraceae	S
26.	*Euphorbia hirta* L.	Kywe-kyaung-mymi-si	Euphorbiaceae	S
27.	*Ficus glomerata* Roxb.	Thapan	Moraceae	T
28.	Flueggea virosa (Roxb.ex.Willd.) Voigt	Ye-chinya	Euphorbiaceae	S
29.	*Fordiophyton peperomiifolium* (Oliv.)C.Hansen.	Myay-phayon	Melastomataceae	S
30.	*Indigofera linifolia* Retz.	Than-ma-naing-kyauk-ma-naing	Fabaceae	S
31.	*Ipomoea turbinata* Lagasca	Kazun-nwe	Convolvulaceae	C
32.	*Jasminum multiflorum* (Burn.f.) Andrews	Tawsabe	Oleaceae	C
33.	*Jussiaea suffruticosa* L.	Lay-nyin-gyi	Onagraceae	H
34.	*Lepidagathis incurva* Buch.Ham.ex D.Don.	Not known	Acanthaceae	H
35.	*Lygodium palmatum* (Bernh.)Sw.	Fern-pin	Lygodiaceae	F
36.	*Markhamia stipulata* (Wall.) Seem.ex.K.Schum	Ma-hlwa	Bignoniaceae	T
37.	*Microcos paniculata* L.	Mya-yar	Malvaceae	ST
38.	*Mimosa pudica* L.	Tikayon	Mimosaceae	H
39.	*Moringa oleifera* Lam.	Dan -da-lun	Moringaceae	T
40.	*Musa sapientum* L.	Nyet-pyaw	Musaceae	H
41.	*Myrica nagi* Thumb.	Kat-pho	Myricaceae	T
42.	*Nephelium lappaceum* L.	Kyet-mauk	Sapindaceae	T
43.	*Oldenlandia diffusa* (Willd.) Roxb.	Sula-napha	Rubiaceae	H
44.	*Oxalis corniculata* L.	Hmo-nado	Oxalidaceae	H
45.	*Peperomia pellucida* Kunth.	Thit-yay-kyi	Piperaceae	H
46.	*Phyllanthus urinaria* L.	Mye-ziphyu	Euphorbiaceae	H
47.	*Scoparia dulcis* L.	Dana-thuka	Scrophulariaceae	H
48.	*Serissa serissoides* (DC.)Druce	Not known	Rubiaceae	S
49.	*Setaria viridis* (L.) P.Beauv.	Myet 1	Poaceae	G
50.	*Sida rhombifolia* L.,s.l.	Katsi-ne	Malvaceae	H
51.	*Synedrella nodiflora* (L.) Gaertn.	Ka-lar-nagut	Asteraceae	H
52.	*Syzygium grande* (Wight) Walp.	Thabye-gyi	Myrtaceae	T
53.	*Terminalia catappa* L.	Banda	Combretaceae	T
54.	*Vernonia cinerea* (L.)Less.	Kadu-pyan	Asteraceae	H
55.	*Ziziphus jujuba* Lam.	Zi	Rhamnaceae	T

T = Tree, S = Shrub, H = Herb, C = Climber, ST = Small tree, F = Fern, G = Grass.

Table 3. Diversity Indices and Evenness of Kyaik-Inn and Ah-lel Ywar

Sr.	Description	Kyaik-Inn		Ah-Lel Ywar	
		T	H	T	H
1.	No. of species	5	35	2	29
2.	Shannon-Wiener (H)	1.5	3.71	0.7	3.2
3.	Simpson index (D)	0.5	0.88	0.3	0.9
4.	Shannon evenness (E)	0.7	0.7	0.7	0.7

Table 4. Ranking of Relative Density in Kyaik-Inn

Sr.	Scientific Name	Myanmar Name	Density	Relative. Density (%)
1.	*Aristida depressa* Retz.	Thamin-mwe-myet	35.05	26.05
2.	*Oldenlandia diffusa* (Willd.) Roxb	Sula-napha	18.72	13.91
3.	*Eupatorium cannabium* L.	Hkwe-thay-pan	10	7.43
4.	*Vernonia cinera* (L.) Less.	Kadu-pyan	10	7.43
5.	*Digitaria adscendens* (Kunth) Henrard	Myet-hnankar	8.44	6.27
6.	*Syzygium grande* (Wight) Walp.	Thabye-gyi	6.94	5.16
7.	*Euphorbia hirta* L.	Kywe-kyaung-mymi-si	5.78	4.29
8.	*Cleome viscosa* L.	Gant-galar	5.33	3.96

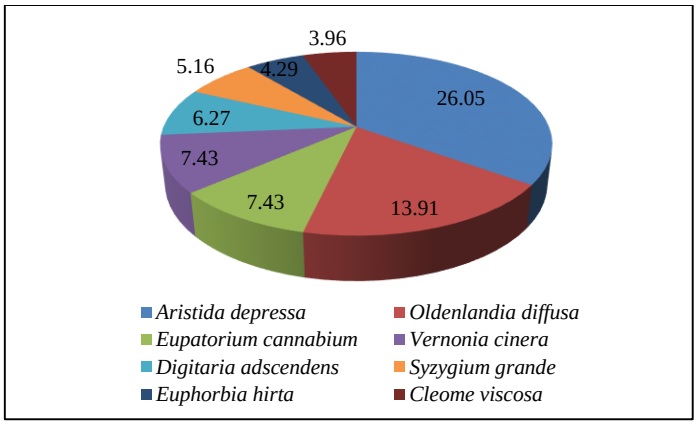

` Fig. 3. Relative Density of Eight Common Species in Kyaik-Inn

Table 5. Ranking of Relative Frequency in Kyaik-Inn

Sr.	Scientific Name	Myanmar Name	Frequency	Relative Frequency (%)
1.	*Aristida depressa* Retz.	Thamin-mwe-myet	0.94	7.91
2.	*Oldenlandia diffusa* (Willd.) Roxb	Sula-napha	0.94	7.91
3.	*Cleome viscosa* L.	Gant-galar	0.61	5.12
4.	*Eupatorium cannabium* L.	Hkwe-thay-pan	0.61	5.12
5.	*Vernonia cinera* (L.) Less	Kadu-pyan	0.61	5.12
6.	*Jussiaea suffruticosa* L.	Lay-nyin-gyi	0.61	5.12
7.	*Digitaria adscendens* (Kunth) Henrard	Myet-hnankar	0.61	5.12
8.	*Echinochloa crus-galli* (L.) P. Beauv	Myet-cho	0.56	4.65

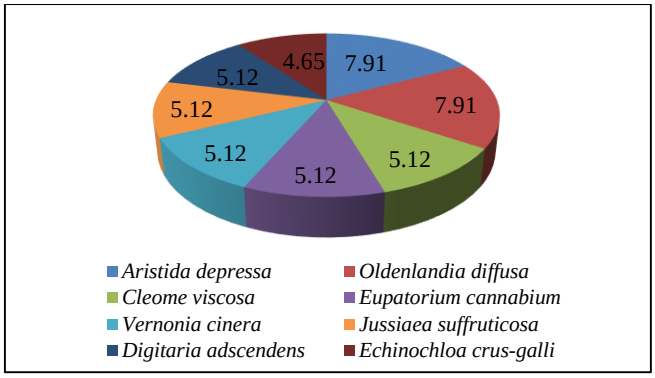

Fig. 4. Relative Frequency of Eight Common Species of Kyaik-Inn

Table 6. Ranking of Relative Density in Ah-Lel Ywar

Sr.	Scientific Name	Myanmar Name	Density	Relative Density (%)
1.	*Mimosa pudica* L.	Tikayon	53.56	20.16
2.	*Indigofera linifolia* Retz.	Than-ma-naing-kyauk-ma-naing	51.17	19.26
3.	*Euphorbia hirta* L.	Kywe-kyaung-mymi-si	45.17	17
4.	*Digitaria adscendens* (Kunth) Henrard	Myet-hnankar	33.17	12.49
5.	*Echinochloa crus-galli* (L.) P. Beauv	Myet-cho	27	10.17
6.	*Jasminum multiflorum* (Burn.f.) Andrews	Tawsabe	14	5.27
7.	*Eleocharis acicularis* (L.)Roem.& Schult.	Myet 2	11	4.14
8.	*Acacia auriculiformis* A. Cunn.	Malaysia-padauk	9.39	3.53

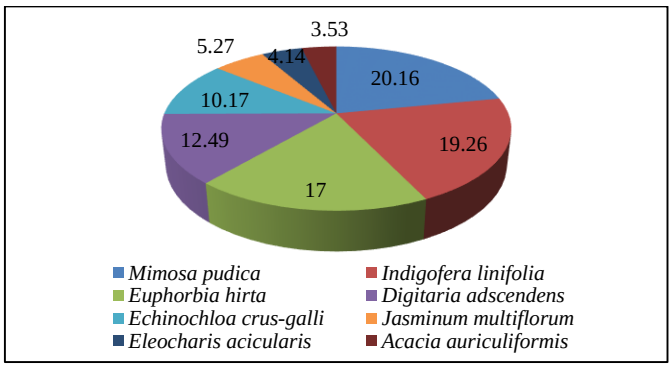

Fig. 5. Relative Density of Eight Common Species in Ah-Lel Ywar

Table 7. Ranking of Relative Frequency in Ah-Lel Ywar

Sr.	Scientific Name	Myanmar Name	Frequency	Relative Frequency (%)
1.	*Mimosa pudica* L.	Tikayon	1	9.28
2.	*Euphorbia hirta* L.	Kywe-kyaung-mymi-s	0.94	8.76
3.	*Acacia auriculiformis* A. Cunn.	Malaysia-padauk	0.83	7.73
4.	*Anacardium occidentale* L.	Thiho-thayet	0.83	7.73
5.	*Jasminum multiflorum* (Burn.f.) Andrews	Tawsabe	0.78	7.22
6.	*Eupatorium cannabium* L.	Hkwe-thay-pan	0.72	6.7
7.	*Vernonia cinera* (L.) Less	Kadu-pyan	0.67	6.19
8.	*Digitaria adscendens* (Kunth) Henrard	Myet-hnankar	0.56	5.15

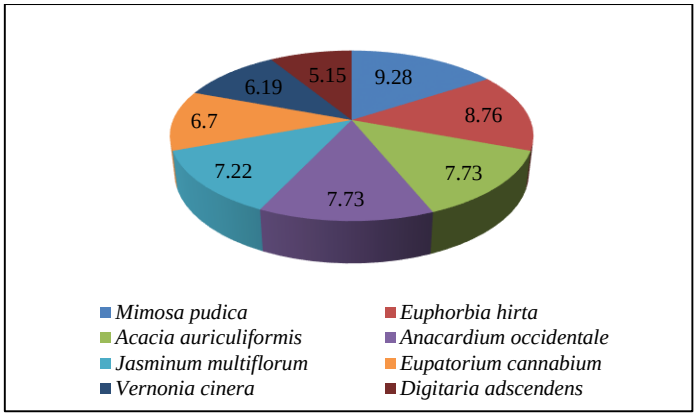

Fig. 6. Relative Frequency of Eight Common Species in Ah-Lel Ywar

Table 8. Soil pH, Moisture and Texture of Study Sites

Sr.		Soil pH	Soil Moisture	Soil Texture	Sand(%)	Silt(%)	Clay(%)
1.	Kyaik-Inn	4.38 Extremely acid	0.44	Silt Loam	30.50	50.10	18.30
2.	Ah-Lel Ywar	5.19 Strongly acid	7.51	Sandy Loam	53.75	31.80	12.50

Source: Myanmar Agriculture Service (Land Use), Insein, Myanmar.

Table 9. Nutrient Content of Soil in Study Sites

Sr.		Total N_2 (%)	Available Nutrients		Exchangeable Cations	Organic Carbon %
			P (ppm)	K_2O (meq/100g)	K (meq/100g)	
1.	Kyaik-Inn	0.11 Very low	194.21 High	3.61 Low	0.08 Very low	0.77 Very low
2.	Ah-Lel Ywar	0.11 Very low	11.63 Low	6.48 Low	0.14 Low	0.94 Very low

Source: Myanmar Agriculture Service (Land use), Insein, Myanmar

Plate 1. Sample plots in Kyaik-Inn for Tree layer

Plate 2. Sample Plots in Kyaik-Inn for Herb layer

Plate 3. Sample Plots in Ah-Lel Ywar for Tree layer

Plate 4. Sample Plots in Ah-Lel Ywar for Herb layer

Plate 5 *Aristida depressa* Retz. (Thamin-mwe-myet) (Dominant Species in Kyaik-Inn)

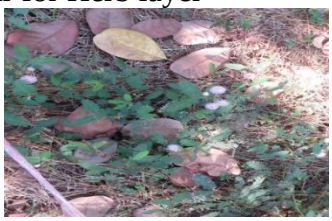

Plate 6 *Mimosa pudica* L. (Tikayon) (Dominant Species in Ah-Lel Ywar)

Discussion and Conclusion

To find out the plant species diversity in the Kyaik-Inn and Ah-Lel Ywar, Thanlyin Township, 2 large quadrats for trees (15 × 15 meters) were set up. Then, each large was equally subdivided into 9 small quadrats (5 × 5 meters) for herbs in two different sites. In the present study, total numbers of plant species in the study area is 55 species, including 53 genera and 33 families. Among them 12 are trees, 4 are small trees, 8 are shrubs, 21 are herbs, 3 are climbers, 6 are grasses and fern is only one (Table 1). In Kyaik-Inn, composed of 39 species, 38 genera, and 24 families. Among them trees are 9, small trees are 3, shrubs are 3, herbs are 16, climbers are 2, grasses are 5 and fern is 1. In Ah-Lel Ywar, a total of 30 species, 29 genera, and 20 families. Among them trees are 6, shrubs are 8, herbs are 9, climbers are 2, grasses are 3, small tree and fern are 1. Among two study sites Kyaik-Inn was more diverse than the Ah-Lel Ywar. The comparison of plant species diversity in two sites are shown in (Table 2 and Fig. 2). So, it can be concluded that the species composition of Kyaik-Inn is more diverse than Ah-Lel Ywar. According to the present study, species richness is variable depending on conditional differences of two sites. According to the results of Shannon-Wiener Index (H), it was observed that the diversity index of Kyaik-Inn were (1.5, 3.71) for trees and herbs respectively and (0.7, 3.2) in Ah-Lel Ywar. Simpson Index (D) of Kyaik-Inn showed (0.5, 0.88) for all layers and for (0.3, 0.9) in Ah-Lel Ywar. Kyaik-Inn was relatively higher than that of Ah-Lel Ywar (Table 3). Evenness of all layers in Kyaik-Inn and Ah-Lel Ywar were (0.7) respectively (Table 3). Eight common species in both study sites were chosen for calculation of population density and frequency. According to calculation, In Kyaik-Inn, *Aristida depressa* Retz. (Thamin-mwe-myet) has the highest degree of density and frequency. The relative density of this species is (26.05%), and relative frequency is (7.91%). (Table 4, 5, Fig. 3, 4 and Plate 5). *Aristida depressa* Retz. (Thamin-mwe-myet) belongs to the family Poaceae. The Poaceae are the world's single most

important source of food. They rank among the top five families of flowering plants in term of the number of species, but they are clearly the most abundant and important family of the Earth's flora. marine habitats, and at all but the highest elevations. In Ah-Lel Ywar, *Mimosa pudica* L. (Tikayon) has the highest degree of density and frequency. The relative density of this species is (20.16%) and relative frequency is (9.28%) (Table 6, 7, Fig. 5, 6 and Plate 6). *Mimosa pudica* L. (Tikayon) belongs to the family Mimosaceae and it is also called "Sensitive Plant". It was found in all studied plots and occur as most dominant species in this area. "Sensitive Plant" folds up its leaves when touched or exposed to a flame. This plant requires a medium light exposure, an evenly moist soil, and temperatures between 60 and 85 degrees. It is spread throughout the hotter parts of Myanmar. The relative density and relative frequency of species in Kyaik-Inn, such as *Oldenlandia diffusa* (Willd.) Roxb. (Sula-napha), *Eupatorium cannabinum* L. (Hkwe-thay-pan), *Vernonia cinerea* (L.)Less. (Kadu-pyan), *Digitaria adscendens* (Kunth) Henrard (Myet-hnankar), *Syzygium grande* (Wight) Walp. (Thabye-gyi), *Euphorbia hirta* L. (Kywe-kyaung-mymi-si), *Cleome viscosa* L. (Gant-galar), are in order (Table 4,5 and Fig. 3,4). The relative density and relative frequency of species in Ah-Lel Ywar, such as *Indigofera linifolia* Retz. (Than-ma-naing-kyauk-ma-naing), *Euphorbia hirta* L. (Kywe-kyaung-mymi-si), *Digitaria adscendens* (Kunth) Henrard (Myet-hnankar), *Echinochloa crus-galli* (L.) P.Beauv. (Myet-cho), *Jasminum multiflorum* (Burn.f.) Andrews (Tawsabe), *Eleocharis acicularis* (L.) Roem. & Schult. (Myet 2), *Acacia auriculiformis* A.Cunn. (Malaysia-padauk), are in order (Table 6, 7 and Fig. 5, 6). This study can clarify the plant species diversity of two study sites; In Kyaik-Inn, Asteraceae family members are highest in number (6 species), Poaceae family members are second highest in number (5 species). In Ah-Lel Ywar, Asteraceae family members are highest in number (4 species), Poaceae family members are second highest in number (3 species). It can also make clear that between the two different site conditions, Kyaik-Inn is more diverse than Ah-Lel Ywar. In addition the common species of study area can be differentiates and their relative density and relative frequency can be evaluated.

Acknowledgements

The author is indebted to Dr Nay Win Oo, Rector of East Yangon University and Dr Aye Aye Ko, Dr Wah Wah Lwin and Dr Thidar Aung, Pro-Rectors of East Yangon University for their kind permission to carry out this research. Special thanks are also due to Professor and Head, Dr. Htay Htay Lwin, Botany Department of East Yangon University for her invaluable encouragement and suggestions.

References

Backer, C.A and R. C. B. Van Den Brink, 1963-1968. *Flora of Java* (Vol. I – III). NV.P. Noordhoof Groningen, The Netherlands.

Hooker, J. D. (1875-1885). *Flora of British India (Vol. I – VII).* L. Reeve and Company, London.

Hundley, H. G. and Chit Ko Ko 1961. *List of trees, shrubs, herbs and principal climbers, etc.*, Forest Department, Yangon, Myanmar.

Krebs, J.C., 1998. *Ecological Methodology***.** Addison Wesley Longman Inc., ISBN:

Kress, W. J., R. A. De Filipps, F. Ellen, and Yin Yin Kyi 2003. A checklist of trees, shrubs, herbs and climbers of Myanmar, Washington DC.

Lawrence, G. H. M. 1969. *Taxonomy forest ecosystems and their long-term utilization. Silviculture in the tropics:* (GTZ) GmbH, Eschborn, Germany.

Magurran, A.E., 1988. *Ecological diversity and its measurement*. Princeton University Press, New Jersey

Naeem, S., Hakanson, K., Lawton, J. H. et al. 1996. *Biodiversity and plant productivity in a model assemblage of plant species.* – Oikos

Shannon, C.E. and W. Wiener, 1963. *The mathematical theory of communication*. University of Illinois Press, Urbana, USA.

Weaver, J. E. and F. E. Clements. 1996. *Plant succession: An analysis of the development of vegetation.* Carnagie Inst, Washington.

Weidelt, H.J. 2000. *Lectures Notes on Tropical Silviculture I and II. Tropical Silviculture,* Institute of Silviculture, Sec. II, Gottingen University, Germany (Unpublished).

Whittaker R.H (1980), *s* Kluwer Academic Publishers, Printed in the Netherlands.

ANTIPYRETIC EFFECT OF *KAEMPFERIA GALANGA* L. RHIZOMES

Phyo Moh Moh Zin[1], Khin Cho Cho Oo[2]

Abstract

Kaempferia galanga L. is the medicinal plant which belongs to the family Zingiberaceae. It is known as Kun-sar-gamone in Myanmar. This plant was collected from Ka-wa- Township, Bago Region. The morphological characters of this plant were identified and microscopical characters of dried powder of this plants were also investigated. The acute toxicity tests on albino mice have been conducted by using 70 % ethanolic extracts of rhizomes from *Kaempferia galanga* L. according to the method of OECD Guideline 423(2001).The maximum dose of the extracts of 5000 mg/ kg (body weight) showed no toxic effect and lethality during the test period of 14 days. The antipyretic activity of 70 % ethanolic extracts of rhizomes of this plant were evaluated using Brewer's yeast induced pyrexia in albino rats. It was found that 70 % ethanolic extract of rhizomes from *Kaempferia galanga* L. had effective antipyretic activity. Therefore, the results showed that this plant can be useful to reduce the fever.

Keywords: *Kaempferia galanga* L., acute toxicity, antipyretic activity, 70 % ethanolic extracts

Introduction

The Zingiberaceae family occur mainly in the tropics and subtropics. Asia and consists of over 40 genera and about 1,000 species (Dassanayake, 1983). The powder of rhizomes mixed with honey are given in coughs and pectoral affections and oil from the rhizomes is externally applied to stoppages of the nasal organs (Kirtikar and Basu, 1995).

Acute systematic toxicity testing is the estimation of the human hazard potential of a substance by determining its systematic toxicity in a test system (currently animals) based on acute exposure. Its assessment has traditionally been based on the medium lethal dose (LD_{50}) value-an estimate that kills 50 % of the test animals. Acute toxicity is generally measured by using an assay to determine the lethal dose; rodents are given single doses and the numbers that died 14 days later is recorded (American Heritage Science Dictionary, 2002).The organization for Economic Cooperation and Development (OECD) had established guidelines for the acute toxicity study. The acute toxicity of 70 % ethanolic extract from *Kaempferia galanga* L. is tested on albino mice.

Fever (medically called pyrexia) is a term used to describe increased body temperature. When the body's defense (immuse) system is activated by a bacteria or a virus, many reactions occur in the body. The normal human body temperature ranges between 36 ºC - 37 ºC (98 - 100 ºF). This temperature may vary depending on several factors. In other countries, antipyretic activity of extracts of plants on rats was tested. Borikar (2009) stated that the study was conducted to screen the antipyretic activity of alcoholic extract of the stem bark of *Bauhinia racemosa* Lam. on albino rats. In this research showed that 70 % ethanolic extract of rhizomes from *Kaempferia galanga* L. had effective of antipyretic activity.

The aim of the present research is to promote the wide application of Myanmar traditional or herbal medicine scientifically. The objective of this research is to ascertain the morphological and diagnostic characters of *Kaempferia galanga* L. and to examine acute toxicity and antipyretic activity of 70 % ethanolic extract of this plant.

[1] Dr, Lecturer, Department of Botany, East Yangon University
[2] Dr, Professor and Head, Department of Botany, Panglong University

Materials and Methods

Plant materials

The plant specimens of *Kaempferia galanga* L. were collected from Ka-wa Township, Bago Region during the flowering and fruiting periods from June to October, in the year 2013. For morphological study, the specimens were measured, described in detail and identified with the help of available literatures (Hooker, 1894; Backer, 1968; Dassanayake, 1983; Wu Delin and Kai Larsen; 2000). The specimens such as habit, leaves, inflorescences and flowers were recorded with the photographs. Herbarium specimens were prepared and kept in the Herbarium, Department of Botany, University of Yangon.

Preparation of powdered samples

The collected samples were washed with water to remove impurities. After washing, the sample was air dried and ground to get powder and stored in air tight container to prevent moisture content and other contaminations. The diagnostic characters of powder samples were observed by using the powder of the rhizomes.

Powdered sample (100) g was extracted with aqueous and 70 % ethanol by decoction on water bath for 6 hours at 70°C. The solution was filtered and the filtrate was concentrated on the water bath at 100°C and finally they were evaporated to dryness and obtain a paste. The extract was stored in a desiccators at 4°C until use.

Acute toxicity test of 70 % ethanolic extracts of rhizomes from *Kaempferia galanga* L. by using albino mice

Materials and Methods

The acute toxicity test on mice was carried out according to the guide lines described in OECD TG-423 (2001) of Department of Medical Research (DMR).

Laboratory animals

Adult, albino mice, Dutch Donken Yoken (DDY) strain of female sex, weighing between 22-30 g, were used for acute toxicity study. These animals were provided by the Laboratory Animal Services Division, Department of Medical Research, Yangon.

Animal used	-	18 female albino mice (body weight 22-30 kg)
Drug used	-	70 % ethanolic extracts of rhizomes
Chemical used	-	10 % tween 80
Apparatus used	-	Mice cage, Animal balance, intragastric needle and 10 ml syringes, rubber glove and mask
Dose schedule	-	(1) 70 % ethanolic extract Control = 10 % tween 80 2 g/Kg (body weight) 5 g/Kg (body weight)
Period of observation	-	Two weeks

Acute toxicity test of 70 % ethanolic extract of rhizomes from *Kaempferia galanga* L.

Acute toxicity test was performed according to OECD guideline TG 423. Female mice, weighing between 22 - 30 g were randomly selected and kept in their cages for at least 5 days prior to dosing to allow for acclimatization for laboratory condition. The test substance was administered in a single dose by gavage using intragastric needle. The animals were kept fasting overnight for 18 hours but were allowed with free access to water. Following period of fasting, mice were weighed and test substance was administered. One group served as the control and only 10 % tween 80 (drug vehicle) was given orally. In this study, starting dose 2000 mg/kg was chosen. 70 % ethanolic extract of rhizomes from *Kaempferia galanga* L. was dissolved in 10 % tween 80. *Kaempferia galanga* L. rhizomes extracts of 2000 mg/kg was given to 6 mice (3 mice for each step).

After administration of the test agent orally, they were allowed to have food and water. The sign of toxicity such as changes in skin and fur, eyes and mucous membrane, respiratory, circulatory, autonomic and central nervous systems and somatomotor activity and behavior were observed on test animals. Mice were observed individually after dosing at one time during the first 24 hours hourly up to 4 hours for first 30 minutes. After that, all the mice were monitored daily and weighed weekly. They were found to survive at the dose of 2000 mg/kg during 14 days. So, another 6 mice (3 mice for each step) were administered 5000 mg/kg. Individual weights of animals were determined shortly before the test substances (i.e., control) were administered and once weekly thereafter. Weight changes were calculated and recorded.

Figure. 1 Groups of mice cages (each contain 6 mice)

Figure.2Administration of drug vehicle to mouse (control)

Figure.3Administration of extract suspension to mouse

Antipyretic activity of 70 % ethanolic extracts of rhizomes from *Kaempferia galanga* L.

Material and Methods

Animal used were 24 both sex albino rats (Wister strain) of (body weight 220 - 300 g)

Animal used	-	24 both sex albino rats (body weight 220 - 300 g)
Extracts and drug used	-	70 % ethanolic extract, 10 % tween 80,
	-	Standard drug, paracetamol tablets (150 mg, MPF), Brewer's Yeast
Apparatus used	-	Aluminium rats cages, animal balance, thermometer, 10ml syringes, spirit socked, cotton wools, rubber glove and masks
Dose schedule	-	70 % ethanolic extract of 1.5 g/kg and 3 g/kg (body weight)

The determination of antipyretic activity of the aqueous and 70 % ethanolic extracts of rhizomes from *Kaempferia galanga* L. were done by using the method of Gupta *et al.*, (2003). Wister strain albino rats, both sexes, weighing between 220 -300g were used for evaluation of antipyretic activity. Rats are weighed randomly divided into four groups of six rats. The body temperature of the rats were taken by inserting a thermometer into their anal cavities about 2 cm and for about 2 mins.

Antipyretic activity of the 70 % ethanolic extract of rhizomes from *Kaempferia galanga* L.

Firstly, temperature was recorded as the pre-treatment temperatures. Pyrexia was induced in the rats by the subcutaneous injection of 10 ml/kg (body weight) of 15 % Brewer's yeast suspension to back of the neck and 19hours later the rectal temperature were measured again. 70 % ethanolic extract were dissolved in 10 % tween 80. Group I served as control and administered orally with 10 % tween 80. Group II was administered orally with 70 % ethanolic extract of rhizomes, 1.5 g/kg. Group III was administered orally with 70 % ethanolic extract of rhizomes, 3 g/kg. Group IV was administered orally with standard drug, paracetamol, 150 mg/kg (body weight). The rectal temperatures were then measured by using thermometer and the temperatures were recorded at 1 hour, 2 hours, 3 hours, 4 hours and 5 hours after administration of the 70 % ethanolic extract. After 19 hours

of yeast injection, the rats showing an increase of rectal temperatures > 0.5°C were selected for this study.

Calculation of percent reduction in rectal temperature

Percent reduction in rectal temperature was calculated by using the following formula. The total fall in rectal temperature from the elevated to normal level was considered as 100 %.

$$\% \text{ reduction} = \frac{\text{Elevated temperature} - \text{temperature at different intetval}}{\text{Elevated temperature} - \text{initial temperature}} \times 100$$

(Mantena *et al*., 2004)

Data Management and Analysis

Standard statistical methods were used in the calculation of arithmetic mean (X), Deviation (SD) and standard Error (SE). The data was analyzed using student 't' test and $P < 0.05$ was considered statistically significant.

Figure. 4 Metal cage which contained 3 rats

Figure. 5 Subcutaneous injection of yeast into nape of neck of Wister albino rat

Figure. 6 Measuring rectal temperature

Figure. 7 Administration of drug vehicle to rat (control)

Figure. 8 Administration of extract suspension to rat

Results

Morphological characteristics of *Kaempferia galanga* L.

Scientific name - *Kaempferia galanga* L.
Myanmar name - Kun-sar-gamone
English name - Sand ginger, Aromatic ginger
Family - Zingiberaceae

Herbs with aromatic rhizome, rhizomes yellowish white inside, fragrant. Leaves opposite and distichous, simple, the lamina broadly elliptic to slightly orbicular, 12.0 - 15.5 cm long and 10.0 -13.1 cm wide, the bases cuneate, the margins entire, the tips acuminate, both surfaces glabrous; shortly petioles; leaf-sheath open,10.0 - 23.0 cm long and 0.35 - 0.5 cm wide. Inflorescence terminal, compact spike; bracts lanceolate, 5.8 - 6.0 cm long and about 1.0 cm wide. Flower white with violet center, 5.6 - 5.8 cm long and 2.6 - 2.8 cm wide,

complete, bisexual, irregular, zygomorphic, trimerous, epigynous; sepals (3), synsepalous, tubular, 2.0 - 2.3 cm long and about 0.3 cm wide, spathaceous splitting, white; petals (3), synpetalous, tubular, the tubes 3.6 - 3.8 cm long and about 0.3 cm wide, the lobes 1.6 - 1.8 cm long and 0.25 - 0.35 cm wide, white; stamens 1+ (2)st+2st, epipetalous, 1 fertile stamen 4.5 mm long and 5.0 mm wide , 2 - outer staminodes fused to form a labellum, 17.0 mm long and 18.0 mm wide, white with violet center and 2 - inner lateral petaloid free staminodes, 12.0 mm long and 8.0 mm wide , filaments grooved, exserted, anthers dithecous, introrse, dorsifixed, longitudinal dehiscence; ovary inferior, ovoid, 2.5 mm long and 2.0 mm wide, tricarpellary, syncarpous, trilocular, axile placentation, the style long and slender, 37.0 mm long and 0.5 mm wide the stigma capitate as shown in Figures (9 to 22). Fruits and seeds not seen. Flowering and fruiting time is June to October.

Morphological characteristics of *Kaempferia galanga* L.

.

Figure. 9 Plants in natural habit

Figure. 10 Habit

Figure. 11 Rhizome

Figure. 12 Ventral view of leaves

Figure. 13 Dorsal view of leaves

Figure. 14 Bract with flower

Figure. 15 Bract

Figure. 16 L.S of flower

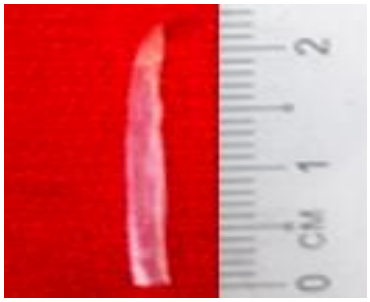

Figure. 17 Calyx

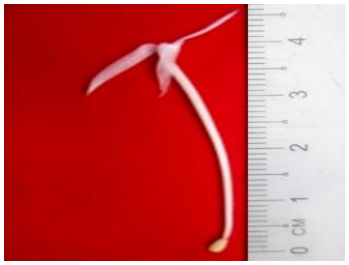

Figure. 18 Corolla

Figure. 19 Corolla with

Figure. 20 Pistil

petaloid staminodes
and fertile stamen

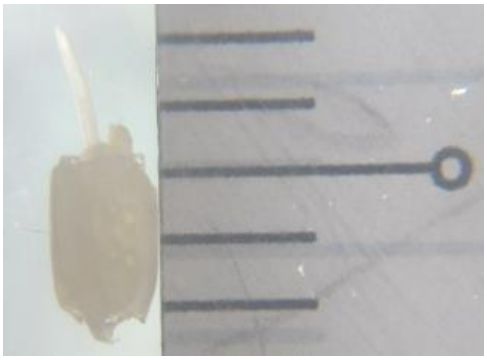

Figure. 21 L.S of ovary

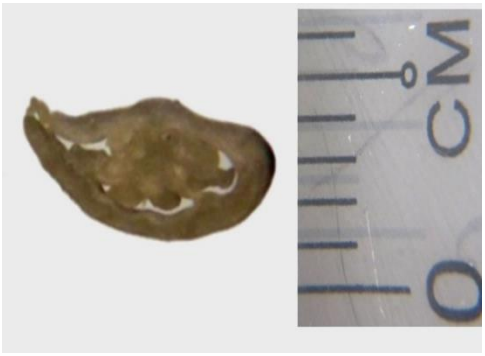

Figure. 22 T.S of ovary

Diagnostic characteristics of powdered of rhizomes of *Kaempferia galanga* L.

The powdered rhizomes was cream colour and strongly aromatic in odour. It was also warm and bitter in taste and fibrous in texture. It consists of pieces of parenchyma cells, reticulate vessel, prism- shaped calcium oxalate crystals, fiber and single starch grains as shown in Figures (23 to 28).

Diagnostic characters of powdered rhizomes of *Kaempferia galanga* L.

Figure. 23 Powdered rhizomes

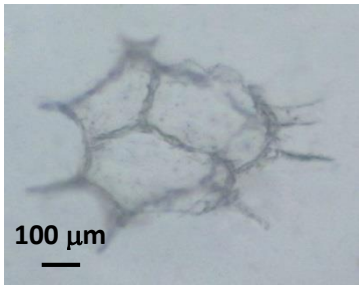

Figure. 24 Pieces of parenchyma cells

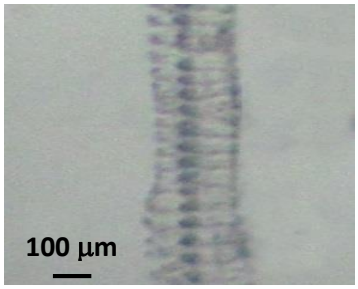

Figure. 25 Reticulate vessel

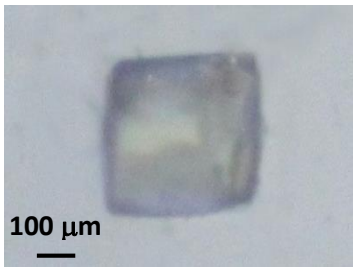

Figure. 26 Prism -shaped calcium oxalate crystals

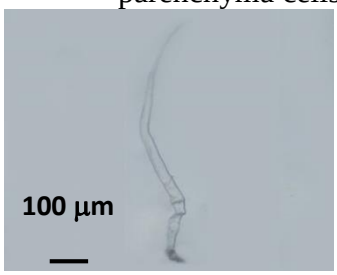

Figure. 27 Fiber

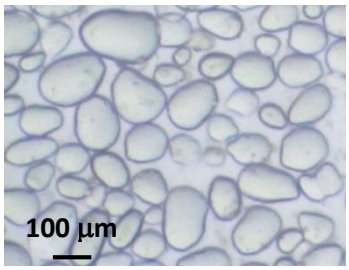

Figure. 28 Single starch grains

Acute toxicity test of 70 % ethanolic extracts of rhizomes from *Kaempferia galanga* L. on albino mice

Acute toxicity was performed according to OECD guideline TG 423. The aqueous and 70 % ethanolic extracts of rhizomes from *Kaempferia galanga* L. showed no lethal effects and toxicity on albino mice up to the maximum dose of 5 g/ kg. Therefore, LD_{50} values of 70 % ethanolic extracts was more than 5 g/kg. The extracts were non-toxic.

Table. 1 Acute toxicity test with 70 % ethanolic extract of rhizomes from *Kaempferia galanga* L.

Group No.	Number of mice	Type of Drugs	Dosage g/kg	Observed period	Dead Tested
I	6	Control (10 % tween 80)	10ml/kg	14days	0/6
II	6	70 % ethanolic extract	2g/kg	14days	0/6
III	6	70 % ethanolic extract	5g/kg	14days	0/6

Antipyretic activity of 70 % ethanolic extracts of rhizomes from *Kaempferia galanga* L. on yeast induced pyrexia in albino rats

Regarding the induction of fever by subcutaneous injection of Brewer's yeast to the albino rats, it was found that the rectal temperatures of all the rats increased 0.5°C at 19 hours after subcutaneous injection of Brewer's yeast. The temperatures significantly increased from basal temperature.

Antipyretic activity of 70 % ethanolic extract of rhizomes from *Kaempferia galanga* L. on yeast induced pyrexia in albino rats

In the control group, the result of mean rectal temperature of six albino rats at 1 hour, 2 hours, 3 hours, 4 hours, and 5 hours after administration of 10 % tween 80 (i.e. at 20 hours, 21 hours, 22 hours, 23 hours and 24 hours after subcutaneous injection of Brewer's yeast 10 ml/kg) were found to be 39.0.7 °C ± 0.13 °C, 39.23 °C ± 0.16 °C, 39.37 °C ± 0.18 °C, 39.5 °C ± 0.16 °C and 39.48 °C ± 0.14 °C respectively as shown in Tables (2, 6) and Figure (29). It was found that significant increase in rectal temperature started at 1hour and lasted up to 5 hours.

The results of mean rectal temperature of six albino rats treated with 70 % ethanolic extract of *Kaempferia galanga* L. rhizomes (1.5 g/ kg) at 1 hour, 2 hours, 3 hours, 4 hours and 5 hours after administration of the extract (i.e at 20 hours, 21 hours, 22 hours, 23 hours and 24 hours after subcutaneous injection of Brewer's yeast (10 ml/kg) were found to be 37.52 °C ± 0.07 °C, 37.23 °C ± 0.11°C, 36.75 °C ± 0.11 °C, 36.52 °C ± 0.09 °C and 36.47 °C ± 0.09 °C respectively. Significant reductions of rectal temperature were observed at 1 hour, 2 hours, 3 hours, 4 hours and 5 hours after administration of the extract ($P < 0.001$) when compared with those of the control group as shown in Tables (3, 6).

The results of mean rectal temperature of six albino rats treated with 70 % ethanolic extract of *Kaempferia galanga* L. rhizomes (3 g/kg) at 1hour, 2 hour, 3 hours, 4 hours and 5 hours after administration of the extract (i.e at 20 hours, 21 hours, 22 hours, 23 hours and 24hours after subcutaneous injection of Brewer's yeast (10 ml/kg) were found to be 36.88 °C ± 0.07 °C, 36.27 °C ± 0.17 °C, 36.07 °C ± 0.21 °C, 35.8 °C ± 0.25 °C and 35.78 °C ± 0.24 °C respectively. Significant reductions of rectal temperature were observed at 1 hour, 2 hours, 3 hours, 4 hours and 5 hours after administration of the extract ($p < 0.001$) when compared with those of the control group and as shown in Tables (4, 6).

The results of mean rectal temperature of six albino rats treated with standard drug, paracetamol (150 mg/kg), at 1 hour, 2 hours, 3 hours, 4 hours and 5 hours after administration of the extract (i.e. at 20 hours, 21 hours, 23 hours and 24 hours after subcutaneous injection of Brewer's yeast (10 ml/kg) found to be 36.63 °C ± 0.09 °C, 35.92 °C ± 0.19 °C, 35.73 °C ± 0.17 °C, 35.5 °C ± 0.15 °C and 35.22 °C ± 0.14 °C respectively. Significant reductions of rectal temperature were observed at 1 hour, 2 hours, 3 hours, 4 hours and 5 hours after

administration of the extract ($p < 0.001$) when compared with those of the control group as shown in Tables (5, 6).

Means percent reductions of rectal temperature of albino rats in different doses of drug treatments were shown in Tables (7 to 10) and Figures (29 to 31). The results showed that the paracetamol as well as 70 % ethanolic extract (1.5 g/kg and 3 g/kg) of rhizomes from *Kaempferia galanga* L. reduced fever in yeast induced pyrexia on albino rats.

Table.2 Effect of 10 % tween 80 on rectal temperature (in °C) of individual rats on yeast-induced pyrexia in albino rats of control group (Mean ± SE)

No. of rat	Mean rectal temperature (in °C)						
	Before extract		After administration of extract				
	0 hr	19 hr	20 hr	21 hr	22 hr	23 hr	24 hr
1	36.8	38.9	38.9	38.9	38.9	39.0	39.0
2	37.0	39.0	39.0	39.1	39.2	39.3	39.4
3	38.0	38.7	38.7	39.0	39.2	39.5	39.4
4	37.4	39.0	39.3	39.5	39.9	39.9	39.9
5	38.4	38.9	38.9	39.0	39.1	39.3	39.3
6	38.4	39.2	39.6	39.9	39.9	40.0	39.9
Sum	226	233.7	234.4	235.4	236.2	237	236.9
Mean	37.67	38.95	39.07	39.23	39.37	39.5	39.48
SD	0.7	0.16	0.33	0.39	0.43	0.38	0.35
SE	0.29	0.07	0.13	0.16	0.18	0.16	0.14

Table. 3 Effect of 70 % ethanolic extract of rhizomes from *Kaempferia galanga* L. 1.5 g/kg on rectal temperature (in °C) of individual rats on yeast induced pyrexia in albino rats (Mean ± SE)

No. of rat	Mean rectal temperature (in °C)						
	Before extract		After administration of extract				
	0 hr	19 hr	20 hr	21 hr	22 hr	23 hr	24 hr
1	37.1	37.8	37.5	37.3	37.0	36.8	36.8
2	37.0	37.7	37.4	37.3	36.8	36.6	36.5
3	37.2	37.9	37.7	37.5	37.0	36.5	36.5
4	37.2	37.9	37.7	37.5	36.7	36.6	36.5
5	37.0	37.7	37.5	37.0	36.7	36.5	36.4
6	37.0	37.7	37.3	36.8	36.3	36.1	36.1
Sum	222.5	226.7	225.1	223.4	220.5	219.1	218.8
Mean	37.08	37.78	37.52	37.23	36.75	36.52	36.47
SD	0.1	0.1	0.16	0.28	0.26	0.23	0.23
SE	0.04	0.04	0.07	0.11	0.11	0.09	0.09
P value	0.0710	0.0000	0.0000	0.0000	0.0000	0.0000	0.0000
	NS	< 0.001	< 0.001	< 0.001	< 0.001	< 0.001	< 0.001

Statistical comparison made between temperature of the control and the extract receiving group.

Table.4 Effect of 70 % ethanolic extract of rhizomes from *Kaempferia galanga* L. 3 g/kg on rectal temperature (in °C) of individual rats on yeast-induced pyrexia in albino rats (Mean ±SE)

No. of rat	Mean rectal temperature (in °C)						
	Before extract		After administration of extract				
	0 hr	19 hr	20 hr	21 hr	22 hr	23 hr	24 hr
1	37.0	37.7	36.8	36.0	36.0	36.0	36.0
2	37.0	37.7	36.7	36.0	35.4	35.1	35.1
3	37.1	37.8	36.8	36.0	35.7	35.3	35.3
4	37.0	37.7	36.8	36.1	36.0	35.5	35.5
5	37.0	37.7	37.0	36.5	36.5	36.2	36.2
6	37.1	37.7	37.2	37.0	36.8	36.7	36.6
Sum	222.2	226.3	221.3	217.6	216.4	214.8	214.7
Mean	37.03	37.72	36.88	36.27	36.07	35.8	35.78
SD	0.05	0.04	0.18	0.41	0.51	0.61	0.58
SE	0.02	0.02	0.07	0.17	0.21	0.25	0.24
P value	0.0517	0.0000	0.0000	0.0000	0.0000	0.0000	0.0000
	< 0.05	< 0.001	< 0.001	< 0.001	< 0.001	< 0.001	< 0.001

Statistical comparison made between temperature of the control and the extract receiving group.

Table.5 Effect of paracetamol (150 mg/kg) on rectal temperature (in °C) of individual rats on yeast-induced pyrexia in albino rats (Mean ± SE)

No. of rat	Mean rectal temperature (in °C)						
	Before extract		After administration of extract				
	0 hr	19 hr	20 hr	21 hr	22 hr	23 hr	24 hr
No	0 hr	19 hr	20 hr	21 hr	22 hr	23 hr	24 hr
1	37.1	37.8	36.8	36.3	36.0	36.0	35.9
2	37.0	37.7	36.5	35.2	35.1	35.0	35.0
3	37.1	37.8	36.5	36.0	36.0	35.5	35.0
4	37.0	37.7	36.5	36.3	36.0	35.8	35.2
5	37.0	37.8	36.5	35.5	35.3	35.2	35.2
6	37.3	38.0	37.0	36.2	36.0	35.5	35.0
Sum	222.5	226.8	219.8	215.5	214.4	213	211.3
Mean	37.08	37.8	36.63	35.92	35.73	35.5	35.22
SD	0.12	0.11	0.22	0.46	0.42	0.37	0.35
SE	0.05	0.04	0.09	0.19	0.17	0.15	0.14
P value	0.0129	0.0057	0.0000	0.0000	0.0000	0.0000	0.0000
	< 0.05	< 0.01	< 0.001	< 0.001	< 0.001	< 0.001	< 0.001

Statistical comparison made between temperature of the control and paracetamol receiving group.

Table.6 Mean rectal temperature of albino rats with different doses of 70 % ethanolic extract of rhizomes from *Kaempferia galanga* L. and paracetamol (Mean ± SE)

Different type of treatments	Rectal temperature at hourly interval (Mean ± SE) (in °C)						
	Before treatment		After treatment				
	0hr	19hr	20hr	21hr	22hr	23hr	24hr
Control	37.67±0.29°C	38.95±0.07°C	39.07±0.13°C	39.23±0.16°C	39.37±0.18°C	39.5±0.16°C	39.48±0.14°C
70 % ethanolic extract 1.5 g/ kg	37.08±0.04°C	37.78±0.04°C	37.52±0.07°C	37.23±0.11°C	36.75±0.11°C	36.52±0.09°C	36.47±0.09°C
70 % ethanolic extract 3 g/ kg	37.03±0.02°C	37.72±0.02°C	36.88±0.07°C	36.27±0.17°C	36.07±0.21°C	35.8±0.25°C	35.78±0.24°C
Paracetamol 150 mg/ kg	37.08±0.05°C	37.8±0.04°C	36.63±0.09°C	35.92±0.19°C	35.73±0.17°C	35.5±0.15°C	35.22±0.14°C

Table.7 Mean percent reductions of rectal temperature of albino rats with different doses of 70 % ethanolic extract of rhizomes from *Kaempferia galanga* L. and paracetamol treatment

Different type of treatments	% Reduction of rectal temperature at hourly interval (Mean ± SE)				
	% reduction at 1hr after treatment	% reduction at 2hr after treatment	% reduction at 3hr after treatment	% reduction at 4hr after treatment	% reduction at 5hr after treatment
70 % ethanolic extract 1.5 g/ kg	38 ± 5 %	79 ± 12 %	148 ± 13 %	181 ± 13 %	188 ± 12 %
70 % ethanolic extract 3 g/ kg	121 ± 10 %	210 ± 22 %	239 ± 28 %	278 ± 34 %	281 ± 32 %
Paracetamol 150 mg/ kg	163 ± 7 %	262 ± 23 %	288 ± 20 %	321 ± 20 %	361 ± 23 %

Different type of treatments	Rectal temperature at hourly interval (Mean ± SE) (in °C)						
	Before treatment		After treatment				
	0hr	19hr	20hr	21hr	22hr	23hr	24hr
Control	37.67±0.29°C	38.95±0.07°C	39.07±0.13°C	39.23±0.16°C	39.37±0.18°C	39.5±0.16°C	39.48±0.14°C
70 % ethanolic extract 1.5 g/ kg	37.08±0.04°C	37.78±0.04°C	37.52±0.07°C	37.23±0.11°C	36.75±0.11°C	36.52±0.09°C	36.47±0.09°C
70 % ethanolic extract 3 g/ kg	37.03±0.02°C	37.72±0.02°C	36.88±0.07°C	36.27±0.17°C	36.07±0.21°C	35.8±0.25°C	35.78±0.24°C
Paracetamol 150 mg/ kg	37.08±0.05°C	37.8±0.04°C	36.63±0.09°C	35.92±0.19°C	35.73±0.17°C	35.5±0.15°C	35.22±0.14°C

Table.8 Comparison between percent reductions of rectal temperature of albino rats with 70 % ethanolic extract of rhizomes from *Kaempferia galanga* L. 1.5 g/kg and 3g/ kg

Different doses of 70 % ethanolic extract	% reduction of rectal temperature at 1hr	% reduction of rectal temperature at 2hr	% reduction of rectal temperature at 3hr	% reduction of rectal temperature at 4hr	% reduction of rectal temperature at 5hr
1.5 g/ kg	38 ± 5 %	79 ± 12 %	148 ± 13 %	181 ± 13 %	188 ± 12 %
3g/ kg	121 ± 10 %	210 ± 22 %	239 ± 28 %	278 ± 34 %	281 ± 32 %
P values	0.0001	0.0007	0.0154	0.0222	0.0223
	< 0.001	< 0.001	< 0.05	< 0.05	< 0.05

Table.9 Comparison between percent reductions of rectal temperature of albino rats with the 70 % ethanolic extract of rhizomes from *Kaempferia galanga* L. 1.5g/kg and standard drug, paracetamol

Different doses of 70 % ethanolic extract	% reduction of rectal temperature at 1hr	% reduction of rectal temperature at 2hr	% reduction of rectal temperature at 3hr	% reduction of rectal temperature at 4hr	% reduction of rectal temperature at 5hr
70 % ethanolic extract 1.5 g/ kg	38 ± 5 %	79 ± 12 %	148 ± 13 %	181 ± 13 %	188 ± 12 %
Paracetamol 150 mg / kg	163 ± 7 %	262 ± 23 %	288 ± 20 %	321 ± 20 %	361 ± 23 %
P values	0.0000	0.0001	0.0005	0.0002	0.0000
	< 0.001	< 0.001	< 0.001	< 0.001	< 0.001

Table.10 Comparison between percent reductions of rectal temperature of albino rats with the 70 % ethanolic extract of rhizomes from *Kaempferia galanga* L. 3g/kg and standard drug, paracetamol

Different doses of 70 % ethanolic extract	% reduction of rectal temperature at1hr	% reduction of rectal temperature at 2hr	% reduction of rectal temperature at 3hr	% reduction of rectal temperature at 4hr	% reduction of rectal temperature at 5hr
70 % ethanolic extract3 g/ kg	121 ± 10 %	210 ± 22 %	239 ± 28 %	278 ± 34 %	281 ± 32 %
Paracetamol 150 mg / kg	163 ± 7 %	262 ± 23 %	288 ± 20 %	321 ± 20 %	361 ± 23 %
P values	0.0561	0.1946	0.2452	0.3250	0.0667
	NS	NS	NS	NS	NS

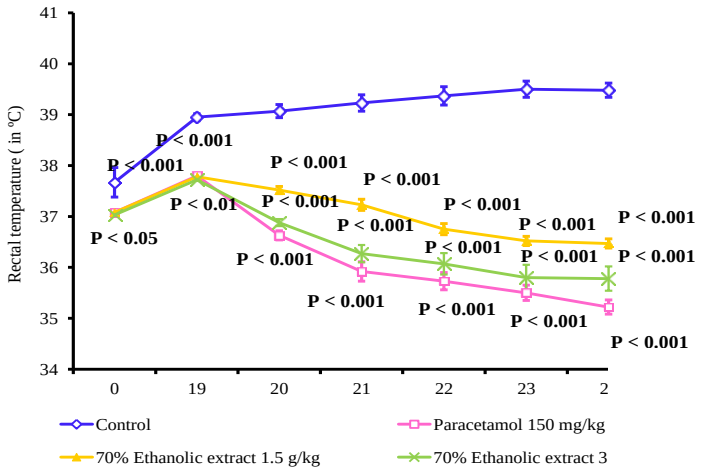
Rectal temperature (in ℃)
41
40
39
38
37
36
35
34
0
19
20
21
22
23
2
P < 0.001
P < 0.001
P < 0.001

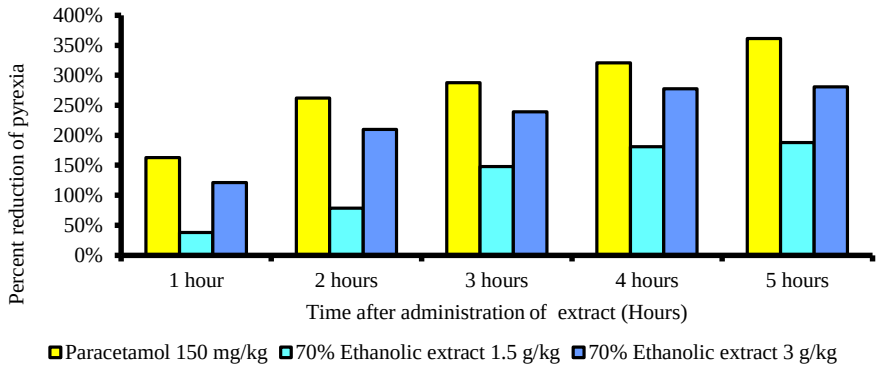

Figure. 31 Mean percent reduction of pyrexia in rats with different doses levels of 70 % ethanolic extract of rhizomes from *Kaempferia galanga* L. and standard drug, paracetamol. Values are in mean SE, n = 6

Discussion and Conclusion

Kaempferia galanga L. (Kun-sa-gamone) is a medicinal plant belongs to the family Zingiberaceae. In the present research, the outstanding characters of *Kaempferia galanga* L. are rhizomatous herbs with yellowish white. Leaves are opposite and distichous and broadly elliptic lamina with shortly petiole and leaf-shealth. Inflorescence compactly spike, white with violet center flower. Sepals are (3), tubular, white and spathaceous splitting. Petals are (3), tubular with reflexed lobes, white. Stamens are 1+ (2^{st}) + 2^{st}, epipetalous, one fertile stamens, white with violet center labellum, lateral petaloid staminodes. Ovary is tricarpellary, trilocular, axile placentation and stigma capitate. These characters were agreement with those given by Lawrence (1964), Ridley and Hutchinson (1967), Dassanayake (1983) and Jiang ke (2000).

The microscopical characteristics of dried powdered of rhizomes *Kaempferia galanga* L. showed that pieces of parenchyma cells, reticulate vessel, prism-shaped calcium oxalate crystals, fiber and single starch grains for their standardization in medicine. The characters are in agreement with those mentioned by (Esau, 1965; Waillis, 1967; Trease and Evans, 2002; Pandey, 1998 and Tunsaringkarn *et.al*., 2007).

Umar *et al*. (2012) revealed that acute toxicity of *Kaempferia galanga* L. rhizomes extracts on albino mice was found to be safe at dose level of 5000 mg/ kg. In this study, the result of acute toxicity study revealed that aqueous and 70 % ethanolic extracts neither have no lethality and toxic effect up to the maximum doses of 5 g/kg. So, LD_{50} values of aqueous and 70 % ethanolic extracts were more than 5 g/kg. The extracts were non- toxic.

The antipyretic activity was investigated on Brewer's yeast induced pyrexia in albino rats with 70 % ethanolic extracts of *Kaempferia galanga* L. at the dose of 1.5 g/ kg and 3g/ kg. These results revealed that antipyretic effect of 70 % ethanolic extract at the dose of 1.5 g/kg and 3 g/kg (body weight) showed significant reduction of fever, at 1 hour up to 5 hours, ($p < 0.001$), after administration of the extract. The standard drug, paracetamol showed significant reduction of fever at 1 hour up to 5 hours ($p< 0.05$- $p< 0.001$). When the different doses of plant extracts were compared with standard drug, paracetamol, it was observed that antipyretic effects of paracetamol was more than 70 % ethanolic extracts of *Kaempferia galanga* L.

Several studies conducted on medicinal plants revealed the presence of secondary metabolites like flavonoids and alkaloids which have been linked to possess analgesic and antipyretic activities (Subedi *et al*., 2016). In this study, antipyretic activity of the extracts of rhizomes from *Kaempferia galanga* L. may be due to phytochemical constituents like alkaloids and flavonoids present in this plant. The results showed that 70 % ethanolic extracts

possessed significant antipyretic effect in rats model. Therefore, it showed that this plant can be useful to reduce the fever like paracetamol.

Acknowledgements

I would like to acknowledge my sincere gratitude to Rector Dr. Nay Win Oo, East Yangon University, for his permission to present this research. I must especially express my deep gratitude to Pro-Rectors Dr. Aye Aye Ko, Dr. Wah Wah Lwin, Dr. Thida Aung, East Yangon University for her giving permission and suggestions. I would like to thanks Dr. Htay Htay Lwin, Professor & Head, Department of Botany, East Yangon University for providing the departmental facilities and their invaluable suggestions. I would like to express my deepest gratitude to my supervisor Dr. Khin Cho Cho Oo, Professor & Head, Department of Botany, Panglong University for her overall supervision, in valuable opinions and collaboration in every aspect of my research.

References

Backer, C. A. (1968). *Flora of Java*, Vol. III, Wolters Neordhaff N. V. Groningen, The Netherlands

Borikar, V. I., C. R. Jangde, P. Philip, D. S. Rekhe and S. K. Atole. (2009). *Study of Antipyretic Activity of Bauhinia racemosa Lam. in Rats*. Nagpur (440006), Maharashtra, India.

Dassanayake, M. D. (1983). *A revised Handbook to the Flora of Ceylon*. (Vol. IV). University of peradeniya, Washington, DC. Amerind Publishind Co. Pvt. Ltd.

Esau, K. (1965). *Plant Anatomy*. 2nd Ed, John Wiley and Sons, Inc. New York, London.

Gupta, M., U. K. Mazumder and R. S. Kumar. (2003). *Studies on Anti-inflammatory, Analgesic and Antipyretic Properties of Methanolic Extract of Caesalpinia bonducella Leaves in Experimental Animal Models*, Department of Pharmaceutical Technology, Jabalpur University and Calcutta: India.

Hooker, J. D. (1894). *The Flora of British India*, Vol. VI, Reeve Co., Ltd., The Oast House, Brock, NR. Ashford, Kent. England.

Jiang Ke, Wu Delin and Kai Laren. (2000). *Flora of China*. Vol.24, Pg. 322- 377, South China Institue of Botany, Guangdong, Republic of China.

Kirtikar K. R. and B. D Basu, K. R. (1995). *Indian Medicinal Plants*, Vol. IV, 3rd ed. Prabasi Press, Upper Circular Road, Calcutta, India.

Lawrence, G. H. M. (1964). *Taxomy of Vascular Plants*, 10thed.The macmillian, Company, New York, London.

Mantena S. K., S. Mutalik, H. Srinivasa, G.S. Subramanian, K. R. Prabhakar, K. R. Reddy, K.K. Srinivasan and]M.K. Unnikrishnan. (2004). "Antiallergic, Antipyretic, Hypoglycemic and Hepatoprotective Effects of Aqueous Extract of *Coronopus didymus* Linn". *Bio. Pharm. Bull*; **28**(3) 468-72.

Pandey, S. N. and A. Chadha. (1998). *Plant Anatomy and Embryology*. Vikas Publishing House Pvt. Ltd ., New Delhi.

Ridley, H. N and J. Hutchinson. (1967). *The Flora of the Malay Peninsula*. Vol. IV. Brook Nr. Ashford, Grat Britain.

Subedi, N.K *et.al*., (2016). *Analgesic and Antipyretic Activities of Methanol Extract and Its Fraction from the Root of Schoenoplectus grossus*.Vol.12, Bangladesh.

Trease G.E. and W.C. Evans. (1978, 2002, 2009). *Pharmacognosy*.11th, 13th, 16th ed. Elsevier Limited. London.

Tunsaringkarn T., C. Palanuvej and A. Rungsiyothin. (2007). *Pharmacognostic Specification of Kaempferia galanga L. rhizomes in Thailand.*Vol.21 (3), Pg.207-214, Chulalongkorn University, Bangkok.

Umar, M. I *et. al.* (2012). *Bioactivity-Guided Isolation of Ethyl-p-methoxycinnamate, an Anti- inflammatory constituent from Kaempferia galanga* L. Extracts, Department of Pharmacology, Penang, Malaysia.

Waillis, T. E. (1967). *Textbook of Pharmacognosy*, 5th ed. Gloucester Place London; J and A. Churchill Limited.

Wu Delin and Kai Larsen. (2000). *Flora of China*. Chinese Academy of Sciences, Wushan Guangzhou, China.

American Heritage and Science Dictionary. (2002). *Toxicology; Define Toxicology of Dictionary*. Com., Houghton Mifflin.

Organization for Economic Co-operation and Development (OECD)423. 2001. *Guideline for testing of chemical Acute oral toxicity- Acute Toxic Class Method* 423, Pg. 1-14.

LITHOFACIES ASSOCIATION OF KALAW FORMATION IN WESTERN PART OF THE SHAN PLATEAU

Than Than Thwe[1], Thura Oo[2]

Abstract

The Kalaw Formation exposed along the western margin of the Shan Plateau is a Cretaceous fluvial clastic units which is an upper part of the discrete and thick parallic sequence (Shweminbon Formation, Loin-an Formation, Kalaw Formation) bearing Mesozoic fossils. Lithologically, the Kalaw Formation can be subdivided into several lithofacies based on the field evidence. These lithofacies and lithofacies association are used as parameters for the stratigraphic correlation, for reconfiguration of the sedimentary bodies, for the interpretation of the paleoenvironment. At least five lithofacies can be recognized from the formation, Lithofacies A, Polymitic paraconglomerate, Lithofacies B, Oligomitic paraconglomerate, Lithofacies C, Sandstone-siltstone interbeds, Lithofacies D, Mudstone with intercalation of thin sandstone layer, Lithofacies E, Mudstone with intercalated of thin sandstone and conglomerate. The lithofacies varied laterally into each other within a kilometre. The red and purple sandstone-mudstone alteration is predominated in the sequence of the Kalaw Formation, while the oligomitic paraconglomerate are found as proximal fan deposits where as polymitic paraconglomerate are found as distal fan deposits.

Keyword: paralic sequence, Lithofacies, paleoenvironment

Introduction

Several lithostratigraphic units of the Mesozoic age have been established from the western part of the Shan Plateau, and among them some are homotaxial and showing variation in lithofacies reflected by the changes of local environmental condition. Figure (2) Therefore, various stratigraphic columns reported by previous authors from the different localities along the Shan Plateau were visited and examined for the regional lithostratigraphic correlation and stratigraphic synthesis. The Kalaw Formation has been recorded as key horizon in the upper part of the Mesozoic paralic successions as it stratigraphically overlies all older units of the western part of Shan Plateau. However, post-Mesozoic tectonics of Myanmar has caused the sequence not only fragmented in stratigraphic column but also repeated and omitted in outcrop sections.

In addition, up-side-down positions and overturned sections are also observed due to the intense tectonic transpression during and after deposition of Kalaw Formation.

Objectives of the research

Present research was carried out to do the regional stratigraphic correlation of Mesozoic units of eastern Myanmar based on the easily recognizable lithofacies and lithofacies associations of the Kalaw Formation observed elsewhere on the the Shan Plateau.

Besides, it was done for the configuration of the paleodepositional environments and reconstruction of the paleogeographic setting of Shan Plateau in geologic past, in relation to the Kalaw Formation based on the sedimentological deduction on the identified lithofacies and lithofacies associations.

Study areas

The red beds and associated rocks are widely distributed in the Ywa-ngan, Pindaya, Kalaw, Heho and Pinlaung Townships. Topographic map and google image showing studied localities for present research are as shown in (Figure 1). Well-exposed sections were found along the road-cuts, rail-cuts and cart-tracks, for example along the car-road between Nampandat village and Kalaw. Some are well exposed on the hill slope covered with sparse vegetation, for example along the Taungni-Aungban-Legya range, and the Shwe-myin-din

[1] Professor and Head, Department of Geology, East Yangon University.
[2] Rector, Monywa University

range of Hsikhip area. The Mesozoic rocks including present studied Kalaw Formation exposed in the following areas were examined for the present research.

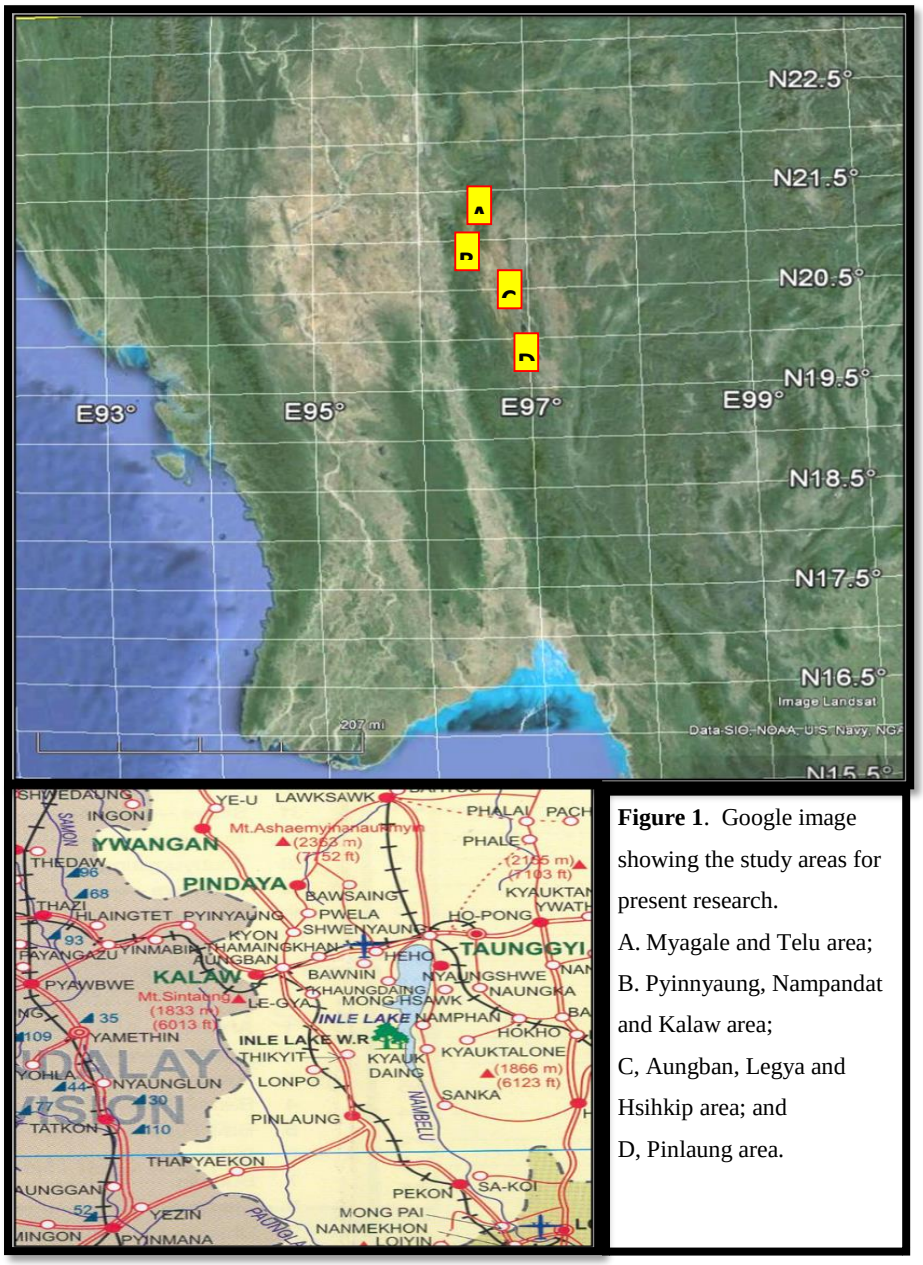

Figure 1. Google image showing the study areas for present research.
A. Myagale and Telu area;
B. Pyinnyaung, Nampandat and Kalaw area;
C, Aungban, Legya and Hsihkip area; and
D, Pinlaung area.

Materials and method of the study

Present research was carried out according to follow the procedure described below.

- Literature survey and critical reading on the previous works on lithostratigraphic classification of the Mesozoic rock units exposed in the areas,
- Preparation of topographic maps (base maps) and satellite images of the study areas for field observation and spot-checking,
- Field observation and geological data collection at outcrops of Kalaw Formation and juxtaposing rock units exposed around the Ywa-ngan, Kalaw, Legya, Hsikhip, and Pinlaung, in southern Shan State,
- Megascopic study of the texture and structure of the sedimentary beds and clasts

lithology of conglomerates at outcrops,
- Petrographic study of the thin-sections of collected samples,
- Data compilation, interpretation and documentation.

Common Lithofacies Association

The Kalaw Formation is composed of three principal facies associations:

(1) lithofacies association I; alluvial fans and pebbly braided rivers (conglomerates and sandstones) with mudflat,
(2) lithofacies association II; low-sinuosity distal sandy braided rivers with flood plain (sandstones and mudstones) and
(3) lithofacies association III; terminal fan with mudflats (conglomerate, shell beds and mudstones).

Lithofacies association I: ***Alluvial fans and pebbly braided rivers*****:**

Alluvial fan and pebbly braided river sediments occur at the base of the sequence. The inner fan zone is characterized by debris-flows or mud-flows, the mid fan zone is dominated by sheet floods, and the outer fan zone is governed by stream flood and stream flow which might be passing into pebbly braided rivers located in front of the fans.

The predominate lithofacies of this association is "angular polymictic paraconglomerate", lithofacies A. The conglomerate is made up of largely of poorly bedded (about 10 to 25 cm thick), hard, red to purple, and weathered to red colour on the surface. The pebbles are subrounded to angular clasts of, indurated mudstone, limestone, quartz, chert, reddish fine-grained sandstone and dark red gritty quartzose sandstone, in order of abundance. The rock is matrix-supported by the reddish arenaceous matrix, which is locally calcareous. There are few thin interbeds of red calcareous gritty sandstone which are cross-bedded and ripple-marked. This type of conglomerate is well exposed on the walls and roof of the Shwe-u-min pagoda cave, in Kalaw. Shown in Figure (2)

The second predominate is "lithic arenaceous sandstone-siltstone lithofacies", lithofacies C. Shown in Figure (3). The sandstone is 3-10 cm thick beds, sharp and erosive based, red and purple, fine- to mediun-grained. Microscopic examination of the rocks has shown that the detrital clasts are clouded quartz (45 %), micas (both detrital and authigenic mica, less than 5 %), opaque minerals (about 5 %), reddish brown iron pigment (both hematite and limonite, about 10 %), calcite cement (about 5 %) and matrix (more than 10 %). The allochems are set together by a calcareous and sericitic matrix. Among this lithofacies, the intercalated thin sandstones with wavy cross lamination and ripple-marks are interpreted as shifting channels. The geometry of the intercalated channel sands exhibits convex sharp base with relatively flat top in cross-section. The beds range in thickness from 5 to 45 cm. Basal soles, such as, flute-casts, and tool-marks are common and asymmetrical current-ripples are observed on the top of the channel sand beds. The lithofacies association is interpreted to represent a broad and shallow braided channel on smooth mudflat.

The less common lithofacies is "subangular oligomictic paraconglomerate", lithofacies B. It is found as a debris flow deposit composed mainly of angular limestone and dolomitic limestone fragments with a range of size between 1 cm and 6 cm, and an average size less than 3 cm, maximum size of 30 cm is exceptional. A phenoclast-count indicates reddish sandstone clasts (5%), calcitic limestone (20%), dolomitic limestone (50%), calcitic cement and matrix impregnated with ferruginous materials (25%). The facies is well developed on the northwestern slope of Legya hill, near Legya village and 3 km southwest of Hsikhip. Shown in Figure (2).

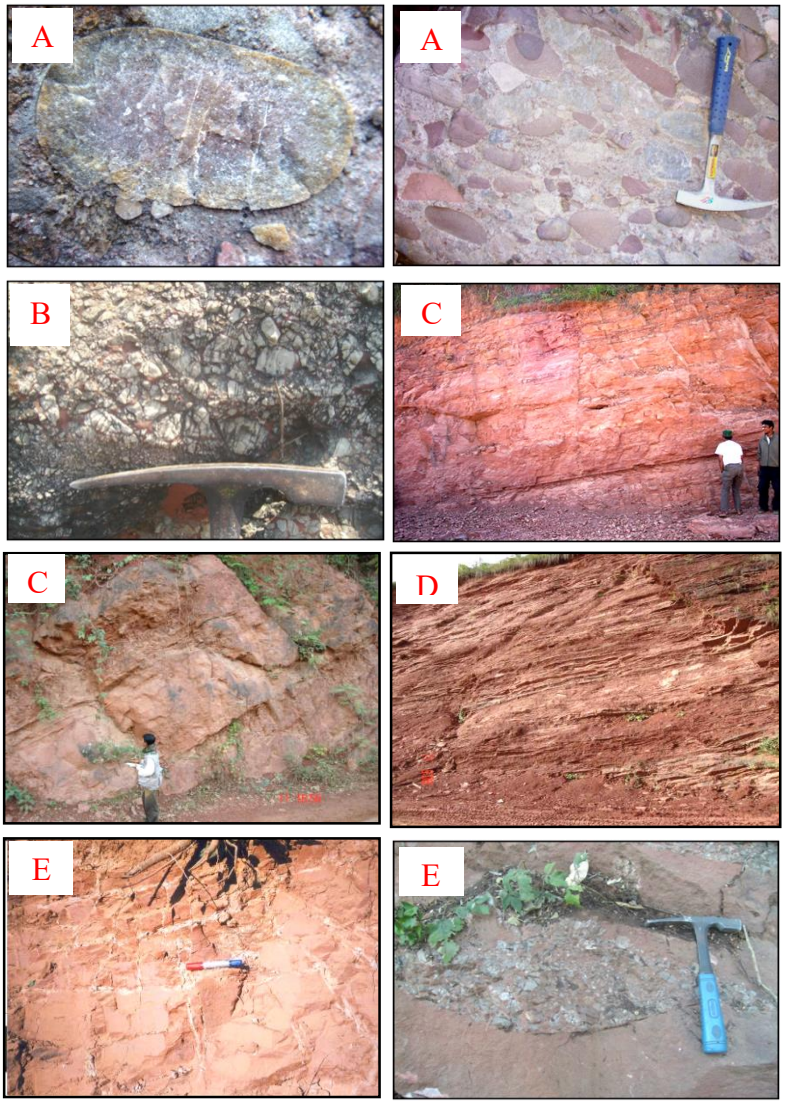

Figure 2. Lithofacies A, Polymictic paraconglomerate, with well rounded orthoquartzite pebble. Lithofacies B, Oligomictic paraconglomerate, comprising angular and unsorted dolomitic
limestone clast, Lithofacies C, Sandstone-siltstone interbeds, Lithofacies D, Mudstone with intercalation of thin sandstone layers, Lithofacies E, Mudstone with intercalation of thin channel sandstone and conglomerate legs.

Lithofacies association II : ***Low-sinuosity distal sandy braided rivers with floodplains***: With transition from restricted alluvial fans to an open braided plain, the pebbly rivers soon evolve both vertically and horizontally into sandy stream networks consisting of channels and floodplains. The floodplain facies is divided into proximal and distal part. The proximal floodplain facies comprises interbedded sandstones and mudstones containing some layers of nodular pedogenic carbonates and originates by overbank sheet-flood, levee overtopping and crevasse-splay sedimentation.

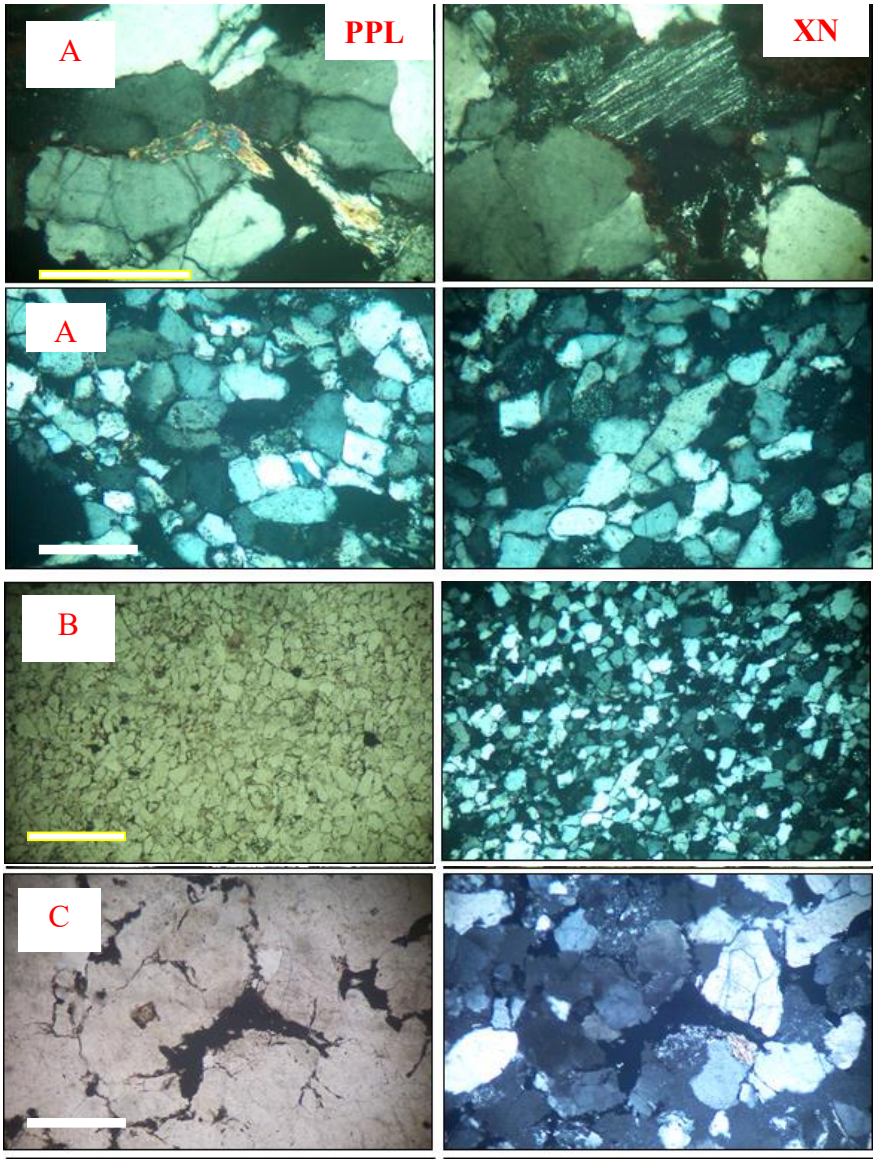

Figure 3. (A). Lithofacies C, Sandstone-siltstone interbeds. (**B)**. Lithofacies D, Mudstone with intercalation of thin sandstone layers. (**C)**. Lithofacies E, Mudstone with intercalation of thin channel sandstone and conglomerate legs. Photomicrographs showing the mineral composition, texture and iron-pigment occurrence in the sandstones of Kalaw Formation, Legya area. (Scale bar is 0.5 mm in length).

The most predominate is "lithic arenaceous sandstone-siltstone lithofacies". The petrographic characteristics are as same as previous sandstones (Lithofacies C).

The second predominate is "polymictic paraconglomerate lithofacies", Lithofacies A. There is a marked variation in the roundness of the pebbles and lithology of the clasts. The conglomerate is made up of largely of poorly bedded (about 3 to 15 cm thick), hard, light grey, and weathered to red colour on the surface. The pebbles are subrounded to well-rounded clasts of porphyritic volcanic rock, limestone, reddish fine-grained sandstone and dark red gritty quartzose sandstone. In some places as in the Myagale, Telu and Pinlaung areas, the well-rounded light coloured algal limestones become abundant. A pebble of white marble was found at the road-cut, near the Myatheintan Pagoda point, east of Hsikhip. The conglomerates are matrix-supported with a reddish arenaceous matrix, which is locally

calcareous. There are few thin interbeds (up to 10 cm thick) of red calcareous gritty sandstone which are cross-laminated and ripple-marked.

Lithofacies association III: Terminal fan with mudflats: The terminal fan facies is built up of mud with minor layers of silt and conglomerate with intercalations of calcareous shell beds and originates in estuarine mudflats. Depositional sequences within the sandy braided river series comprise major sequences that are produced by migration of alluvial subenvironments during course of their aggradation, and minor sequences that are related to alternating high- and low-water stages with changing channel abandonment and stream neoformation.

The poorly bedded mudstone is intercalated with siltstone-sandstone which is 5-30 cm thick and polymictic paraconglomerate (Lithofacies D and A) which is 4 to 15 cm thick beds. The mudstone which tends to be shaly and the siltstone-sandstone lithofacies is locally calcareous. As the lithofacies is a multicyclic thin sandstone and mudstone, the facies is considered to represent an overbank-flow deposit formed by gravitational settling of suspended fines away from the active feeder channels. The individual thickness of the lithofacies varies both laterally and vertically in the association. Lithofacies A in this association dominates in the lower part of the formation (proximal fan) where as the Lithofacies B predominate in the upper part of the formation (distal fan). Bleaching spots (up to 3 cm in diameter) are common and unaltered nucleus (mostly limestone clasts, calcareous bioclasts) are observed in places. Horizontal grazing burrows and vertical bioturbation are found in the mudstone of this association. In the Legya area, the lower part of the formation consists a thick sequence of Lithofacies D and yields sand-volcanoes and climbing ripples.

Apart from the conglomerates, extensive outcrops of the formation are covered by the red mudstone of this distal fan and overbank association. The exposed Lithofacies association III along the Huba chaung, east of Wetphyuye and northeast of Legya village represent the upper part of the Kalaw Formation. The association is well exposed at road-cut near Nampandat village and on the beautiful natural wall at the northern gate of Kalaw.

Summary and Conclusion

As a reference section of the Kalaw Formation, the rail-cuts between Myindaik and Kalaw stations were observed. In addition, the sections exposed along the Hkagyingu and Nampandat streams, road-cuts between Pinlaung and Pyinmana, and those exposed near Legya village are also good for the reference sections. The red and purple sandstone-mudstone alternation is predominated in the sequences of the formation, while the oligomictic paraconglomerate are found as proximal fan deposits whereas the polymictic paraconglomerate are observed as distal fan deposits. Locally, sediments of the various zones of alluvial fans were found. The inner fan facies consists of debris-flow and mud-flow deposits. The mid-fan sediments are built up of conglomerates, sandstones and mudstones arranged in fining-upwards sequences. The distal fan and pebbly braided river deposits are characterized by conglomerates, sandstones and mudstones associated with fluvial channels which also display fining-upwards sequences.

Acknowledgments

Thanks are indebted to Prof. Dr. Nay Win Oo (Rector of the East Yangon University) for his kind financial allowance for present research. Thanks are also due to the Township Administrative Committees of Pinlaung and Ywa-ngan Townships.

I would like to express my heartfelt thanks to my Master thesis and Doctoral thesis supervisor Prof. Dr. Thura Oo (Rector of Monywa University) who encourages me to carry out further researches and studies in the Stratigraphy of Myanmar. Several discussion followed by literature survey and field observation, compilation and synthesis on Myanmar tectonics and stratigraphy of Myanmar leading to reconstruction of paleogeography, and integration with sedimentological and paleontological evidences of several previous authors for the regional stratigraphic correlation were done under his guidance. In addition, most of the photographs with geologic notes were provided by him.

References

BENDER, F., 1983. *Geology of Burma*. Gebrüder Borntraeger, Berlin, 293 pp.

BROWN, J. C., and SONDHI, (1933) "The geology of the country between Kalaw and Taunggyi, southern Shan State, Burma" Geol. Surv. India, Rec., Vol. 67, pp. 166-247.

CHHIBBER, H.L., 1934. *Geology of Burma*. Macmillan, London, 538 pp.

CLEGG, E.L.G., 1941. The Cretaceous and associated rocks of Burma. *Geol. Surv. India, Mem*., **74**: 1-101.

DUNHUM, R.J., 1962. Classification of carbonate rocks according to depositional texture. *Amer. Assoc. Petr. Geol*., Mem. **1**: 108-121.

METCALFE, I., 1988. Origin and assembly of southeast Asian continental terranes. In: AUDLEY-CHARLES, M.G. and HALLAN, A., (Eds.), Gondwana and Tethys, Geol. Soc. London, Spec. Publ., 37: 101-118.

METCALFE, I., 1996. Pre-Cretaceous evolution of SE Asian terranes. In; HALL, R. and BLUNDELL, D., (Eds.); Tectonic evolution of Southeast Asia. Geological Soci. London, Special Publication No. 106: 97-122.

METCALFE, I., 1997. The Paleo-tethys and Paleozoic-Mesozoic tectonic evolution of Southeast Asia. p. 260-272.

MITCHELL, A.H.G., 1981. Phanerozoic plate boundaries in mainland SE Asia, the Himalayas and Tibet. Jour. Geol. Soci. London, 138:109-122.

MITCHELL, A.H.G., 1989. The Shan Plateau and Western Burma: Mesozoic-Cenozoic plate boundaries and correlation with Tibet. In: ŞENGÖR, A.M.C., (Ed.), Tectonic evolution of the Tethyan region, Kluwer Academic Publ., p. 567-583.

MITCHELL, A.H.G., 1992. Late Permian-Mesozoic events and the Mergui Group Nappe in Myanmar and Thailand. Jour. S. E. Asia. Earth Science, 7: 165-178.

MITCHELL, A.H.G., 1993. Cretaceous-Cenozoic tectonic events in the western Myanmar (Burma)-Assam region. Jour. Geol. Soci. London, 150: 1089-1102.

MITCHELL, A.H.G., 1998. Myanmar as a nappe stack and relationship to plate collisions and the Himalayas. Siminar paper read at Myanma Oil and Gas Enterprise, 12 pp.

MITCHELL, A.H.G., TIN HLAING and ZAW PE, 1978. Structural units and post-Devonian geological history of Burma. Unpubl. report, Geological Survey and Exploration Project, Myanmar, 57 pp.

MIDDLEMISS, C.S. 1900. General Report of the Geological Survey of India (1899-1900). p. 128.

THURA OO (2000) A biostratigraphic synthesis on the Cretaceous Foraminifers in Myanmar. Ph D Dissertation, Geology Department, Yangon University (Unpublished).

THAN THAN THWE (2004) Lithofacies and biofacies analysis of the Kalaw Formation, Legya Area, Kalaw Township M. Sc. Thesis. Geology Department, Yangon University (Unpublished).

ENGINEERING GEOLOGICAL INVESTIGATION OF MYO GYI MULTIPURPOSE DAM PROJECT, YWA-NGAN TOWNSHIP, SHAN STATE (SOUTH)

Myint Myint Soe[1], Kyaw Htun[2]

Abstract

The Myo Gyi Multipurpose Dam project is located on Zaw Gyi River near Myo Gyi village in Ywa Ngan Township, Southern Shan State. It is bounded at a Latitude 21˚ 26' 36" N to 21˚ 28' 45" N and Longitude 96˚ 22' 10" E to 96˚ 25' 00" E of one inch to one-mile scale topographic map index of 93/C7. Myo Gyi Dam is a zone type filled dam. Engineering geological study data analysis is used for investigation of Myo Gyi Multipurpose Dam projects. The study area is mainly composed of lithostratigraphic units ranging in age from Precambrian to Silurian. With thoroughly site investigation many times to implement Myo Gyi Multipurpose Dam Project. Engineering geological investigation of Myo Gyi Multipurpose Dam Project is carried out in order to provide engineering geological information, especially for foundation of the dam and parts of dam construction structures. The rock outcrops observed at power tunnel inlet are black slate, moderately weathered, hard and joint 2 sets. The outcrops observed at power tunnel outlet are phyllite and metagreywacke, which are light grey, moderately weathered, very hard and 2 sets of joints with quartz veins. The project area consists of main dam (zone filled type), spillway (chute type), diaphragm wall, diversion tunnel (at right abutment), power tunnel (at right abutment), power house and switch yard are major structures of this project.

Keywords: power tunnel (at right abutment), spillway (chute type), diaphragm wall, power house and switch yard

Introduction

The dam site, spillway and their appurtenant structures and tunnels are located in different geological formations. Therefore, the studies of site investigation, all methods of geotechnical testing, engineering geological conditions of dam sites and tunnels are focused and described separated for the convenience.

Engineering geological investigation of Myo Gyi Multipurpose Dam Project is carried out in order to provide engineering geological information, especially for foundation of the dam and parts of dam construction structures. For convenience, the discussion on the foundation is focused dividing into different section like the River Section, the Left and Right abutment sections. The engineering geological map and cross-section of the project area is shown in Figure 1

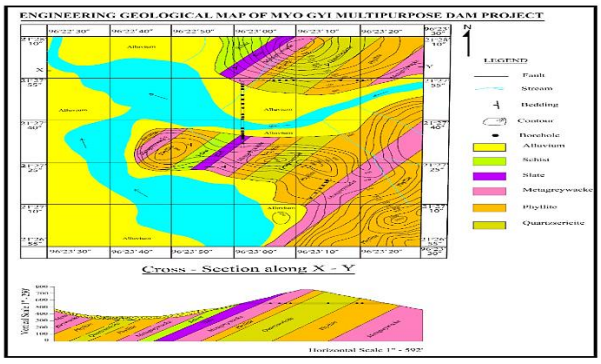

Figure 1. Engineering Geological Map and Cross-Section

[1] Lecturer, Department of Geology, East Yangon University.

[2] Visiting Associate Professor, Dr, Engineering Geology Department, Yangon Technical University, Myanmar

Geology of Dam Site Area

The major rock types are metagreywacke and phyllite. In the left abutment of main dam, metagreywacke and phyllite are found. In the right abutment of the main dam chlorite phyllite, black slate, metagreywacke and quartzite are found. At the downstream of the left abutment, weathered meta-greywacke and phyllite are found as highly jointed. Parts the dam site, several local faults are found.

Drilling Investigation for Myo Gyi Multipurpose Dam Project Area

The investigation programme is based on the diamond core drilling works with core sampling and water pressure testing. Detailed core logging works with core sampling. Water pressure testing and rock quality designation records are taken at diversion tunnel works for investigation. Total number of (17) drill holes were sunk to about bed rocks and its characteristics and for confirmation of gravel bed thickness in the dam obtaining the information site area.

Engineering Geological Condition of Main Dam Axis

Drill Hole data from the main dam axis and its diaphragm area showed that the whole dam base area was occupied by a thick gravel and boundary deposit. Its thickness is 16 feet in shallow portion and maximum depth is 62 feet. These gravels or boundary deposits are underlined by a clay, soft and cohesive materials in diaphragm alignment. The thickness of the intermediate layer is 4 feet to 8 feet in maximum. In fact, The dam site area falls in a final gravel basin of Zaw Gyi river and construction of an impervious seepage barrier. In the dam foundation, treatment was made by means of consolidation grouting in gravel or boulder layer and curtain grouting about 30 feet in bed rock.

Engineering Geological Condition of Right Abutment of Dam

To know the detailed subsurface conditions, twelve bore-holes such as DH-1, CDH-2, DH-2, CDH-3, DHN-5, DHN-4, CDH-4, CHN-3, DH-3, DAH-07-01, DAH-07-02 and DAH-07-03 are performed along the dam axis of right abutment. The depths of the bore-holes are 84 ft, 120 ft, 200 ft, 130 ft, 150 ft, 120 ft, 100 ft, 120 ft, 107 ft, 100 ft, 100 ft and 63 ft respectively.

According to the bore-hole data, average thickness of overburden soil is about 6 ft. In CDH-3, gravel formation is about 55 ft thick. Phyllite is also found between 60 ft and 130 ft and lugeon values range from 42 Lu to 130 Lu.

In DHN-5, highly to completely weathered are found from 50 ft to 65 ft in depth. Lugeon values are from 6.4 Lu to 53.5 Lu. In DHN- 4, Lugeons values range from 4.6 to 30.4 Lu. In CHN-3, there is phyllite in the lower portion and Lugeon values are from 4.3 Lu to 85.5 Lu. Two water loss zones are found in DH-3. Therefore, these zones can be regarded as highly weathered zone. Phyllite occurs from 6 ft to 107 ft in depth. Metagreywacke is in the lower portion of DAH-07-01. RQD values are good. Phyllite is also found in DAH-07-02 and DAH-07-03. Therefore, it is necessary to perform the treatment for the required foundation condition.

Engineering Geological Condition of the Left Abutment of Dam

Altogether five bore-holes are examined along the dam axis of the left abutment to investigate the foundation condition.

The five bore-holes are DHN-1 (100ft) (Incline hole), DHN-2 (120 ft), CDH-1 (80 ft), DHN-6 (100 ft) and DHN-7 (100 ft). According to the test result, Lugeon values are high in remaining three bore-holes except an incline hole. The lithology of the left abutment is overburden soil in the upper portion. In the middle part, gravel formations and phyllite are

found in middle and lower sections. Metagraywacke and phyllite are observed in the left abutment of Myo Gyi dam. It is medium to thick bedded, grey to reddish brown colour. Phyllite is thin to medium bedded, light green to reddish brown colour. Metagraywacke and phyllite are high angle and nearly vertical. Both kind of rocks interlayered on both abutment degree of differential weathering in phyllite may lead to rock slide at thickly bedded metagraywacke portion.

The rock formations are interbedded of Phyllites and Metagreywacke; and 1´ to 4´ thick, curshed zones are also observed within the above rock stratas. White rock powder (Gpige) filled joint 2 sets are observed at Metagreywacke and iron oxide stained joint 2 sets and slicken sided bedding plane surfaces are observed at phyllite strata. Core loss % is low along the entire drill hole and the permeabilities (k) are DHN-1; 43.5 Lu between 10 ft and 30 ft in depth in DHN 2; 35.6 at 30 ft and 50 ft, CDH1; 23.7 Lu at 50 ft and 70 ft in depth , DHN 6; 15.3 Lu between 70 ft and 90 ft in depth.

Engineering Geological Condition of the Spillway

There are seven bore holes in spillway, namely EXTRA-1, SPW-1, SPW-2, CHT-1, SPW-4, BSN-1and SPW5. Spillway is located at the left abutment of the reservoir. Lithology of the spillway is similar with main dam site. Up welling of groundwater occurs at spillway basin site along bedding plane because its design bed level is lower than the existing Than Bo stream. Rock slide of the spillway is still in slow progress. Shotcreting is necessary to give further treatment during dry season period with wire meshing and rock bolting at downstream site of the slope and inner side slope of the left abutment at upstream side.

Engineering Geological Condition of the Power House

Power House is located at the right abutment. Lithology of the power house is fresh, hard and strong metagreywacke. They are downstream dipping bed with high angle and moderately to thickly bedded characteristics. Further grouting treatment works on right hand side and upstream side of the Power house area would be necessary to prevent from seepage water encroachment to surrounding area of the Power House at shown in Figure 2.

Engineering Geological Condition of the Weir Site

Myo Gyi weir is located on the Aungban- Hanmyintmo motor car bad between Kinn village and Thanywa village. It is about 5 miles from Main Dam. Lithology of the weir site is milky white limestone with traces of karst development. Limestone on weir site alignment is slightly to moderately weathered. This alignment is rejected at first and proposed for shifting to light green zone of phylite rocks. Unfortunately, this site has a thick gravel layer resting on foundation rock and river valley is very broad at the same time. Second alignment for weir site is investigated again at upstream portion of the Zaw Gyi River by geophysical method. In this alignment, gravel bed thickness in stream area is about 14´. It is favorable for construction of a weir.

Part of Dam Construction

Part of the Myo Gyi Dam construction consists of diaphragm wall, diversion tunnel, power tunnel, power steel penstock, tailrace structure, tail water canal, and switchyard.

Diaphragm Wall

The first alignment is at 550 feet upstream from main dam axis and later it was shifted to present location at RD-445 feet up stream from main dam axis. The length of diaphragm wall is 1695 feet and 48 feet in depth. There encountered a swampy pocket between panel No. 44 and right abutment of dam as shown in Figure 3.

Diversion Tunnel

Diversion tunnel is located on the right abutment of Myo Gyi dam. The shape of diversion tunnel is in standard horse shoe. It is 486 meter in length and 5.5 meter in diameter.

The distance of diversion tunnel is about 5 meters away from the end point of the main dam. Lateral distance from diversion tunnel to power tunnel is about 15 meters. Leading channel portion of this diversion tunnel is composed of river materials and groundwater table is very close to natural ground surface level as shown in Figure 3.6. Six numbers of drillhole were sunk at diversion tunnel outlet area for confirmation of lithology, permeability inlet rock R.Q, and for their in-situ joint setting as shown in Figure 4.

Diversion Tunnel Inlet

Moderately weathered metagreywacke are majority and Phyllites outcrops are minority. The outcrops are observed as 2 sets of joint. Joint planes are filled with iron oxide stained and white rock powder (gouge). Although it had a high dip angle (dip60°) and its weathering stage and scarp-slope side, no rock slides (landslides) were observed at the inlet portion.

Diversion Tunnel Outlet

The outcrops are highly to completely weathered phyllite and metagreywacke with thin quartzite veins. The metagreywacke outcrops are weak and crushed, brecciated and highly jointed with 3 sets. Join planes are weak and iron oxide stained and filled with white rock powder (gouge). Phyllite strata having smooth slicken size bedding plane surface show high dip angle dip 57. Therefore, high dip angle of the strata, highly jointed rock structure, weathering state and dip-slope side are causing steep slope and rock sliding (landslide) downward trending towards the tunnel alignment.

Main Structures of Power Tunnel at Myo Gyi Multipurpose Dam

Myo Gyi Hydropower Project is located at the upstream of Ngapyaung weir which was built for supplying irrigation water in Kyaukse area. The project comprises principally of two 15 MW generators with installed capacity of 2x15MW, a rated head of 52.4 m, and a quantitative discharge of 84 m^3/s. The main structures of the power tunnel are intake structure, power tunnel, power steel penstock, power house, tailrace structure, tail water canal and switchyard.

Figure 2. Power House

Figure 3. Diaphragm Wall

Main Structures of Power Tunnel at Myo Gyi Multipurpose Dam

Myo Gyi Hydropower Project is located at the upstream of Ngapyaung weir which was built for supplying irrigation water in Kyaukse area. The project comprises principally of two 15 MW generators with installed capacity of 2x15MW, a rated head of 52.4 m, and a quantitative discharge of 84 m^3/s. The main structures of power tunnel are intake structure, power tunnel, power steel penstock, power house, tailrace structure, tail water canal and switchyard.

Intake Structure

The intake structure is laid out of the right bank of the dam with a design putative discharge of 84 m^3/s, the intake is provided with two 4.5 x 18.0 m trash racks and on 6x6m quick-acting emergency plate gate. The minimum pool level is 179.00 m, normal level is 197.00 mm, design flood level is 210 m, and check flood level is 216.18 m. The intake is 29 m long, 16 m wide, and 55.15 m high, with a foundation elevation of 162.35 m, base plate top elevation of 166.35 m, and maintenance platform elevation of 217.50 m. On the maintenance platform, a gate hoist room is set, and reinforcement concrete structure is adopted as shown in Figure 5.

Power Tunnel

The power tunnel is 406.103 m long and the design discharge is 84 m^3/s. The tunnel is composed of the inlet transition section, and tunnel body section, etc. The inlet transition section is 10 m long with a bottom slope of 166.35 m and the tunnel body section is 406.103 m long, with a bottom slope of 1/40.

The section is in horse-shoe shape. After the concrete lining, the section is changed to round shape with an inner diameter of 6 m. The steel penstock is covered with a concrete lining. According to the preliminary calculation 0.5 m thick reinforced concrete lining is used. The investigation programmed is based on the diamond core drilling works with core sampling and water pressure testing. Detail core logging works with core sampling and water pressure testing and R.Q.D records are taken at power tunnel investigation works.

Drill holes were sunk to know about bed rocks and their characteristics and for confirmation of gravel bed thickness in dam seat area. The power tunnel is located on right abutment. The level difference to diversion tunnel is 20.5 m. Lateral distance from diversion tunnel to power tunnel is about 15 m.

Power tunnel is in circular form and its diameter and length is 6 m and 416 m each. At first six numbers of alignments are chosen for tunneling works. Alignment No 1, 2, 3 are on the right abutment and No 4, 5, 6 are on the left abutment.

Based on drilling logs, R.Q.D, degree of rock core, and fracturing from left abutment drill holes were unsuitable for tunneling works and abandoned for them. Also, from the drill hole data of P.D.H-2 on alignment No (2) had the less R.Q.D and bad rock core fracturing. Drill hole No (3) (D.H-3) on right abutment has good core recovery and good R.Q.D and it was used as a reference for selection of power tunnel alignment.

Figure 4. Diversion Tunnel of Myo Gyi Dam

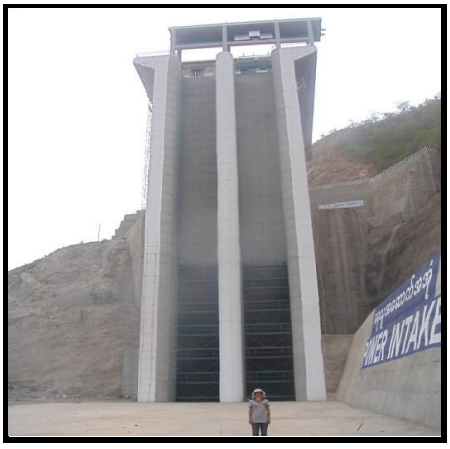

Figure 5. Intake Structure

Power Tunnel Outlet

The outcrops observed at power tunnel outlet are phyllite and metagreywacke, which are light grey, moderately weathered, very hard and 2 sets of joints with quartz veins. The dip direction of the phyllite rock strata is S 80 W and dip amount is 50 W. They are dipping towards the power house side (downstream). The dip slope causes gentle slope at the power tunnel outlet site and scarp slope causes steep slope at the power intake site.

Power Steel Penstock

The power steel penstock consists of the common pipe, irrigation pipe, and the power generation pipe. The common pipe with a diameter of 6000 mm includes the 114 m long tunnel steel lining section and pipe wrapping section. The irrigation pipe with a diameter of 2500 mm is 21 m long. The generation pipe consists of 2 crescent bifurcated pipes and two branch pipes with a diameter of 3000 mm and a length of about 51.5 m for each branch. All the above steel pipes are buried in concrete.

The penstock is laid out by connection to the pressure diversion tunnel at the joint of bifurcated pipe. The penstock is composed of one main pipe; one hem reinforced bifurcated pipe and one Y-shaped reinforced crescent bifurcated pipe, two branch pipes, one irrigation pipe and accessories as shown in Figure 6.

Tailrace Structure

Tail water of the two units flows into the main river channel through the draft tune, tail water gate, linkage section of rectangle tail water canal, and trapezoid tail water open canal. Two tail water gates are arranged, and the orifice size is 6.408 x 2.31 m. Tailrace platform elevation is 150.11 m, and one movable electric hoist is arranged on the platform to carry out open and close operations for the fates. Rectangular cross section is used for the tail water canal, its bottom width is 19.6 m and its base plate and side walls are reinforced concrete lined as shown in Figure 7.

Tail Water Canal

On condition that the upstream and downstream water levels are kept unchanged, the tail water weir crest elevation of the hydropower station shall be 141.12 m. Reservoir open diversion channel can be used as a tail water outlet of a hydropower station, according to the on-site investigation, topographic map of the power house area and base plate elevation points of the open diversion channel provided. The open diversion channel only needs to be modified slightly at shown in Figure 8.

Switchyard

The switchyard is arranged at the end side of the power house, and the booster station floor elevation is 150.11 m. Two oil immersed type transformers, three SFO circuit breakers, seven groups of disconnecting switches, and the 66 kV pressure power distribution units, such as potential transformers, current transformers, and surge arresters are arranged in the switchyard. The length and width of the switchyard is 50 m and 30.5 m as shown in Figure 9.

Figure 6. Power Steel Penstock (Power Generation Pipe)

Figure 7. Tailrace Structure

Figure 8. Tail Water Canal

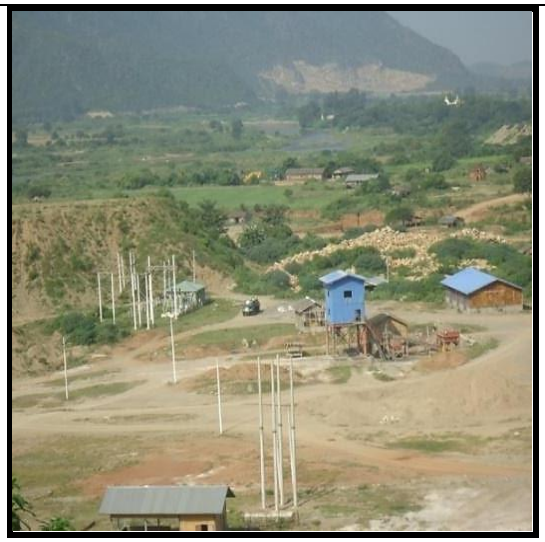

Figure 9. Switchyard

Engineering Geology of The Project Area

During the feasibility and preliminary design stages of a project, when very little detailed information is available on the rock mass and its stress and hydrologic characteristics, the use of a rock mass classification scheme can be of considerable benefit. At its simplest, this may involve using the classification scheme as a check-list to ensure that all relevant information has been considered.

At the other end of the spectrum, one or more rock mass classification schemes can be used to build up a picture of the composition and characteristics of a rock mass to provide initial estimates of support requirements, and to provide estimates of the strength and deformation properties of the rock mass.

Therefore, common rock mass classification system is described separately for the convenience.

Rock Quality Designation Index (RQD)

The Rock Quality Designation index (RQD) was developed by Deere et al. to provide a quantitative estimate of rock mass quality from drill core logs. RQD is defined as the percentage of intact core pieces longer than 100 mm (4 inches) in the total length of core. The

core should be at least NW size (54.7 mm or 2.15 inches in diameter) and should be drilled with a double-tube core barrel. The correct procedures for measurement of the length of core pieces and the calculation of RQD are summarized in Figure 10.

When no core is available but discontinuity traces a visible in surface exposures or exploration admits, the RQD may be estimated from the number of discontinuities per unit volume. The suggested relationship for clay-free rock masses is:

RQD =115-3.3 Jv

Where, Jv is the sum of the number of joints per unit length for all joint (discontinuity) sets known as the volumetric joint count.

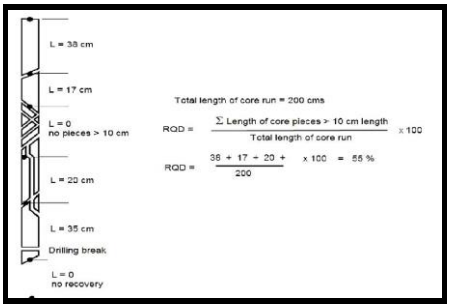

Figure 10 . Procedure for Measurement and Calculation of RQD
Source: Deere and Deere (1988)

Deere proposed the following relationship between the numerical value of RQD and RMR the engineering quality of the rock as shown in Table 1

Table 1. Relationship between RQD Value and Rock Quality

No	RQD	Rock Quality
1	<25	Very poor
2	25-50	Poor
3	50-75	Fair
4	75-90	Good
5	90-100	Very good

Table 3. Rating Adjustment for Discontinuity Orientation

Strike and Dip Orientation of Joints	Very Favorable	0

Table 4. Rock Mass Classes Determined from Total Rating

Rating	Class No.	Description
39	IV	Poor Rock

Source: Deere and Deere (1988)

Table2. Geomechanics Rock Mass Classification of Power Tunnel (Inlet Portion)

Parameter		Description	Rating
1	Strength of intact rock material	<25 MPa	2
2	R.Q.D	<50%	8
3	Spacing of joints	60 mm	5
4	Condition of joints	Slightly rough surface, separation <1mm highly weathered wall	20
5	Ground water	Dripping	4
B	Adjustment for joint orientation	Note 2	0
		Total	39

According to the UCS (Unconfined Compressive Strength) results of the laboratory test and borehole data, the Geomechanics classification (RMR) is mentioned Tables 2, 3, 4, 5, 6, 7

Table 5. Geomechanics Rock Masses Classification of Power Tunnel (Outlet Portion)

	Parameter	Description	Rating
1	Strength of intact rock material	<27.5MPa	4
2	R.Q.D	50%-75%	13
3	Spacing of joints	0.6-2m	15
4	Condition of joints	Slightly rough surface, separation<1mm highly weathered wall	20
5	Ground water	Completely dry	15
B	Adjustment for joint orientation	Note 2	-5
		Total	62

Table 6. Rating Adjustment for Discontinuity Orient

Strike and Dip Orientation of Joints	Fair	-5

Table 7. Rock Mass Classes Determined from Total Rating

Rating	Class No.	Description
62	II	Good Rock

The inlet portion of the tunnel rock mass obtained rating 39, class IV and describes as poor rock, and the outlet portion of the tunnel rock mass obtained rating 62, class II and also described as good rock.

Conclusion

Myo Gyi Multipurpose Dam Project is located on Zaw Gyi River about 0.5 mile away from Kyaukse-Ywa-Ngan motor car road, near Myo Gyi village, Ywa-Ngan Township, Southern Shan State. In the study area, the Zaw Gyi River is the principal drainage feature running in the nearly E-W direction. The tributaries join to the major stream as parallel drainage pattern. The major rock types are cropping out at diversion and power tunnels are; chlorite phyllite, metagraywacke, black slate, and quartz-sericite schist. Dominant rocks are phyllite and metagraywacke. Their general strike is nearly N-S and perpendicular to tunnel axis. All kinds of these rocks belong to Chaungmagyi Series. They required shotcreting treatment with steel wire mesh and rock bolting at every excavated rock surface, to prevent from rock slides in inlet area of power tunnel.The main structures of power tunnel at Myo Gyi Multi-Purpose Project are: intake structure, power tunnel, power steel penstock, power house, tailrace structure, tail water canal, and switchyard.

Diversion tunnel is about 5 m distance from the end point of the main dam. Diversion tunnel is located on the right abutment of Myo Gyi Dam. Diaphragm Concrete Wall has 1695 ft in length and 48 ft average depth under the dam. Spillway site is located at the left side of the reservoir rim at a distance of 2200 ft from the main dam. The spillway is Ogee type and the full R.C width of the spillway is 295.3 ft.

Rocks Mass Classification Method (RMR) has been used to classify the rock mass quality. The strength parameter of rock mass was determined and each parameter had obtained the average value. The two diamond drill holes were drilled at the Power Tunnel Inlet and Outlet. Rock Mass Rating values of the Power Tunnel are in the range of 39 to 62, poor to good rock and class IV to II. Myo Gyi Dam is a zone type filled dam with two impervious center cores and it's both upstream and downstream portion is made up of previous river bed materials as shell earth dam.

Acknowledgements

The authors wish to express their thanks to Dr Nay Win Oo, Rector, East Yangon University, for his permission to carry out present research. We are indebted to Dr Aye Aye Ko and Dr Wah Wah Lwin and Dr Thidar Aung, Pro-Rectors, East Yangon University, for their permission to carry out this research. Finally, we would like to thank the researchers from the Engineering Geology Department at the Yangon Technological University, for their advice.

References

Bieniawski, Z. T. 1989. **Engineering Rock Mass Classification**. Wiley, New York.

Chibber, H.L. 1934. **Stratigraphy of Burma**. London, MacMillan Co.Ltd.

Deere, D. U., and Deere, D. W. 1988. "The Rock Quality Designation (RQD) Index in Practice". In Rock Mass Classification Systems for Engineering Purposes, (ed. L. Kirkaldie), ASTM Special Publication 984: 91-101. Philadelphia: Am. Soc.Test. Mat.

Department of Geology. 1971. "Geology and Mineral Resources, Myo Gyi South, Kinda-Yechanbyin, Nyaunggyat-Yengan area, Kyakse and Taunggyi Districts." R.A.S.U.

Engineering Geology Office 2. 2004. "Technical Report on Engineering Geology of Myo Gyi Multipurpose Dam Project". Ministry of Agriculture and Irrigation.

Field Parties. 1974 to 1978. "Geology of the Myo Gyi Area", R.A.S.U.

Field Party. 1982. "The Geology and Geochemistry of the Rock Units Exposed at the Environs of Hseywa", D.G.S.E.

Field Party. 1985. "The Geology of the Myo Gyi Area and Mapped on a Reconnaissance Level", M.O.C.

Hla Min. 1980. "Geology and Structures of the area, north Thanywa, Kyaukse Township": M.Sc. Thesis, Dept. Geol., R.A.S.U.

Ko Ko Myint. 1989. "Geology of the Myo Gyi Area, Ywa-Ngan Township". M.Sc. Thesis, Department of Geology, University of Mandalay.

HYDROCARBON EXPLORATION TARGETS IN SECOND LINE OF STRUCTURE MAGWE AND MANDALAY REGIONS

Daw Kay Khine Yu[1]

Abstract

These second line well known as the Tuyintaung –Gwegyo Thrust Belt.These Belt is situated on the east flank of Central Myanmar Basin(CMB). The shallow Padaung Oil sands currently exploiting by local peoples in Ngashandaung and Payagyigon area and Tetma oil field indicate the hydrocarbon prone of nature this belt.Most of the Petroleum Geologist considers that this belt has lower hydrocarbon potential than the First Line of Structure (Sabe-Thargyitaung- Chauk- Yenangyaung Oil Field indicates that there must have active source pod the Kyaukpadaung Syncline.The prospectivity of the study area is also high at first line of structure, However due to lack of detailed seismic measurements and insufficient well data, the locations of commercial oil accumulations cannot be identified yet. In the presents study a total of five prospects and four leads are identified in the second line structure of Tuyintaun-Gwegyo Thrust Belt. There are two main play types in the present study area i.e, Structural Play (Thrust related Anticlinal Trap) and Stratigraphic Play (Oligocene- Pliocene Unconformity Trap). In the prospects areas, it can resume exploratory drilling based on the existing data but in the lead areas it will need additional seismic surveys and geological investigation.

Key Words: prospect, lead, play type

Introduction

Location

Second line of structure is located on the east bank of Ayeyarwady River covering Nyaung-U Township, Mandalay Region and Chauk Township, Magwe Region. The geographical coordinates of the study area are between latitude 21°15′ to 21°35′ N and longitude 94°15′ to 94° 45′ E as seen in Figure (1).

Method of the Study

Literature research of the published papers and reports. To conduct a geological transverse to observe the stratigraphy, distribution of rock units, geological structures developed in the study area. Petrophysical analysis of the wireline logs of the wells drilled and reinterpretation of the available seismic data in the study area. Integration of geological and production data for prospect evaluation ranking of the prospect for drilling.

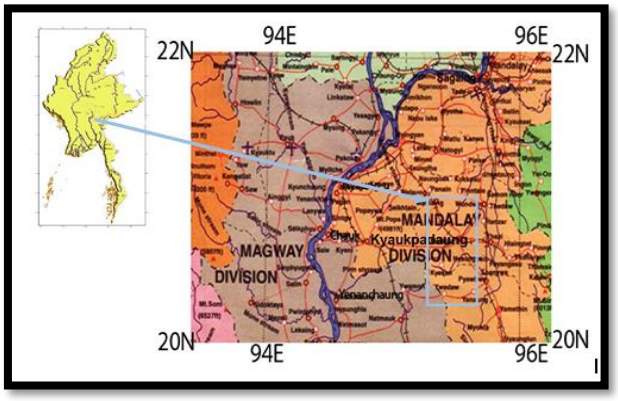

Figure (1) Location Map of the Study Area

[1] Lecturer, Department of Geology, East Yangon University.

Stratigraphy

The stratigraphic succession of the second line well known as the Tuyintaung –Gwegyo Thrust Belt is shown in the table below;

FORMATION	AGE	LITHOLOGY	THICKNESS	DEPOSITIONAL ENVIRONMENT
Irrawaddy	Pliocene	Coarse-grained, yellowish Sandstone	10000+	Fluvial
.....	..... Unconformity.....	.....	.....	.....
Okhmintaung	Upper Oligocene	Sandy unit with distinct shale horizons	6000+	Shallow, marginal marine
Padaung	Middle Oligocene	Thick shale beds with subordinate thin Sandstones	4000+	Shallow marine
Shwezetaw	Lower Oligocene	Sandstone & Clay	3000+	Shallow marine
Yaw	Upper Eocene		2820+	Shallow Marine
Pondaung	Upper Eocene	Hard fine grained Sandstones	3000+	swampy to shallow marine to lake environment

The research area is mainly composed of sedimentary rocks. In this area, Cenozoic age rocks are found in Pegu Group in Okhmintaung Formation, Padaung Formation and Shwezetaw Formation have cropped out to the surface along the thrust.

Geological Structure

The second line of structure is the developed on the east flank on the Central Myanmar Basin. These second line well known as the Tuyintaung –Gwegyo Thrust Belt.This belt trends in N-S direction in the distance of extension is over 50 km along the strike. As seen in (Figure 2) the thrust belt can be subdivided into three structural segments namely Tuyintaung, Gwegyo and Ngashandaung. All three segments are trending in NW-SE direction in the length of segments are 20 km, 25 km and 10 km respectively.

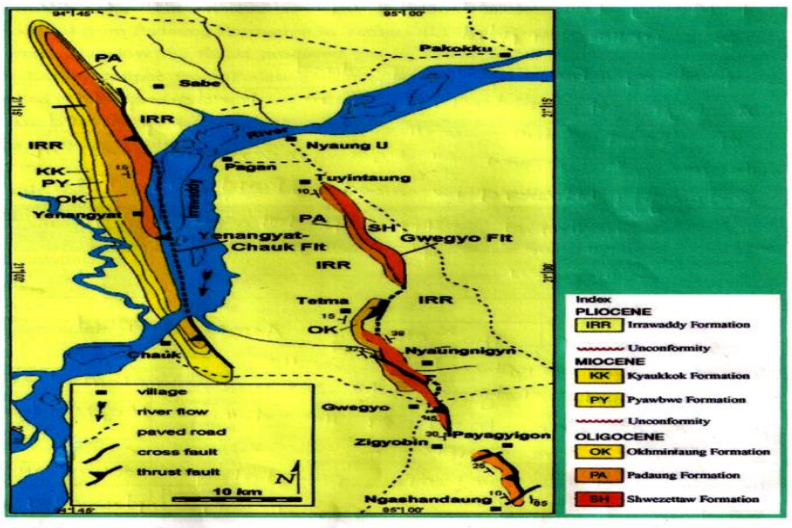

Figure (2) A simplified Geological Map of Study area (source MOGE)

Identification Targets

In the petroleum industry, the terms **"Lead", "Prospect" and "Play Type"** are commonly used for identification of exploration targets. There are two main play types. In the present study area i.e Structural Play (Thrust related Anticlinal Trap) and Stratigraphic Play (Oligocene- Pliocene Unconformity Trap). The leads and prospects which were developed in the study area are identified by integrated evaluation of the surface geological data, oil and rock geophysical data, exploratory well log data and well testing data. As a result of integrated evaluation, **(5) prospects, (4) leads** are identified in the study areas. The prospects are immediate drillable areas while leads are potential area but need further evaluation.

Exploration Targets

Structural Prospect

Tuyintaung Prospect

Tuyintaung structure is located at Latitude 21° 05′ N and Longitude 94° 55′ E and lies in the area bounded by Nyaung – U township (North) and Taungzin village (south). This structure trends is NNW-SSE direction. It is thrusted asymmetrical anticline Figure (3). Tuyintaung structure bears good condition of petroleum accumulation and the key exploration target horizons exist in Padaung and Shwezetaw formations. BOC resumed test drilling 1n 1963 and drilled Pagan Hill Well 3 to a final depth of 11,014 ft and hydrocarbons were tested from sub-thrust Pondaung Formation. MOGE drilled 3 wells during the years 1981 to 1987 produced oil and gas from Padaung and Shwezetaw Formations are well No.1 reached 9832 ft and tested waxy crude oil and gas from Pondaung sandstones.

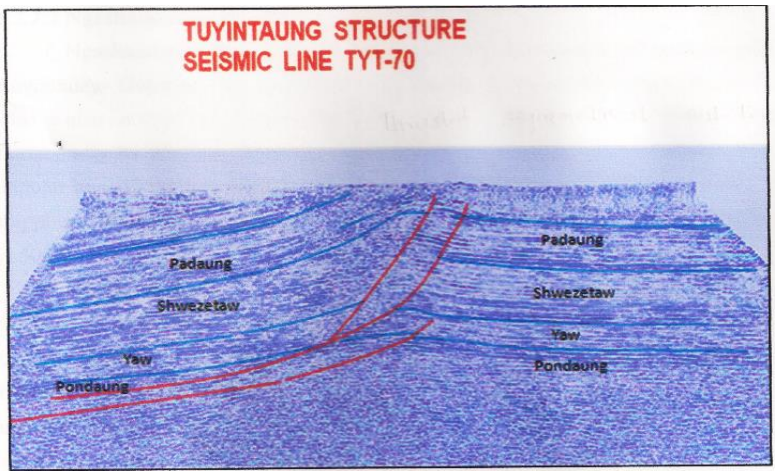

Figure (3) N-S Seismic Section of the Tuyintaung Structure (Source MOGE)

Tetma Prospect

The Tetma structure is a thrusted anticline trending north-south direction as shown in Figure (4) near Tetma village and then swings S-S-E direction from Chaungmagyi Chaung till 41/2 miles north – east of Ayadaw village. Most of the cross faults are trending NE-SW direction. There seems to be a concealed major Shwezetaw Formation and Padaung Formation suddenly disappear near Shawbin village. This fault is probably Pre -Irrawaddian in age. In Tetma area, BOC drilled three wells during 1961-63. Well NO.1 to a depth of 1060 ft had gas shows at 275 ft and 512 ft, well NO.2 to a depth of 561 ft had indication of gas at 376 ft and well NO.3 to a depth of 2275 ft had gas show at 600 ft and 700 ft and encountered on oil show at 1855 ft . MOGE drilled 24 wells during the years 1981 to 1987 and produced oil and gas

from Padaung and Shwezetaw formations. Tetma Oil Filed has a very high remaining hydrocarbon potential but needs further evaluation by using high resolution 2D and 3D seismic surveys.

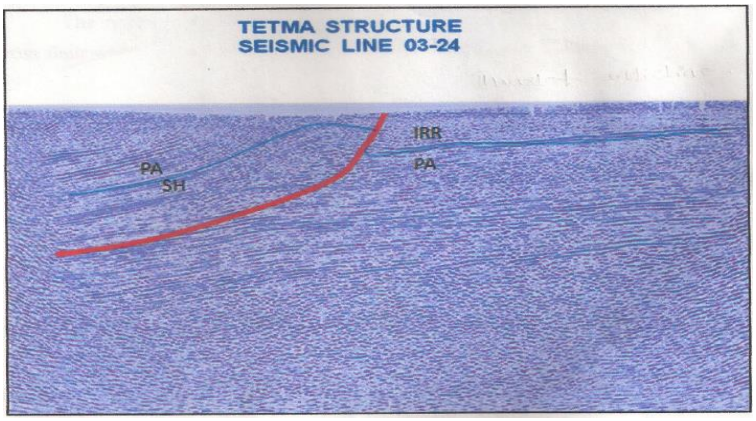

Figure (4) N-S Seismic Section of the Tetma Structure (Source MOGE)

Ngashandaung Prospect

This is also an anticline structure which is located in the down thrown side of southern part of Tuyintaung- Gwegyo structure belt. Its axis is cut by a N-S normal fault. and this is also an anticline structure Figure (5). The northern and southern part of Ngashadaung structure is separated by a cross fault with the down thrown side in the north. Thenorthern closure is higher than the southern one. The northern closure is cut by a longitudinal reverse fault in the east. In 1925 – 1926, BOC 6 wells test drilled noth of Ngashandaung area several shows of oil and gas were recorded in between 600-1700 ft from Padaung sandstones. In 1985 -1984, 4 wells were drilled by the MOGE at Ngashandaung area and produced Oil and gas from Padaung sandstones. In the present study, oil and gas local produced from in the RSF-3 of Ngashandaung area.

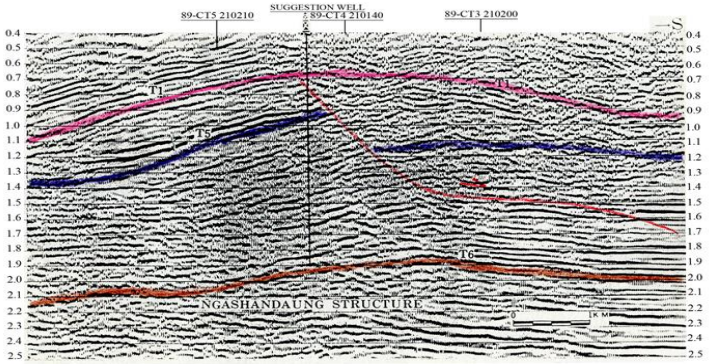

Index

T1- Irrawaddy Formation, T5- Padaung Formation, T6- Shwezetaw Formation

Figure (5) North- South Seismic Section of the Ngashandaung Structure (Source MOGE)

Payagyigone Prospect

Payagyigone structure is situated in southern end the second line structure of the Tuyintaung- Gwegyo thrust. The structure is located ½ mile from south of Payagyigon village. Seismic time contour map shows one major high in Payagyigone area as shown in figure (6). The structure is appeared as two incomplete small anticlines cut by four N-E direction normal fault.The trap area is totally 11.73 square kilometers, the top of its depth is 4930 ft and the

closure magnitude is 100 ft. The trapping area in T5 formation is 5.6 square kilometers the maximum height of closure is 200 ft and the top of the structure is at the depth of 4800 ft. MOGE drilled 2 wells in the Payagyigone area during the years 1982. No. 1 well test oil at 3374 ft and No.2 well test oil at 3800 ft of Padaung Formation.

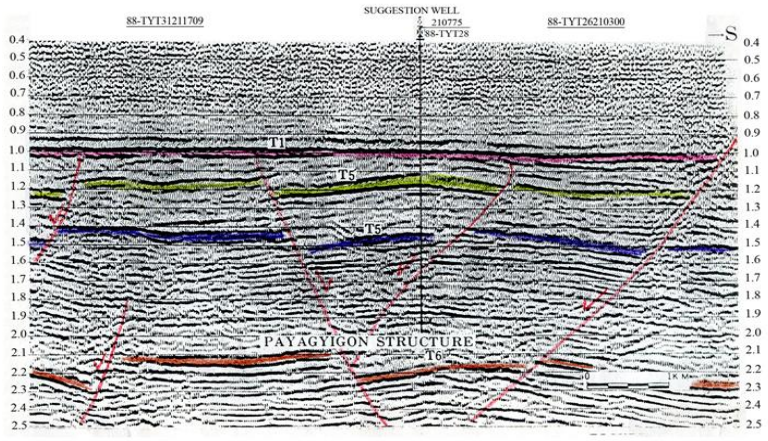

Index

T1- Irrawaddy Formation, T5'- 3700 ft Sand in Padaung Formation, T5-Bottom of the Padaung Formation, T6- Shwezetaw Formation.

Figure (6) North-South Seismic Section Payagyigon of the Structure

Gwegyo Prospect

The Gwegyo Prospect is located about one mile South of Ngashandaung village. The major anticline structural trend is in a NNW-SSE direction and disappears at Pyinma Chaung, where it is covered by the alluvium. One mile south of Nyaungnigyin village the anticlinal axis is again observed in the Shwezetaw Formation trending in a NNW-SSE direction. On the Gwegyo area two test wells were drilled during 1984 – 1985 by MOGE. Gwegyo well NO.1 reached 7332 ft produced very heavy wax content crude traces from Shwezetaw sandstones. Well NO.2 reached 2630 ft -6800 ft no hydrocarbon indication were observed in Gwegyo area.

Structural Leads

Kaungnyo Lead

The Kaungnyo structure is also a main feature of the study area. In the year 2003, Chinnery Assects Limited implemented 2D influseismic data acquisition in Bagan blocks of RSF-2/3 and IOR-3. Totally 43 seismic lines were surveyed of Which 5 cover the Kaungnyo prospect. Data interpretation and mapping on the Kaungnyo area has indicated that Kaungnyo propect is a well-defined fauted 4-way dip inticline as shown in Figure (7). Which is developed under the nearly N-S trending thrust, and is cut by normal faults trensdind NNW-SSE is middle part. The first test well drilled by Chinnery Assets Limited is not tested. So the hydrocarbon potential of this lead should not be downgraded and it can still be considered as a potential exploration target in the study area.

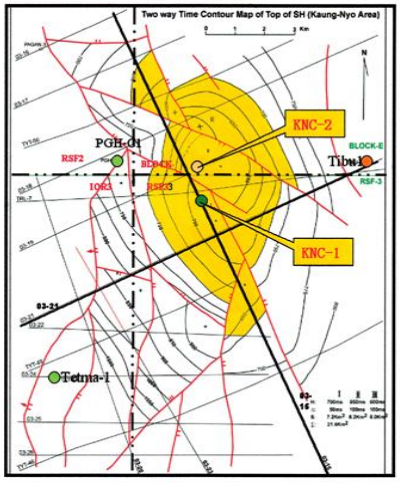

Figure(7) Contour Map(TWT) Top of Shwezetaw Formation Kaungnyo Structure (Source MOGE)

Kanyet Lead

The Kanyet Lead is a trap of fault block type and developed on anticline background in saddle between the southern plunge of Myaing and the second line of Tuyintaung –Gwegyo thrust Belt. Kanyet prospect is a two-way dip closure as seen in Figure (8). Its east and north boundaries are formed by two normal faults. The Chinese company CAL drilled one exploratory well in Kanyat Lead and not tested. However should not be downgraded and revisit evaluation. well KYT C-1 is located at the center of Block RSF-2, on the north bank of Irrawaddy River. In the year 2003, Chinnery Assets Limited implemented 2D infill seismic data acquisition in the Bagan Blocks of RSF-2/3 and IQR-3. Existing seismic interpretation and mapping the results show an expected value of 148.92 MMBO, with maximum and minimum values of 717.44 MMBO and 20.8 MMBO respectively.

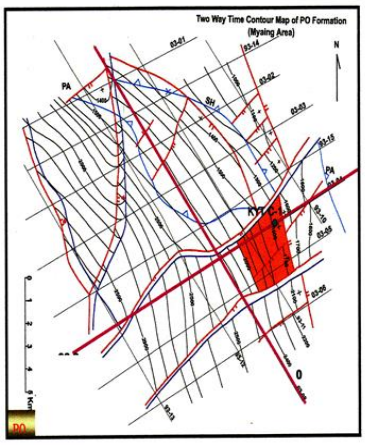

Figure (8) Contour Map(TWT) Top of Pondaung Formation, Kanyet Structure (Source: MOGE)

Stratigraphic Leads

Thanbo Lead

It is an anticline structure is located near Thanbo village. The trapping area of is 14.4 square kilometers, the height of the closure is 150 ft and the depth of top of the structure is 3624 ft Figure (9).

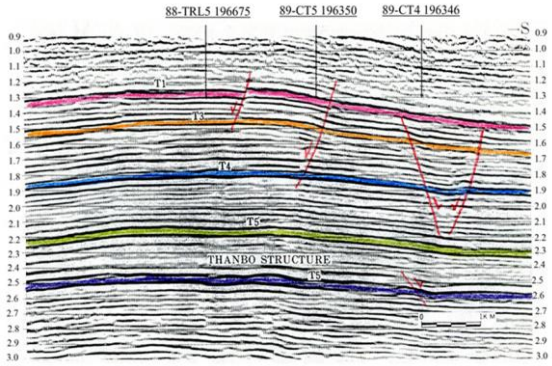

Index

T1-Irrawaddy Formation, T3- Bottom of Pyawbwe Formation,
T4- Bottom of Okhmintaung Formation, T5-Padaung Formation

Figure (9) North- South Seismic Section of the Thanbo Structure (Source MOGE)

Western Tuyintaung Gwegyo unconformity

This unconformity is located in the west of Tuyintaung-Gwegyo thrust belt formed by truncation of Okhmintaung and Padaung formations. The strike of it is nearly N-S direction with the length of 40 km. Cross fault striking W-E joined with pinch out to constitute separate unconformity traps. The total trap area is 35.625 sq.km. Its shape plane and section view is shown in Figure (10).

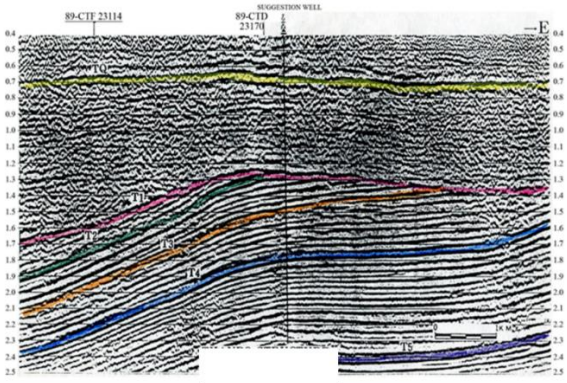

Index

TQ-Bottom of Quanterany, T1-Irrawaddy Formation, T2 –Top of Pyawbwe Formation, T3- Bottom of Pyawbwe Formation, T4- Bottom of Okhmintaung Formation, T5-Padaung Formation

Figure (10) West-East Seismic Section of the Western Tuyintaung-Gwegyo Unconformity (Source MOGE)

Discussion

In the presents study, a total of five prospects and four leads are identified in the second line structure of Tuyintaun-Gwegyo Thrust Belt. In the prospects areas, it can resume exploratory drilling based on the existing data but in the lead areas it will need additional seismic surveys and geological investigation. The leads and prospects which were developed in the study area are identified by integrated evaluation of the surface geological data, oil and geophysical data, exploratory well log data and well testing data. As a results of integrated evaluation (5) prospects and (4) leads are identified in the study area. Five prospects are

Tuyintaung, Tetma, Ngashandaung, Payagyigone and Gwegyo areas. Four leads are Kaungnyo, Kanyet, Thanbo areas and Western Tuyintaung Gwegyo unconformity. The prospects are of immediate drillable areas while leads are of potential areas but need further evaluation.

Conclusion and Recommendations

Conclusion

Tuyintaung- Gwegyo Thrust Belt is located on the east bank of Ayeyarwady River covering Nyaung-U Township, Mandalay Region and Chauk Township, Magwe Region. The study area has serious topographic relief and full of stromed cracks. The dominated hilly terrains are Tuyintaung range, Gwegyo-Taungzin and Ngashandaung range which elevation ranges from 300-400 meter above sea level and trending in NNW-SSE direction.The research area is mainly composed of sedimentary rocks. In this area, Cenozoic age rocks are found in Pegue Group. In this area, Okhmintaung Formation, Padaung Formation and Shwezetaw Formation have cropped out to the surface along the thrust. The four ways closed structure, fault related three ways and two ways structures, stratigraphic pinch out and unconformities have trapping Potential. *In the presents study a total of five prospects and four leads are identified in the Tuyintaun-Gwegyo Thrust Belt.*

Recommendations

The prospects are immediate drillable areas while leads are potential area need further evaluation. The follwings are recommended;

(1) To re-evaluate Tetma Oil field by 3D seismic survey.
(2) To acquire infill 2D seismic survey in Tuyintaung prospect . To conduct a research work for application of suitable production technique for production of thick crude.
(3) To conduct 3D seismic survey in Ngashandaung and Payagyigon prospects to indentify stratigraphic and structural aspects of the shallow and medium oil sands.

Acknowledgements

Firstly, we would like to express our thanks to Dr. Nay Win Oo, Rector, Dr. Aye Aye Ko, Dr. Wah Wah Lwin and Dr. Thidar Aung, Pro-Rectors, East Yangon University for their permissions an encouragements to do this research. We wish to express our heartfelt gratitude to Dr. Than Than Thwe, Professor and Head, Department of Geology, East Yangon University for her encouragements and advice.

Thanks are also expressed to the organizers of the committee of East Yangon University Research Journal for giving the chance in publishing this research paper in EYU research journal.

References

Ligui X and Z Shihua (1990) *The Interpretation Results Of Second Phase Seismic Exploration In Chauk- Gwego Area Central Myanma Basin , Myanma ,* Second.

Maung Maung Kyaw (2007) *Sesismic Interpretation Report On Tuyintaung – Tetma – Gwegyo – Payagyigon – Ngashandaung – Nyaunggon - Area* , Geophical Report No. 04/93.

Croft (1991) *Myanmar Regional Geology And Prospectivity Report* .

Chinnery Assets Limited (CNPC 1. 2005) *Block E, adjacent Blocks RSF- 3, Bagan Area, KNC-2 well Geochemical Report,* Huabei Mudlogging Company.

Chinnery Assets Limited (CNPC 1. 2005) *Block E, adjacent Blocks RSF- 3, Bagan Area, KNC-2 well Final Well Report t,* Huabei Mudlogging Company.

Chinnery Assets Limited (CNPC 1. 2005) *Block RSf -2 , Bagan Area, KYT-1 well Geochemial Report,* Huabei Mudlogging Company.

M.O.G.E, 1984. Write – up of Chauk-Gwegyo Area in Central Burma Depression; Unpublished Reports.

CARBONATE PETROLOGY AND LEAD MINERALIZATION OF THE BAWBYU-TAUNG AND NYAUNGLWE AREA, KALAW TOWNSHIP, SHAN STATE (SOUTH), MYANMAR

Zaw Moe Lwin[1], Thet Tin Nyunt[2], Suang Kham Pau[3]

Abstract

The present research work is carried out in BawByu-Taung and NyaungLwe Area, Kalaw Township which is situated about 13.2 km east of Pindaya, Shan State (South). It lies between the North Latitude 20˚ 55′ 10″N to 20˚ 51′ 40″N and the East Longitude 96˚ 44′ 30″E to 96˚ 46′ 50″E, part of one inch topographic map number 93 D/9 and 93 D/13. The comparative studied areas mainly situated in the Eastern Highlands province. Regionally, Bawsaing area is predominantly made up of Pindaya Group (Ordovician), Mibayataung Group (Silurian) and Plateau Limestone Group (Middle Permian to Middle Triassic). In the Bawsaing area, the main ore body occurred in Wunbye Formation (Middle Ordovician). Wunbye Formation are well distributed in the study area and is composed dominantly of medium to thick bedded, bluish grey limestone and distinguished by the presence of irregular silt partings and patches, this is also called "burrowed limestone" is sometimes used. Petrography of Wunbye Formation can be classified as Oosparite, Oosparite (dolomitized), Pelsparite, Pelmicrite, Biomicrite, Biopelmicrite, Pelbiosparite, Oopelsparite and Dolostone by according to Folk's (1959) classification. The major ore minerals are galena, barite and cerussite. The associated ore minerals are pyrite, chalcopyrite, sphalerite, covellite, malachite and azurite. Gangue mineral consists of calcite and dolomite. The prominent alternations are Dolomitization and Pyritization. Textural studies indicate that colloform texture, fissure and Vug filling texture, growth zoning and rim replacement texture which are the characteristics of Mississippi Valley Type (MVT) deposit. The formation of ores can be interpreted as the stratiform as well as stratabound nature which is conformable with host carbonate strata. These facts support that ore deposit of research area is MVT. The mineralization of Bawsaing is stratigraphically controlled by the Ordovician Wunbye and it deposits have different mineralization styles, alterations and textures. Moreover, structural control is also favorable for the mineralization of research areas.

Keywords: Wunbye Formation, Oosparite, Pelsparite, Pelmicrite, Biomicrite, Biopelmicrite, Pelbiosparite, Oopelsparite and galena

Introduction

The present research work is carried out in Bawsaing area which is situated about 13.2 km east of Pindaya and about 28.5 km north of Heho, Kalaw Township, Shan State (South). It lies between the North Latitude 20˚ 55′ 10″N to 20˚ 51′ 40″N and the East Longitude 96˚ 44′ 30″E to 96˚ 46′ 50″E, part of one inch topographic map number 93 D/9 and 93 D/13 (part of UTM-Map no. 2096-09 and -13). The Location map of the study area is shown in (Figure 1).

Regional Geologic Setting

The study areasis mainly situated in the Eastern Highlands province. Most of the mountain ranges are roughly trending from north to south, trending N–S, NNW–NW or NNE–NE. In the Southern Shan Plateau, there are three N–S trending ranges, Taunggyi range in the east, Bawsaing range in the middle and Pindaya range in the west (Theingi Moe Pwint, 2015). Generally, The Paleozoic and Mesozoic strata are exposed in the study area.

The regional structure of Bawsaing–Heho area is a double plunging anticline (Myint Lwin Thein, 1972).The thrust faults are trending N–S. The numerous minor drag folds occurred in

[1] Demonstrator, Department of Geology, East Yangon University
[2] Director General, Department of Geological Survey and Mineral Exploration (DGSE)
[3] Assistant Lecturer, Department of Geology, East Yangon University

the Linwe Formation and Nan-on Formation. Mineralization of the study area can be related with regional structure**.** The Bawsaing range is predominantly made up of Pindaya Group and portions of northern, western and eastern flanks have the exposures of Mibayataung Group. In the western part of the study area, Permo-Triassic units are being extensively developed, the carbonate rock units of the plateau exhibits karst topography.The succession of the Paleozoic rocks in the study area is described by (Brown and Sondhi, 1993; Reed, 1936 and Myint Lwin Thein, 1972). In the study area, the Ordovician Formation of Pindaya Group is conformably overlain by the Silurian Formation of Mibayataung Group, and this Formation is also unconformably overlain by Permo-Carboniferous age of the Plateau Limestone Group. Mineralization of the research area can be related with the regional structure. The regional geological map of the study area is shown in (Figure 2).

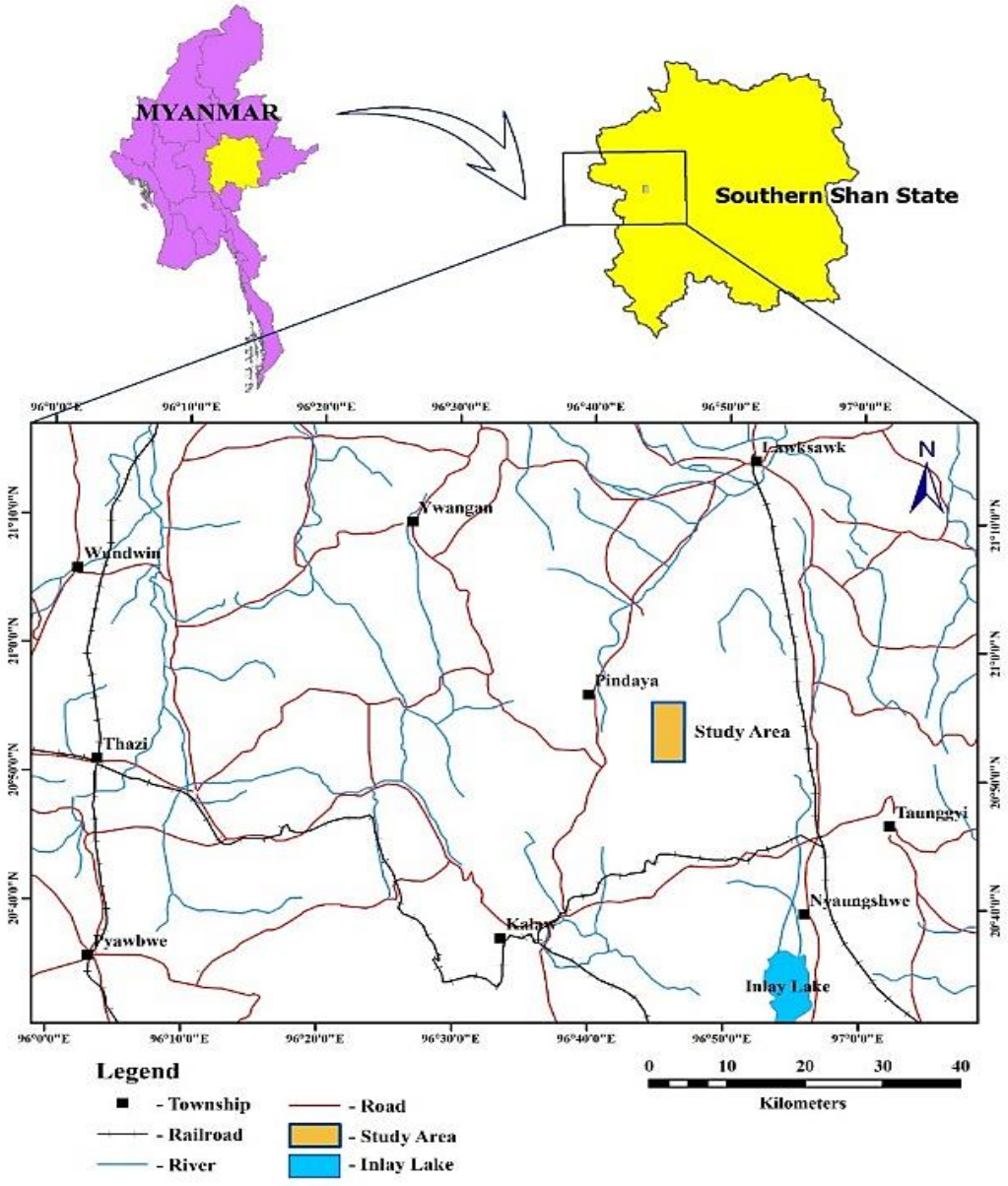

Figure 1. Location map of research area

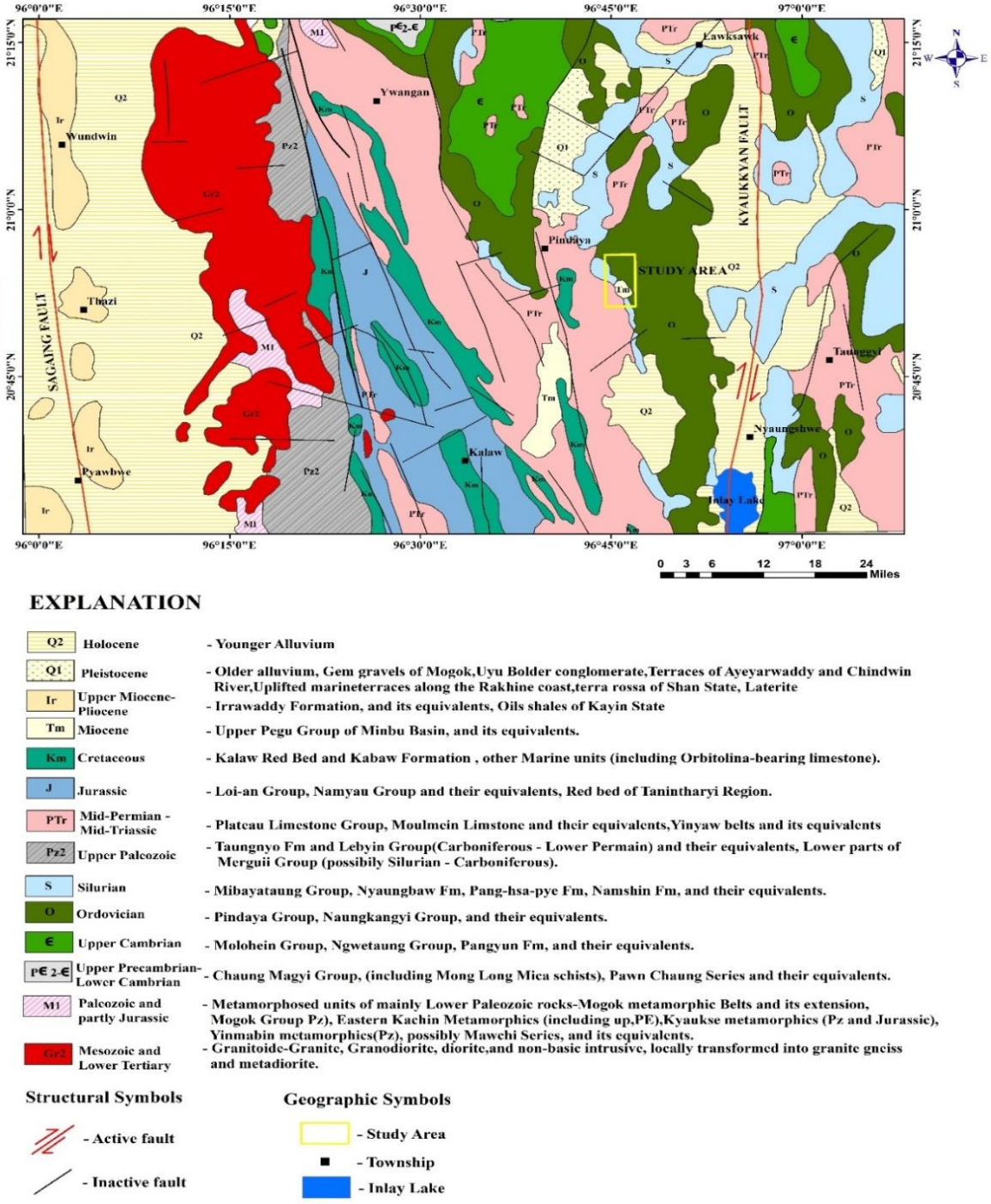

Figure 2. Regional Geological map of the Bawsaing and Sitha area

(After Soe Thura Tun etal., 2014)

Stratigraphic Succession of the Bawsaing area

Stratigraphic classification of the Ordovician units and the Silurian units of Bawsaing area is shown in Table 1.

Table 1 The stratigraphic succession of the study area in ascending order from older to younger is described as follows: (after Myint Lwin Thein, 1973, 1979)

Stratigraphic Units	Age
Plateau Limestone Group	Middle Triassic to Middle Permian
Unconformity	
Linwe Formation (Mibayataung Group)	Lower Silurian
Nan-on Formation (Pindaya Group)	Upper Ordovician
Wunbye Formation (Pindaya Group)	Middle to Lower Ordovician

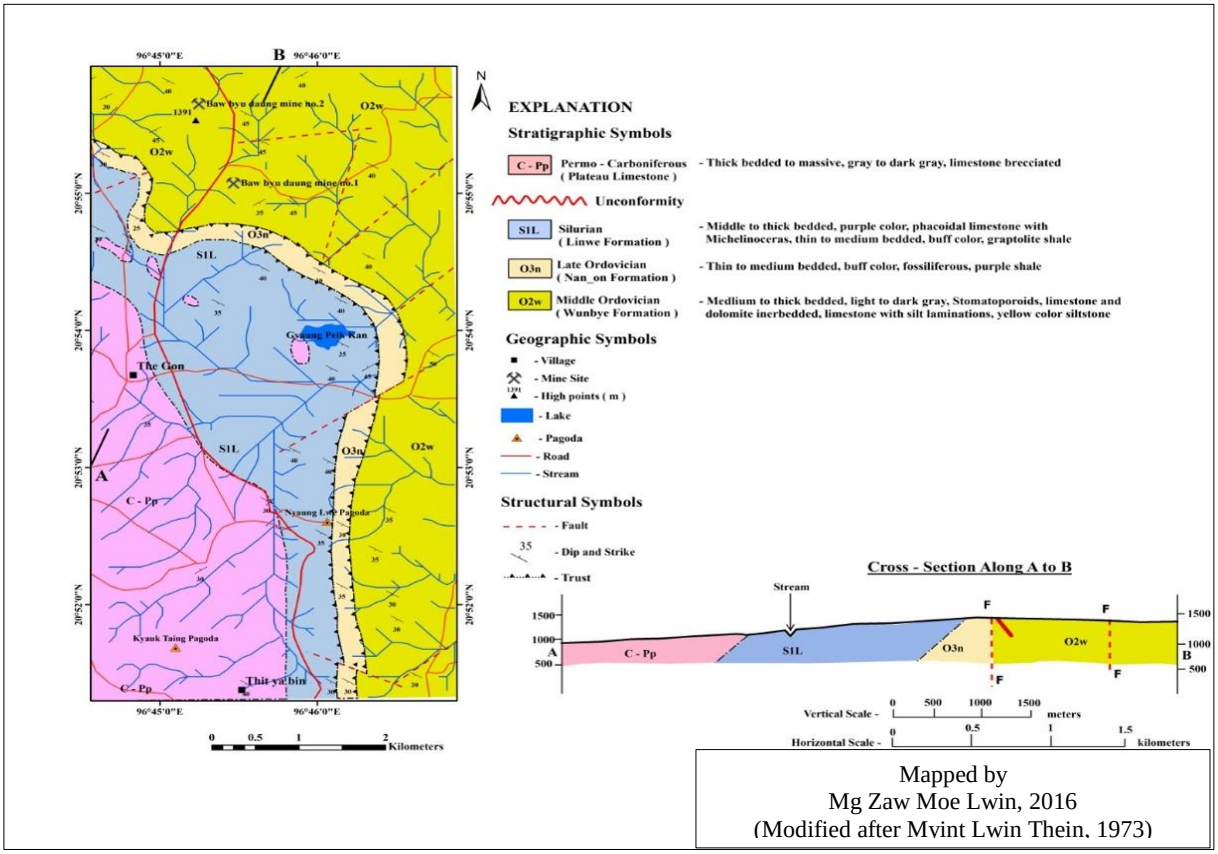

Figure 3. Geological map of the Bawsaing area (Modified after Myint Lwin Thein, 1973)

Pindaya Group

The Wunbye Formation and Nan-on Formation of the rocks of the Pindaya Group are exposed in the study area. Wunbye Formation (Myint Lwin Thein, 1973) is the limestones of Ordovician age in the Southern Shan State and Bawbyutaung, east of the Thegon village and Nyaunglwe pagoda are the best exposed area of the Wunbye Formation. Geological map of the study area is shown in (Figure 3). It is composed dominantly of medium to thick bedded, bluish grey limestone and it can be easily distinguished by the presence of irregular silt partings and patches and also called the name "burrowed limestone". The well-bedded character is seen clearly near the eastern part of the study area (Figure 4a, b). Myint Lwin

Thein (1973) assigned the Wunbye Formation as Lower to Middle Ordovician age and it can be correlated with the Lower Naungkangyi stage of Shan State (North), La Touche (1913)

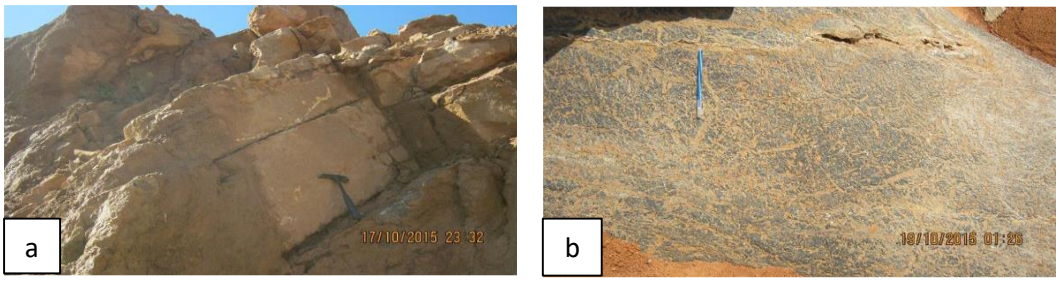

Figure 4a. Outcrop nature of the dark grey color, thick-bedded Wunbye Formation, N of the Bawbyutaung, location 47Q KD 266387E/N2315705, Facing- N290˚, b. Burrow structure and silt patches in the Wunbye Formation, SE of Bawbyutaung, location 47Q KD 267935E/N2314489, Facing- N20˚E

Petrography

The representative samples of Wunbye Formation are collected randomly the investigated area. The fifty numbers of thin sections were studied by polarizing microscope, to describe the petrolograhic name and depositional environment. The study area is mainly exposed with Wunbye Formation. Upper horizons of Wunbye Formation and Lower horizons of Nan-on Formation are the host rock for lead mineralization and associated ore minerals. The Wunbye Formation was studied by thin section under polarizing binocular microscope. According to Folk's (1959) classification (Table -2), they occur as, (1) Oosparite, (2) Oosparite (dolomitized), (3) Pelsparite, (4) Biomicrite, (5) Pelmicrite, (6) Biopelsparite, (7) Biopelmicrite, (8) Oopelsparite and (9) Dolostone.

Oosparite

It shows light gray or dark gray on the fresh surface, medium to thick bedded, irregular silt patches and small calcite veins. Petrographically, the oolite principally dominates grain assemblage, the amounts ranging from 50 – 60% of framework. Quartz and other allochems contain about 10% of the framework. The oolites are cemented by sparry calcite cement, containing 20 – 30% of the framework. The ooids are well developed with internal radial and concentric structure (Fig.5a). Oolitic limestones commonly have detrital intraclasts or pellets as nuclei cemented in the micritic matrix. The ooids usually range in size about 0.5mm to 2mm in diameter. Ooids shows outer layer of foliation due to compaction and pressure solution contact between ooids. According to Folk's Classification (1959), this rock can be named as Oosprite. The deposition environment of the oosparite may be possible high energy of current transportation and subtidal environment.

Oosparite (dolomitized)

This rock shows light grey to reddish brown or light grey in fresh colour, medium to thick bedded, highly joints on surface and composed mainly of 50% of the total volume are dolomite minerals , 40% of the oolite, iron oxide and minor amount of quartz occur in 5 – 10% of the rock volume. Dolomitized ooids varies in size range from 0.5 to 2mm (Fig.5b). Dolomitic oolite show no radial structure and concentric structure but composed of anhedral grains of dolomite with concentric growths. This rock in which the matrix has been replaced by more finely crystalline dolomite than the originally ooids. According to the composition of ooids, dolomite and sparry calcite cements, this rock can be named as oosprite (dolomitized)

by Folk's (1959). The deposition environment of the oosparite (dolomitized) and bioclasts were formed under high energy condition and subtidal environment.

Table (2) A Classification of Limestone (after Folk's, 1959)

Volumetric allochems composition			>10% allochems		<10% allochems			
			Sparry calcite > Micrite	Micrite > Sparry calcite	1-10% allochems		<1% allochems	
>25% Intraclasts			INTRASPARITE	INTRAMICRITE	Most abundant allochems	Intraclasts INTRACLAST-BEARING MICRITE	present DISMICRITE	Undisturbed reef and bioherm rocks
< 25% Intraclasts	>25% Ooids		OOSPARITE	OOMICRITE		Ooids OOID-BEARING MICRITE		
	< 25% Ooids Volume ratio, bioclasts: peloids	>3:1	BIOSPARITE	BIOMICRITE		Bioclasts FOSSILIFEROUS MICRITE	MICRITE, or if sparry patches	
		3:1 to 1:3	BIOPELSPARITE	BIOPELMICRITE		Peloids PELOID-BEARING MICRITE		BIOLITHITE

Pelsparite

This rock shows dark grey to bluish grey, medium to thick bedded and silt patches layer on the bedding surface forming burrowing features and composed of dominantly allochem and containing pellets, sparry calcite, ferrugeneous matrix and small amount quartz. The composition consists of 55% of sparry calcite, 40% of pellets, 5% minor amount of ferruginous matrix and quartz. The pellets showing oval shape, moderately sorted fecal pellets are parallel oriented along the microlamination plane (Fig.5c).They are an average diameter is 0.1 to 0.3 mm and neospar is the most common cementing material. Pellet grains are producing horse-tail structure under the effect of compaction. According to the field observation and petrographic description this facies is named as pelsparite by Folk's Classification (1959). The depositional environment of the pelsparite may be possible low energy and subtidal environment. (Win Naing, 1991)

Biomicrite

These rocks are grey to bluish grey, poorly moderately exposed, medium bedded of Wunbye Formation and composed of 20 to 30% of allochem grains, which are found to bebioclasts, pellets, crinoids and intraclasts, broken unidentifiable bioclasts. This rock consists of 5 to 10% of dolomite rhombs and minor amoun t of quartz. The gastropods, brachiopods and echinoderm fragments are also common. The rectangular crinoidal fragment composed by single calcite crystal with markedly twin plane (Fig.5d).The primary cavity partly dissolved and filled by calcite cement in residue of molluscan shell fragment with micrite envelope. Microcrystalline micrite contains 50 to 60% of the framework. According to Folk's (1952) classification the rock can be named as biomicrite. Abundant accumulation of bioclasts and micrite reflects a low energy of current transportation and subtidal deposition environment.

Pelmicrite

These exposures show grey to bluish grey, thick bedded and silt layer lamination. The burrows are filled with silty fine sediment. This facies consists mainly of 55% micrite matrix, 35% pellets, 10% terrigeneous sediment and minor amount of bioclast. The pellets are spherical to ellipsoidal shape (size range from 0.1 to 0.4mm), well sorted and not easy to differentiate with micrite (Fig.5e). Due to their size and shapes, is commonly taken to be of fecal. In some place, the micrite matrix is neomorphosed to psuedospar. According to field observation and microscopic description, this facies is defined as pelmicrite by Folk's Classification (1952). The pellets reflect the deposition of the supratidal to intertidal environment with low to moderately agitated condition.

Biopelsparite

The rock is grey to bluish grey in fresh colour. They are medium to thick bedded, medium grains. Microscopically, this unit composed mainly of 35% bioclasts, 20% pellets, 5% terrugeneous grains and 40% of sparry calcite cement. The bioclasts include molluscan and other shell fragments. These bioclasts are usually lined by micritic envelopes and the central shell cavities are filled up by the moasic of sparry calcite.The micritized grains of molluscan shell fragment are bored (Fig.4.11) and burrow filled with bioclasts and micrite (Fig.4.12). Pellets show round to ovoid in shape (average 0.3mm) and poorly sorting.Terrugeneous grain quartz and muscovite mica such also common. The framework grains cemented by micritic matix are microspar to pseudospar. According to Folk's Classification (1959), this rock can be named as biopelsparite. The depositional environment of biopelsparite reflects as the rapid deposition of shallow-subtidal environment. (Laporte, 1971).

Biopelmicrite

The rock is light grey to grey, medium to thick bedded, fine grained and well exposed.This unit composed mainly of 30% bioclasts, 25% pellets, 5% terrugeneous clasts and 40% of microcrystalline carbonate mud. Crinoid and trilobite fragments are also common. Pellets are showing round, spherical to oval shape and slightly compaction (Fig.5g). Crinoid fragment composed of single calcite crystal. Terrigeneous grains of fine quartz silts and muscovite flakes are observed in the burrow filled sediment and parental rock. Crinoid fragment composed of singal calcite crystal. According to microscopic description, this rock is named as biopelmicrite by Folk's (1952). The depositional environment of the biopelmicrite interpreted as the deposition of quiet water, relatively deep and open circulated subtidal environment.

Oopelsparite

These exposures show bluish grey, medium bedded and calcite veinlets on weathered surface.This rocks occur in the section consists of 50 to 60% of the allochemical grains which are packed by sparry calcite cement. The allochem grains are ooids and pellets. The ooids

content in these rocks are approximately 35% ooids by volume of the rock. Commonly the rocks contain the grain to grain pressure solution of ooids (range in size from 0.5 to 1.5mm) and avoid of concentric lamellae (Fig.5h). The nucleus of oolite is pellet and quartz. The pellets make up of 25% of the total rock volume. They are rounded to elongated shape and composed of microcrystalline calcite. The sparry calcite cement covers approximately of 30 to 40 % sparry calcite of the rock volume. According to field observation and microscopic description, this facies is named as oopelsparite by Folk's (1952) Classification. Abundant accumulation of oolites and pellets indicates as low to moderate energy of water agitation and shallow-subtidal environment (Laporte, 1971).

Dolostone

These rocks occur are grey to light grey, thick bedded to massive and well distributed. Microscopically, the rock mainly composed of 70% of dolomite, 10% of quartz and 10% of iron oxide occurs in this slide. Anhedral to subhedral grain of calcite range from 0.2 in diameter occurs polysynthetic twin and striation. Euhedral to anhedral dolomite rhombs are observed and crystal fabric is interlocking (Fig.5i). The dolomite rhombs has replaced original micrite. Occurs as anhedral quartz grains occur in this slide. According to field observation and microscopic study, this facies is named as dolostone by Folk's (1952) Classification. The deposition environment of the dolostone indicates as supratidal environment.

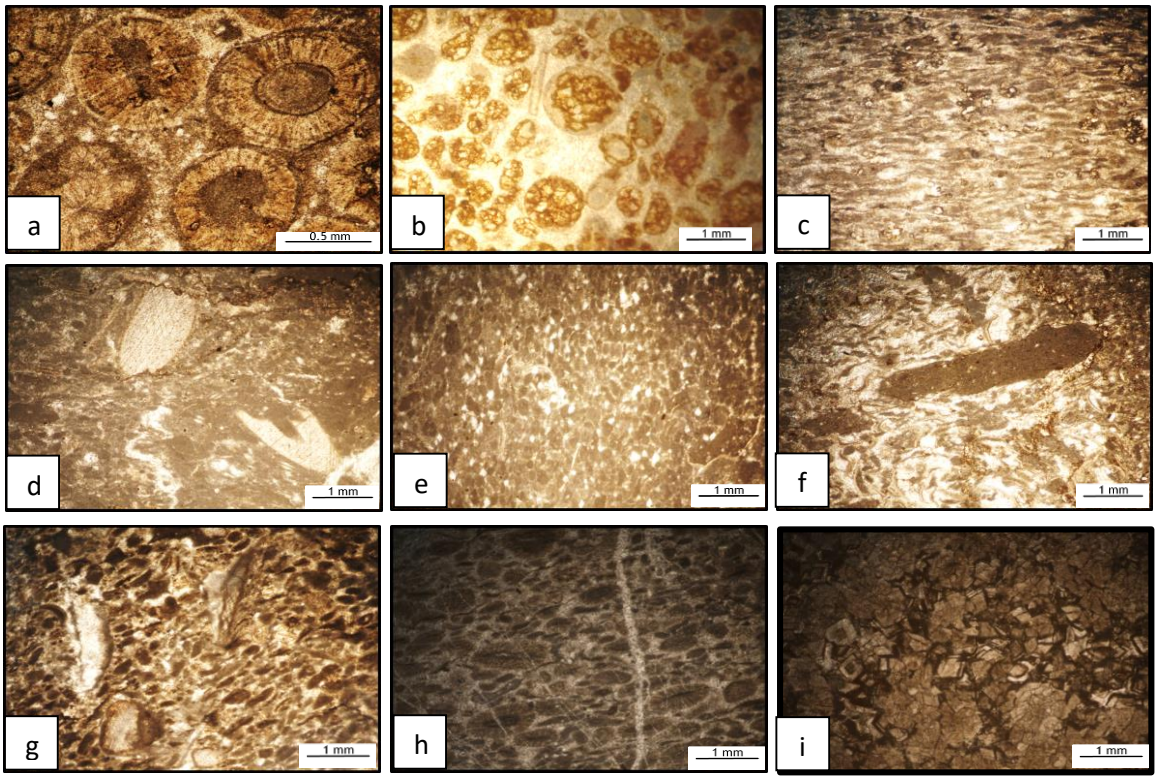

Fig.5a Photomicrograph showing well developed ooids with internal radial structure and concentric structure ellipsoidal of Wunbye Formaion. (Under PPL, 10X)

Fig.b Photomicrograph showing sized range from 0.5 to 2 mm, dolomitized ooids show no internal structure of Wunbye Formation. (Under PPL, 4X)

Fig.c Photomicrograph showing oval shape, moderately sorted fecal pellets are parallel oriented along the microlamination plane of Wunbye Formation. (Under PPL, 4X)

Fig.d Photomicrograph showing the rectangular crinoidal fragment composed by single calcite crystal with markedly twin plane of Wunbye Formation. (Under PPL, 4X)

Fig.e Photomicrograph showing well sorted and spherical to ellipsoid shape pellets (size

range from 0.1 to 0.4mm) in Pelmicrite of Wunbye Formation. (Under PPL, 4X)

Fig.f Photomicrograph showing bored and micritized grains of molluscan shell fragment of Wunbye Formation. (Under PPL, 4X)

Fig.g Photomicrograph showing pellets show round, spherical to oval shape and slightly compaction of Wunbye Formation. (Under PPL, 4X)

Fig.h Photomicrograph showing moderately sorted and average ranging from 0.1 to 0.4mm in diameter of pellets of Wunbye Formation. (Under PPL, 4X)

Fig.i Photomicrograph showing euhedral to anhedral dolomite rhombs are observed and crystal fabric is interlocking of Wunbye Formation. (Under PPL, 4X)

Mineralization Of The Study Area

At the Bawbyutaung, the study area includes Line-Kyal Mine, Pin-Sein-Pin Mine Hsa-pye-pin, Dike Ma and Myayngar. Line-Kyal Mine was studied in this study and Pin-Sein-Pin Mine was flooded during the field season. The Bawbyutaung-Ngwetaung ranges are trending in NNW-SSE direction. A cross fault cut cross the range in the middle which had separated Ngwetaung hill from Bawbyutaung hill. The main ores that occurred in the study area are galena, barite and cerussite. The associated ore minerals are pyrite, chalcopyrite, sphalerite, covellite, malachite and azurite. Line-Kyal Mine was exposed medium to thick bed, fine grained, grey or bluish grey limestone of Wunbye Formaton. Galena is the mainly mineralization in this mine, Galena often found between limestone layers and sometimes ore zone is concealed by soil. The depth of mine is about 30.48 meters, Galena mineralizaton ore zone occur three characters about the depth of 24.38 meters in this mine. The galena occurrences in bedrock are stratiform, largely layered and parallel to the bedding (Fig. 7e-h). Galena occurs as medium to fine grained, massive to subhedral forms. The thickness of galena ore body is about 1.3 meter and its length is about 6.09 meters. In generally, The host rock is trending north to south and dipping eastward. Galena occurred as pocket or massive types. In the study area, the localization of ore is generally controlled by the primary features such as lithologic control. Dolomitic limestone (dolostone) and oolitic limestone (oosparite) of the Wunbye Formation are the principal primary features. Faults, minor displacement, folds and coarse and fine breccia are the secondary features that controlled the localization of secondary ores from the study area (Figure 7a-d)

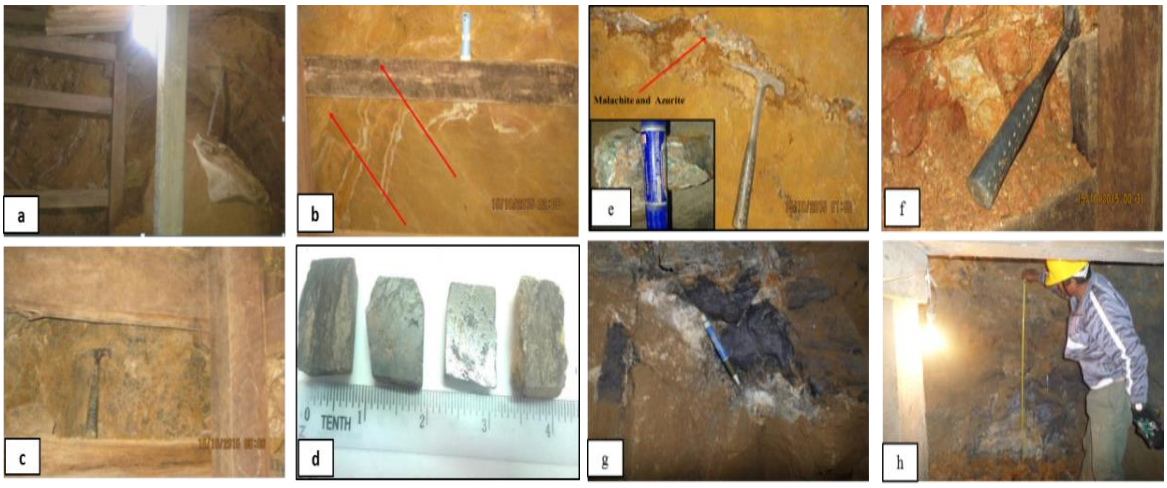

Figure 7a. Photographs of cerussite mineralization associated with the minor fold, at the Hsa-Pye-Pin Mine, Facing-S70˚E; b. Minor fault of mineralized zone, Facing-N280˚W; c. Cerussite mineralization formed near the brecciated zone, Facing-N40˚; d. Fissure filling ore sample from the study area. e. outcrop nature of malachite and azurite (minor amount, only

identified under ore microscope), inset photo is the identified sample. F. Barite occurs in the limestone of Wunbye Formation at the Hsa-Pye-Pin Mine. g. Galena segregation in Wunbye Limestone which is parallel to the bedding (stratiform type) at the Line-Kyal Mine, Looking-SW. h. Nature and distribution of galena ore zone in the Wunbye Formation at the Line-Kyal Mine, Looking- SW.

Ore Mineralogy

In the Bawsaing area, the major ore recognized in polished section are galena, cerussite and barite. The minor amount of ore minerals are pyrite, chalcopyrite, malachite, azurite, sphalerite and covellite. The gangue minerals consist of calcite, dolomite and quartz. Textural studies indicate that colloform texture, fissure and Vug filling texture, growth zoning and rim replacement texture which are the characteristics of Mississippi Valley Type (MVT) deposit (Fig. 9a-f).

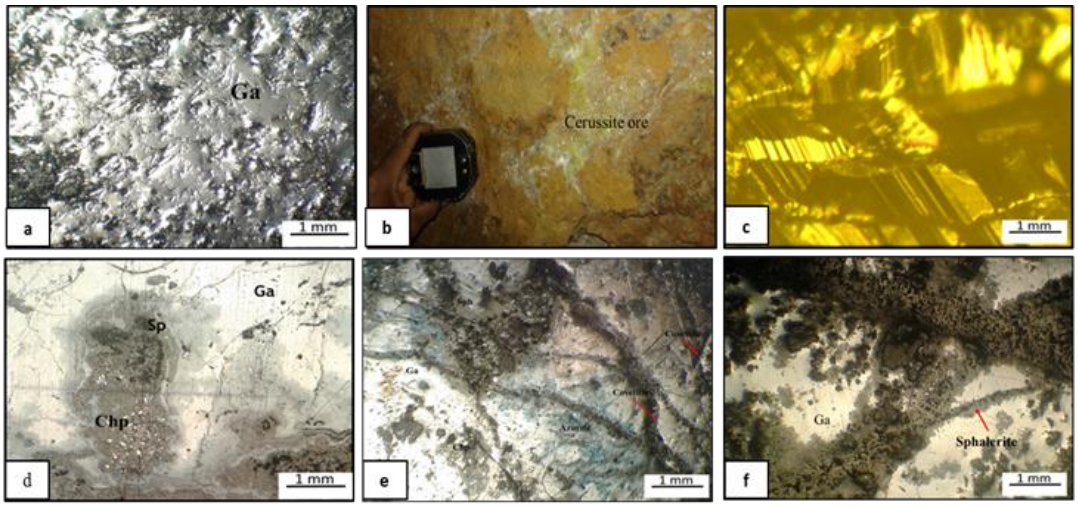

Figure 9a. Photograph of typical feature, triangular pits of galena (Ga) from the analysed ore; b. High grade cerussite ore in the mineralization zone, at the Hsa-Pye-Pin Mine, Facing-N50˚E; c. Growth zoning texture is mainly found in the cerussite where the successive growth of it developed during the formation; d. Colloform texture occurs in a series of concentric curved layers around the galena which transformed to sphalerite from Zinc bearing lead ore; e. Covellite shows rim replacement texture which is mainly developed around the grain boundaries of galena and chalcopyrite; f. Covellite shows rim replacement texture which is mainly developed around the grain boundaries of galena and chalcopyrite.

Types of Alteration

In Bawsaing area, Wunbye Formation is mineralization hosted rock. Dolomitization and pyritization are the major alteration processes that occurred in the study area.

Discussion and Conclusion

The main ores that occurred in Bawbyu-Taung and Nyaunglwe area (Bawsaing) are galena, barite and cerussite. The Mississippi Valley Type-deposit MVT and similar occurrences of ore deposits such as galena, sphalerite and supergene ore, cerussite are found in the study area. These ore are mainly confined to the dolomitized (dolostone) and oolitic limestone of the Ordovician (Wunbye Formation) units. Moreover, there has lack of significant igneous activity around the study area, expect a small rhyolite body which is quite far from the study area (Myint Lwin Thein, 1981). The occurrence of ore deposits are generally restricted to the specific stratigraphic unit, not to the whole carbonate sequences

(i.e., Wunbye Formation). The mineralogy of ores is simple with dominant sulphide minerals such as Lead sulphide (PbS) and Zinc Sulphide (ZnS) and pyrite with minor chalcopyrite. Gangue minerals are calcite and dolomite. Petrography of Wunbye Formation can be classified as Oosparite, Oosparite (dolomitized), Pelsparite, Pelmicrite, Biomicrite, Biopelmicrite, Pelbiosparite, Oopelsparite and Dolostone by according to Folk's (1959) classification.

Myint Lwin Thein (1981) also stated that the interlaminations of barite and galena, barite and limestones, and galena and limestones are typical features of the stratiform ore deposits. Some available data from field and laboratory analyses indicate that the formation of ores from the study area can be concluded as it may probably be the stratabound as well as stratiform deposit as described by Myint Lwin Thein (1979, 1981).

Stanton (1966) stated that the ideal occurrence of galena and barite at specific stratigraphic horizons on the regional scale cannot be due to epigenetic diffusions and this can only be explained by the sedimentary history and physico-chemical conditions of deposition in a marine environment. He also interpreted that lead and barium carrying barines were deposited in the as Galena and Barite during the early Mid Ordovician under the oxidizing environment.

The occurrence of lead carbonate (cerussite) is probably due to supergene ore formed at the upper portion of the limestone or under the siltstones. At BawByutaung, it is found on and along the surface of the limestones of Upper Wunbye Formation and along the fractured zone overlain by the siltstone unit. Ohn Myint (1980) also interpreted the mineralization of Bawsaing-Heho area as stratabound-syngenetic rather than hydrothermal epigenetic origin. Htay Win (2002) interpreted the genetic aspects of ore minerals from Bawsaing area as two different ways: as stratabound syngenetic and hydrothermal epigenetic types.

The occurrences of ores are stratiform as well as stratabound nature which is conformable with host carbonate strata Cavity filling and replacement type occurred in the open space of dolomitic and oolitic limestone indicates that these ore deposits were epigenetic in origin. Khin Zaw *et al.*, (1984) compared the principal Mississippi Valley Type-deposit with Bawsaing lead deposit (including present study area) on the basis of country rock stratigraphy, structural criteria for the mineralization and mineralogy. They also explained that the presence of tetrahedrite-tennantite and argentite are product of hydrothermal origin. But, in present study, these minerals have not yet been identified and so that it is difficult to interpret as hydrothermal origin. Khin Zaw et al., (1984) also explained that the associated alteration such as dolomitization, pyritization and recrystallization and fluid inclusions study indicated that Pb-Zn deposit of Bawsaing area were deposited by highly saline brines which are about 10 times more saline than the normal sea water. They also estimated that the formation temperature of this deposit was range from 80˚C to 120˚C and rarely up to 200˚C. These facts support that ore deposit of research area is MVT. The mineralization of Bawsaing is stratigraphically controlled by the Ordovician Wunbye and it deposits have different mineralization styles, alterations and textures. Moreover, structural control is also favorable for the mineralization of research areas.

Acknowledgements

Firstly, We would like to express are thanks to Dr Nay Win Oo (Rector), Dr Aye Aye Ko, Dr Wah Wah Lwin, Dr Thidar Aung, (Pro Rectors East Yangon University for their permissions an encouragement to do this research. We would like to mention my deep gratitude to Dr Than Than Thwe, (Professor and Head of the Department of Geology, East Yangon University), for her valuable suggestion, useful guidance, encouragement and provision of necessary departmental facilities. We would like to extend our gratitude to Dr Cho Cho Aye and Dr. Htay Win, (Retired Professor and Department of geology, East Yangon University). Dr Mee Mee Thein, (former Associate Professor of the Geology Department, East Yangon

University) for their advice and fruitful suggestion. Thanks are also to U Aung Kyaw Htoon, (Part time, Assistant Lecturer) for his explanation and valuable suggestion during the field time.

Reference

Aye Ko Aung, 2012. The Paleozoic Stratigraphy of Shan Plateau, Myanmar-An Updated Version. *Journal of the Myanmar Geosciences Society,* Special Vol. 5, No.1, p 1-73.

Bender, F. 1983. *Geology of Burma*. Beitre. Reg. Geol. Erde, p-55-75.

Bernhard, P. 2008. *The Ore Minerals Under the Microscope: An Optical Guide*: Editor. Atlases in Geosciences, 3. Elsevier Amsterdam, 894.

Brown, J.C., and Sondhi, V.P. 1993a. Geological reconnaissance in the Southern Shan States. Rec. Geol. Surv. India 67, 2: Calcutta, pl.3-5, 135-165 P.

Folk, R.L.,1959. Practical Petrographic Classification of Limestone, *Bull. Amer. Asso. Petro*l.43. 1-38.

Htay Win, 2002. *The study of Ore Minerals of the Bawsaing Mine*, Unpublished Master of Research Thesis, Department of Geology, Yangon University. 45-47P

IGCP (Burmese National Committee), 1980. Stratigraphic Committee field excursion in the Maymyo-Yadanatheingi -Hsipaw and Bawdwin areas. Field Excursion No.7, 29P.

Khin Mg Nyo, 1970. Geology and Ore Deposits of Heho-Bawzaing Area. Revolutinary Government of the Union of Burma Mineral Development Corporation Mineral and Geological studies Department, Unpublished Departmental Report. 8, 16-18P.

Khin Zaw, Aung Pwa & Thet Aung Zan, 1984. Pb-Zn Mineralization at Theingon Mine, Bawsaing, Southern Shan State, Burma; A Mississippi Valley-type deposit: Geol.Soc, Malaysia Bull. 17:283- 306.

La Touche, T. H. D. 1913. Geology of the northern Shan States. *Memoir of the Geological Survey of India* 39, pt. II, Calcutta, 283p.

Lee, C. P., 2009. Paleozoic stratigraphy. In, *Geology of Peninsular Malaysia*. (Eds.) C. S. Hutchison, and D. N. K. Tan, 55-86

Myint Lwin Thein, 1973. The Lower Paleozoic Stratigraphy of Western part of the Southern Shan State, Burma, *Geol. Soc. Malaysia, Bull*. 6, 143-163.

Myint Lwin Thein, 1981. Barite and Galena Occurrences in the Ordovician Rocks of the Western Part of the Shan State, Buma, *Contr. Burm Geol*., Vol. 1, No. 1., 17-22.

Nackowski, M. P., Khin Zaw and Aung Myint Thein, 1977. Field Training in Mineral Exploration Bawsaing area, Kalaw Township, Shan State (south), Burma. Dept. Applied Geol, Staff Rept. No. 35.

Ohn Myint, 1980. *Detailed Stratigraphic and structural analysis of lithostratigraphic units in relationship to mineralization at Bawsaing Area. Southern Shan State*, (Unpublished M.Sc. Thesis. Department of Geology, Rangoon Arts and Science University, 80-97p.

Soe Thura Tun, Maung Thein, Nyunt Htay & Kyaing Sein. 2014. *Geological Map of Myanmar 1:2,250,000*. Myanmar Geosciences Society, Yangon, Myanmar.

Stanton, R.L., 1966. Composition of stratiform ores as evidience of depositional processes: *Trans. Inst. Min. Metall*. (ect. B: Appl. Earth Sci.), V. 81, p. B141-B148.

The Ore Minerals Under the Microscope: An OpticalGuide. BERNHARDPRACEJUS, Editor. Atlases in Geosciences, 3. 2008. Elsevier, Amsterdam

Theingi Moe Pwint, 2015. *Geology and Barite Mineralization of Nyaunglwet-LegGyaikDaik Village, Kalaw Township, Shan State (South).* Unpublished MSc. Thesis, Yangon University. 10-11p.

Wongwanich, T., W. Tansathien, S. Leevongcharoen, W. Paengkaew, P. Thiamwong, J. Chaeroenmit & W. Saengsrichan 2002. The Lower Paleozoic rocks of Thailand. *The Symposium on Geology of Thailand, Bangkok, Thailand*, 16-21.

Zaw Moe Lwin, 2017. *Petrology and Barite mineralization of the Sitha Area, Pyin Oo Lwin Township, Mandalay Region*, Unpublished M.Res. Thesis, Department of Geology, East Yangon University. 75p.

DISTRIBUTION AND ECOLOGY OF RECENT FORAMINIFERA IN THE MYEIK COASTAL AREA, TANINTHARYI REGION, MYANMAR

Thet Paing Soe[1] and Soe Moe Lwin[2]

Abstract

The distribution and ecology of recent foraminifera are analyzed along the shoreline around the Myeik area. The total species ranges from Myeik coastal area are range from 153 from 250. The richest of species which is found in Myeik coastal area are *Pyramillina* sp., *Tubinella* sp. *Bathsiphone spinosus, Bathsiphone* sp., *Spiroloculina anderseni, Miliammina pariaensis, Triloculina* sp., *Spiroloculina grata, Q. frigida, Q. atlantica, Q. seminula, Asterorotalia trispinosa, Elphidium discoidale, E. crispum, E. advena*. The rare occurrence of all Rotalia group are controlled by the substrate condition. High nutrient environments in Myeik coastal area are low energy area which has been used up in the decomposition of the organic materials providing the nutrients. There is some indication that the distribution of certain benthonic such as *Quinqueloculina* and a few of planktonics may be actually adapted to low oxygen environment. The Myeik coastal are muddy and rich in food for foraminifera, so the species diversity and species population of foraminifera is moderate to high. Only a few planktonic species have been found due to the presence of sediments in the deep sea without the presence of sediments in the deep sea.

Keywords: Foraminifera, benthonic, planktonic, Myeik coastal area

Introduction

The research area is situated in the Tanintharyi Region in Myanmar. The Myeik coastal area is situated in the Myeik Township, it lies between latitude 12° 28′47" N to 12° 25' 40"N and longitude 98° 33' 45" E to 98° 35' 57" E. Transport and communication of research area are easily accessible. The research area can be reached by car or cycle. The location map of the research area is show figure (1).

Figure.1 Location map of the research area

[1] Demonstrator, Department of Geology, East Yangon University.
[2] Pro-Rector, Myeik University.

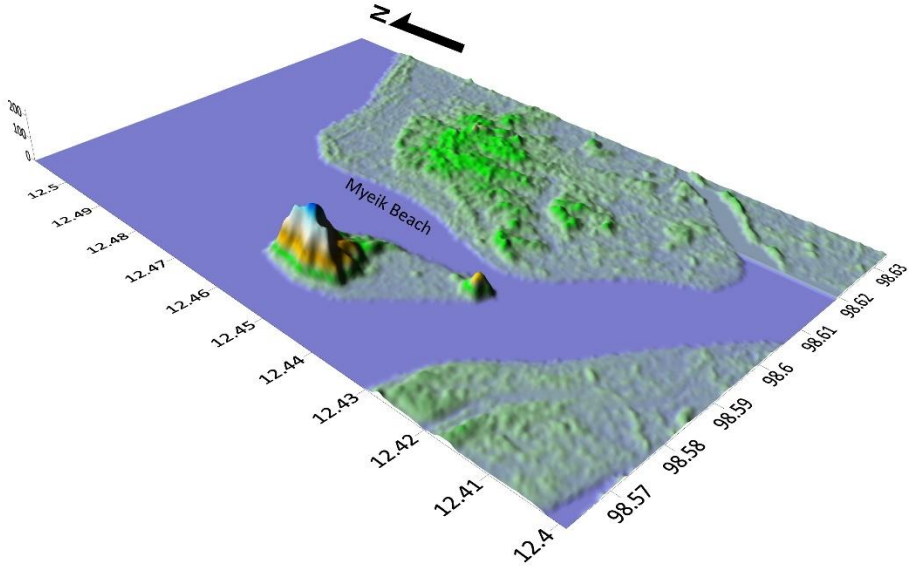

Figure.2 3D Map of Myeik Coastal Area

Method of the Study

Sediments which were collected at seven locations (generally 3 – 5 meters depth) in the Myeik coastal area, Tanintharyi Region, Myanmar. Sediments washed over the brass sieve have normal opening of 0.18 or Mesh 180.The washed residue was again dried and separated into four fractions of sieve meshes of sizes 30, 60, 90 respectively. Microscopic examination of all fractions was done very carefully. All collected foraminiferal fossils were picked up by means of stable hair brush and put into the sample micro-slides with bee wax. The foraminiferal examination and taxonomic classification were made according to Le Roy (1941, 1944), Boomgaart (1949), Bolli (1957), Blow (1959) and Bolli (1988). Respectively type species was photographed with Microscopic Camera MODEL NO.SZM CTV1/2. All established species are revealed on corresponding Plates.

Regional Geological Setting

The Research area lies in is the southern continuation of the Shan-Tanintharyi Block of Maung Thein (1974-2000) on Sino-Burma Range of Bender (1983). The study area forms a part of the Tanintharyi granite belts, which is actually a part of western tin-bearing batholiths called Western Tin Belt of South East Asia tin provinces of Michell (1977),Thein(1983), Nyan Thin (1984) and Cobbing et.al (1992).The study area is mainly composed of granitoid rocks Coastal Range Granite of Bender (1983). The regional geologic setting of the study area is shown in (Fig.2). There are six major granitoid plutonism the Tavoy area, but detail mapping of the major pluton has yet to be undertaken. The granitoid plutons intruded into the metasedimentary rocks of the Mergui Group of Brown and Heron (1923), Chhibber (1934) and Pascoe (1959). Tanintharyi Region is composed of north-south trending, narrow, Mountainous, Coastal stretch of the mainland part of Myanmar. It is generally considered to be the southern part of the eastern most geotectonic beltof Myanmar, which is referred to as the Shan-Tanintharyi massif or as the Eastern Highlands Province.

The granitoids crop out in three north-south trending belts along Thai-Myanmar border on the east, along the central range of hills, and the last isolated islands and high islands on the west (Win Swe, 2012).

The Research area corresponds to a part of central Granitoid belt of Khin Zaw (1990). He described that Central Granitoid belt forms a narrow belt of 1450 km long which is dominantly calc-alkaline and falls in peraluminous field according to petrographic and geochemical data. The geological map of Myanmar prepared by Bannert et. al. (1981) and the geological map based on Tertiary map of Southeast Asia prepared by Jacques, 2009 are shown in (Fig.2) provide descriptions of the rock formations, but it is beyond the scope of the study to discuss them in details.

Regionally, alluvium can be found along the valley of Tainintharyi River and coastal plain. Younger alluviums have Holocene age and these were deposited mainly in channel, point-bar and flood plain. Alluvium has light to medium grey and yellowish grey color, fine-coarse grained gravel, sand, silt and clay.

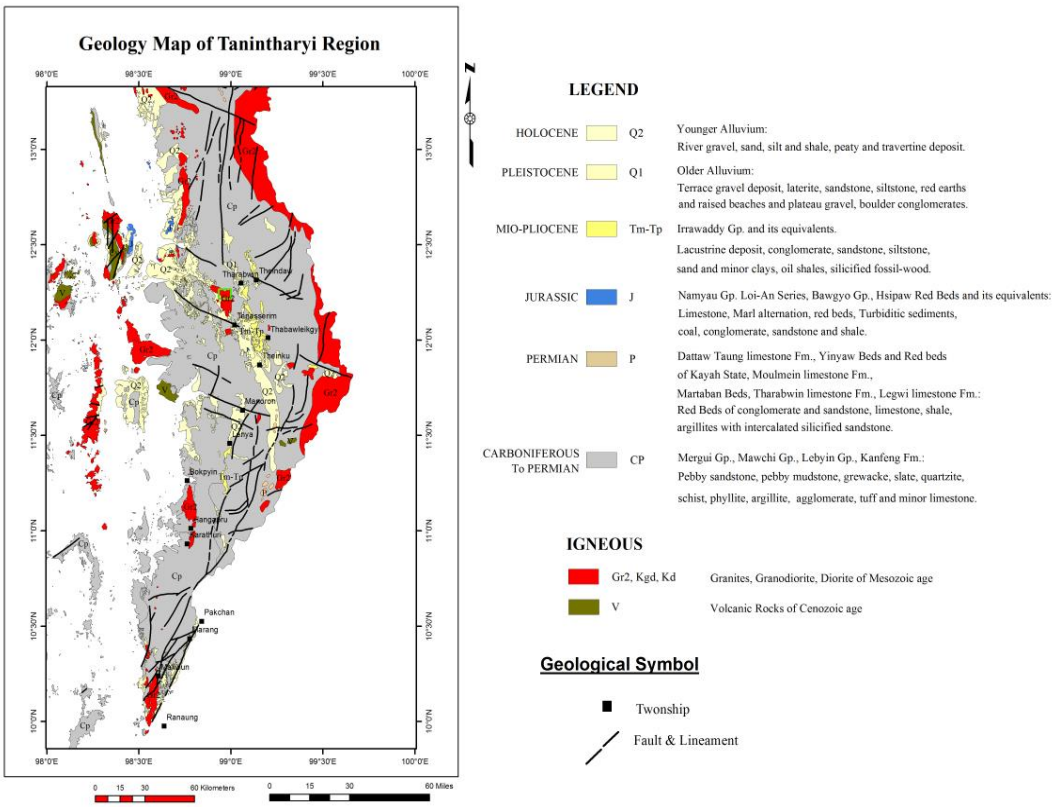

Figure.3 Regional Geology Setting Map of Tanintharyi Region

Mergui Series was given by Oldham (1956) to the unfossiliferous strata consisting of shales, agglomerates, limestones and quartzites which widely distributed within the Tanintharyi Region and occur stratigraphically between below Moulmein Limestone (Carboniferous) and upper the Devonian rock unit, Geological map of Myanmar.

The age of the Mergui Group is one of the record provocative difficulties in Burmese Geology. The Mergui Group was once correlated with the Precambrain Chaung Ma Gyi Group of the Shan State and with the Mawchi Group of Kayah State, both of with were also considered to be Precambrian in stage. However, similar lithology of Mergui strata also occur in the Pa-an and Mottaban areas which were referred to as Taungnyo Series and Martaban Series of Carboniferous and Permian. Poorly preserved Carboniferous fossils have been recently obtained from the Mergui strata of Taungnyo range near Mawlamyine from the Yadanabon Mine area on the mainland to confirm their correlation. However, the age of the Mergui Group remains an open question.

Coastal Morphology of the Research Area

Coastal morphology is the science of natural morphodynamic processes, which are responsible for shaping the coastal zone. These natural processes, which involve wind, tides, currents, waves, soil and sea-level changes, interact with the materials from which the coastal zone is built. Coastal zones around the world are shaped in highly diverse ways.

Landforms found unit are beach ridges, beach ridges complex, swale, mud flats, brackish water and spit of recent origin. Landforms are paleo-beach ridges, paleo-beach ridges complex, swale and coastal sand. Coastal plain is raised, wedged shaped sedimentary platform containing signature of marine influences.

Table 1. Coastal Geomorphology Classifications

Origin	Coastal Geomorphic Features
Marine Origin	Mud Flat Beach Spit Beach Ridges Swales and Backwater zone Off-shore island and coral reefs Wave cut platform Sea cliff Sea cave
Fluvio-marine origin	Deltas Deltaic Plain
Fluvial origin	Natural levee Flood plain
Aeolian origin	Sand dune complex
Other	Flood basin Salt pan / Salt flat Strand line Water logged land Aquaculture pond Source: SAC (1991)

Myeik costal area is mostly made up mudflats which are developed where enough fine sediment is available and the wave action is not strong enough to disturb the sediments (Reineck and Singh, 1980).

Mostly, such a kind of condition favorable for their progress is behind the barrier, lagoons and near estuaries. Coastal areas of the inner Gulf of Andaman are very much suitable sites for the deposition of mudflats because of the availability of sediments (mostly suspended very fine grained), low wave velocity and flat gradient.

The striking features of the mudflats are tidal channels developed within them which are branched towards the landward side. The mudflats which are not in connection with the

active processes and are flanking the active mudflats are termed as paleo mudflats. This unit is also remarkable in the research area.

4 (a)

4 (b)

4 (c)

4 (d)

Figure 4. (a to d) Coastal deposition landforms along Myeik coastal area

Mangroves are trees and shrubs that grow in saline coastal habitats in the tropics and subtropics. The areas covered by mangroves have muddy sediments with a very high amount of water saturation and are known as the mangrove swamps (Figure 4, a to d).

5 (a)

5 (b)

5 (c)

Figure 5 (a to c) Coastal deposition landforms near Myeik coastal area

Foraminifera distribution and Ecology

There are a total of (29) foraminiferal species in which all are benthonic species where have been identified from the seven points near the Myeik coastal area. All of these recent foraminifera species are mostly distributed of the Latitude N 12˚26' 20" Longitude E 98˚ 35' 32" of Myeik coastal area (Figure 5).

Figure 6. Map of the Myeik Coastal Area, showing the locations of the surface samples were taken from 2 m water depth

The Myeik coastal area is characterized by moderately distribution as there are a medium number of species occurring. The total species ranges from 18 to 23 in number, which is said to be the most distinctive part among the three study areas. The Myeik sample contains 29 species whereas the sample 7 yields a total of 23 species. The species diversity (Figure 6) and species population are higher in the southern part of the study area. The whole population strength is counted about 1342 species (Figure 7). The richest of species which is found in Myeik shoreline area are as follow: *Pyramillina* sp., *Tubinella* sp., *Bathsiphone spinosus, Bathsiphone* sp., *Spiroloculina anderseni*, *Miliammina pariaensis*, *Triloculina* sp., *Spiroloculina grata*, *Quinqueloculina frigida*, *Quinqueloculina atlantica*, *Quinqueloculina seminula*, *Asterorotalia trispinosa*, *Elphidium discoidale*, *Elphidium crispum*, *Elphidium advena*. Other *Rotalia* spp. species occur from rare to commonly. They are; *Tubinella funalis, Amphistegina radiata, Amphistegina radiata* var.*papillosa, Amphistegina radiata var.venosa, Rotalia beccarii, Rotalia* cf. *"*R*". japonica, Rotalia murrayi, Rotalia ozawai, Rotalia papillosa, Rotalia calcar, Pelosina cylindrica, Laevidentalina ariena, Siphogenerina raphanus, Tiphotrocha comprimata*.

The rare occurrence of all Rotalia group are controlled by the substrate condition. High nutrient environments in Myeik shoreline area are low energy area which has been used up in the decomposition of the organic materials providing the nutrients. Distribution of certain benthonic such as *Quinqueloculina* and a few planktonic may be actually adapted to low oxygen environment.

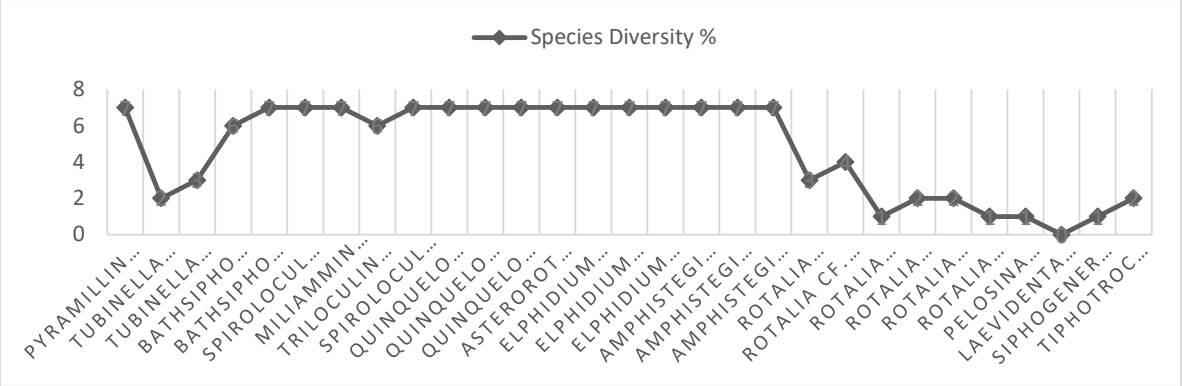

Figure 7. Graph showing benthonic species diversity present in Myeik Shoreline Area

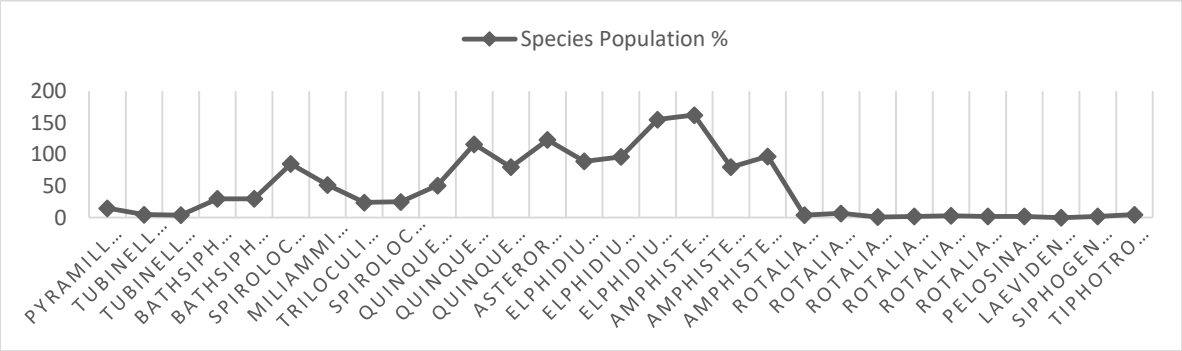

Figure 8. Graph showing benthonic species population present in Myeik shoreline Area

Table 2. Distribution of Recent Foraminifera Species in Myeik Shoreline Area

Recent Foraminifera Species	The Distributions of Recent Foraminifera Species in Myeik Shoreline Area																													
	Benthonic Species																													
	Foraminiferal Species	*Pyrabinella* sp.	*Tubinella funalis*	*Tubinella* sp.	*Baculogypsinoides spinosus*	*Bathysiphon* sp.	*Spiroloculina anderseni*	*Miliammina pariaensis* sp.	*Triloculina* sp.	*Spiroloculina grata* sp.	*Quinqueloculina frigida*	*Quinqueloculina atlantica*	*Quinqueloculina Seminula*	*Asterorotalia trispinosa*	*Elphidium discoidale*	*Elphidium crispum*	*Elphidium advenum*	*Amphistegina radiata*	*Amphistegina radiata* v ar.papillosa	*Amphistegina radiata* var.venosa	*Rotalia beccarii*	*Rotalia cf. "R". japonica*	*Rotalia murrayi*	*Rotalia ozawai*	*Rotalia papillosa*	*Rotalia calcar*	*Pelosina cylindrica*	*Laevidentalina ariena*	*Siphogenerina raphanus*	*Tiphotrocha comprimata*
	Sample No:	1	2	3	4	5	6	7	8	9	10	11	12	13	14	15	16	17	18	19	20	21	22	23	24	25	26	27	28	29
Myeik Shoreline Area	N 12°26' 30" E 98° 35' 50"	1			1	4	2	8	1	2	11	16	16	15	7	26	10	9	11	9		1			2					2
	N 12°26' 20" E 98° 35' 49"	3			6	1	11	3	3	1	2	14	11	20	13	21	19	21	14	21	1	2								
	N 12°26' 04" E 98°35' 48"	2			3	3	6	5	3	1	2	15	10	19	6	13	32	27	16	11				1						
	N 12°26' 36" E 98° 35' 44"	2				3	12	11	2	1	13	16	11	16	4	3	27	25	21	10		2								3
	N 12°26' 34" E 98° 35' 41"	2	2	1	4	2	22	10	3	2	5	21	22	11	17	6	20	27	2	10	2			1			2			
	N 12°26' 28" E 98° 35' 36"	3		1	10	2	21	12		2	2	21	4	21	11	11	24	32	7	21			1			2				
	N 12°26' 20" E 98° 35' 32"	2	3	2	11	15	11	3	12	16	16	13	6	21	31	16	23	21	9	15	1	2			1				2	

1.Pyrabinella sp., 2. *Spiroloculina anderzeni* , 3.*Spiroloculina anderzeni*, 4.*Spiroloculina anderzeni*, 5.*Miliammina pariaensis* , 6.*Triloculina* sp., 7.*Spiroloculina grata* , 8.*Quinqueloculina frigida* , 9.*Quinqueloculina atlantica*, 10.*Quinqueloculina Seminula*, 11.*Asterorotalia trispinosa*, 12.*Asterorotalia trispinosa*, 13.*Asterorotalia trispinosa*, 14.*Asterorotalia trispinosa*, 15.*Asterorotalia trispinosa*, 16*Elphidium discoidale*, 17.*Elphidium crispum*,18. *Elphidium advenum*,19.*Elphidium advenum*, 20.*Elphidium crispum*

Figure 9. Plate showing selected foraminifera species in Myeik Coastal Area

Distribution of living foraminifera species, genera and families. Norton (1930) examined the living foraminifera in Florida and West Indian regions. Four groups based on the depth and temperature has been divided. They are: Group A 0-5 fathoms and 21.5° to 31.4°C. *Miliolidae* and *Peneroplidae* are common to abundant. *Vulvulinidae, Calcarinidae, Homotremidae* and *Nonionidae* are rather common.Group B 5-60 fathoms and 18.9° C to 31.4° C.*Miliolidae* and *Peneroplidae* decrease and *Lagenidae, Textularidae, Buliminidae* and *Amphisteginidae* are common.Group C 500-825 fathoms and 4°C to 7.5°C

Benthonic Foraminifera reduce and *Globigerinidae* and *Globorotalidae* are predominant. Group D 2035 and 2849 fathoms and 1.83°C to 2°C.*Lagenidae* and *Buliminidae* persist to great depths but usually small numbers. *Rotaliidae* and *Anomalinidae* are rather uniformly present at nearly all depths.

The general results of Norton's work are in agreement with those obtained by Natland (1933) who examined the living Foraminifera in Southern California. Natland (1933) divided into (5) groups based on the depths, temperature and abundant Foraminiferal species characteristics.

Very low salinity correlated with reduced size of tests as well as reduced calcium carbonate and thinner shells. Other recent foraminifera living in water of very low salinity are species of *Quinqueloculia* and *Elphium* found in Venezuela (1/ 30 of normal salinity). Typical example of a fossil brackish water assemblages consists of a few species of *Elphidium, Nonion.* As a rule, salt bearing and gypsiferous beds do not contain Foraminifera, but interbedded clays or limestones may contain rich Foraminifera assemblages.

The top 500m of sea water are said to be saturated with respect to calcium carbonate which reflects the high alkalinity in the region. Below 550 m, water is considered under saturated with respect calcium carbonate and thus carbonate may begin to go into solution. Below this depth the lower alkalinities tend to cause calcium carbonate to dissolve. In general alkalinity decreases with the increasing depth and also if CO2 pressure increased, temperature decreased.

The benthonic foraminifera species of *Rotalia* spp. which survived at the depth of 20 m and more than 21.4ºC, can be abundantly found in sandy beach.

Almost all the common and dominant species described in the present work are cosmopolitan, occurring in other estuaries all over the world (Sen Gupta, 1999) and several of them were previously recorded by Ruiz et al. (1996, 2005) and Gonzalezet al. (2000) in Guadiana Estuary. A finding is that both *Miliolina* such as *Quinqueloculina frigida*, and *Spiroloculina grata* and Rotalia such as *Elphidium advena* which are currently abundant and along the Myeik Coastal Area.

Quinqueloculina seminula is one of the species with the greatest scientific consensus in terms of life position and ecological indicator value, its relative abundance is very useful in sea-level change studies because it reflects the elevation of the depositional environment in relation to the high-water level, where it may represent 100% of foraminiferal assemblages, decreasing towards the low marsh, where it is almost absent (Scott and Medioli, 1978, 1980).

Discussion and Conclusion

The Myeik coastal area is characterized by moderate distribution as there are a medium number of species occurring. The total species ranges from Myeik costal area are *Pyramillina* sp., *Tubinella* sp. *Bathsiphone spinosus, Bathsiphone* sp., *Spiroloculina anderseni, Miliammina pariaensis, Triloculina* sp., *Spiroloculina grata, Q. frigida, Q. atlantica, Q. seminula, Asterorotalia trispinosa, Elphidium discoidale, E. crispum, E. advena***.** The rare occurrence of all Rotalia group are controlled by the substrate condition. High nutrient environments in Myeik shoreline area are low energy area which has been used up in the decomposition of the organic materials providing the nutrients. There is some indication that the distribution of certain benthonics such as *Quinqueloculina* and a few planktonics may be actually adapted to low oxygen environment. It has been observed that the distribution of foraminifera and species diversity and species population depends largely on the type of coast and substrate. The Myeik coastal area are muddy and rich in food for foraminifera, so the species diversity and species population of foraminifera is high. In particular, all three are Textularid, Miliolid and Rotalid, but more abundant are found in the miliolid and rotalid groups. Only a few planktonic species have been found due to the presence of sediments in the deep sea without the presence of sediments in the deep sea. In summary, Muddy Beach shallow marine areas have higher diversity and population of foraminifera than other beaches.

Acknowledgements

The authors thanks Dr Nay Win Oo, Rector of East Yangon University, and Pro-Rectors Dr Aye Aye Ko, Dr Wah Wah Lwin and Dr Thidar Aung for their kind permission to submit this research paper. The author would also like to express sincere gratitude to Professor Dr Than Than Thwe, Head of Geology Department, East Yangon University for her encouragements, suggestions and discussions.

References

Aye San, (1981) "Geology of King Island, Mergui (West), Tenasserim Division". Field Report, Department of Geological Survey and Mineral Exlporation, Ministry of Mines (Unpulished).

Bender, F., (1983) Geology of Burma, 1st ed., Gebruder Borntraeger, Berlin.

Brown, J.C., Heron, A.M., (1923) "The Geology and ore deposits of the Tavoy district". https://www.britannica.com/place/Mergui

Memoirs of the Geological Survey of Indian, 44(2), 167-354, pl. 8.

Chhibber, H.L., (1934) *The Geology of Burma, London, Mac Millan*, 538pp. https://quizlet.com/395399247/sociology-ch-15-questions-flash-cards/

Chit Saing, (1972) Recent foraminifera from the Bay of Bengal of the Arakan Coast. M.Sc Thesis. Department of geology, Arts & Sci University Rangoon.

Earth Sciences Research Division, (1977) *The Geological map of Burma 1:1000,000 (with explanatory brochure).* Rangoon. https://en-us.topographic-map.com/

Kar (1993)., Coastal Geomorphology of the Kachchh coast, late Quaternary Morphodynamic., western India 47-75p. https://www.aboutcivil.org/coarse-grained-vs-fine-grained-comparison

Marial. Machain. Castillo., 2007, Recent planktonic foraminifera distribution patterns and their relation to hydrographic conditions of the Gulf of Tehuantepec, Mexican Pacific. http://taxonomicon.taxonomy.nl/Reference.aspx?id=8415

Oldham, T. (1856) "Notes on the coal-fields and tin-stone deposits of the tenasserim Provinces".Sel. Records of Government of India, 10, 31-67. https://www.merriam-webster.com/dictionary/widely%20distributed

Prinsep, J., (1838) "Report on Mergui coal". Journal of the Asiatic Society of Bengal. 7,705-706.

Rau, Sethu Rama, S., (1930) The geology of the Mergui district. *Memoirs of the Geological Survey of India*, 55(1), 1-62, 10 pls. https://catalog.lib.kyushu-u.ac.jp/opac_download_md/4060151/eng2967.pdf

Subba Rao, M., Vedanatam, D. and Nageswara Ra0, S., distribution and ecology of Benthic foraminifera in the sediment of Visahapatnaam shelf, East Coast of India. https://link.springer.com/chapter/10.1007/978-94-009-8498-1_2.

Paleogeography, Paleochimatology, Palaecology, 1979,27,349-369. https://www.mynces. org/download/ 2018/ ProceedingMNCES2018/48_Win%20Lai%20Lai.pdf

Searl, D.L., Ba Than Haq, (1964) The Mogok Belt of Burma and its relationship to the Himalayan orogeny. *Proceeding of the International Geological Congress*, New Delhi, India, 22, pp. 133-161.

Win Swe & Than Tun Chein, (1975) 10th Burma Research Congress, Rangoon (Unpublished).

Win Swe, (1977) Progress report of the Field Mapping Division, Annual Geological Report (1975-76), Department of Geological Survey and Mineral Exploration, Ministry of Mines.

Online sources

https://www.nationalgeographic.org/article/cause-effect-tides/

https://mynces.org/download/2019/ProceedingMNCES2019/80_HlaYinMin.pdf

https://quizlet.com/303039415/local-anesthesia-chapter-13-mandibular-flash-cards/

https://slcc.pressbooks.pub/physicalgeography/chapter/4-1/

https://plants.ces.ncsu.edu/plants/rohdea-japonica/

https://www.nationalgeographic.com/science/article/coastlines

https://wandofknowledge.com/landform-types-processes-in-formation-gradation-of-landform/

https://www.researchgate.net/publication/303586824_Coastal_Geomorphology_An_Introduction

https://en.wikipedia.org/wiki/Quinqueloculina

https://pubmed.ncbi.nlm.nih.gov/33170955/

https://en.wikipedia.org/wiki/High-nutrient,_low-chlorophyll_regions

https://pubmed.ncbi.nlm.nih.gov/30159463/

https://www.researchgate.net/publication/228544768_Shoreline_Definition_and_Detection_A_Review

https://www.chegg.com/homework-help/questions-and-answers/equilibrium-concentration-carbonate-ion-saturated-lead-carbonate-solution-m-q37848411

https://www.gbif.org/species/7757981

https://www.sciencedirect.com/topics/earth-and-planetary-sciences/foraminifera

https://www.khanacademy.org/science/biology/ecology/biogeography/a/tolerance-ranges-of-species

http://novascotia.com/

https://brainly.com/question/18942615

https://www.researchgate.net/publication/283703718_Mediterranean_coastal_lagoons_sustainable_management_and_interactions_among_aquaculture_capture_fisheries_and_the_environment_Studies_and_Reviews_General_Fisheries_Commission_for_the_Mediterranean_No_

https://www.sciencedirect.com/topics/earth-and-planetary-sciences/alkalinity

https://serc.carleton.edu/hydromodules/steps/168500.html

https://fishtankadvisor.com/brackish-water-fish/

https://pubs.geoscienceworld.org/cushmanfoundation/jfr/article-abstract/43/1/14/294741/The-Ecology-of-Asterorotalia-Trispinosa-Thalmann

https://pubs.geoscienceworld.org/cushmanfoundation/jfr/article-abstract/36/4/355/77048/taxonomy-and distribution-of-the-uvigerina

https://en.wikipedia.org/wiki/Rotaliida
https://depts.washington.edu/forams/by-species-order-rotaliida/genus-buliminella/
https://www.nature.com/articles/s41477-018-0250-6
https://up.codes/s/use-group-5
https://convertilo.com/3-125-inches-to-feet
https://marinespecies.org/aphia.php/www.oceandocs.org/handle/1834/rest/aphia.php?p=taxdetails&id=814782